Received: 8 July 2021 | Revised: 24 August 2021 | Accepted: 25 August 2021

DOI: 10.1002/cne.25243

RESEARCH ARTICLE

JCN RESEARCH IN SYSTEMS NEUROSCIENCE THE JOURNAL OF COMPARATIVE NEUROLOGY WILEY

Cellular resolution anatomical and molecular atlases for prenatal human brains

Song-Lin Ding[1] | Joshua J. Royall[1] | Phil Lesnar[1] | Benjamin A.C. Facer[1] | Kimberly A. Smith[1] | Yina Wei[2] | Kristina Brouner[1] | Rachel A. Dalley[1] | Nick Dee[1] | Tim A. Dolbeare[1] | Amanda Ebbert[1] | Ian A. Glass[3] | Nika H. Keller[1] | Felix Lee[1] | Tracy A. Lemon[1] | Julie Nyhus[1] | Julie Pendergraft[1] | Robert Reid[1] | Melaine Sarreal[1] | Nadiya V. Shapovalova[1] | Aaron Szafer[1] | John W. Phillips[1] | Susan M. Sunkin[1] | John G. Hohmann[1] | Allan R. Jones[1] | Michael J. Hawrylycz[1] | Patrick R. Hof[4] | Lydia Ng[1] | Amy Bernard[1] | Ed S. Lein[1]

[1]Allen Institute for Brain Science, Seattle, Washington, USA

[2]Zhejiang Lab, Hangzhou, Zhejiang, P. R. China

[3]Department of Pediatrics and Medicine, University of Washington School of Medicine, Seattle, Washington, USA

[4]Nash Family Department of Neuroscience and Friedman Brain Institute, Icahn School of Medicine at Mount Sinai, New York, New York, USA

Correspondence
Song-Lin Ding and Ed S. Lein, Allen Institute for Brain Science, Seattle, WA 98109, USA.
Email: songd@alleninstitute.org; EdL@alleninstitute.org

Funding information
National Institute of Mental Health, Grant/Award Number: RC2MH089921

Abstract

Increasing interest in studies of prenatal human brain development, particularly using new single-cell genomics and anatomical technologies to create cell atlases, creates a strong need for accurate and detailed anatomical reference atlases. In this study, we present two cellular-resolution digital anatomical atlases for prenatal human brain at postconceptional weeks (PCW) 15 and 21. Both atlases were annotated on sequential Nissl-stained sections covering brain-wide structures on the basis of combined analysis of cytoarchitecture, acetylcholinesterase staining, and an extensive marker gene expression dataset. This high information content dataset allowed reliable and accurate demarcation of developing cortical and subcortical structures and their subdivisions. Furthermore, using the anatomical atlases as a guide, spatial expression of 37 and 5 genes from the brains, respectively, at PCW 15 and 21 was annotated, illustrating reliable marker genes for many developing brain structures. Finally, the present study uncovered several novel developmental features, such as the lack of an outer subventricular zone in the hippocampal formation and entorhinal cortex, and the apparent extension of both cortical (excitatory) and subcortical (inhibitory) progenitors into the prenatal olfactory bulb. These comprehensive atlases provide useful tools for visualization, segmentation, targeting, imaging, and interpretation of brain structures of prenatal human brain, and for guiding and interpreting the next generation of cell census and connectome studies.

KEYWORDS
amygdala, brain development, cerebral cortex, ganglionic eminence, gene expression, hippocampal formation, thalamic nuclei

This is an open access article under the terms of the Creative Commons Attribution-NonCommercial-NoDerivs License, which permits use and distribution in any medium, provided the original work is properly cited, the use is non-commercial and no modifications or adaptations are made.
© 2021 The Authors. *The Journal of Comparative Neurology* published byWiley Periodicals LLCWiley Periodicals LLC.

Contents

Main text . . . 7
TABLE 1: Abbreviations and ontology of brain structures . . . 37
APPENDIX 1: Anatomical atlas plates for the prenatal human brain at PCW 15 . . . 56
APPENDIX 2: Spatial expression of 37 genes in the brain at PCW 15 . . . 98
APPENDIX 3: Anatomical atlas plates for the prenatal human brain at PCW 21 . . . 281
APPENDIX 4: Spatial expression of five representative genes in the brain at PCW 21 . . . 422

1 | INTRODUCTION

Anatomical brain atlases are essential tools for visualizing, integrating, and interpreting experimental data about brain structure, function, circuits, cell types, and structure-function-behavior relationships (Evans et al., 2012; Wang et al., 2020). We previously generated brain-wide detailed microarray-based transcriptomic atlases for the prenatal human brain at postconceptional weeks (PCW) 15, 16, and 21 (Miller et al., 2014), and single-cell genomic studies are now increasingly profiling prenatal brains to define cellular diversity, developmental trajectories, and gene regulatory mechanisms (Eze et al., 2021; Fan et al., 2020; Nowakowski et al., 2017). To provide an anatomical and ontological framework for these prior and future studies of human brain development, here we aimed to create detailed and accurate reference atlases that densely sample the whole developing brain at PCW 15 and 21. These prenatal human brain atlases can also be important tools to guide increasing neuroimaging studies of prenatal human brains and developmental deficits and malformations (Kostović et al., 2019; Oishi, Chang, & Huang, 2019).

Two highly detailed comprehensive anatomical atlases are available for the adult human brain (Ding et al., 2016; Mai et al., 2016). Fewer anatomical references are available for developing human brains, and especially for prenatal stages. Only one series of prenatal human brain atlases is available, generated on a limited set of Nissl-stained sections from different brain specimens (Bayer & Altman, 2003, 2005, 2006). While heroic efforts at the time, these atlases have relatively low sampling density, are limited to Nissl stain, and have much fewer structural annotations than the adult atlases. For example, only 15 and 13 coronal sections were annotated for the human brain atlases from prenatal weeks (PW) 13.5 and 17, respectively (Bayer & Altman, 2005). Furthermore, certain developmental stages, such as PW 15 and 16, are not available in this atlas series.

In this study, we aimed to create a plate-based atlas with coverage of essentially all anatomical structures, a complete developmental structural ontology, and a high information content gene expression analysis that allows accurate structural delineation. Whole brain serial sectioning was performed on each brain, with interdigitated histochemistry and in situ hybridization (ISH) spanning the entire brain specimens, which were scanned at 1 μm/pixel resolution. We annotated representative Nissl-stained coronal sections spanning the brain (46 sections for the PCW 15 brain and 81 sections for the PCW 21 brain) based on a combined analysis of cytoarchitecture, acetylcholinesterase (AChE) staining, and expression patterns of selected genes from the same brain. Annotations were also performed on a series of the ISH images that often delineate particular structures well (sections for 37 and 5 selected genes from the PCW 15 and 21 brains, respectively). Finally, these atlases are presented as freely accessible online interactive data resources (www.brain-map.org or www.brainspan.org).

2 | MATERIALS AND METHODS

2.1 | Prenatal human brain specimens

Two postmortem human brain specimens at PCW 15 (male; Caucasian) and PCW 21 (female; Asian), respectively, were used for generation of anatomical and molecular atlases. Both specimens were procured from Laboratory of Developmental Biology at the University of Washington, Seattle, USA. All work was performed according to guidelines for the research use of human brain tissue and with approval by the Human Investigation Committees and Institutional Ethics Committees of University of Washington. Appropriate written informed consent was obtained and all available nonidentifying information was recorded for each specimen. The criteria for tissue selection include no known history of maternal drug or alcohol abuse, potential teratogenic events, or HIV1/2, HepB or HepC infection, and no neuropathological defects were observed in histological data derived from these tissues. Eligible tissue was also screened to ensure cytoarchitectural integrity (analysis of Nissl-stained sections) and high RNA quality. Both brains met above criteria and showed normal appearance and high RNA quality with an average RNA integrity number of 8 and 9 for PCW 15 and 21, respectively. Both brains were bisected, and the left hemisphere was used for DNA microarray analysis (see Miller et al., 2014) and right hemisphere was used for histology and ISH stains. For the right hemisphere, two and four coronal slabs were cut for the PCW 15 and 21 brains, respectively, based on the size of the hemisphere. These slabs were frozen in isopentane chilled to −50°C and stored at −80°C until sectioning. Serial sectioning was performed through the whole hemisphere, slab by slab. Nissl, AChE, and ISH stains for 43 gene probes were carried out on sequential series of sections (see below). For both stages, sequential sections for Nissl and AChE stain were regularly spaced and flanked by series of ISH for marker genes. All histology and ISH sections were digitally scanned at 1.0 μm/pixel. To generate anatomical atlases for PCW 15 and 21 brains, 46 out of the 115, and 81 out of the 174 Nissl-stained sequential sections were selected, respectively.

2.2 | Nissl staining

After sectioning 20 μm-thick sections in the coronal plane from an entire hemisphere of the specimens, slides were baked at 37°C for 1 to

5 days and were removed 5 to 15 min prior to staining. Sections were defatted with xylene or the xylene substitute Formula 83, and hydrated through a graded series containing 100, 95, 70, and 50% ethanol. After incubation in water, the sections were stained in 0.213% thionin, then differentiated, and dehydrated in water and a graded series containing 50, 70, 95, and 100% ethanol. Finally, the slides were incubated in xylene or xylene substitute Formula 83, and coverslipped with the mounting agent DPX. After drying, the slides were analyzed microscopically to ensure staining quality.

2.3 | AChE staining

A modified AChE protocol was used to help delineate subcortical structures at high resolution. AChE staining was performed using a direct coloring thiocholine method combined with a methyl green nuclear counterstain to improve tissue visibility (Karnovsky & Roots, 1964). Glass slides with fresh-frozen tissue sections were removed from 4°C, allowed to equilibrate to room temperature, fixed in 10% neutral buffered formalin, and washed briefly in ultra-pure water. Sections were then incubated for 30 min in a solution of acetylthiocholine iodide, sodium citrate, cupric sulfate, and potassium ferricyanide in a 0.1 M sodium acetate buffer (pH 6.0), washed in 0.1 M Tris-HCl buffer (pH 7.2), incubated with 0.5% diaminobenzidine in 0.1 M Tris-HCl with 0.03% hydrogen peroxide. Slides were incubated in 0.2% methyl green, briefly dipped in 100% ethanol, cleared with Formula 83 and coverslipped with DPX.

2.4 | ISH staining

A colorimetric, digoxigenin-based method for labeling target mRNA was used to detect gene expression on human prenatal tissue sections with 43 selected genes (see Lein et al., 2007). These genes include canonical morphological and cell-type markers and disease-related genes associated with neocortical development. Gene selection was preferential toward data available through the Allen Developing Mouse Brain Atlas (Thompson et al., 2014), allowing a direct phylogenetic comparison of gene expression patterns between mouse and human. Gene lists and details of the ISH process are available online (http://help.brain-map.org/display/devhumanbrain/Documentation). Gene list is also shown in the legend of Appendix 2.

2.5 | Digital imaging and image processing

Digital imaging of the stained slides was done using a ScanScope XT (Aperio Technologies Inc., Vista, CA) with slide autoloader. The final resolution of the images was 1 μm/pixel. All images were databased and preprocessed, then subjected to quality control (QC) to ensure optimal focus and that no process artifacts were present on the slide images. Images that passed this initial QC were further assessed to ensure that the staining data were as expected. Once all QC criteria were met, images became available for annotation of anatomical structures.

2.6 | Generation of whole-brain structure ontology

To generate a unifying hierarchical ontology for both developing and adult human brains with each structure having a unique identification code, we first subdivided the brain into three major parts: forebrain, midbrain, and hindbrain. Under each major part, we created four main branches: gray matter, white matter, ventricles, and surface structures (e.g., cortical sulci and gyri). Under the gray matter branches two types of brain structures were separated: transient and permanent ones. Under the transient structures, we listed all structures that only appear during development and not exist in adult brain (see Table 1 for detailed transient structures). Under the permanent structures, we listed all structures that exist in both developing and adult brains (for details see Table 3 of Ding et al., 2016). Table 1 also lists abbreviations for the main brain structures shown in this study.

2.7 | Creation of prenatal human brain atlases

For the specimen at PCW 15, a total of 115 Nissl-stained sections were produced at 1.04 mm spacing. For annotation 46 slides were chosen, including 23 from slab 1 (~1 mm sampling density for the first 7 Nissl-stained levels, ~0.5 mm for the remaining 16 ones), and 22 from slab two (~0.5 mm sampling density for the first 16 Nissl-stained levels, ~1 mm for the remaining 6 ones), and a single additional section effectively between slabs one and two. For the specimen at PCW 21, four slabs were generated due to its larger size than the PCW15 brain. Each of these four slabs were sectioned into 174 Nissl-stained sections with 3 per 1.2 mm. A total of 81-stained levels were chosen for annotation for anatomical atlas of this stage including 13 from slab 1 (~1.2 mm sampling density), 32 from slab 2 (~0.5 mm sampling density), 22 from slab 3 (~0.5 mm sampling density for the first 16, ~1.2 mm sampling density for the remaining 6), and 14 from slab 4 (~1.2 mm sampling density). These particular sections were chosen to represent the anatomy with a frequency that corresponded with the structural complexity of the regions contained at that plane of section. In very frontal and occipital regions, for example, it is not necessary to densely sample cortical regions that are large and do not change much from section-to-section. In contrast, in middle regions containing many small subcortical regions the sampling density was increased to match that complexity and not miss any small structures (i.e., more Nissl-stained sections were chosen for annotation). The position of each chosen section in a given slab was marked.

Annotation of the present brain atlases was performed similarly to that of our digital adult human brain atlas (Ding et al., 2016). Briefly, annotation drawings were done on printouts of the Nissl-stained sections and then digitally scanned. Digital cartographic translation of expert-delineated Nissl printouts was performed using Adobe Creative Suite 5. The resulting vector graphics were then converted to Scalable Vector Graphics (SVG). Each polygon was then associated with a structure from the ontology (see Table 1). Collating polygons in this way allows the flexibility to create various presentation modes (e.g., with or without colorization and transparency). The brain

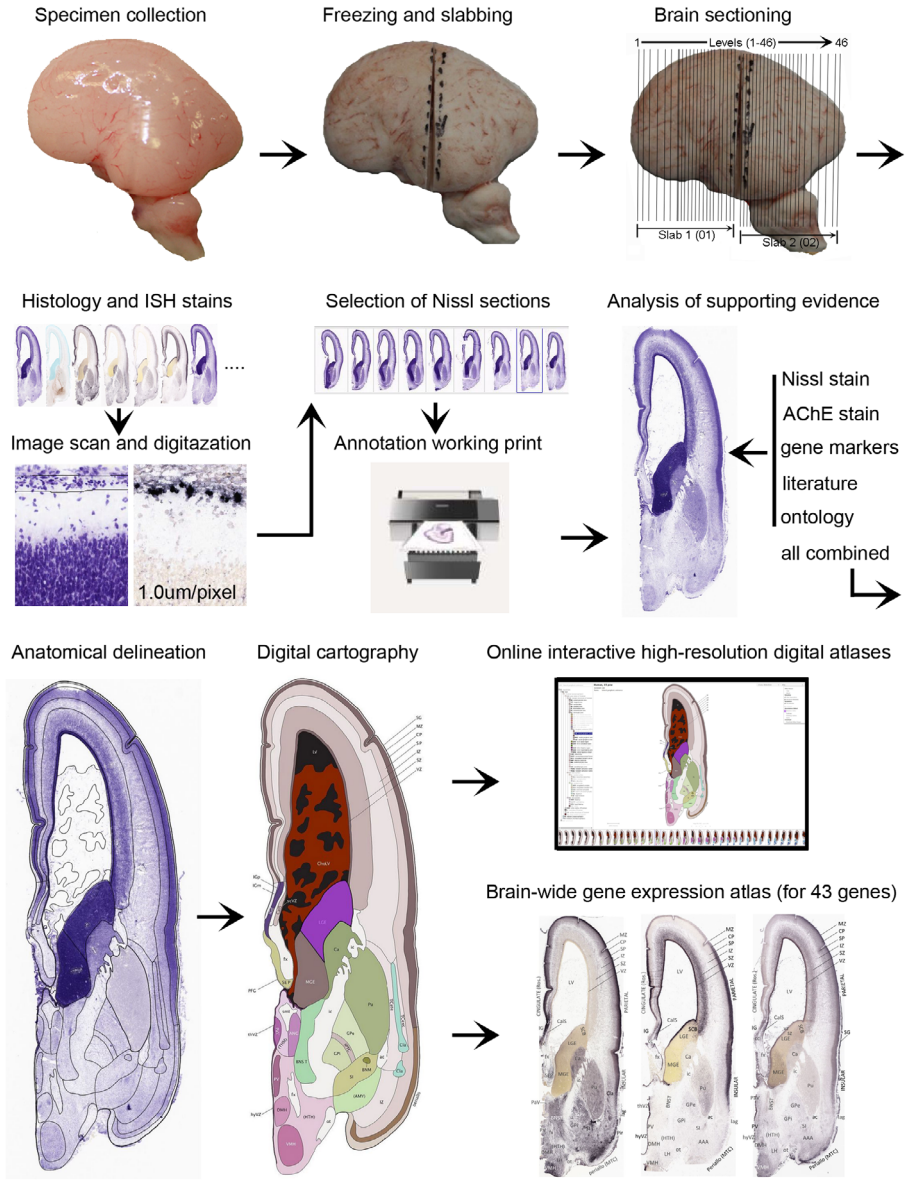

FIGURE 1 Workflow for atlas generation

structures were colorized to assist users with identifying structures across different sections (see Appendices 1 and 3). Gross ontological groups ("parents") were assigned hues from a range of the color spectrum. Each structure within a given parent group ("child") was given a variation of the parent hue according to its relative cellular contrast in Nissl stain. The following general principle was applied: the higher the density, the deeper the shade (i.e., addition of black to hue); the lower the density, the deeper the tint (i.e., addition of white to hue). Large parent groups (e.g., thalamus) were assigned uniformly light variations of their principal hues to provide a visually subtle, cohesive backdrop for component substructures, which often exhibit a range of relative cellular contrasts (reflected by shades and tints). To create gene expression atlases for PCW 15 and 21 brains, we applied annotations from the anatomical atlases for each age onto the interleaved coronal ISH sections for 37 (PCW15) and 5 (PCW21) genes out of 43 (see Appendices 2 and 4). The workflow for generation of the prenatal human brain atlases is similar to the one described in our adult human brain atlas (Ding et al., 2016) and is briefly summarized in Figure 1.

3 | RESULTS

3.1 | Structural annotation of histological and molecular prenatal human brain datasets

To generate accurate and detailed anatomical brain atlases, we performed both histological stains (Nissl and AChE) and ISH for 43 gene probes on sequential sets of coronal cryosections from right hemisphere of two midgestation brains (PCW 15 and 21). With the anatomical atlases as a guide, we also annotated the spatial expression of 37 and 5 genes in the brain at PCW 15 and 21, respectively; these are treated as prenatal molecular brain atlases. The anatomical and

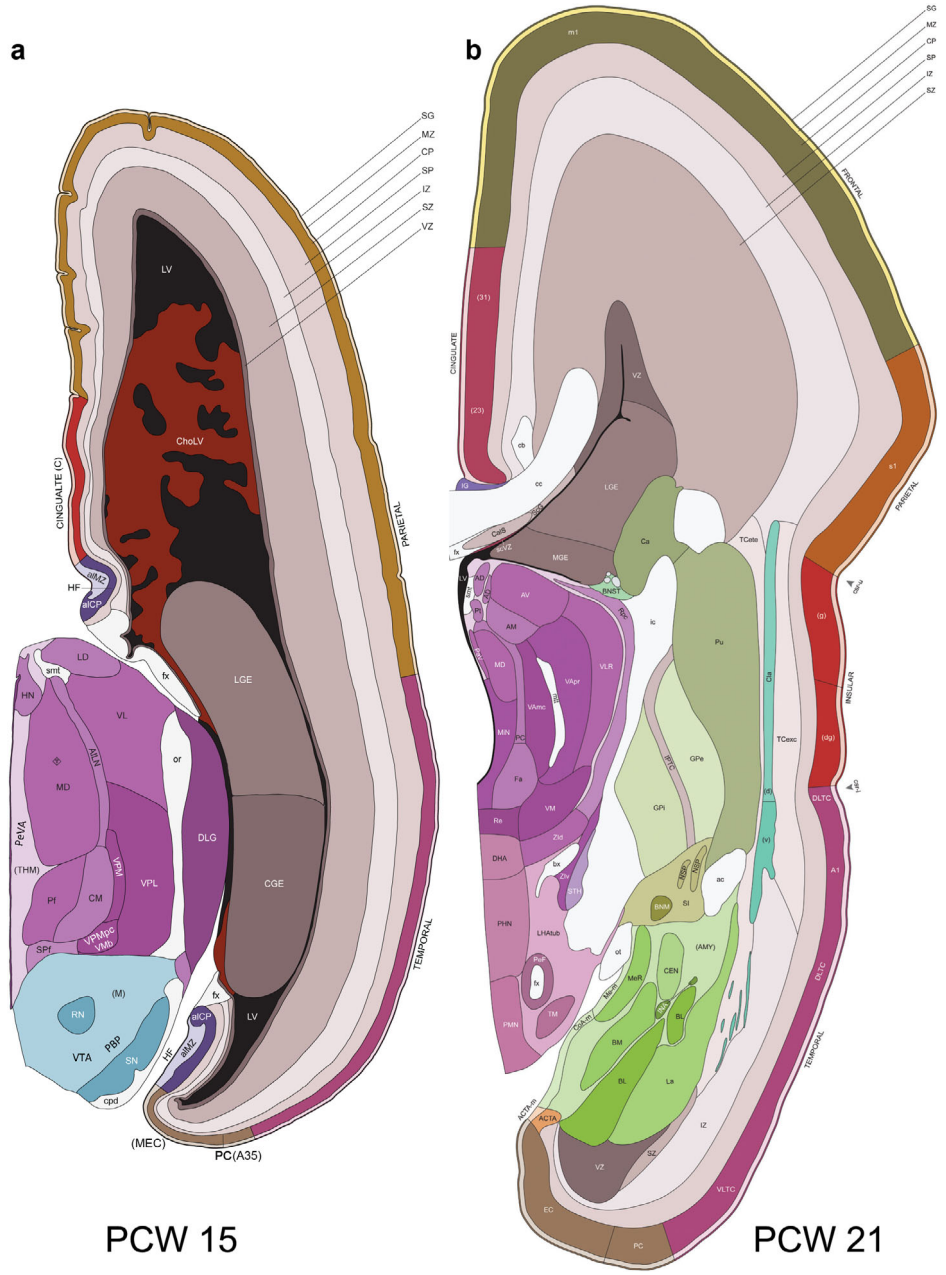

FIGURE 2 Example of anatomical atlas plates from PCW 15 (a) and 21 (b) brains

molecular atlases for the brain at PCW 15 are presented in Appendices 1 and 2, respectively. The similarly generated anatomical and molecular atlases for the brain at PCW 21 are presented in Appendices 3 and 4. All appendices have online links for cellular resolution histology and ISH images (1.0 μm/pixel). Example plates of annotated anatomical atlases from the two brains are shown in Figure 2 (where a and b designate PCW 15 and PCW 21, respectively). Delineation of anatomical boundaries of different cortical layers and brain regions are detailed below with emphasis mainly on the brain at PCW 15 although some major molecular features from the brain at PCW 21 are also described for comparison.

3.2 | Delineation of prenatal neocortical layers

PCW 15. In Nissl preparations, seven neocortical layers can be generally identified. For example, from the pia to the lateral ventricle (LV) of the medial occipital cortex, these layers include the subpial granular zone (SG), marginal zone (MZ), cortical plate (CP), subplate (SP), intermediate zone (IZ), subventricular zone (SZ), and ventricular zone (VZ) (Figure 3a). The SZ can be further subdivided into less densely packed outer and more densely packed inner parts (SZo and SZi, respectively) with SZi adjoining VZ, which is the most densely packed zone near the LV (Figure 3a). However, evidence for the existence of two

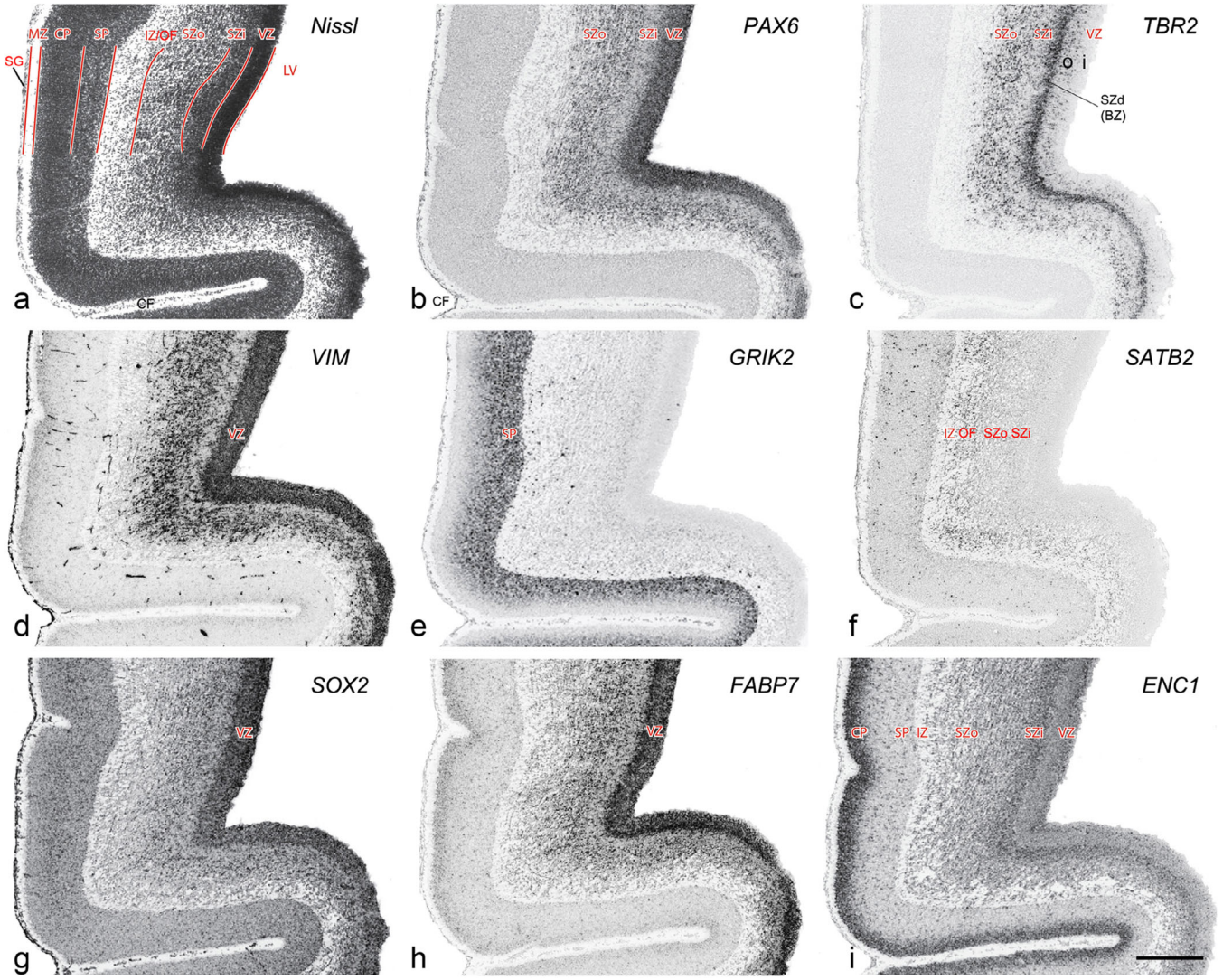

FIGURE 3 Molecular marker expression in medial occipital cortex at PCW15. (a) A Nissl-stained section showing the lamination of the cortex near the calcarine fissure (CF). (b-i) Expression patterns of *PAX6* (b), *TBR2* (c), *VIM* (d), *GRIK2* (e), *SATB2* (f), *SOX2* (g), *FABP7* (h), and *ENC1* (i). Note that a dense zone of *TBR2* expression at the border between SZi and VZ is termed as deep SZ zone (SZd) or border zone (BZ). The thickness ratio of SZo to VZ is about 3:1. SG, subpial granular zone; MZ, marginal zone; CP, cortical plate; SP, subplate; IZ, intermediate zone; OF, outer fiber zone; SZ, subventricular zone; SZo and SZi, outer and inner SZ; VZ, ventricular zone; LV, lateral ventricle. These terms apply to main text and all related figures below. Scale bar: 400 μm in (i) for all panels

subdivisions of the SP is not observed although the two portions were reported for human brains at PCW 13 and 14 (Kostovic & Rakic, 1990). At PCW15, the outer fiber zone (OF) begins to appear in the outermost part of the SZo, deep to the IZ. The OF is positive for AChE staining (see the AChE plates in Appendix 1). To confirm and accurately to delineate the developing neocortical layers, we analyzed the large set of ISH data described above and found that many genes display layer-specific expression patterns. For instance, in the medial occipital/visual cortex (Figure 3), *PAX6* and *TBR2* (*EOMES*) are selectively expressed in the proliferative zones VZ and SZ with strongest *PAX6* and *TBR2* expression in VZ and deepest SZ (SZd), respectively (Figure 3b and c). SZd was sometimes termed as the border zone (BZ) between SZ and VZ. Interestingly, inner part of the VZ (VZi, near LV) does not show *TBR2* expression (Figure 3c). *VIM*, *SOX2*, and *FABP7* are also dominantly expressed in VZ and SZ (VZ > SZ) but with weak expression in CP (Figure 3d, g, and h). In contrast, *GRIK2* and *SATB2* are selectively expressed in the postmitotic zones IZ/OF, SP, and CP. Specifically, *GRIK2* is dominantly expressed in SP and deep CP with weak expression in IZ while *SATB2* is mainly expressed in IZ/OF with weak expression in SP and CP (Figure 3e and f). Some genes (e.g., *ENC1*) are strongly expressed in both proliferative (VZ, SZ) and postmitotic (CP) zones (Figure 3i).

To examine whether more anterior neocortical regions display similar or different laminar organization, we investigated the same set of genes expressed in the dorsomedial frontal neocortex (Figure 4). In this region, all the cortical layers are visible with relatively thick SP compared to CP (Figure 4a). Compared to the occipital region, the

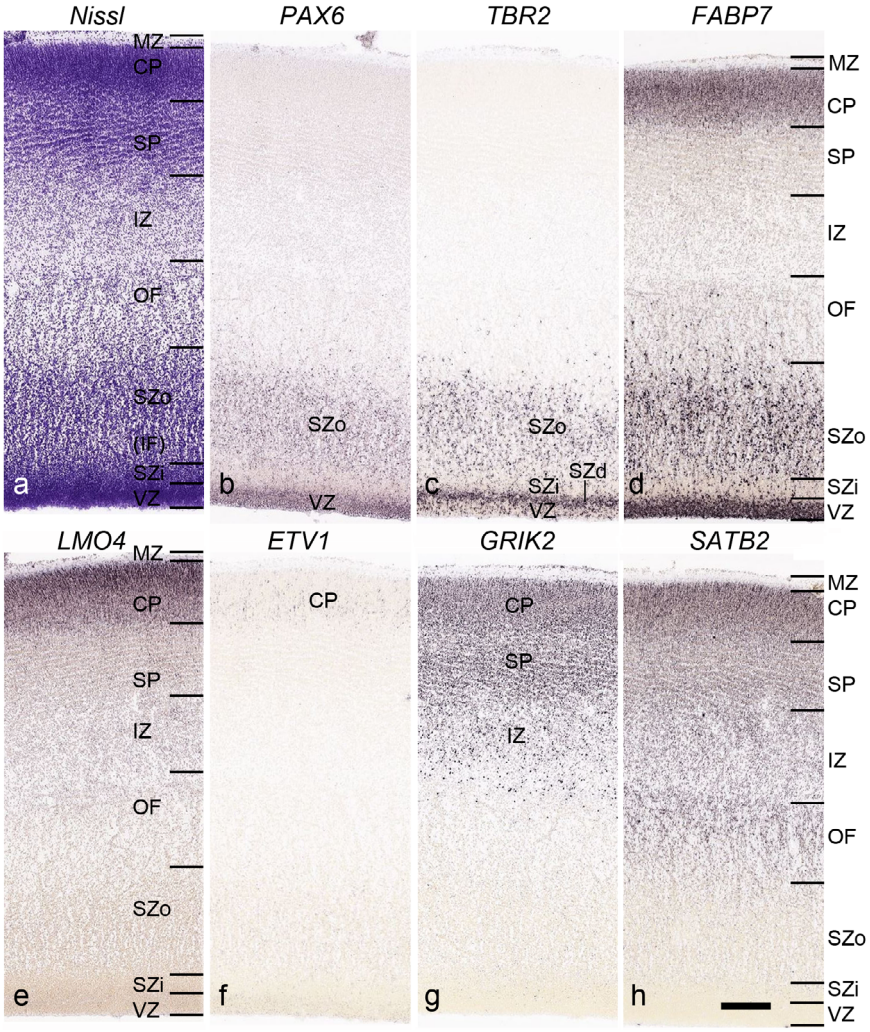

FIGURE 4 Gene expression in medial frontal cortex at PCW 15. (a) Nissl-stained section showing the laminar organization of the cortex. (b-h) Expression patterns of *PAX6* (b), *TBR2* (c), *FABP7* (d), *LMO4* (e), *ETV1* (f), *GRIK2* (g), and *SATB2* (h). Note that the thickness ratio of SZo to VZ is about 5:1. Scale bar: 330 μm in (h) for all panels

existence of the OF in the frontal cortex is more visible and thicker. The OF contains many radially oriented SZ cells (Figure 4a) and is, thus, included in the outermost part of SZo in the present atlas (i.e., the OF is not annotated separately from the SZo in Appendix 1). In the frontal cortex, *VIM*, *SOX2*, *PAX6*, and *TBR2* have similar expression patterns as in the occipital cortex (e.g., Figure 4a-c). Compared to the occipital cortex, *FABP7* shows stronger expression in CP (Figure 4d) although expression in other zones is comparable to the occipital cortex. *LMO4* is selectively expressed in the CP (Figure 4e) while this expression in the occipital cortex is not obvious (see Appendix 2). *GRIK2* display strong expression in CP, SP, and IZ of frontal cortex (Figure 4g), while it is mainly expressed in SP of occipital cortex (Figure 3e). *SATB2* in the frontal cortex has strong expression in CP, SP, IZ, and OF (Figure 4h), while only the OF has strong expression in the occipital cortex. In addition, *ETV1* expression appears in the deep CP (Figure 4f), but is not detected in the occipital cortex (not shown). The differential gene expression could reflect differential maturation across the cortex as well as regional differences. Additional data on later stages are needed to address this issue. Finally, it is noted that the inner fiber zone (IF), which is a cell-sparse zone located between SZo and SZi (see Figure 5a), is not clearly distinguishable in most of the neocortical regions at PCW 15 (e.g., Figure 4a) except in the middle lateral region (mainly parietal cortex, see the Nissl plates in Appendix 1).

PCW 21. On Nissl-stained sections, all the cortical layers that appeared at PCW 15 can be identified at PCW21, although changes in their relative thickness are observed. In the occipital/visual cortex, the thickness of CP and SZo is greatly increased and outer and inner CP (CPo and CPi) are distinguishable (Figure 5a). A major feature of the neocortex at PCW 21 is the clear presence of the IF across all neocortical regions (e.g., Figure 5a). The IF was reported to be immunoreactive to SLIT-ROBO Rho GTPase activating protein 1 (see Molnár & Clowry, 2012). Some callosal fibers may contribute to this IF zone since the callosal fibers appear to extend in this zone from medial to lateral aspects (see Nissl plates in Appendices 1 and 3). Tangential migrating cortical interneurons, which are derived from the ganglionic eminence (GE), are mainly located in this zone before invading the CP. At PCW 21, *NPY* expression is mainly located in the SP of all neocortical regions and in the middle CP layers (future layers 3 and 4) of V1 (Figure 5e). Strong *PAX6*, *TRB2*, and *VIM* expression is restricted in the proliferative zones (SZo, SZi, and VZ) of the neocortex, similar to the findings from PCW 15. The OF and IF at PCW 21 still contain a lot of SZo cells and,

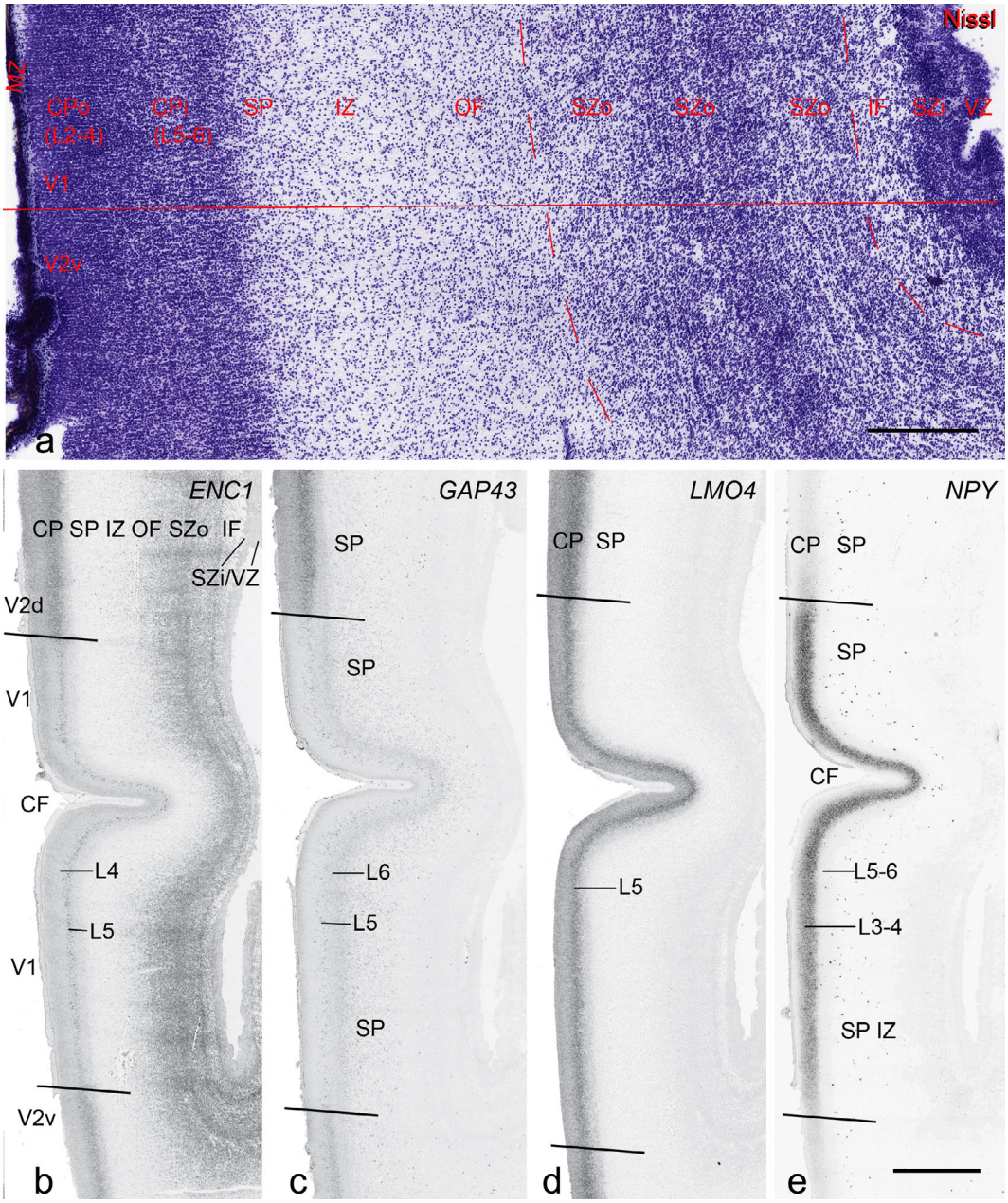

FIGURE 5 Cytoarchitecture and gene expression in the medial occipital cortex at PCW 21. (a) A Nissl-stained section showing the lamination of the cortex. CPo (future layers 2 to 4) and CPi (future layers 5 and 6) can be appreciated but differentiation between V1 and V2 (here V2v) is not yet clear in Nissl preparations. Inner fiber zone (IF) can be identified as a cell-less zone between SZi and SZo. (b-e) Expression patterns of *ENC1* (b), *GAP43* (c), *LMO4* (d), and *NPY*(e). Note the obvious difference of the gene expression patterns between V1 and the dorsal and ventral V2 (V2d and V2v, respectively). Scale bars: 400 μm in (a); 1600 μm in (b) for panels (b-e)

thus, are included in the SZ (SZo) in our atlas plates (Appendix 3). *SST* is an additional marker for the SP at PCW21 (Appendix 4).

3.3 | Delineation of prenatal neocortical areas

PCW 15. On Nissl-stained sections, obvious differences among neocortical regions were not observed at PCW 15. However, an anterior-posterior (A-P) gradient of gene expression in neocortex was observed. For instance, *LMO4* displays strong expression in the CP of frontal and temporal cortices with gradually weaker expression in parietal and occipital cortices (Figure 6a and b). In contrast, *NPY* expression in the CP is stronger in temporal (Figure 6c) and occipital cortices than in parietal (Figure 6c) and frontal (Figure 6d) cortices. *NPY* expression in the SP also shows regional difference with relatively stronger expression in posterior and lateral neocortex and weaker expression in anterior and medial neocortex (Figure 6c and d). In addition, *NTRK2* shows weak expression in the SP and CPi of frontal neocortex but gradually stronger expression in parietal, temporal, and occipital cortices, and is strongest in occipital neocortex (see Appendix 2). A-P differences

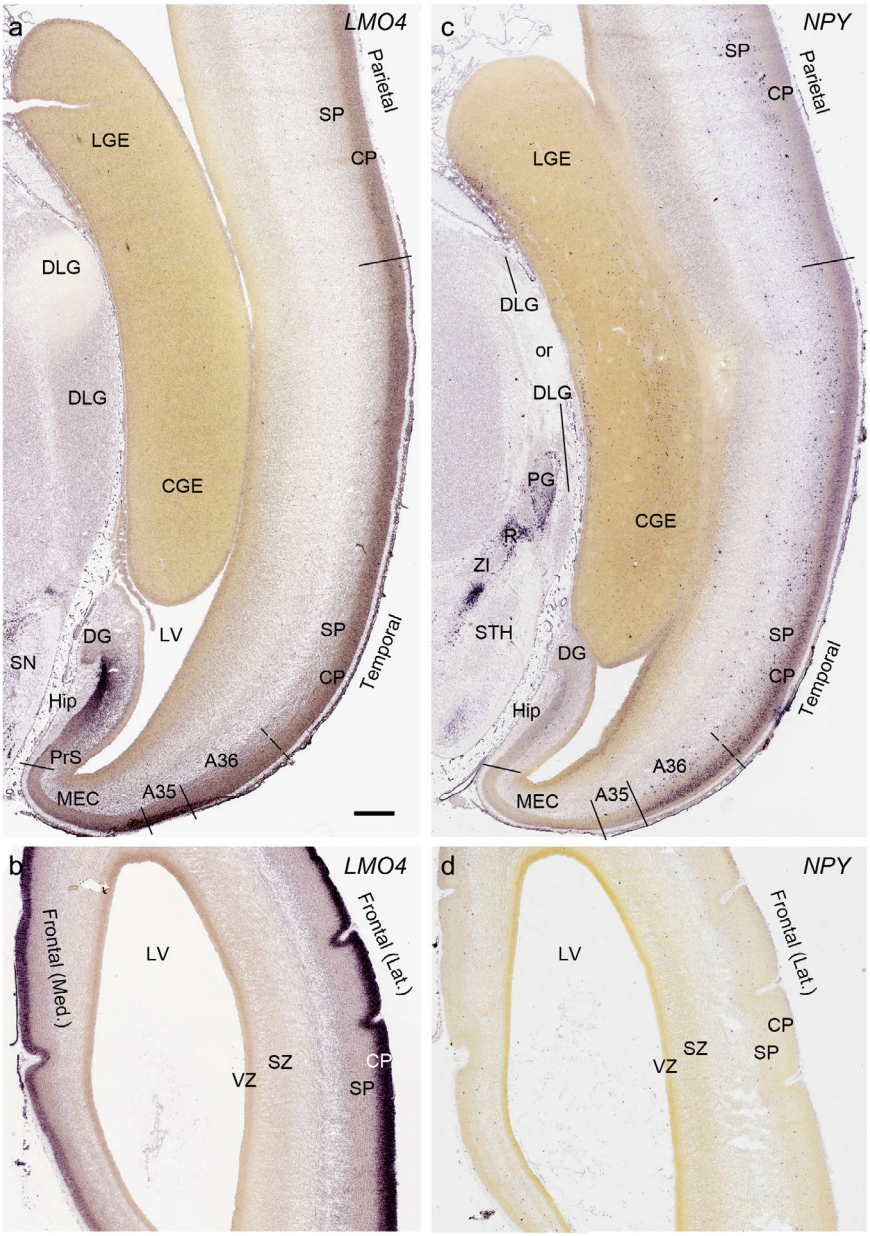

FIGURE 6 Differential gene expression across neocortex at PCW15. (a,b) Expression of *LMO4* in parietal, temporal (a), and frontal (b) cortices. Note the strong expression in the hippocampus (Hip). (c,d) Differential expression of *NPY* in parietal, temporal (c), and frontal (d) cortices. *NPY* is also expressed in the pregeniculate (PG) and reticular thalamic (R) nuclei. DLG, dorsal lateral geniculate nucleus; SN, substantia nigra; ZI, zona incerta; STH, subthalamic nucleus. Scale bar: 790 μm in (a) for all panels

in *FABP7*, *LMO4*, *GRIK2*, and *SATB2* expression in different layers also occur between dorsomedial frontal and occipital cortices (compare Figure 3–4). However, primary sensory (V1, A1 [primary auditory] and S1 [somatosensory]) cortices and primary motor cortex (M1) are not distinguishable from adjoining areas at PCW 15. The cingulate cortex can be identified based on its differential expression patterns of genes, such as *ETV1*, *ENC1*, and *LMO4*, from adjoining regions (see Appendix 2). Therefore, frontal, parietal, temporal, occipital, and cingulate cortices can be roughly identified at PCW 15.

PCW 21. In addition to the identified major neocortical regions described above, one important feature at PCW 21 is that V1 can be distinguished from the secondary visual cortex (V2) on *ENC1*-, *GAP43*-, *LMO4*-, and *NPY*-ISH sections (Figure 5b-e) although the borders are not yet discernable based on Nissl staining (Figure 5a). Generally, the former three genes are much less expressed in V1 than in V2 (Figure 5b-d), while *NPY* is strongly expressed in the deep CP of V1 compared to V2 (Figure 5e). However, A1 and S1 cannot be well distinguished from adjoining cortices. Subtle difference between M1 and S1 appears at PCW 21, for example, on *ENC1*-, *PLXNA2*-, *NRGN*-, and *ETV1*-ISH sections. These gene markers clearly display layer 5 of the neocortex. As M1 has a well-developed and thicker layer 5 than S1, which shows a weaker layer 5, the border between M1 and S1 can be roughly established at PCW 21 (see Appendix 4). Similarly, the cingulate cortex can be identified at PCW 21 more easily than at PCW 15 based on the expression patterns of *ETV1*, *ENC1*, *LMO4*, *PLXNA2*, and *NRGN* (see Appendix 4). For example, *ETV1* and *NRGN* are strongly expressed in both anterior and posterior cingulate cortex but only weakly in the adjoining neocortex (see Appendix 4). Finally, the dysgranular and granular insular cortex (Idg and Ig, respectively) can also be identified at PCW 21 based on Nissl stain, gene expression

patterns, and its relationship with the claustrum, located deep to the insular cortex and displaying strong *GRIK2* and *LMO4* expression.

3.4 | Delineation of the layers in prenatal allocortex and periallocortex

In contrast to the neocortex, which typically has six well-defined cortical layers, the allocortex, which includes the hippocampal formation (HF or archicortex) and olfactory cortices (mainly the piriform cortex, Pir), generally displays three major layers in mature cortex. As in the mature brain, the prenatal Pir is a three-layered, easily identified structure, and as such is not further described in this study. The HF in this study mainly contains the hippocampus [dentate gyrus [DG] and hippocampal subfields (CA1-4)] and the subicular cortex [prosubiculum (ProS) and subiculum proper (S)]. The cortical region located between allocortex and neocortex is usually termed periallocortex which includes peripaleocortex and periarchicortex. The former mainly includes agranular insular cortex (Iag) and agranular temporal insular cortex (area TI) while the latter includes entorhinal cortex (EC), perirhinal cortex (PC or area 35), presubiculum (PrS), parasubiculum (PaS), and retrosplenial cortex (RSC: areas 29 and 30) (see Table 1 and Ding et al., 2016). The periallocortex has more than three layers (4 to 6 or 7 layers) and these layers are usually not equivalent to the neocortical layers. Note that other related terms were also used in literature. For example, subicular complex was used to include ProS, S, PrS, and PaS (e.g., Ding, 2013). The medial temporal cortex (MTC) was used to contain PrS, PaS, EC, and PC (i.e., area 35) (similar to periarchicortex without RSC). The following description mainly focuses on the HF and MTC.

PCW15. On Nissl preparations, the typical laminar organization of the HF is obvious at this stage (Figure 7a). Many genes show clear expression patterns in distinct layers or sublayers of the HF. The expression patterns of 16 genes are shown as examples (Figure 7b-p). Specifically, the CP of the HF (i.e., hippocampal plate) expresses *FADS2*, *FOXP1*, *ETV1*, and *SYNGAP1* in its full thickness, while the inner CP (CPi) expresses additional genes such as *FEZF2*, *NRTK2*, *NRGN*, and *SHANK3*. *FABP7*, *FADS2*, and *NTRK2* are strongly expressed in the VZi while strong expression of *VIM* is seen throughout the VZ. Interestingly, *TBR2* expression appears to concentrate at SZi/VZo border or SZd. The SP expresses *GRIK2*, while *GAP43*, *FOXG1*, and *ENC1* are strongly expressed in the SZi, CP, and SP, but weakly in IZ. In the MZ, strong expression was found for *GAP43* (Figure 7c), *ERBB4*, *DCX*, *RELN*, and *CALB2* (see Appendix 2). Interestingly, SZo is not identified in the HF and MTC. As shown in Figure 8, only the thinner VZ and SZi, but not the thicker SZo, extend from temporal neocortex into the MTC and HF. The SZi is recognizable by lower expression of *TBR2* (Figure 8a) and *VIM* (Figure 8b) compared to the VZ and SZo. The existence of SZi in the MTC and HF are also revealed by the strong expression of *TBR2* in the SZd (Figure 8a).

PCW 21. All the layers of the HF and MTC seen at PCW 15 can be identified on Nissl-stained and ISH sections at PCW 21. These layers include MZ, CP, SP, IZ, SZi, and VZ (Figure 9a). Layer-specific gene expression is also observed. *SOX2*, *FOXG1*, *ENC1*, *GAP43*, *NTRK2*, *SHANK3*, *SYNGAP1*, *LBX1*, *LHX2*, *NRGN*, *LMO4*, *DCX* (see Appendix 4), and *NES* (Figure 9a) are strongly expressed in the CP while *FOXP1* and *CNTNAP2* expression (Figure 9c) are strongly expressed in the inner CP (CPi). *RELN* is expressed in MZ (Figure 9b), and *NPY*, *SST*, *PLXNA2* (see Appendix 4), and *GRIK2* (Figure 9d) in SP. Finally, *PAX6* is lightly expressed in SZi (Figure 9e) and *SOX2*, *VIM* (not shown), and *GFAP* strongly in VZ (Figure 9f). The thick SZo does not extend from the temporal neocortex into the MTC and HF, as demonstrated using SZo markers such as *FABP7* (not shown), *NES*, *PAX6*, *TBR2*, and *VIM* (Figure 9a and e; 10a and d). In the MTC, *ETV1* and *NRXN1* are also mostly expressed in layers 5–6 of the EC (Figure 11a-c). In contrast, *GRIK2* and *LMO4* are mainly expressed in layers 2–3 of the EC with relatively lower expression in L5-6 (Figure 11d and e).

In summary, a striking feature of the HF and MTC appears to be its lack of SZo, which is one of the thickest neocortical layers at PCW15 and 21. The thickness of SZo in temporal neocortex is dramatically reduced toward the border with the PC (Figure 8) and the SZo is not observed in the MTC and HF (Figures 8, 9, 10). At PCW 21, the VZ and SZi extend from the temporal neocortex into the HF with gradually narrowing of their thickness towards the DG (Figures 9a, 10a and d).

3.5 | Delineation of the subregions in prenatal allocortex and periallocortex

PCW 15. To investigate whether regional difference can be distinguished in the prenatal allocortex and periallocortex, we analyzed and compared gene expression patterns in different regions of the HF and MTC, and between the MTC and neocortex. At PCW 15, the granular layer of the DG (DGgr) is recognizable from the remaining HF (Figure 7a and b). The polymorphic layer of the DG (DGpm) can also be roughly identified in *GRIK2*, *GAP43*, *FABP7*, and *ENC1*- ISH sections (Figure 7b-d and h). However, subfields CA1-3 are not yet distinguishable within the HF although the boundary between the HF and MTC is appreciable (Figure 7d, e, g, h, k, and l). Interestingly, strong *VIM* and *TBR2* expression is observed in the so-called dentate neuroepithelial stem cell zone (DNS; see Nelson et al., 2020) while *VIM* and *NTRK2* are strongly expressed in another transient zone called dentate-hippocampal transient cell zone (DHTC), which is located immediately dorsal to the DNS (Figure 7i and m). The boundaries between the MTC and neocortex are identifiable based on expression patterns of some genes in addition to the lack of SZo in the MTC. For instance, *SATB2* displays strong expression in the entire CP and IZ and moderate expression in the SP of the insular and temporal neocortex (Figure 12a and b). In contrast, strong *SATB2* expression is only seen in the IZ and CPi (layers 5–6) of the lateral EC (LEC; Figure 12a) and in layer 5 of the medial EC (MEC; Figure 12b and the inset in b).

In addition, differential gene expression patterns in LEC versus MEC can also be identified. For example, strong expression of *NTRK2* (Figure 13a), *GRIK2* (Figure 13b), *ETV1* (Figure 13c), and *GAP43* (Figure 13d) is observed in layer 2 of the LEC, which is located anteriorly

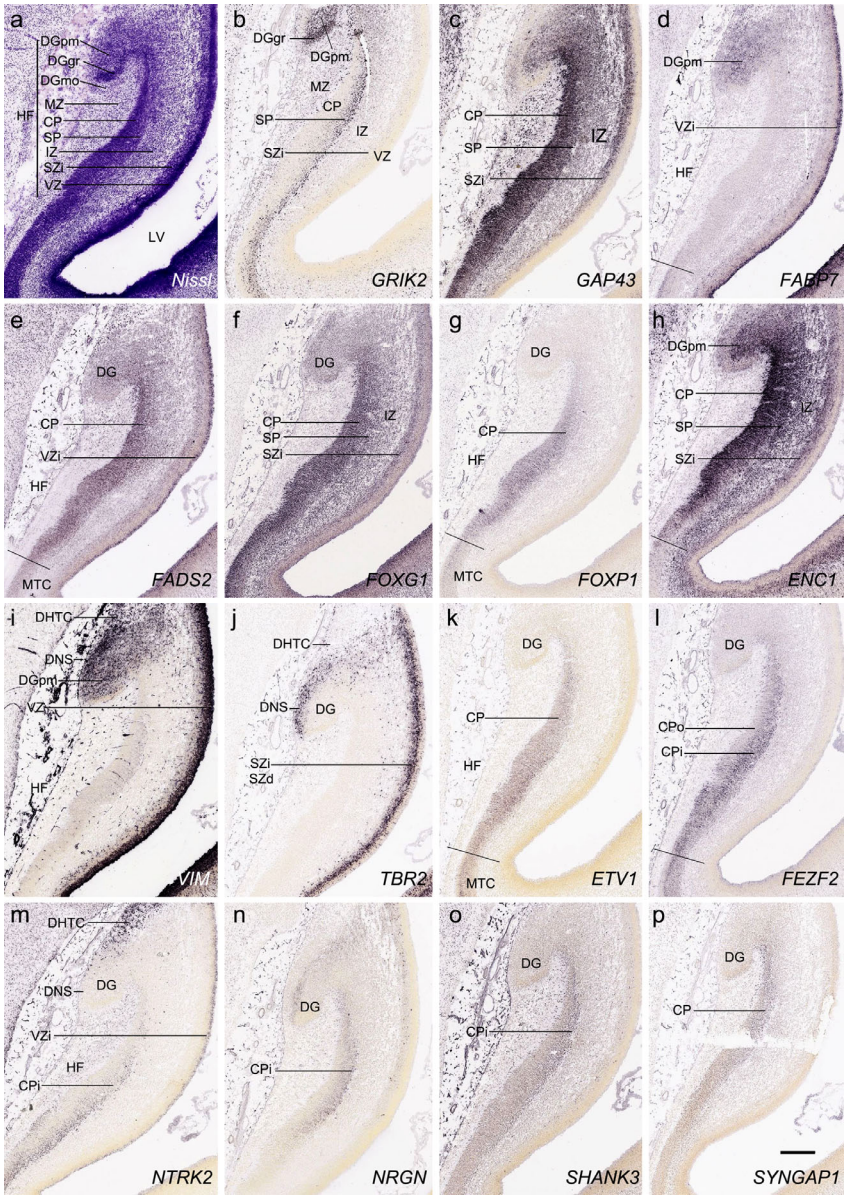

FIGURE 7 Gene expression in hippocampal formation (HF) at PCW15. (a) A Nissl-stained section showing the laminar organization of the HF. (b-p) Expression patterns of 15 genes as indicated in (b-p). Note the layer-specific gene expression in HF and the expression of *VIM* (i) and *NTRK2* (m) in the migrating dentate-hippocampal transient cells (DHTC). VZi, inner VZ; DG, dentate gyrus; DGmo, DGgc and DGpm, molecular, granular, and polymorphic layers (zones) of the DG. Scale bar: 400 μm in (p) for all panels

at the level of the amygdala. In contrast, *ETV1* (Figure 13e) and *NTRK2* (Figure 13h) are not expressed in layer 2 of the MEC, which is at the posterior levels and adjoins the HF. Layer 2 in both LEC and MEC expresses GAP43 (Figure 13d and g) and areas 35 (A35) and 36 (A36) extend along both LEC and MEC. The borders of A35 with the EC and A36 can also be appreciated at both anterior (Figure 13a-d) and posterior (Figure 13e-h) levels based on combined gene expression patterns. At the anterior level, for example, *GRIK2* is strongly and weakly expressed in layers 2–3 of the LEC and A35, respectively (Figure 13b) and the reverse is true for *ETV1* expression (Figure 13c). At the posterior level, clear and faint *CNTNAP2* expression is observed in layer 2 of the MEC and A35, respectively (Figure 13f). The border between A35 and A36 can be identified based on *ETV1* expression since strong and faint expression exists in A35 and A36, respectively (Figure 13e). In contrast, the border between A36 and the laterally adjoining temporal cortex is relatively difficult to be placed. However, subtle expression difference exists in the density and intensity of certain genes. For instance, the density and intensity of *ETV1* expression is lower in A36 than in the lateral neocortex (Figure 13e).

PCW 21. Regional differences within the HF are clear at PCW 21. For instance, the subiculum (S) strongly expresses *CNTNAP2*, *GRIK2* (Figure 9c and d), *ETV1*, *and FEZF2* (Figure 10b and c) while adjoining HF regions (e.g., ProS, CA1-3) display very low expression of these genes. Alternatively, some genes, such as *TBR2* and *VIM*, show strong expression in the DGpm and DNS but not or little expression in other HF regions (Figure 10a and d). The DNS also strongly expresses *PAX 6*, *GFAP* (Figure 9e and f), *SOX2*, and *NTRK2* while the DHTC express strong *GFAP*, weaker *VIM*, *SOX2*, and *NTRK2*, and no or low *TBR2* and *PAX6* (see Appendix 4). The regional difference between MTC and neocortex at PCW 21 is even more obvious than that at PCW 15 (Figure 12c and d). LEC and MEC have strong *SATB2* expression in layers 5–6 and layer 5, respectively (Figure 12c and d). In the PrS and

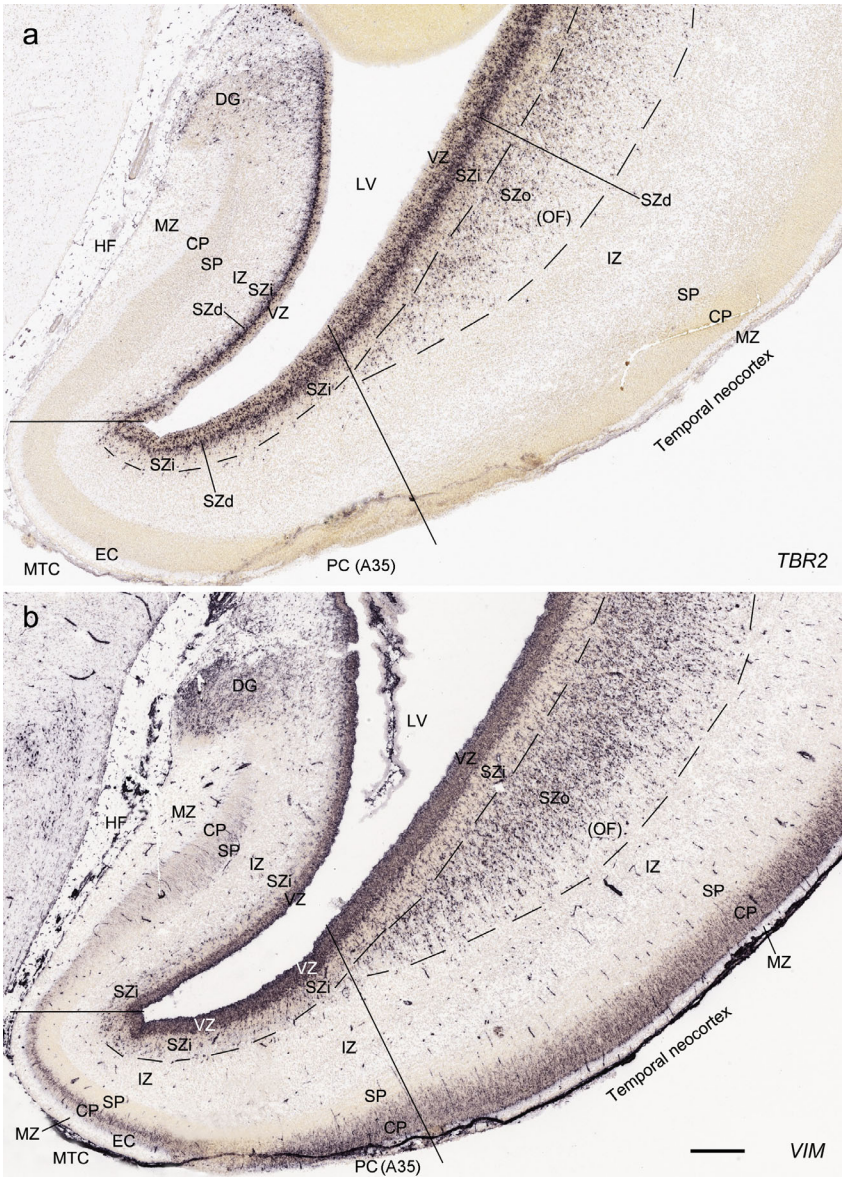

FIGURE 8 Comparison of the layers in allocortex, periallocortex, and neocortex at PCW 15. *TBR2* (a) and *VIM* (b) are expressed in the VZ and SZi of these three types of cortex as well as in the SZo of the neocortex. Note that the SZo in the temporal neocortex does not extend into periallocortex [mainly entorhinal cortex (EC) and perirhinal cortex (PC)] and hippocampal formation (HF). *VIM* is also strongly expressed in the CP of the neocortex and PC (i.e., area 35) but weakly in the CP of the EC (b). Scale bar: 400 μm in (b) for (a, b)

PaS, strong *SATB2* expression is seen in the superficial rather than deep layers (Figure 12d). In contrast, no *SATB2* expression is observed in the subiculum and hippocampus (Figure 12d). The borders of A35 with the LEC and A36 can be identified based on the relatively weaker expression of *ETV1*, *NRXN1*, and *GRIK2* in A35 compared to the LEC and A36 (Figure 11a-d). The border between A36 and the lateral temporal neocortex can also be roughly determined based on the relatively weaker expression of *ETV1*, *GRIK2*, and *NRGN* in A36 than in the temporal cortex (Figure 11b, d, and f).

3.6 | Delineation of cerebral nuclei

PCW 15. Strong gene expression was found in specific cerebral nuclei and these are helpful in their delineation. For example, *CALB2* expression is observed in the medial (Me), anterior cortical (CoA), and parts of the lateral (La) nuclei of the amygdala (Figure 14a). Other such regional expression patterns are *NPY*, *SST*, *FOXG1*, and *DLX1* in the bed nucleus of terminalis (BNST); *ETV1* expression in the external part of globus pallidus (GPe), and basolateral nucleus (BL; Figure 13c) of the amygdala; *NTRK2*, *GRIK2* (Figure 13a and b), and *SST* expression in central nucleus (CEN) of the amygdala; *FOXP1* and *NPY* expression in caudate nucleus (Ca) and putamen (Pu); *GRIK2* (Figure 13b) and *LMO4* expression in claustrum; *NKX2.1* and *ZIC1* expression in GPe; and *RELN* and *LMO4* expression in GPi. In addition, *ZIC1* is strongly expressed in septal nucleus (SEP) and basal nucleus of Meynert (BNM). It should also be pointed out that strong transient expression of *CALB2* (Figure 14a) and *PAX6* is observed in the space between the GPe and GPi. We refer to this zone as interpallidal transient cell zone (IPTC; Figure 14a). *CALB2* is also expressed in the transient cells located between GPe and Pu (Figure 14a). Expression of all above mentioned genes is shown in Appendix 2.

PCW 21. In Nissl preparations, the major subdivisions of the amygdala can be identified (Figure 11a). In ISH sections, *ETV1* is mostly

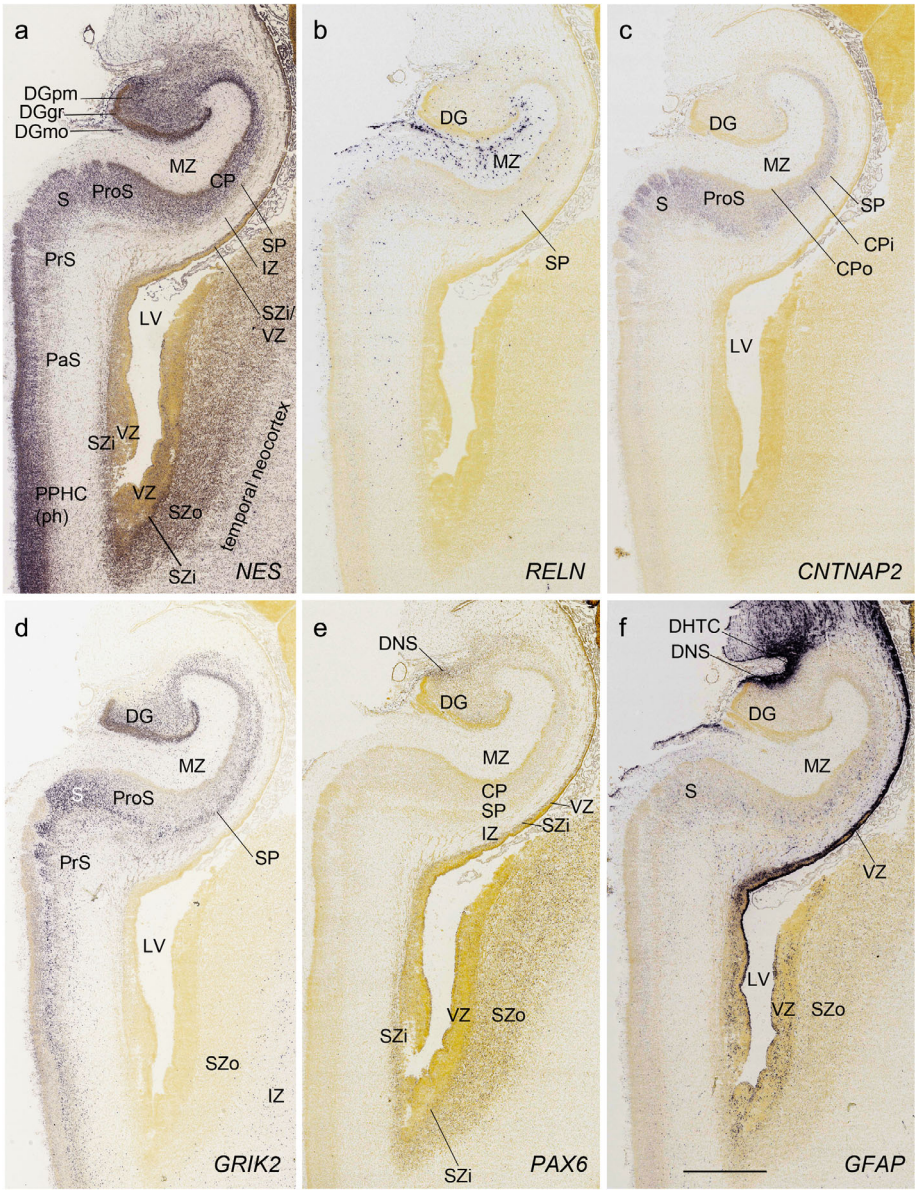

FIGURE 9 Layer-selective gene expression in the hippocampus at PCW 21. (a) *NES* expression in the CP but not the SP of the hippocampus. (b) *RELN* expression in the MZ and SP of the hippocampus and DGmo. (c, d) *CNTNAP2* (c) and *GRIK2* (d) expression in the inner CP (CPi) of the hippocampus and superficial layers of the subiculum (S). (e) *PAX6* expression in the SZi of the hippocampus and both SZi and SZo of the temporal neocortex as well as in the DNS. (f) *GFAP* expression in the VZ of the hippocampus and DNS of the DG. Scale bar: 1590 μm in (f) for all panels

expressed in the BL, while *NRXN1*, *GRIK2*, *LMO4*, and *NRGN* are expressed in the BM, BL, and La with various intensity in each subdivision (Figure 11c-f). Strong *GRIK2* and *NRGN* expression is also observed in the anterior cortical nucleus of the amygdala (CoA; Figure 11d and f). Gene expression patterns in other cerebral nuclei are similar to those at PCW 15 (see Figure 14).

3.7 | Delineation of the thalamic and hypothalamic nuclei

Delineation of the thalamic nuclei at PCW 15 and 21 is mainly based on multiple region-specific gene markers, such as *CALB2* (Figures 14 and 15), *CNTNAP2*, *PLXNA2*, *GRIK2*, *ETV1*, *NTRK2*, *ZIC1*, and *ENC1* (see Appendices 2 and 4) as well as AChE staining (Figure 16). *CALB2* is expressed in many thalamic nuclei, including paraventricular (PaV), central medial (CeM), central lateral (CL), lateral dorsal (LD), ventral anterior (VA), ventral lateral (VL), reticular (R), subparafascicular (SPf), medial geniculate (MG), posterior intralaminar (PIL), limitans-suprageniculate (LSG), and lateral posterior (LP) nuclei, as well as anterior nuclear complex (ANC; mainly AV and AM), pulvinar (Pul), and dorsal lateral geniculate nucleus (DLG) (Figure 14a-c; 15a-g). Strong expression of *CNTNAP2* occurs in mediodorsal (MD), centromedian (CM), habenular (HN) nuclei, and DLG of the thalamus, and *PLXNA2* expression in CM, parafascicular (Pf), and ventral posterior lateral (VPL) nuclei. In addition, *ZIC1* is a reliable marker for

FIGURE 10 Region-selective gene expression in the HF at PCW 21. (a) *TBR2* expression in the DNS and DGpm. Strong *TBR2* expression is also seen in the SZo of the temporal neocortex. (b,c) *ETV1* (b) and *FEZF2* (c) expression in the subiculum (S) and deep prosubiculum (ProS). *FEZF2* is also expressed in the deep CP of the hippocampus (CA1-3). (d) Strong *VIM* expression in DNS, DHTC, DGpm, and VZ of the hippocampus as well as in the VZ and SZo of the temporal neocortex. (e) Strong *SATB2* expression in the presubiculum (PrS) and parasubiculum (PaS) as well as in the IZ of the temporal neocortex. (f) Strong *SHANK3* expression in the CP of the hippocampus. Scale bar: 1590 μm in (f) for all panels

ANC, PaV, DLG, LD, Pul and medial HN (MHN) while *NRGN*, *SOX2*, *ZIC1*, and *ETV1* are strongly expressed in MHN (see Appendices 2 and 4). As shown in Figure 14b and d, gene expression patterns are more helpful in the delineation of the thalamic nuclei than Nissl. For instance, strong and weak *CALB2* expression, respectively, in DLG and PG (VLG) allows an easy differentiation of the two structures (Figure 14b) whereas this is difficult in Nissl-stained sections (Figure 14d). Interestingly, we observe a region that is the likely equivalent of the mouse PIL (Wang et al., 2020) in terms of its topographical relationship with adjoining regions and molecular signature. As in mouse, the PIL adjoins MG, SPf, posterior thalamic nucleus (Po), VPM, LSG, peripeduncular nucleus (PP), and pretectal nucleus (PTN) and has strong expression of *CALB2*, *GRIK2*, *LHX2*, *NRGN*, and *NTRK2* (see Appendices 2 and 4). Finally, it should be mentioned that AChE is a useful marker for the identification of the MD at PCW 15 (Figure 16a) and 21 (Figure 16b and c) and of the ventral posterior medial nucleus (VPM) and its parvocellular part (VPMpc) at PCW21 (Figure 16c).

Genes with regional expression in hypothalamus at PCW 15 and 21 includes *CALB2*, which has strong expression in the ventromedial

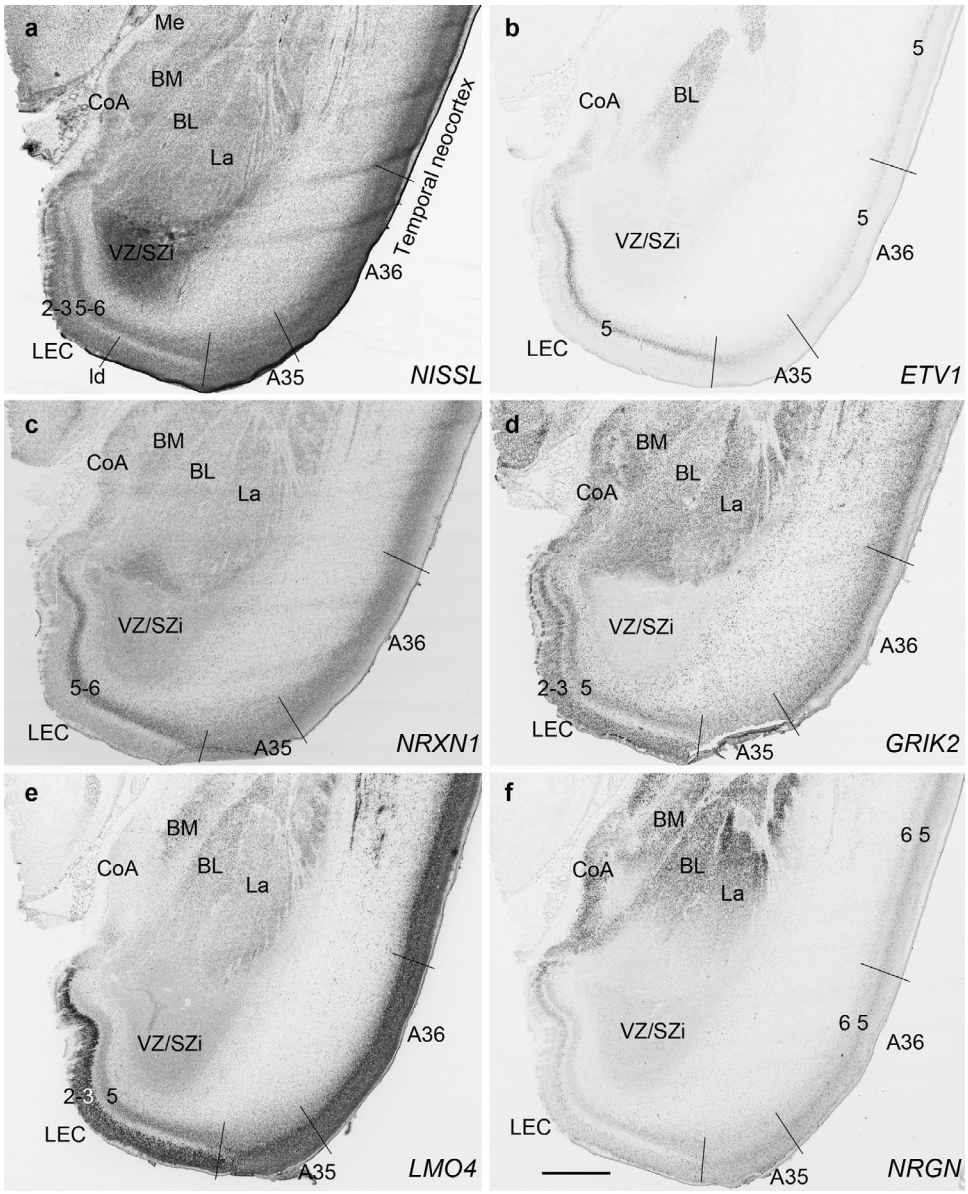

FIGURE 11 Gene expression in lateral entorhinal cortex (LEC), perirhinal area 35 (A35), and amygdala at PCW 21. (a) A Nissl-stained section showing the cytoarchitecture in the LEC, A35, and amygdaloid nuclei. (b-f) Expression patterns of *ETV1* (b), *NRXN1* (c), *GRIK2* (d), *LMO4* (e), and *NRGN* (f) in the LEC, A35, and amygdaloid nuclei. Note that the borders of A35 with LEC and temporal neocortical area 36 (A36) can be identified based on gene expression difference. A35 displays overall lower expression of *ETV1* (b), *NRXN1* (c), and *GRIK2* (d) than LEC and A36. Subtle difference could also be noted at the border between A36 and more dorsally located temporal cortex with less expression of *ETV1* (b), *GRIK2* (d), and *NRGN* (f) in A36. Scale bar: 1590 μm in (f) for all panels

nucleus (VMH), perifascicular nucleus (PeF), and posterior hypothalamic nucleus (PHN) (Figure 14a and b), and *SST*, which is expressed in the dorsomedial nucleus (DMH), paraventricular nucleus (PV), and lateral hypothalamic region (LH) (see Appendices 2 and 4). Other genes with region-specific expression include *GRIK2* in DMH; *DLX1* in anterior hypothalamic nucleus (AHN); *ZIC1* in suprachiasmatic nucleus (SCN) and PeF; *FOXG1* in medial preoptic nucleus (MPN); *LMO4* and *RELN* in the PV; *NKX2.1*, *CDH4*, and *NTRK2* in VMH, and *NRXN1* in PHN and arcuate nucleus (Arc) (see Appendices 2 and 4).

3.8 | Delineation of cerebellum and major brainstem structures

Cerebellar cortex at PCW 15 displays an immature shape with clear and thick external granular layer (EGL) and upper rhombic lip (URL) superficially, while deep cerebellar nuclei (CbDN) have formed in the center of the cerebellum (Figure 17a-j). The EGL has strong expression of *PAX6* (Figure 17b and c) and *ZIC1* while *ERBB4* and *GRIK2* are mainly expressed underneath the EGL (Figure 17h). The URL contains strong *ZIC1* and *TBR2* expression (Figure 17j). CbDN shows strong

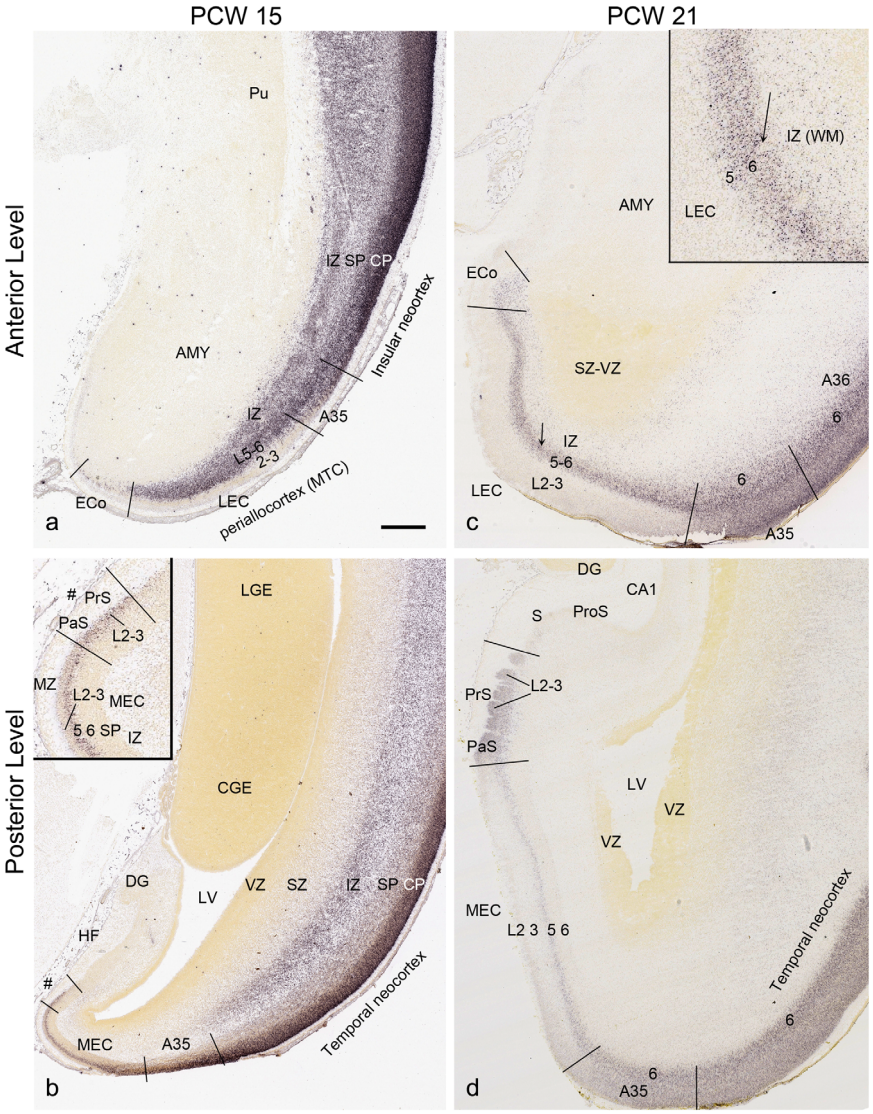

FIGURE 12 Identification of lateral and medial entorhinal cortex at PCW 15 and 21. (a, b) Lateral (a) and medial (b) entorhinal cortex (LEC and MEC, respectively) identified on *SATB2*-stained section at PCW15. The inset in (b) is a higher power view of the MEC (#s indicate the same location). (c, d) LEC (c) and MEC (d) identified on *SATB2*-stained section at PCW21. The inset in (c) is a higher power view of the LEC (the arrows indicate the same location). *SATB2* expression is seen in both layers 5 and 6 of the LEC, including the olfactory part (ECo) (c), but only in layer 5 of the MEC (d). At both PCW 15 and 21, strong *SATB2* expression is seen in layer 5 of the MEC and layers 2–3 of the presubiculum (PrS) and parasubiculum (PaS). Pu, putamen; AMY, amygdala; LGE and CGE, lateral and caudal ganglion eminence. Scale bar: 790 μm in (a) for all panels

expression of *GAP43*, *CALB2*, *NRNX1*, *ERBB4* in the fastigial (Fas), interpositus (InP), and dentate (DT) nuclei (Figure 17e-h), while *GRIK2* is mainly expressed in DT (Figure 17i). These results are consistent with patterns observed in the mouse (e.g., Figure 17n-q). It should be noted that *RELN* is not expressed in CbDN but present in surrounding cerebellar regions (Figure 18e and f). In addition, some genes are mostly expressed in EGL of the vermis (e.g., *SST*) while others are strongly expressed in transient Purkinje cell clusters (TPC) (e.g., *CNTNAP2* and *NRXN1*; see Appendix 2).

In the midbrain, a rough lamination in the superior colliculus (SC) has formed at PCW15 with *FOXP1* and *VIM* expressed in the inferior gray layer (InG). *VIM* is also expressed in the periaqueductal gray region (PAG) (see Appendix 2). In the inferior colliculus (IC), central IC nucleus (Figure 17k) has strong expression of *ENC1* (Figure 17l), *NRGN*, and *NPY*, the latter being also strongly expressed in the cuneiform nucleus (CnF; Figure 17m). The cortical (or external) IC (CxIC) displays expression of *RELN* (Figure 18c-e). The red nucleus (RN) shows strong expression of *CNTNAP2*, *GRIK2*, and *NTRK2*, while the substantia nigra (SN) strongly expresses *ENC1* and *FABP7*. In addition, the parabrachial pigmented nucleus (PBP) located between RN and SN has strong *RELN* expression (Figure 18a). *RELN* is also strongly expressed in the median raphe nucleus (MnR) and the oculomotor nucleus (3N) (Figure 18b and c). In the lower brainstem (pons and medulla), *ZIC1*, *RELN*, and *SST* are strongly expressed in the vestibular nuclei (8Ve) and external cuneate nucleus (ECu) (Figure 18f and g) while *ENC1*, *ETV1*, *FOXP1*, and *PLXNA2* (see Appendix 2) are expressed strongly in the inferior olive (IO). *RELN* is strongly expressed in the reticulotegmental nucleus (RtTg), lateral lemniscus nucleus (LLN), IO, and medullary reticular formation (MoRF) (Figure 18b, d, e, and f). *VIM* expression is found in 3N, Edinger-Westphal nucleus (EW), and abducens nucleus (6N) (see Appendix 2). Finally, the pretectal nuclear complex (PTN) contains strong expression of *RELN* (Figure 18b), *FABP7*, and *NPY* (see Appendix 2).

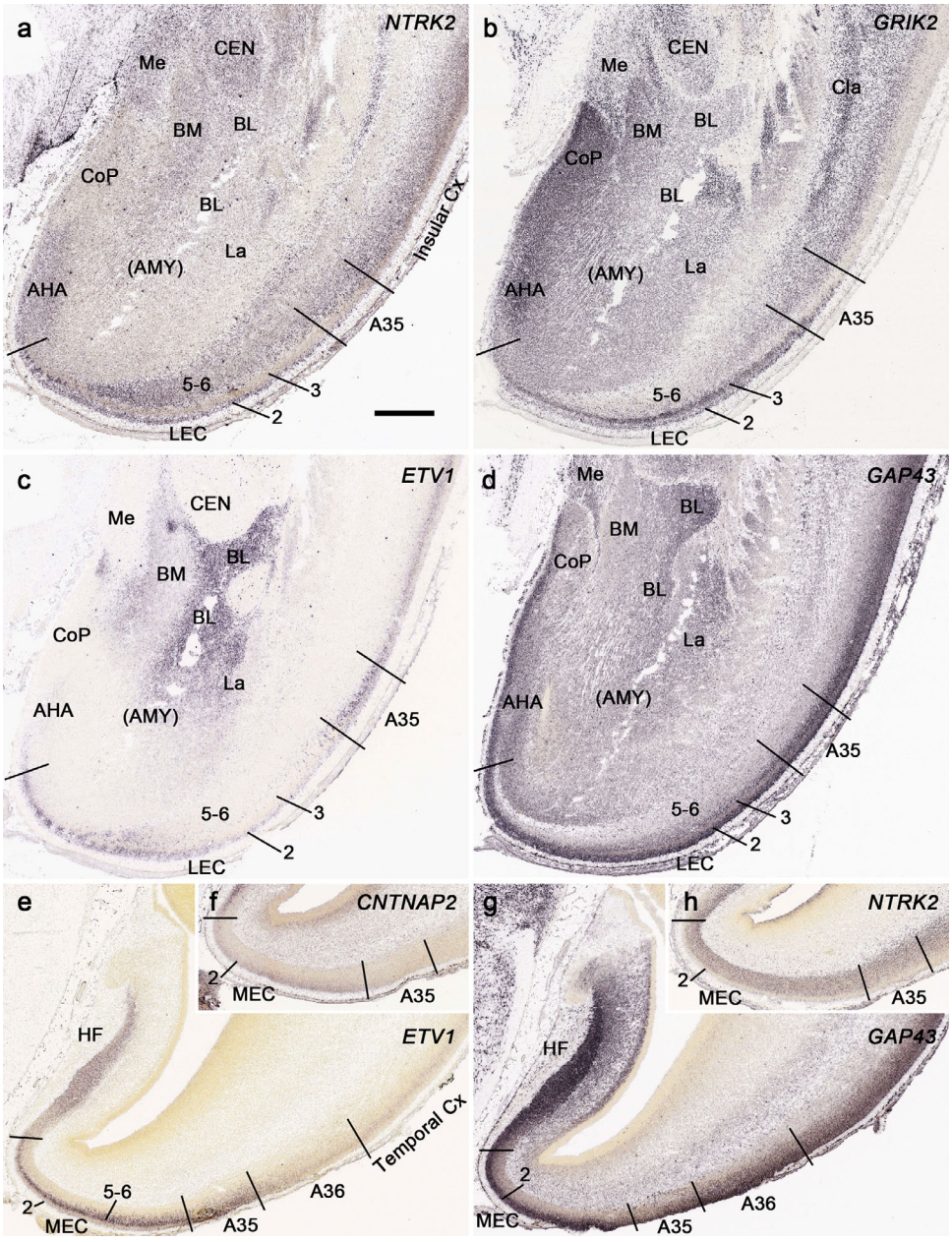

FIGURE 13 Identification of LEC, MEC, and areas 35 and 36 at PCW15. The borders of these four areas can be identified based on combined gene expression patterns. Strong expression of *NTRK2* (a), *GRIK2* (b), *ETV1* (c), and *GAP43* (d) is observed in layer 2 of the LEC. In contrast, *ETV1* (e) and *NTRK2* (h) are not expressed in layer 2 of the MEC. Layer 2 in both LEC and MEC expresses GAP43 (d, g). The borders of A35 with the EC (LEC and MEC) and A36 can also be appreciated on the base of combined gene expression patterns. At the anterior level (a-d), *GRIK2* is strongly and weakly expressed in layers 2–3 of the LEC and A35, respectively (b) and the reverse is true for *ETV1* expression (c). At the posterior level (e-h), clear and faint *CNTNAP2* expression is observed in layer 2 of the MEC and A35, respectively (f). The border between A35 and A36 can be identified based on *ETV1* expression since strong and faint expression exists in A35 and A36, respectively (e). The density and intensity of *ETV1* expression is lower in A36 than in the lateral neocortex (e)

3.9 | Delineation of the ganglionic eminence subdivisions

The GE mainly consists of three major parts, MGE, LGE, and CGE (Hansen et al., 2013; Ma et al., 2013). In this study, the boundary between GE and adjoining cortical regions can be clearly identified with the gene markers *TBR2* and *DLX2* or *DLX1*. *TBR2* (i.e., *EOMES*) reveals no expression in GE but strong expression in cortical regions, while the reverse pattern is seen for *DLX2* and *DLX1* (Figure 19a, b, g, and h). Complementary expression patterns of *NKX2-1* and *ERBB4* are observed in MGE and LGE, making it easy to distinguish them (Figure 19d and e). The border between LGE and CGE is not sharp but CGE has much stronger expression of *CALB2* than LGE (Figure 14b), and the reverse patterns occurs for *ERBB4* (CGE < LGE; Figure 20a-c).

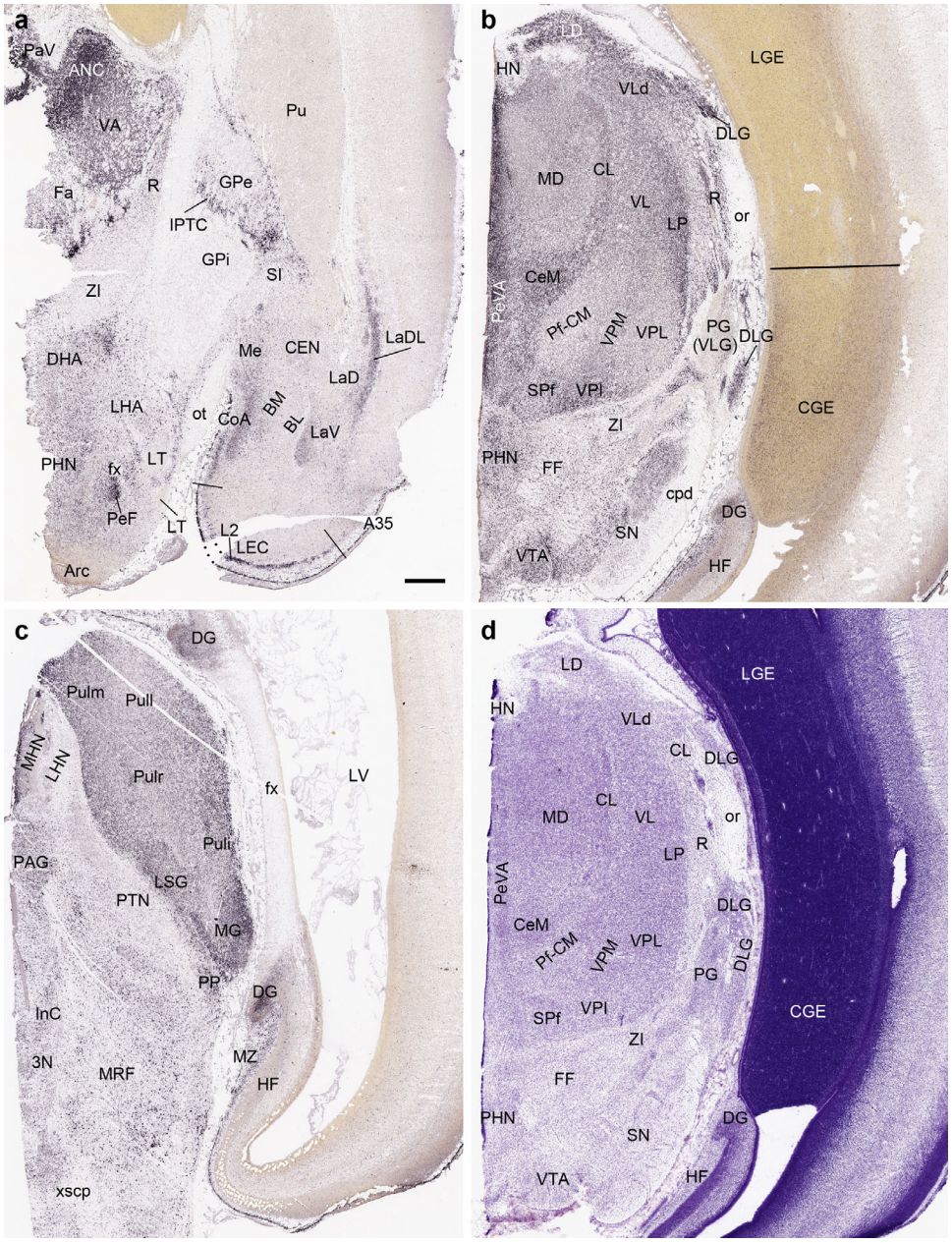

FIGURE 14 *CALB2* expression in the brain at PCW 15. (a) *CALB2* expression in the anterior thalamic region, basal ganglion, amygdala, and lateral entorhinal cortex (LEC). Note the strong *CALB2* expression in anterior thalamic nuclear complex (ANC), medial hypothalamic region, anterior cortical nucleus of the amygdala (CoA), interpallidal transient cell zone (IPTC), and layer 2 of the LEC. (b) *CALB2* expression in middle thalamic region, midbrain, and caudal ganglionic eminence (CGE). Strong *CALB2* expression is seen in the lateral dorsal nucleus (LD), ventral lateral nucleus (VL), dorsal lateral geniculate nucleus (DLG), central medial nucleus (CeM), and subparafascicular nucleus (SPf) of the thalamus as well as in the ventral tegmental area (VTA) and CGE. Note the much stronger expression of *CALB2* in CGE than in LGE. (c) *CALB2* expression in posterior thalamic region, midbrain, and HF. Note the strong *CALB2* expression in the pulvinar (Pul), medial geniculate nucleus (MG), limitans/supragenicular nucleus (LSG), medial habenular nucleus (MHN), and the dentate gyrus (DG). (d) A Nissl-stained section adjacent to (b) showing the cytoarchitecture of the thalamic regions. It is not easy to identify the different thalamic nuclei in Nissl-stained sections. In contrast, this is much easier in the *CALB2* ISH section (b). Scale bar: 800 μm in (a) for all panels

Therefore, in this study, the LGE-CGE border was placed based on complementary expression of *CALB2* and *ERBB4*. This border has been shown previously on the basis of *COUP-TFII* expression (Alzu'bi, Lindsay, Harkin et al., 2017; Reinchisi et al., 2012), and we find that the pattern of *CALB2* is similar to that of COUP-TFII. The sulcus located between the striatum (GE) and the cortex, termed here striatal-cortical sulcus (SCS; indicated by arrows in Figure 19a-c, g-i), does not appear to be a reliable landmark for the striatal-cortical border. As shown in Figure 19, the *NTRK2*-enriched striatal-cortical boundary (SCB, or subpallial–pallial or pallial–subpallial boundary, see Carney et al., 2009; Puelles et al., 2000; Figure 19c and i) is located at the striatal side at PCW 15 (Figure 19a-c), while at PCW 21 it is at the cortical

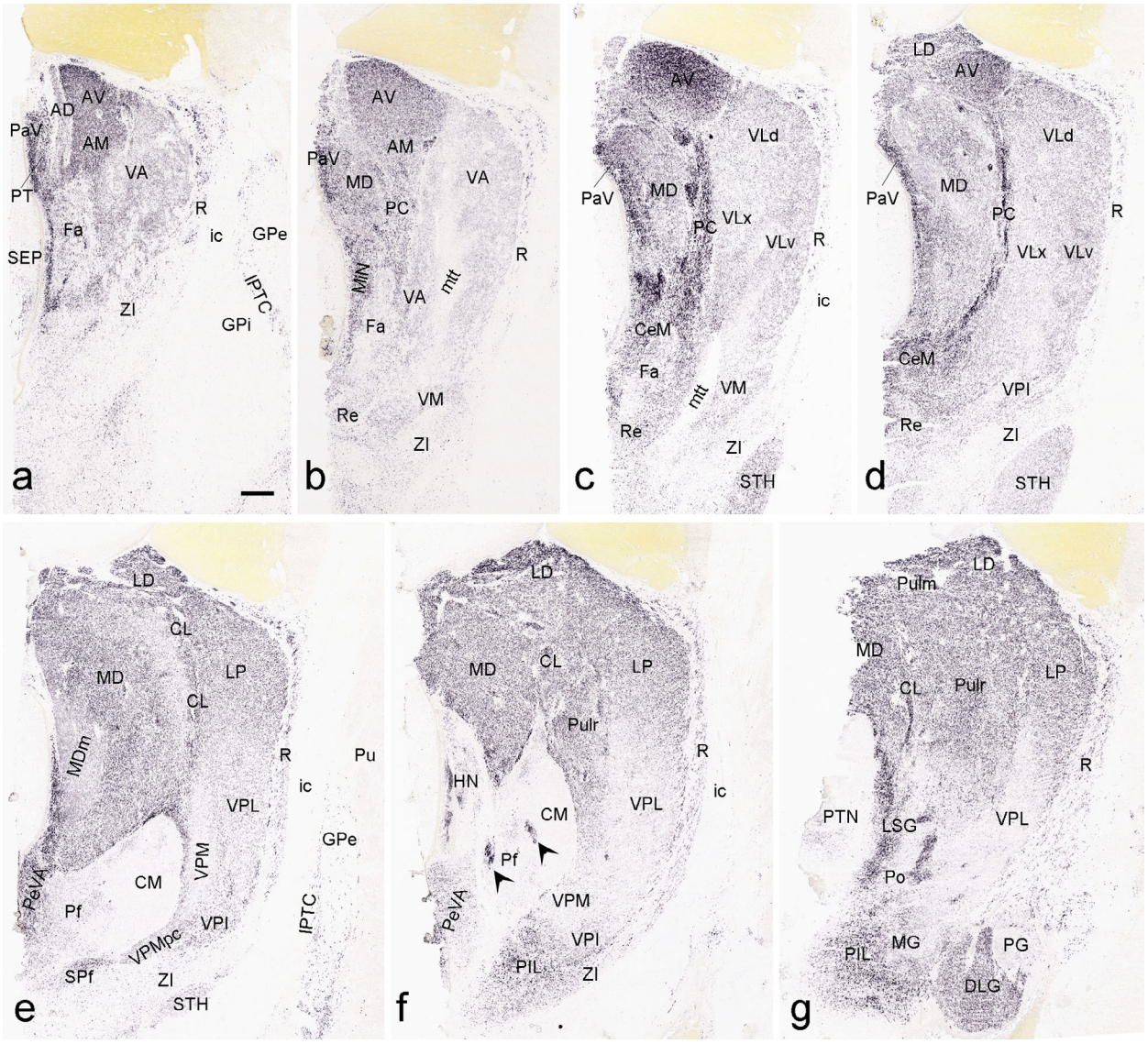

FIGURE 15 *CALB2* expression in the thalamus at PCW 21. (a-g) Sequential sections showing *CALB2* expression in the anterior ventral (AV) and anteromedial (AM) thalamic nuclei, paraventricular nucleus (PaV), midline nuclear complex (MiN), ventral anterior nucleus (VA), ventral lateral nucleus (VL), centromedian nucleus (CeM), reuniens nucleus (Re), and paracentral nucleus (PC) (a-d). Clear *CALB2* expression is also seen in the mediodorsal nucleus (MD), ventromedial nucleus (VM), lateral dorsal nucleus (LD), central lateral nucleus (CL), habenular nucleus (HN), periventricular area (PeVA), subparafascicular nucleus (SPf), lateral posterior nucleus (LP), pulvinar (Pul), dorsal lateral geniculate nucleus (DLG), and limitans/supragenicular nuclei (LSG) (c-g). In contrast, faint *CALB2* expression is observed in ventral posterior lateral (VPL), ventral posterior medial (VPM), parafascicular nucleus (Pf), central medial nucleus (CM), pregeniculate nucleus (PG), and zona incerta (ZI) (e-f). Note the *CALB2* expression in the patches within Pf/CM (f). Note also the *CALB2* expression in the subthalamic nucleus (STH; c-e) and interpallidal transient cell zone (IPTC; a). Strong *CALB2* expression is also found in a region that appears to be equivalent to mouse posterior intralaminar nucleus (PIL). Scale bar: 800 μm in (a) for all panels

side (Figure 19g-i). Also, the SCB is enriched with *CALB2*, *DLX2*, *ERBB4*, *PAX6*, and *DLX1* (Figure 19b, e, f, and h).

In general, gene expression in the GE of the prenatal human brains is heterogenous with some gene expression in different zones within the GE. In MGE, for instance, distinct gene expression between its VZ or inner part and SZ or outer part and among different regions of the SZ is observed. Specifically, some genes are expressed in both VZ and SZ (e.g., *NES*, *VIM*, and *NKX2-1*, see Figure 19d) with others exclusively or dominantly in SZ (e.g., *DCX*, *DLX5*, *DLX1*, and *DLX2*; see Figure 19b and h) or VZ (e.g., *VIM*, *NTRK2*, and *PAX6;* see Figure 19c, f, and i). In LGE, heterogenous gene expression in its VZ and SZ is also observed for genes such as *FABP7*, *DLX2*, *NTRK2*, *ERBB4*, and *DLX1* (Figure 19b, c, e, h, and I, and 20a–c). Within the SZ of both LGE and MGE, region-dominant or complementary gene expression is visible, with stronger expression of *DCX*, *DLX1*, and *DLX5* in the inner portion of the SZ than in the outer portion and a reverse expression pattern for *ERBB4*, *NES*, and *VIM* (see Appendix 2).

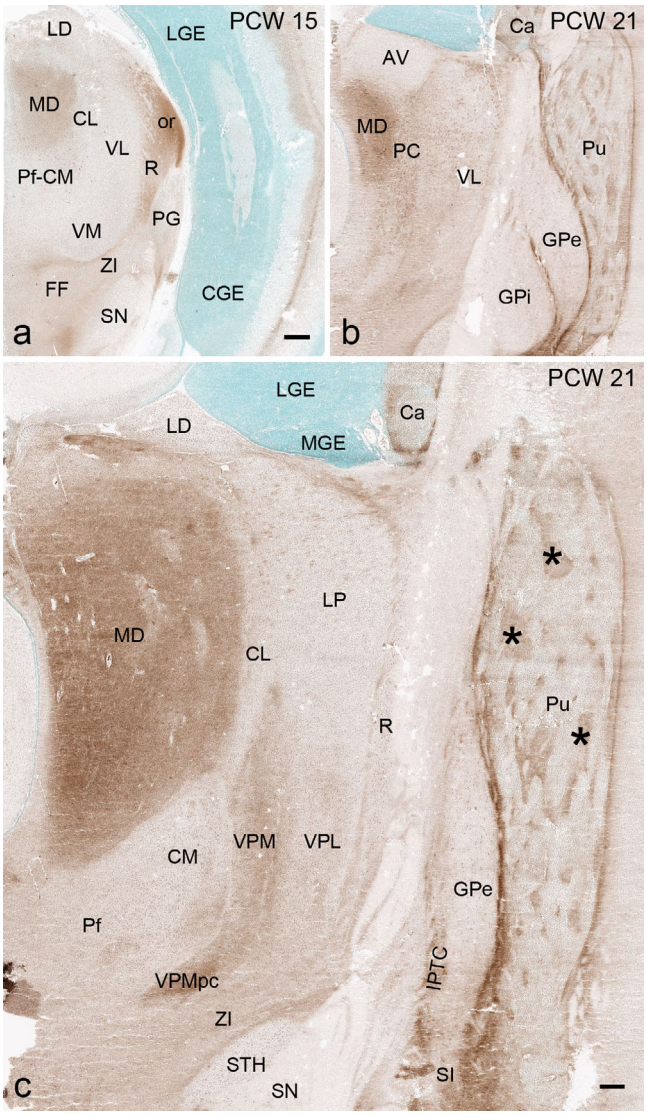

FIGURE 16 AChE staining patterns in the thalamus and basal ganglia. (a) AChE staining showing its enriched expression in the mediodorsal thalamic nucleus (MD) and some fiber regions such as optic radiation (or) at PCW 15. (b,c) AChE staining showing its enriched expression in the MD and two subdivisions of ventroposterior medial nucleus (VPM and VPMpc) as well as in the patches (*) of the putamen (Pu), substantia innominata (SI), and some fiber regions such as interpallidal transient cell zone (IPTC). Scale bars: 800 μm in (a) for (a-b); 400 μm in (c)

3.10 | Gene expression in olfactory bulb and anterior olfactory nucleus

At PCW 15, the olfactory bulb (OB) has obvious but immature lamination. From its outer to inner aspects, these layers include olfactory nerve (ON), glomerulus (GL), mitral cell (MC), and granular cell (GC), SZ, and VZ (Figure 21a-p). An incipient external plexus layer (ep) is also observed between GL and MC but the internal plexus layer is not well defined. A number of genes show a strong expression in GL (*VIM*, *NTRK2*, *FADS2*, *SOX10*, and *LMO4*), MC (*TBR2*, *GRIK2*, *LBX1*, *NTRK2*, *RELN*, *TBR1*, *LHX2*, *GAP43*, *DCX*, *DLX1*, *DLX5*, *NES*, *SYNGAP1*, *MECP2*, *SHANK3*, *FEZF2*, *CNTNAP2*, *GFAP*, *CDH4*, and *LMO4*), GC (*DCX*, *FEZF2*, *LBX1*, *DLX1*, *SHANK3*, *CNTNAP2*, and *LHX2*), SZ (*CALB2*, *DCX*, *PAX6*, and *ZIC1*), and VZ (*VIM*, *TBR2*, *PAX6*, *FABP7*, *LHX2*, *FADS2*, *FOXG1*, *LBX1*, *ZIC1*, *ETV1*, and *CDH4*). The SZ and VZ is part of the proliferative rostral migratory system (RMS). Note that the dorsal but not ventral walls of the VZ in the RMS strongly expresses TBR2 (Figure 21p). Interestingly, in addition to the OB lamination there exist patches within the OB (marked with # in Figure 21) that are positive for *ENC1*, *GRIK2*, *LBX1*, *TBR1*, *LHX2*, *MECP2*, *CDH4*, *FEZF2*, *DCX*, *LMO4*, *PLXNA2*, *NKX2.1*, *FADS2*, and *GAP43*, and negative for *TBR2*, *RELN*, *CALB2*, *PAX6*, *ZIC1*, and *DLX1* (Figure 21).

The anterior olfactory nucleus (AON) is featured by strong expression of *ENC1*, *GRIK2*, *LBX1*, *GAP43*, *TBR1*, *CDH4*, *LHX2*, and *MECP2* (Figure 21f, g, j, l, n, and o). The AON shows no expression of *PLXNA2*, *LMO4*, *TBR2*, *CALB2*, and *RELN* (e.g., Figures 21k and p). Small patches are often seen in OB that have a pattern similar to that of the AON (e.g., Figure 21c-g). The gene expression patterns observed in OB and AON at PCW 15 are comparable to those at PCW 21 (Figure 22).

3.11 | Brain-wide detailed anatomical and molecular atlases for prenatal human brains

Based on combined analysis of Nissl and AChE histology as well as laminar and regional gene expression patterns described above, anatomical boundaries of different cortical regions and subcortical nuclei can be accurately delineated on Nissl-stained sections. In this study, 46 and 81 selected Nissl-stained sequential coronal sections at PCW 15 and 21, respectively, were annotated in detail to generate two brain-wide anatomical atlases. The anatomical atlases for the brains at PCW 15 and 21 are presented in Appendices 1 and 3, respectively, with online links to high-resolution images. In these atlases, all cortical layers and many subcortical structures and their subdivisions are accurately demarcated based on cytoarchitecture and gene expression patterns. Furthermore, allocortex (HF and olfactory cortex), periallocortex (MTC and Iag), and their subdivisions are annotated. However, for neocortex only major cortical regions (e.g., frontal, parietal, temporal, occipital, and insular cortices) could be roughly identified at PCW 15 as molecular makers did not reveal detailed regional patterns at this age although more detailed cortical segmentation could be generated for the brain at PCW 21. Finally, using the anatomical atlases as a guide, we have also annotated spatial expression of 37 and 5 genes from the brains at PCW 15 and 21, producing two brain-wide molecular atlases, which are presented in Appendices 2 and 4, with online links to high-resolution images. Although the expression of 38 genes from the brain at PCW 21 was not annotated the online links to their sequential high-resolution ISH images are presented in Appendix 4. Therefore, spatial mapping of these genes can be achieved by users using the detailed anatomical atlas (Appendix 3) as a guide, the ISH data and Nissl-stained sections used for the anatomical atlas being derived from the same brain hemisphere.

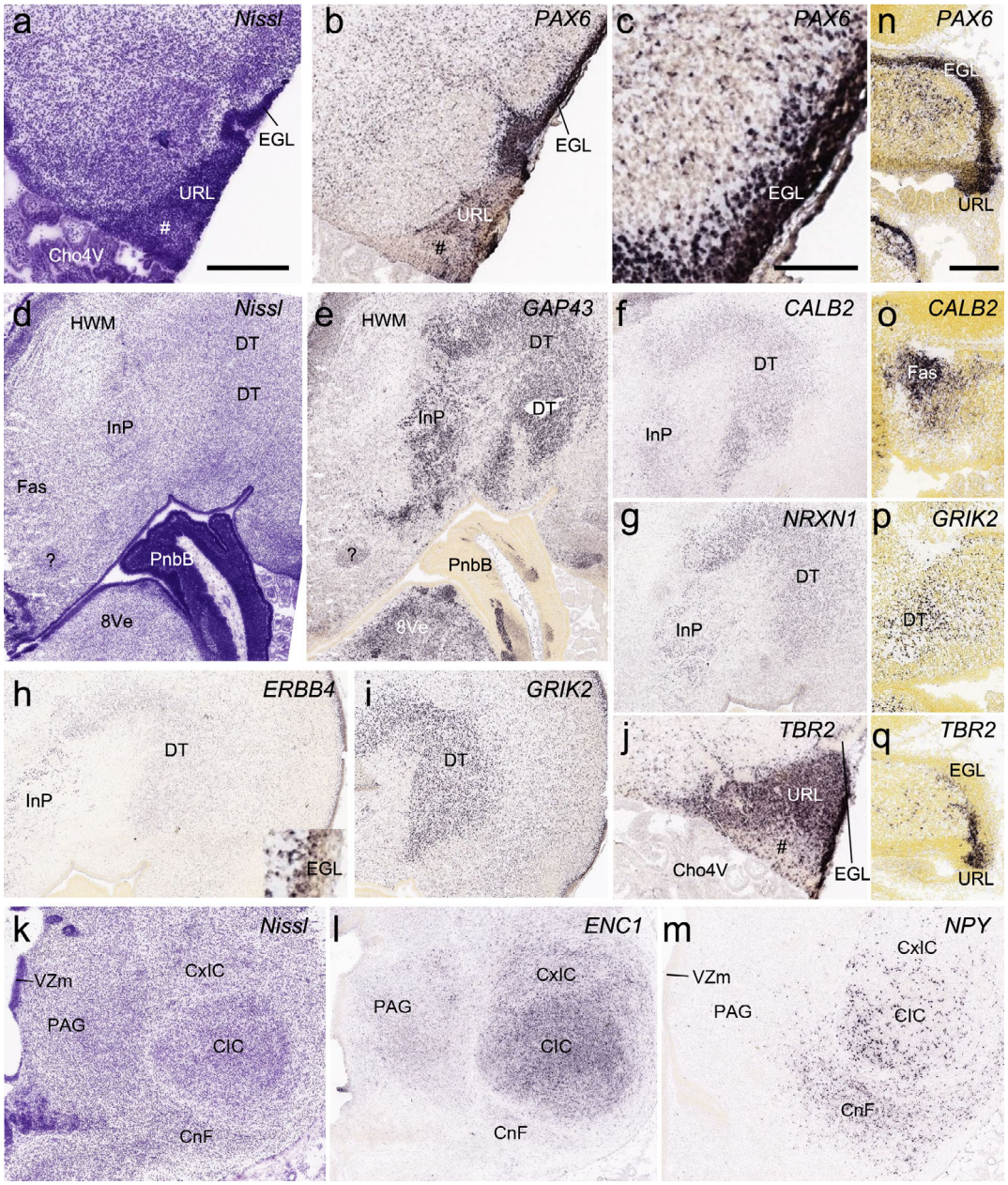

FIGURE 17 Cytoarchitecture and gene expression of the cerebellum and inferior colliculus. (a-l) From human brain at PCW 15; (n-q) from mouse brain at E15.5. (a) A Nissl-stain section showing the cytoarchitecture of the upper rhombic lip (URL) and external granular layer (EGL). This sectioning level is at about the level 40 of the atlas plates (see Appendix 1). (b, c) Low (b) and higher (c) power views of the *PAX6* expression in EGL. (d) A Nissl-stain section showing the cytoarchitecture of the cerebellar deep nuclei (CbDN), which include fastigial nucleus (Fas), interpositus nucleus (InP), and dentate nucleus (DT), and the pontobulbar body (PnbB), which is located at the junction of the cerebellum and pons. (e-i) Expression of *GAP43* (e), *CALB2* (f), *NRXN1* (g), *ERBB4* (h), and *GRIK2* (i) in the CbDN. Note that *ERBB4* and *GRIK2* are also strongly expressed in the region underneath the EGL (h, i). The inset in (h) is a higher power view of the EGL. (j) *TBR2* expression in the URL. The URL appears to have two parts with the less *TBR2 expression* part indicated by #. (K) A Nissl-stain section showing the cytoarchitecture of inferior colliculus (IC) and periaqueduct gray (PAG). (l, m) Expression of *ENC1* (l) and *NPY* (m) in the IC regions. (n-q) Comparative expression of *PAX6* (n), *CALB2* (o), *GRIK2* (p), and *TBR2* (q) in the cerebellum at E15.5 (on sagittal sections). Scale bars: 400 μm in (a) for (a-m; except c); 100 μm in (c); 220 μm in (n) for (n-q)

3.12 | Highly interactive digital atlases for web users

The prenatal brain atlases presented in this study were used to make interactive digital resources (Figure 23), and are publicly accessible through the Allen Institute web portal: www.brain-map.org or directly at the BrainSpan project portal: www.brainspan.org/static/atlas. The atlases may be of interest to diverse groups including students and educators as resources of detailed anatomy of the prenatal human brains. For basic anatomy, the location, shape, and relationship of general structures such as forebrain, midbrain, and hindbrain, as well as cerebral cortex, thalamus, hypothalamus, amygdala, hippocampus,

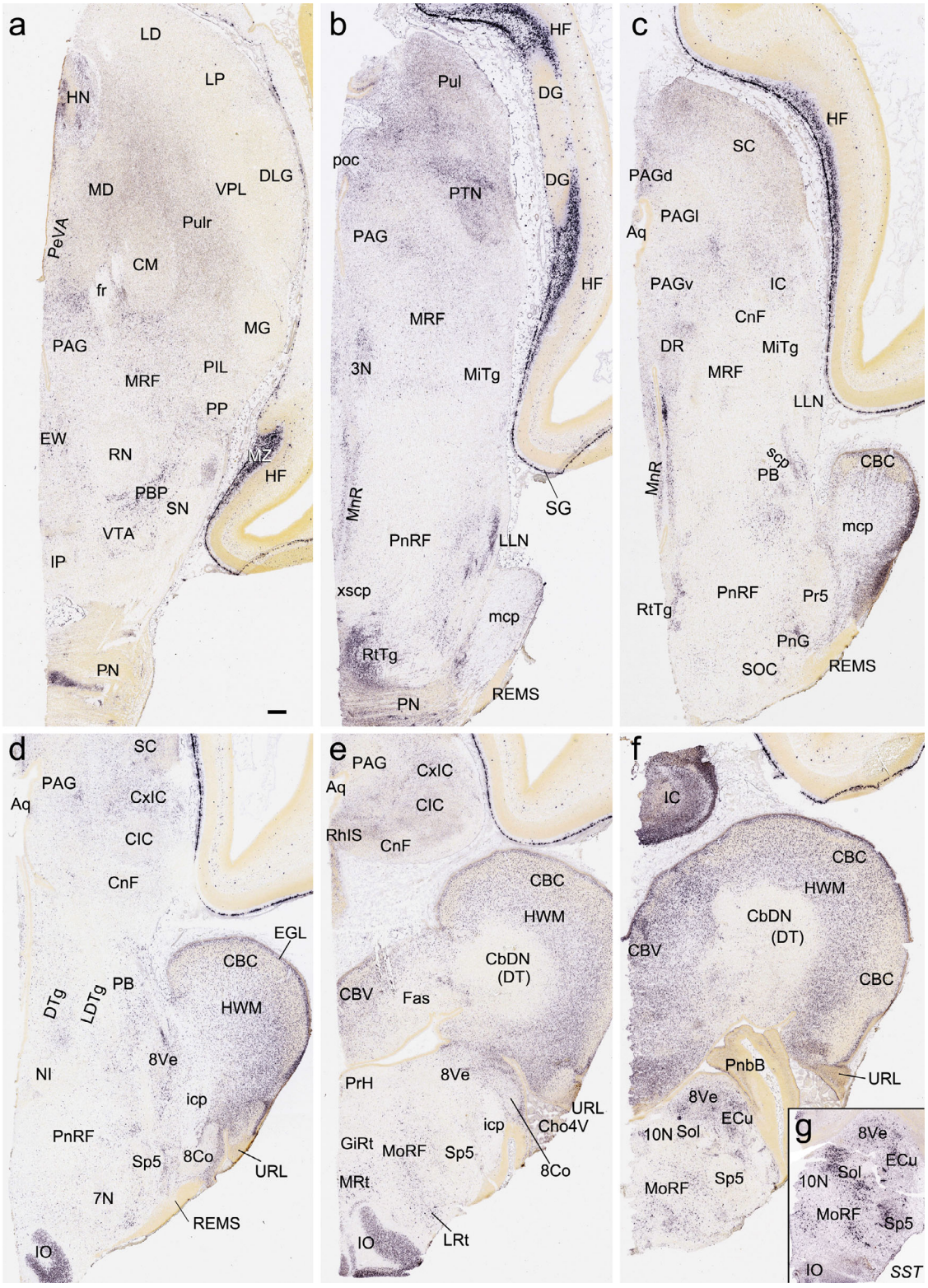

FIGURE 18 Gene expression in the brainstem and cerebellum at PCW 15. (a-f) *RELN* expression in brainstem nuclei and cerebellar cortex (CBC). Note the negative expression in cerebellar deep nuclei (CbDN) and strong expression in the hindbrain white matter (HWM). Note also the strong *RELN* expression in marginal zone (MZ in a) of the hippocampus and subpial granular zone (SG in b) of the cortex. (g) *SST* expression in the medullar nuclei. Scale bars: 400 μm in (a) for all panels. **Abbreviations**: 3N, oculomotor nucleus; 7N, facial nucleus; 8Co, cochlear nucleus; 8Ve, vestibular nucleus; 10N, vagal nucleus; Aq, aqueduct; CBV, cerebellar vermis; Cho4V, choroid plexus of fourth ventricle; CM, centromedian nucleus; CnF, cuneiform nucleus; CxIC, cortex of inferior colliculus; DR, dorsal raphe nucleus; DTg, dorsal tegmental nucleus; ECu, external cuneate nucleus; EW, Edinger–Westphal nucleus; GiRt, gigantocellular reticular nucleus; HN, habenular nucleus; icp, inferior cerebellar peduncle; IO, inferior olive; IP, interpeduncular nucleus; LDTg, dorsolateral tegmental nucleus; LLN, nucleus of lateral lemniscus; LP, lateroposterior nucleus; LRt,

cerebellum, and brainstem, can be easily elucidated simply by using the ontology tree (Figure 23, left column). For medical students and neuroscience professionals, deeper systematic learning and teaching of human brain development can be conveniently achieved via the menu and different tools (Figure 23, inset, thumbnails and right column). In particular, one can search or choose any specific brain region and learn its topographic location, subdivisions, cyto-, and chemoarchitectures. One can also choose specific A-P levels and study which structures occurs on these planes. As needs dictate, structures can be recolorized prior to printing plates using the menu (Figure 23, inset). The ontology itself serves as an essentially complete index of brain structures and their relationships (Figure 23, left column; Table 1).

4 | DISCUSSION

Anatomical atlases are essential resources as for the research community, providing a detailed mapping and synthesis of knowledge about brain structure and function. Although detailed modern high-resolution human brain atlases are available for adult brains (Ding et al., 2016; Mai et al., 2016), similar atlases for prenatal human brain have not been produced. To our knowledge, only one series of anatomical prenatal human brain atlases is available, generated on limited Nissl-stained sections from different prenatal ages (Bayer & Altman, 2003, 2005, 2006). In addition, anatomical delineation in these developmental brain atlases was based only on cytoarchitecture (Nissl staining), and annotation was not complete enough to create a brain-wide hierarchical structural ontology. In the present study, we have created detailed anatomical atlases for prenatal human brain at PCW 15 and 21, aiming to advance the state of the field through dense whole-brain sampling, high information content histological and gene expression analysis, developmental ontology creation, and generation of web-based interactive tools. This reference atlas was used to guide a large-scale microarray-based transcriptomic project, available as a complementary developmental gene expression resource (Miller et al., 2014; https://www.brainspan.org/lcm/search/index.html; see Table 1 for the regions with transcriptomic data). Thus, these atlases should be valuable tools to guide newer efforts to map cell types and developing circuitry in the developing human brain, both as anatomical and gene expression resources.

A major design principle of the atlas was to use highly informative histological and gene expression datasets from the same brain specimen to guide anatomical demarcation across the entire brain at PCW 15 and 21. As demonstrated above, the combined analysis of Nissl-based cytoarchitecture, AChE staining features, and spatial expression patterns of 43 genes by ISH allowed an accurate delineation of brain structures. This information was used to annotate Nissl-stained sections, but also to annotate the gene expression images and illustrate the high utility of individual genes as markers of developing brain structures. Together, these atlases provide a reference for midgestational human brain development and can be used to annotate other timepoints in this period. For example, we used the anatomical atlas for the brain at PCW 15 (Appendix 1) to guide a dense transcriptomic atlas of the PCW 16 brain, which was effective due to its similar cortical lamination and subcortical structures (see Miller et al., 2014). The anatomical atlas for the brain at PCW 21 (Appendix 3) was similarly created and could be applied to the human brains at ages close to PCW 21 (e.g., PCW 19–24). With guidance of these anatomical atlases, spatial expression of 37 and 5 genes was annotated to generate two brain-wide molecular atlases, which are presented in Appendices 2 and 4, respectively.

In general, this study reveals many developmental features of human brain structures that are similar to rodent as well as some human-specific or dominant developmental features. Many of the latter features have been reviewed in detail recently (e.g., Kostović et al., 2019; Molnár et al., 2019), including thick SP, very thick SZo (enriched with intermediate progenitor cells), large extent of SP8 and COUP-TFI expression overlap in the VZ, and an extended period of interneuronal generation and migration from the GE into the cerebral cortex in human compared to mouse. In addition, some migratory routes of interneurons were reported in human but not in mouse (Alzu'bi, Lindsay, Kerwin et al., 2017; Alzu'bi & Clowry, 2019; Paredes et al., 2016; Rubin et al. 2010). In this study, we have observed additional human features not observed in other species. In addition to typical scattered expression in the SP, for instance, strong expression of *NPY* is found in the CP of the V1 at PCW 21 (Figure 5e). This was not reported in mouse (e.g., Thompson et al., 2014) and monkey (Bakken et al., 2016). Another example is the existence of *CALB2* positive patches within the Pf-CM (Figure 15f), which were also not found in monkey and mouse (data available in the Allen Brain Atlas). The third example is that strong *CALB2* expression is seen in the DLG at PCW 15 and 21 (e.g., Appendix 2) but not in mouse DLG at all prenatal stages (Allen datasets). In postnatal mice, *CALB2* expression in the DLG was only observed at P14 (Allen datasets). Finally, it should be point out that the DLG at both PCW 15 and 21 is not yet laminated as in adult and, thus, the two subdivisions (magnocellular and parvocellular parts) of the DLG are not visible at these two stages (see Appendices 1 and 3).

lateral reticular nucleus; mcp, middle cerebellar peduncle; MiTg, microcellular tegmental nucleus; MnR, median raphe nucleus; MoRF, medullar reticular formation; MRF, midbrain reticular formation; MRt, medial reticular nucleus; NI, nucleus incertus; PB, parabrachial nucleus; PBP, parabrachial pigmented nucleus; PeVA, periventricular area; PIL, posterior intralaminar nucleus; PN, pontine nucleus; PnG, pontine gamma nucleus; PnRF, pontine reticular formation; poc, posterior commissure; PP, peripeduncular nucleus; Pr5, principal sensory nucleus of the trigeminal nerve; PrH, prepositus hypoglossal nucleus; PTN, pretectal nucleus; Pulr, rostral pulvinar; REMS, rostral extramural migration system; RhIS, rhombencephalic isthmus; RN, red nucleus; RtTg, reticular tegmental nucleus; scp, superior cerebellar peduncle; SN, substantia nigra; SOC, superior olivary complex; Sol, solitary nucleus; Sp5, spinal trigeminal nucleus; VPL, ventroposterior lateral nucleus; xscp, decussation of superior cerebellar peduncle

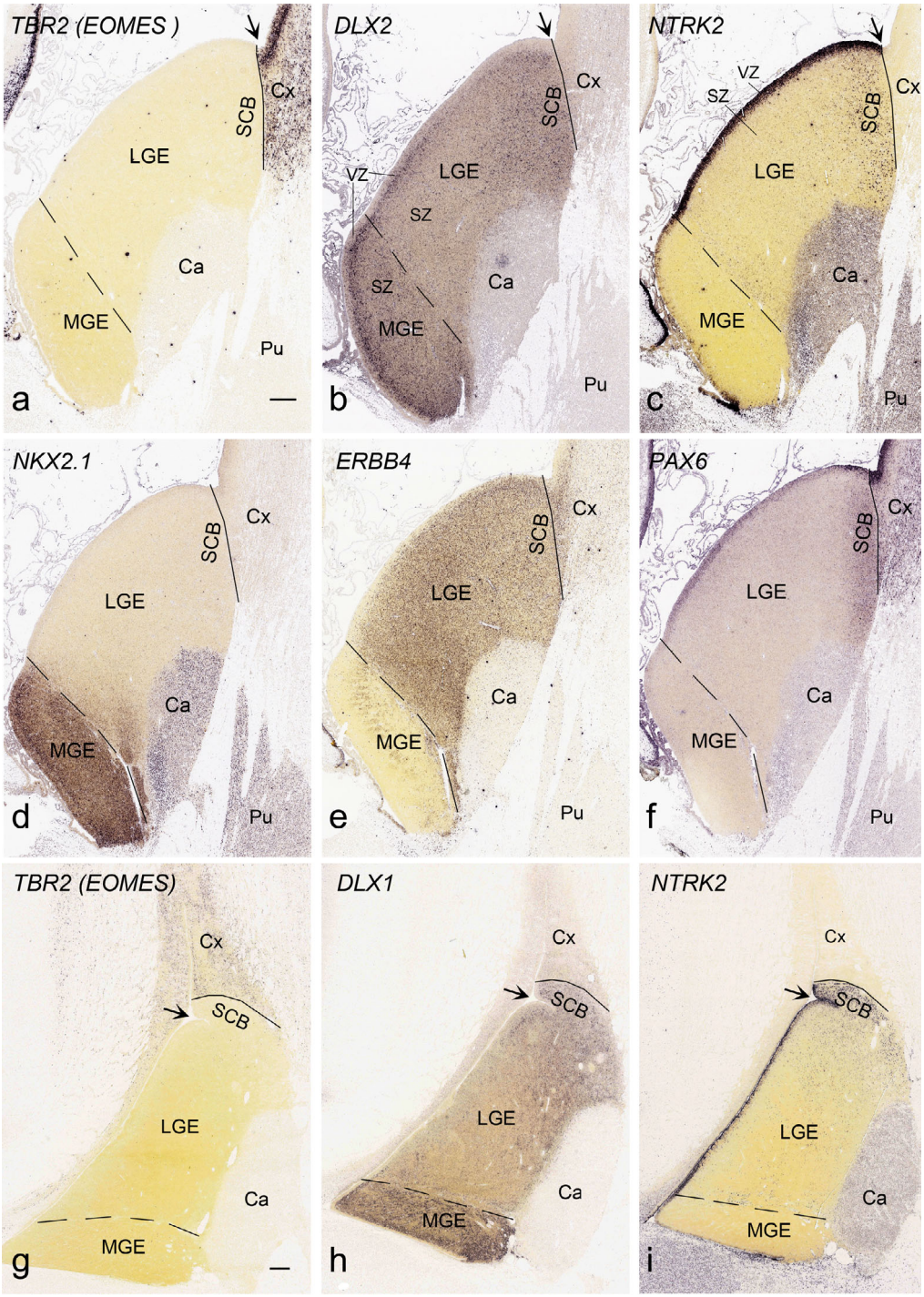

FIGURE 19 Identification of lateral and medial ganglionic eminence (LGE and MGE) and striatal-cortical border (SCB). Solid and dashed lines indicate the striatal-cortical border and MGE-LGE border, respectively. VZ and SZ are ventricular and subventricular zones of the GE, respectively. (a-f) Gene expression in the GE and neocortex at PCW 15. *TBR2* (a) and *DLX2* (b) is expressed in the SZ/VZ of the cortex (Cx) and GE (LGE and MGE), respectively. *NTRK2* (c) and *PAX6* (f) are mostly expressed in the VZ of the LGE and SCB. *NKX2.1* (d) and *ERBB4* (e) are mainly expressed in SZ/VZ of MGE and LGE, respectively. Note *DLX2* and *ERBB4* expression also exists in SCB. (g-i) Gene expression in the GE and neocortex at PCW 21. Expression patterns of *TBR2* (g), *DLX1* (h), *NTRK2* (i), as well as *DLX2*, *NKX2.1*, *ERBB4*, and *PAX6* (not shown) are similar to those at PCW 15. Surprisingly, the striatal-cortical sulcus (SCS, indicated by arrows) is not a reliable landmark for the striatal-cortical border. Thus, the SCB, as marked by rich NTRK2 expression, is located at the striatal side at PCW 15 (c), while at PCW 21 it is located at the cortical side (i). Scale bars: 400 μm in (a) for (a-f); 400 μm in (g) for (g-i)

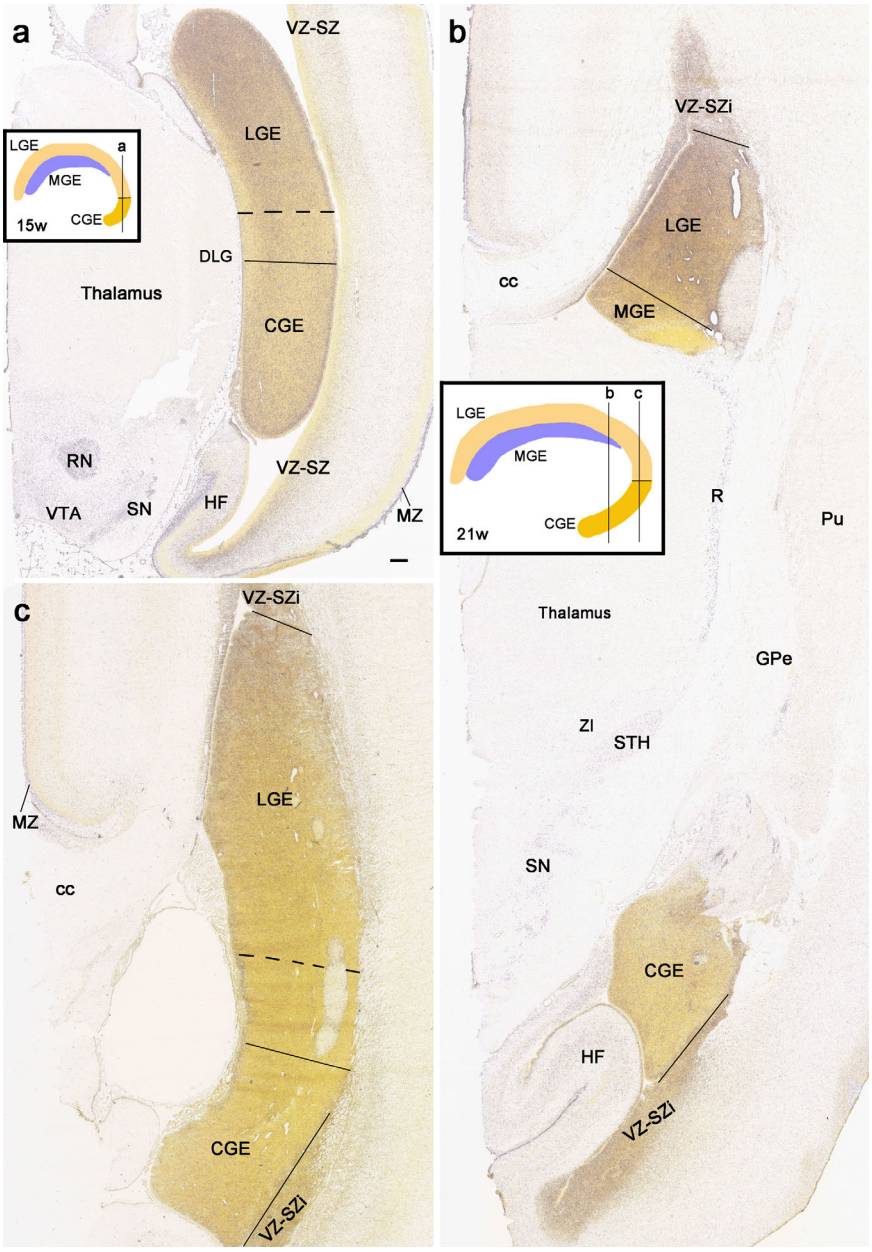

FIGURE 20 Determination of the border between lateral and caudal ganglionic eminence (LGE and CGE). The diagrams in the insets in (a) and (b) show the locations of the sections displayed in (a) and (b, c), respectively. In general, LGE shows much stronger expression of *ERBB4* than CGE at both PCW 15 (a) and 21 (b, c). However, the border is not clear-cut since the expression displays clear gradient. The transition zone between the LGE and CGE is identified between the solid and dashed lines based on the expression of *ERBB4* (a, c) and *CALB2* (much stronger in CGE than in LGE; see Figure 14b). In this study, the LGE-CGE border is placed at the solid lines (a, c) to be conservative for the CGE. Note the *ERBB4* expression in the red nucleus (RN in a), substantia nigra (SN in a, b), and ventral tegmental area (VTA in a) of the midbrain, and in the reticular thalamic nucleus (R), subthalamic nucleus (STH), and zona incerta (ZI) of the thalamus (b). *ERBB4* is also expressed in the marginal zone (MZ) and ventricular-subventricular zone (VZ-SZ or VZ-SZi) of the cortex (a-c). Scale bar: 400 μm in (a) for (a-c)

Several interesting developmental features of prenatal human brain also emerged from our analysis. First, we found that the prenatal HF and EC lack the outer subventricular zone (SZo) that is prominent in developing human neocortex and thought to drive the differential expansion of supragranular layers in primate evolution. The SZo is the major site of supragranular neuron production in the macaque monkey neocortex (Lukaszewicz et al., 2005), and is also present (albeit smaller) in rodents, where common gene expression in SZo and supragranular neurons suggests they are generated from SZo (Nieto et al., 2004; Tarabykin et al., 2001; Zimmer et al., 2004). The thicker SZo in human compared to mouse is also consistent with single-cell transcriptomic findings of increased number, diversity, and phenotypic specialization of supragranular neurons (Berg et al., 2021; Ortega et al., 2018). Histologically, the HF and EC obviously lack equivalent supragranular neurons in layers 2 and 3 of the neocortex (Bakken et al., 2016; Ding et al., 2009; Ding & van Hoesen, 2015). While layers 2 and 3 exist in the EC, the neurons in these two layers are not equivalent to those in the neocortex. For example, layer 2 neurons in the neocortex are very small round and ovoid neurons, while those in the EC are usually very large stellate or pyramidal neurons (Braak & Braak, 1991; Ding et al., 2009; Ding & van Hoesen, 2010). Gene expression and connectivity patterns of layers 2 and 3 in the HF and EC are also different from the neocortex (e.g., Bakken et al., 2016; Ding et al., 2020; Yao et al., 2021). Pathologically, layer 2 neurons in the EC are among the earliest neurons with tau lesions in aging and Alzheimer's disease (AD) populations (Arnold et al., 1991; Braak & Braak, 1991; Ding & van Hoesen, 2010). However, this is not true for layers 2 and 3 neurons in the neocortex, which are affected at later stages of AD (Arnold et al., 1991; Braak & Braak, 1991).

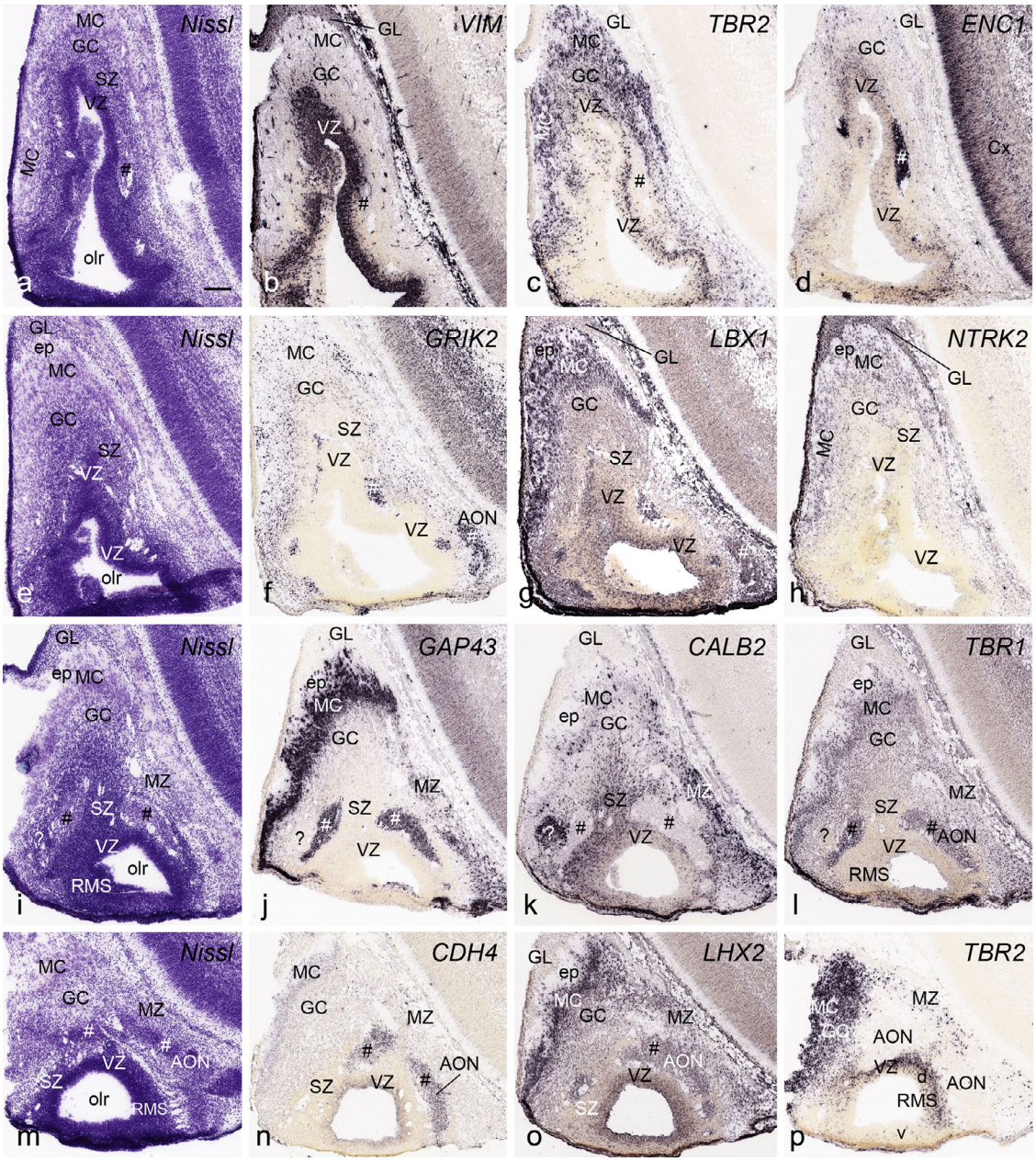

FIGURE 21 Cytoarchitecture and gene expression of olfactory bulb (OB) and anterior olfactory nucleus (AON) at PCW 15. The sections were shown from one rostral level (a-d), two intermediate levels (e-h and i-l), and one caudal level (m-p) with different stains indicated on each panel. OB, rostral migratory stream (RMS) and AON can be identified at PCW15. Some patches in OB and AON (identified by #) express *ENC1*, *GRIK2*, *LBX1*, *GAP43*, *TBR1*, *CDH4*, and *LHX2* but not *CALB2*. Note that the dorsal but not ventral walls of the VZ of RMS strongly expresses TBR2 (panel p) whereas the whole VZ of RMS contains strong expression of *VIM*, *LBX1*, and *LHX2*. One patch (? in i-l) in AON appears to have a very different expression profile. MC, mitral cells; GC, granular cells; GL, glomerular layer; ep, external plexus layer; olr, olfactory recess. Bar: 200 μm in (a) for all panels

Therefore, our findings suggest that layers 2 and 3 neurons in the PrS, PaS, and EC are not likely produced from SZo and instead may directly originate from the SZi. As a previous study suggested, the hippocampal neurons are generated in the VZ while MTC neurons are generated in the VZ and SZ (SZi) with the latter generating the superficial neurons located in lamina principalis externa (Nowakowski & Rakic, 1981).

We found evidence for compartmentalization of the GE in developing human cortex, similar to multiple progenitor domains that have been reported in mouse GE (Flames et al., 2007). In addition to the three well-known subdivisions of the GE (MGE, LGE, CGE), each subdivision can be further divided into VZ and SZ parts that continue at the SCB with cortical VZ and SZ, respectively. The VZ and SZ of the GE displayed differential gene expression within each GE subdivision, and cross over between GE subdivisions (Figure 19). Moreover, complex gene expression patterns within the VZ and SZ of specific GE subdivisions in human were also clearly evident. For example, *NTRK2* is pre-

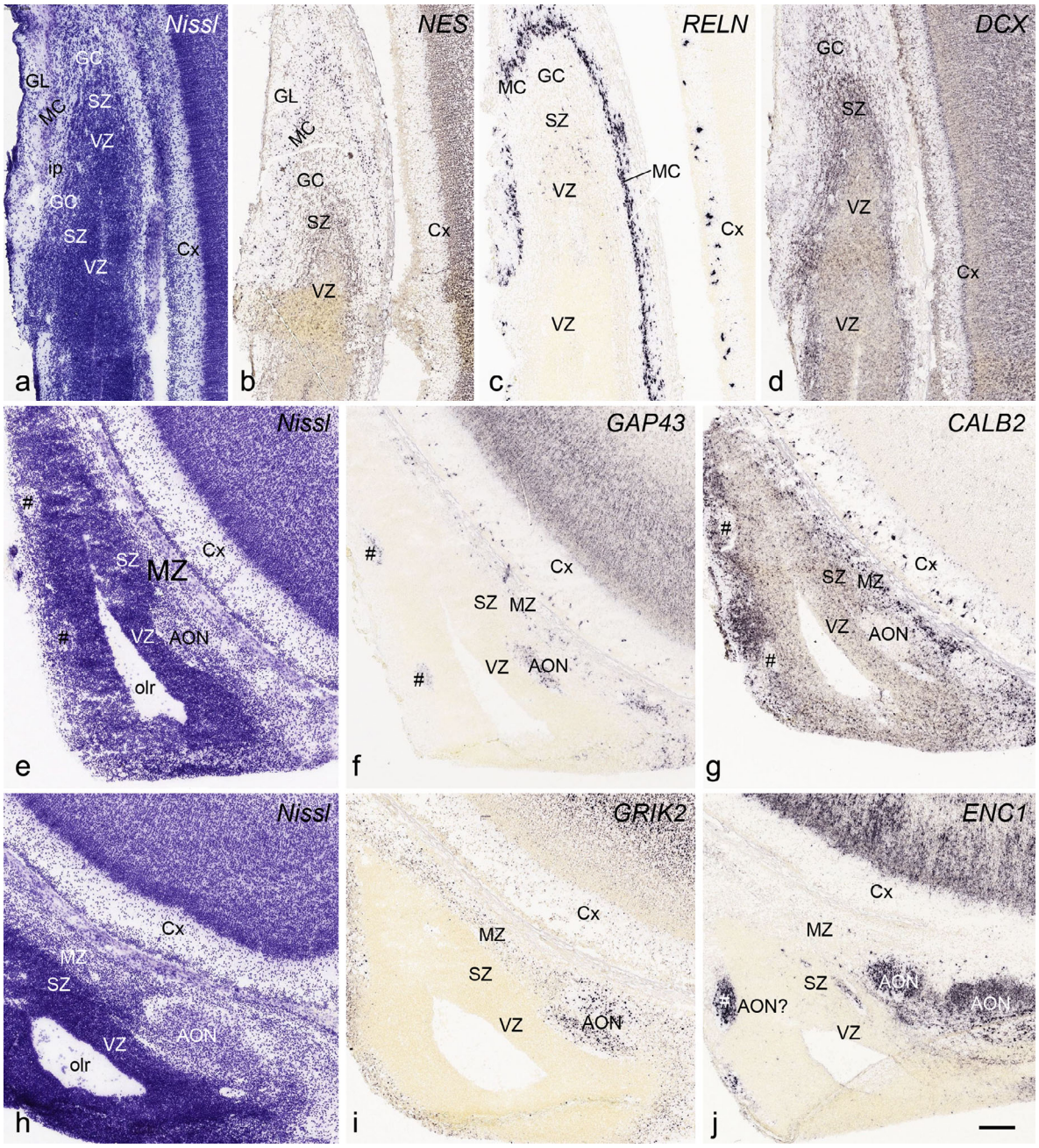

FIGURE 22 Cytoarchitecture and gene expression of olfactory bulb (OB) and anterior olfactory nucleus (AON) at PCW 21. The sections were shown from rostral (a-c), intermediate (d-g), and caudal (h-j) levels with different stains indicated on each panel. The layers of OB and internal plexus layer (ip) can be clearly identified at PCW 21. As at PCW15, AON strongly expresses *GAP43*, *GRIK2*, and *ENC1* but negative for *CALB2*. Note the scattered patches (#s in e-g) which express marker genes for AON (e.g., *GAP43* and *ENC1*). Scale bar: 200 μm in (j) for all panels

dominantly expressed in the VZ of CGE and LGE; furthermore, within the LGE, *NTRK2* expression in the VZ is generally stronger in lateral LGE (and SCB) than in medial LGE (see Appendix 2). Gene expression in the SZ of LGE is also not homogeneous. For instance, *FABP7* expression in the SZ of the LGE is stronger in lateral than medial parts (see Appendix 2), while *NKX2.1* expression is seen in the most medial but not lateral parts of the SZ in addition to strong expression in MGE. Interestingly, *ERBB4* expression displays both A-P and M-L difference in the SZ of the LGE. Specifically, *ERBB4* is much more strongly expressed in the SZ of the laterocaudal part of the LGE (including SCB) compared to the mediorostral part (see Appendix 2). Finally, *SST*, *NPY*, *VIM*, *FABP7*, and *ERBB4* expression is also compartmentalized in MGE (see Appendix 2). These observations likely represent a combination of parcellation of progenitor zones and developmental gradients across the GE.

ERBB4 expression in the GE is significantly different between human and rodents. Previous studies in rat and mouse reported that

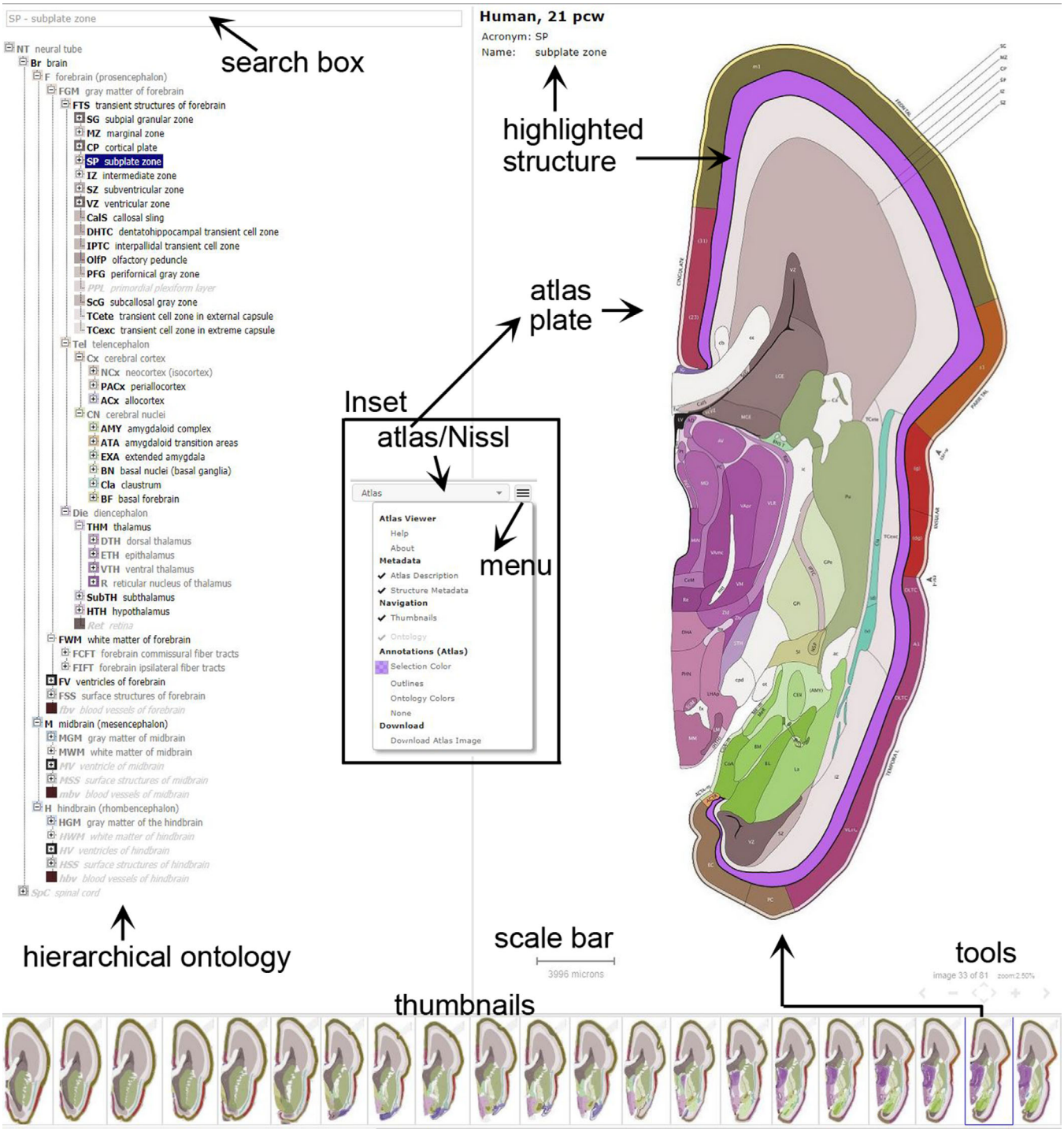

FIGURE 23 Interactive web-based digital atlases for prenatal human brains at PCW 15 and 21. Tools are provided to explore, search, adjust, and download the atlas plates and related structures. These tools include a hierarchical ontology browser and search box (left column), thumbnails (bottom), segmented atlas plates (right column), and atlas menu (Inset), which is placed at the top right corner of the browser and can be used to toggle between Nissl and annotated plates as well as many other functions

ERBB4 is mostly expressed in the SZ of MGE (i.e., not in LGE and CGE) (Fox & Kornblum, 2005; Yau et al., 2003). Rodent *ERBB4* is mainly expressed in MGE-derived GABAergic interneurons migrating to the cerebral cortex, and this expression was reported to be important in this tangential migration (Li et al., 2012; Rakić et al., 2015; Villar-Cerviño et al., 2015). In contrast, we found in human that *ERBB4* is strikingly enriched in LGE rather than MGE. This raises the possibility that human LGE generates cortical interneurons that express *ERBB4* and migrate tangentially through the SZ and VZ (see Appendix 2). Alternatively, this may simply reflect a species difference in *ERBB4*

expression such that OB-bound interneurons from the LGE now express *ERBB4*, or that *ERBB4*-expressing interneurons are mostly generated in MGE as in rodents, but they are immediately channeled to LGE in human. In any event, these findings in human suggest that there may be significant differences in MGE and LGE across species, and that at a minimum *ERBB4* expression and function are not conserved across species.

Another interesting observation was that markers of both cortical and striatal progenitors extend into the RMS. In mouse, the RMS is a pathway mostly consisting of interneurons migrating from LGE and SCB to OB (e.g., Bandler et al., 2017; Kohwi et al., 2005). Glutamatergic neurons also migrate in the RMS, but the source of these neurons has not been clear. In mice, these excitatory neurons derive from *NGN2*-expressing progenitors (Winpenny et al., 2011), and excitatory lineage markers *NGN2*, *PAX6*, and *TBR2* are all expressed in the dorsal wall of the RMS (RMS-d) but also in the SCB region. TBR2, strongly expressed in developing cortical VZ and SZ, is a marker for excitatory neuronal precursors (Englund et al, 2005; Hevner, 2019). Here, we found that *TBR2* is strongly expressed in the developing cortical VZ and SZ and in the RMS-d (Figure 21p), but not the SCB region (Figure 19a and g). These findings suggest that the *TBR2*-expressing VZ and SZ of the neocortex extends rostrally into the OB via the RMS-d, and that excitatory neurons in OB likely originate from the ventral cortical wall rather than from the subpallial–pallial region or SCB region, both during development (this study) and into adulthood (Brill et al., 2009).

Single-cell genomic profiling has become a powerful tool to define cell types (BICCN, 2020; Hodge et al., 2019; Yao et al., 2021) and developmental trajectories, and has begun to be applied in prenatal human brain development (Eze et al., 2021; Fan et al., 2020; Nowakowski et al., 2017). Whole-brain anatomical and molecular atlases, such as those presented here, are important resources to help guide these new cell census efforts and other high-throughput anatomical and connectional efforts in the future. The joint analysis of histology and molecular parcellation creates a needed framework for establishing the cellular and spatial basis of brain development and circuit formation, and a structured ontological framework for defining brain structures across development to adulthood.

ACKNOWLEDGMENTS

We thank the Allen Institute founders, P.G. Allen, and J. Allen, for their vision, encouragement, and support. We are also grateful for the technical support of the staff members in the Allen Institute who are not part of the authorship of this article. The project described was supported by award numbers RC2MH089921 to ESL and MJH from the National Institute of Mental Health. Its contents are solely the responsibility of the authors and do not necessarily represent the official views of the National Institutes of Health and the National Institute of Mental Health.

CONFLICT OF INTEREST

The authors declare that there are no potential sources of conflict of interest.

AUTHOR CONTRIBUTION

SLD and ESL designed the atlas project; SLD generated the anatomical ontology, analyzed histological, and gene expression data and delineated all anatomical boundaries and spatial gene expression. JJR, PL, and BACF performed atlas cartography; KAS led the ISH experiment; IAG, SLD, and ND contributed to specimen processing; TAD, NHK, FL, AS, and LN performed web visualization and application; KB, RAD, AE, TAL, JN, JP, RR, MS, and NVS provided technical support; YW, SLD, JJR, PL, and BACF prepared appendix figures; SLD prepared the figures for the main text; SMS managed the project; AB managed and led the histological pipeline and team; JWP, JGH, ARJ, MJH, PRH, AB, and ESL provided overall supervision. ESL and MJH procured the NIH grant; SLD and ESL wrote the manuscript; all authors had full access to all the data and read the manuscript.

PATIENT CONSENT STATEMENT

Appropriate written informed consent was obtained and all available nonidentifying information was recorded for each specimen.

PERMISSION TO REPRODUCE MATERIAL FROM OTHER SOURCES

We did not reproduce material from other sources.

DATA AVAILABILITY STATEMENT

The data that support the findings and atlas creation of this study are available online (www.brain-map.org or www.brainspan.org), and available from the corresponding authors upon reasonable request.

PEER REVIEW

The peer review history for this article is available at https://publons.com/publon/10.1002/cne.25243.

ORCID

Song-Lin Ding https://orcid.org/0000-0002-7072-5272
Patrick R. Hof https://orcid.org/0000-0002-3208-1154

REFERENCES

Alzu'bi, A., Lindsay, S. J., Harkin, L. F., McIntyre, J., Lisgo, S. N., & Clowry, G. J. (2017). The transcription factors COUP-TFI and COUP-TFII have distinct roles in arealisation and GABAergic interneuron specification in the early human fetal telencephalon. *Cerebral Cortex*, *27*(10): 4971–4987.

Alzu'bi, A., Lindsay, S., Kerwin, J., Looi, S. J., Khalil, F., & Clowry, G. J. (2017). Distinct cortical and sub-cortical neurogenic domains for GABAergic interneuron precursor transcription factors NKX2.1, OLIG2 and COUP-TFII in early fetal human telencephalon. *Brain Structure and Function*, *222*, 2309–2328.

Alzu'bi, A., & Clowry, G. J. (2019). Expression of ventral telencephalon transcription factors ASCL1 and DLX2 in the early fetal human cerebral cortex. *Journal of Anatomy*, *235* (3), 555–568.

Arnold, S. E., Hyman, B. T., Flory, J., Damasio, A. R., & Van Hoesen, G. W. (1991). The topographical and neuroanatomical distribution of neurofibrillary tangles and neuritic plaques in the cerebral cortex of patients with Alzheimer's disease. *Cerebral Cortex*, *1*, 103–116.

Bakken, T. E., Miller, J. A., Ding, S. L., Sunkin, S. M., Smith, K. A., Ng, L., Szafer, A., Dalley, R. A., Royall, J. J., Lemon, T., Shapouri, S., Aiona, K., Arnold, J., Bennett, J. L., Bertagnolli, D., Bickley, K., Boe, A., Brouner, K., Butler, S., …,

Lein, E. S. (2016). A comprehensive transcriptional map of primate brain development. *Nature*, *535*(7612), 367–375.

Bayer, S. A., & Altman, J. (2003). Atlas of human central nervous system development. *Volume 2: The human brain during the third trimester*. CRC Press.

Bayer, S. A., & Altman, J. (2005). Atlas of human central nervous system development. *Volume 3: The human brain during the second trimester*. CRC Press.

Bayer, S. A., & Altman, J. (2006). Atlas of human central nervous system development. *Volume 4: The human brain during the late first trimester*. CRC Press.

Bandler, R. C., Mayer, C., & Fishell, G. (2017). Cortical interneuron specification: the juncture of genes, time and geometry. *Current Opinion of Neurobiology*, *42*, 17–24.

Berg, J., Sorensen, S. A., Ting, J. T., Miller, J. A., Chartrand, T., Buchin, A., Bakken, T. E., Budzillo, A., Dee, N., Ding, S. L., Gouwens, N. W., Hodge, R. D., Kalmbach, B., Lee, C., Lee, B. R., Alfiler, L., Baker, K., Barkan, E., Beller, A., …, Lein, E. S. (2021). Human cortical expansion involves diversification and specialization of supragranular intratelencephalic-projecting neurons. *Nature*, *598*(7879):151–158.

BICCN (Brain Initiative Cell Census Network). (2021). A multimodal cell census and atlas of the mammalian primary motor cortex. *Nature*, *598*(7879):86–102.

Braak, H., & Braak, E. (1991). Neuropathological stageing of Alzheimer-related changes. *Acta Neuropathologica*, *82*, 239–259.

Brill, M. S., Ninkovic, J., Winpenny, E., Hodge, R. D., Ozen, I., Yang, R., Lepier, A., Gascón, S., Erdelyi, F., Szabo, G., Parras, C., Guillemot, F., Frotscher, M., Berninger, B., Hevner, R. F., Raineteau, O., & Götz, M. (2009). Adult generation of glutamatergic olfactory bulb interneurons. *Nature Neuroscience*, *12*(12), 1524–1533.

Carney, R. S. E., Cocas, L. A., Hirata, T., Mansfield, K., Joshua, G., & Corbin, J. G. (2009). Differential regulation of telencephalic pallial–subpallial boundary patterning by *Pax6* and *Gsh2*. *Cerebral Cortex*, *19*(4), 745–759.

Ding, S. L. (2013). Comparative anatomy of the prosubiculum, subiculum, presubiculum, postsubiculum, and parasubiculum in human, monkey, and rodent. *Journal of Comparative Neurology*, *521*, 4145–4162.

Ding, S. L., Royall, J. J., Sunkin, S. M., Ng, L., Facer, B. A., Lesnar, P., Guillozet-Bongaarts, A., McMurray, B., Szafer, A., Dolbeare, T. A., Stevens, A., Tirrell, L., Benner, T., Caldejon, S., Dalley, R. A., Dee, N., Lau, C., Nyhus, J., Reding, M., …, Lein, E. S. (2016). Comprehensive cellular-resolution atlas of the adult human brain. *Journal of Comparative Neurology*, *524*, 3127–3481.

Ding, S. L., & Van Hoesen, G. W. (2010). Borders, extent, and topography of human perirhinal cortex as revealed using multiple modern neuroanatomical and pathological markers. *Human Brain Mapping*, *31*, 1359–1379.

Ding, S. L. & Van Hoesen, G. W. (2015). Organization and detailed parcellation of human hippocampal head and body regions based on a combined analysis of cyto- and chemoarchitecture. *Journal of Comparative Neurology*, *523*, 2233–2253.

Ding, S. L., Van Hoesen, G. W., Cassell, M. D., & Poremba, A. (2009). Parcellation of human temporal polar cortex: a combined analysis of multiple cytoarchitectonic, chemoarchitectonic, and pathological markers. *Journal of Comparative Neurology*, *514*(6), 595–623.

Ding, S. L., Yao, Z., Hirokawa, K. E., Nguyen, T. N., Graybuck, L. T., Fong, O., Bohn, P., Ngo, K., Smith, K. A., Koch, C., Phillips, J. W., Lein, E. S., Harris, J. A., Tasic, B., & Zeng, H. (2020). Distinct transcriptomic cell types and neural circuits of the subiculum and prosubiculum along the dorsal-ventral axis. *Cell Reports*, *31*, 107648. https://doi.org/10.1016/j.celrep.2020.107648

Englund, C., Fink, A., Lau, C., Pham, D., Daza, R. A., Bulfone, A., Kowalczyk, T., & Hevner, R. F. (2005). Pax6, Tbr2, and Tbr1 are expressed sequentially by radial glia, intermediate progenitor cells, and postmitotic neurons in developing neocortex. *Journal of Neuroscience*, *25*, 247–251.

Evans, A. C., Janke, A. L., Collins, D. L., & Baillet, S. (2012). Brain templates and atlases. *Neuroimage*, *62*, 911–922.

Eze, U. C., Bhaduri, A., Haeussler, M., Nowakowski, T. J., & Kriegstein, A. R. (2021). Single-cell atlas of early human brain development highlights heterogeneity of human neuroepithelial cells and early radial glia. *Nature Neuroscience*, *24*(4), 584–594.

Fan, X., Fu, Y., Zhou, X., Sun, L., Yang, M., Wang, M., Chen, R., Wu, Q., Yong, J., Dong, J., Wen, L., Qiao, J., Wang, X., & Tang, F. (2020). Single-cell transcriptome analysis reveals cell lineage specification in temporal-spatial patterns in human cortical development. *Science Advances*, *6*(34), eaaz2978. https://doi.org/10.1126/sciadv.aaz2978

Flames, N., Pla, R., Gelman, D. M., Rubenstein, J. L., Puelles, L., & Marin, O. (2007). Delineation of multiple subpallial progenitor domains by the combinatorial expression of transcriptional codes. *Journal of Neuroscience*, *27*, 9682–9695.

Fox, I. J., & Kornblum, H. I. (2005). Developmental profile of ErbB receptors in murine central nervous system: implications for functional interactions. *Journal of Neuroscience Research*, *79*(5), 584–597.

Hansen, D. V., Lui, J. H., Flandin, P., Yoshikawa, K., Rubenstein, J. L., Alvarez-Buylla, A., & Kriegstein, A. R. (2013). Non-epithelial stem cells and cortical interneuron production in the human ganglionic eminences. *Nature Neuroscience*, *16*(11), 1576–1587.

Hevner, R. F. (2019). Intermediate progenitors and Tbr2 in cortical development. *Journal of Anatomy*, *235*, 616–625.

Hodge, R. D., Bakken, T. E., Miller, J. A., Smith, K. A., Barkan, E. R., Graybuck, L. T., Close, J. L., Long, B., Johansen, N., Penn, O., Yao, Z., Eggermont, J., Höllt, T., Levi, B. P., Shehata, S. I., Aevermann, B., Beller, A., Bertagnolli, D., Brouner, K., …, Lein, E. S. (2019). Conserved cell types with divergent features in human versus mouse cortex. *Nature*, *573*(7772), 61–68.

Karnovsky, M. J., & Roots, L. (1964). A "direct coloring" thiocholine method for cholinesterases. *Journal of Histochemistry and Cytochemistry*, *12*, 219–221.

Kohwi, M., Osumi, N., Rubenstein, J. L., & Alvarez-Buylla, A. (2005). Pax6 is required for making specific subpopulations of granule and periglomerular neurons in the olfactory bulb. *Journal of Neuroscience*, *25*(30), 6997–7003.

Kostovic, I., & Rakic, P. (1990). Developmental history of the transient subplate zone in the visual and somatosensory cortex of the macaque monkey and human brain. *Journal of Comparative Neurology*, *297* (3), 441–470.

Kostović, I., Sedmak, G., & Judaš, M. (2019). Neural histology and neurogenesis of the human fetal and infant brain. *Neuroimage*, *188*, 743–773.

Lein, E. S., Hawrylycz, M. J., Ao, N., Ayres, M., Bensinger, A., Bernard, A., Boe, A. F., Boguski, M. S., Brockway, K. S., Byrnes, E. J., Chen, L., Chen, L., Chen, T. M., Chin, M. C., Chong, J., Crook, B. E., Czaplinska, A., Dang, C. N., Datta, . S., …, Jones, A. R. (2007). Genome-wide atlas of gene expression in the adult mouse brain. *Nature*, *445*(7124), 168–176.

Li, H., Chou, S. J., Hamasaki, T., Perez-Garcia, C. G., & O'Leary, D. D. M. (2012). Neuregulin repellent signaling via ErbB4 restricts GABAergic interneurons to migratory paths from ganglionic eminence to cortical destinations. *Neural Development*, *7*, 10. https://doi.org/10.1186/1749-8104-7-10

Lukaszewicz, A., Savatier, P., Cortay, V., Giroud, P., Huissoud, C., Berland, M., Kennedy, H., & Dehay, C. (2005). G1 phase regulation, area-specific cell cycle control, and cytoarchitectonics in the primate cortex. *Neuron*, *47*, 353–364.

Ma, T., Wang, C., Wang, L., Zhou, X., Tian, M., Zhang, Q., Zhang, Y., Li, J., Liu, Z., Cai, Y., Liu, F., You, Y., Chen, C., Campbell, K., Song, H., Ma, L., Rubenstein, J. L., & Yang, Z. (2013). Subcortical origins of human and monkey neocortical interneurons. *Nature Neuroscience*, *16*(11), 1588–1597.

Mai, J. K., Majtanik, M., & Paxinos, G. (2016). *Atlas of the human brain* (4th ed.). Elsevier Academic Press.

Miller, J. A., Ding, S. - L., Sunkin, S. M., Smith, K. A., Ng, L., Szafer, A., Ebbert, A., Riley, Z. L., Royall, J. J., Aiona, K., Arnold, J. M., Bennet, C., Bertagnolli, D., Brouner, K., Butler, S., Caldejon, S., Carey, A., Cuhaciyan, C., Dalley, R. A., …, Lein, E. S. (2014). Transcriptional landscape of the prenatal human brain. *Nature*, *508*, 199–206.

Molnár, Z., & Clowry, G. J. (2012). Cerebral cortical development in rodents and primates. *Progress in Brain Research*, *195*, 45–70.

Molnár, Z., Clowry, G. J., Šestan, N., Alzu'bi, A., Bakken, T., Hevner, R. F., Hüppi, P. S., Kostović, I., Rakic, P., Anton, E. S., Edwards, D., Garcez, P., Hoerder-Suabedissen, A., & Kriegstein, A. (2019). New insights into the development of the human cerebral cortex. *Journal of Anatomy*, *235*(3), 432–451.

Nelson, B. R., Hodge, R. D., Daza, R. A., Tripathi, P. P., Arnold, S. J., Millen, K. J., & Hevner, R. F. (2020). Intermediate progenitors support migration of neural stem cells into dentate gyrus outer neurogenic niches. *elife*, *9*, e53777. https://doi.org/10.7554/eLife.53777.

Nieto, M., Monuki, E. S., Tang, H., Imitola, I., Haubst, N., Khoury, S. J., Cunningham, J., Gotz, M., & Walsh, C. A. (2004). Expression of Cux-1 and Cux-2 in the subventricular zone and upper layers II–IV of the cerebral cortex. *Journal of Comparative Neurology*, *479*, 168–180.

Nowakowski, R. S., & Rakic, P. (1981). The site of origin and rout and rate of migration of neurons to the hippocampal region of the rhesus monkey. *Journal of Comparative Neurology*, *196*, 129–154.

Nowakowski, T. J., Bhaduri, A., Pollen, A. A., Alvarado, B., Mostajo-Radji, M. A., Di Lullo, E., Haeussler, M., Sandoval-Espinosa, C., Liu, S. J., Velmeshev, D., Ounadjela, J. R., Shuga, J., Wang, X., Lim, D. A., West, J. A., Leyrat, A. A., Kent, W. J., & Kriegstein, A. R. (2017). Spatiotemporal gene expression trajectories reveal developmental hierarchies of the human cortex. *Science*, *358*(6368), 1318–1323.

Oishi, K., Chang, L., & Huang, H. (2019). Baby brain atlases. *Neuroimage*, *185*, 865–880.

Ortega, J. A., Memi, F., Radonjic, N., Filipovic, R., Bagasrawala, I., Zecevic, N., & Jakovcevski, I. (2018). The subventricular zone: a key player in human neocortical development. *Neuroscientist*, *24*, 156–170.

Paredes, M. F., James, D., Gil-Perotin, S., Kim, H., Cotter, J. A., Ng, C., Sandoval, K., Rowitch, D. H., Xu, D., McQuillen, P. S., Garcia-Verdugo, J. M., Huang, E. J., & Alvarez-Buylla, A. (2016). Extensive migration of young neurons into the infant human frontal lobe. *Science*, *354*, aaf7073.

Puelles, L., Kuwana, E., Puelles, E., Bulfone, A., Shimamura, K., Keleher, J., Smiga, S., & Rubenstein, J. L. (2000). Pallial and subpallial derivatives in the embryonic chick and mouse telencephalon, traced by the expression of the genes Dlx-2, Emx-1, Nkx-2.1, Pax-6, and Tbr-1. *Journal of Comparative Neurology*, *424*, 409–438.

Rakić, S., Kanatani, S., Hunt, D., Faux, C., Cariboni, A., Chiara, F., Khan, S., Wansbury, O., Howard, B., Nakajima, K., Nikolić, M., & Parnavelas, J. G. (2015). Cdk5 phosphorylation of ErbB4 is required for tangential migration of cortical interneurons. *Cerebral Cortex*, *25*, 991–1003.

Reinchisi, G., Ijichi, K., Glidden, N., Jakovcevski, I., & Zecevic, N. (2012). COUP-TFII expressing interneurons in human fetal forebrain. *Cerebral Cortex*, *22*(12), 2820–2830.

Rubin, A. N., Alfonsi, F., Humphreys, M. P., Choi, C. K. P., Rocha, S. F., & Kessaris, N. (2010). The germinal zones of the basal ganglia but not the septum generate GABAergic interneurons for the cortex. *Journal of Neuroscience*, *30*, 12050–12062.

Tarabykin, V., Stoykova, A., Usman, N., & Grass, P. (2001). Cortical upper layer neurons derive from the subventricular zone as indicated by Svet1 gene expression. *Development*, *128*, 1983–1993.

Thompson, C. L., Ng, L., Menon, V., Martinez, S., Lee, C. K., Glattfelder, K., Sunkin, S. M., Henry, A., Lau, C., Dang, C., Garcia-Lopez, R., Martinez-Ferre, A., Pombero, A., Rubenstein, J. L. R., Wakeman, W. B., Hohmann, J., Dee, N., Sodt, A. J., Young, R., …, Jones, A. R. (2014). A high-resolution spatiotemporal atlas of gene expression of the developing mouse brain. *Neuron*, *83*, 309–323.

Villar-Cerviño, V., Kappeler, C., Nóbrega-Pereira, S., Henkemeyer, M., Rago, L., Nieto, M. A., & Marín, O. (2015). Molecular mechanisms controlling the migration of striatal interneurons. *Journal of Neuroscience*, *35*, 8718–8729.

Wang, Q., Ding, S. L., Li, Y., Royall, J., Feng, D., Lesnar, P., Graddis, N., Naeemi, M., Facer, B., Ho, A., Dolbeare, T., Blanchard, B., Dee, N., Wakeman, W., Hirokawa, K. E., Szafer, A., Sunkin, S. M., Oh, S. W., Bernard, A., …, Ng, L. (2020). The Allen mouse brain common coordinate framework: a 3D reference atlas. *Cell*, *181*, 936–953.

Winpenny, E., Lebel-Potter, M., Fernandez, M. E., Brill, M. S., Götz, M., Guillemot, F., & Raineteau, O. (2011). Sequential generation of olfactory bulb glutamatergic neurons by Neurog2-expressing precursor cells. *Neural Development*, *6*, 12. https://doi.org/10.1186/1749-8104-6-12

Yao, Z., van Velthoven, C. T. J., Nguyen, T. N., Goldy, J., Sedeno-Cortes, A. E., Baftizadeh, F., Bertagnolli, D., Casper, T., Chiang, M., Crichton, K., Ding, S. L., Fong, O., Garren, E., Glandon, A., Gouwens, N. W., Gray, J., Graybuck, L. T., Hawrylycz, M. J., Hirschstein, D., …, Zeng, H. (2021). A taxonomy of transcriptomic cell types across the isocortex and hippocampal formation. *Cell*, *184*, 3222–3241.

Yau, H. - J., Wang, H. F., Lai, C., & Liu, F. - C. (2003). Neural development of the neuregulin receptor ErbB4 in the cerebral cortex and the hippocampus: preferential expression by interneurons tangentially migrating from the ganglionic eminences. *Cerebral Cortex*, *13*, 252–264. https://doi.org/10.1093/cercor/13.3.252

Zimmer, C., Tiveron, M. C., Bodmer, R., & Cremer, H. (2004). Dynamics of Cux2 expression suggests that an early pool of SVZ precursors is fated to become upper cortical layer neurons. *Cerebral Cortex*, *14*:1408–1420.

How to cite this article: Ding, S.-L., Royall, J. J., Lesnar, P., Facer, B. A. C., Smith, K. A., Wei, Y., Brouner, K., Dalley, R. A., Dee, N., Dolbeare, T. A., Ebbert, A., Glass, I. A., Keller, N. H., Lee, F., Lemon, T. A., Nyhus, J., Pendergraft, J., Reid, R., Sarreal, M., …, Lein, E. S. (2022). Cellular resolution anatomical and molecular atlases for prenatal human brains. *Journal of Comparative Neurology*, *530*(1), 6–503. https://doi.org/10.1002/cne.25243

TABLE 1 Abbreviations and ontology of brain structures*

Abbreviations	Ontology of brain structures	Transcriptome data available (A)		
		pcw 15	pcw 16	pcw 21
F	Forebrain			
FGM	grey matter of forebrain			
FTS	transient structures of forebrain			
SG	subpial granular zone			
fSG	SG in frontal neocortex			A
pSG	SG in parietal neocortex			A
tSG	SG in temporal neocortex	A		A
oSG	SG in occipital neocortex			A
iSG	SG in insular neocortex			A
cSG	SG in cingulate neocortex			A
peSG	SG in periallocortex			
SGpc	SG in perirhinal cortex		A	
SGpas	SG in parasubicular cortex			
SGec	SG in entorhinal cortex			A
SGprs	SG in presubicular cortex			
SGrs	SG in retrosplenial cortex			
SGiag	SG in agranular insular cortex			
alSG	SG in allocortex			
SGhip	SG in hippocampal proper			
SGsub	SG in subicular cortex			
SGpir	SG in piriform cortex			
MZ	marginal zone			
fMZ	MZ in frontal neocortex			
fMZfp	MZ in frontal polar cortex	A	A	A
fMZdl	MZ in dorsolateral prefrontal cortex	A		A
fMZvl	MZ in ventrolateral prefrontal cortex	A		A
fMZor	MZ in orbital frontal cortex			A
fMZm1	MZ in posterior frontal cortex (motor cortex)			A
pMZ	MZ in parietal neocortex			
pMZs1	MZ in primary somatosensory cortex		A	A
pMZdm	MZ in dorsomedial parietal cortex			A
pMZpd	MZ in posterodorsal (superior) parietal cortex			A
pMZpv	MZ in posteroventral (inferior) parietal cortex	A	A	A
tMZ	MZ in temporal neocortex			
tMZsl	MZ in superolateral temporal cortex	A	A	A
tMZil	MZ in inferolateral temporal cortex	A		A
tMZmt	MZ in medial temporal-occipital cortex	A	A	A
tMZlt	MZ in lateral temporal-occipital cortex	A		A
tMZph	MZ in posterior parahippocampal cortex		A	A
oMZ	MZ in occipital neocortex			
oMZv1	MZ in primary visual cortex	A	A	A
oMZdm	MZ in dorsomedial extrastriate cortex (V2)	A	A	A
oMZvm	MZ in ventromedial extrastriate cortex (VP)		A	A

(Continues)

TABLE 1 (Continued)

Abbreviations	Ontology of brain structures	Transcriptome data available (A)		
		pcw 15	pcw 16	pcw 21
oMZml	MZ in midlateral extrastriate cortex (area 19)	A		A
iMZ	MZ in insular neocortex			
iMZdg	MZ in dysgranular insular neocortex		A	A
iMZgr	MZ in granular insular neocortex			A
cMZ	MZ in cingulate neocortex			
cMZr	MZ in rostral cingulate cortex	A	A	A
cMZc	MZ in caudal cingulate cortex			A
peMZ	MZ in periallocortex			
MZpc	MZ in perirhinal cortex	A	A	A
MZpas	MZ in parasubicular cortex			
MZec	MZ in entorhinal cortex			A
MZprs	MZ in presubicular cortex			
MZrs	MZ in retrosplenial cortex			A
MZiag	MZ in agranular insular cortex			
alMZ	MZ in allocortex			
MZhip	MZ in hippocampal proper			
MZsub	MZ in subicular cortex			
MZpir	MZ in piriform cortex			
CP	cortical plate			
fCP	CP in frontal neocortex			
fCPfp	CP in frontal polar cortex	A	A	A
fCPdm	CP in dorsomedial frontal cortex	A		A
fCPdl	CP in dorsolateral prefrontal cortex	A	A	A
fCPvl	CP in ventrolateral prefrontal cortex	A		A
fCPor	CP in orbital frontal cortex	A	A	A
fCPm1	CP in posterior frontal cortex (motor cortex)	A	A	A
pCP	CP in parietal neocortex			
pCPs1	CP in primary somatosensory cortex	A	A	A
pCPdm	CP in dorsomedial parietal cortex (area 7m)	A	A	A
pCPpd	CP in posterosuperior (dorsal) parietal cortex	A	A	A
pCPpv	CP in posteroinferior (ventral) parietal cortex	A	A	A
tCP	CP in temporal neocortex			
tCPdl	CP in dorsolateral temporal cortex			
tCPa1	CP in primary auditory cortex		A	A
tCPsl	CP in superolateral temporal cortex	A	A	A
tCPps	CP in polysensory temporal cortex			
tCPpi	CP in parainsualr temporal cortex			
tCPvl	CP in ventrolateral temporal cortex			
tCPml	CP in midlateral temporal cortex	A		
tCPil	CP in inferolateral temporal cortex	A	A	A
tCPmi	CP in midinferior temporal cortex			A
tCP36	CP in rostral midinferior temporal cortex (area 36)	A	A	
tCPtf	CP in caudal midinferior temporal cortex (area TF)	A	A	

(Continues)

TABLE 1 (Continued)

Abbreviations	Ontology of brain structures	Transcriptome data available (A)		
		pcw 15	pcw 16	pcw 21
tCPph	CP in posterior parahippocampal cortex	A	A	A
tCPmt	CP in medial temporal-occipital cortex	A	A	A
tCPlt	CP in lateral temporal-occipital cortex	A		A
tCPtp	CP in temporal polar cortex	A		A
oCP	CP in occipital neocortex			
oCPpro	CP in area prostriata			
oCPv1	CP in primary visual cortex	A	A	A
oCPexs	CP in extrastriate cortex			
oCPdm	CP in dorsomedial extrastriate cortex (V2d)	A	A	A
oCPvm	CP in ventromedial extrastriate cortex (VP)	A	A	A
oCPml	CP in midlateral extrastriate cortex (area 19)	A		A
iCP	CP in insular neocortex			
iCPdg	CP in dysgranular insular cortex	A	A	A
iCPgr	CP in granualr insular cortex	A	A	A
cCP	CP in cingulate neocortex			
cCPr	CP in rostral cingulate cortex	A	A	A
cCPmi	CP in midcingulate cortex		A	
cCPc	CP in caudal cingulate cortex	A	A	A
cCPsg	CP in subgenual (subcallosal) cingulate cortex	A	A	
peCP	CP in periallocortex			
CPpc	CP in perirhinal cortex			
CPpcr	CP in rostral perirhinal cortex		A	A
CPpcc	CP in caudal perirhinal cortex	A	A	
CPpas	CP in parasubicular cortex			
CPec	CP in entorhinal cortex			
CPlec	CP in lateral (anterior) entorhinal cortex			
CPmec	CP in medial (posterior) entorhinal cortex			
CPprs	CP in presubicular cortex			
CPrs	CP in retrosplenial cortex		A	A
CPiag	CP in agranular insular cortex			
alCP	CP in allocortex			
CPhip	CP in hippocampal proper			
CPhipr	CP in rostral hippocampus	A	A	
CPhipc	CP in caudal hippocampus		A	
CPsub	CP in subicular cortex			
CPsubr	CP in rostral subicular cortex			
CPsubc	CP in caudal subicular cortex	A		
CPpir	CP in piriform cortex			
SP	subplate zone			
fSP	SP in frontal neocortex			
fSPfp	SP in frontal polar cortex	A	A	A
fSPdm	SP in dorsomedial frontal cortex		A	A
fSPdl	SP in dorsolateral prefrontal cortex	A	A	A

(Continues)

TABLE 1 (Continued)

Abbreviations	Ontology of brain structures	Transcriptome data available (A)		
		pcw 15	pcw 16	pcw 21
fSPvl	SP in ventrolateral prefrontal cortex	A		A
fSPor	SP in orbital frontal cortex	A	A	A
fSPm1	SP in posteror frontal cortex (motor cortex)	A	A	A
pSP	SP in parietal neocortex			
pSPs1	SP in primary somatosensory cortex	A	A	A
pSPdm	SP in dorsomedial parietal cortex (area 7m)	A	A	A
pSPpd	SP in posterosuperior (dorsal) parietal cortex	A	A	A
pSPpv	SP in posteroinferior (ventral) parietal cortex	A	A	A
tSP	SP in temporal neocortex			
tSPdl	SP in dorsolateral temporal cortex			
tSPa1	SP in primary auditory cortex		A	A
tSPsl	SP in superolateral temporal cortex	A	A	A
tSPps	SP in polysensory temporal cortex			
tSPpi	SP in parainsular temporal cortex			
tSPvl	SP in ventrolateral temporal cortex			
tSPml	SP in midlateral temporal cortex	A		A
tSPil	SP in inferolateral temporal cortex	A	A	A
tSPmi	SP in midinferior temporal cortex			A
tSP36	SP in rostral midinferior temporal cortex (area 36)	A	A	
tSPtf	SP in caudal midinferior temporal cortex (area TF)	A	A	
tSPph	SP in posterior parahippocampal cortex		A	A
tSPmt	SP in medial temporal-occipital cortex		A	A
tSPlt	SP in lateral temporal-occipital cortex	A		A
tSPtp	SP in temporal polar cortex			A
oSP	SP in occipital neocortex			
oSPpro	SP in area prostriata			
oSPv1	SP in primary visual cortex	A	A	A
oSPexs	SP in extrastriate cortex			
oSPdm	SP in dorsomedial extrastriate cortex (V2d)	A	A	A
oSPvm	SP in ventromedial extrastriate cortex (VP)	A	A	A
oSPml	SP in midlateral extrastriate cortex (area 19)	A		A
iSP	SP in insular neocortex			
iSPdg	SP in dysgranular insular cortex	A	A	A
iSPgr	SP in granular insular cortex	A	A	A
cSP	SP in cingulate neocortex			
cSPr	SP in rostral cingulate cortex	A	A	A
cSPmi	SP in midcingulate cortex		A	
cSPc	SP in caudal cingulate cortex	A	A	A
cSPsg	SP in subgenual (subcallosal) cingulate cortex	A	A	
peSP	SP in periallocortex			
SPpc	SP in perirhinal cortex		A	A
SPpas	SP in parasubicular cortex			
SPec	SP in entorhinal cortex			A

(Continues)

TABLE 1 (Continued)

Abbreviations	Ontology of brain structures	Transcriptome data available (A)		
		pcw 15	pcw 16	pcw 21
SPlec	SP in lateral (anterior) entorhinal cortex			
SPmec	SP in medial (posterior) entorhinal cortex			
SPprs	SP in presubicular cortex			
SPrs	SP in retrosplenial cortex			
SPiag	SP in agranular insular cortex			
alSP	SP in allocortex			
SPhip	SP in hippocampal proper			
SPhipr	SP in rostral hippocampal proper			
SPhipc	SP in caudal hippocampal proper	A		
SPsub	SP in subicular cortex			
SPsubr	SP in rostral subicular cortex			
SPsubc	SP in caudal subicular cortex	A		
SPpir	SP in piriform cortex			
IZ	intermediate zone			
fIZ	IZ in frontal neocortex			
fIZfp	IZ in frontal polar cortex	A	A	A
fIZdm	IZ in dorsomedial frontal cortex			A
fIZdl	IZ in dorsolateral prefrontal cortex			A
fIZvl	IZ in ventrolateral prefrontal cortex	A		A
fIZor	IZ in orbital frontal cortex	A	A	A
fIZm1	IZ in posteror frontal cortex (motor cortex)	A	A	A
pIZ	IZ in parietal neocortex			
pIZs1	IZ in primary somatosensory cortex	A	A	A
pIZdm	IZ in dorsomedial parietal cortex (area 7m)	A	A	
pIZpd	IZ in posterosuperior (dorsal) parietal cortex	A	A	A
pIZpv	IZ in posteroinferior (ventral) parietal cortex	A	A	A
tIZ	IZ in temporal neocortex			
tIZdl	IZ in dorsolateral temporal cortex			
tIZa1	IZ in primary auditory cortex			A
tIZsl	IZ in superolateral temporal cortex	A	A	A
tIZps	IZ in polysensory temporal cortex			
tIZpi	IZ in parainsular temporal cortex			
tIZvl	IZ in ventrolateral temporal cortex			
tIZml	IZ in midlateral temporal cortex	A		
tIZil	IZ in inferolateral temporal cortex	A	A	A
tIZmi	IZ in midinferior temporal cortex			
tIZ36	IZ in rostral midinferior temporal cortex (area 36)			
tIZtf	IZ in caudal midinferior temporal cortex (area TF)		A	
tIZph	IZ in posterior parahippocampal cortex		A	A
tIZmt	IZ in medial temporal-occipital cortex	A	A	
tIZlt	IZ in lateral temporal-occipital cortex	A		
tIZtp	IZ in temporal polar cortex			
oIZ	IZ in occipital neocortex			

(Continues)

TABLE 1 (Continued)

Abbreviations	Ontology of brain structures	Transcriptome data available (A)		
		pcw 15	pcw 16	pcw 21
oIZpro	IZ in area prostriata			
oIZv1	IZ in primary visual cortex	A		A
oIZexs	IZ in extrastriate cortex			
oIZdm	IZ in dorsomedial extrastriate cortex (V2)	A	A	A
oIZvm	IZ in ventromedial extrastriate cortex (VP)			
oIZml	IZ in midlateral extrastriate cortex (area 19)			A
iIZ	IZ in insular neocortex			
iIZdg	IZ in dysgranular insular cortex	A	A	A
iIZgr	IZ in granular insular cortex	A	A	A
cIZ	IZ in cingulate neocortex			
cIZr	IZ in rostral cingulate cortex	A	A	A
cIZmi	IZ in midcingulate cortex		A	A
cIZc	IZ in caudal cingulate cortex	A	A	A
cIZsg	IZ in subgenual (subcallosal) cingulate cortex	A	A	
peIZ	IZ in periallocortex			
lZpc	IZ in perirhinal cortex	A		
lZec	IZ in entorhinal cortex			
lZlec	IZ in lateral (anterior) entorhinal cortex			
lZmec	IZ in medial (posterior) entorhinal cortex			
lZprs	IZ in presubicular cortex			
lZrs	IZ in retrosplenial cortex			
alIZ	IZ in allocortex			
lZhip	IZ in hippocampal proper			
lZsub	IZ in subicular cortex			
SZ	subventricular zone			
fSZ	SZ in frontal neocortex			
fSZfp	SZ in frontal polar cortex			
fSZfpo	outer SZ in frontal polar cortex	A	A	A
fSZfpi	inner SZ in frontal polar cortex	A	A	
fSZdm	SZ in dorsomedial frontal cortex			
fSZdmo	outer SZ in dorsomedial frontal cortex	A		
fSZdmi	inner SZ in dorsomedial frontal cortex	A		
fSZdl	SZ in dorsolateral prefrontal cortex			
fSZdlo	outer SZ in dorsolateral prefrontal cortex	A	A	A
fSZdli	inner SZ in dorsolateral prefrontal cortex	A	A	
fSZvl	SZ in ventrolateral prefrontal cortex			
fSZvlo	outer SZ in ventrolateral prefrontal cortex	A		A
fSZvli	inner SZ in ventrolateral prefrontal cortex	A		
fSZor	SZ in orbital frontal cortex			
fSZoro	outer SZ in orbital frontal cortex	A	A	A
fSZori	inner SZ in orbital frontal cortex	A	A	
fSZm1	SZ in posteror frontal cortex (motor cortex)			
fSZm1o	outer SZ in posteror frontal cortex (motor cortex)	A	A	A

(Continues)

TABLE 1 (Continued)

Abbreviations	Ontology of brain structures	Transcriptome data available (A)		
		pcw 15	pcw 16	pcw 21
fSZm1i	inner SZ in posteror frontal cortex (motor cortex)	A	A	
pSZ	SZ in parietal neocortex			
pSZs1	SZ in primary somatosensory cortex			
pSZs1o	outer SZ in primary somatosensory cortex	A	A	A
pSZs1i	inner SZ in primary somatosensory cortex	A	A	A
pSZdm	SZ in dorsomedial parietal cortex (area 7m)			
pSZdmo	outer SZ in dorsomedial parietal cortex (area 7m)	A	A	A
pSZdmi	inner SZ in dorsomedial parietal cortex (area 7m)	A	A	
pSZpd	SZ in posterosuperior (dorsal) parietal cortex			
pSZpdo	outer SZ in posterosuperior (dorsal) parietal cortex	A	A	A
pSZpdi	inner SZ in posterosuperior (dorsal) parietal cortex	A	A	A
pSZpv	SZ in posteroinferior (ventral) parietal cortex			
pSZpvo	outer SZ in posteroinferior (ventral) parietal cortex	A	A	A
pSZpvi	inner SZ in posteroinferior (ventral) parietal cortex	A	A	A
tSZ	SZ in temporal neocortex			
tSZdl	SZ in dorsolateral temporal cortex			
tSZa1	SZ in primary auditory cortex			
tSZa1o	outer SZ in primary auditory cortex			A
tSZa1i	inner SZ in primary auditory cortex			
tSZsl	SZ in superolateral temporal cortex			
tSZslo	outer SZ in superolateral temporal cortex	A	A	
tSZsli	inner SZ in superolateral temporal cortex	A	A	
tSZps	SZ in polysensory temporal cortex			
tSZpso	outer SZ in polysensory temporal cortex			
tSZpsi	inner SZ in polysensory temporal cortex			
tSZpi	SZ in parainsular temporal cortex			
tSZvl	SZ in ventrolateral temporal cortex			
tSZml	SZ in midlateral temporal cortex			
tSZmlo	outer SZ in midlateral temporal cortex	A		
tSZmli	inner SZ in midlateral temporal cortex	A		
tSZil	SZ in inferolateral temporal cortex			
tSZilo	outer SZ in inferolateral temporal cortex	A	A	A
tSZili	inner SZ in inferolateral temporal cortex	A	A	A
tSZmi	SZ in midinferior temporal cortex			
tSZ36	SZ in rostral midinferior temporal cortex (area 36)			
tSZ36o	outer SZ in rostral midinferior temporal cortex (area 36)			
tSZ36i	inner SZ in rostral midinferior temporal cortex (area 36)			
tSZtf	SZ in caudal midinferior temporal cortex (area TF)			
tSZtfo	outer SZ in caudal midinferior temporal cortex (area TF)		A	
tSZtfi	inner SZ in caudal midinferior temporal cortex (area TF)		A	
tSZph	SZ in posterior parahippocampal cortex			A
tSZpho	outer SZ in posterior parahippocampal cortex		A	
tSZphi	inner SZ in posterior parahippocampal cortex		A	

(Continues)

TABLE 1 (Continued)

Abbreviations	Ontology of brain structures	Transcriptome data available (A)		
		pcw 15	pcw 16	pcw 21
tSZmt	SZ in medial temporal-occipital cortex			A
tSZmto	outer SZ in medial temporal-occipital cortex	A	A	
tSZmti	inner SZ in medial temporal-occipital cortex	A	A	
tSZlt	SZ in lateral temporal-occipital cortex			
tSZlto	outer SZ in lateral temporal-occipital cortex	A		A
tSZlti	inner SZ in lateral temporal-occipital cortex	A		A
tSZtp	SZ in temporal polar cortex			
oSZ	SZ in occipital neocortex			
oSZpro	SZ in area prostriata			
oSZv1	SZ in primary visual cortex			
oSZv1o	outer SZ in primary visual cortex	A	A	A
oSZv1i	inner SZ in primary visual cortex	A	A	A
oSZexs	SZ in extrastriate cortex			
oSZdm	SZ in dorsomedial extrastriate cortex (V2)			
oSZdmo	outer SZ in dorsomedial extrastriate cortex	A	A	A
oSZdmi	inner SZ in dorsomedial extrastriate cortex	A	A	A
oSZvm	SZ in ventromedial extrastriate cortex (VP)			
oSZvmo	outer SZ in ventromedial extrastriate cortex	A	A	A
oSZvmi	inner SZ in ventromedial extrastriate cortex	A	A	A
oSZml	SZ in midlateral extrastriate cortex (area 19)			
oSZmlo	outer SZ in midlateral extrastriate cortex	A		A
oSZmli	inner SZ in midlateral extrastriate cortex	A		A
cSZ	SZ in cingulate neocortex			
cSZr	SZ in rostral cingulate cortex	A	A	A
cSZmi	SZ in midcingulate cortex		A	A
cSZc	SZ in caudal cingulate cortex	A	A	A
cSZsg	SZ in subgenual cingulate cortex	A	A	
peSZ	SZ in periallocortex			
seSZ	SZ in septal region			
VZ	ventricular zone			
fVZ	VZ in frontal neocortex			
fVZfp	VZ in frontal polar cortex	A	A	A
fVZdm	VZ in dorsomedial frontal cortex	A		A
fVZdl	VZ in dorsolateral prefrontal cortex	A		A
fVZvl	VZ in ventrolateral prefrontal cortex	A		A
fVZor	VZ in orbital frontal cortex	A	A	A
fVZm1	VZ in posteror frontal cortex (motor cortex)	A	A	A
pVZ	VZ in parietal neocortex			
pVZs1	VZ in primary somatosensory cortex	A	A	A
pVZdm	VZ in dorsomedial parietal cortex (area 7m)	A	A	
pVZpd	VZ in posterosuperior (dorsal) parietal cortex	A	A	A
pVZpv	VZ in posteroinferior (ventral) parietal cortex	A	A	A
tVZ	VZ in temporal neocortex			

(Continues)

TABLE 1 (Continued)

Abbreviations	Ontology of brain structures	Transcriptome data available (A)		
		pcw 15	pcw 16	pcw 21
tVZdl	VZ in dorsolateral temporal cortex			
tVZa1	VZ in primary auditory cortex			
tVZsl	VZ in superolateral temporal cortex	A		
tVZps	VZ in polysensory temporal cortex			
tVZpi	VZ in parainsular temporal cortex			
tVZvl	VZ in ventrolateral temporal cortex			
tVZml	VZ in midlateral temporal cortex	A		
tVZil	VZ in inferolateral temporal cortex	A	A	A
tVZmi	VZ in midinferior temporal cortex			
tVZ36	VZ in rostral midinferior temporal cortex (area 36)			
tVZtf	VZ in caudal midinferior temporal cortex (area TF)		A	
tVZph	VZ in posterior parahippocampal cortex	A	A	A
tVZmt	VZ in medial temporal-occipital cortex	A	A	A
tVZlt	VZ in lateral temporal-occipital cortex	A		A
tVZtp	VZ in temporal polar cortex			
oVZ	VZ in occipital neocortex			
oVZpro	VZ in area prostriata			
oVZv1	VZ in primary visual cortex	A	A	A
oVZexs	VZ in extrastriate cortex			
oVZdm	VZ in dorsomedial extrastriate cortex (V2)	A	A	A
oVZvm	VZ in ventromedial extrastriate cortex (VP)	A	A	A
oVZml	VZ in midlateral extrastriate cortex (area 19)	A		A
cVZ	VZ in cingulate neocortex			
cVZr	VZ in rostral cingulate neocortex	A	A	A
cVZmi	VZ in midcingulate neocortex		A	A
cVZc	VZ in caudal cingulate neocortex	A	A	A
cVZsg	VZ in subgenual cingulate neocortex	A	A	
peVZ	VZ in periallocortex			
VZpc	VZ in perirhinal cortex			
VZpcr	VZ in rostral perirhinal cortex			
VZpcc	VZ in caudal perirhinal cortex			
VZec	VZ in entorhinal cortex			
VZmec	VZ in medial (posterior) entorhinal cortex			A
VZlec	VZ in lateral (anterior) entorhinal cortex			
VZprs	VZ in presubicular cortex			
VZprsr	VZ in rostral presubicular cortex			
VZprsc	VZ in caudal presubicular cortex			
VZrs	VZ in retrosplenial cortex			
alVZ	VZ in allocortex			
VZhip	VZ in hippocampal proper			
VZhipr	VZ in rostal hippocampal proper			
VZhipc	VZ in caudal hippocampal proper	A		
VZsub	VZ in subicular cortex			

(Continues)

TABLE 1 (Continued)

Abbreviations	Ontology of brain structures	Transcriptome data available (A)		
		pcw 15	pcw 16	pcw 21
VZsubr	VZ in rostral subicular cortex			
VZsubc	VZ in caudal subicular cortex	A		
OF	outer fiber zone in neocortex			
IF	inner fiber zone in neocortex			
GE	ganglionic eminence (VZ in basal nuclei)	A		
SCB	striatal-cortical boundary (subpallium-pallium boundary)			
LGE	lateral ganglionic eminence	A	A	A
LGEo	outer portion of lateral ganglionic eminence (SZ)	A	A	
LGEi	inner portion of lateral ganglionic eminence (VZ)	A	A	
LGEVZ	LGE-VZ border region	A	A	
LMGE	MGE-Lateral region	A	A	
MGE	medial ganglionic eminence	A	A	A
MGEo	outer portion of medial ganglionic eminence (SZ)	A	A	
MGEi	inner portion of medial ganglionic eminence (VZ)	A	A	
CGE	caudal ganglionic eminence		A	A
CGEo	outer portion of caudal ganglionic eminence (SZ)			
CGEi	inner portion of caudal ganglionic eminence (VZ)			
seVZ	VZ in septal region	A	A	
scVZ	VZ in subcallosal region	A	A	
paVZ	VZ in postamygdaloid region			A
thVZ	VZ in thalamic region		A	
hyVZ	VZ in hypothalamic portion		A	
RMS	rostral migratory stream	A	A	A
RMSv	vertical portion of rostral migratory stream			
RMSvv	VZ part of RMSv			
RMSvg	GE part of RMSv			
RMSvs	SZ part of RMSv			
RMSh	horizontal portion of rostral migratory stream			
RMShv	VZ part of RMSh			
RMShg	GE part of RMSh			
RMShs	SZ part of RMSh			
CalS	callosal sling		A	
DHTC	dentatohippocampal transient cell zone			
DNS	dentate neuroepithelial stem cell zone			
IPTC	interpallidal transient cell zone			
OlfP	olfactory peduncle			
PFG	perifornical gray zone			
PPL	primordial plexiform layer			
ScG	subcallosal gray zone			
TCete	transient cell zone in external capsule			
TCexc	transient cell zone in extreme capsule			
LMS	lateral migratory stream			
VMS	ventral migratory stream			

(Continues)

TABLE 1 (Continued)

Abbreviations	Ontology of brain structures	Transcriptome data available (A)		
		pcw 15	pcw 16	pcw 21
DMS	dorsal migratory stream			
SMS	septal migratory stream			
SCS	striatal-cortical sulcus			
CAS	caudal amygdaloid stream			
FPS	permanent structures of forebrain			
Tel	telencephalon (for more details see table 3 in Ding et al. J Comp Neurol, 2016)			
Cx	cerebral cortex			
NCx	neocortex			
FCx	frontal neocortex			
PFC	prefrontal cortex	A		
A10 (FP)	frontal polar cortex			
DFC	dorsolateral prefrontal cortex			
VFC	ventrolateral prefrontal cortex			
OFC	orbital frontal cortex	A		
M1C (A4, M1)	primary motor cortex	A		
PMC (A6)	premortor cortex	A		
PCx	parietal neocortex			
S1C (S1)	primary somatosensory cortex			
SPC	superior parietal cortex			
IPC	inferior parietal cortex	A		
TCx	temporal neocortex			
DLTC	dorsolateral temporal cortex	A		
VLTC	ventrolateral temporal cortex			
PPHC	posterior parahippocampal cortex			
A37	medial temporal-occipital cortex			
A38 (TP)	temporal polar cortex			
Ocx	occipital neocortex			
V1C (V1)	primary visual cortex (striate cortex)			
ESOC	extrastriate occipital cortex			
V2	parastriate cortex			
PSC (A19)	peristriate cortex			
ICx	insular neocortex			
Idg	dysgranular insular cortex			
Ig	granular insular cortex			
CCx	cingulate cortex			
MFC (ACC)	medial frontal cortex (rostral cingulate cortex, areas 32, 24 and 25)	A		A
MCC	midcingulate cortex (area 24mi)			
PCC	caudal cingulate cortex (areas 23 and 31)			
PACx	periallocortex			
PArCx	periarchicortex			
A35	perirhinal cortex (area 35)		A	A
EC	entorhinal cortex			

(Continues)

TABLE 1 (Continued)

Abbreviations	Ontology of brain structures	Transcriptome data available (A)		
		pcw 15	pcw 16	pcw 21
LEC	lateral entorhinal cortex	A	A	A
MEC	medial entorhinal cortex		A	A
PaS	parasubicular cortex			A
PrS	presubicular cortex			A
RSC (RS)	retrosplenial cortex (areas 29 and 30)			
PPCx	peripaleocortex			
Iag	agranular insular cortex	A		A
FI	frontal agranular insular cortex			
TI	temporal agranular insular cortex			
ACx	allocortex			
ArCx	archicortex			
DG	dentate gyrus	A	A	A
Hipp	hippocampal proper (CA1-4)	A	A	A
Sub	subicular cortex			
S	subiculum		A	A
ProS	prosubiculum	A		
IG	indusium griseum			
PalCx	paleocortex			
OB	olfactory bulb		A	
AON	anterior olfactory nucleus			
OT	olfactory tubercle	A	A	A
Pir	piriform cortex	A	A	A
LOA	lateral olfactory area			
PEA	piriform-entorhinal-amygdaloid area			
CN	cerebral nuclei			
AMY	amygdaloid complex	A		
AAA	anterior amygdaloid area			
CEN	central nuclear group		A	A
CMN	corticomedial nuclear group			
Co	cortical amygdaloid nucleus			
CoA	anterior cortical nucleus	A	A	A
CoP	posterior cortical nucleus			A
Me	medial nucleus		A	A
AHA	amygdalohippocampal area			
BLN	basolateral nuclear group			
La	lateral nucleus of amygdala	A	A	A
BL	basolateral nucleus of amygdala	A	A	A
BM	basomedial nucleus of amygdala	A	A	A
INA	intercalated nucleus of amygdala		A	A
ATA	amygdaloid transition area			
ASTA	amygdalostriatal transition area		A	A
ACTA	amygdalocortical transition area			
EXA	extended amygdala			
BNST	bed nucleus of stria terminalis	A	A	A

(Continues)

TABLE 1 (Continued)

Abbreviations	Ontology of brain structures	Transcriptome data available (A)		
		pcw 15	pcw 16	pcw 21
BN	basal nuclei (basal ganglia)			
STR	striatum			
Ca	caudate nucleus	A	A	A
Pu	putamen	A	A	A
NAC	nucleus accumbens	A	A	A
GP	globus pallidus			
GPe	external segment of globus pallidus	A	A	A
GPi	internal segment of globus pallidus	A	A	A
VeP	ventral pallidus	A	A	
Cla	claustrum	A	A	A
BF	basal forebrain			
SEP	septal nuclei			
MSN	medial septal nucleus	A	A	A
LSN	lateral septal nucleus	A	A	A
BNM	basal nucleus of Meynert	A	A	A
NDB	nucleus of diagonal band	A	A	A
SI	substantia innominata			
Die	diencephalon (for more details see table 3 in Ding et al. J Comp Neurol, 2016)			
THM	Thalamus			
DTH	dorsal thalamus			
ANC	anterior nuclear complex of thalamus	A		
AD	anterior dorsal nucleus of thalamus		A	A
AV	anterior ventral nucleus of thalamus		A	A
AM	anterior medial nucleus of thalamus			A
LD	lateral dorsal nucleus of thalamus		A	A
MNC	medial nuclear complex of thalamus			
MD	mediodorsal nucleus of thalamus	A	A	A
Re	Reuniens nucleus	A		
LNC	lateral nuclear complex of thalamus			
VA	ventral anterior nucleus of thalamus	A	A	A
VL	ventral lateral nucleus of thalamus		A	A
VP	ventral posterior nucleus of thalamus			
VPM	ventral posterior medial nucleus of thalamus		A	A
VPL	ventral posterior lateral nucleus of thalamus		A	A
VPI	ventral posterior inferior nucleus of thalamus	A	A	
VM	ventral medial nucleus of thalamus		A	
LP	lateral posterior nucleus of thalamus		A	A
Pul	pulvinar of thalamus	A	A	A
PoN	posterior nuclear complex of thalamus			
LG	lateral geniculate nucleus			
DLG	dorsal lateral geniculate nucleus	A	A	A
PG (VLG)	pregeniculate nucleus			
MG	medial geniculate nucleus	A	A	A

(Continues)

TABLE 1 (Continued)

Abbreviations	Ontology of brain structures	Transcriptome data available (A)		
		pcw 15	pcw 16	pcw 21
LSG	limitans/suprageniculate nucleus	A	A	
PIL	posterior intralaminar nucleus			
Po	posterior nucleus of thalamus			
ILN	intralaminar nuclear complex of thalamus			
Fa	fasciculosus nucleus of thalamus			
PC	paracentral nucleus of thalamus			
CL	central lateral nucleus of thalamus			
CeM	central medial nucleus of thalamus			
Pf	parafascicular nucleus of thalamus	A	A	A
CM	centromedian nucleus of thalamus	A	A	A
SPf	subparafascicular nucleus of thalamus	A	A	
MiN	midline nuclear comlex	A		
PeVA	periventricular area of thalamus			
IMD	intermediodorsal nucleus of thalamus			
ETH	epithalamus			
HN	habenular nucleus			
MHN	medial habenular nucleus	A	A	A
LHN	lateral habenular nucleus	A	A	A
PaV	paraventricular nucleus of thalamus	A	A	A
Pin	pineal body		A	
VTH	ventral thalamus			
FF	nucleus of the field of Forel			
ZI	zona incerta		A	A
R	reticular nucleus of thalamus	A	A	A
SubTH	subthalamus			
STH	subthalamic nucleus		A	A
HTH	hypothalamus			
MnPO	median preoptic nucleus			
PeV	periventricular nucleus	A		
MPN	medial preoptic nucleus			A
SCN	suprachiasmatic nucleus			
SO	supraoptic nucleus	A		A
AHN	anterior hypothalamic nucleus	A	A	A
PV	paraventricular nucleus of hypothalamus	A		
DHA	dorsal hypothalamic area			
TM	tuberomammillary nucleus			
DMH	dorsomedial hypothalamic nucleus	A	A	A
VMH	ventromedial hypothalamic nucleus	A	A	A
Arc	arcuate nucleus of hypothalamus	A	A	A
ME	median eminence			
LT	lateral tuberal nucleus		A	
PMH	posteromedial hypothalamic nucleus			
PMN	premammillary nucleus			

(Continues)

TABLE 1 (Continued)

Abbreviations	Ontology of brain structures	Transcriptome data available (A)		
		pcw 15	pcw 16	pcw 21
PHN	posterior hypothalamic nucleus		A	A
SUM	supramammillary nucleus			
MM	medial mammillary nucleus		A	A
LM	lateral mammillary nucleus			
LHA	lateral hypothalamic area	A	A	A
PeF	perifornical nucleus			
FWM	white matter of forebrain (for details see table 3 in Ding et al. J Comp Neurol, 2016)			
FV	ventricles of forebrain			
LV	lateral ventricle			
3V	third ventricle			
FSS	surface structures of forebrain (for details see table 3 in Ding et al. J Comp Neurol, 2016)			
M	Midbrain			
MGM	grey matter of midbrain			
MTS	transient structures of midbrain			
MNM	mesencephalic neuromere (mesomere)			
MZM	marginal zone of midbrain			
IZM	intermediate (mantle) zone of midbrain			
IZMro	roof plate of midbrain			
IZMal	alar plate (tectal zone) of midbrain			
IZMba	basal plate of midbrain			
IZMfl	floor plate of midbrain			
VZM	ventricular (matrix) zone of midbrain			
MPS	permanent structures of midbrain (for more details see table 3 in Ding et al. J Comp Neurol, 2016)			
PTR	pretectal region			
PTN	pretectal nuclear complex	A	A	A
MTg	midbrain tegmentum			
EW	Edinger-Westphal nucleus		A	
3N	oculomotor nucleus		A	A
4N	trochlear nucleus			
MRF	midbrain reticular formation	A		A
CnF	cuneiform nucleus			
PTg	pedunculotegmental nucleus		A	A
IP	interpeduncular nucleus		A	
RN	red nucleus	A	A	A
SN	substantia nigra	A	A	A
PBP	parabrachial pigmented nucleus			
VTA	ventral tegmental area		A	A
PAG	periaqueductal gray substance		A	A
DR	dorsal raphe nucleus		A	A
InC	interstitial nucleus of Cajal			
PrC	precommissural nucleus			A
MTc	midbrain tectum			
SC	superior colliculus		A	A

(Continues)

TABLE 1 (Continued)

Abbreviations	Ontology of brain structures	Transcriptome data available (A)		
		pcw 15	pcw 16	pcw 21
IC	inferior colliculus	A	A	A
PBG	parabigeminal nucleus		A	A
MWM	white matter of midbrain (for details see table 3 in Ding et al. J Comp Neurol, 2016)			
MV	ventricle of midbrain			
Aq	cerebral aqueduct			
MSS	surface structures of midbrain (for details see table 3 in Ding et al. J Comp Neurol, 2016)			
H	Hindbrain			
HGM	grey matter of hindbrain			
HTS	transient structures of hindbrain			
CBT	transient zones of cerebellar cortex			
VeT	transient zones of cerebellar vermis			
VeTe	external granular (germinal) zone of the vermis			
VeTm	marginal zone of the vermis			
VeTp	Purkinje cell zone of the vermis			
VeTi	inner granular cell zone of the vermis			
VeTv	ventricular (germinal) zone of the vermis			
PRVT	transient zones of cerebellar paravermis			
PRVTe	external granular (germinal) zone of the paravermis			
PRVTm	marginal zone of the paravermis			
PRVTp	Purkinje cell zone of the paravermis			
PRVTi	inner granular cell zone of the paravermis			
PRVTv	ventricular (germinal) zone of the paravermis			
CbLT	transient zones of cerebellar lateral hemisphere			
CbLTe	external granular (germinal) zone of lateral hemisphere			
CbLTm	marginal zone of lateral hemisphere			
CbLTp	Purkinje cell zone of lateral hemisphere			
CbLTi	inner granular cell zone of lateral hemisphere			
CbLTv	ventricular (germinal) zone of lateral hemisphere			
CbFT	transient zones of cerebellar flocculus			
CbFTe	external granular (germinal) zone of flocculus			
CbFTm	marginal zone of flocculus			
CbFTp	Purkinje cell zone of flocculus			
CbFTi	inner granular cell zone of flocculus			
CbFTv	ventricular (germinal) zone of flocculus			
TGCbN	transient glia cell group of cerebellar deep nucleus			
CbP	cerebellar plate			
MZCbP	marginal (subpial stream) zone of cerebellar plate			
IZCbP	intermediate (mantle) zone of cerebellar plate			
NTZ	nuclear transitory zone of cerebellar plate			
CTZ	cortical transitory zone of cerebellar plate			
VZCbP	ventricular (neuroepithelial) zone of cerebellar plate			
CbS	cerebellar swelling			
CbSi	internal cerebellar swelling			

(Continues)

TABLE 1 (Continued)

Abbreviations	Ontology of brain structures	Transcriptome data available (A)		
		pcw 15	pcw 16	pcw 21
CbSe	external cerebellar swelling			
HNM	hindbrain neuromeres			
RhIS	rhombencephalic isthmus			
RhA	rhombomere A			
Rh1	rhombomere 1			
Rh2	rhombomere 2			
Rh3	rhombomere 3			
RhB	rhombomere B			
Rh4	rhombomere 4			
RhC	rhombomere C			
Rh5	rhombomere 5			
Rh6	rhombomere 6			
Rh7	rhombomere 7			
RhD	rhombomere D			
Rh8	rhombomere 8			
RhL	rhombic lip			
URL	upper (rostral) rhombic lip	A	A	
EGL	external granular (germinal) layer of upper rhombic lip	A	A	
LRL	lower (caudal) rhombic lip	A	A	
EGLL	external granular (germinal) layer of lower rhombic lip	A		
TCC	transient cell columns in pons			
MCCP	medial cell column of pons			
ICCP	intermediate cell column of pons			
LCCP	lateral cell column of pons			
TPC	transient Purkinje cell clusters	A		
PkA	cluster A of Purkinje cells			
PkB	cluster B of Purkinje cells			
PkC	cluster C of Purkinje cells			
PkD	cluster D of Purkinje cells			
PkE	cluster E of Purkinje cells			
PkF	cluster F of Purkinje cells			
PkG	cluster G of Purkinje cells			
PkH	cluster H of Purkinje cells			
MSH	migratory streams in hindbrain			
REMS	rostral (anterior) extramural migratory stream	A		
CEMS	caudal (posterior) extramural migratory stream	A	A	
ImMS	intramural migratory stream			
MZH	marginal zone of hindbrain			
MZCb	marginal zone of cerebellum			
MZPn	marginal zone of pons			
MZMo	marginal zone of medulla oblongata			
IZH	intermediate (mantle) zone of hindbrain			
IZHal	alar plate of intermediate zone of hindbrain			

(Continues)

TABLE 1 (Continued)

Abbreviations	Ontology of brain structures	Transcriptome data available (A)		
		pcw 15	pcw 16	pcw 21
IZHba	basal plate of intermediate zone of hindbrain			
IZHfl	floor plate of intermediate zone of hindbrain			
IZHro	roof plate of intermediate zone of hindbrain			
VZH	ventricular (matrix) zone in hindbrain			
VZCb	ventricular (matrix) zone of cerebellum		A	
VZPn	ventricular (matrix) zone of pons		A	
VZMo	ventricular (matrix) zone of medulla			
PnFlx	pontine flexures			
CrSlp	cranial (metacephalic) slope			
CaSlp	caudal (myelencephalic) slope			
PnbB	pontobulbar body	A	A	
RhGv	rhombic grooves			
HPS	permanent structures of hindbrain (for more details see table 3 in Ding et al. J Comp Neurol, 2016)			
Met	metencephalom			
CB	cerebellum			
CBC	cerebellar cortex			
CBV	cerebellar vermis	A	A	
CBPV	paravermis of cerebellum	A	A	
CBL	lateral hemisphere of cerebellum	A	A	
CbDN	cerebellar deep nuclei			
DT	dentate nucleus	A	A	
InP	interpositus nucleus		A	
Fas	fastigial nucleus			
Pn	pons			
PN	pontine nucleus	A	A	
Mo5	motor nucleus of trigeminal nerve	A	A	
Pr5	principal sensory nucleus of trigeminal nerve	A	A	
6N	abducens nucleus	A	A	
7N	facial nucleus	A	A	
8Co	cochlear nuclei	A	A	
MSO	medial superior olive	A	A	
SOC	superior olivary complex			
TrZ	nucleus of trapezoid body			
PnRa	Raphe pontis nucleus			
MnR	median raphe nucleus			
PnG	pontine gamma nucleus			
PB	parabrachial nuclei			
LPB	lateral parabrachial nucleus	A	A	
MPB	medial parabrachial nucleus	A	A	
RtTg	reticulotegmental nucleus	A	A	
NC	nucleus coeruleus	A	A	
LLN	nuclei of lateral lemniscus			
DTg	dorsal tegmental nucleus			

(Continues)

TABLE 1 (Continued)

Abbreviations	Ontology of brain structures	Transcriptome data available (A)		
		pcw 15	pcw 16	pcw 21
LDTg	laterodorsal tegmental nucleus			
PnRF	pontine reticular formation			
Mo	myelencephalon (medulla oblongata)			
Sp5	spinal trigeminal nucleus	A	A	
8Ve	vestibular nuclei	A	A	
Sol	solitary nucleus	A	A	
Psol	parasolitary nucelus	A		
10N	vagal nucleus	A	A	
12N	hypoglossal nucleus	A	A	
Amb	ambiguus nucleus			
PrH	prepositus hypoglossal nucleus		A	
MoRa	raphe nuclei in medulla oblongata			
ROb	raphe obscurus nucleus	A		
RMg	raphe magnus nucleus	A	A	
IO	inferior olive	A	A	
InM	intercalated nucleus of medulla	A		
MoRF	medullary reticular formation		A	
RVRG	rostral ventral respiratory cell group	A		
LRt	lateral reticular nucleus	A		
ECu	external cuneate nucleus			
Cu	cuneate nucleus		A	
Gr	gracile nucleus		A	
HWM	white matter of hindbrain (for details see table 3 in Ding et al. J Comp Neurol, 2016)			
HV	ventricles of hindbrain			
4V	fourth ventricle			
cec	central canal of medulla oblongata			
HSS	surface structures of hindbrain (for details see table 3 in Ding et al. J Comp Neurol, 2016)			

*Lists all transient structures and main permanent structures used in the present study. For complete and detailed list of permanent brain structures, see Ding et al. J Comp Neurol, 2016.

APPENDIX 1: Anatomical atlas plates for the prenatal human brain at PCW 15

Forty-six plates with matching histological (Nissl- or AChE-stained) sections are displayed in anterior-to-posterior (A-P) order. The A-P positions of 46 atlas plates (levels 1–46) and the locations of the two slabs as well as the codes for A-P levels, stains, slabs, and the section number in each slab are indicated in the Inset on top of the first page of the atlas plates. For example, Level 1 (01—015) represents the 15th section of the slab 1, which is atlas plate 1 (i.e., Level 1), and AChE-01-054 represents the 54th section of the slab 1, which is AChE-stained and adjacent to plate 2 [Level 2 (01-053)]. The parcellation and subdivisions of different brain regions as well as the parent–daughter relationship and abbreviation of each structure are detailed in Table 1 (for transient structures) and in our adult human brain atlas (Ding et al., 2016; for permanent structures). Note that all annotated brain structures and their abbreviation in this atlas can be searched in the interactive window of the online version of this atlas (www.brainspan.org or http://brainspan.org/static/atlas).

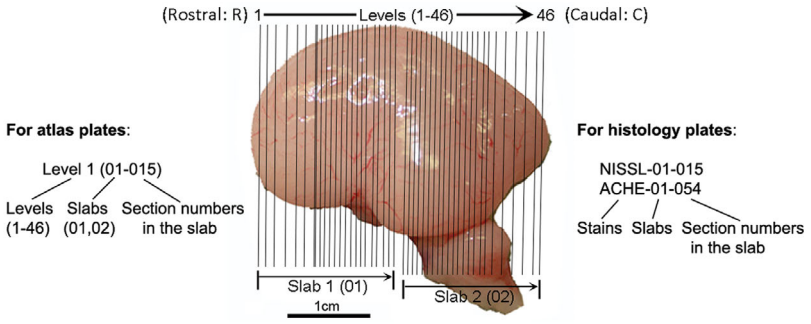

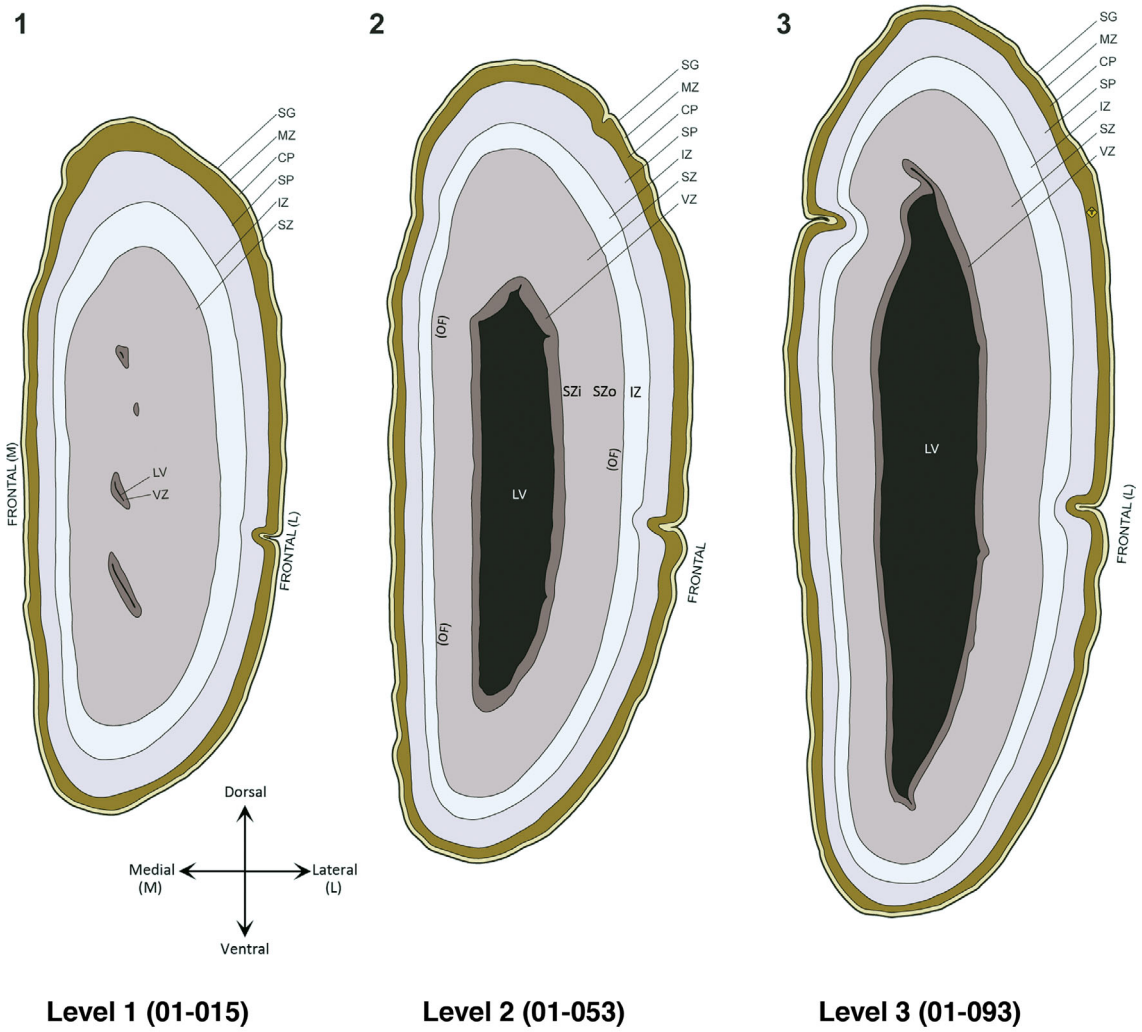

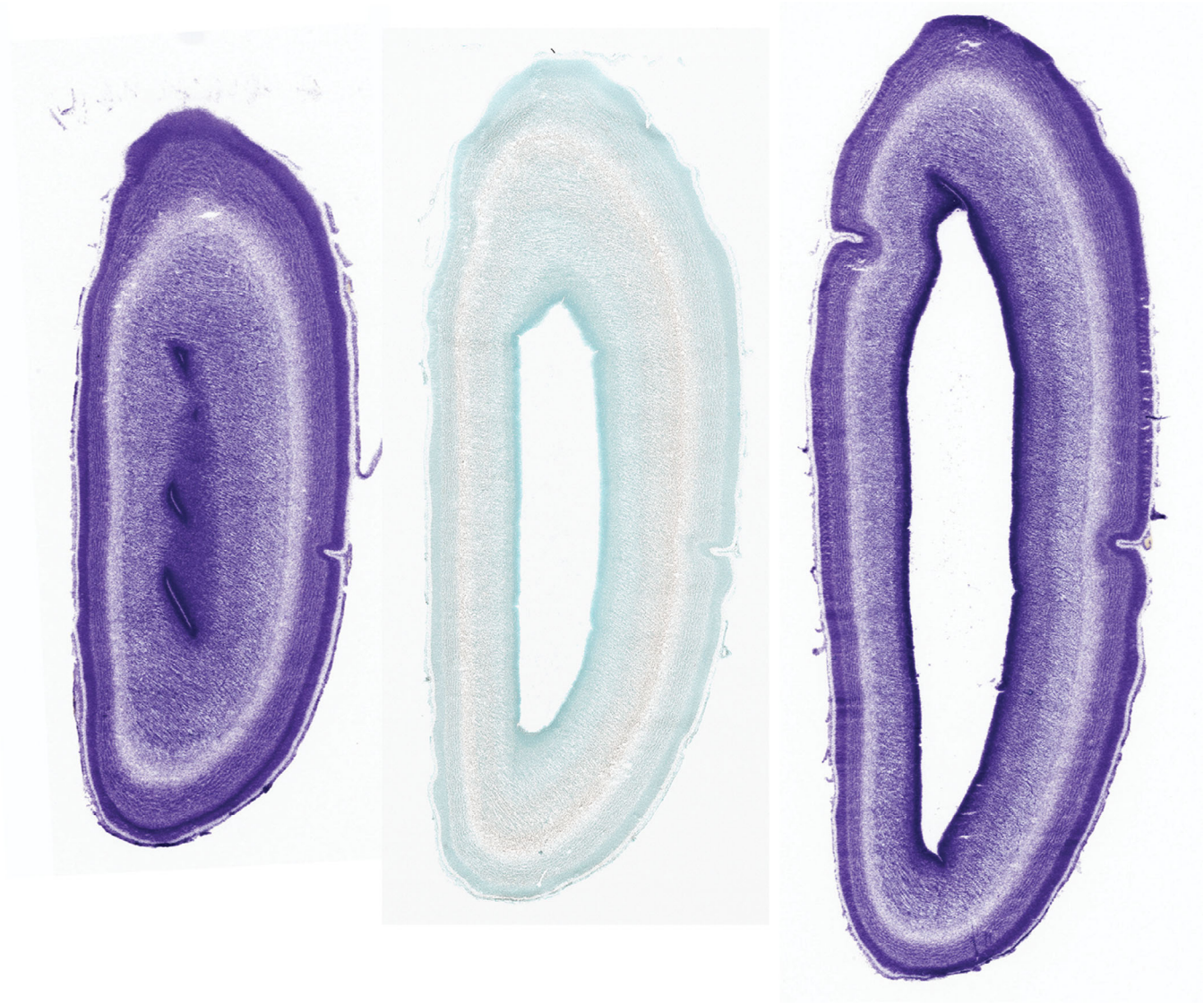

NISSL-01-015 ACHE-01-054 NISSL-01-093

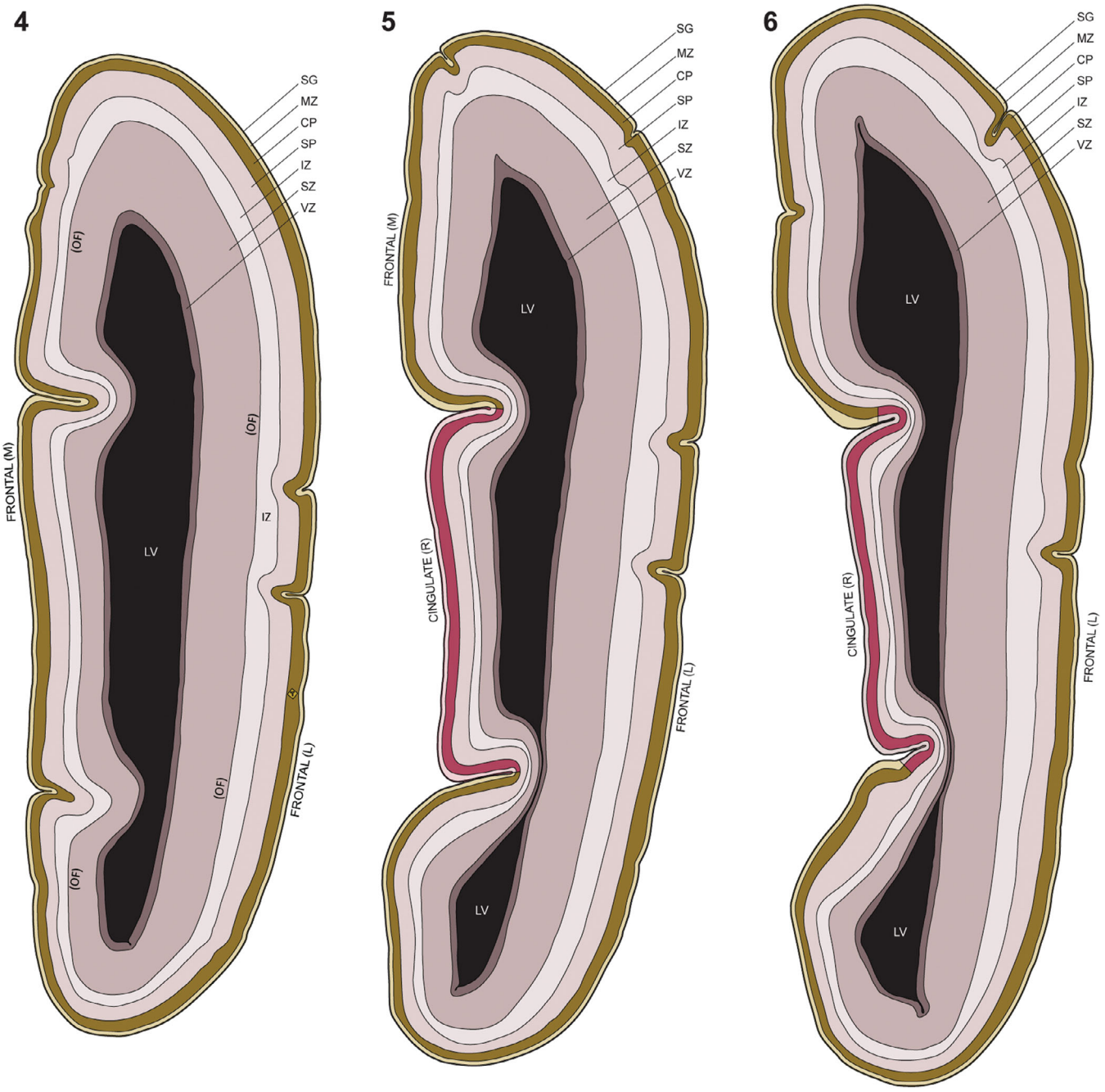

Level 4 (01-157) **Level 5 (01-209)** **Level 6 (01-249)**

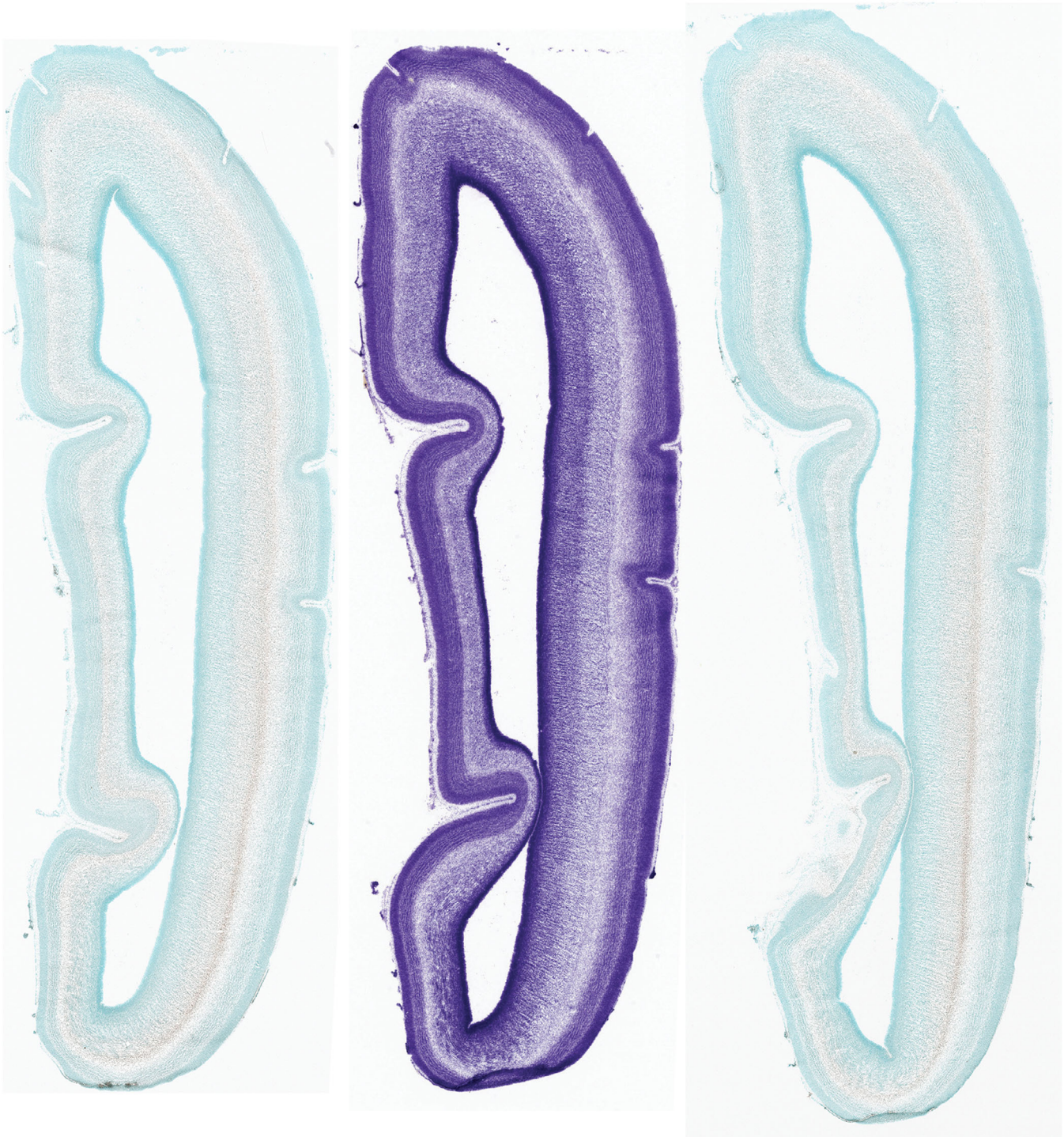

ACHE-01-184 NISSL-01-209 ACHE-01-236

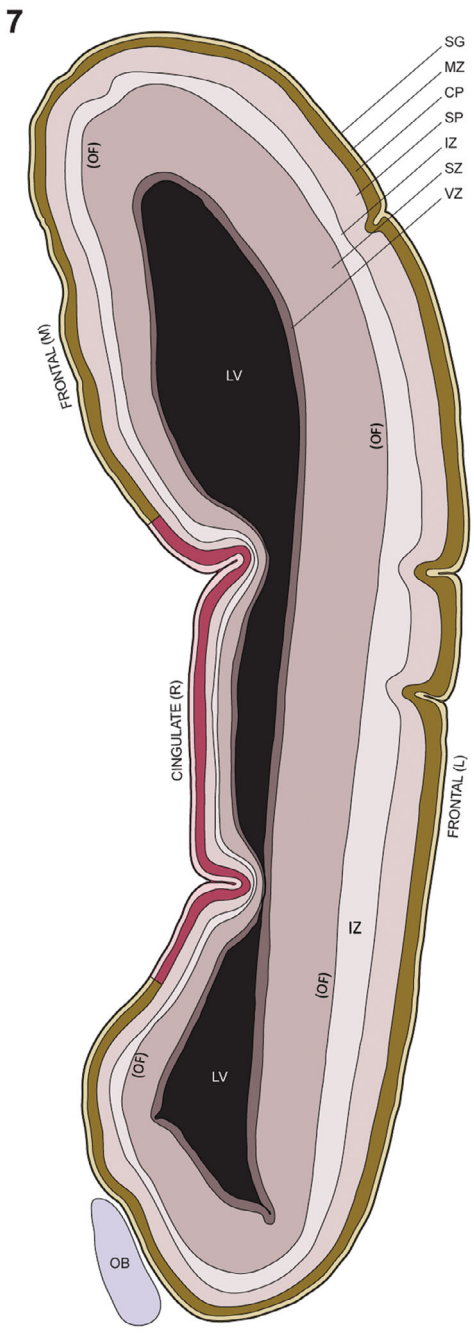

Level 7 (01-301)

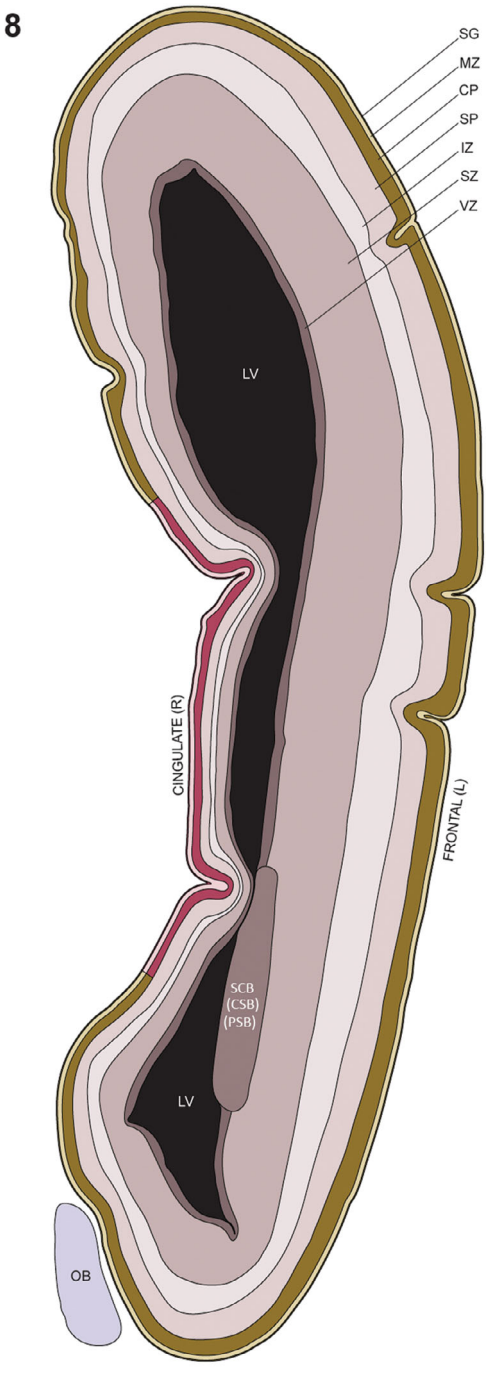

Level 8 (01-313)

NISSL-01-301

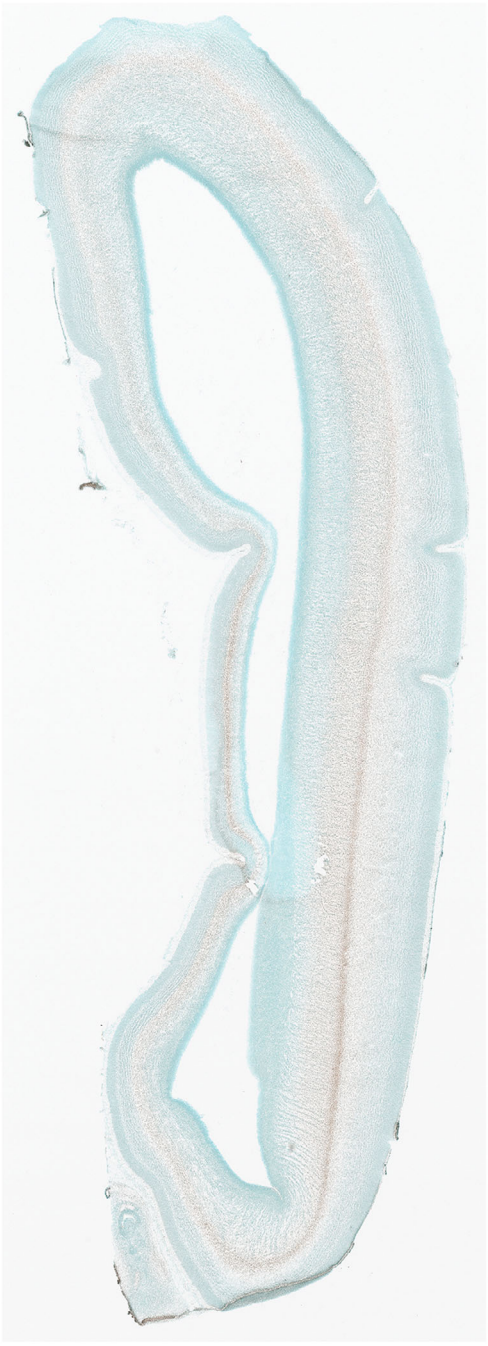

ACHE-01-314

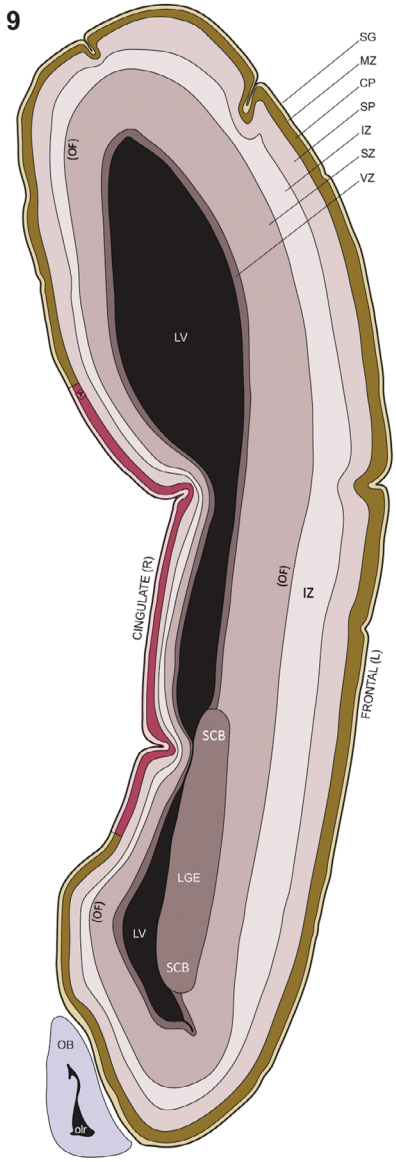

Level 9 (01-339)

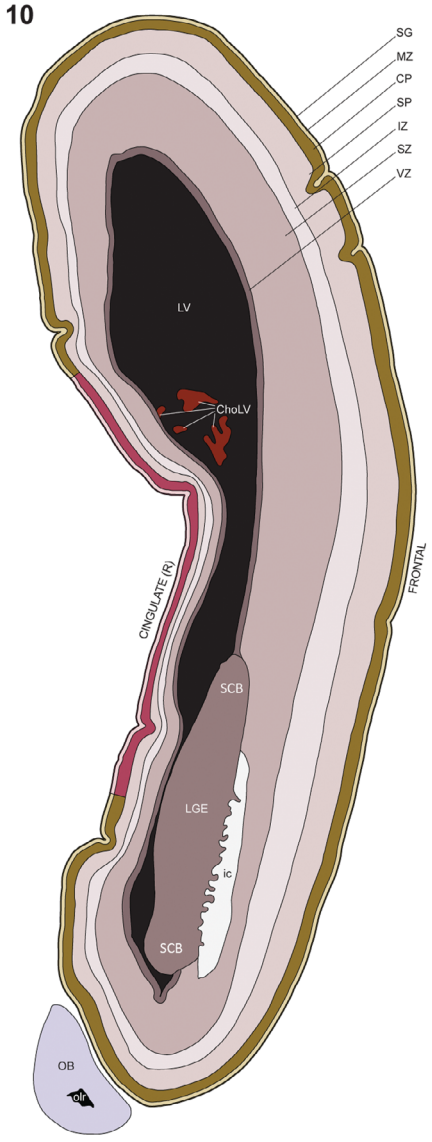

Level 10 (01-365)

NISSL-01-339

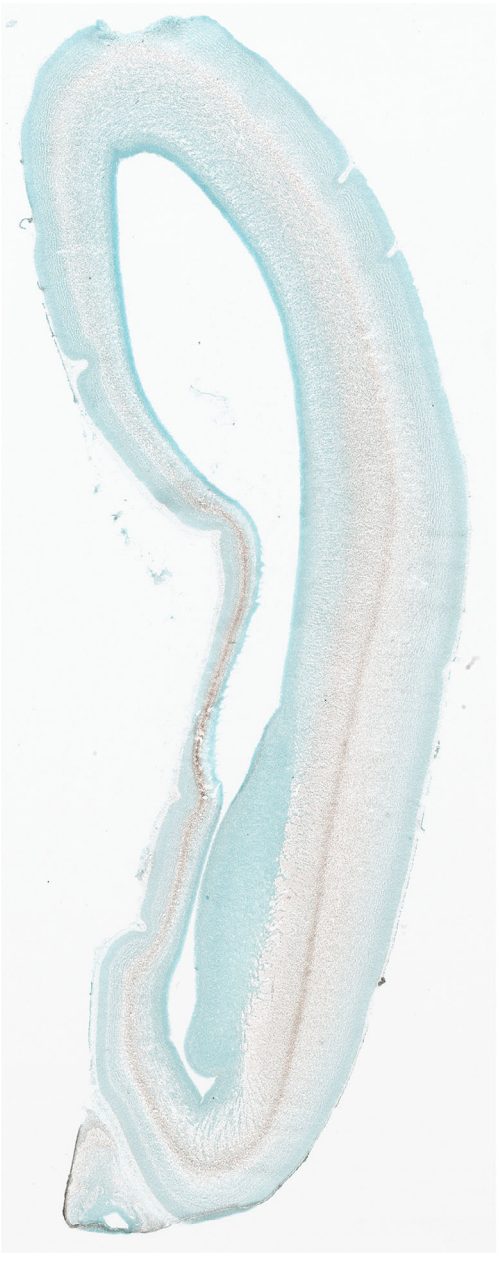

ACHE-01-366

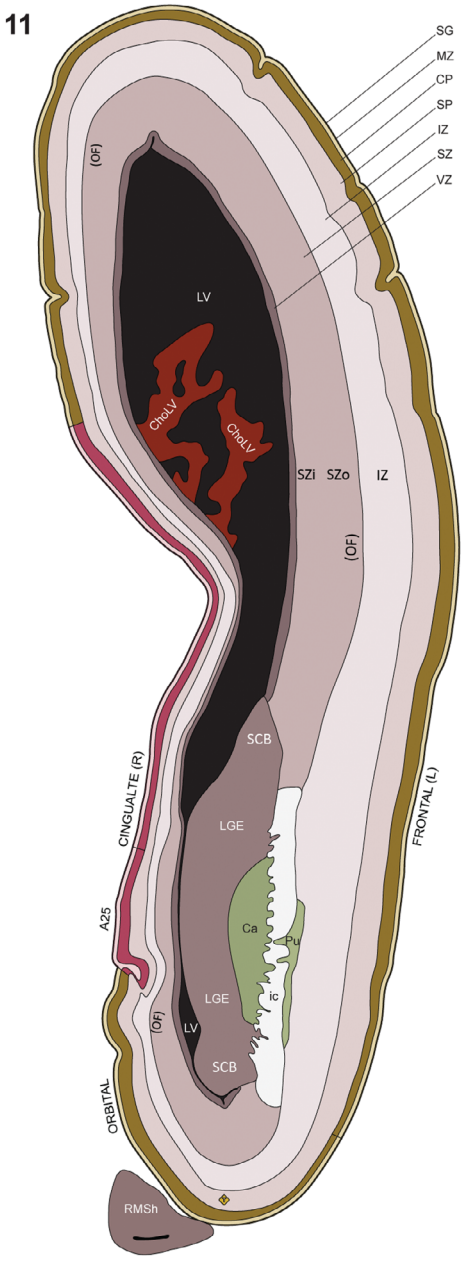

Level 11 (01-391)

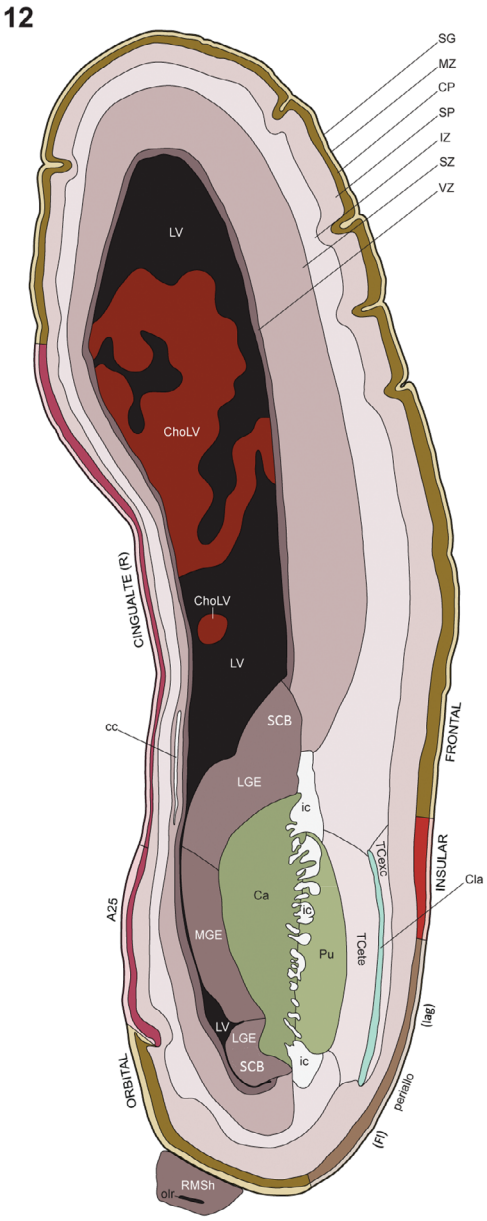

Level 12 (01-417)

NISSL-01-391

ACHE-01-392

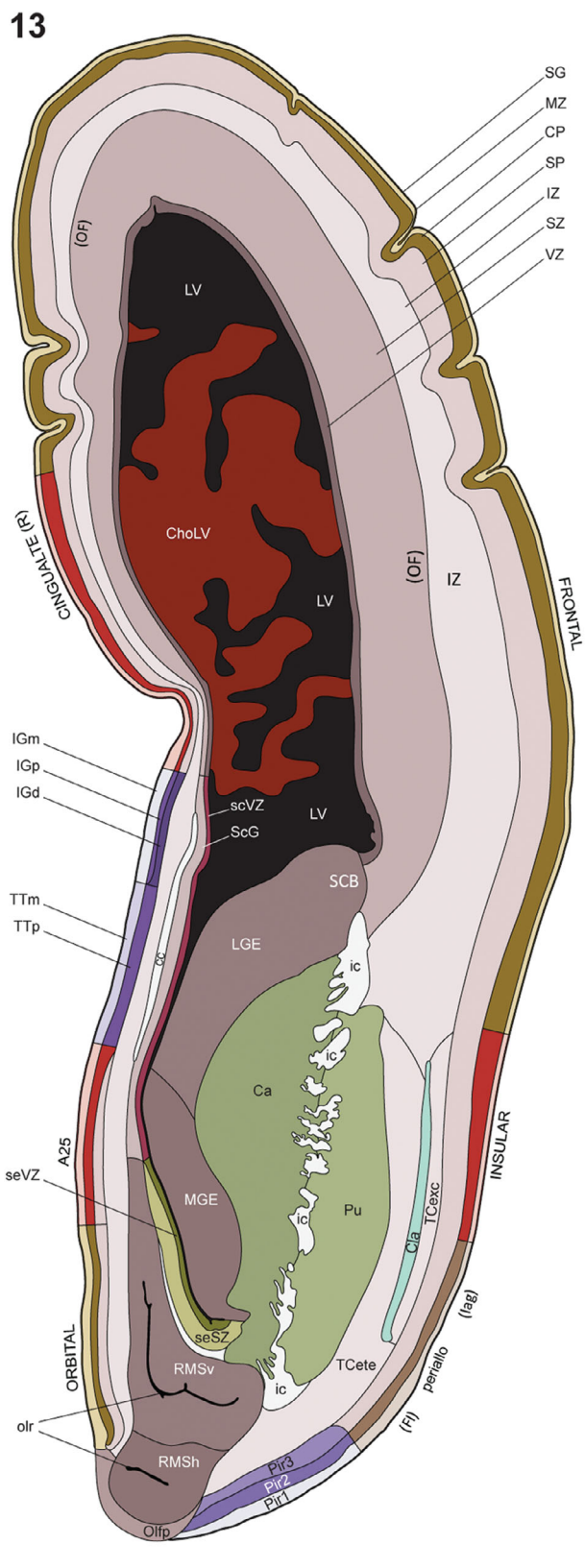

Level 13 (01-443)

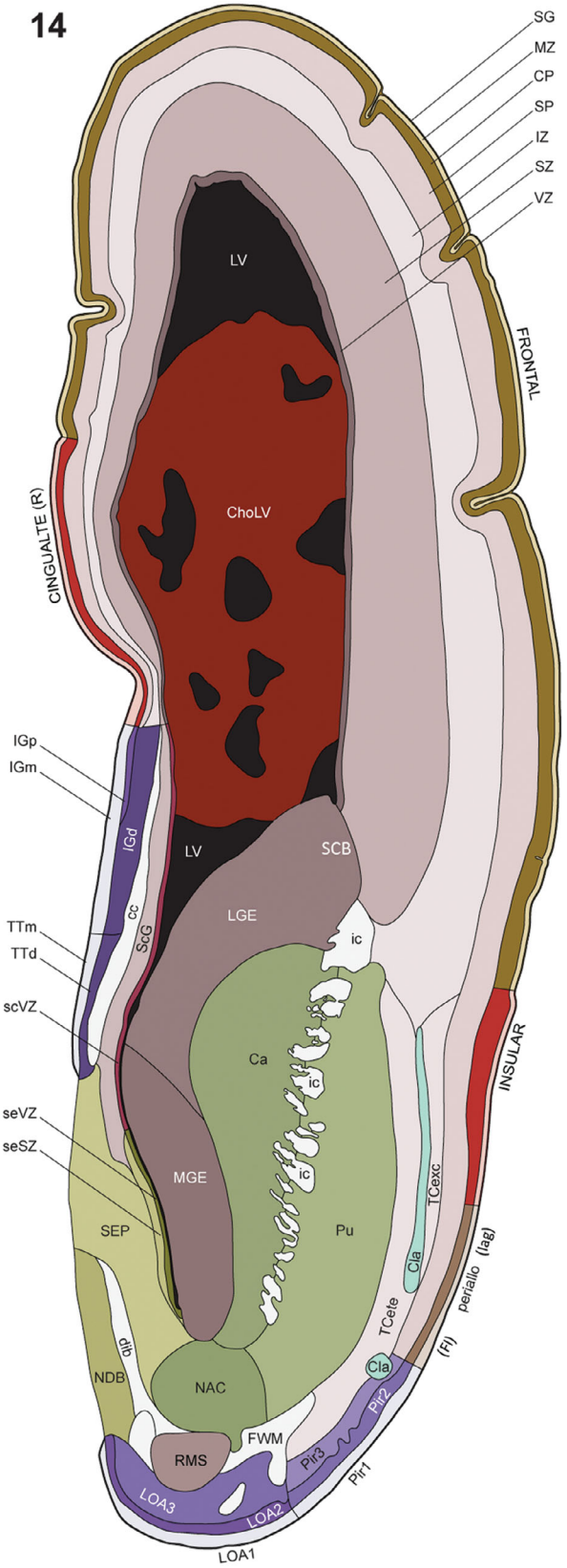

Level 14 (01-469)

NISSL-01-443 ACHE-01-470

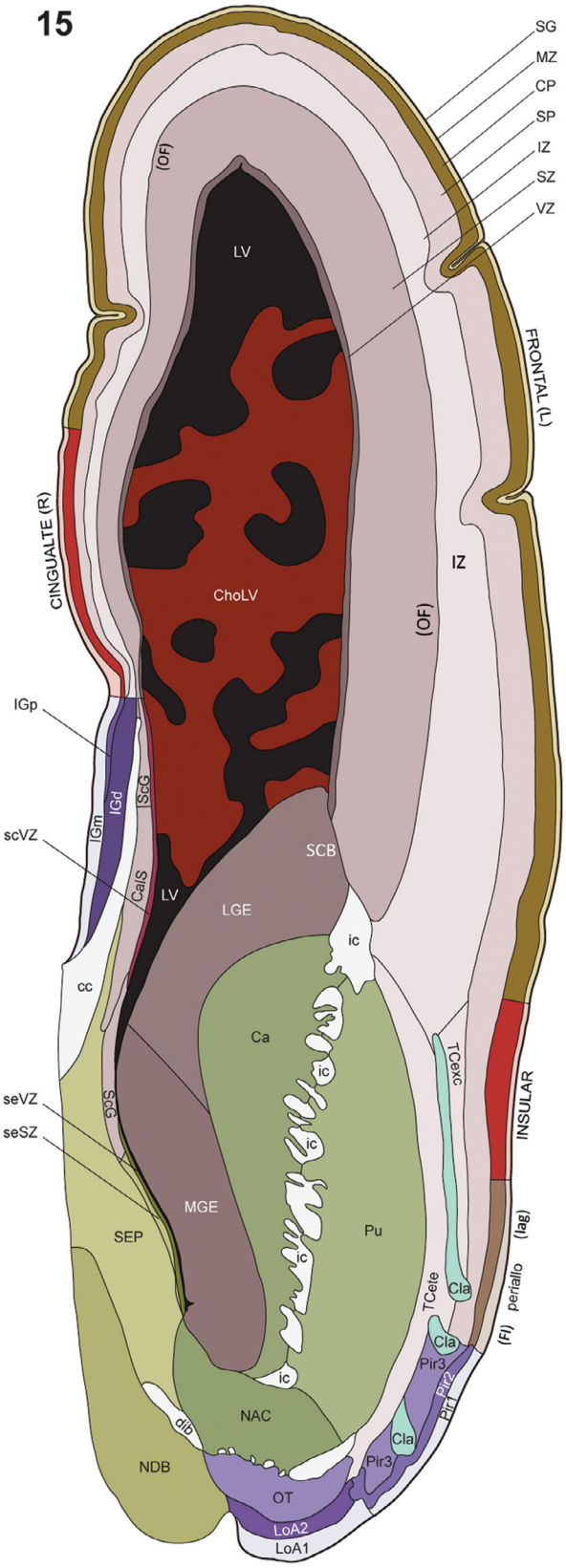

Level 15 (01-495)

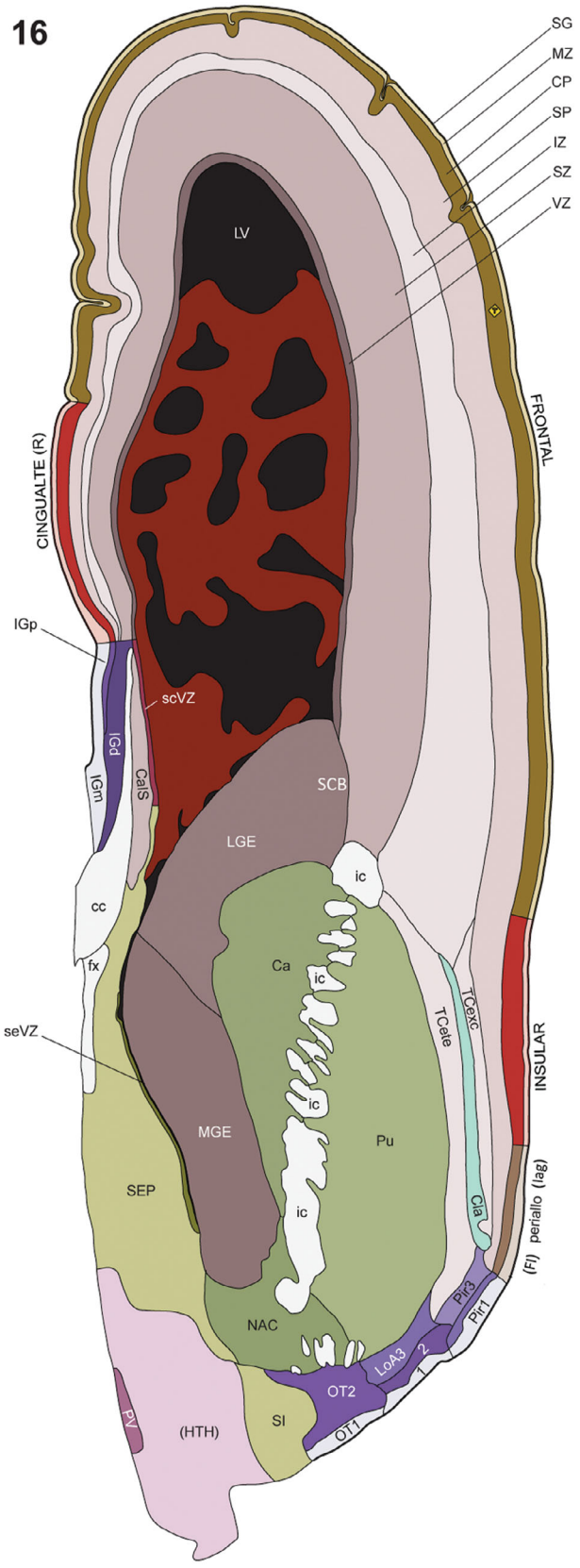

Level 16 (01-521)

NISSL-01-495

ACHE-01-522

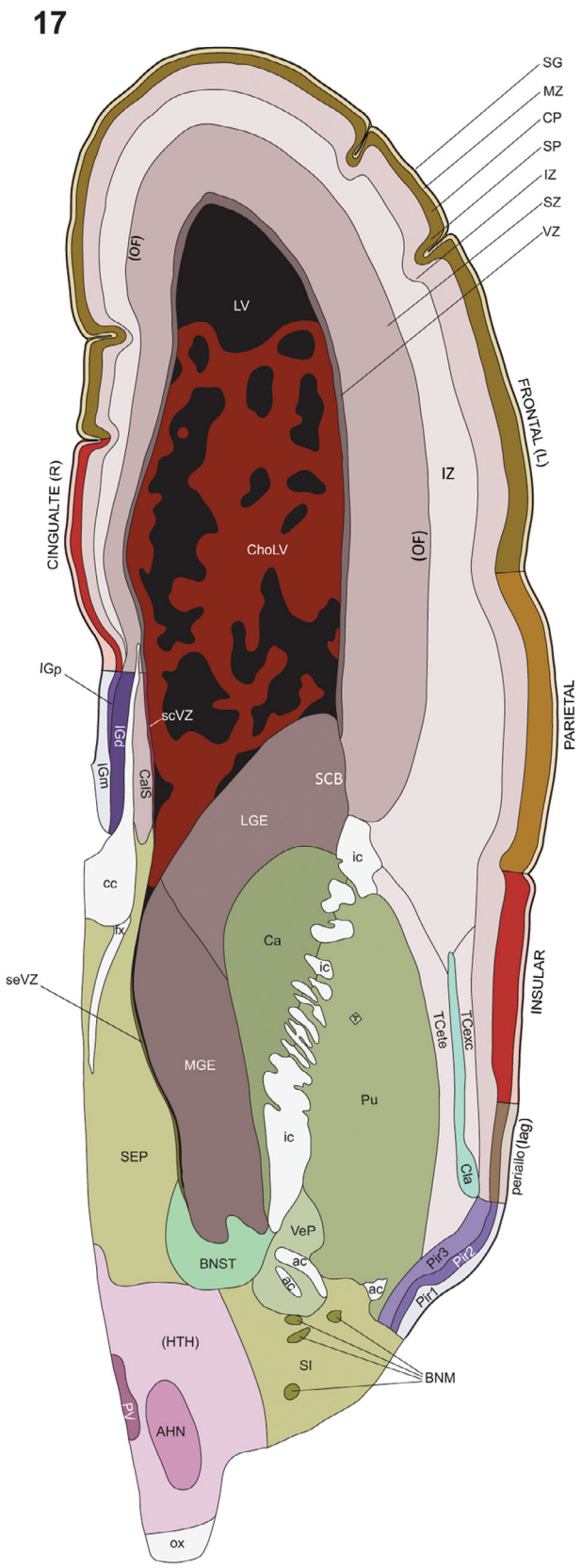

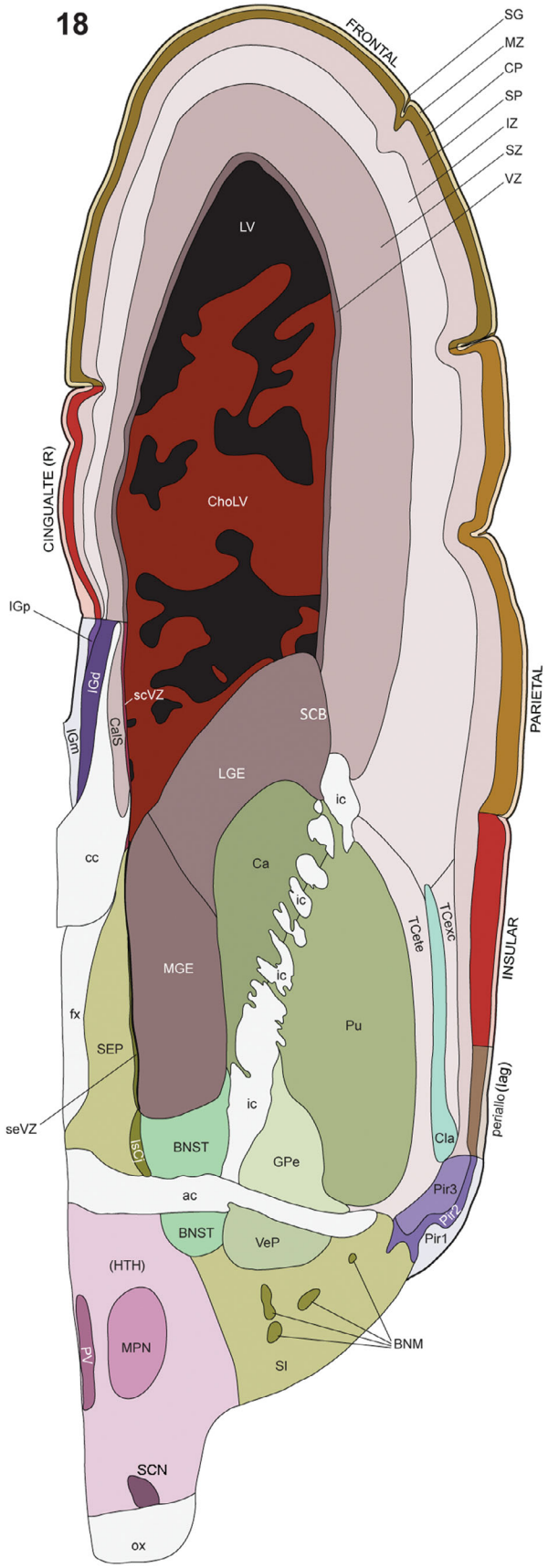

Level 17 (01-547)

Level 18 (01-573)

NISSL-01-547 ACHE-01-574

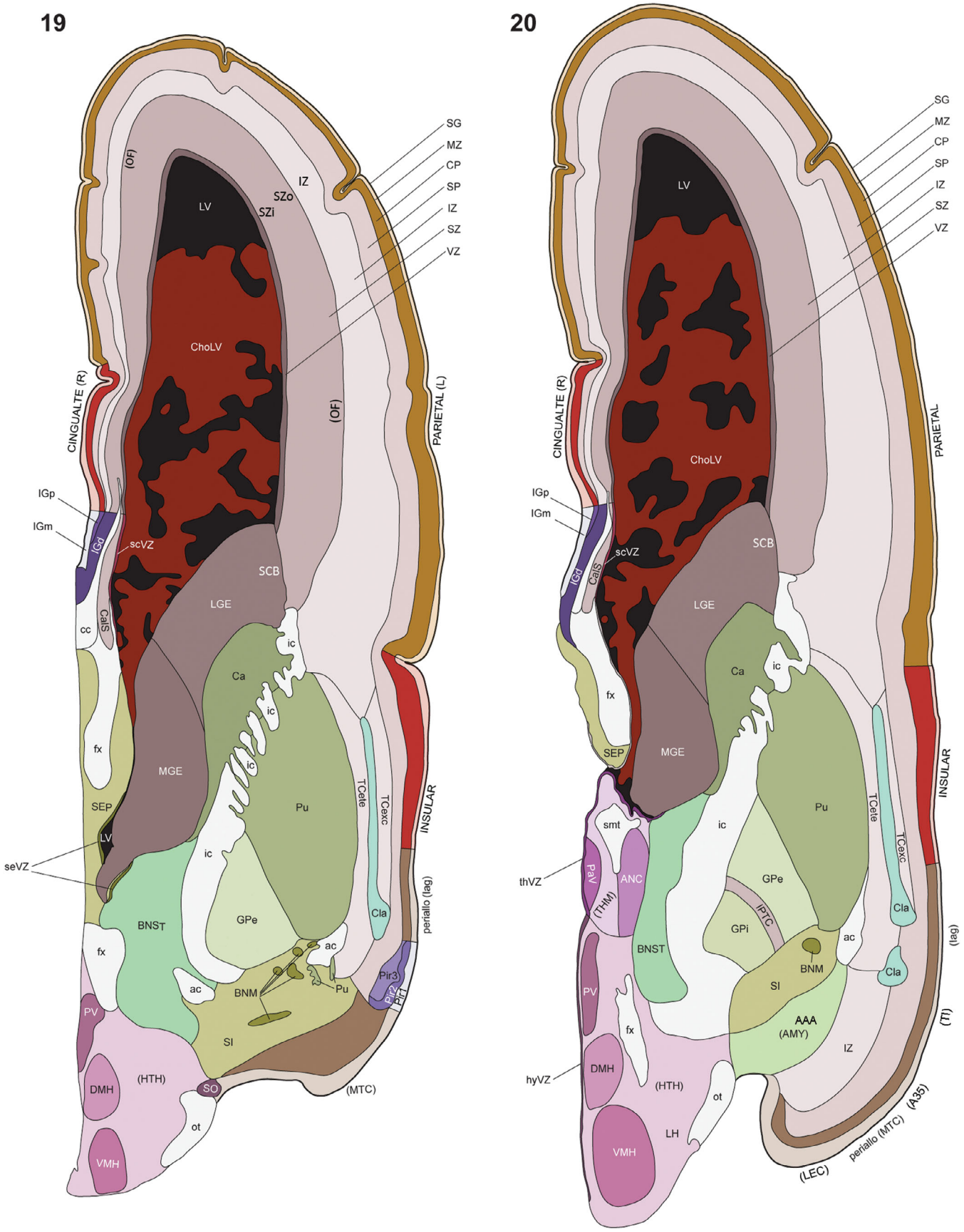

Level 19 (01-613)

Level 20 (01-639)

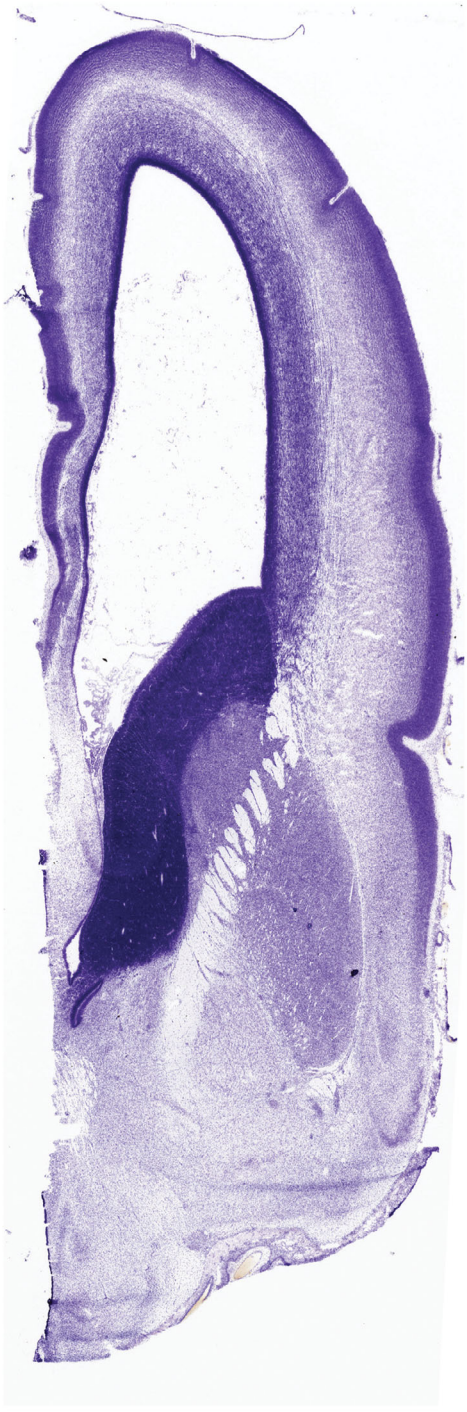

NISSL-01-613

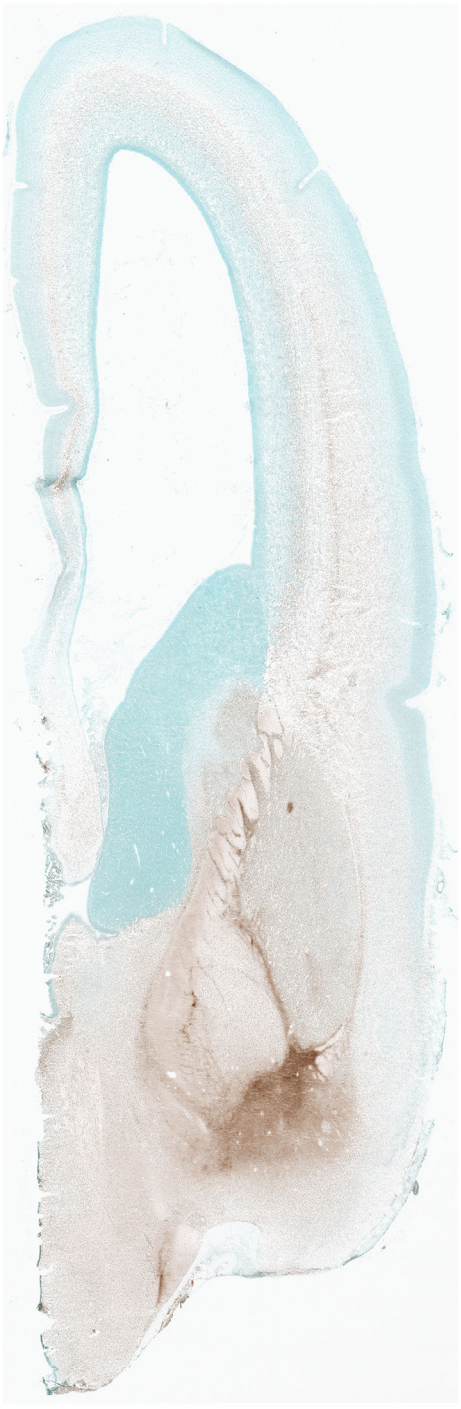

ACHE-01-626

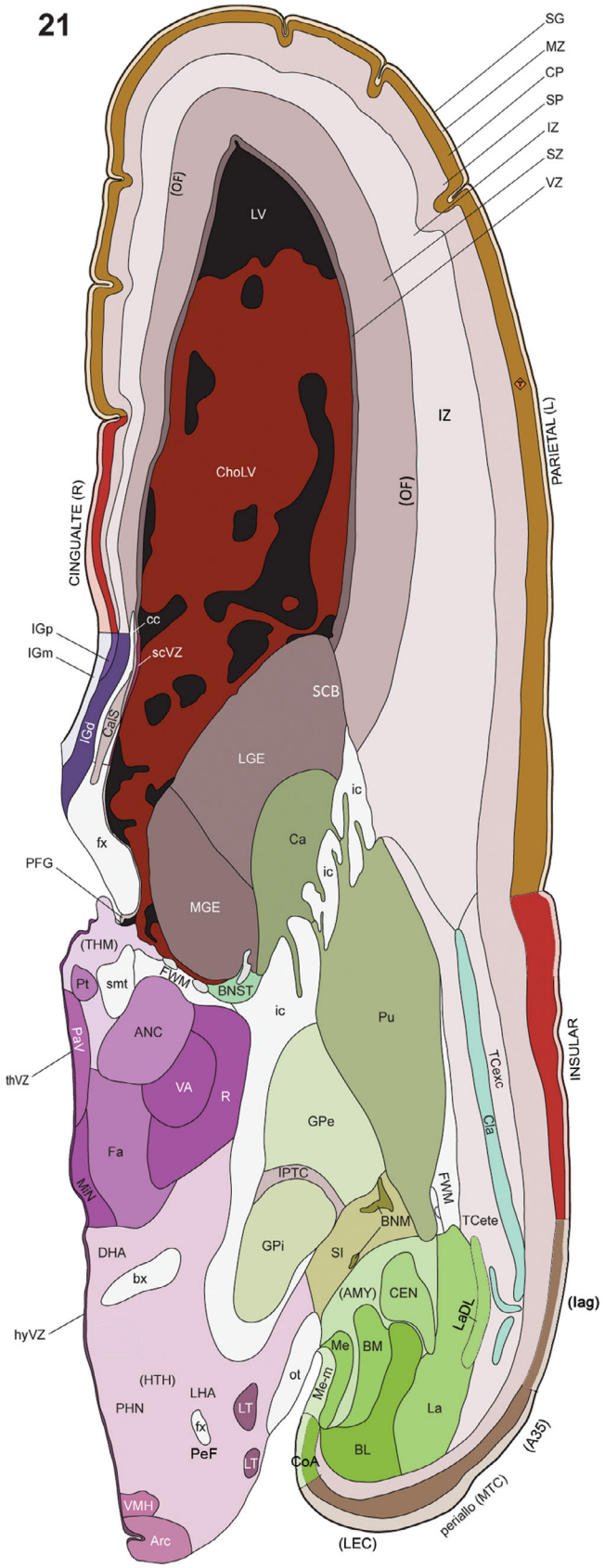

Level 21 (01-677)

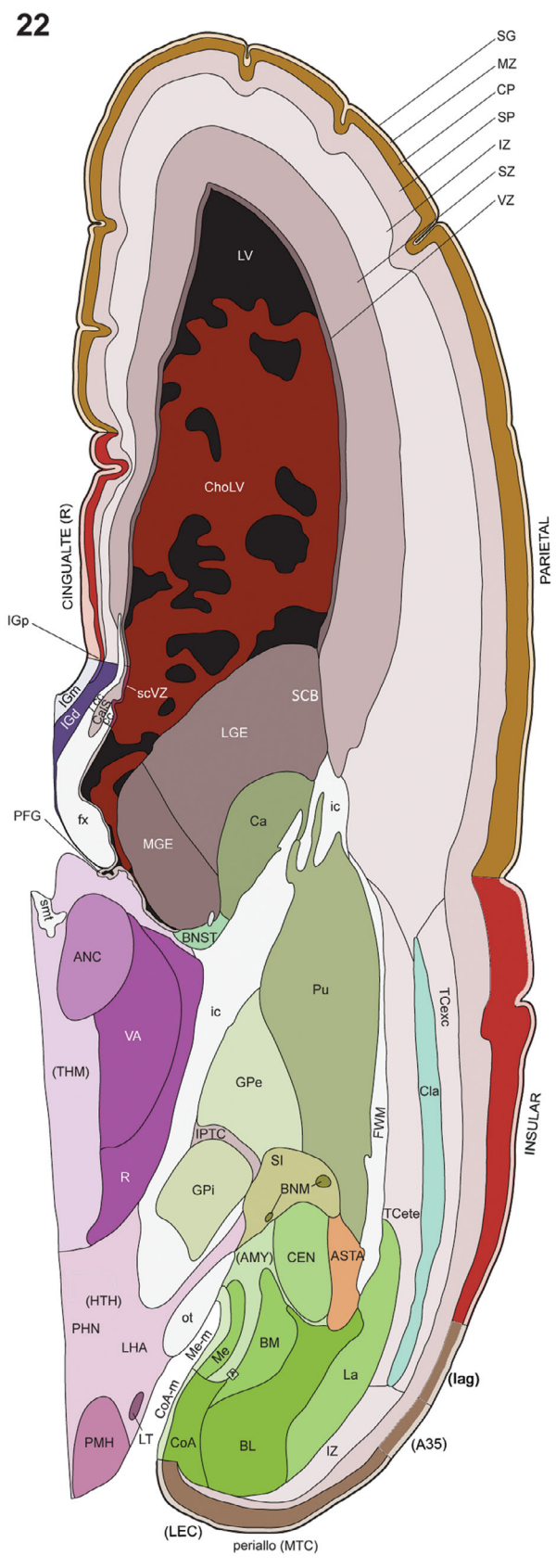

Level 22 (01-703)

NISSL-01-677

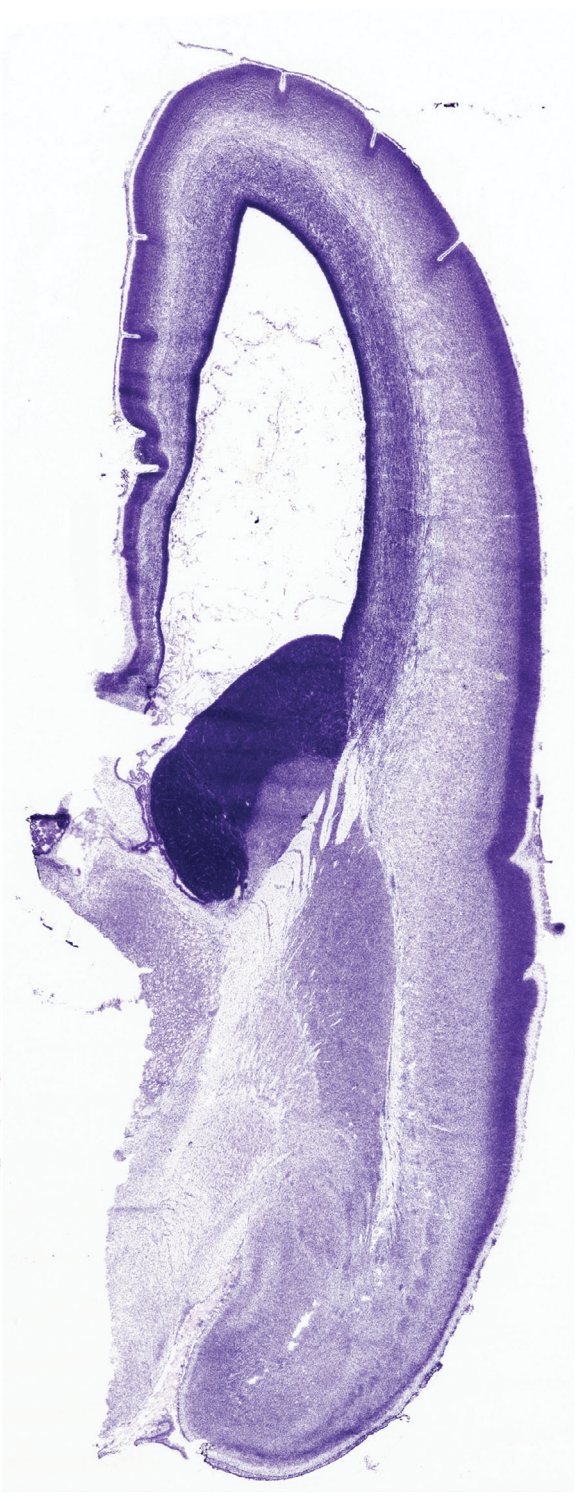

NISSL-01-703

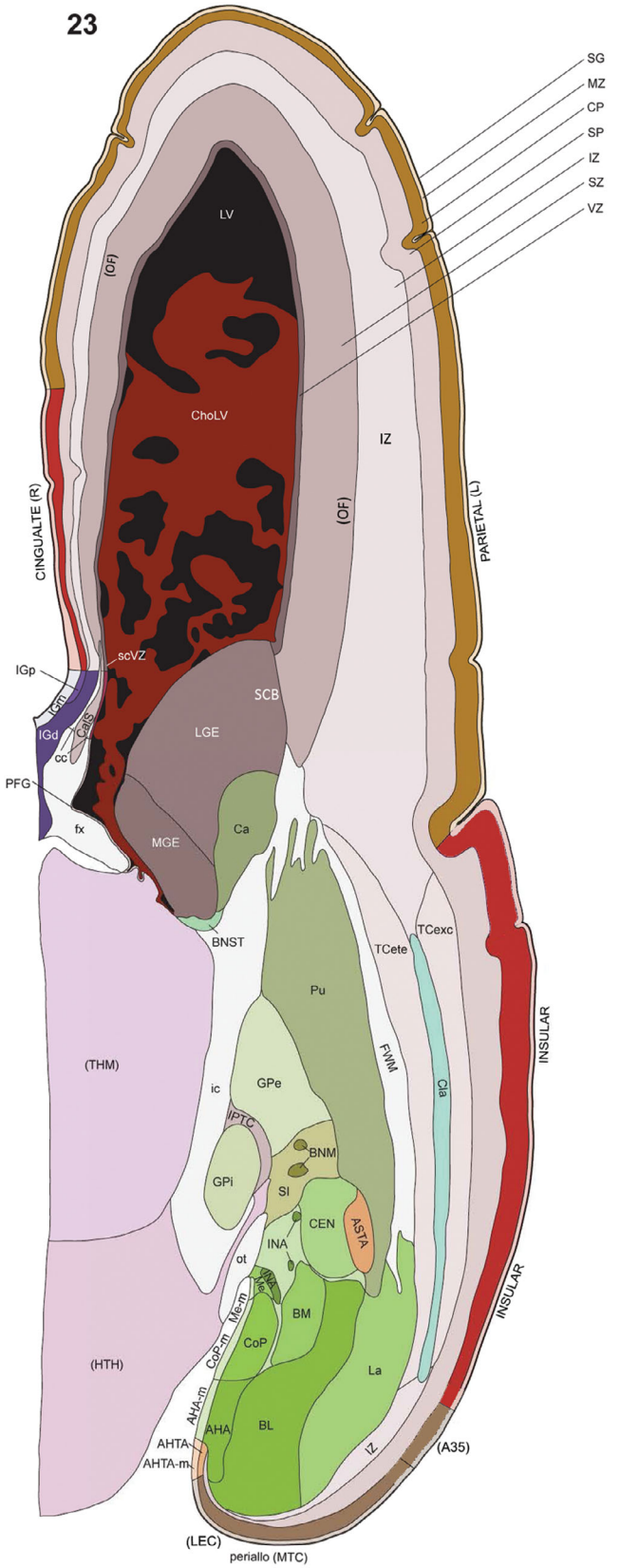

Level 23 (01-729)

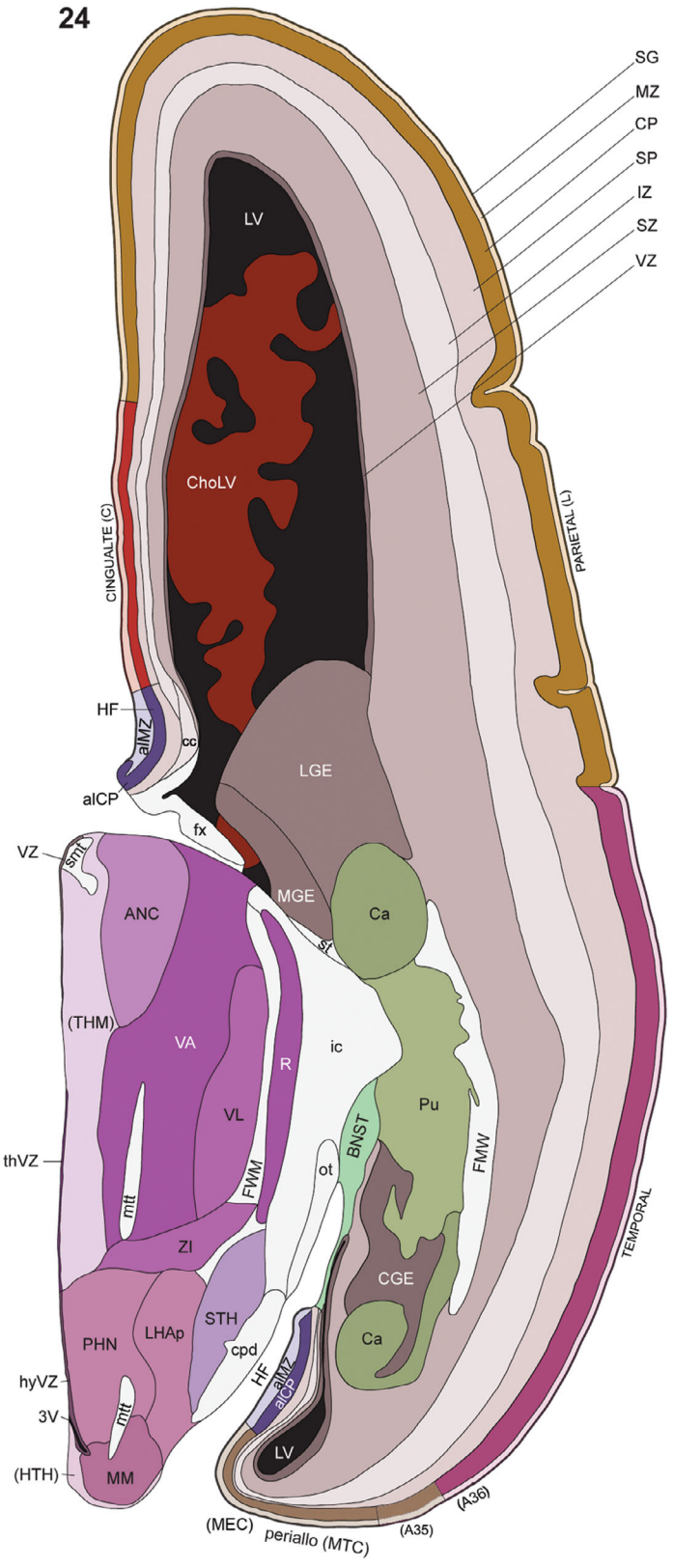

Level 24 (02-001)

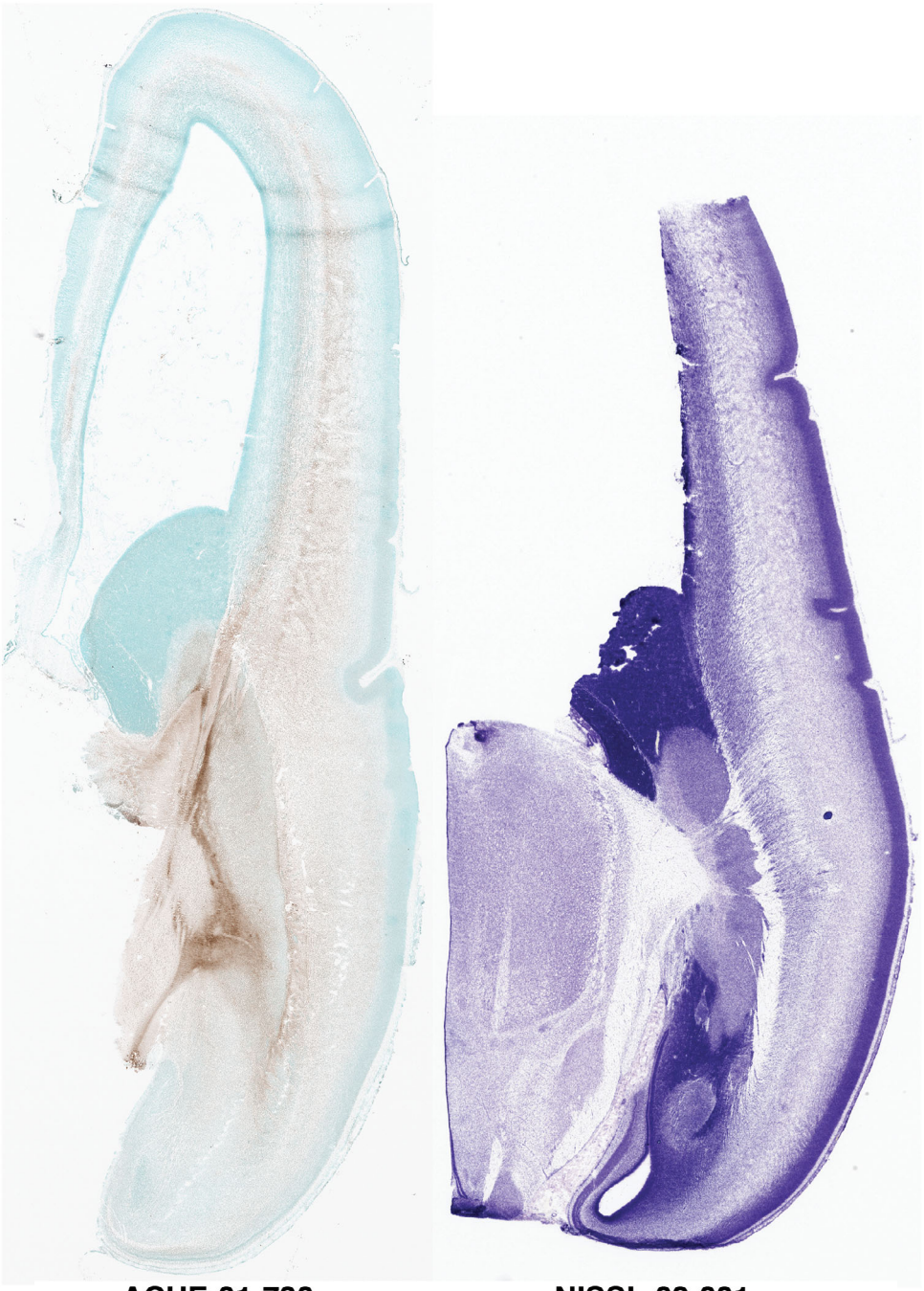

ACHE-01-730 NISSL-02-001

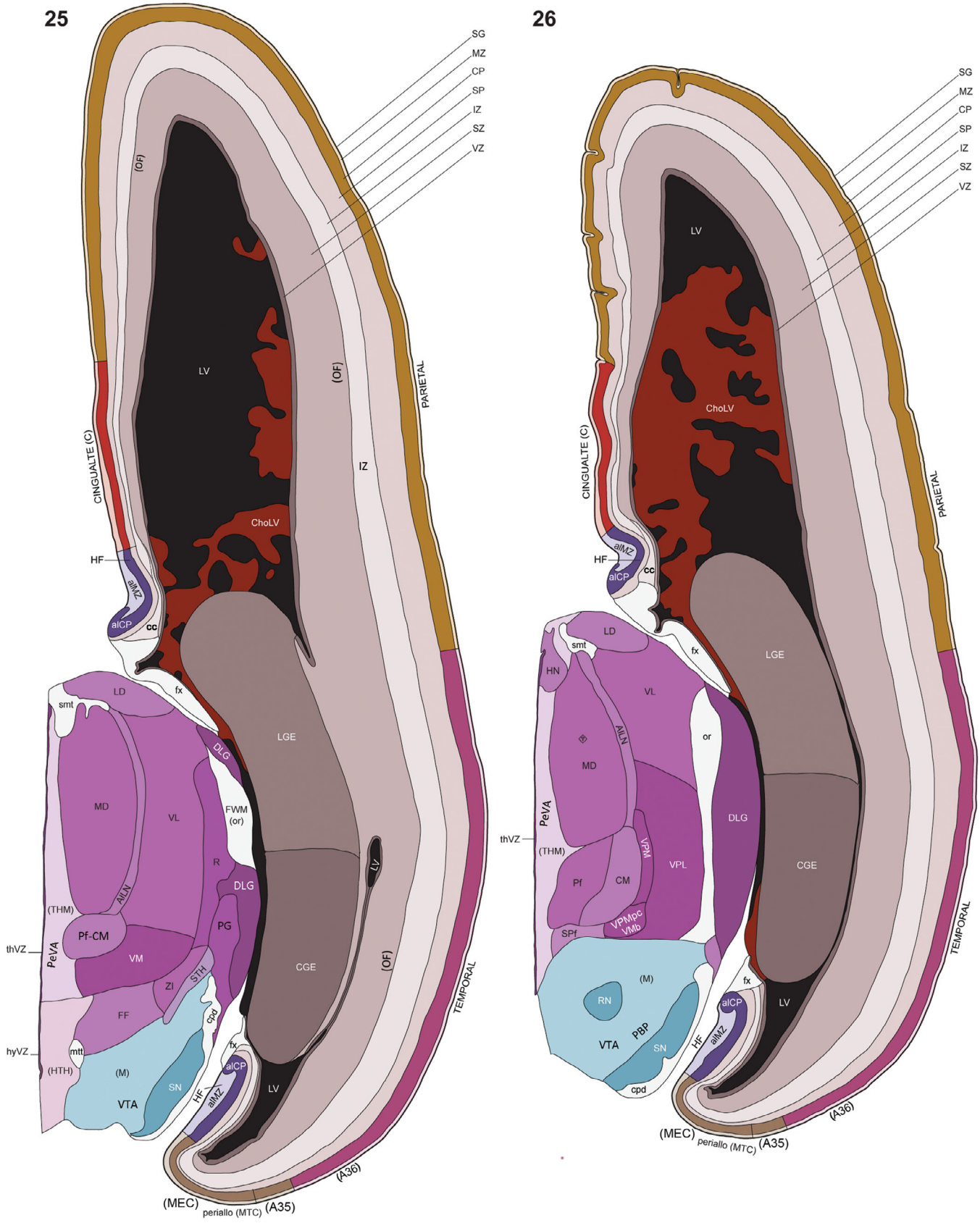

Level 25 (02-015) **Level 26 (02-041)**

ACHE-02-028

NISSL-02-041

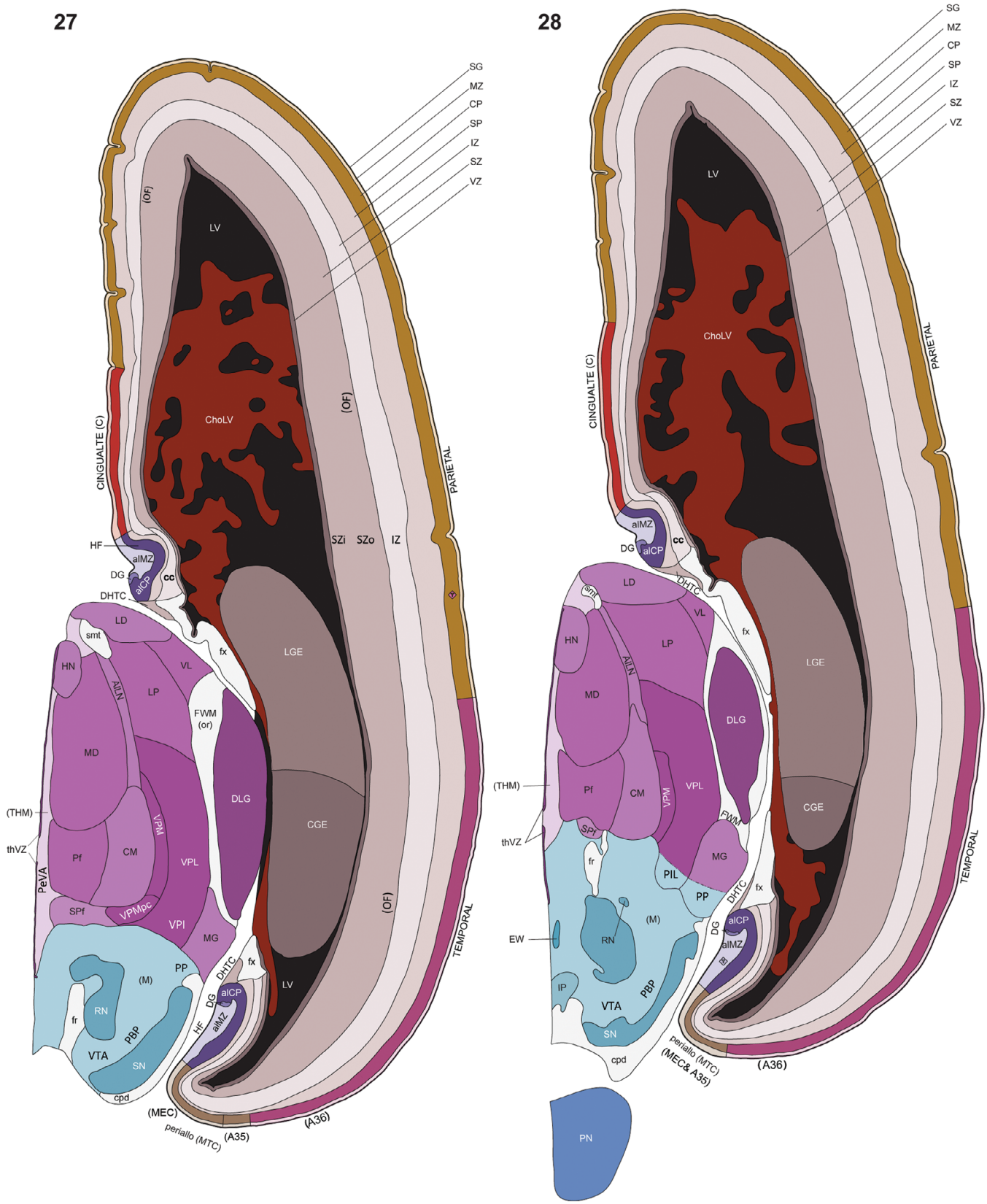

Level 27 (02-067) **Level 28 (02-093)**

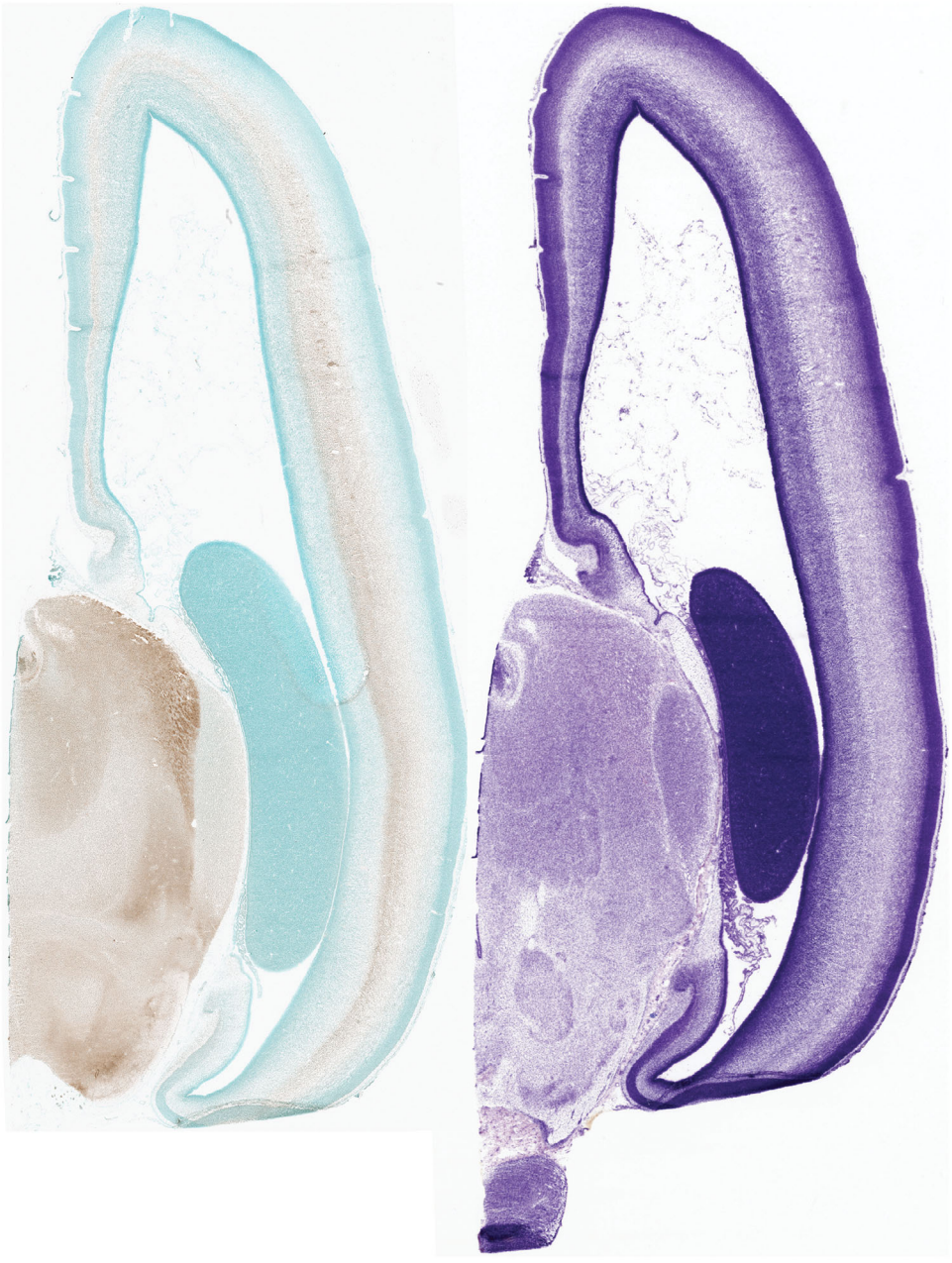

ACHE-02-054 NISSL-02-093

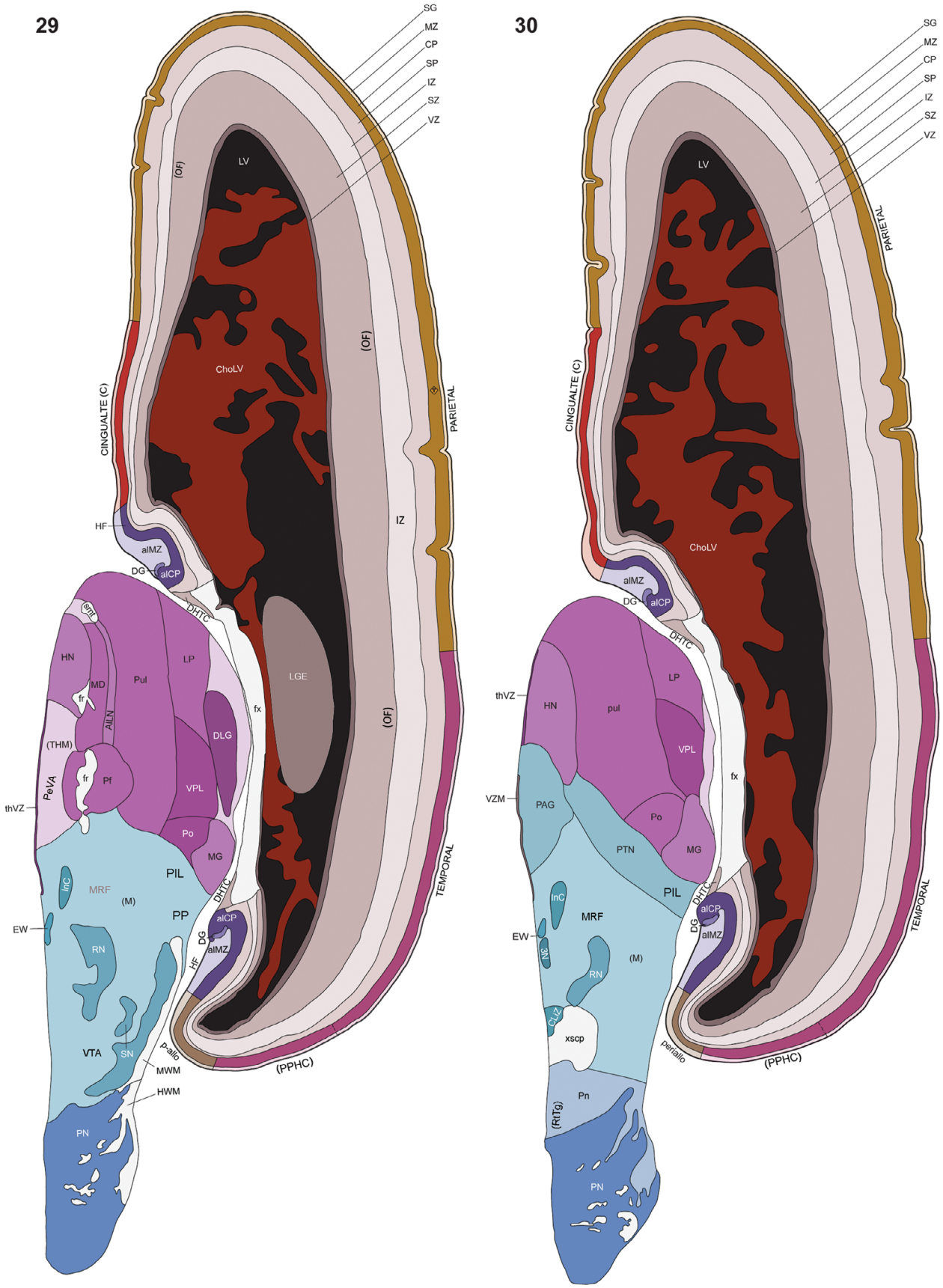

Level 29 (02-119)

Level 30 (02-145)

ACHE-02-106 NISSL-02-145

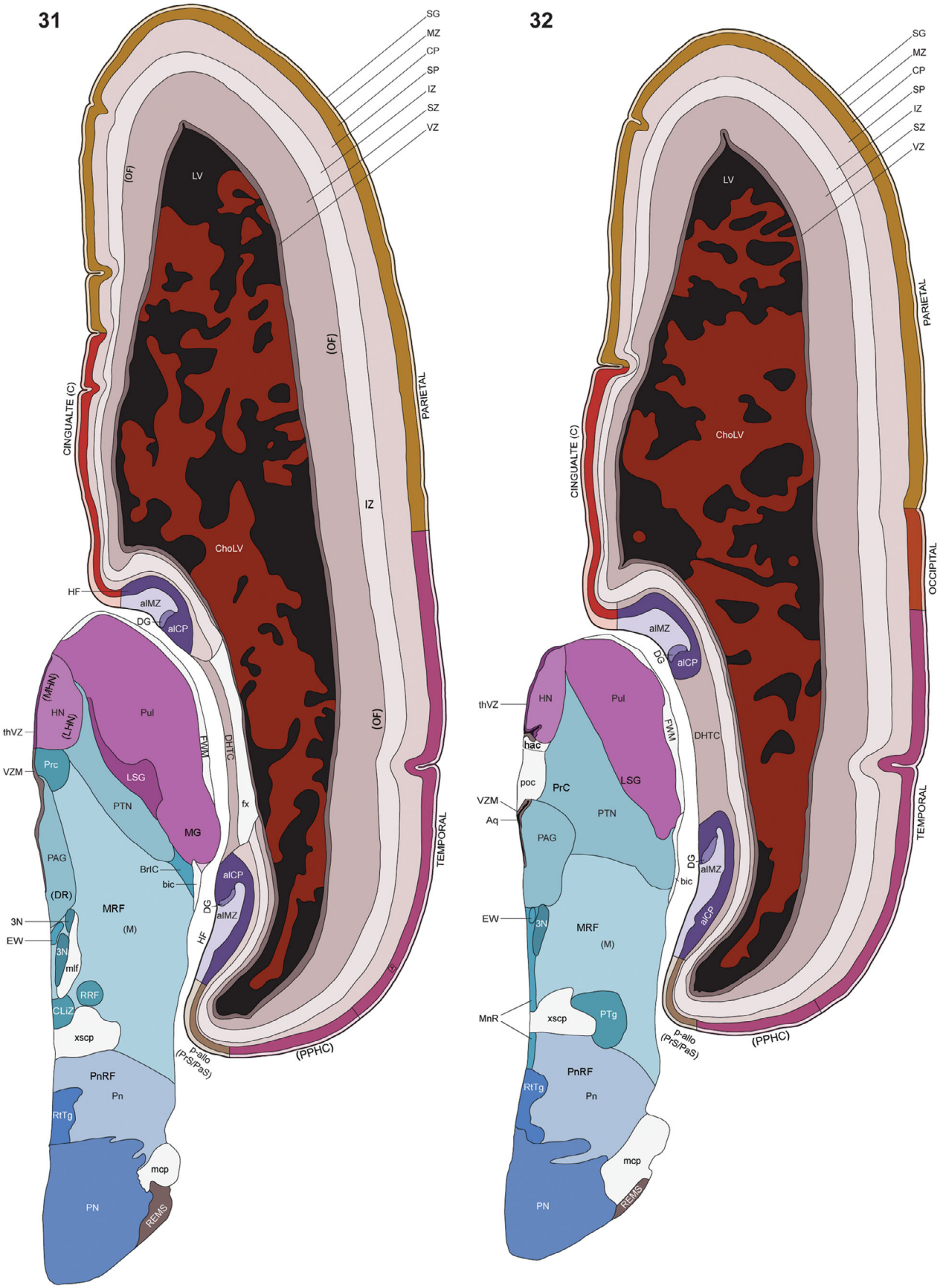

Level 31 (02-171)

Level 32 (02-197)

NISSL-02-171 ACHE-02-184

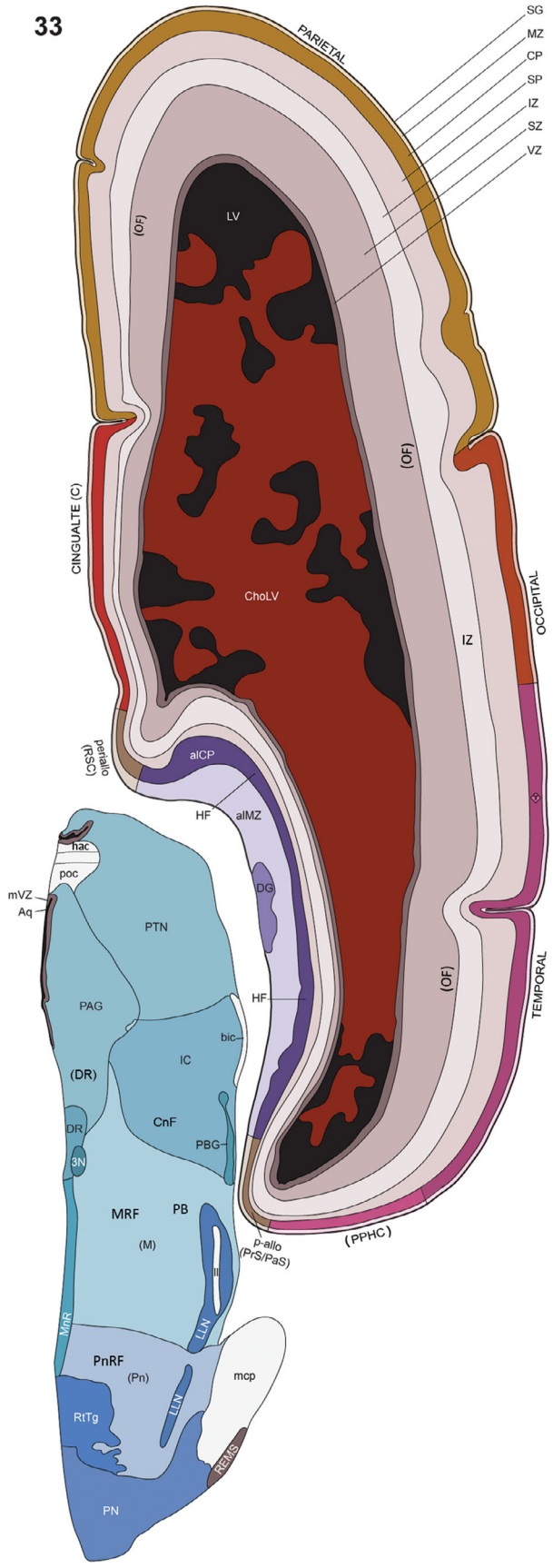

Level 33 (02-223)

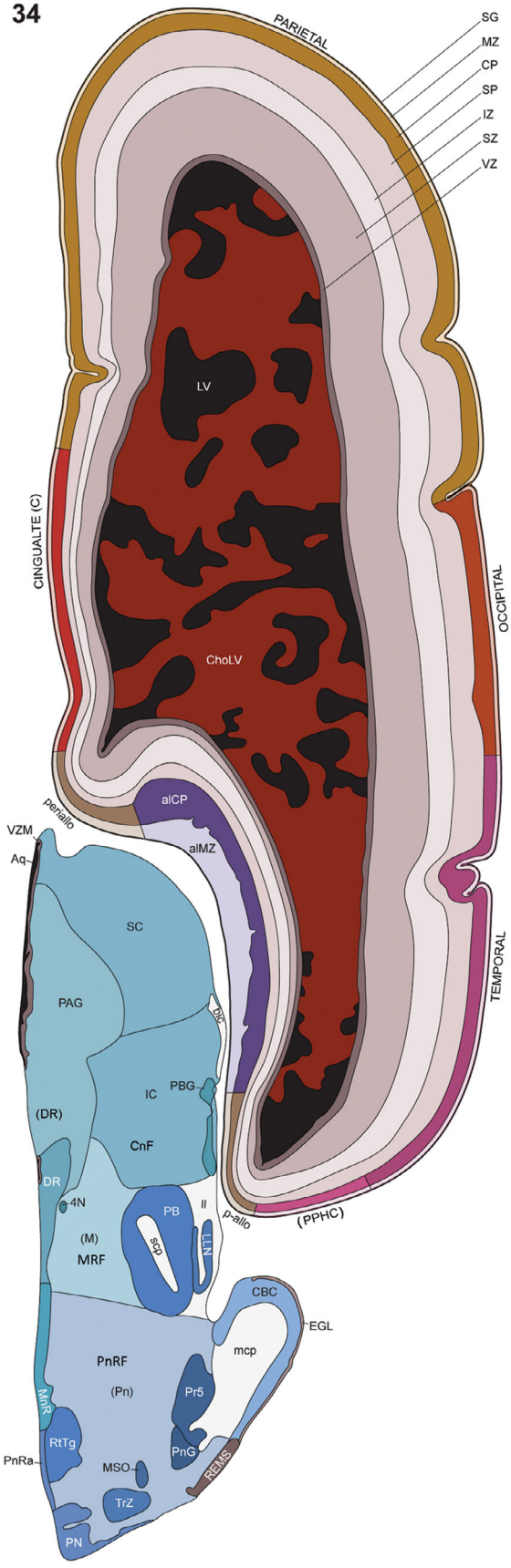

Level 34 (02-249)

NISSL-02-223 ACHE-02-262

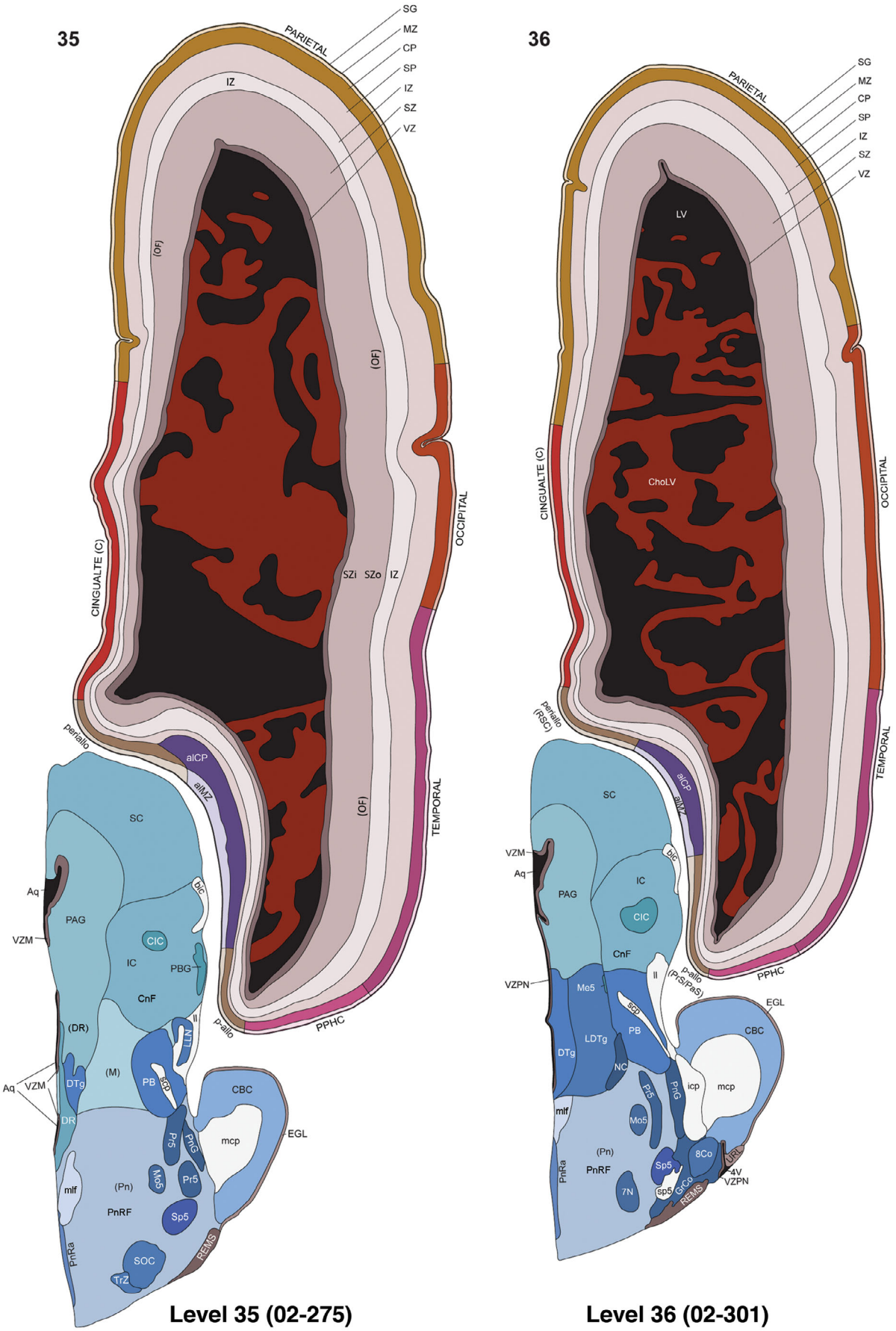

Level 35 (02-275) **Level 36 (02-301)**

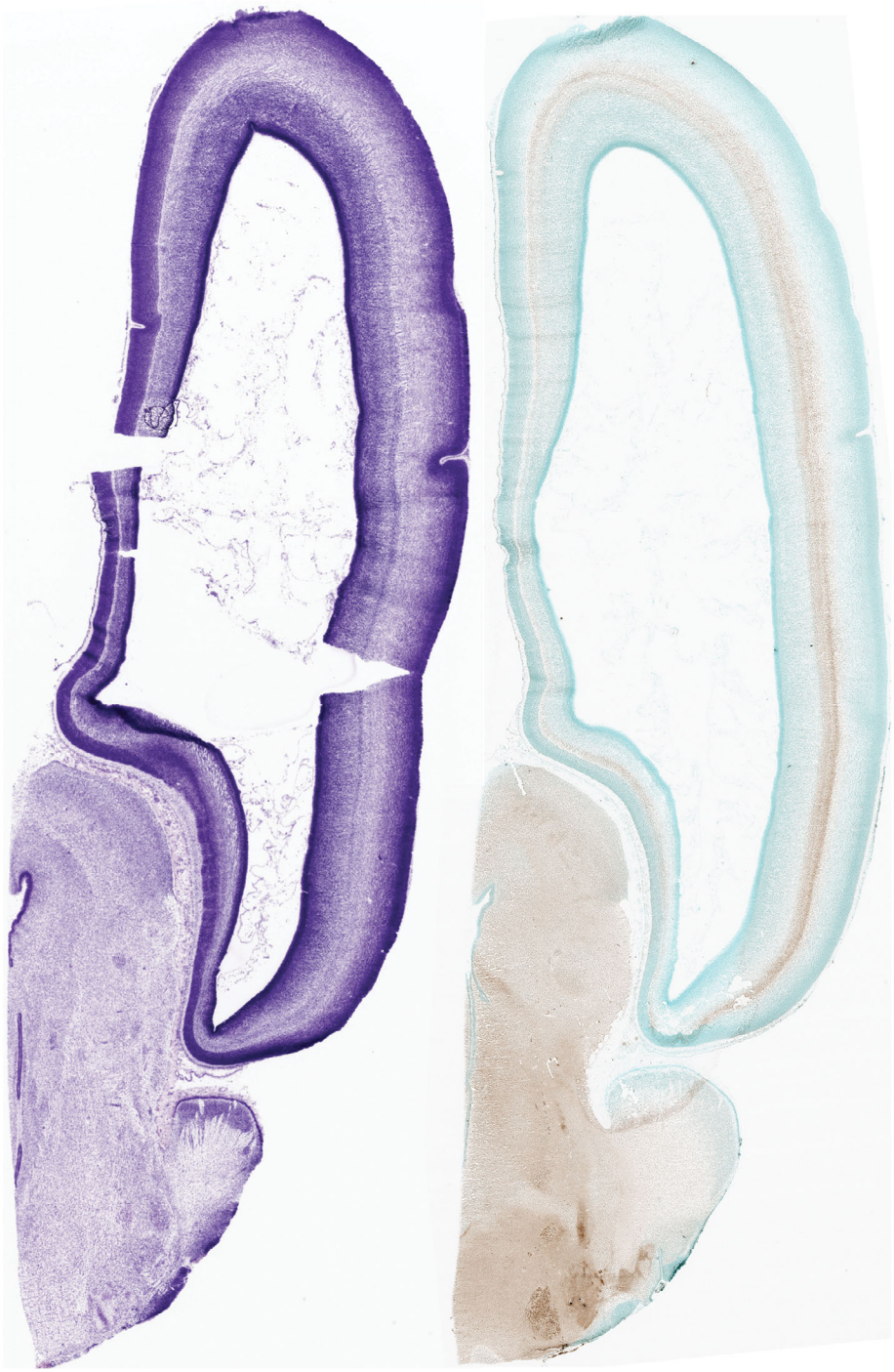

NISSL-02-275 ACHE-02-314

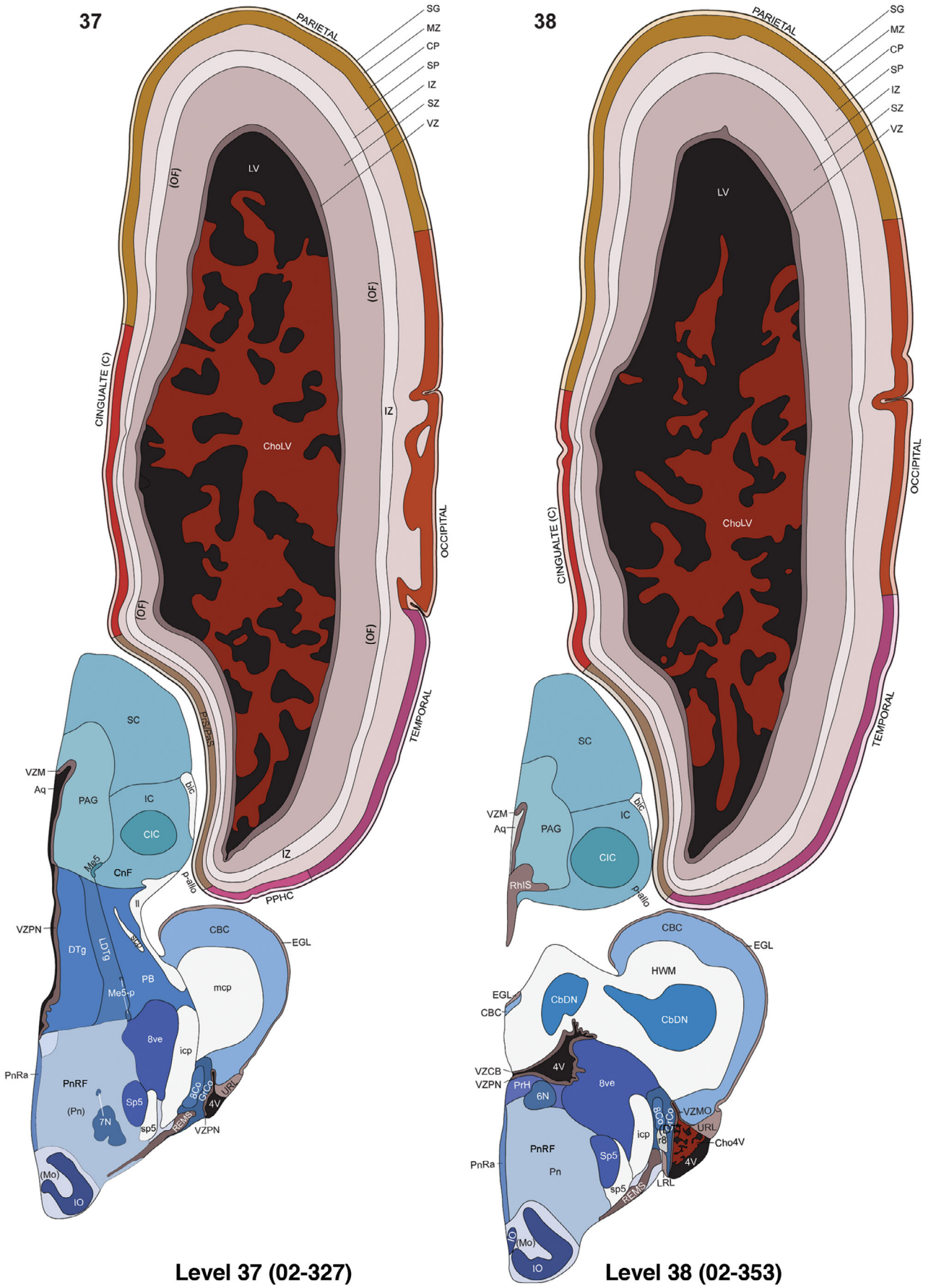

Level 37 (02-327) Level 38 (02-353)

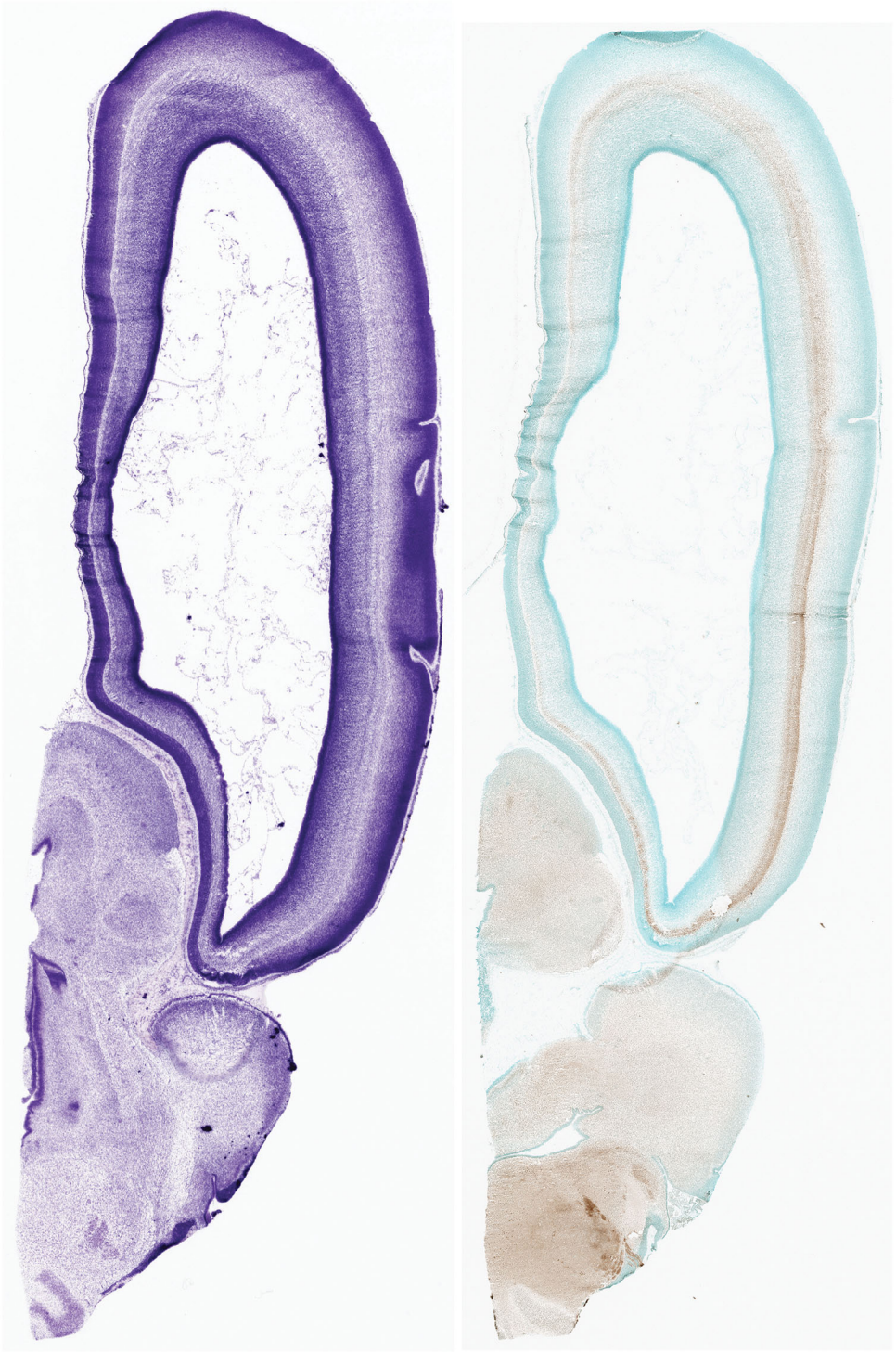

NISSL-02-327 ACHE-02-366

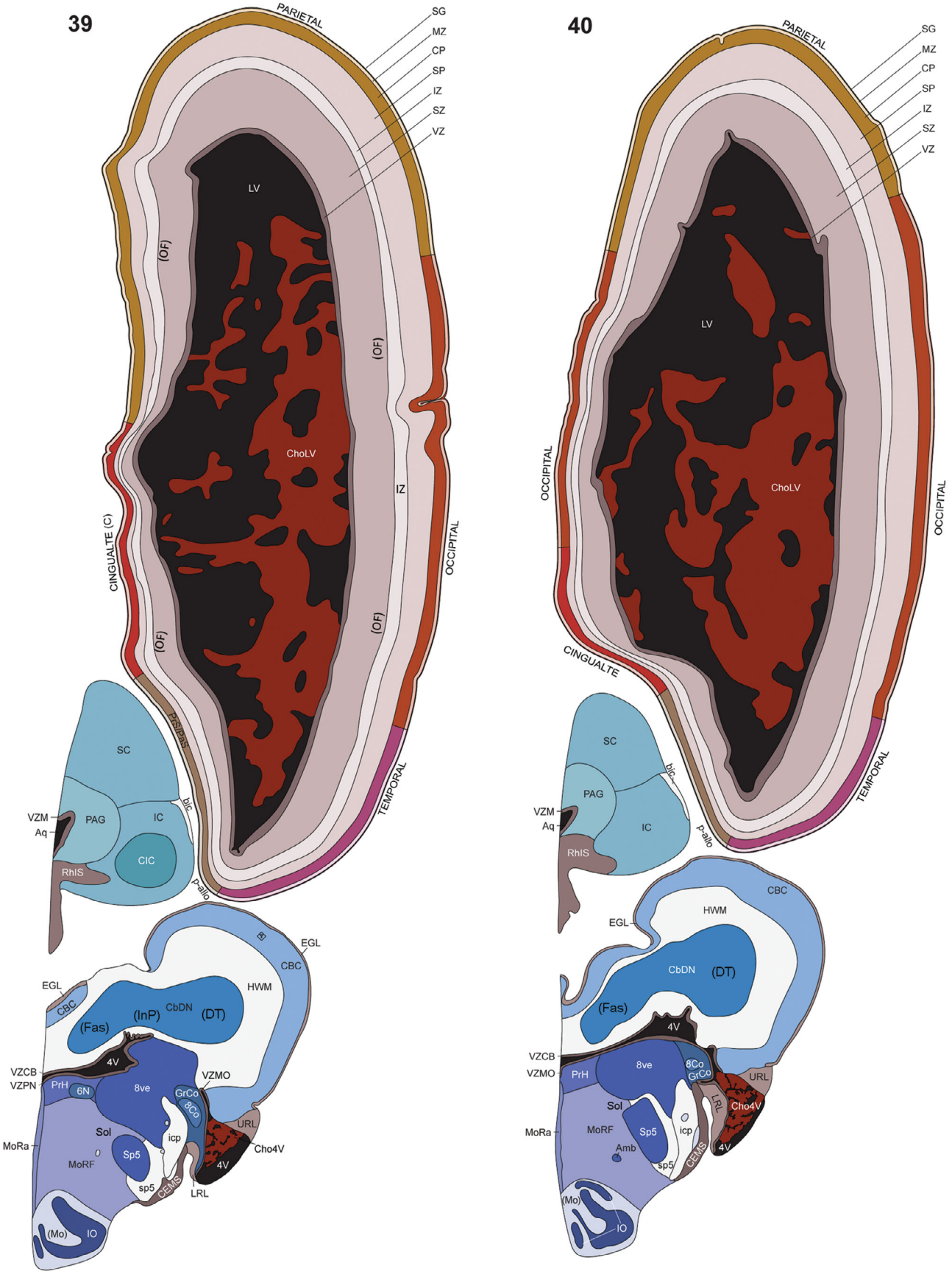

Level 39 (02-365) **Level 40 (02-391)**

NISSL-02-365 ACHE-02-392

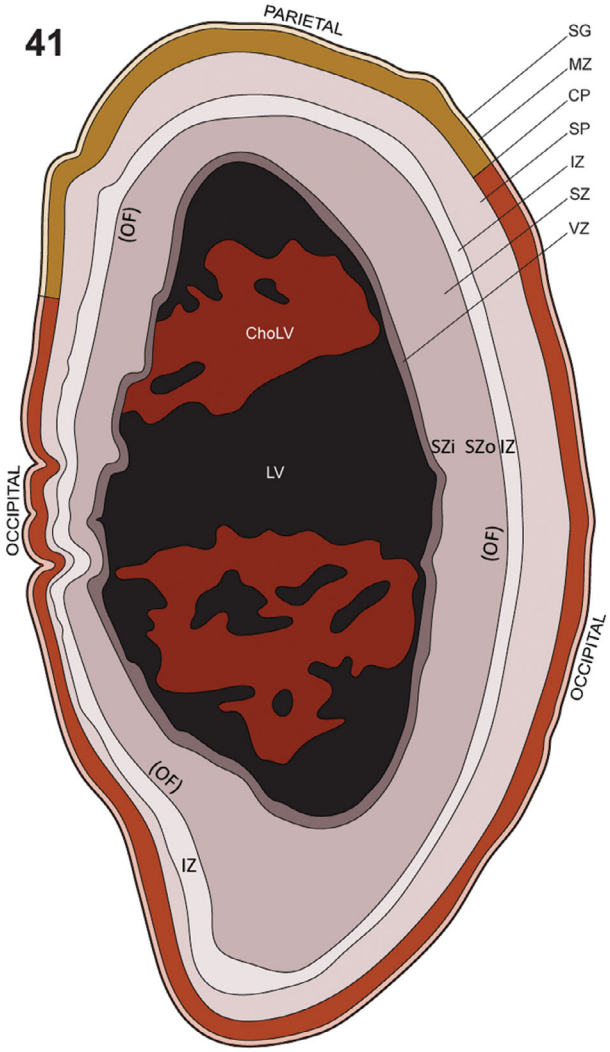

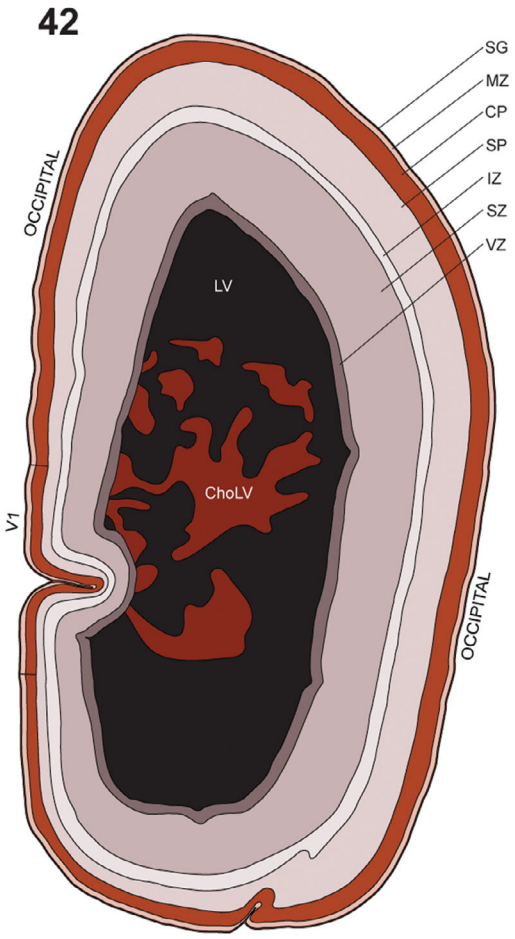

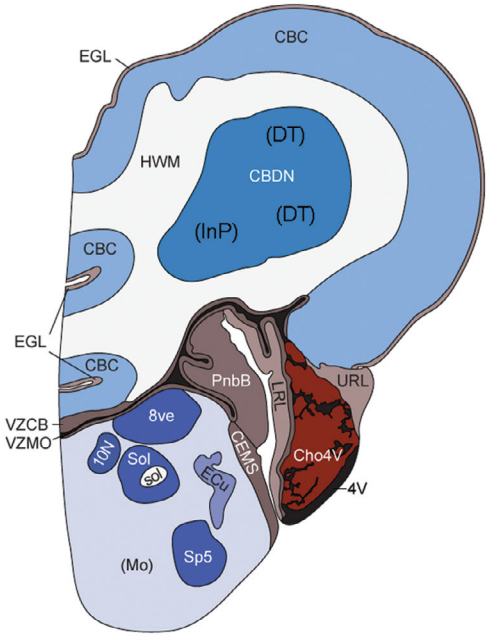

Level 41 (02-431)

Level 42 (02-483)

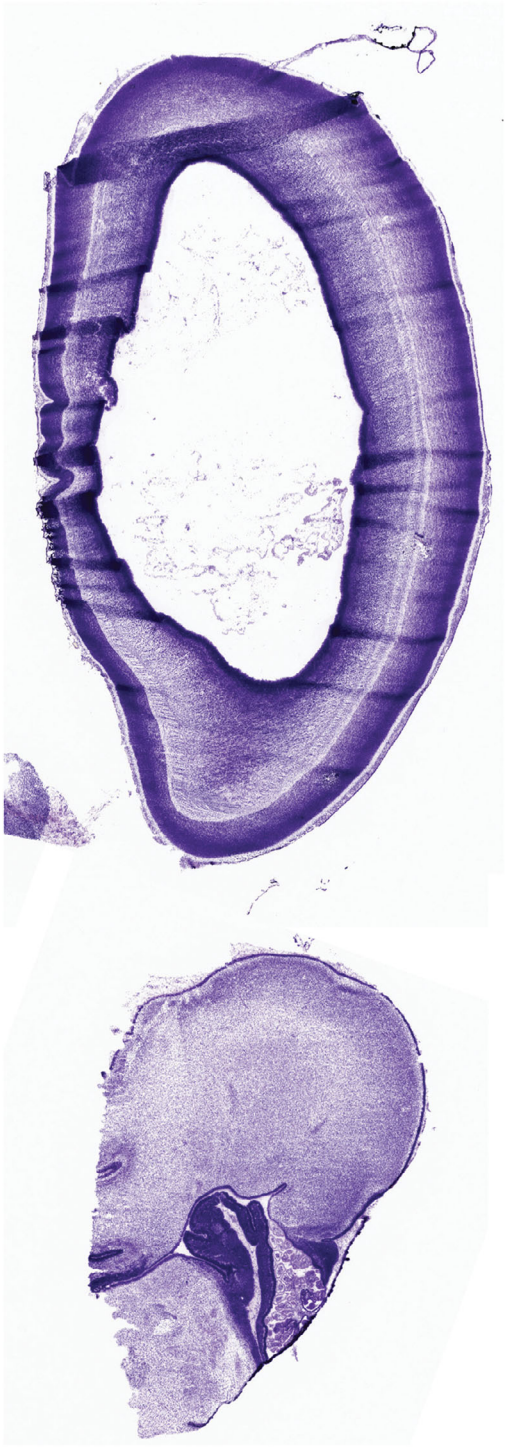

NISSL-02-431

ACHE-02-446

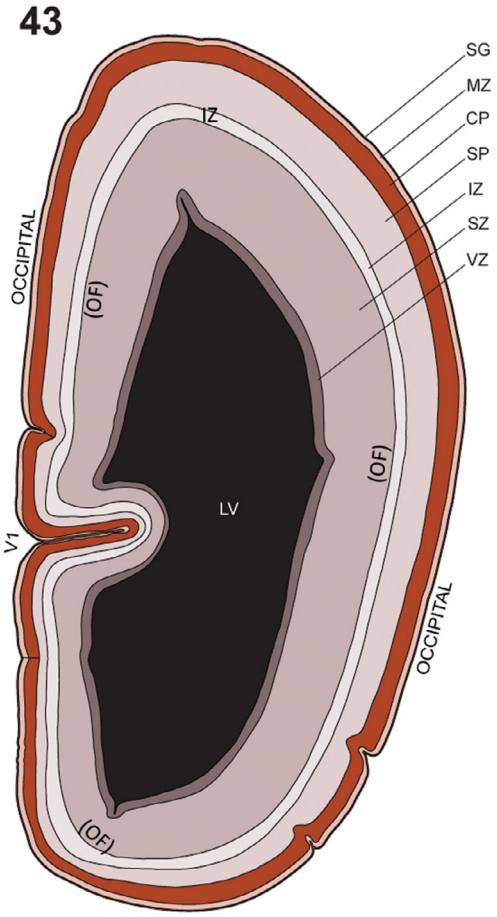

Level 43 (02-535)

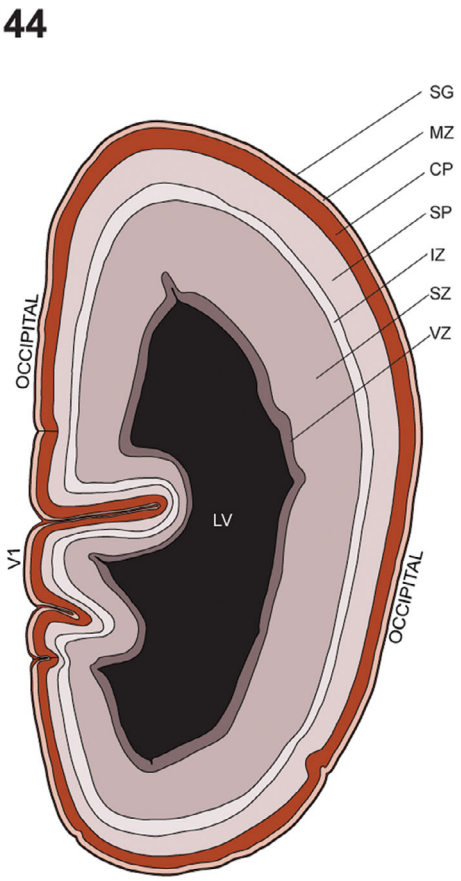

Level 44 (02-587)

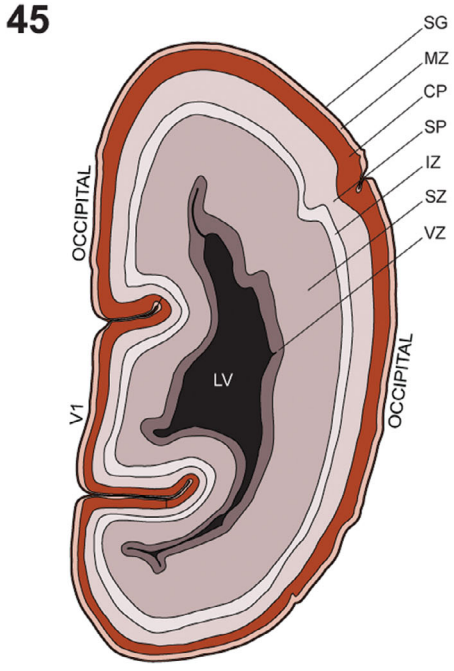

Level 45 (02-639)

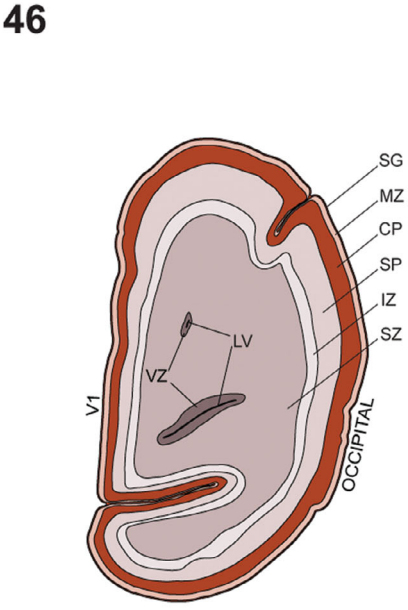

Level 46 (02-677)

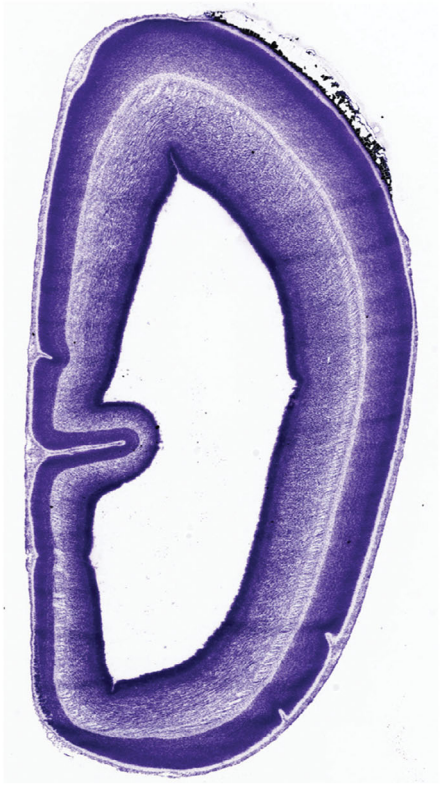

NISSL-02-535

ACHE-02-574

NISSL-02-639

ACHE-02-704

APPENDIX 2: Spatial expression of 37 genes in the brain at PCW 15

Anatomical localizations of the gene expression are based on the anatomical brain atlas (**Appendix 1**) which is derived from the same brain hemisphere. Note that some artifacts like the blank (white) round or oval regions usually caused by air bulbs during ISH staining are indicated by (#). The expression of the other six genes was not annotated mainly because of their faint or sparse expression but the sequential ISH images for these genes are linked online after the 37 genes in this appendix.

CALB2 (calbindin 2) (starting page) 99
(link to online high-resolution sequential ISH images)
CDH4 [cadherin 4, type 1, R-cadherin (retinal)] 104
(link to online high-resolution sequential ISH images)
CNTNAP2 (contactin associated protein-like 2) 109
(link to online high-resolution sequential ISH images)
DCX (doublecortin) 114
(link to online high-resolution sequential ISH images)
DLX1 (distal-less homeobox 1) 119
(link to online high-resolution sequential ISH images)
DLX2 (distal-less homeobox 2) 124
(link to online high-resolution sequential ISH images)
DLX5 (distal-less homeobox 5) 127
(link to online high-resolution sequential ISH images)
ENC1 [ectodermal-neural cortex (with BTB-like domain)] 132
(link to online high-resolution sequential ISH images)
EOMES (eomesodermin) or TBR2 (T-box brain transcription factor 2) 137
(link to online high-resolution sequential ISH images)
ERBB4 [v-erb-a erythroblastic leukemia viral oncogene homolog 4 (avian)] 142
(link to online high-resolution sequential ISH images)
ETV1 (ets variant 1) 147
(link to online high-resolution sequential ISH images)
FABP7 (fatty acid-binding protein 7, brain) 152
(link to online high-resolution sequential ISH images)
FADS2 (fatty acid desaturase 2) 157
(link to online high-resolution sequential ISH images)
FEZF2 (FEZ family zinc finger 2) 162
(link to online high-resolution sequential ISH images)
FOXG1 (forkhead box G1) 167
(link to online high-resolution sequential ISH images)
FOXP1 (forkhead box P1) 172
(link to online high-resolution sequential ISH images)
GAP43 (growth-associated protein 43) 177
(link to online high-resolution sequential ISH images)
GFAP (glial fibrillary acidic protein) 182
(link to online high-resolution sequential ISH images)
GRIK2 (glutamate receptor, ionotropic, kainate 2) 187
(link to online high-resolution sequential ISH images)
LHX2 (LIM homeobox 2) 192
(link to online high-resolution sequential ISH images)
LMO4 (LIM domain only 4) 197
(link to online high-resolution sequential ISH images)
NES (nestin) 202
(link to online high-resolution sequential ISH images)
NKX2.1 (NK2 homeobox 1) 207
(link to online high-resolution sequential ISH images)
NPY (neuropeptide Y) 212
(link to online high-resolution sequential ISH images)
NRGN neurogranin (protein kinase C substrate, RC3) 217
(link to online high-resolution sequential ISH images)
NRXN1 (neurexin 1) 222
(link to online high-resolution sequential ISH images)
NTRK2 (neurotrophic tyrosine kinase, receptor, type 2) 227
(link to online high-resolution sequential ISH images)
PAX6 (paired box 6) 232
(link to online high-resolution sequential ISH images)
PLXNA2 (plexin A2) 237
(link to online high-resolution sequential ISH images)
RELN (reelin) 242
(link to online high-resolution sequential ISH images)
SATB2 (SATB homeobox 2) 247
(link to online high-resolution sequential ISH images)
SOX2 [SRY (sex determining region Y)-box 2] 252
(link to online high-resolution sequential ISH images)
SST (somatostatin) 257
(link to online high-resolution sequential ISH images)
SYNGAP1 [synaptic Ras GTPase activating protein 1 homolog (rat)] 262
(link to online high-resolution sequential ISH images)
TBR1 (T-box brain transcription factor 1) 267
(link to online high-resolution sequential ISH images)
VIM (tripeptidyl peptidase I) 271
(link to online high-resolution sequential ISH images)
ZIC1 [Zic family member 1 (odd-paired homolog, Drosophila)] 276
(link to online high-resolution sequential ISH images)

List of other six genes with only online link for their spatial expression

HOXA4 (homeobox A4): link to online ISH images.

LBX1 (ladybird homeobox 1): link to online ISH images.

MECP2 [methyl CpG-binding protein 2 (Rett syndrome)]: link to online ISH images

SHANK3 (SH3 and multiple ankyrin repeat domains 3): link to online ISH images.

SOX10 [SRY (sex determining region Y)-box 10]: link to online ISH images.

TPP1 (tripeptidyl peptidase I): link to online ISH images.

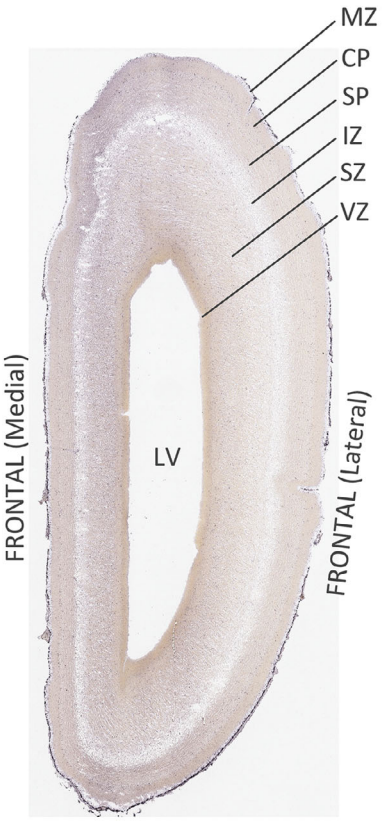

CALB2-01-060 (Level ~2)

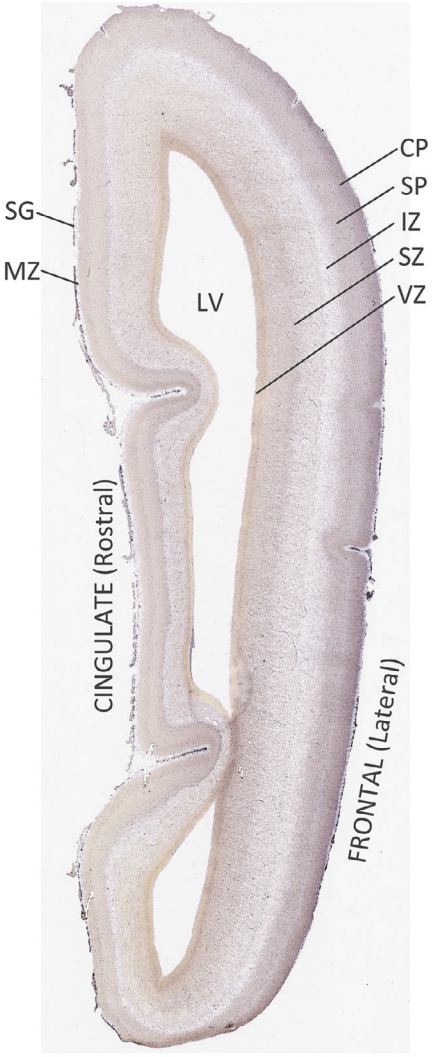

CALB2-01-216 (Level ~6)

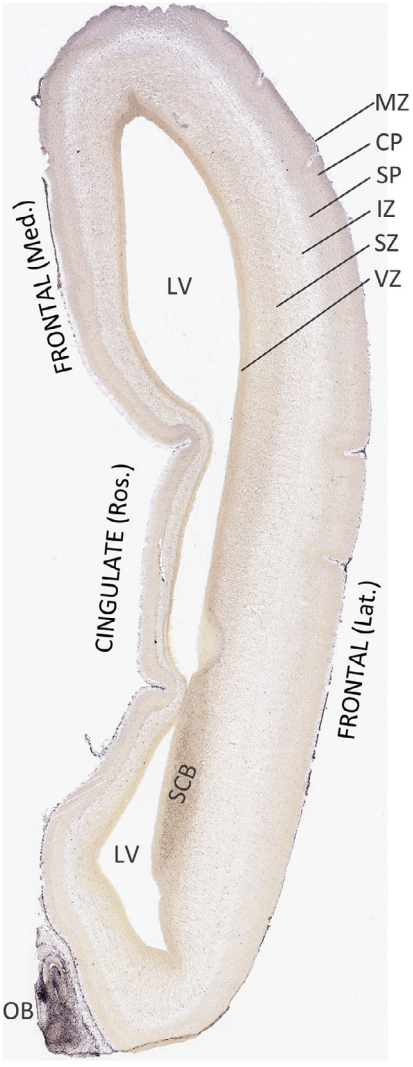

CALB2-01-320 (Level ~8)

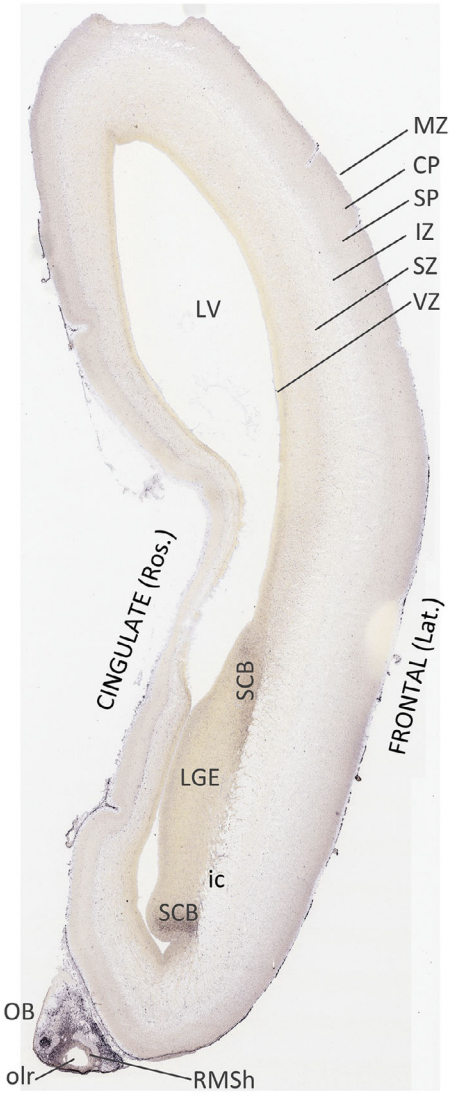

CALB2-01-372 (Level ~10)

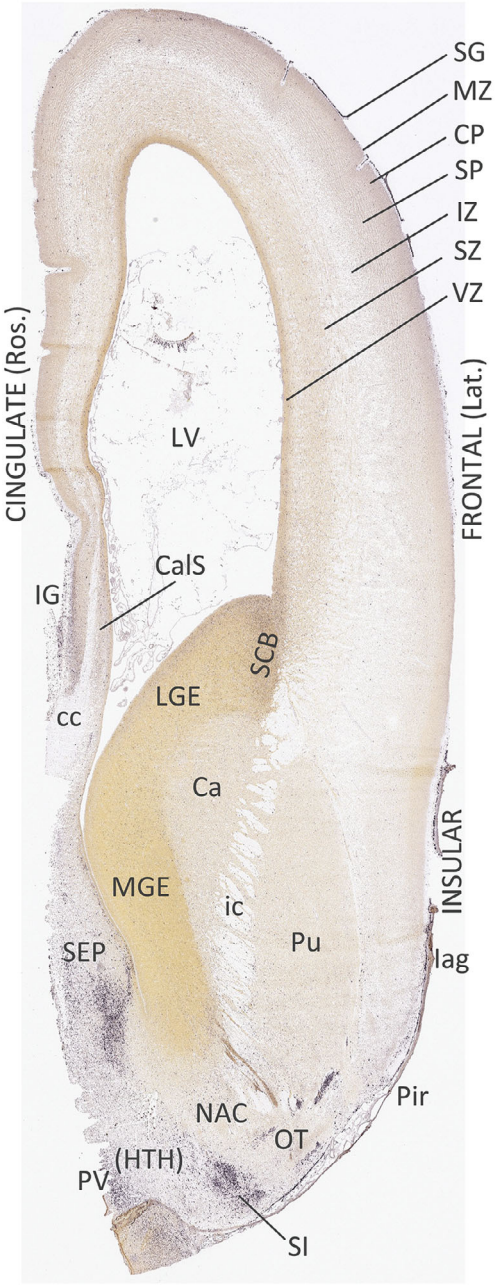

CALB2-01-528 (Level ~16)

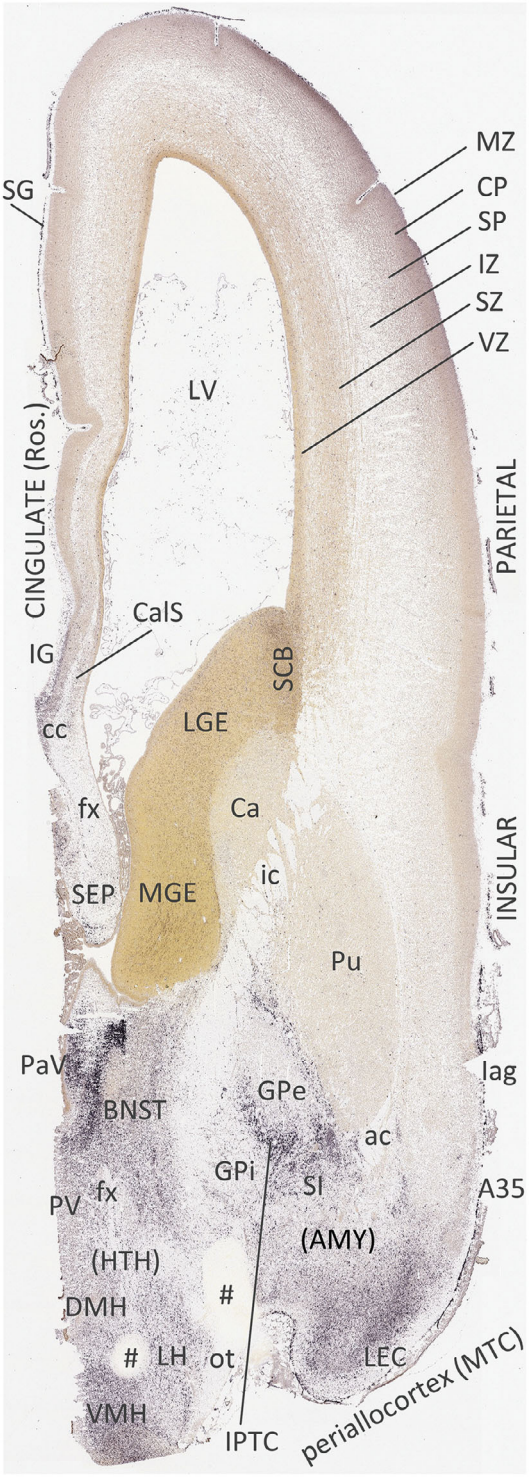

CALB2-01-632 (Level ~20)

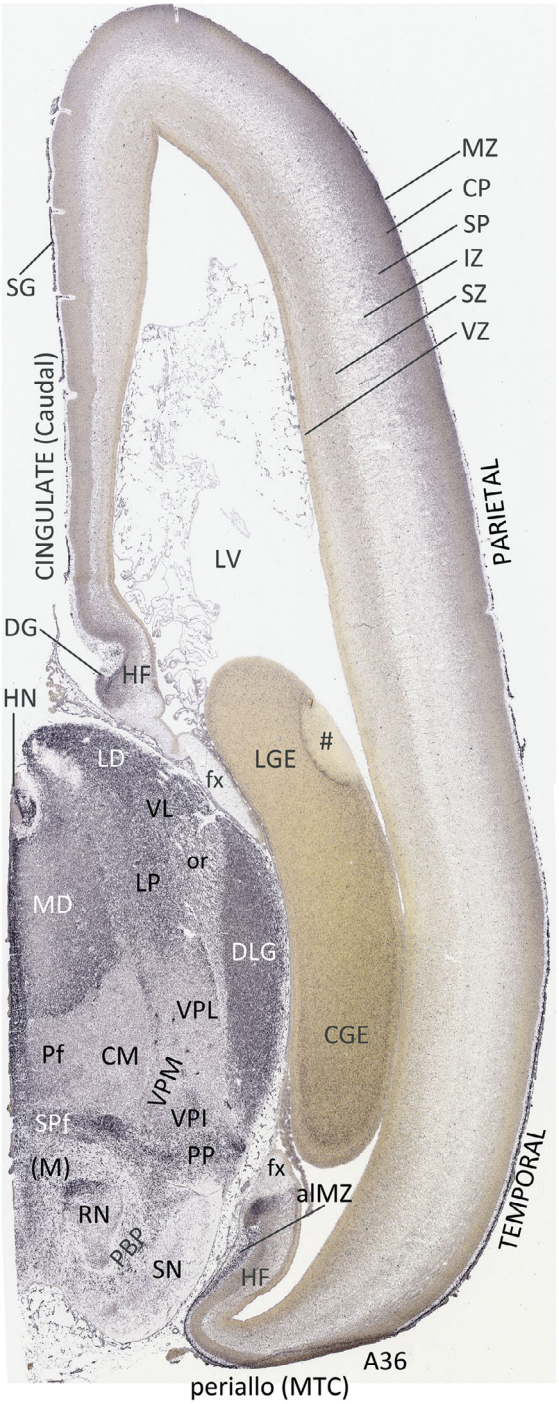

CALB2-02-060 (Level ~27)

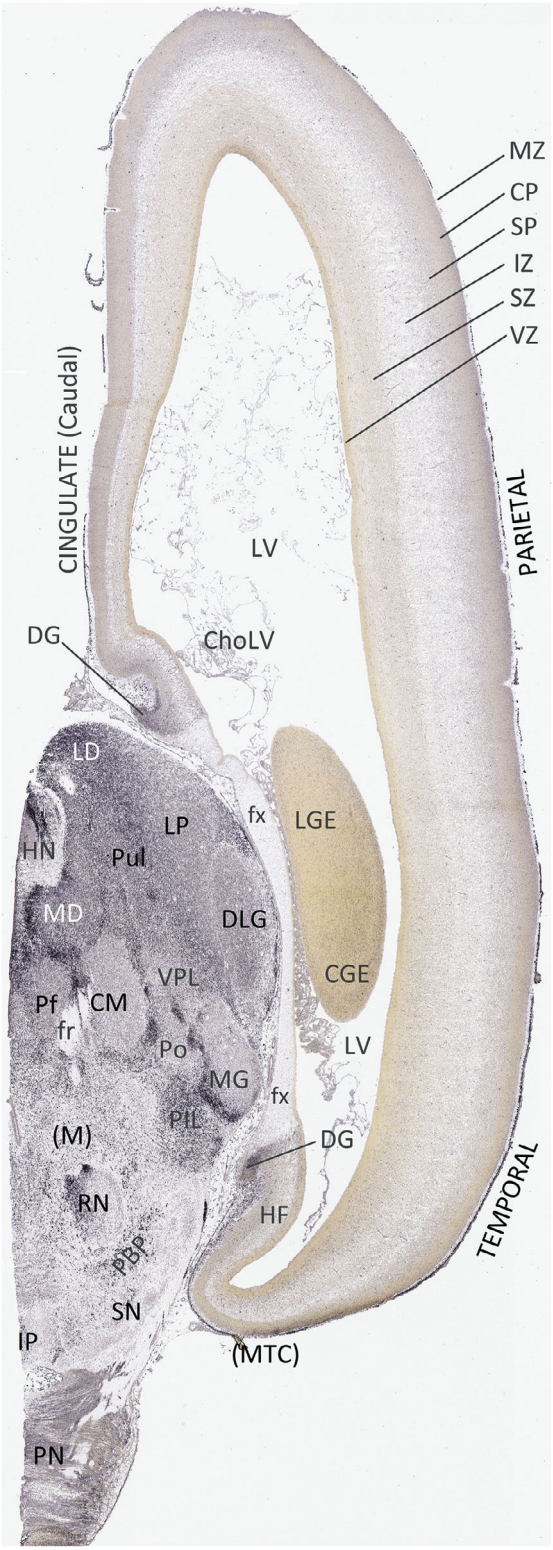

CALB2-02-112 (Level ~29)

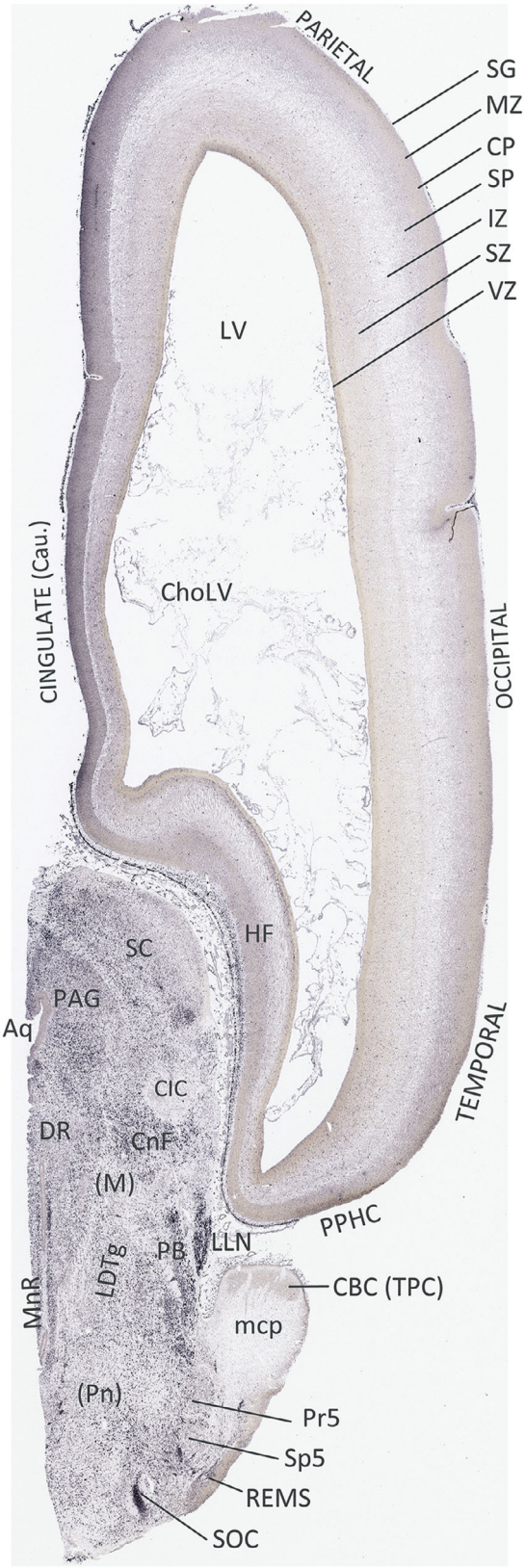

CALB2-02-268 (Level ~35)

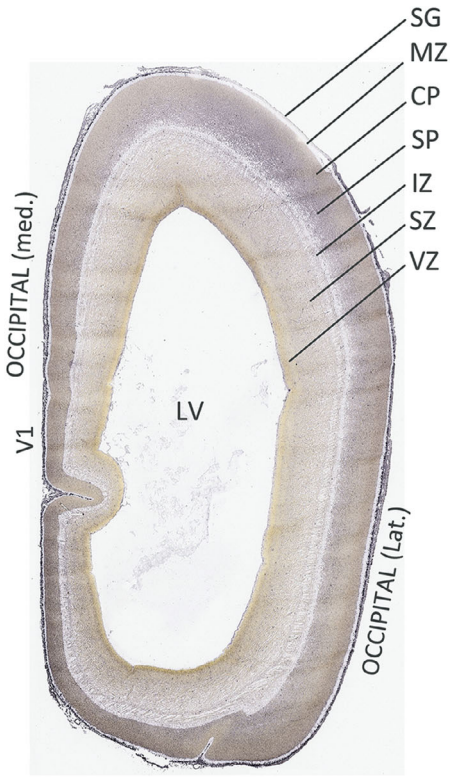

CALB2-02-476 (Level ~42)

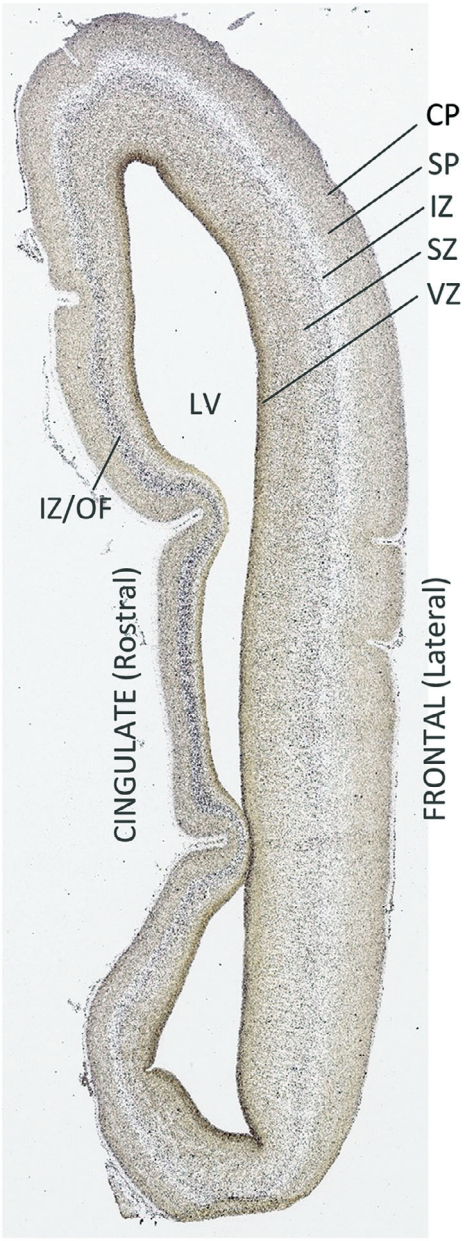

CDH4-01-282 (Level ~7)

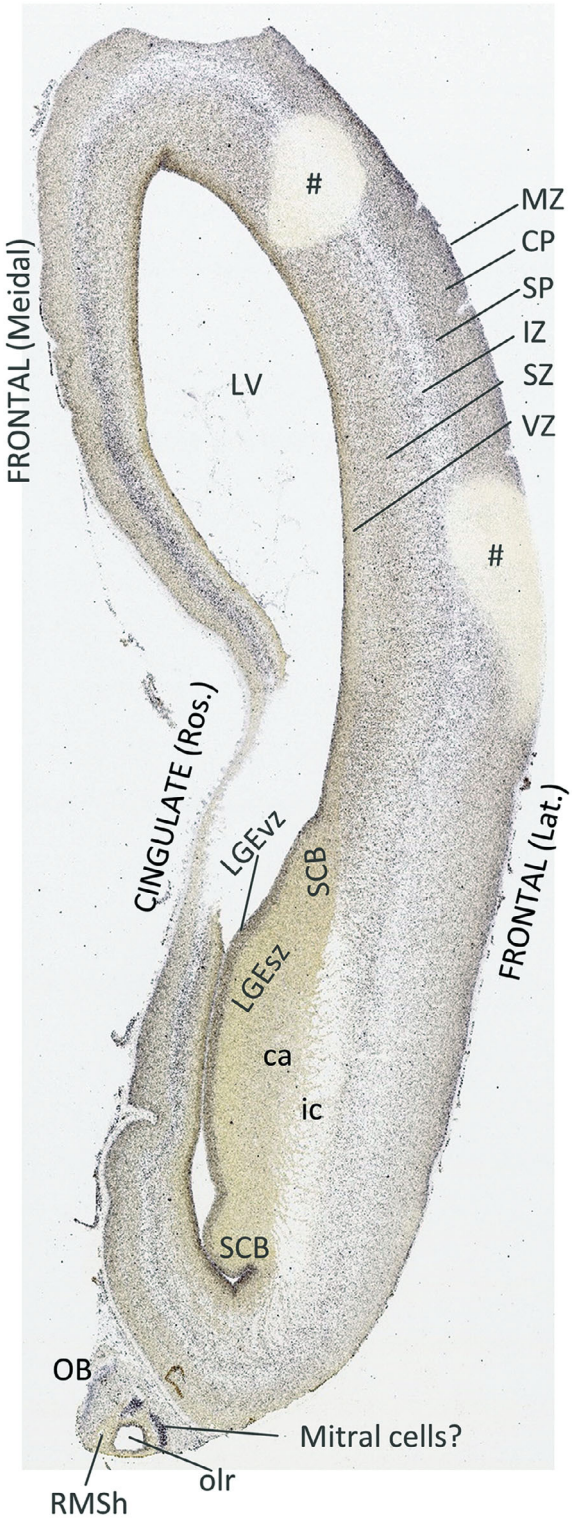

CDH4-01-386 (Level ~11)

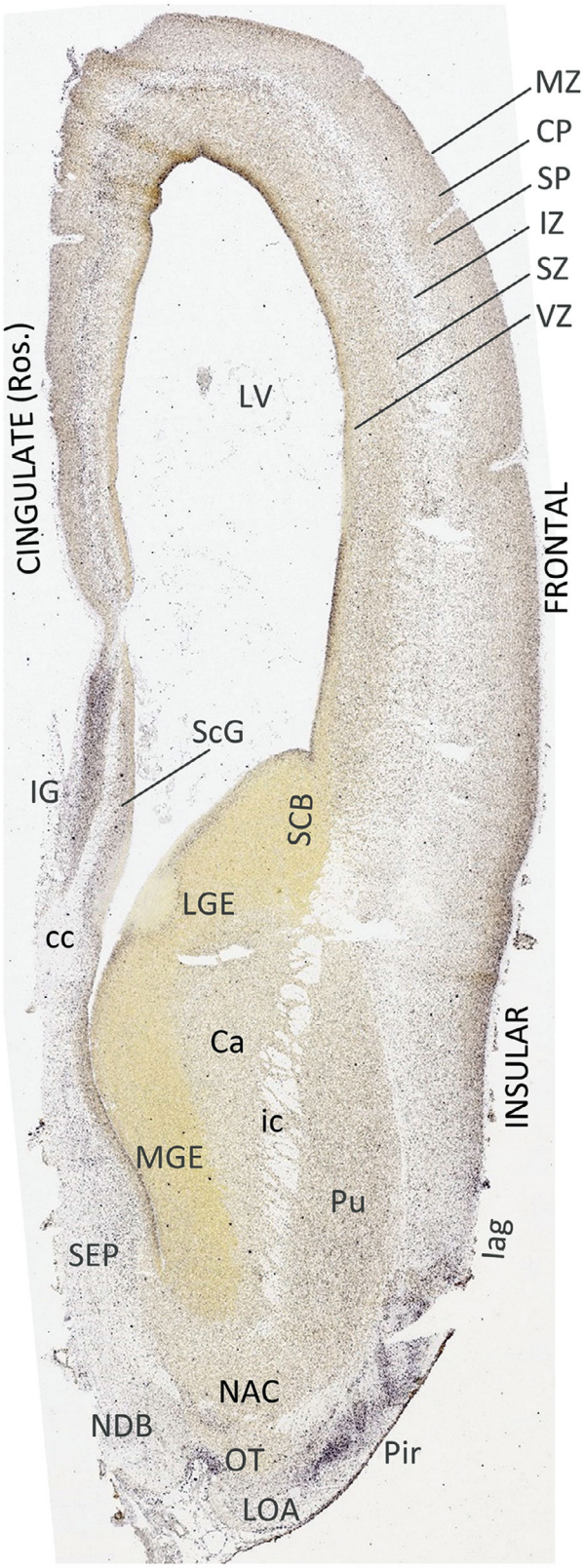

CDH4-01-490 (Level ~15)

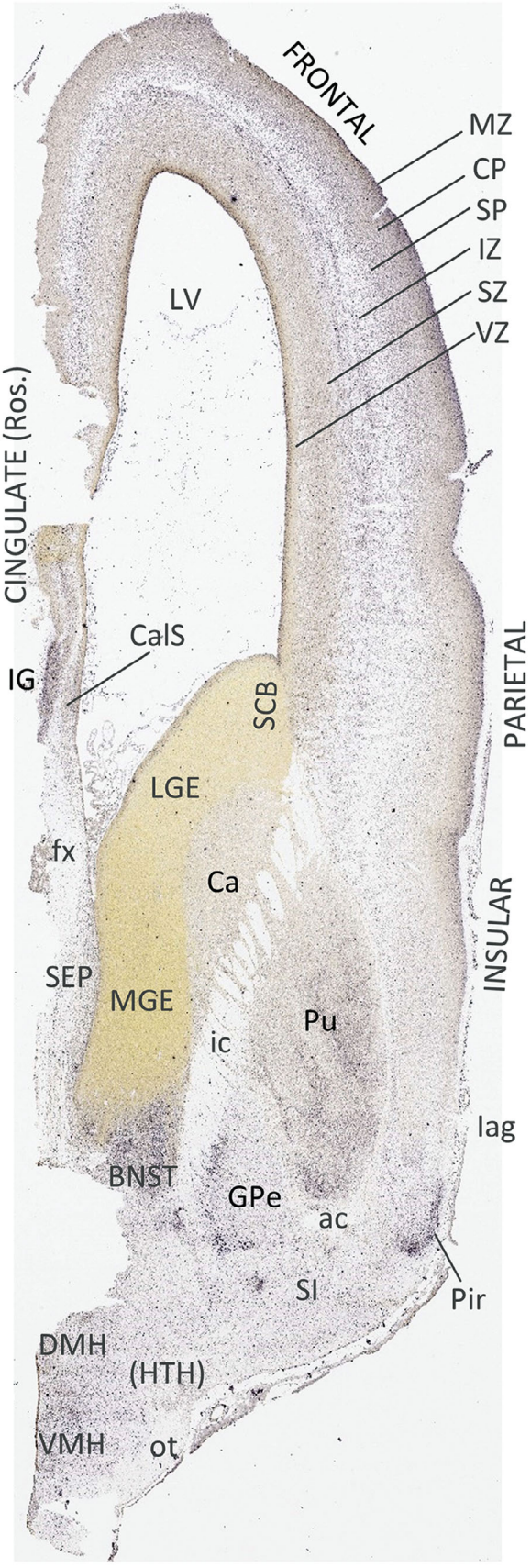

CDH4-01-594 (Level ~19)

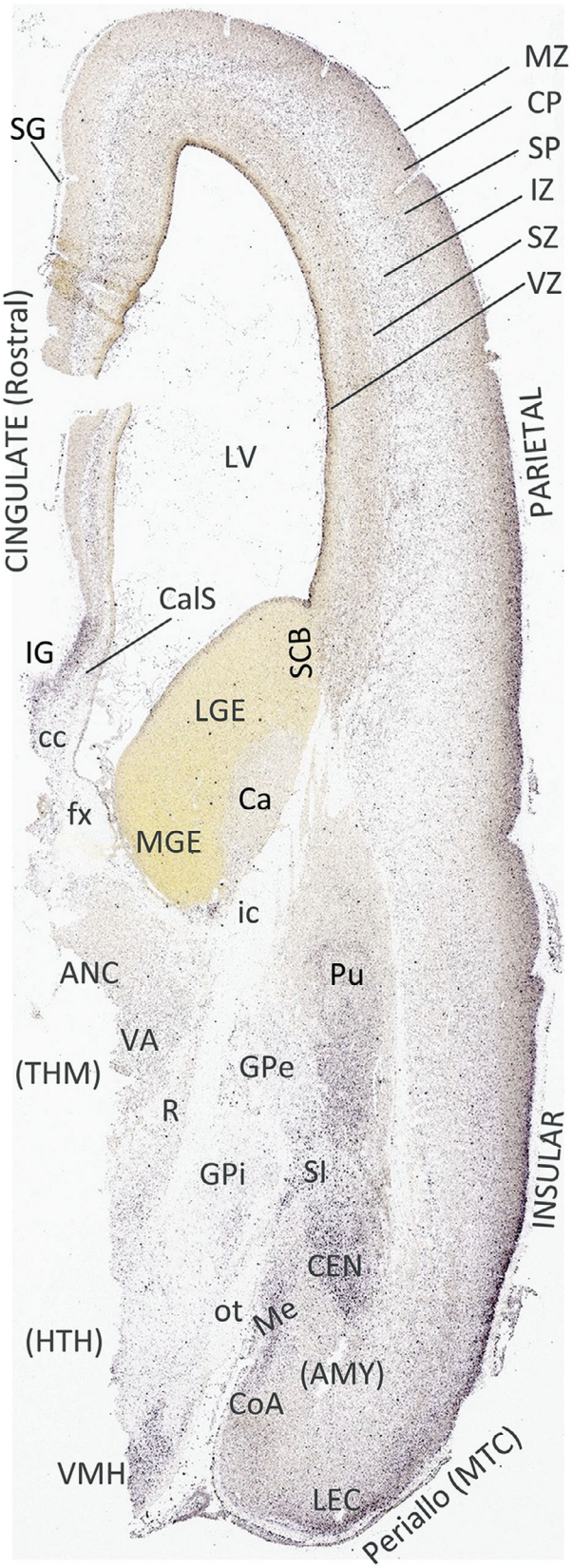

CDH4-01-698 (Level ~22)

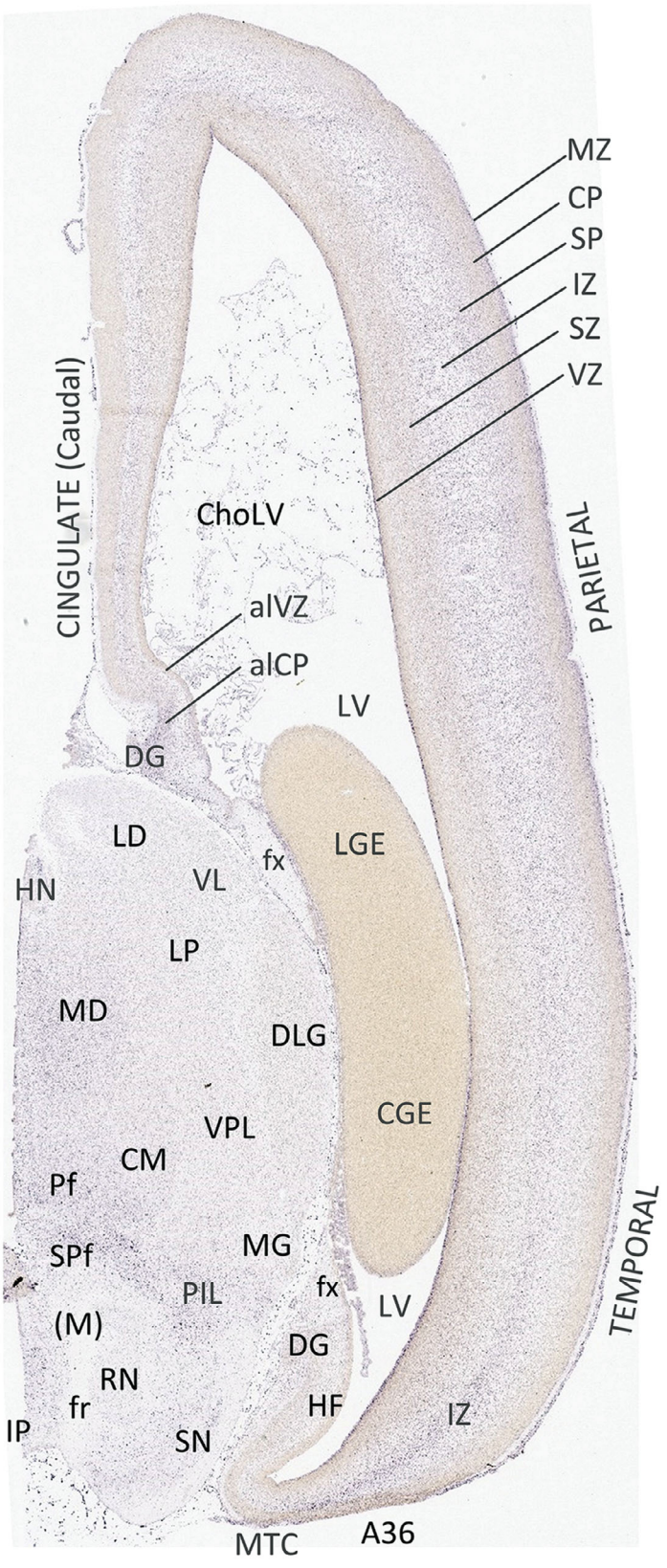

CDH4-02-074 (Level ~27)

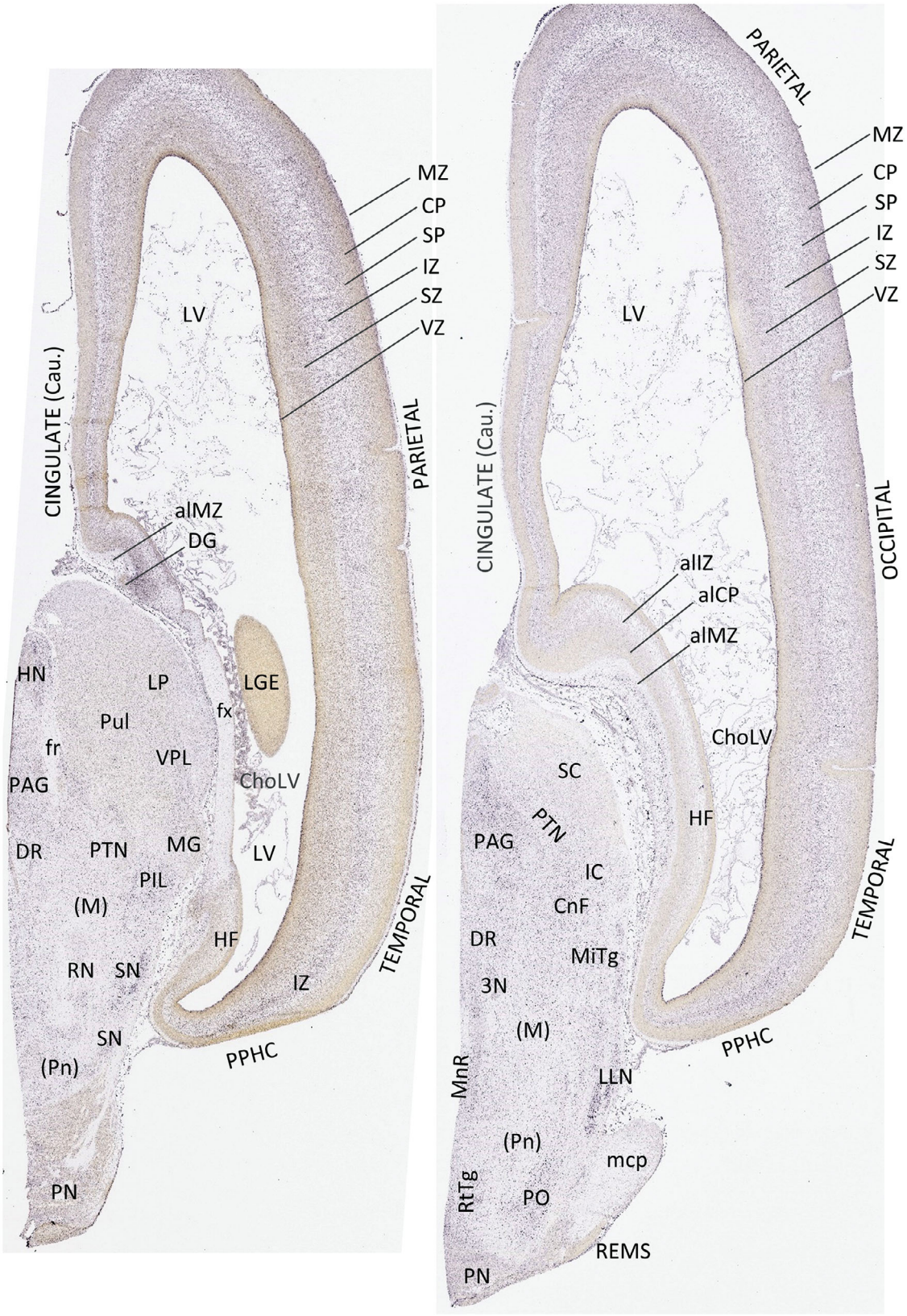

CDH4-02-126 (Level ~29-30) **CDH4-02-230 (Level ~33-34)**

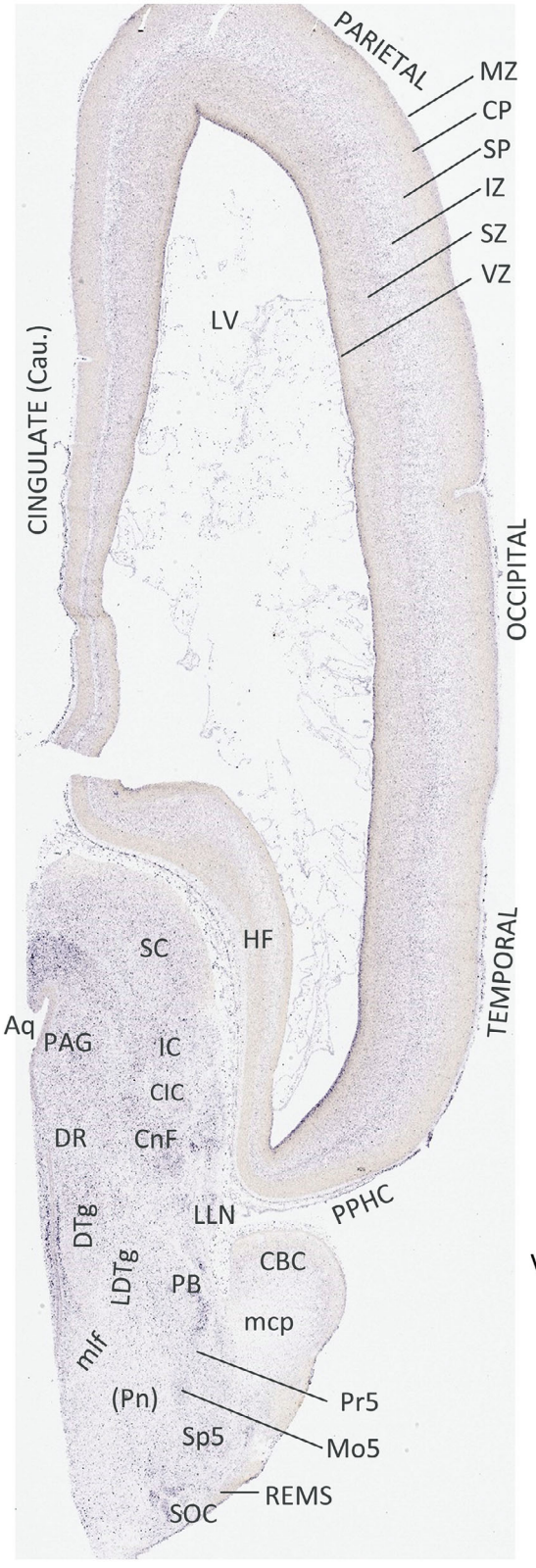

CDH4-02-282 (Level ~35)

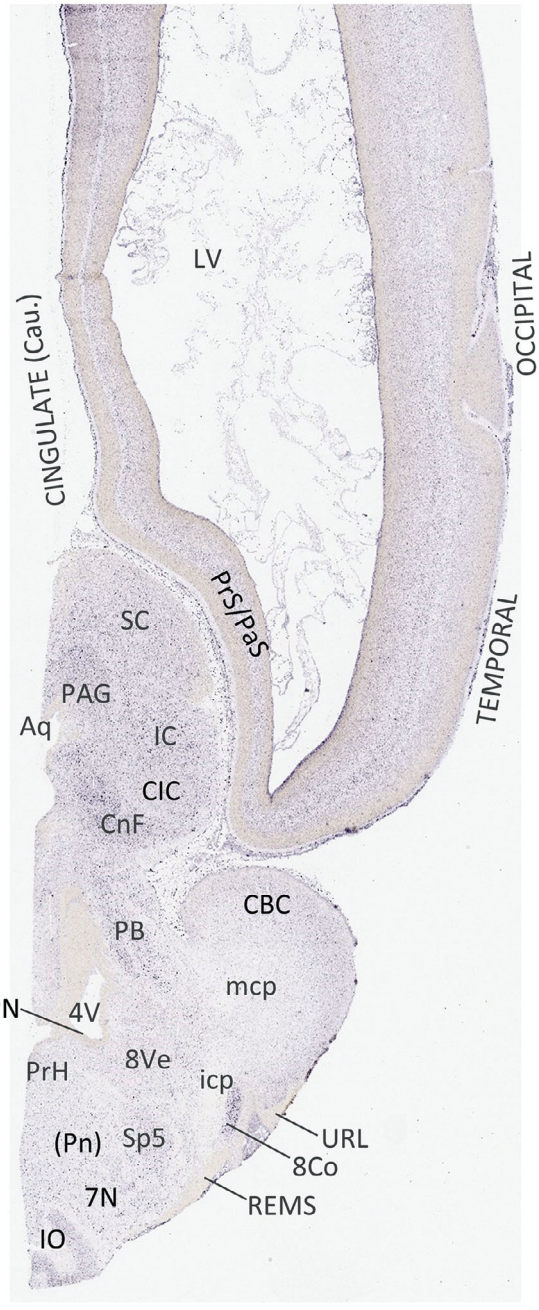

CDH4-02-334 (Level ~37-38)

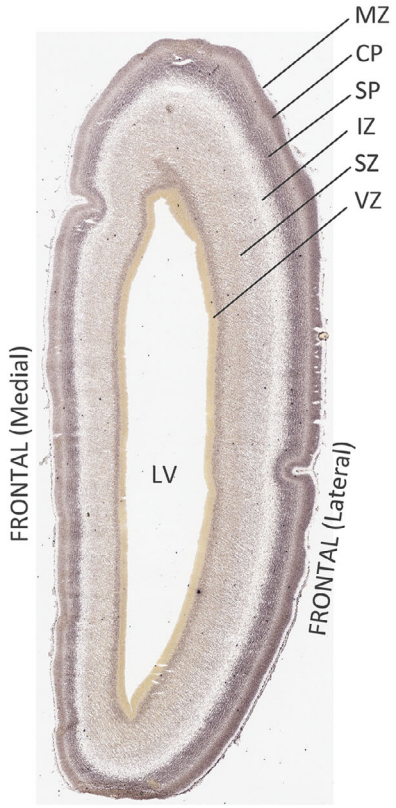

CNTNAP2-01-084 (Level ~3)

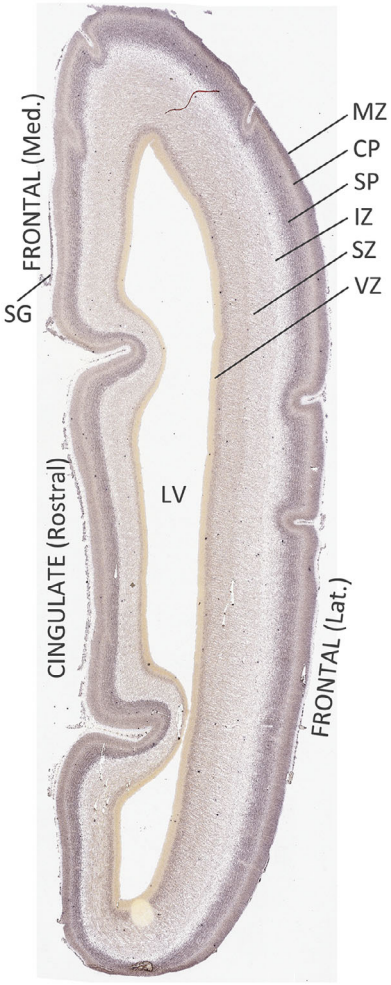

CNTNAP2-01-188 (Level ~5)

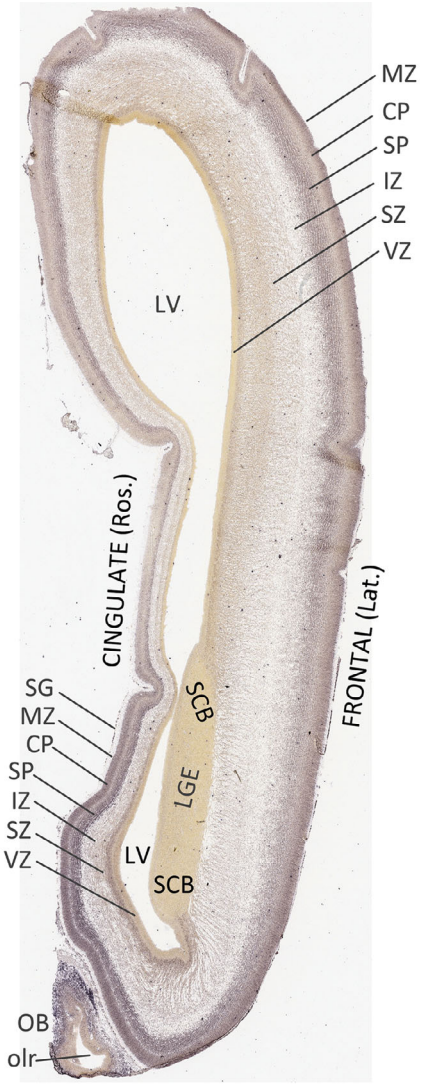

CNTNAP2-01-344 (Level ~9)

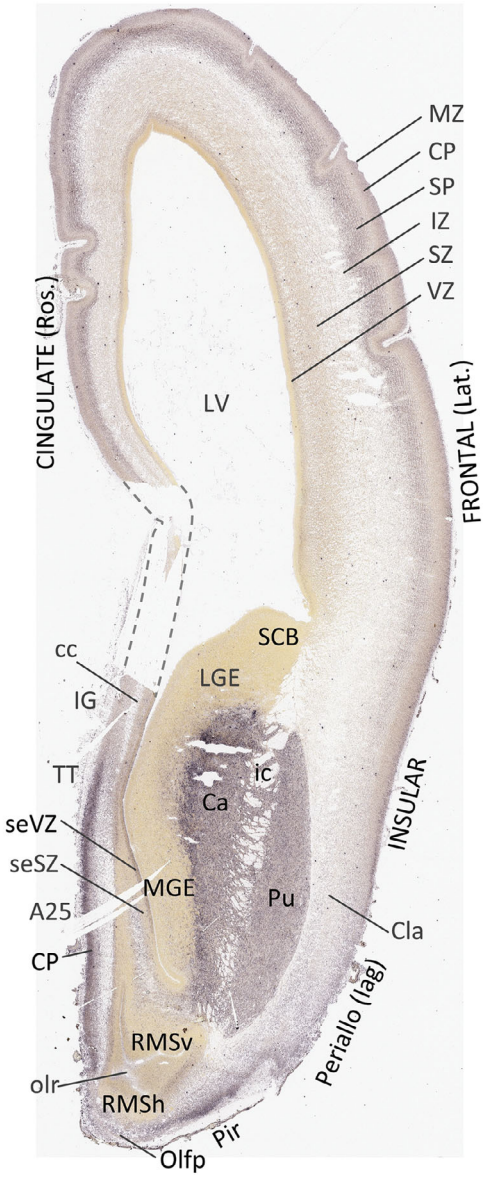

CNTNAP2-01-448 (Level ~13)

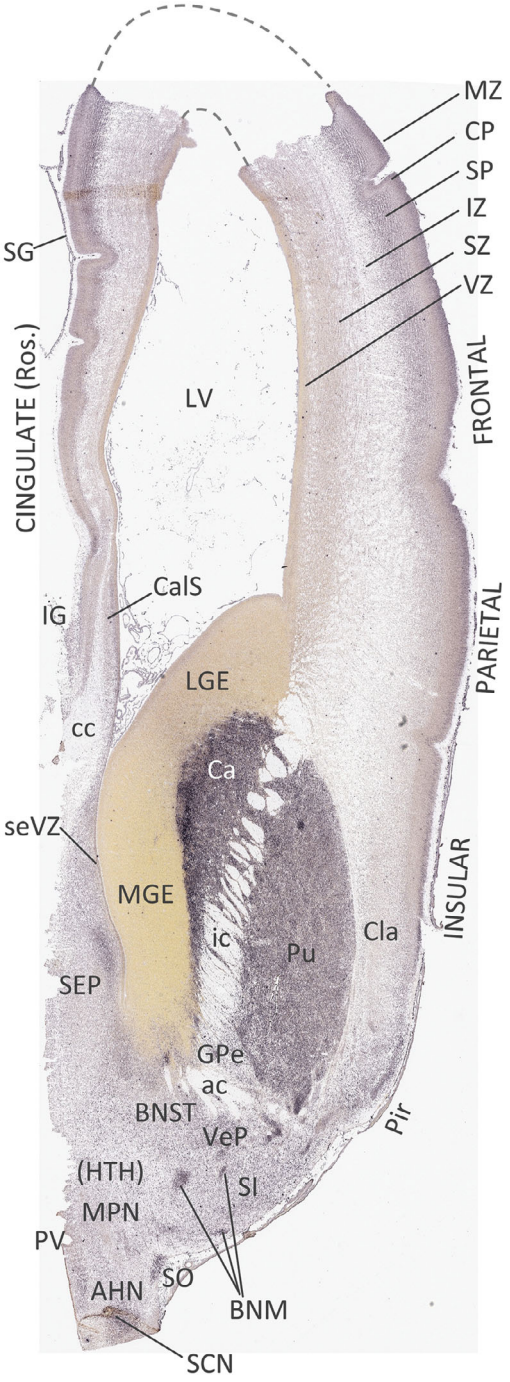

CNTNAP2-01-552 (Level ~17-18)

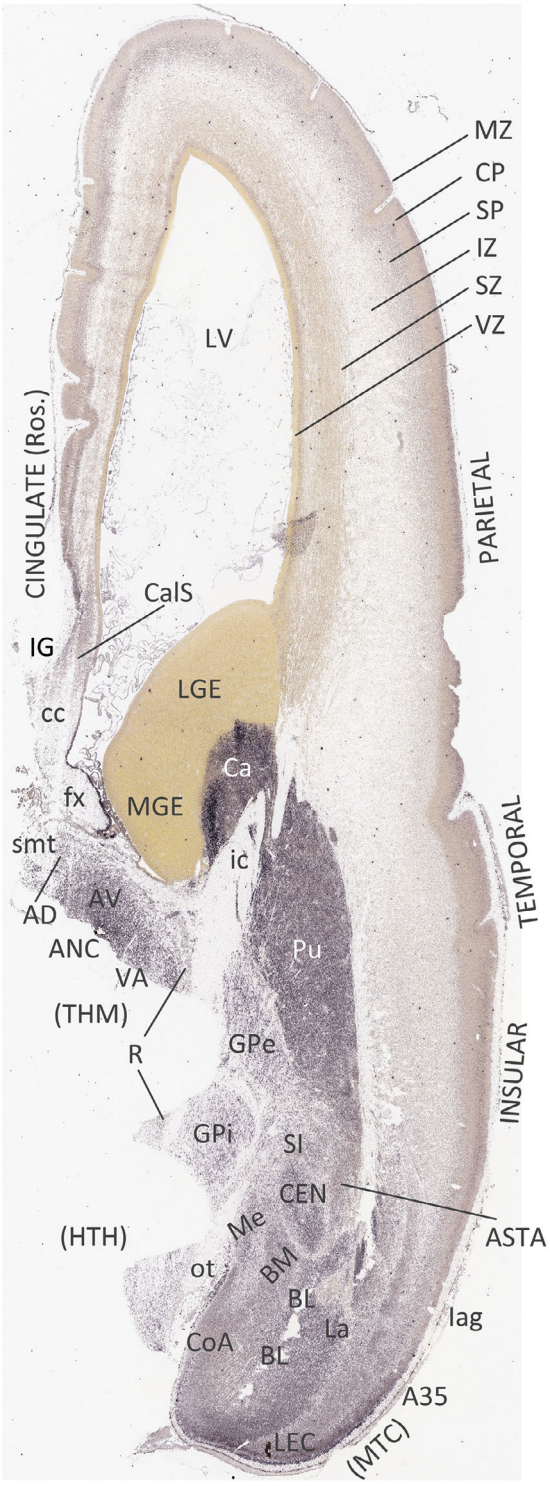

CNTNAP2-01-708 (Level ~22)

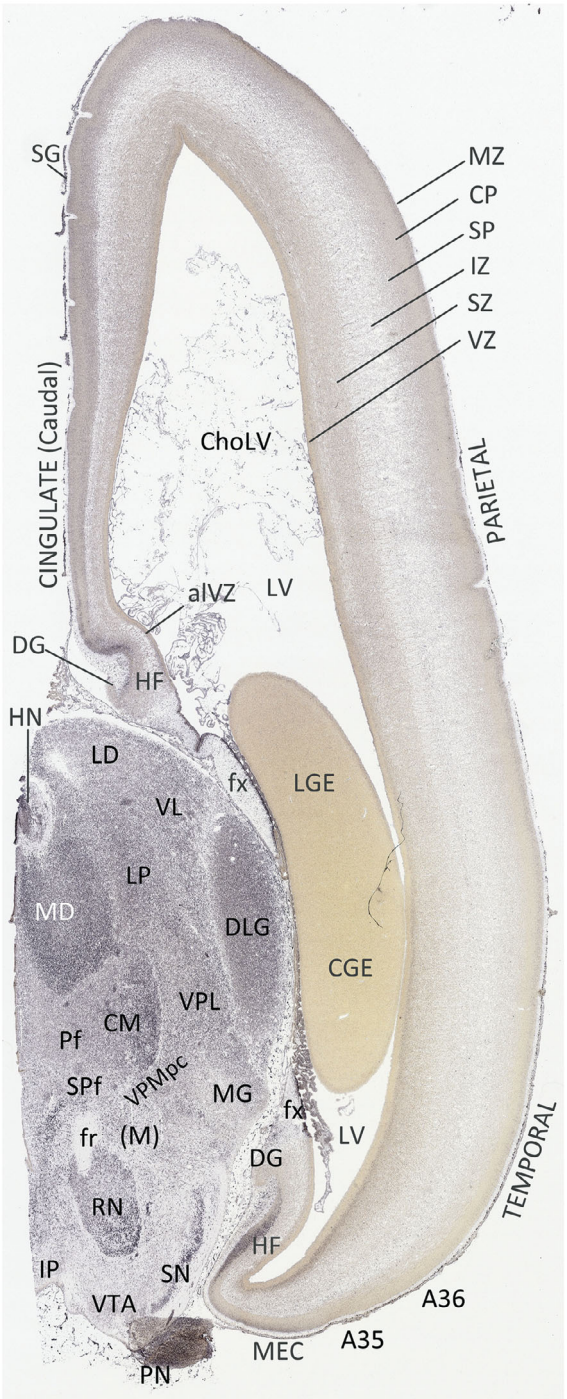

CNTNAP2-02-084 (Level ~28)

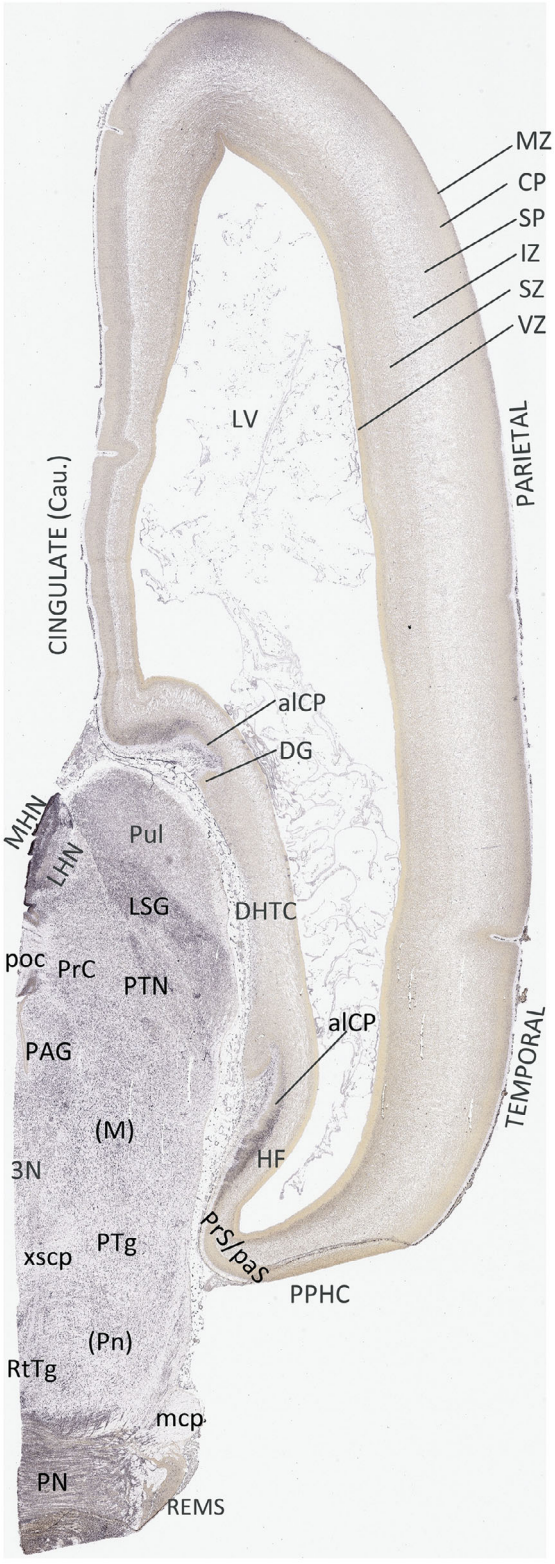

CNTNAP2-02-188 (Level ~32)

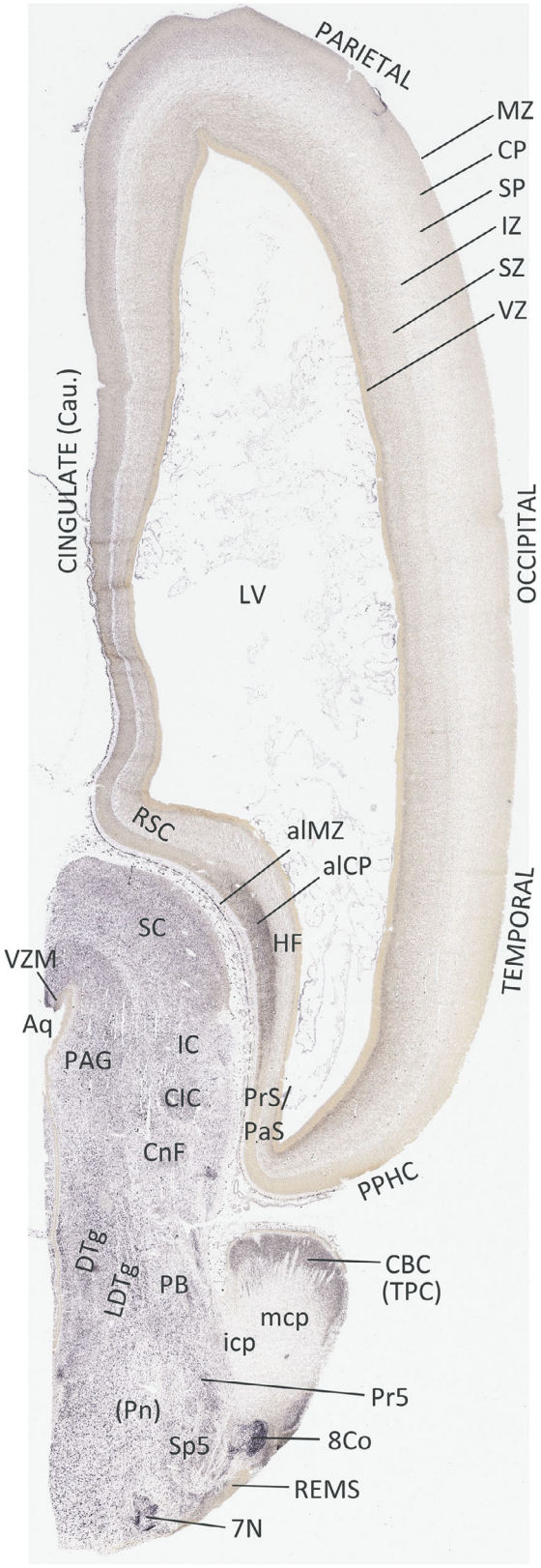

CNTNAP2-02-292 (Level ~36-37)

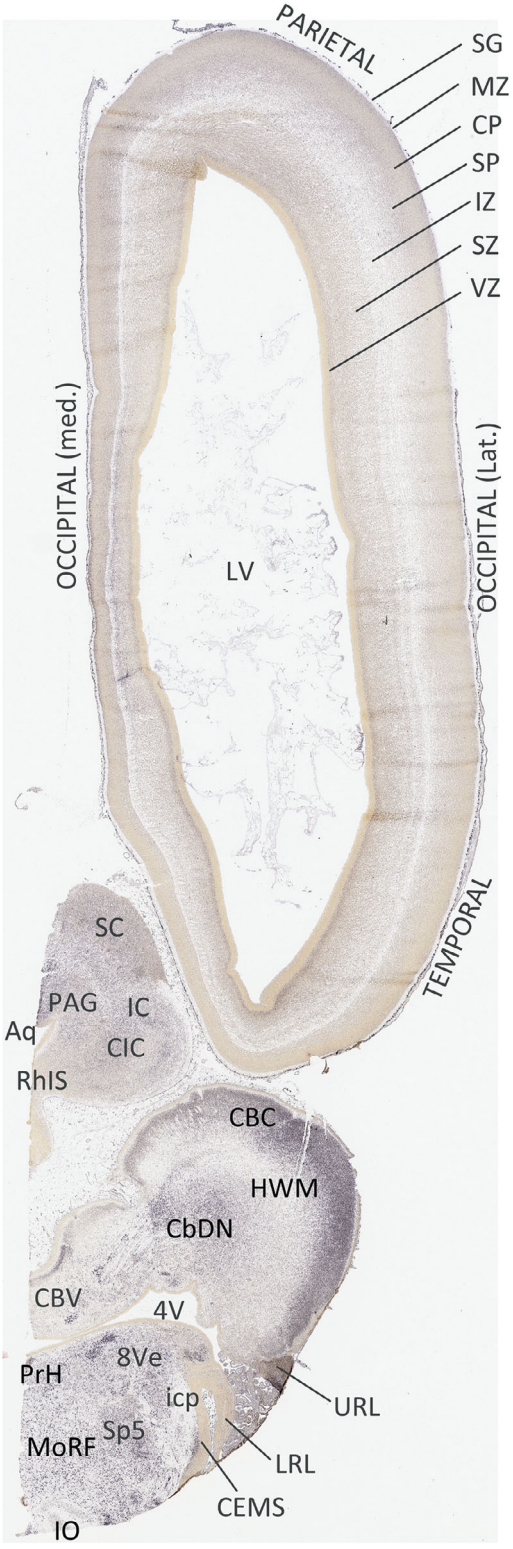

CNTNAP2-02-396 (Level ~40)

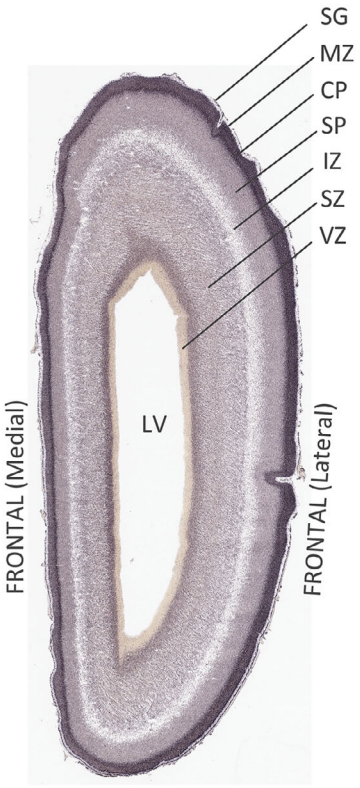

DCX-01-56 (Level ~2)

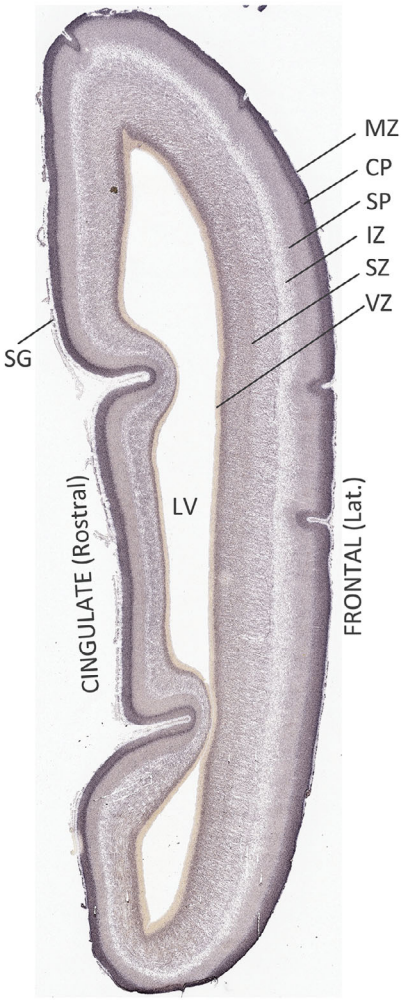

DCX-01-212 (Level ~5)

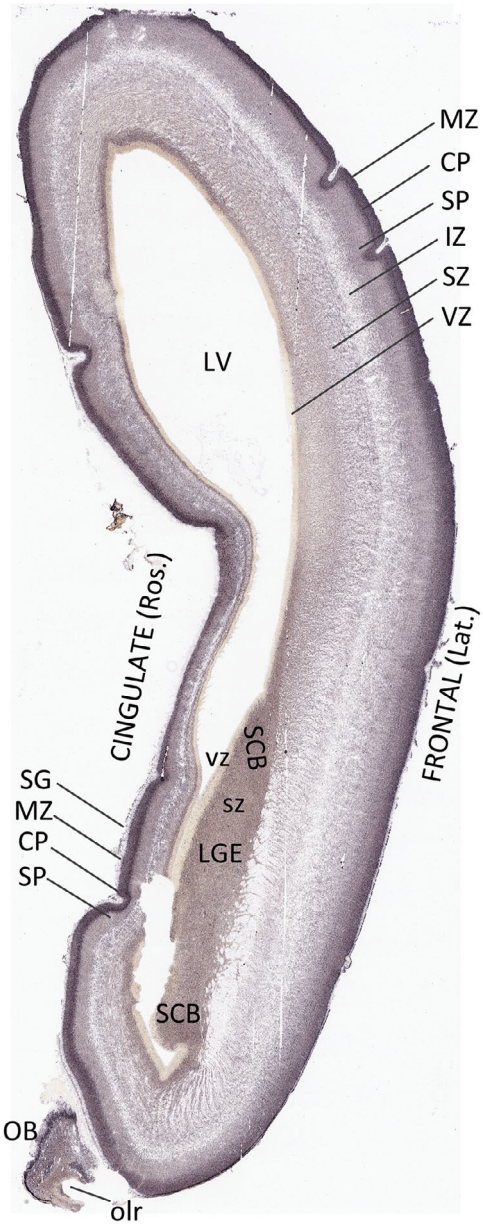

DCX-01-368 (Level ~10)

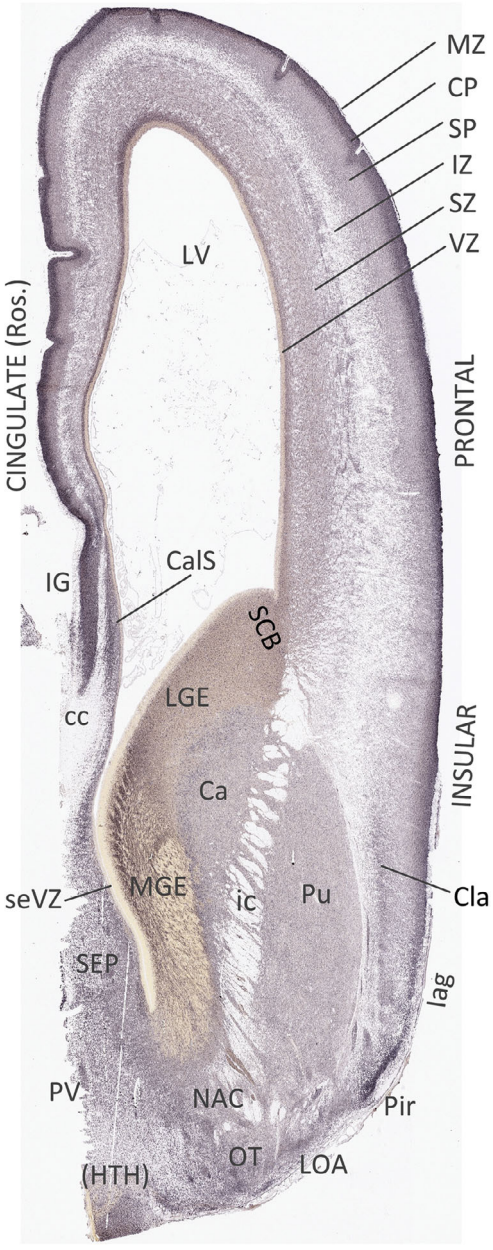

DCX-01-524 (Level ~16)

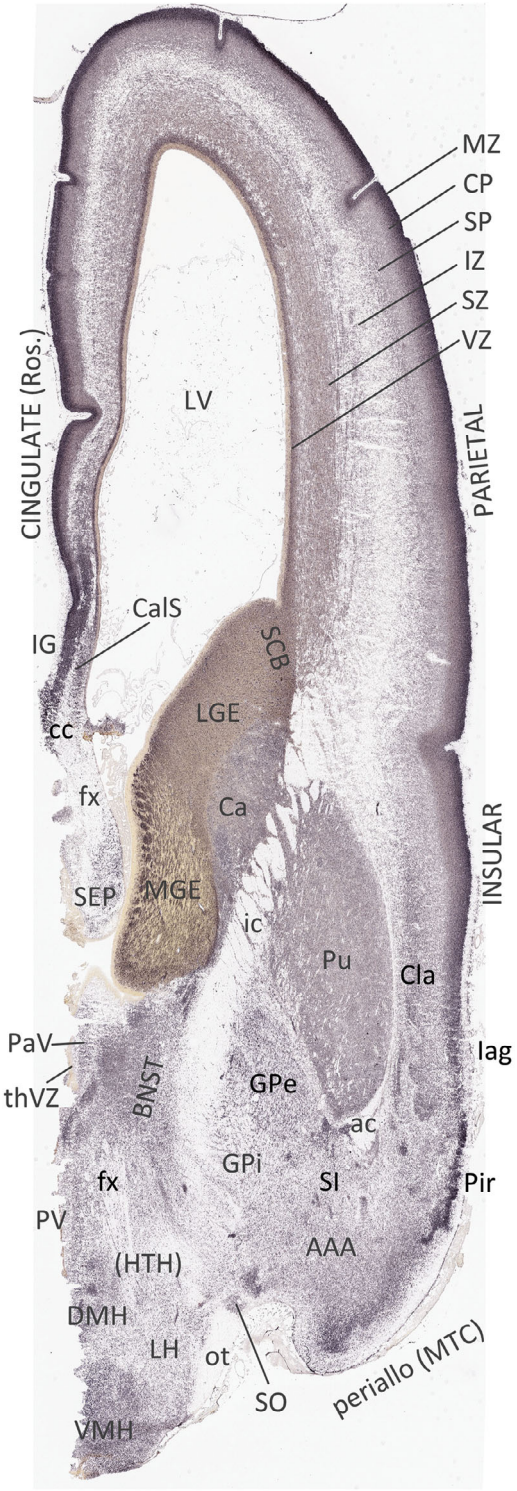

DCX-01-628 (Level ~19-20)

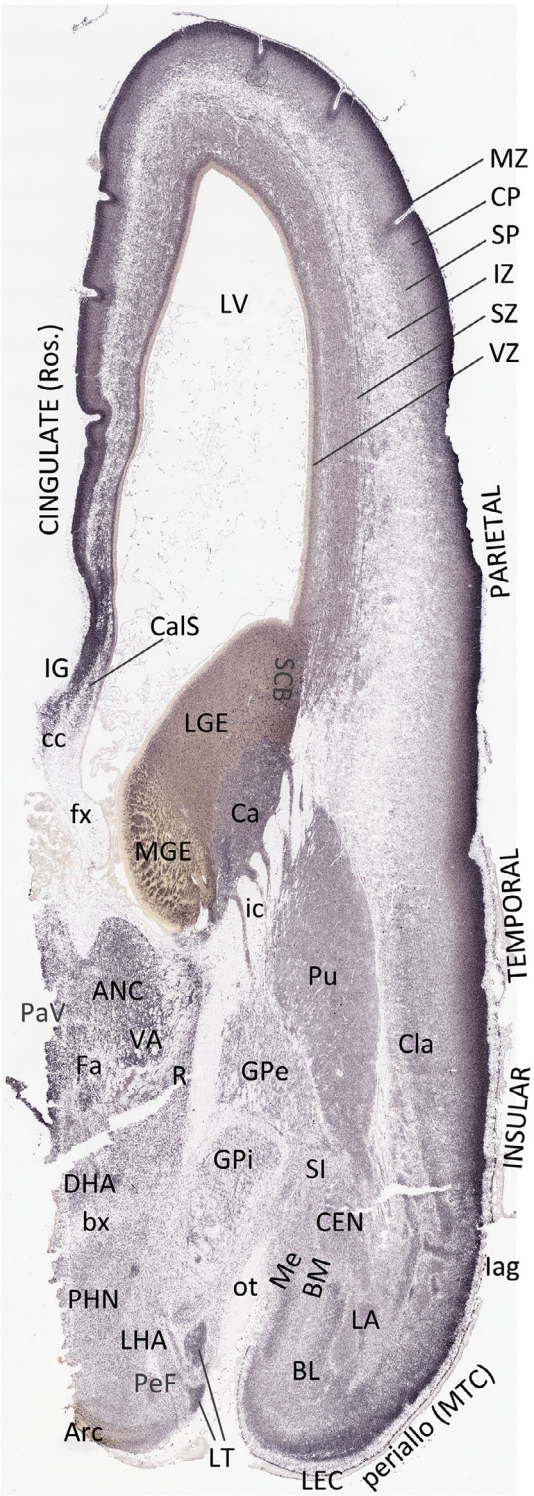

DCX-01-680 (Level ~21)

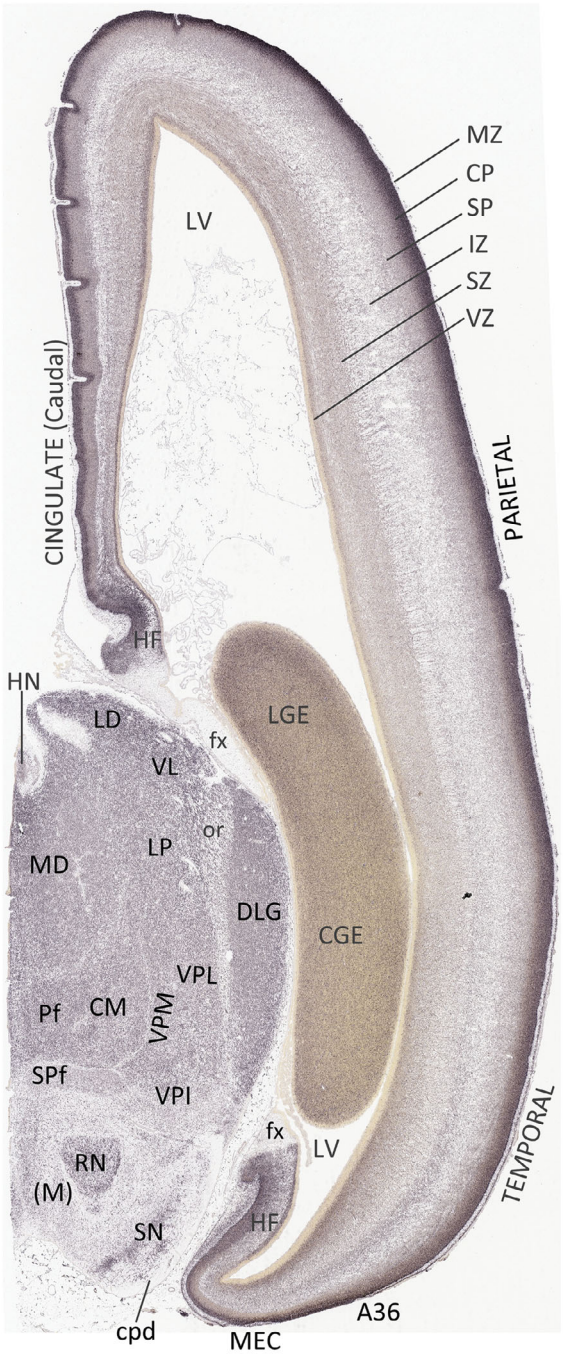

DCX-02-56 (Level ~26-27)

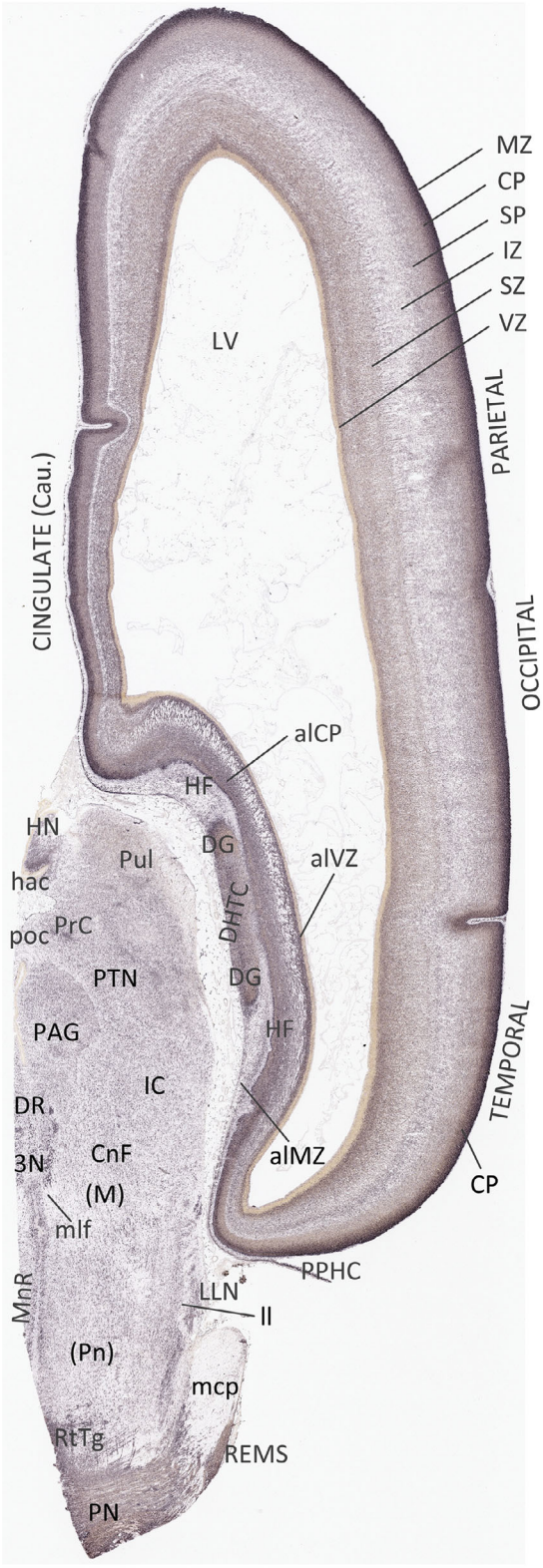

DCX-02-212 (Level ~32-33)

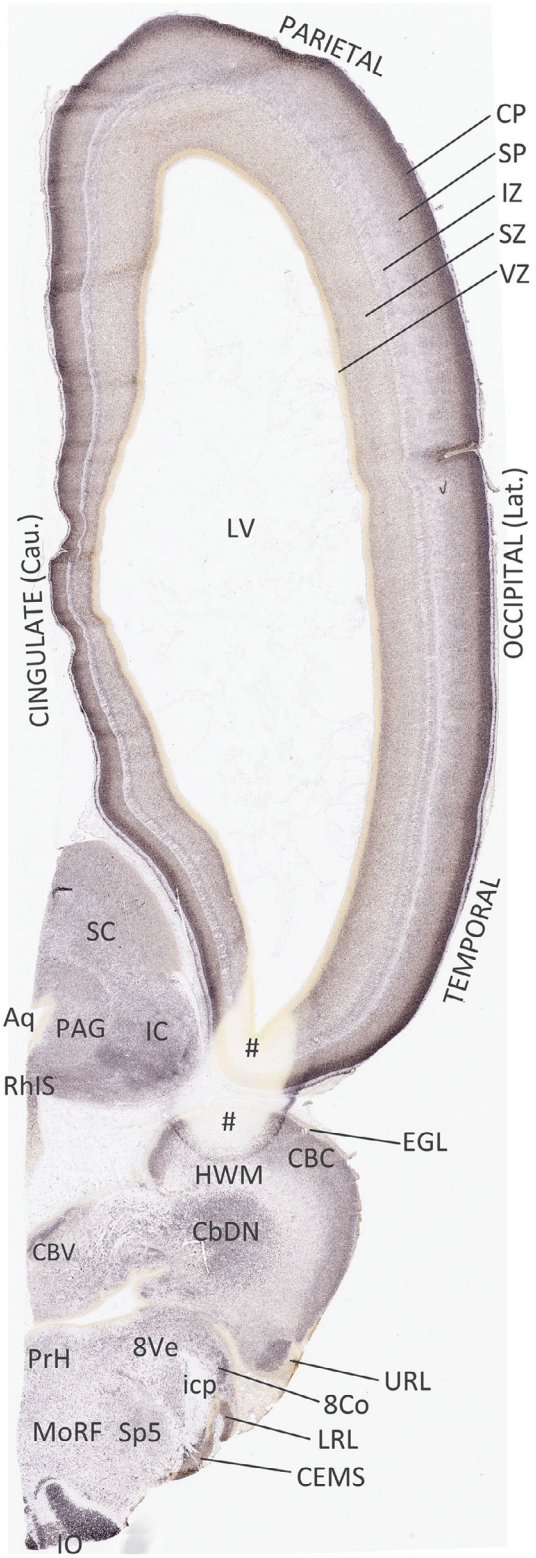

DCX-02-368 (Level ~39)

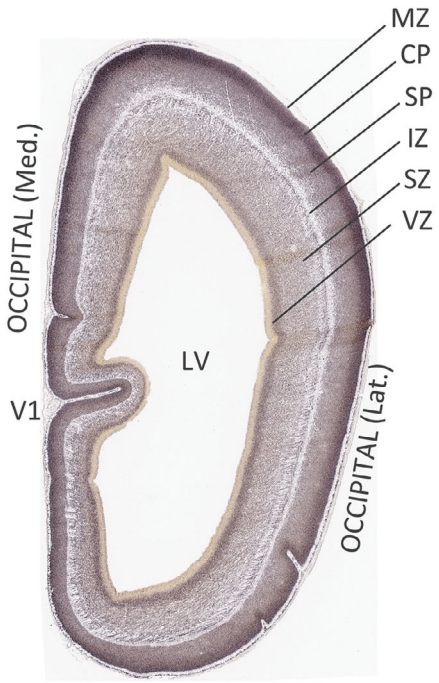

DCX-02-524 (Level ~43)

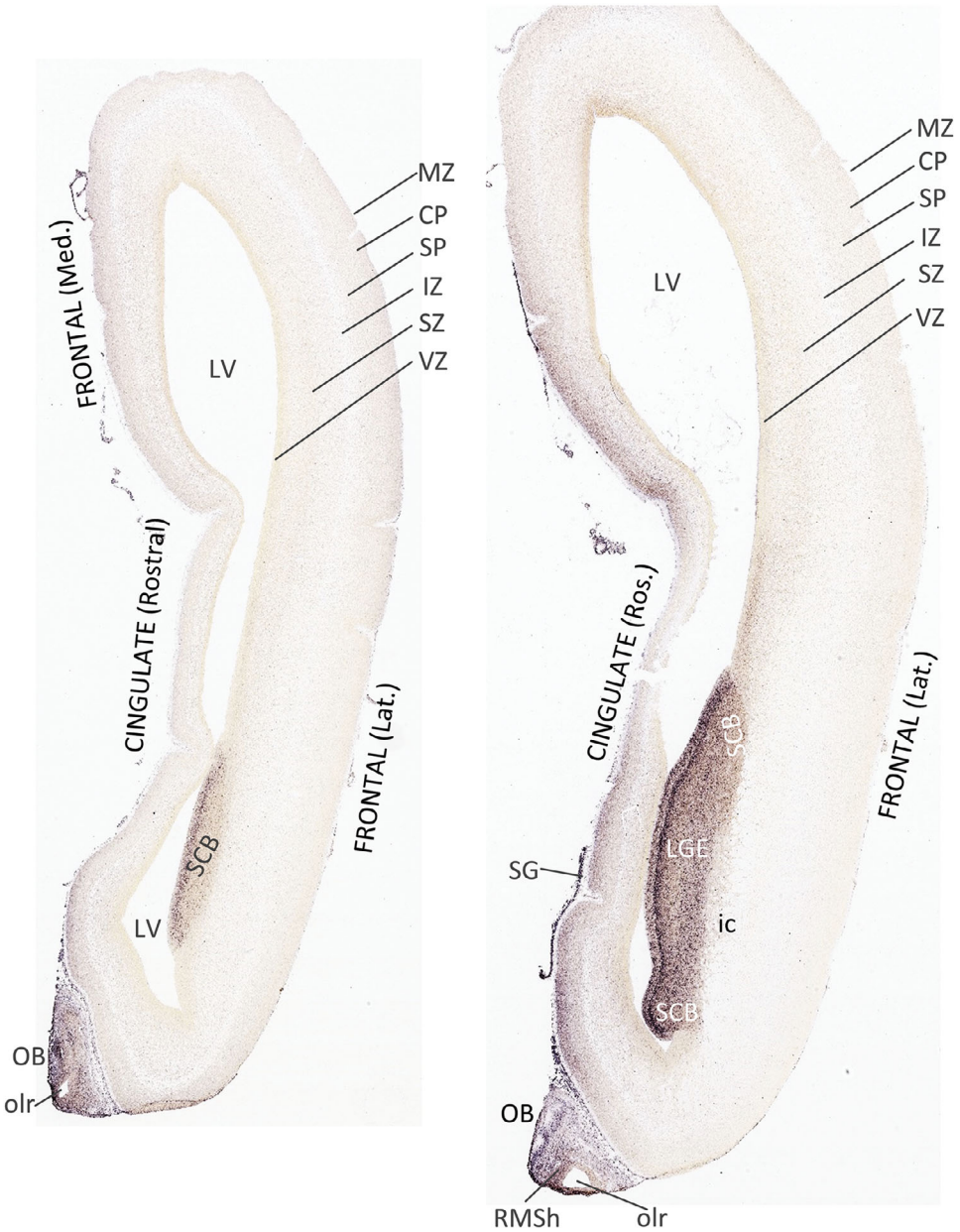

DLX1-01-324 (Level ~8) **DLX1-01-376 (Level ~10-11)**

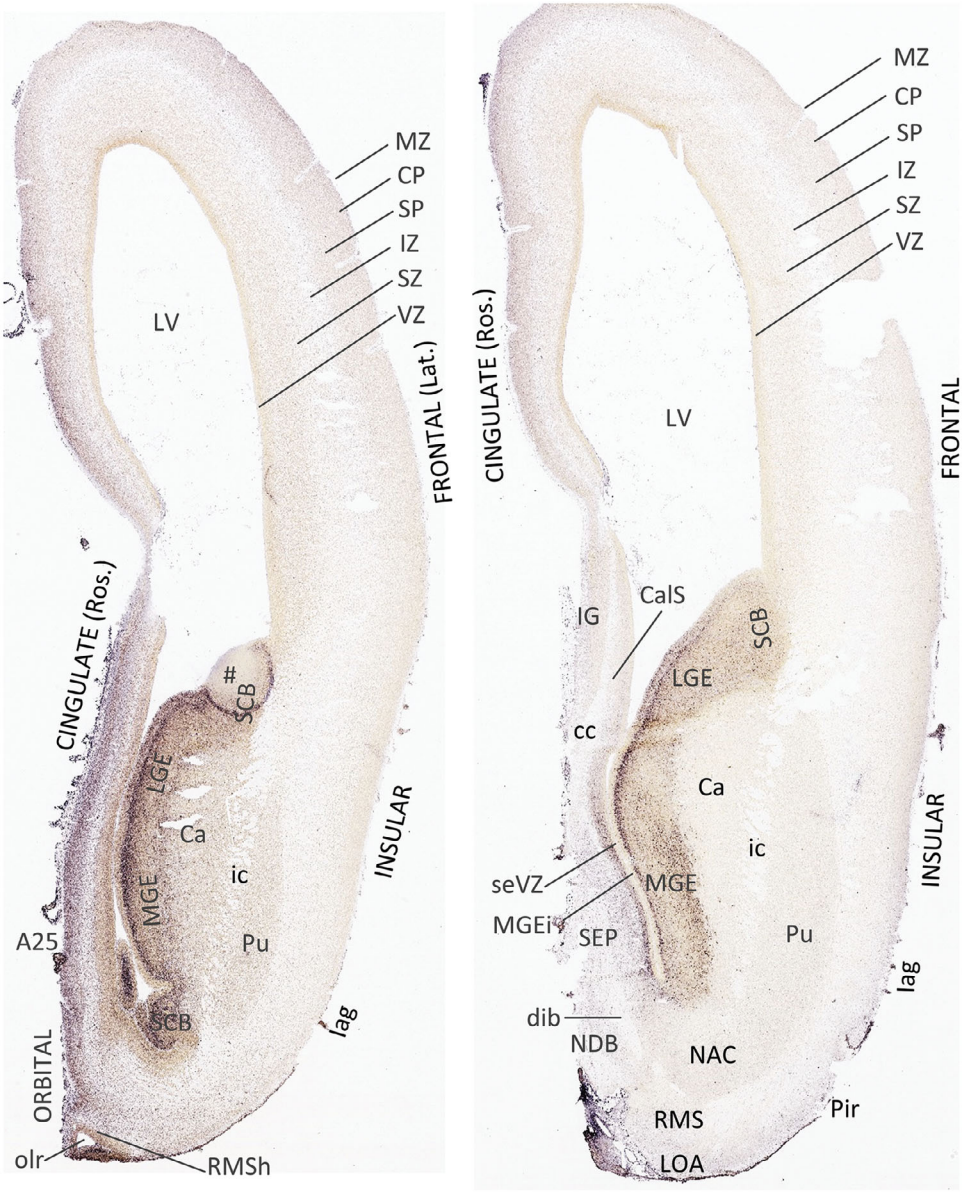

DLX1-01-428 (Level ~12) **DLX1-01-480 (Level ~14-15)**

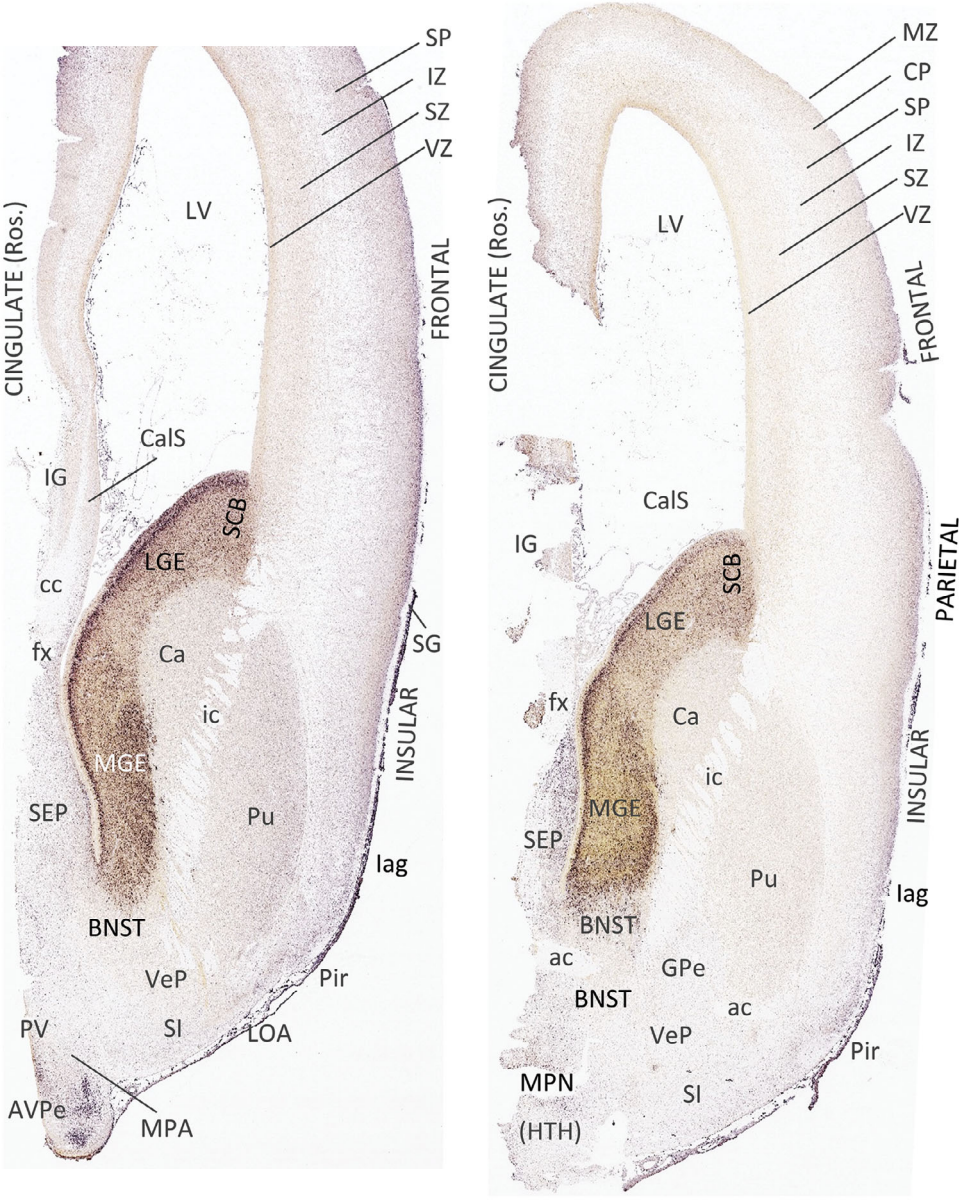

DLX1-01-532 (Level ~16) **DLX1-01-584 (Level ~18)**

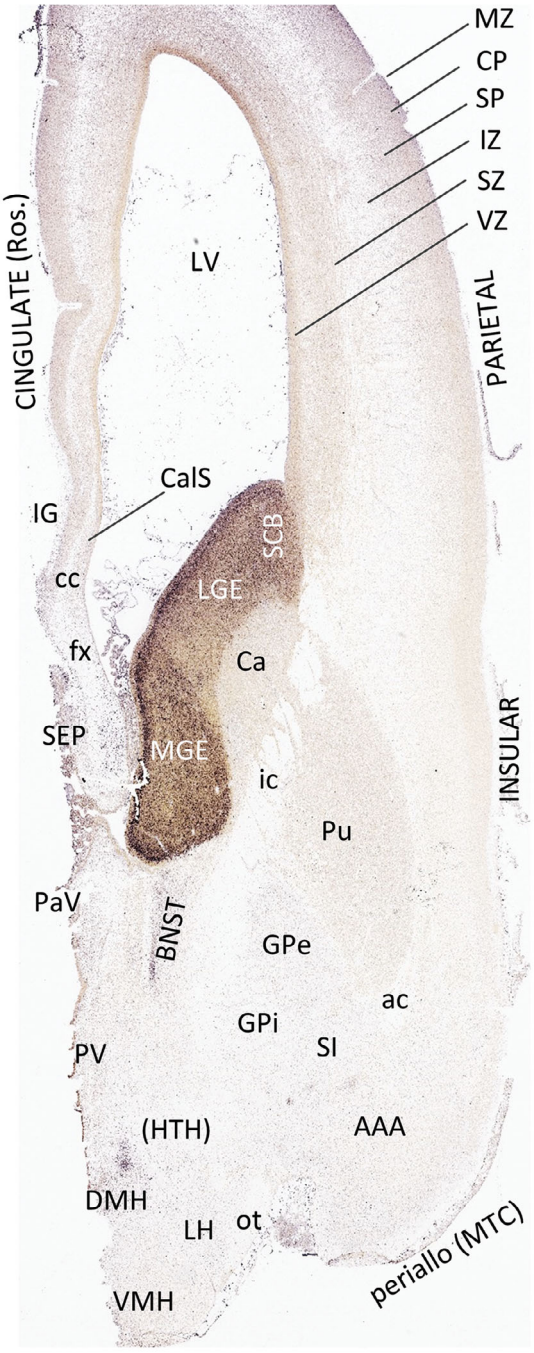

DLX1-01-636 (Level ~20)

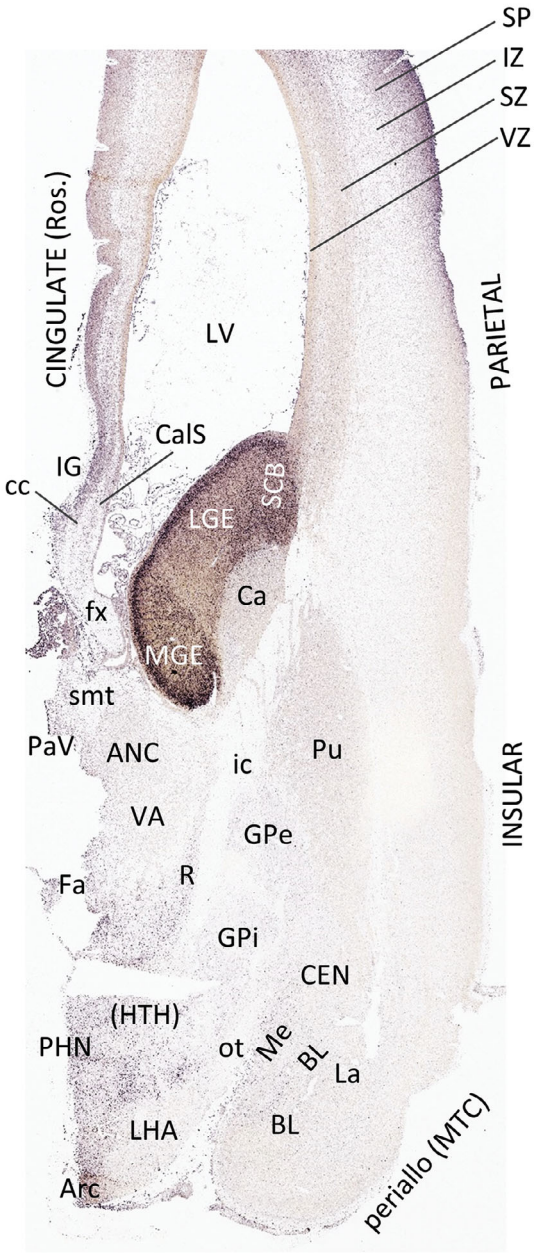

DLX1-01-688 (Level ~21)

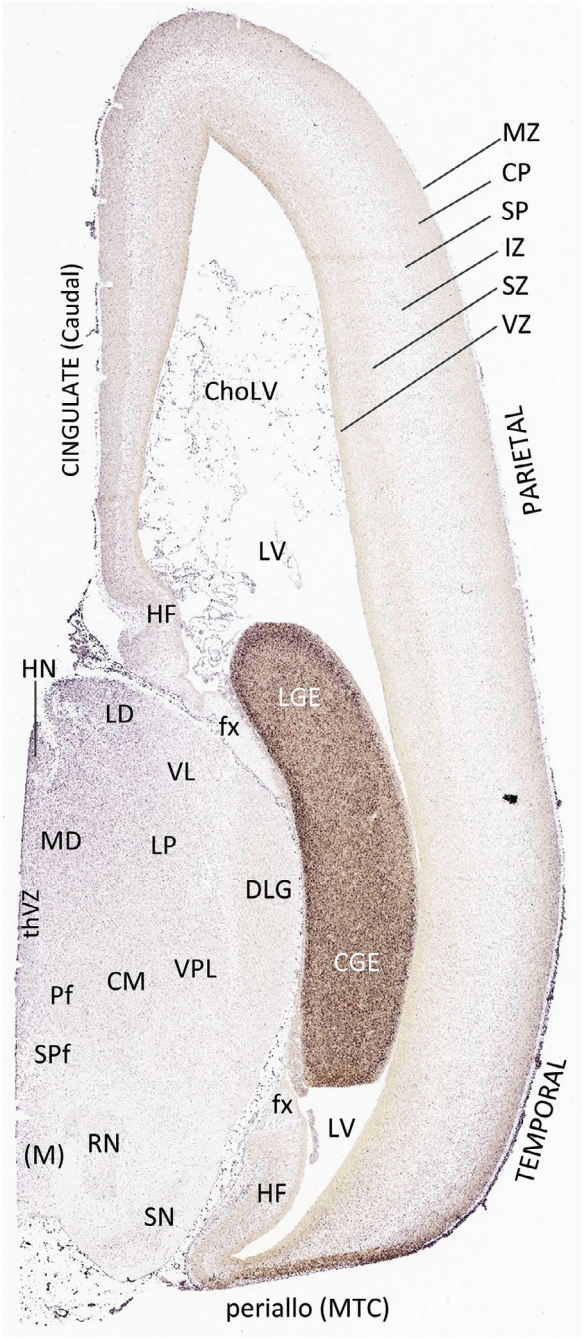

DLX1-02-064 (Level ~27)

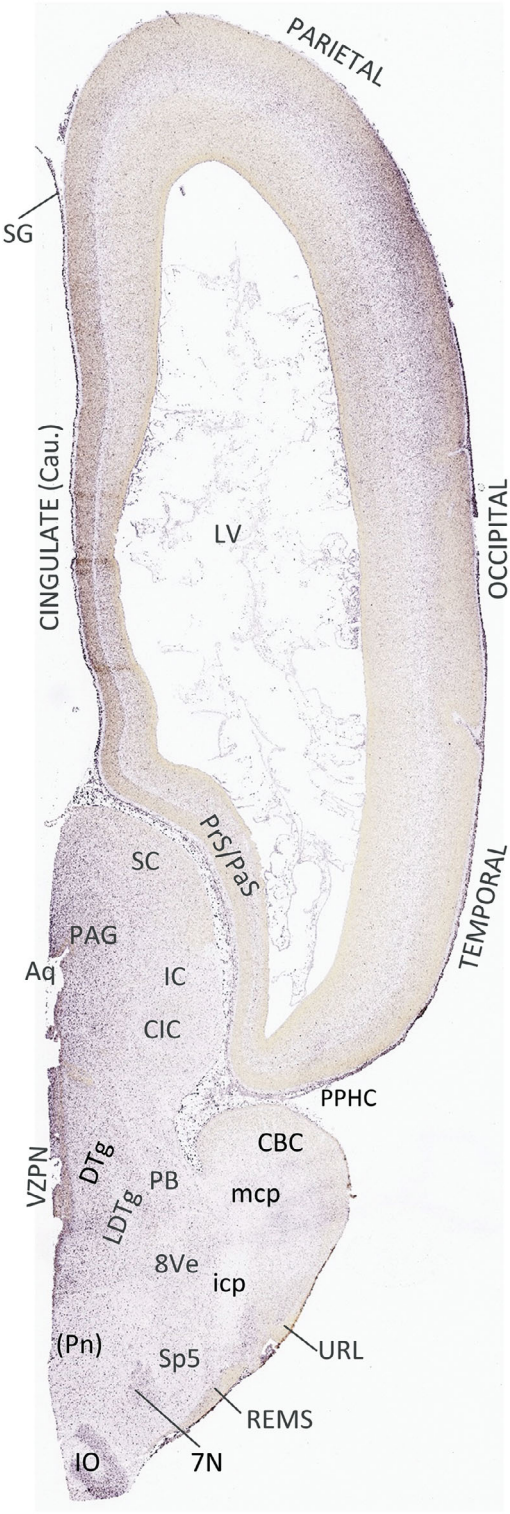

DLX1-02-324 (Level ~37)

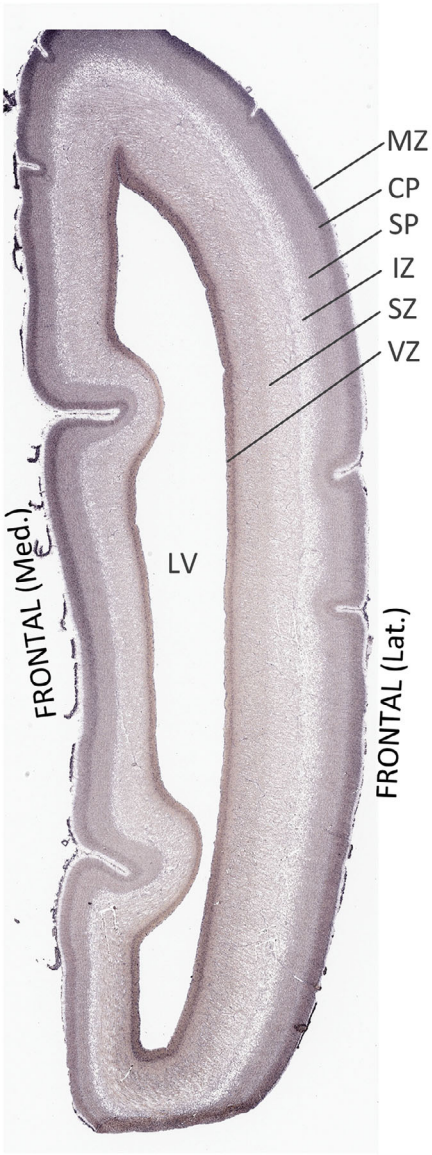

DLX2-01-169 (Level ~4)

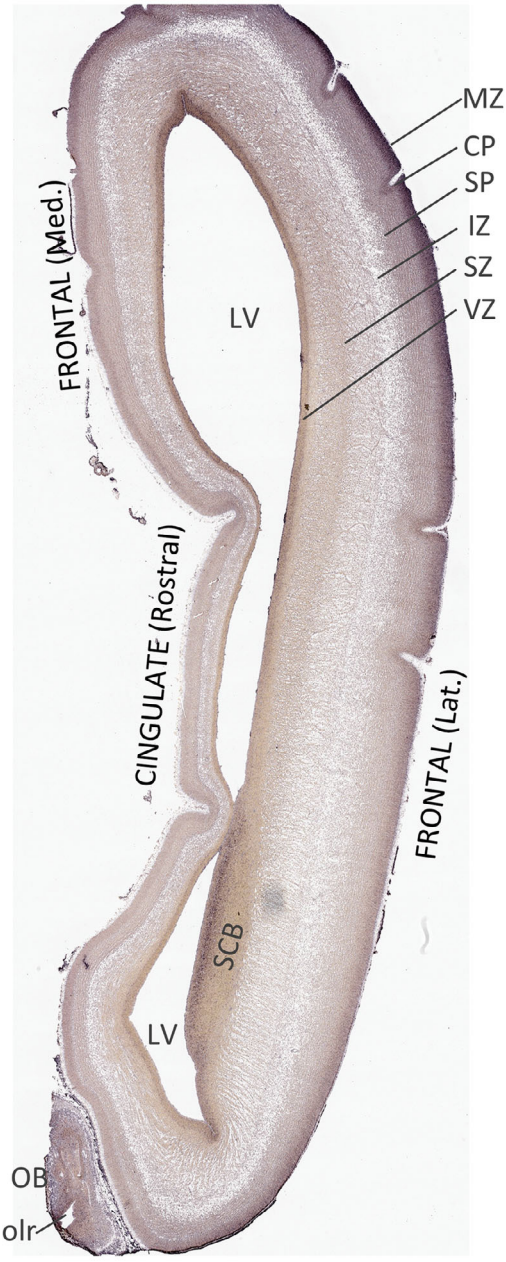

DLX2-01-325 (Level ~8)

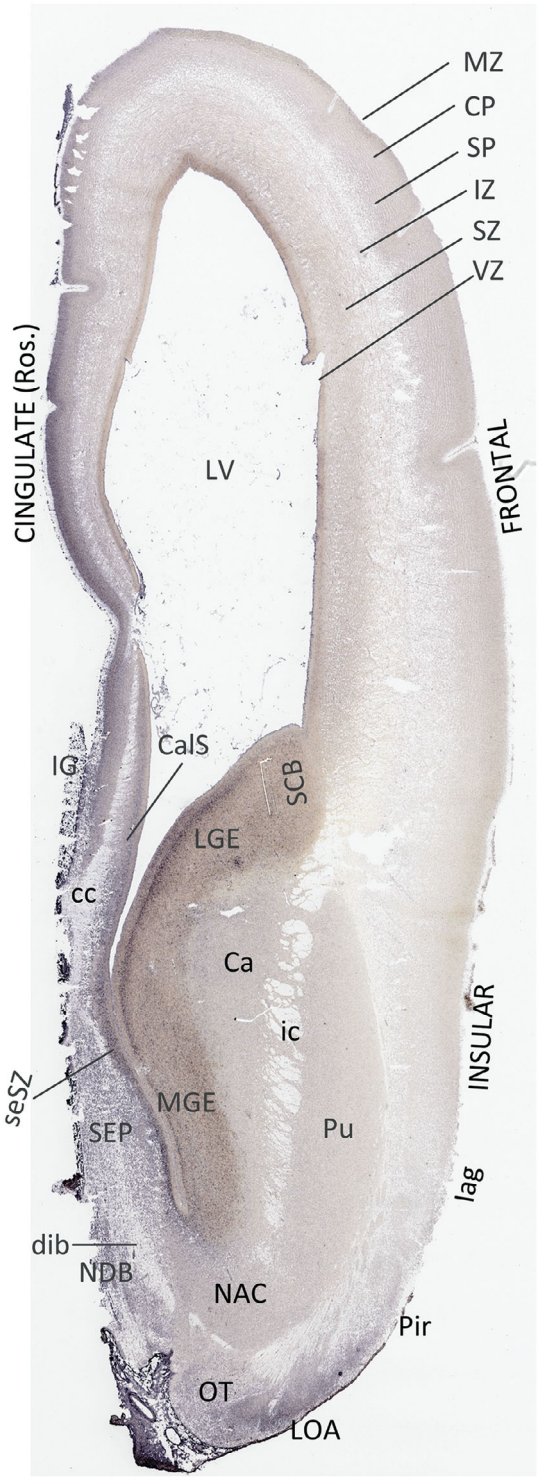

DLX2-01-481 (Level ~15)

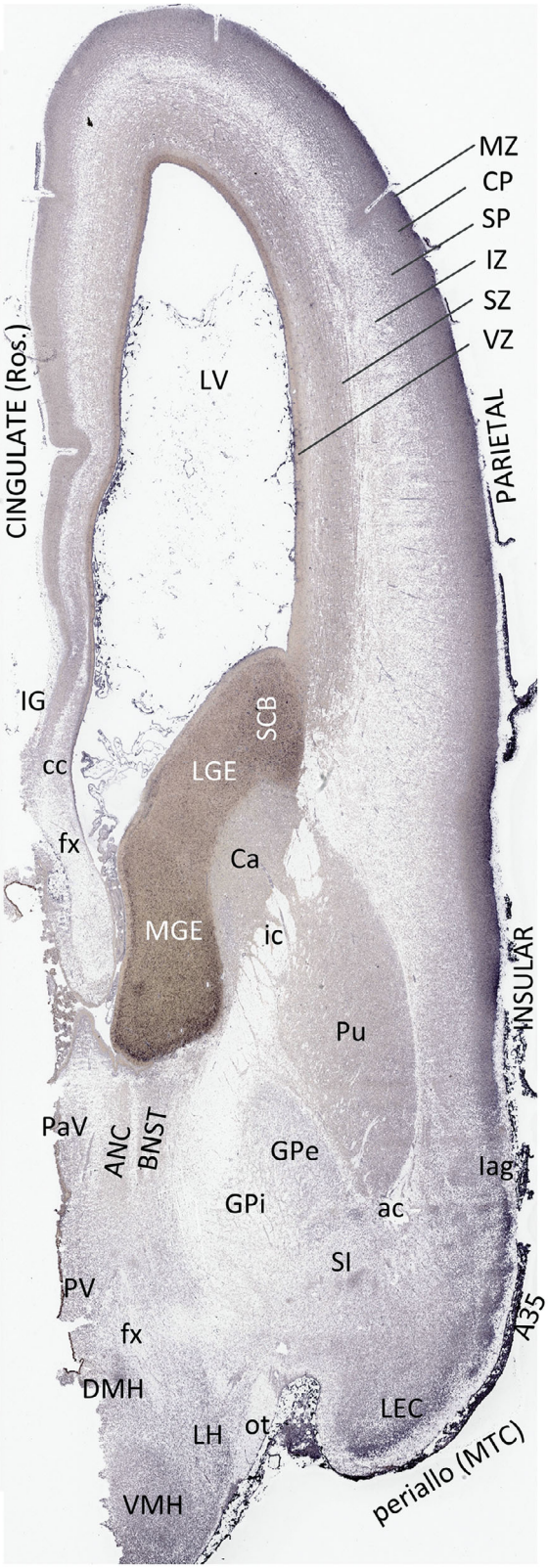

DLX2-01-637 (Level ~20)

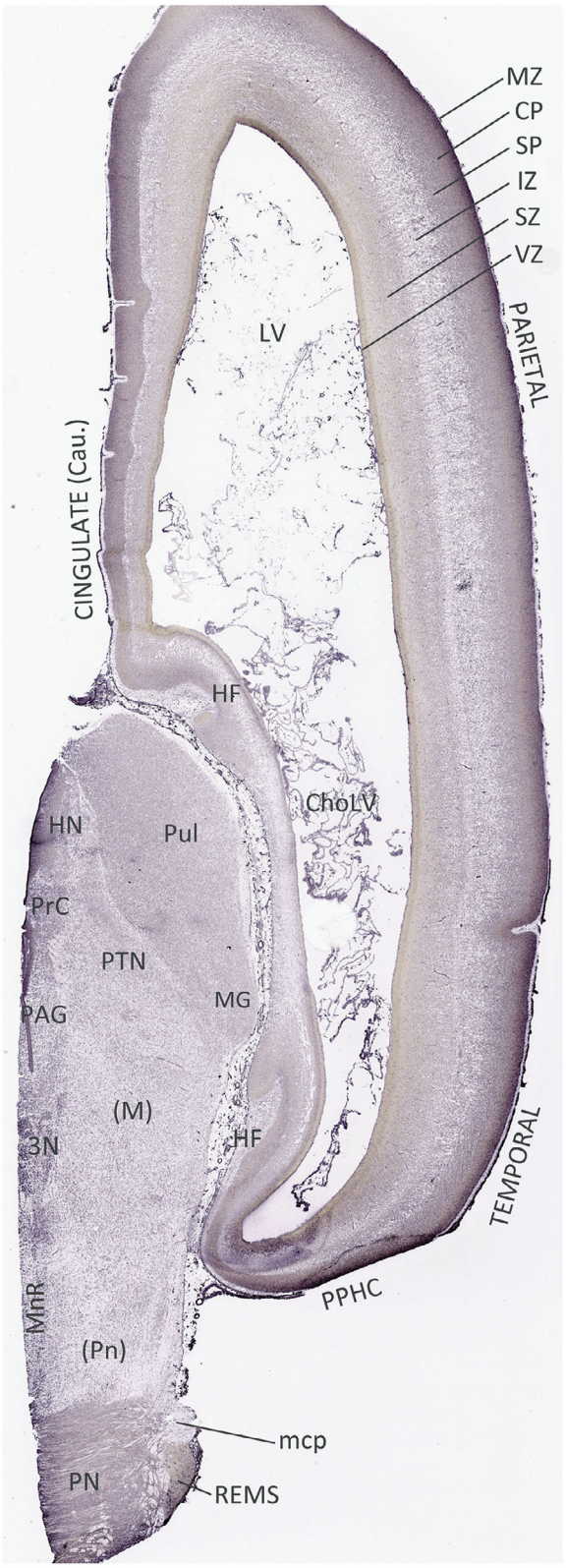

DLX2-02-169 (Level ~31)

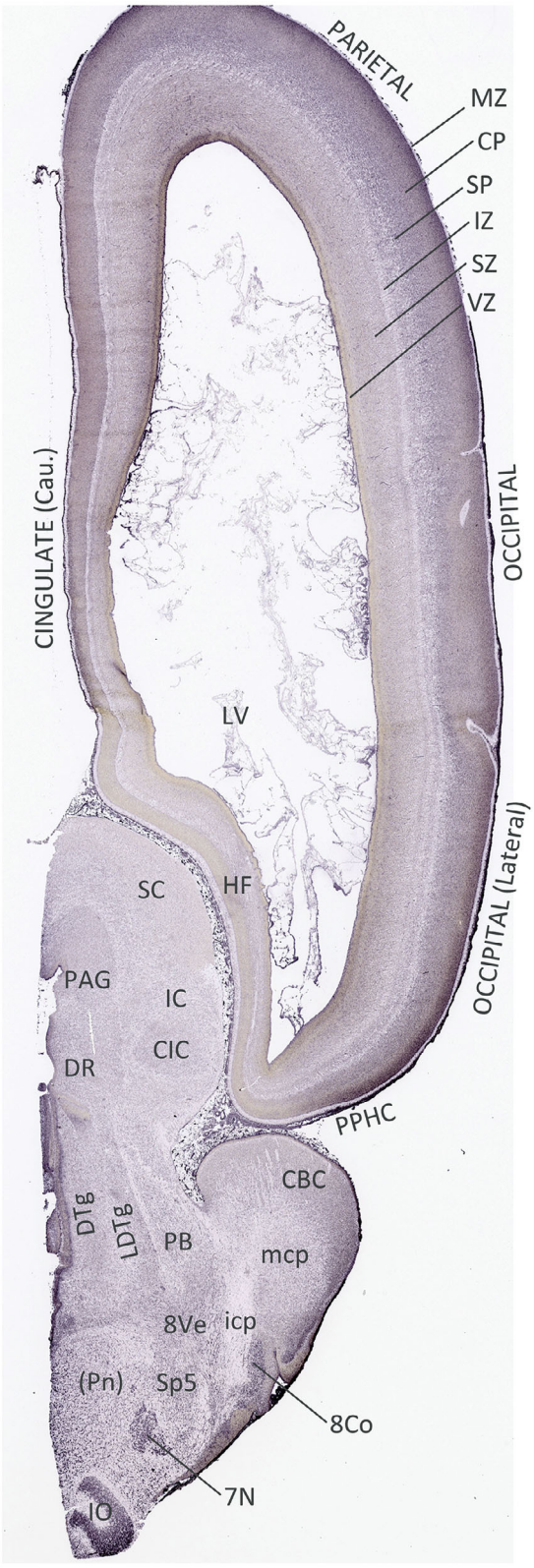

DLX2-02-235 (Level ~37)

DLX5-01-326 (Level ~8-9)

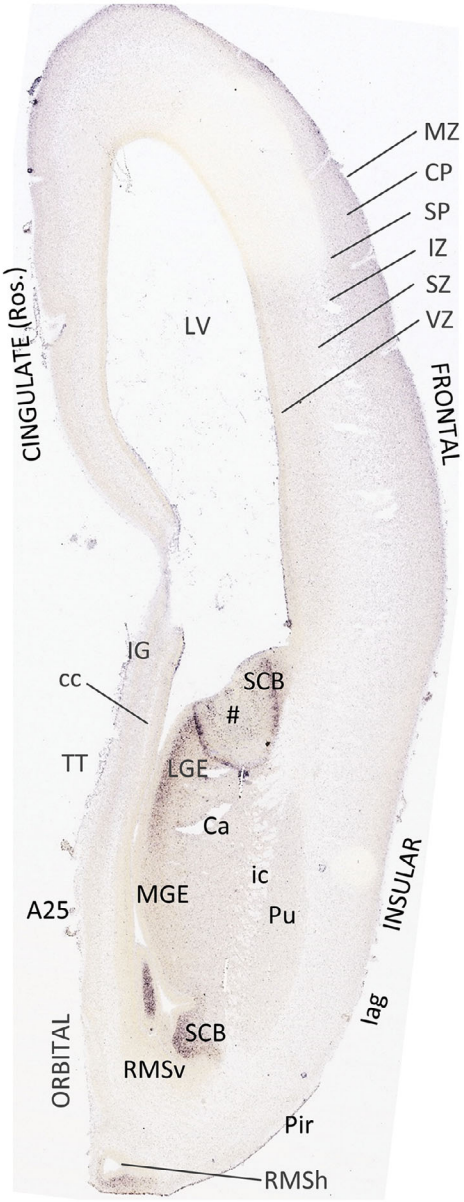

DLX5-01-430 (Level ~12-13)

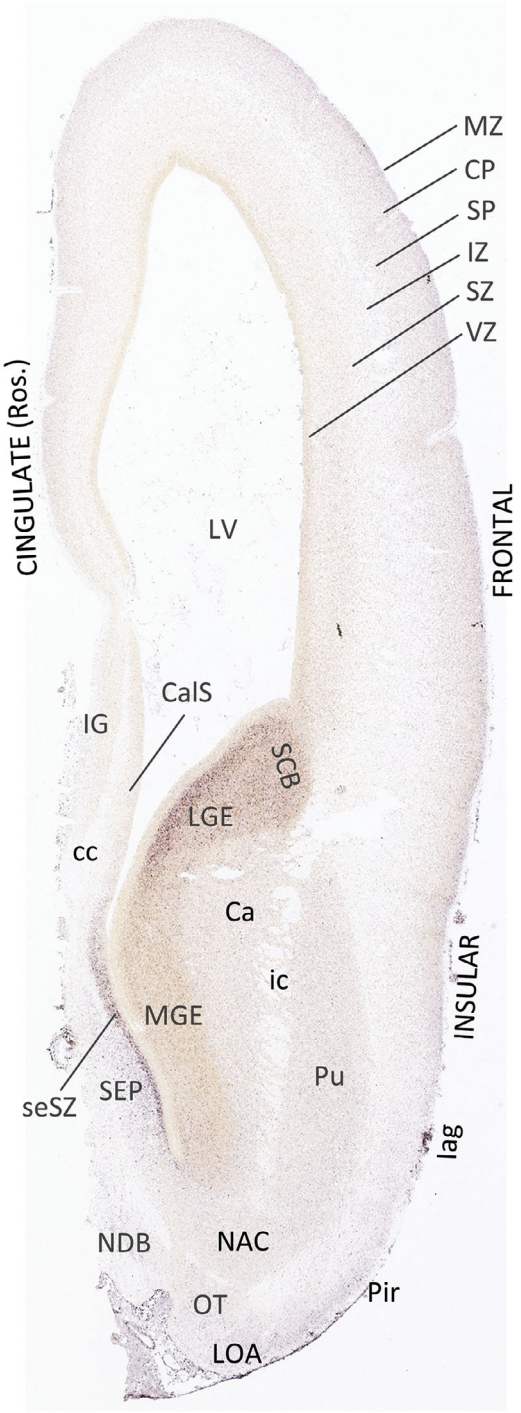

DLX5-01-482 (Level ~14-15)

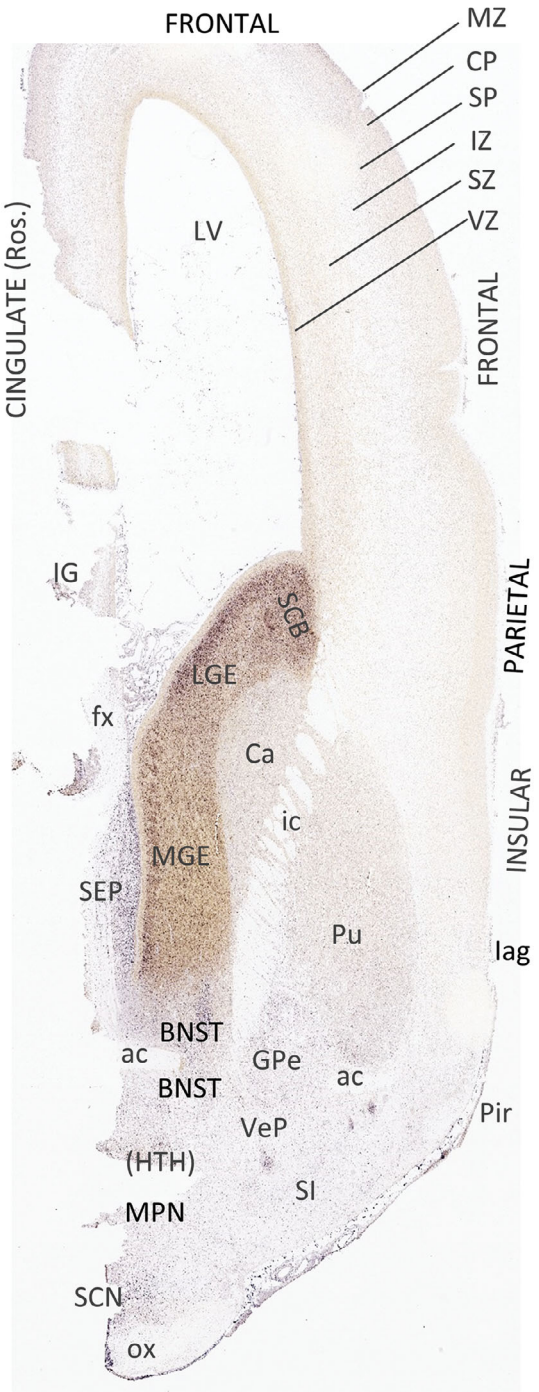

DLX5-01-586 (Level ~18)

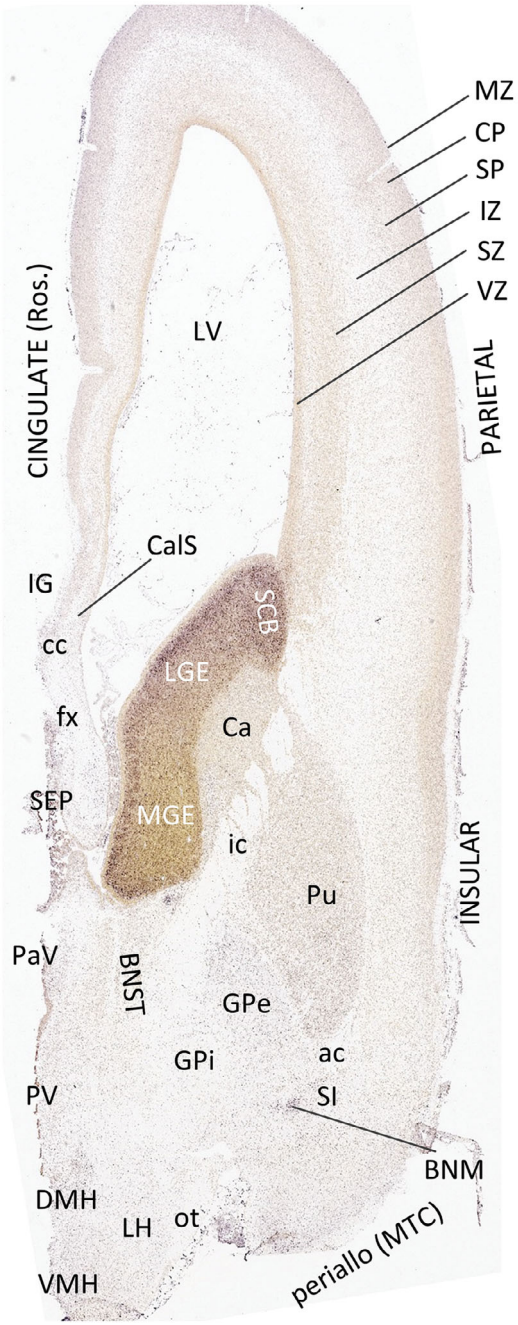

DLX5-01-638 (Level ~20)

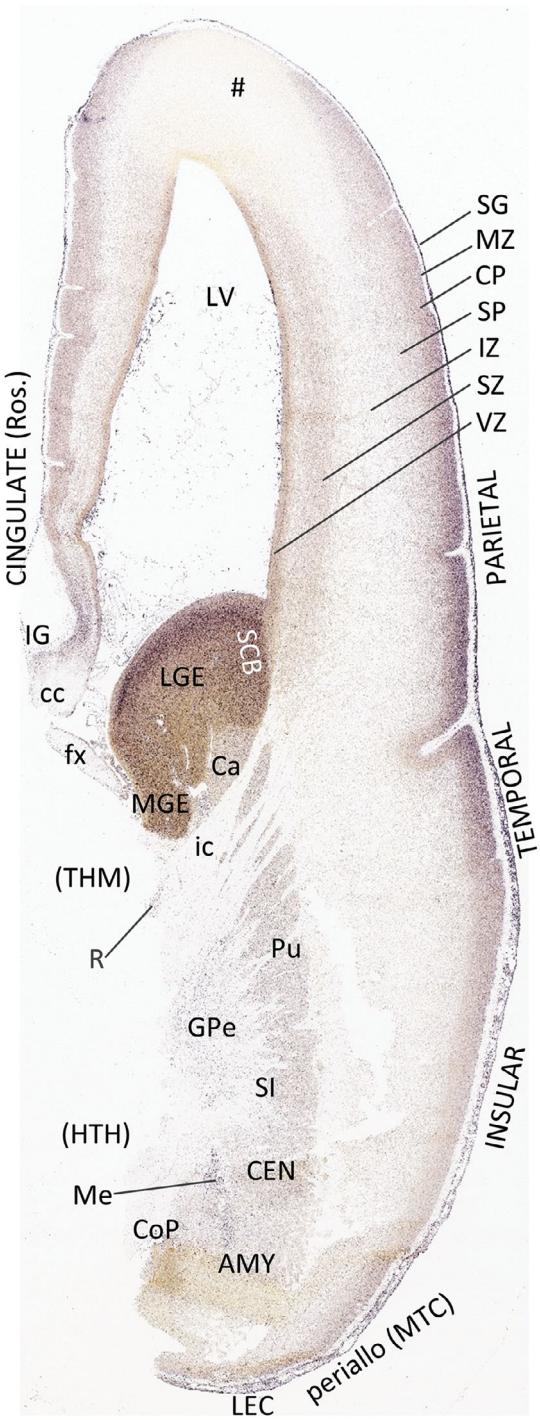

DLX5-01-742 (Level ~23)

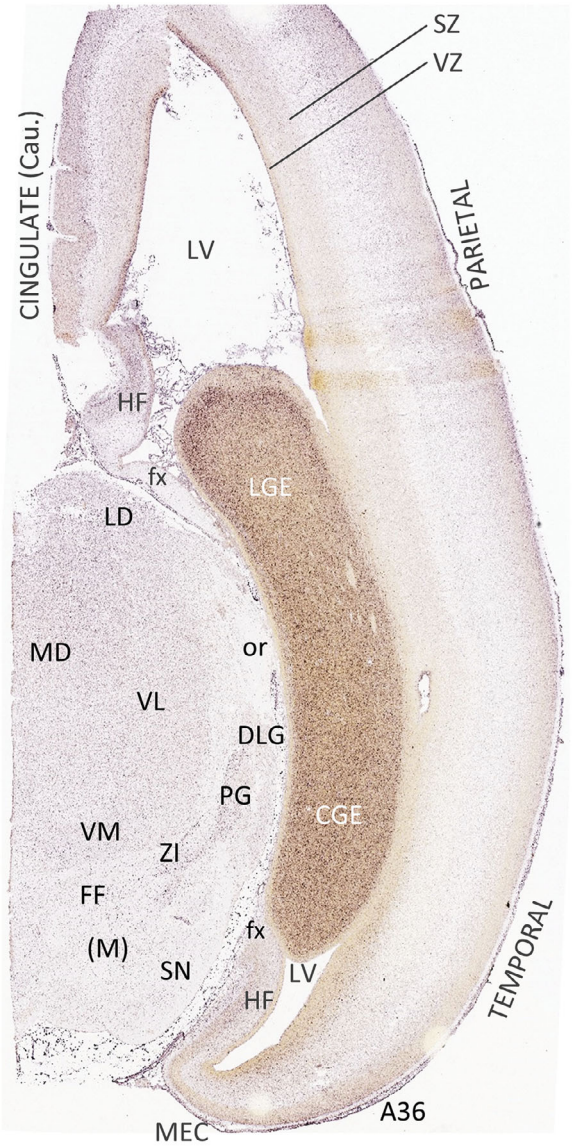

DLX5-02-014 (Level ~25)

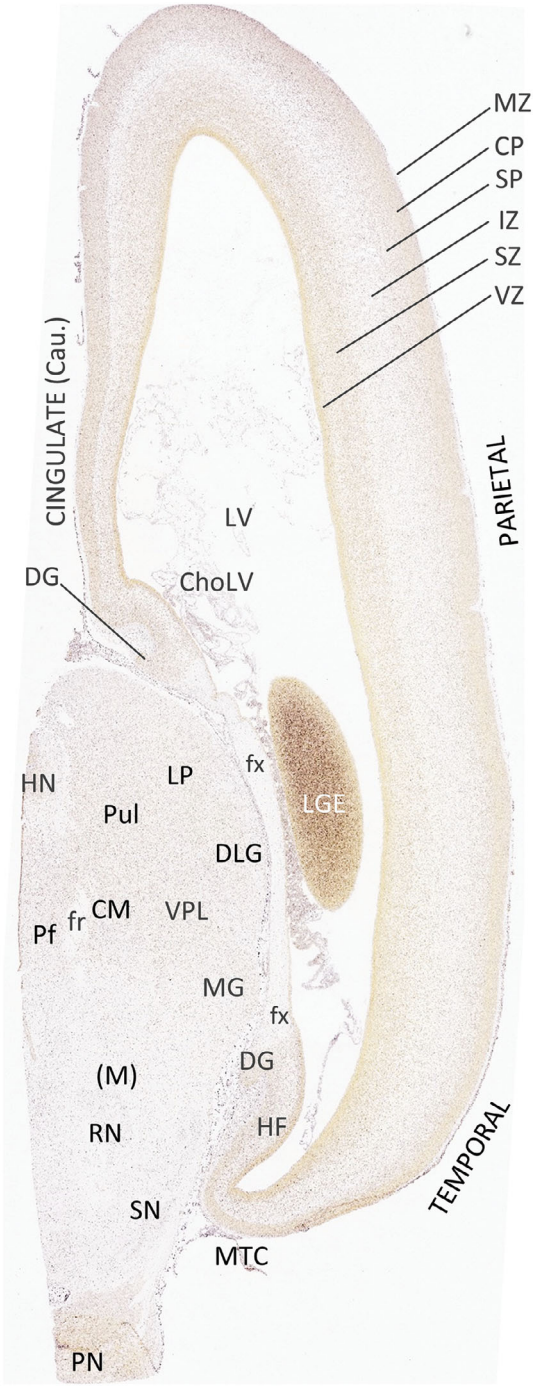

DLX5-02-118 (Level ~29)

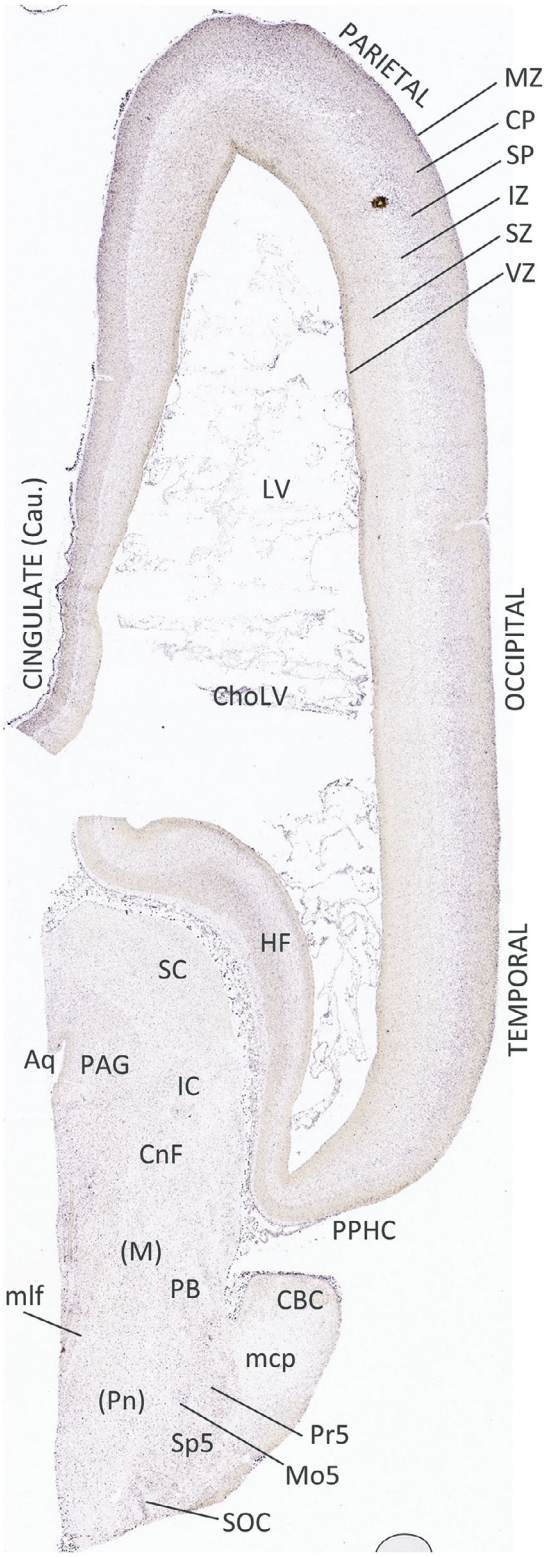

DLX5-02-274 (Level ~35)

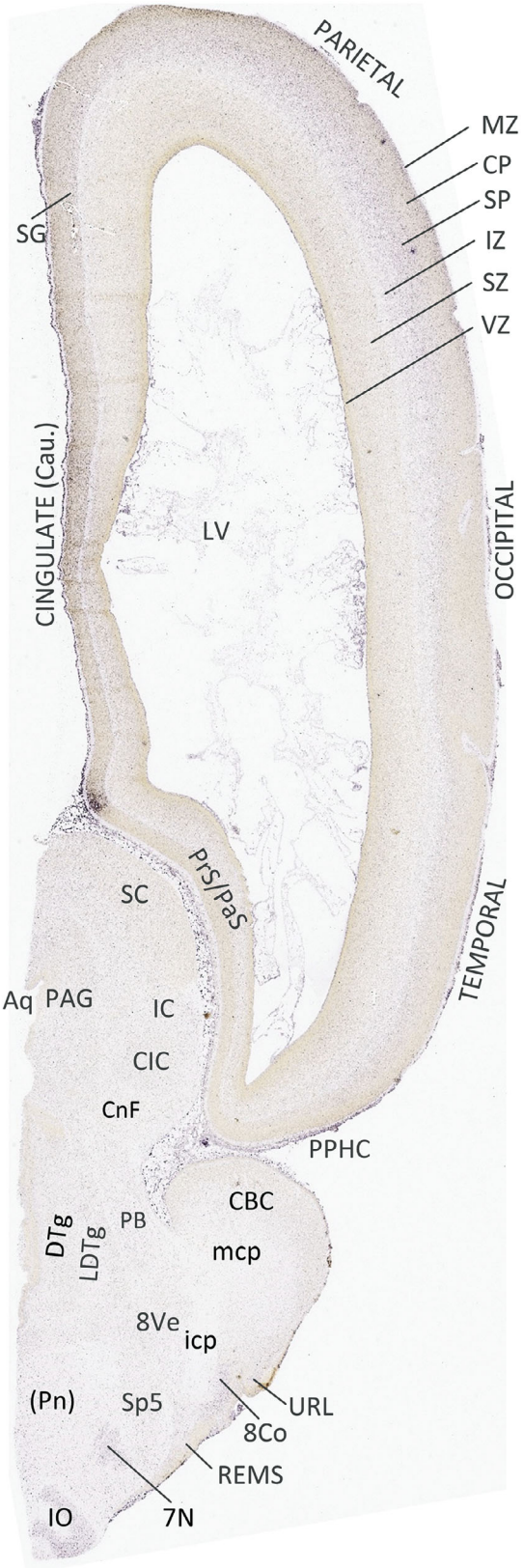

DLX5-02-326 (Level ~37)

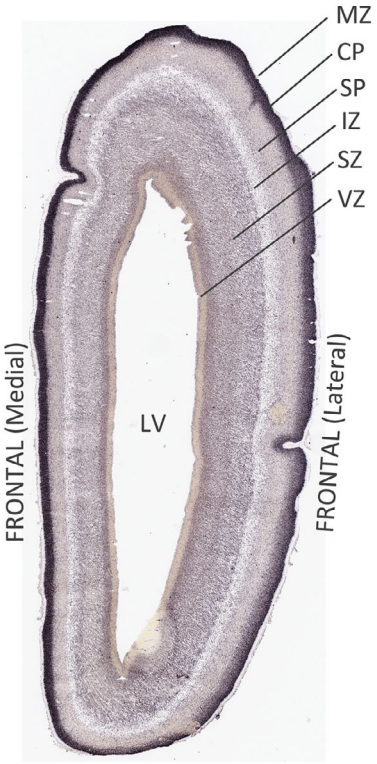

ENC1-01-81 (Level ~3)

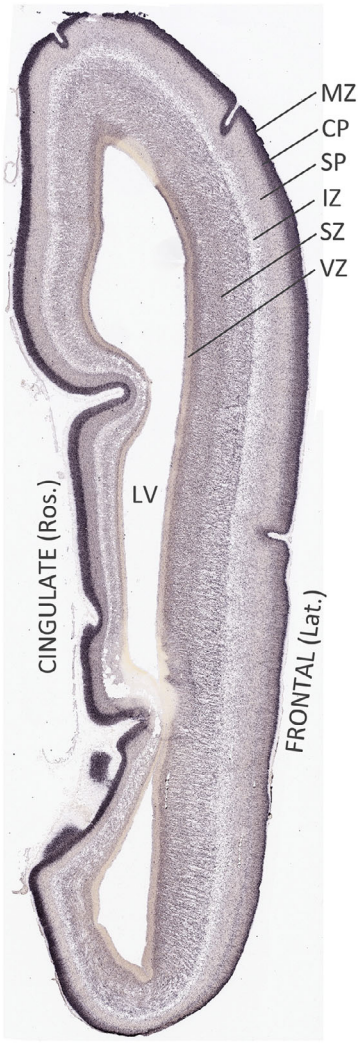

ENC1-01-237 (Level ~6)

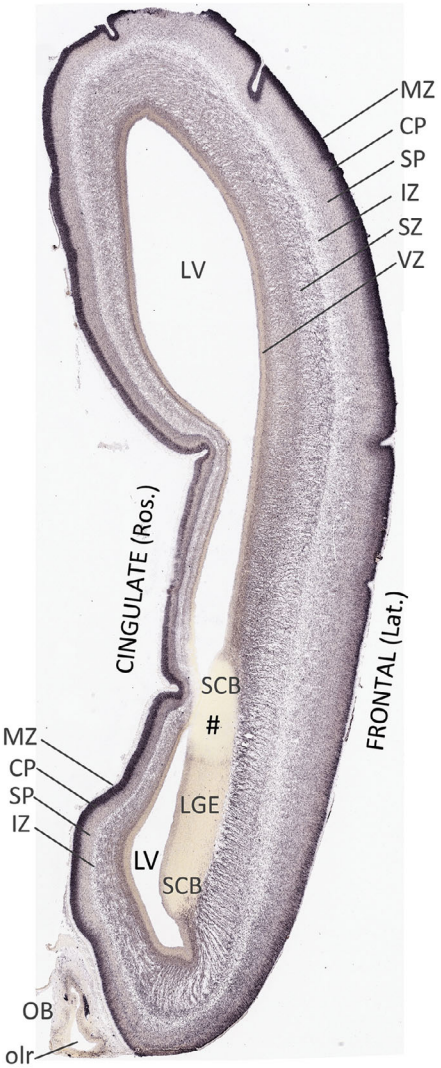

ENC1-01-341 (Level ~9)

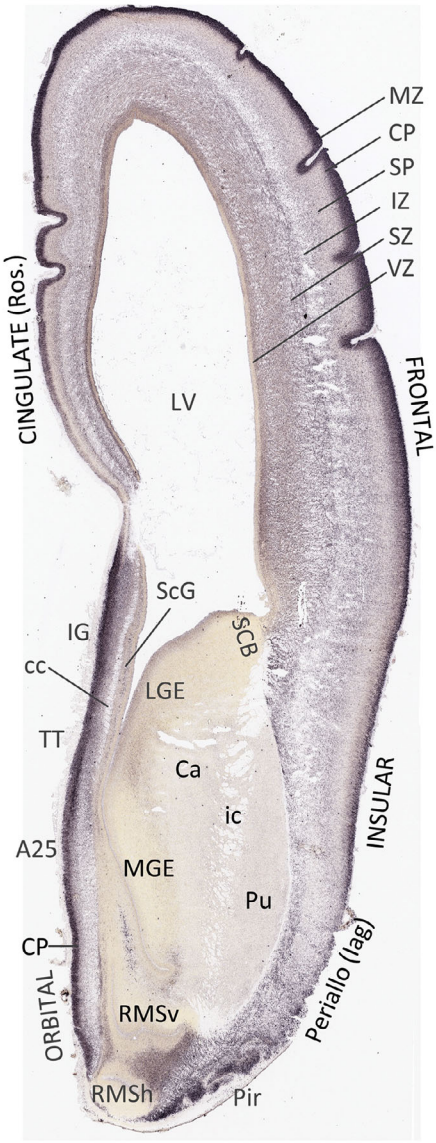

ENC1-01-445 (Level ~13)

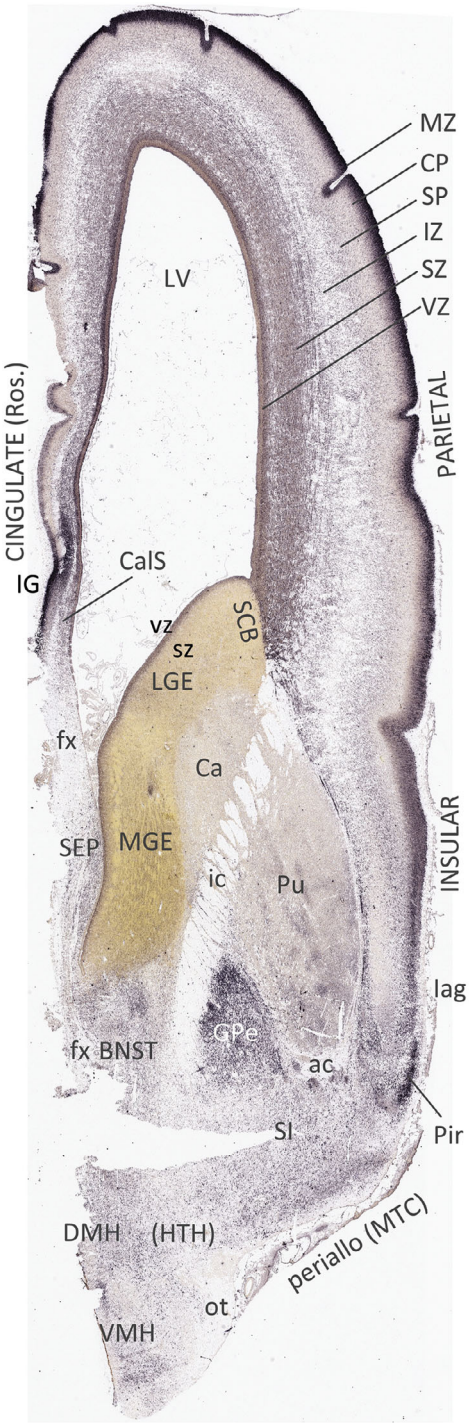

ENC1-01-601 (Level ~19)

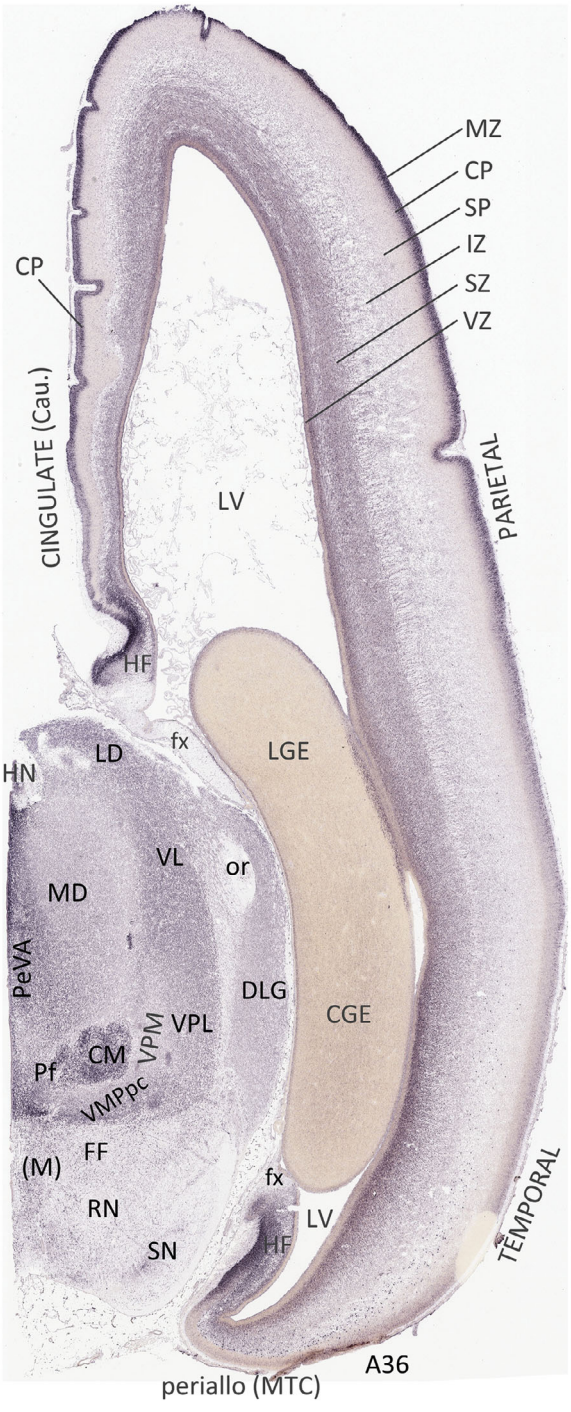

ENC1-02-29 (Level ~26)

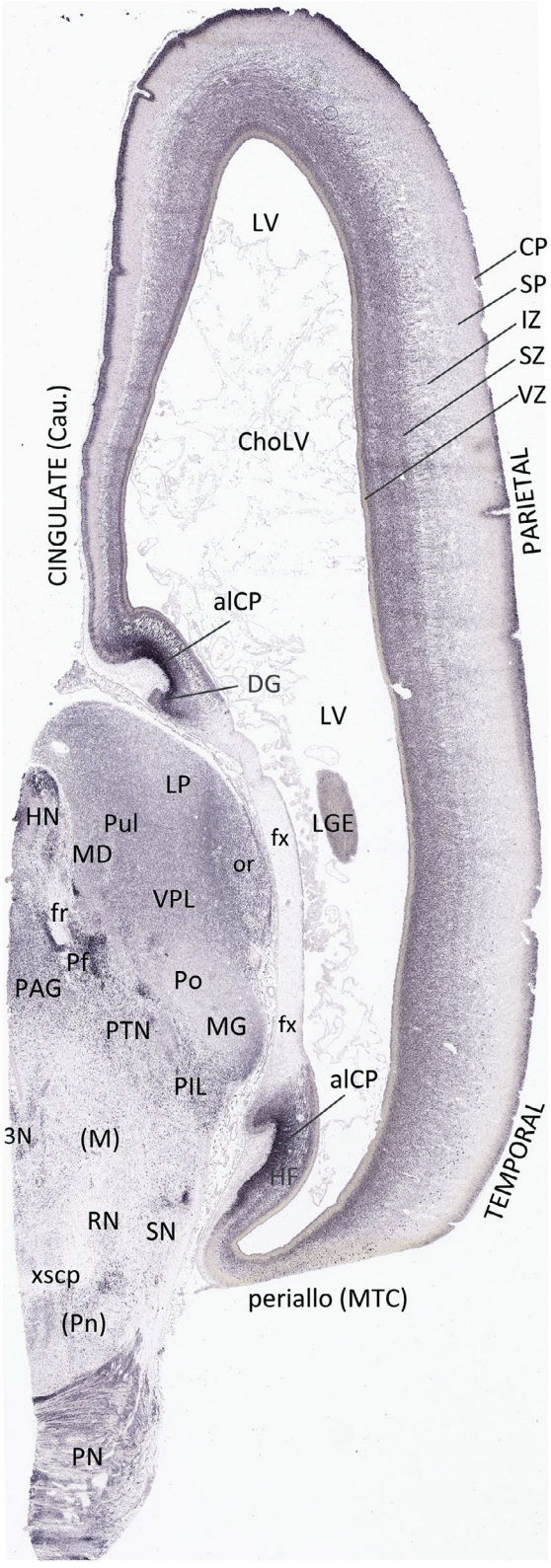

ENC1-02-133 (Level ~29-30)

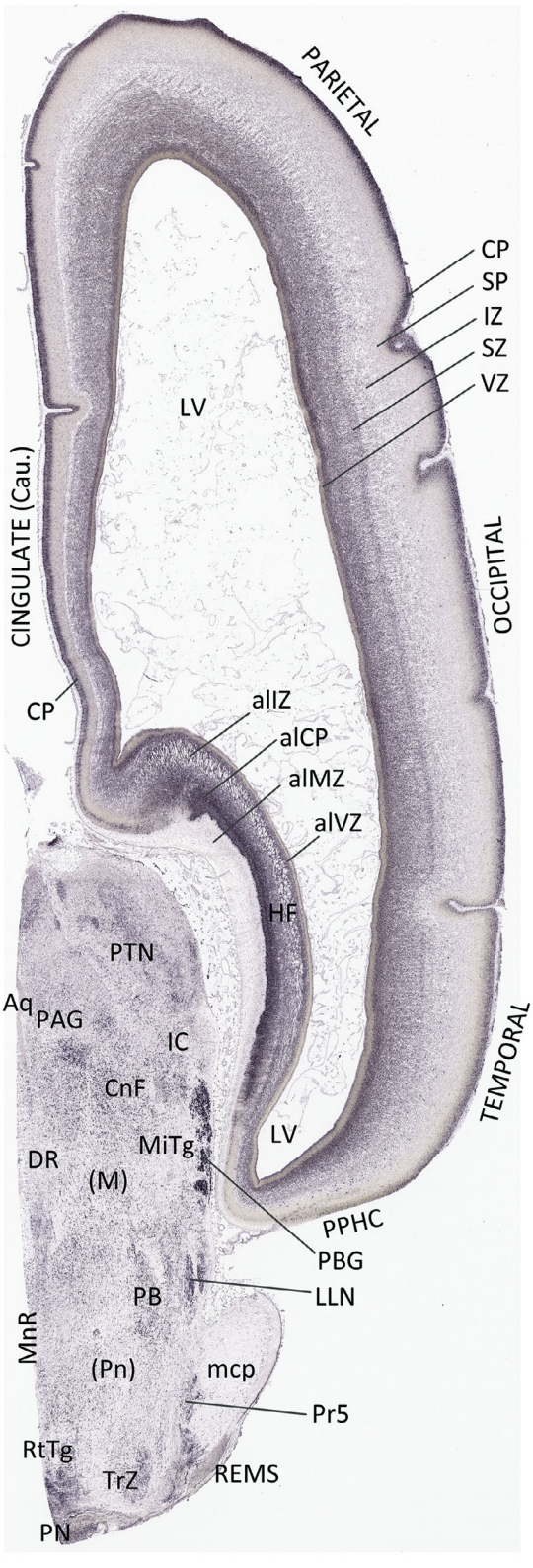

ENC1-02-237 (Level ~33-34)

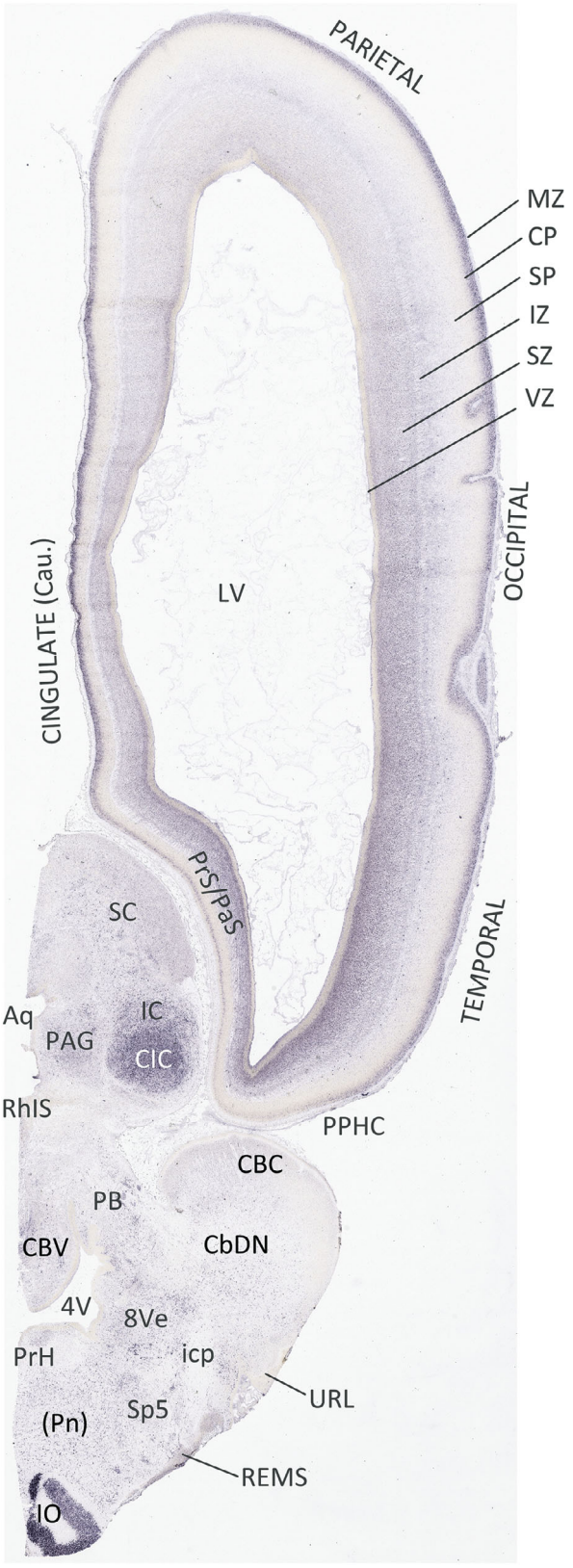

ENC1-02-341 (Level ~37-38)

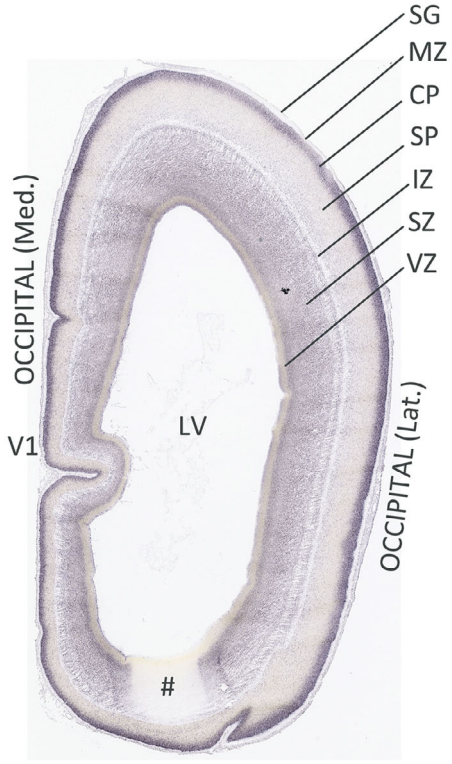

ENC1-02-497 (Level ~42)

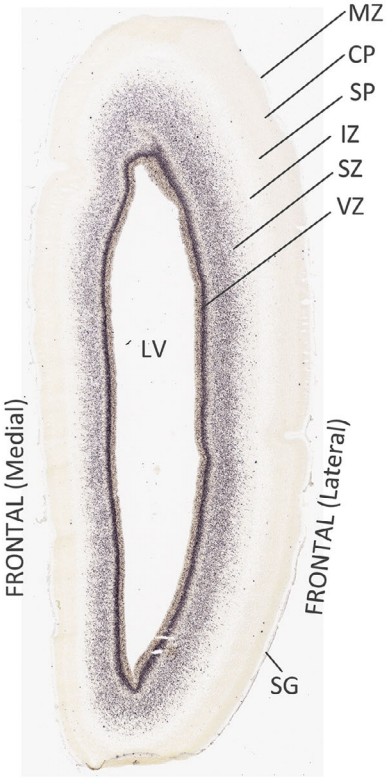

EOMES-01-083 (Level ~3)

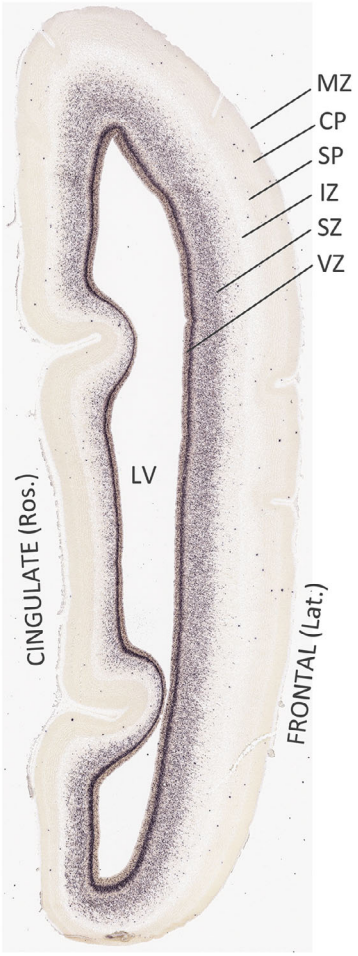

EOMES-01-187(Level ~5)

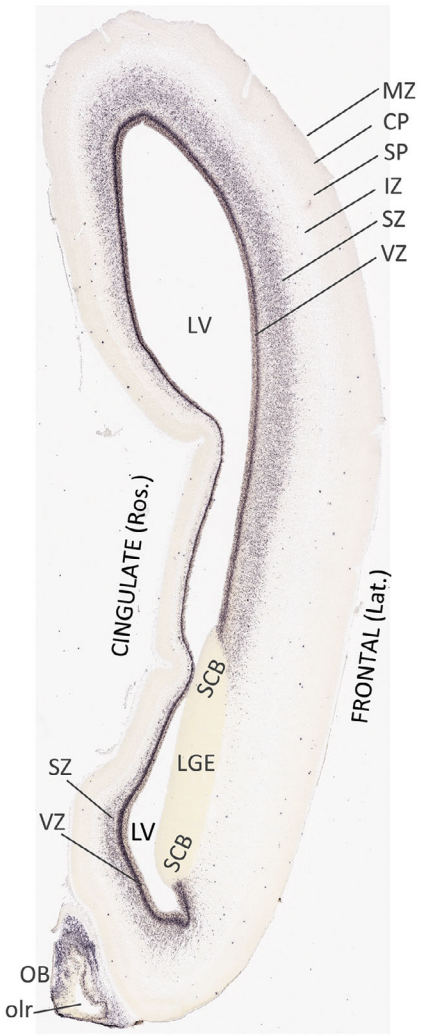

EOMES-01-343 (Level ~9)

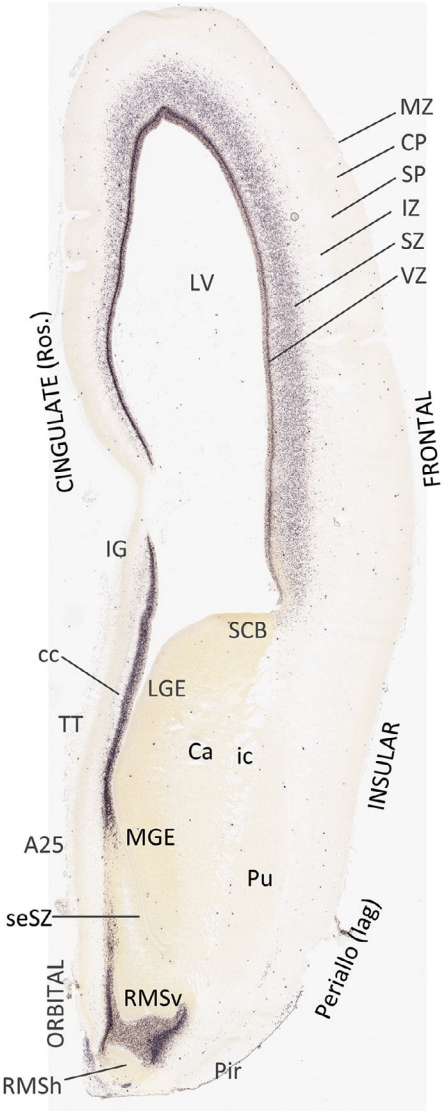

EOMES-01-447 (Level ~13)

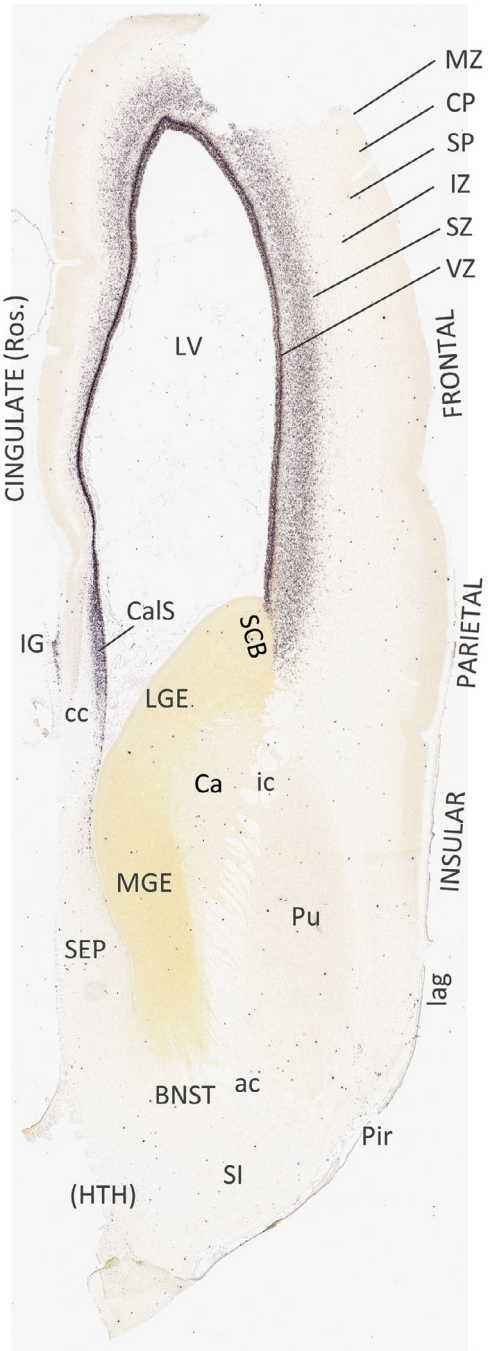

EOMES-01-551 (Level ~17)

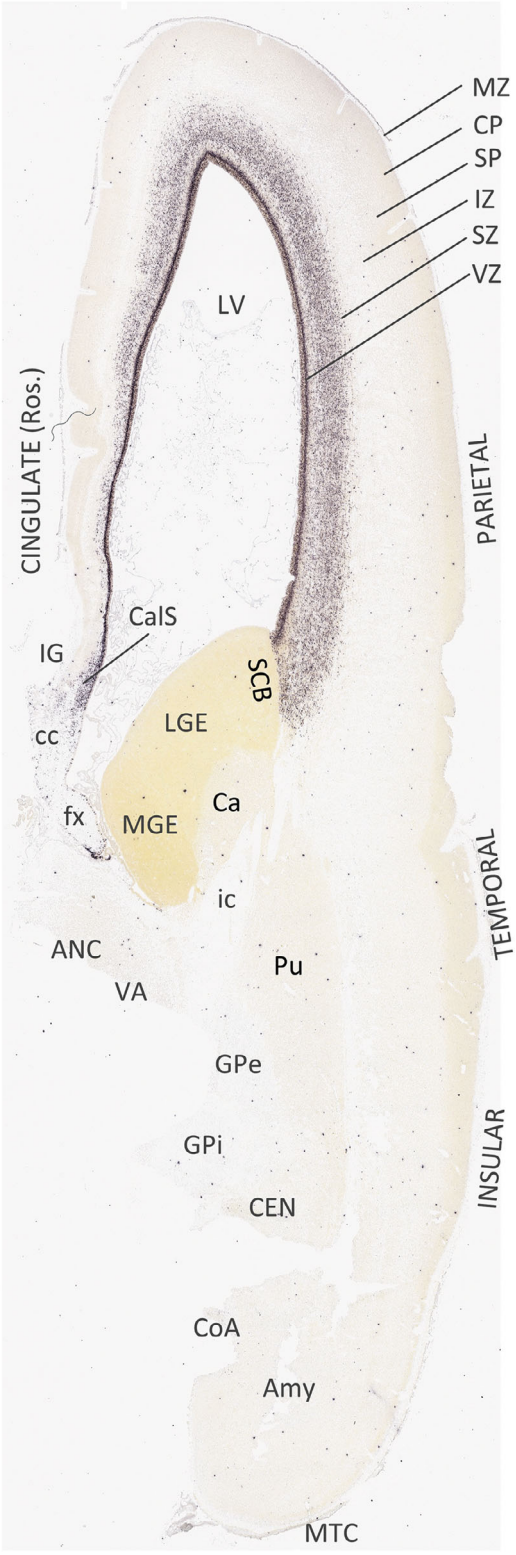

EOMES-01-707 (Level ~22)

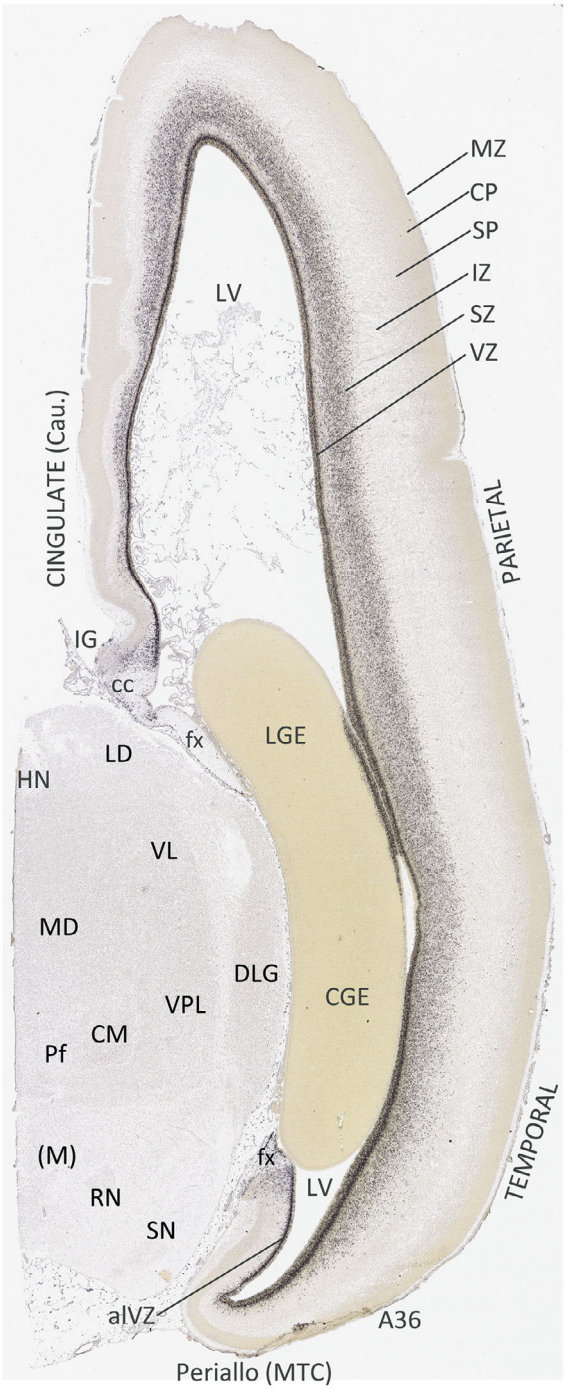

EOMES-02-31 (Level ~26)

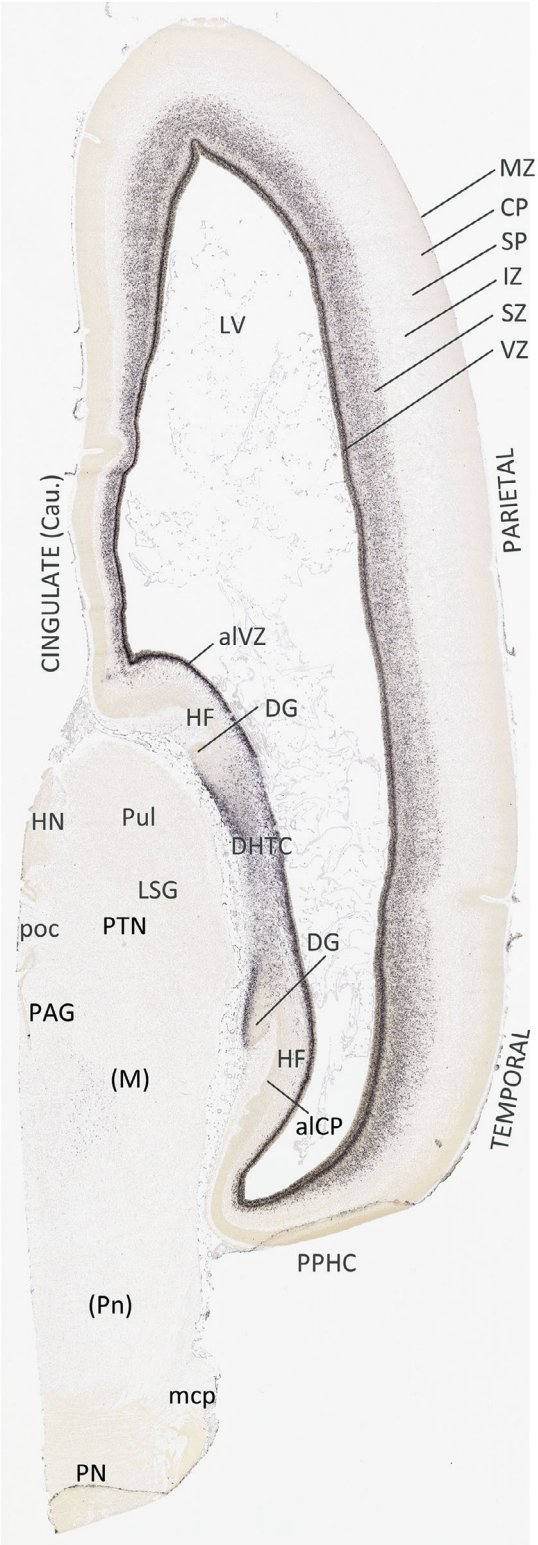

EOMES-02-187 (Level ~31-32)

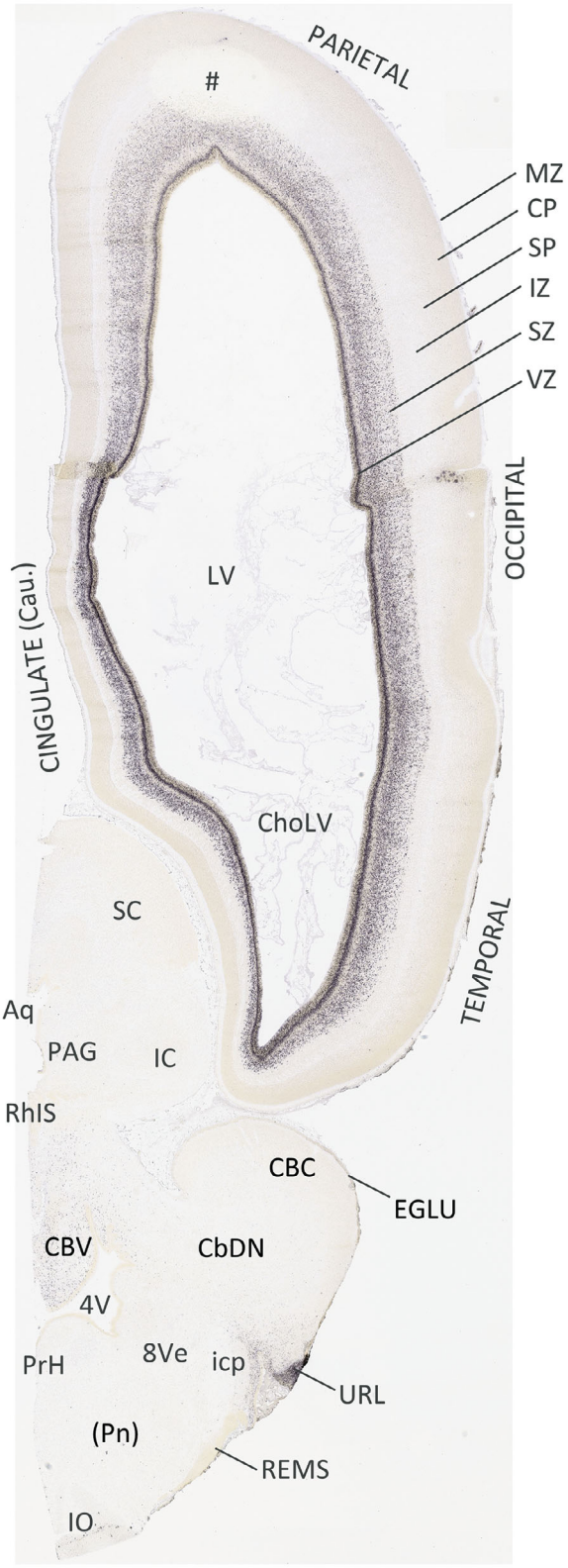

EOMES-02-343 (Level ~37-38)

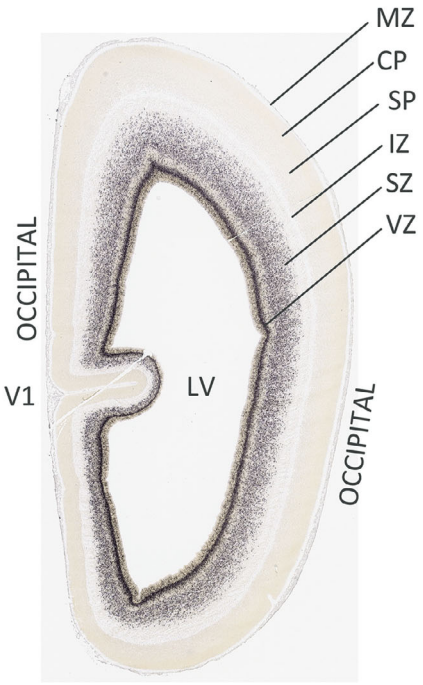

EOMES-02-551 (Level ~43)

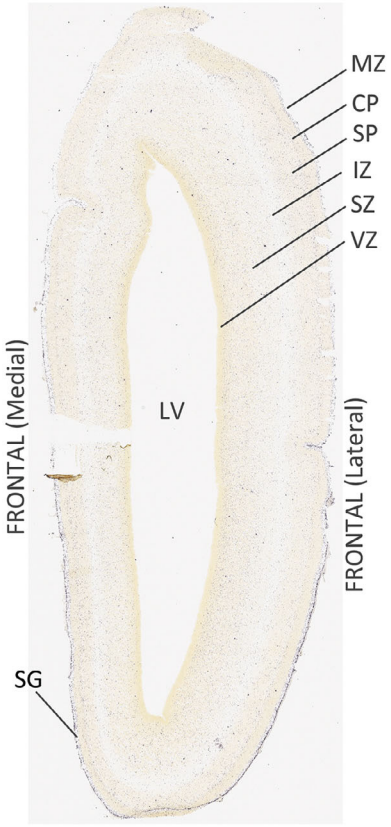

ERBB4-01-099 (Level ~3)

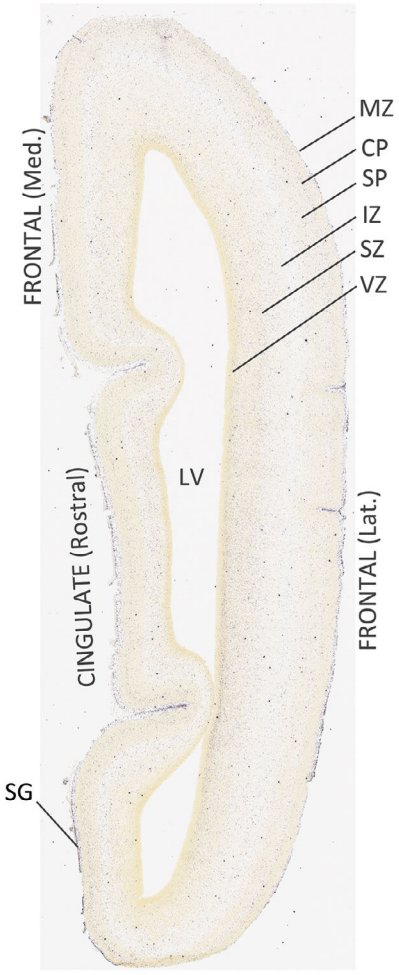

ERBB4-01-203 (Level ~5)

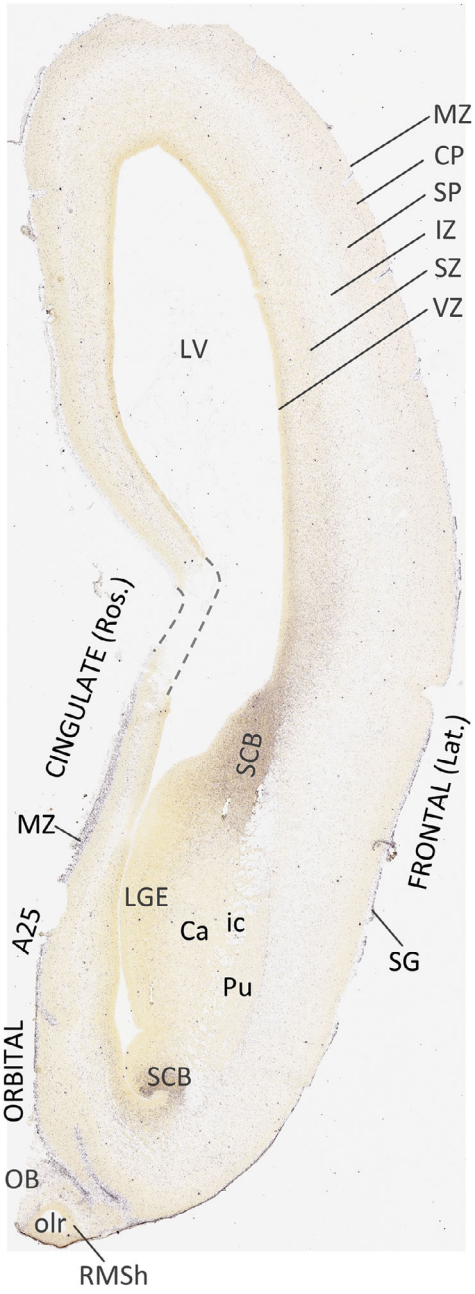

ERBB4-01-411 (Level ~12)

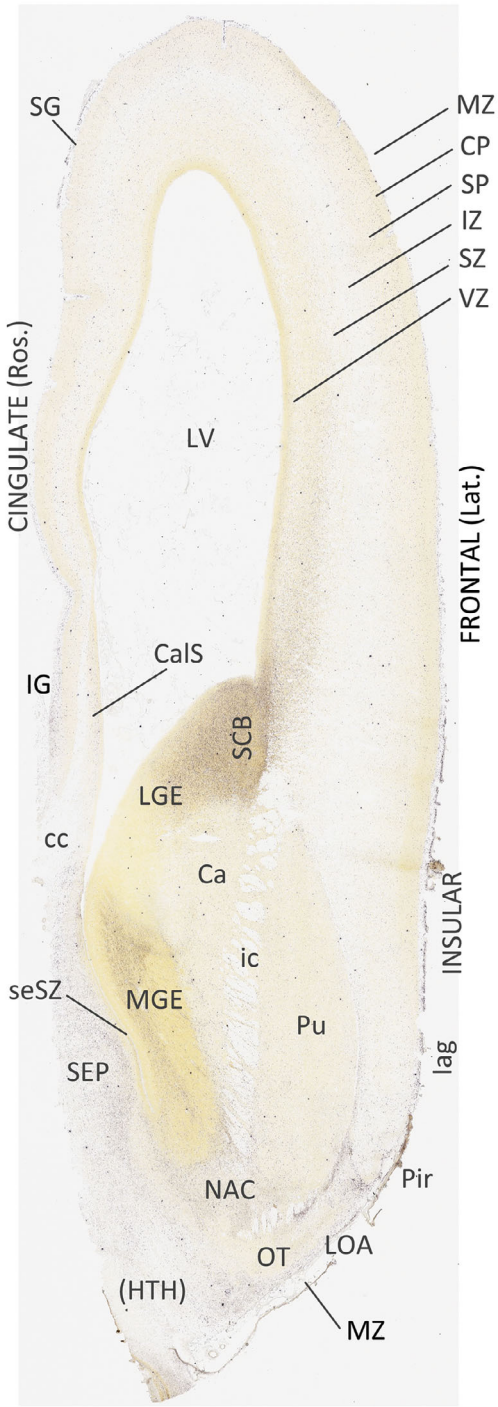

ERBB4-01-515 (Level ~16)

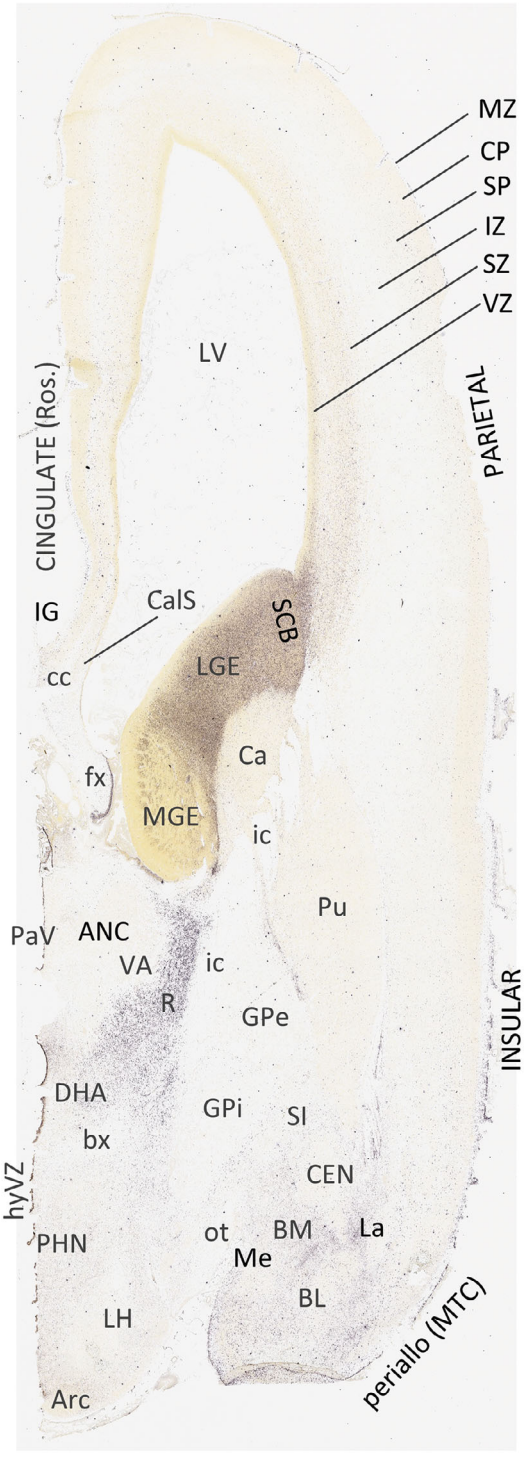

ERBB4-01-671 (Level ~21)

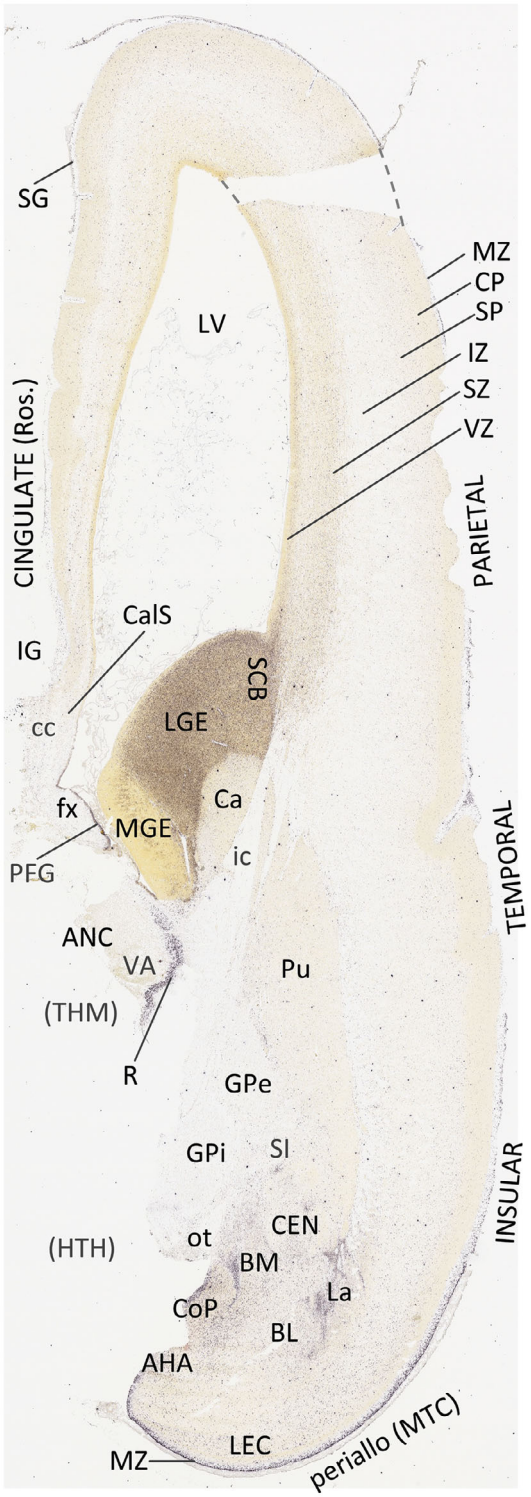

ERBB4-01-732 (Level ~23)

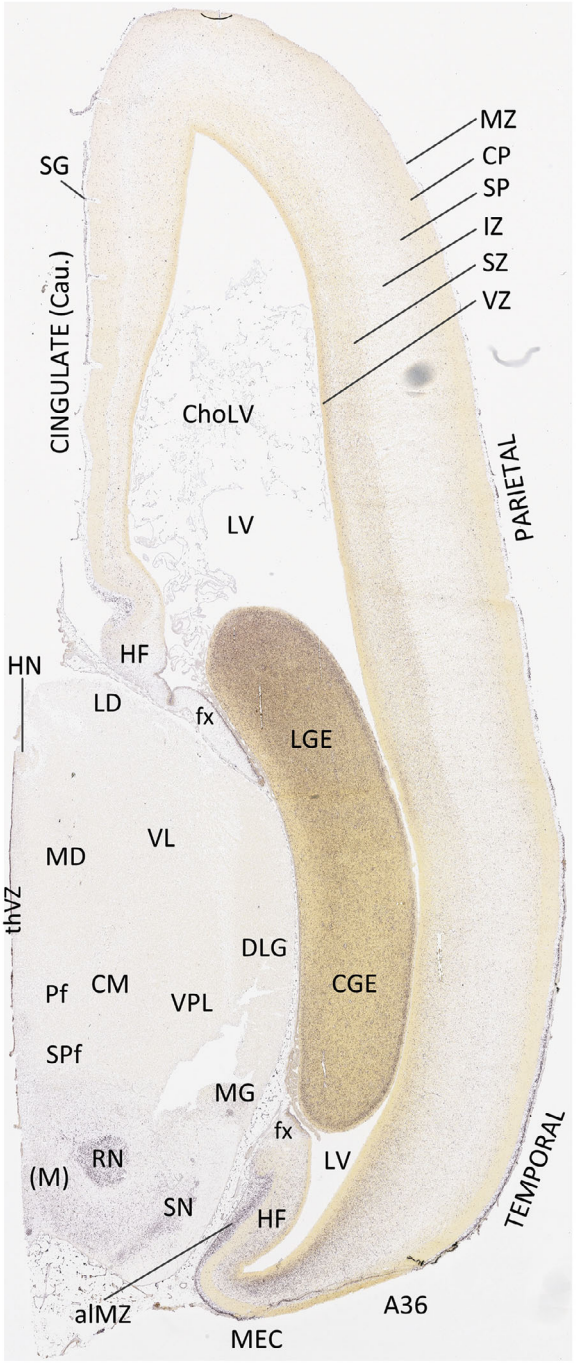

ERBB4-02-047 (Level ~26)

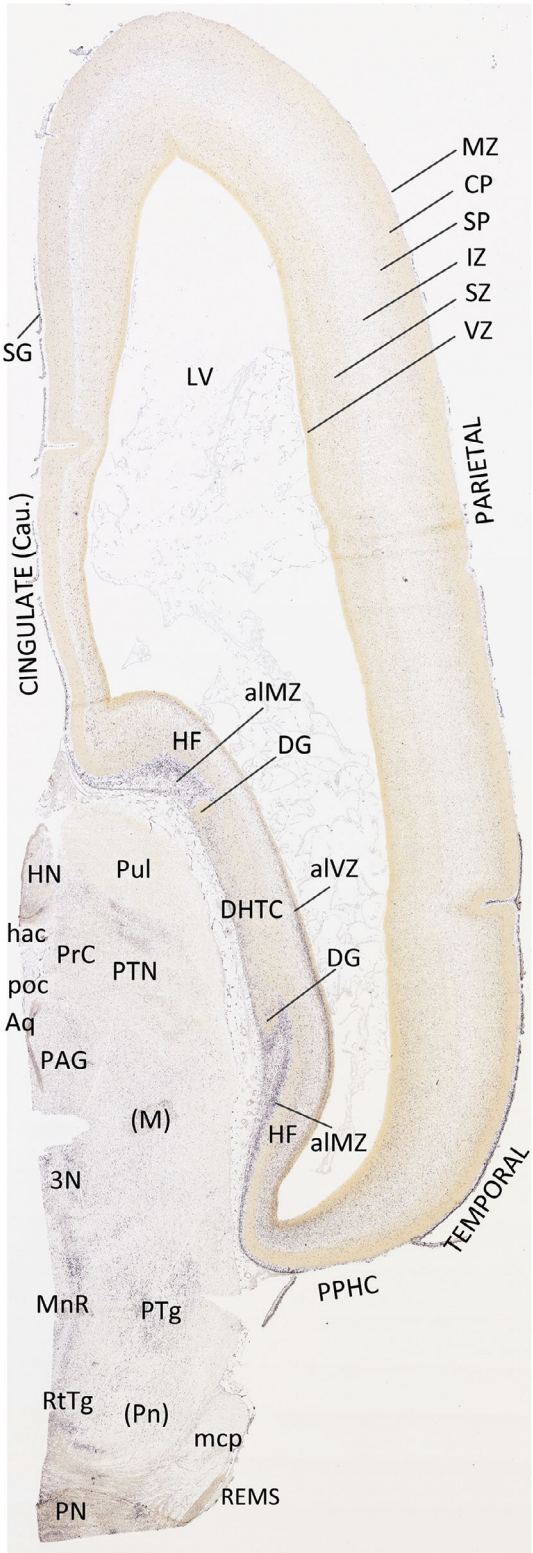

ERBB4-02-203 (Level ~32)

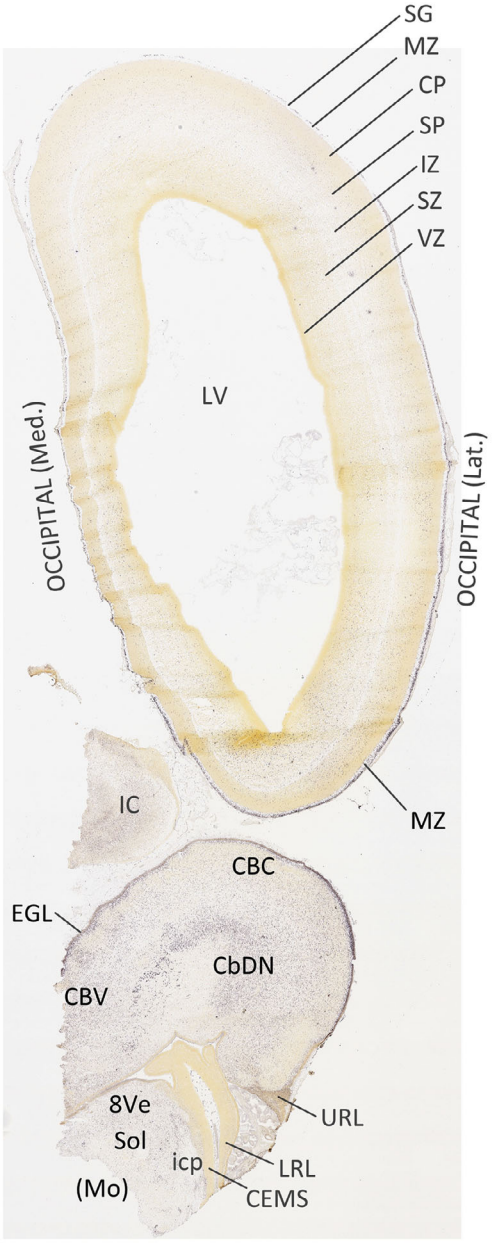

ERBB4-02-411 (Level ~41)

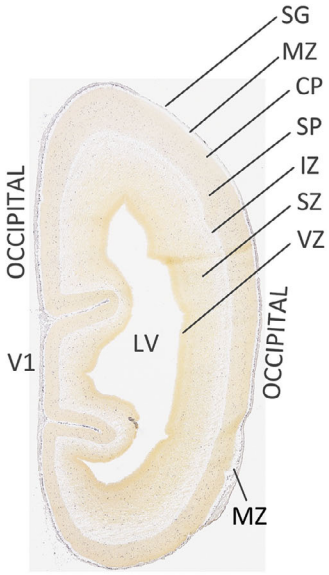

ERBB4-02-619 (Level ~45)

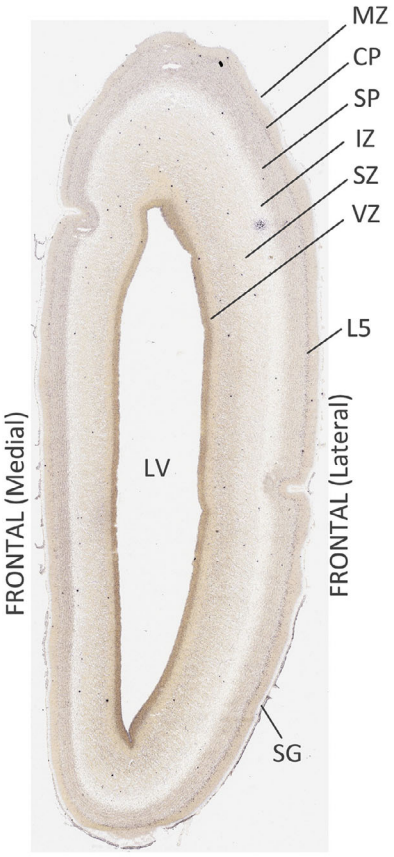

ETV1-01-085 (Level ~3)

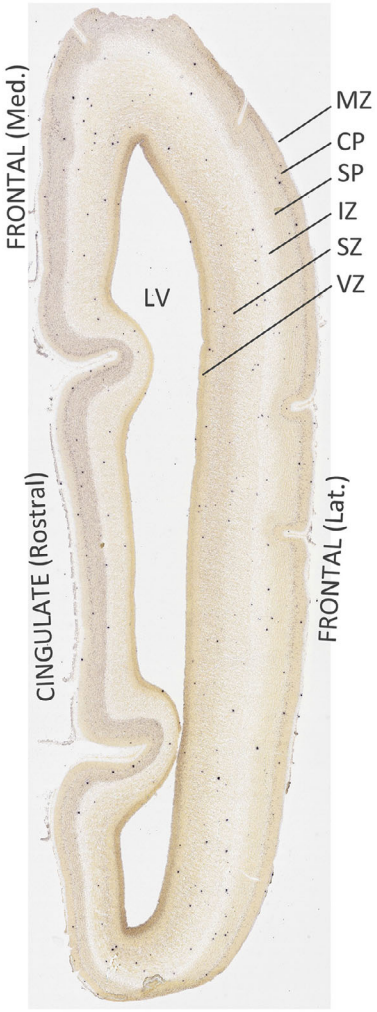

ETV1-01-189 (Level ~5)

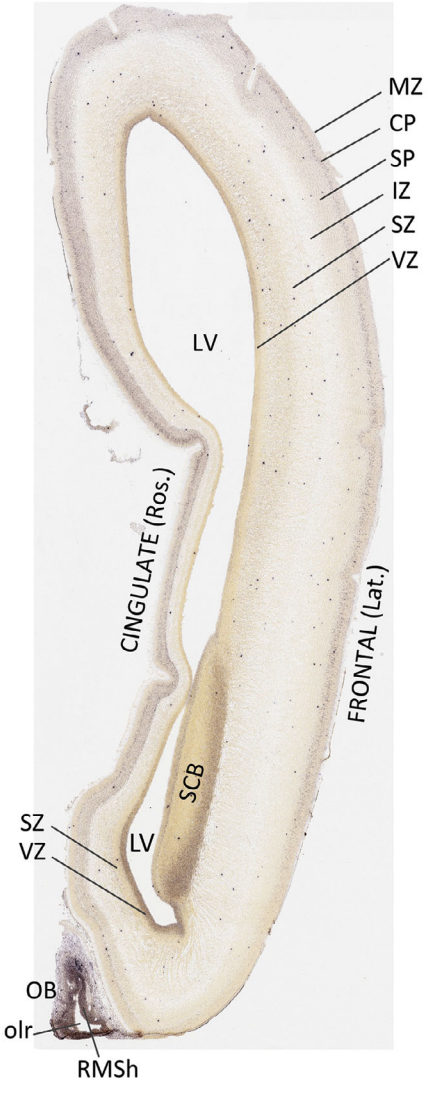

ETV1-01-345 (Level ~9)

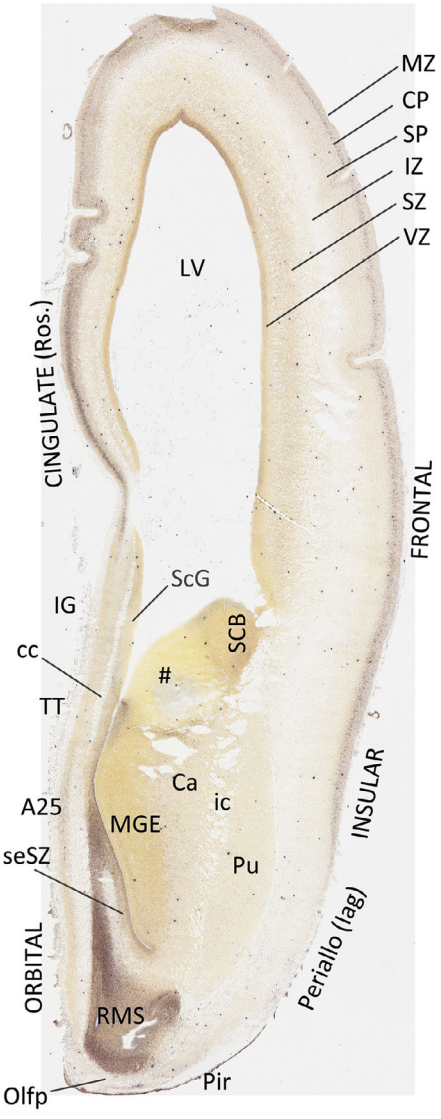

ETV1-01-449 (Level ~13)

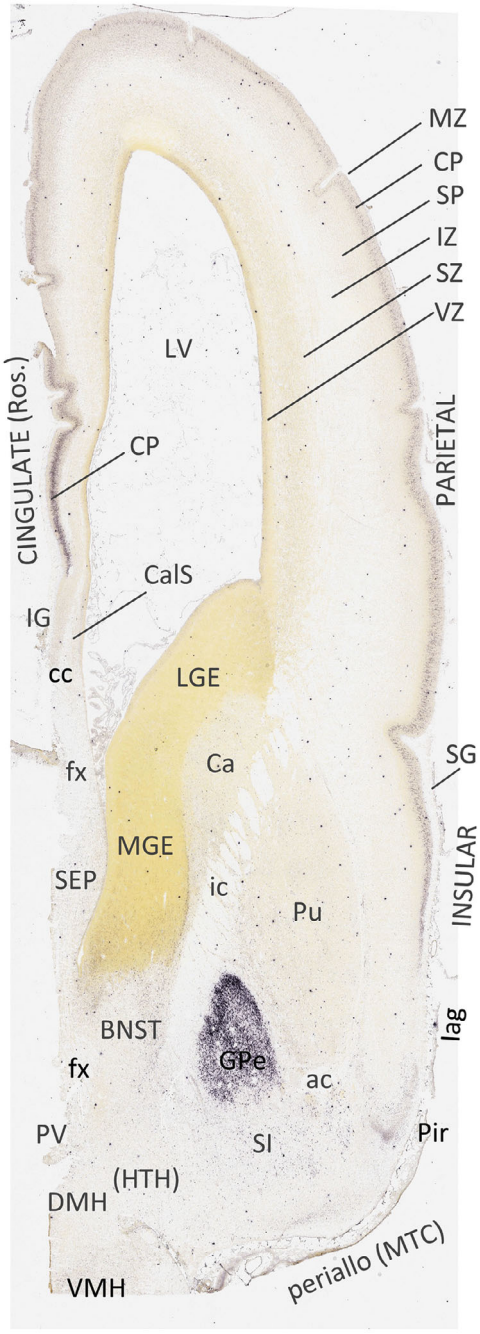

ETV1-01-605 (Level ~19)

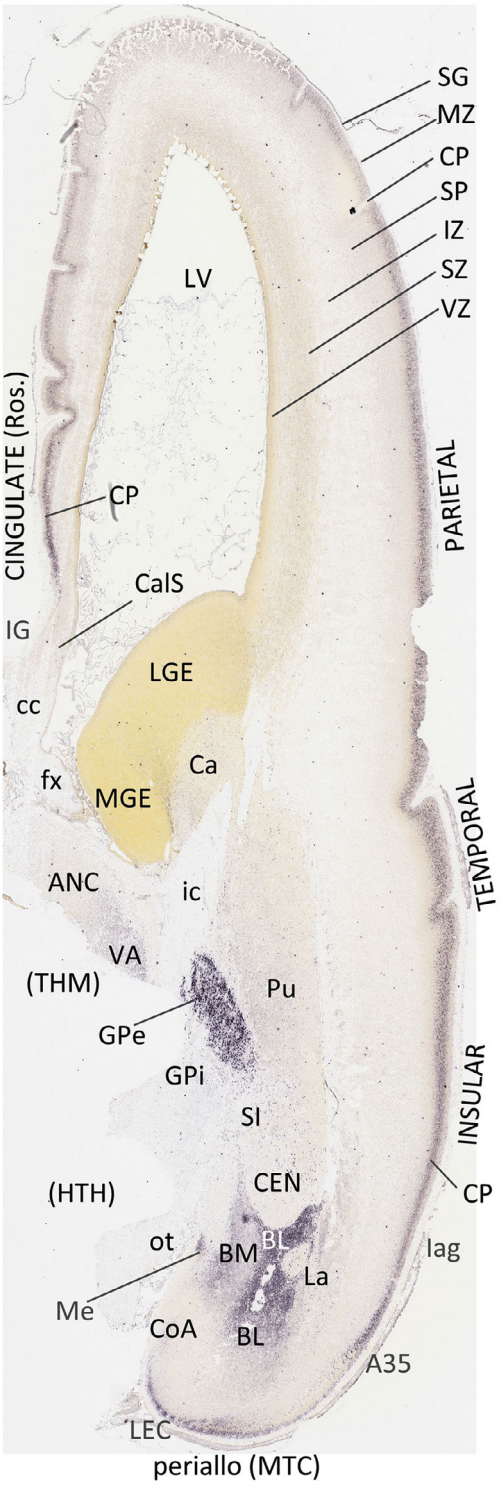

ETV1-01-709 (Level ~22)

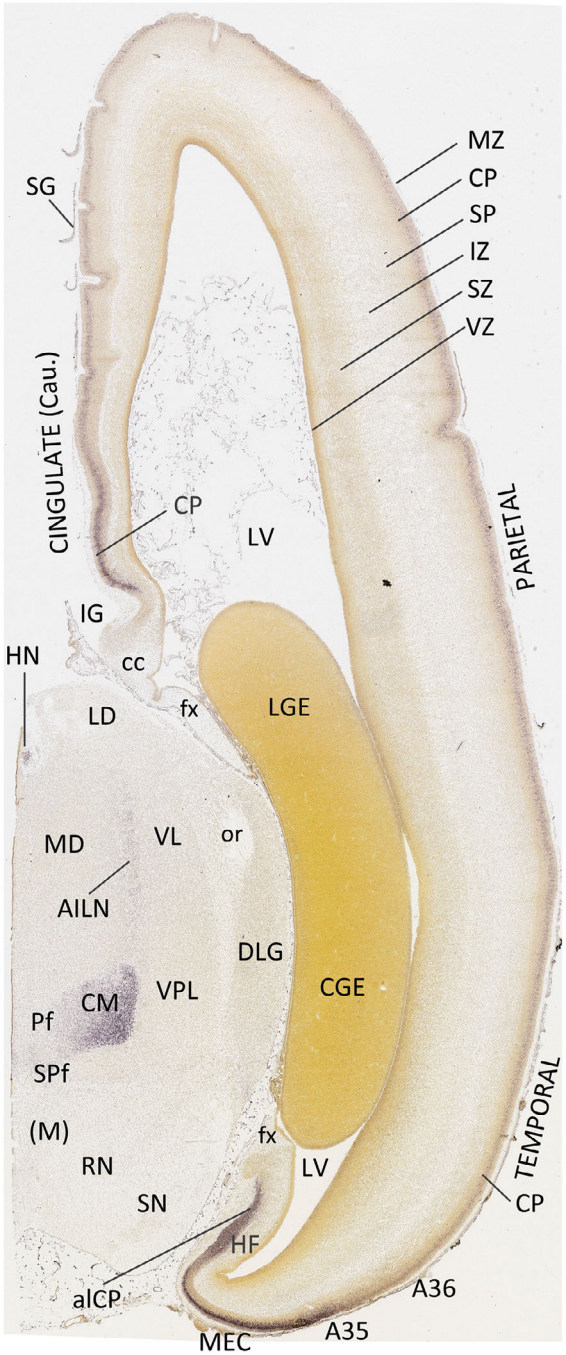

ETV1-02-033 (Level ~26)

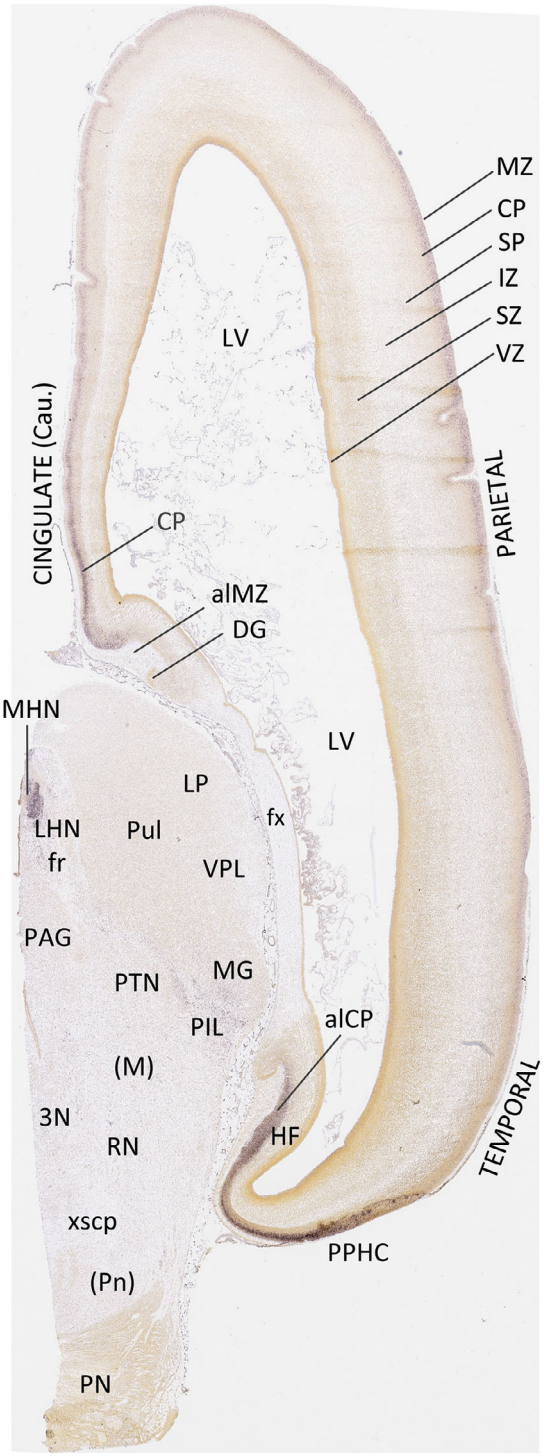

ETV1-02-137 (Level ~30)

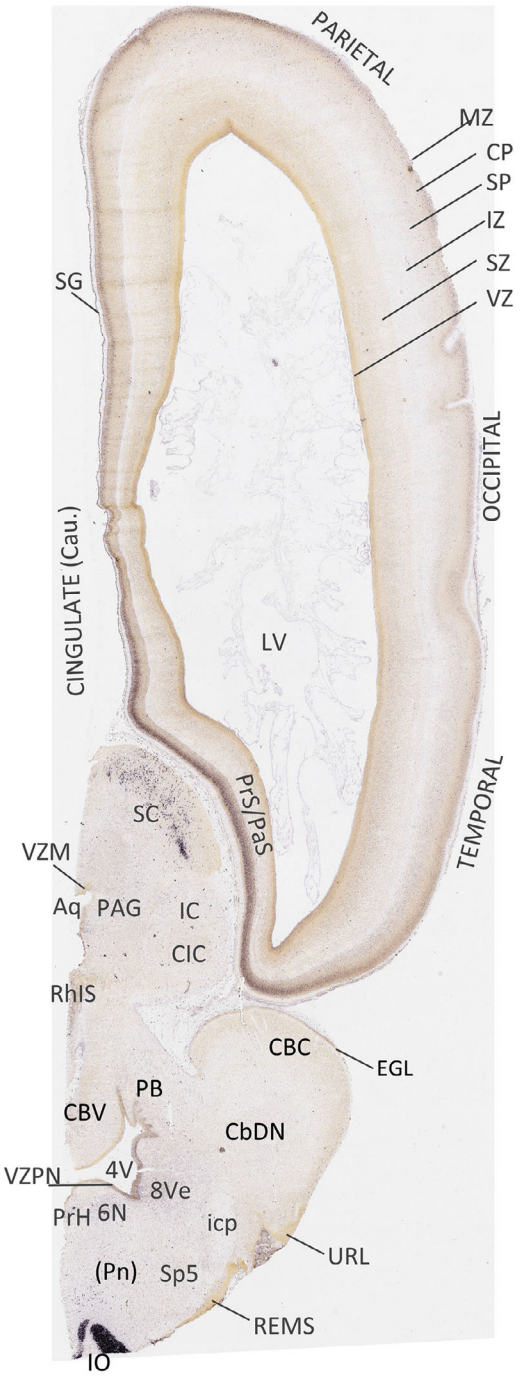

ETV1-02-345 (Level ~37-38)

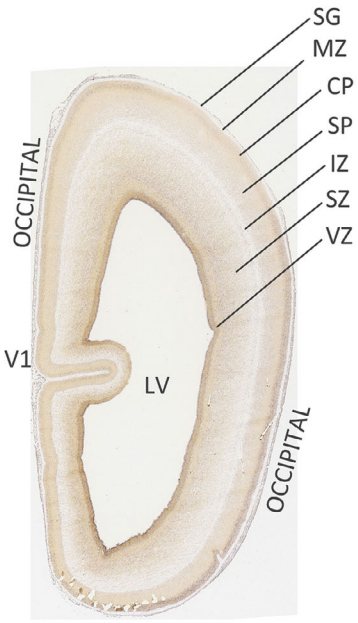

ETV1-02-553 (Level ~43)

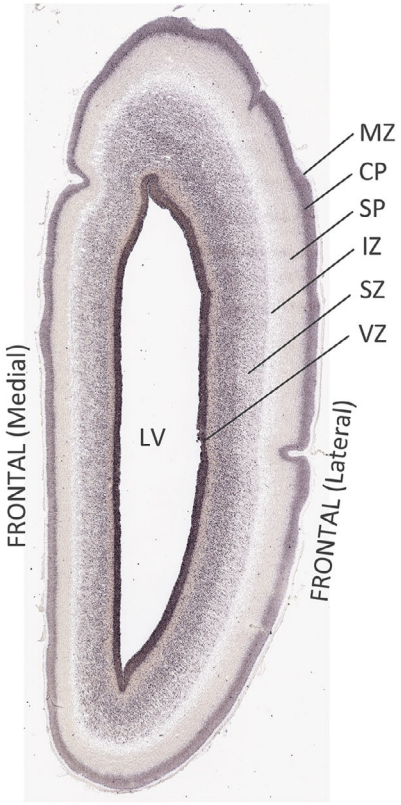

FABP7-01-075 (Level ~2-3)

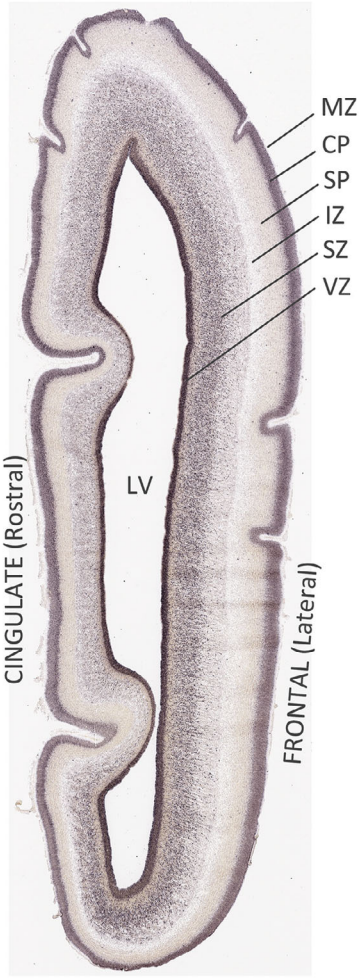

FABP7-01-179 (Level ~4-5)

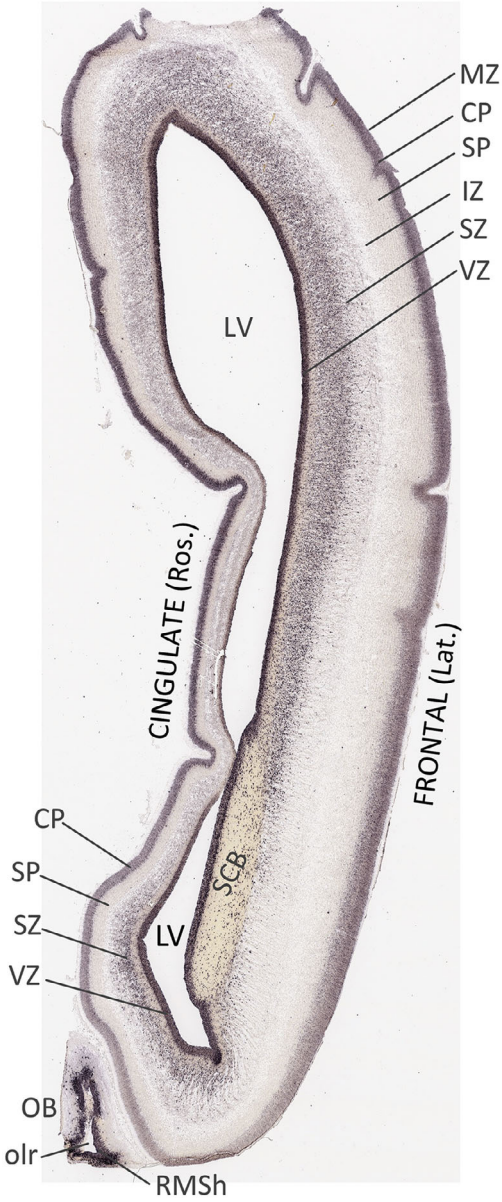

FABP7-01-335 (Leve ~9)

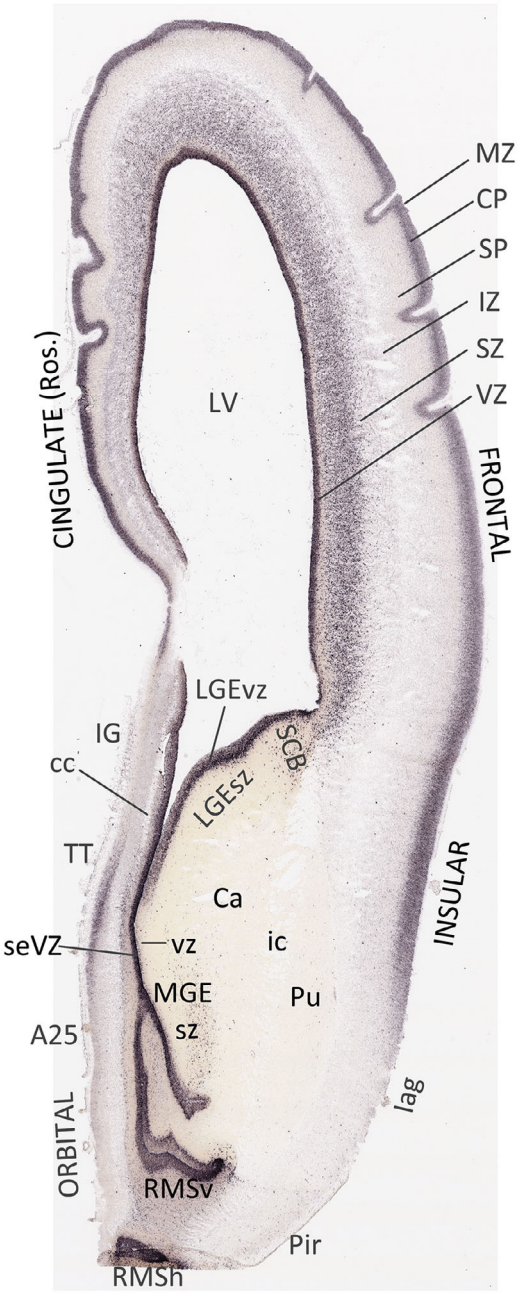

FABP7-01-439 (Leve ~13)

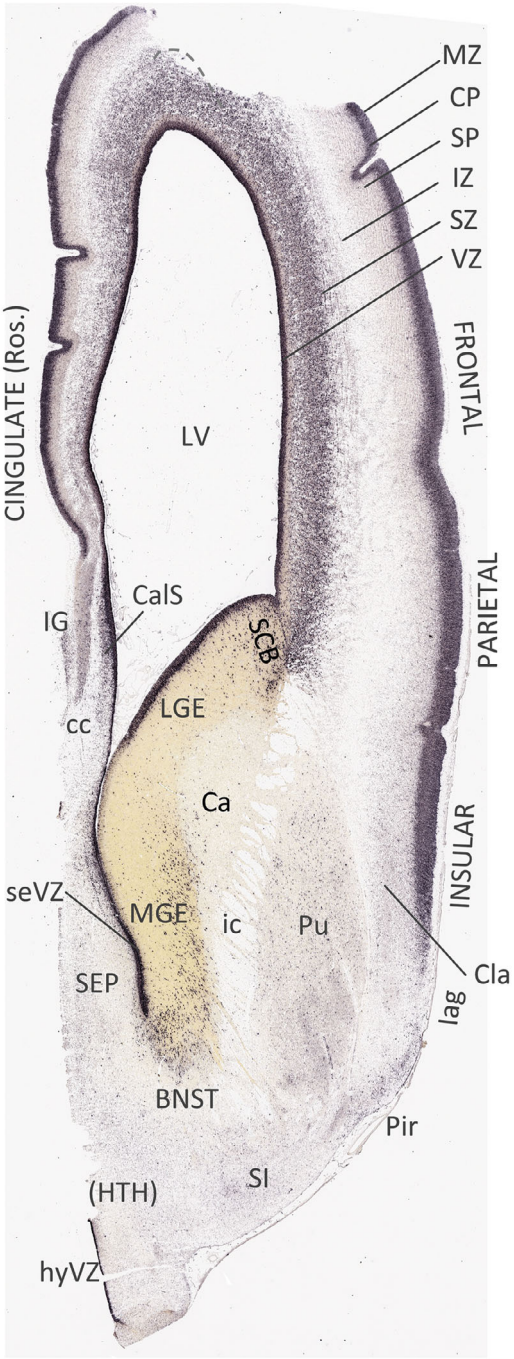

FABP7-01-543 (Level ~17)

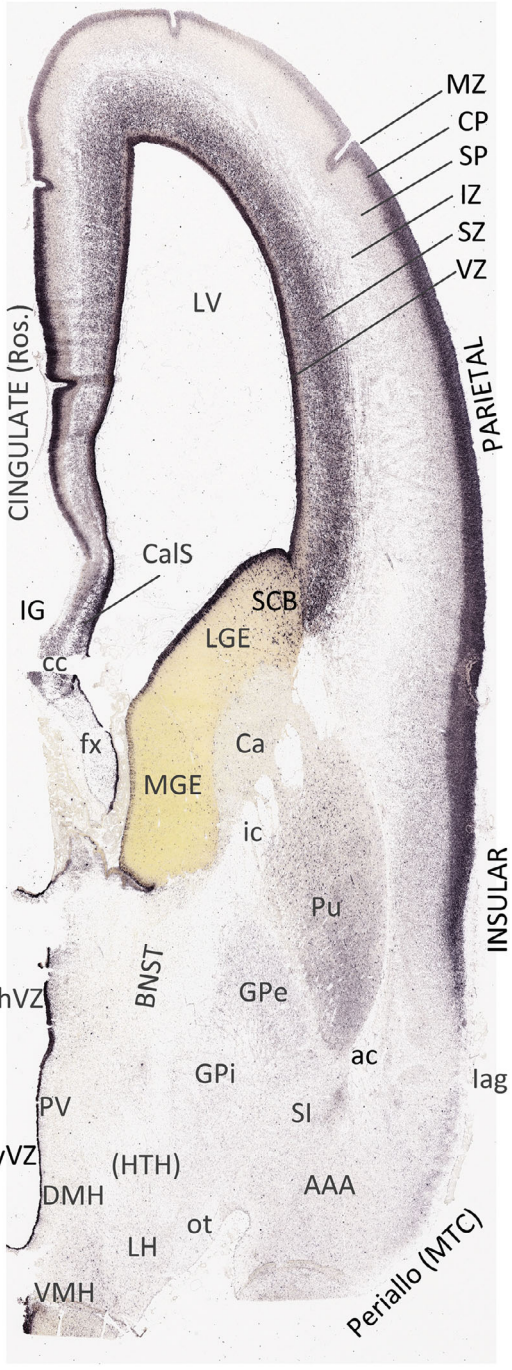

FABP7-01-647 (Level ~20)

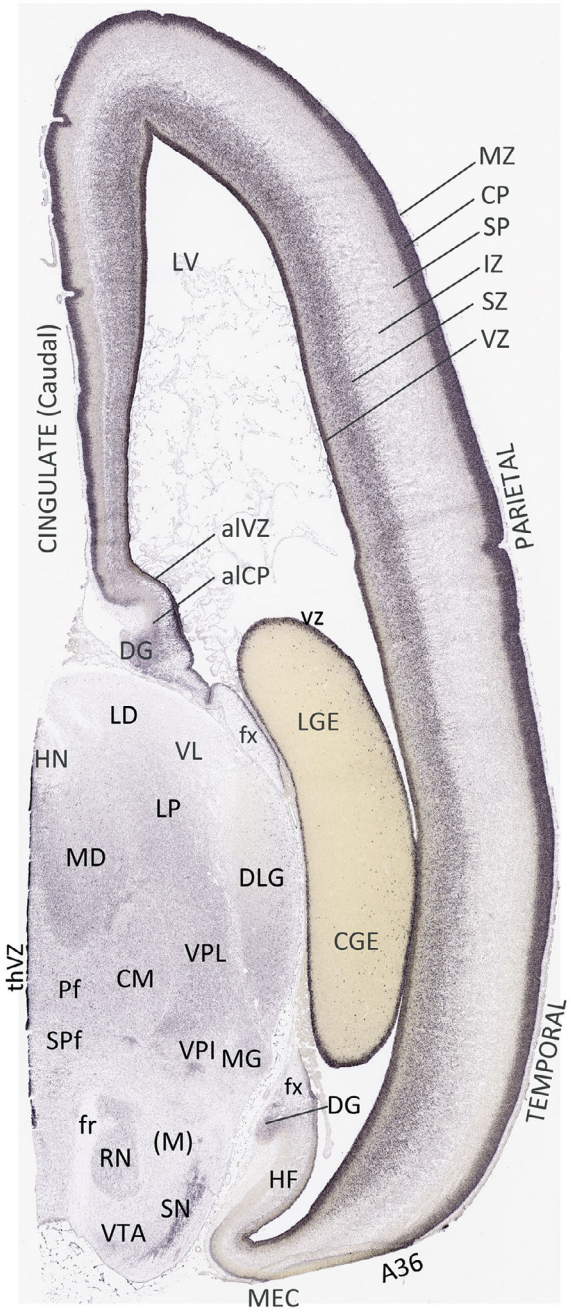

FABP7-02-075 (Level ~27)

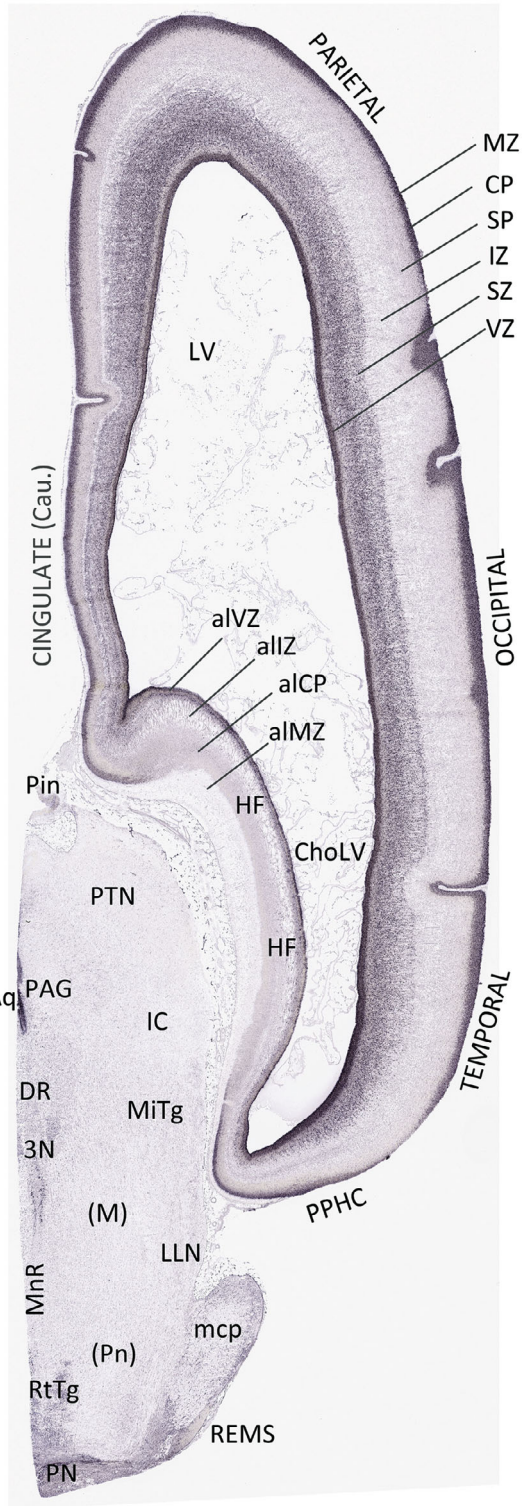

FABP7-02-231 (Level ~33)

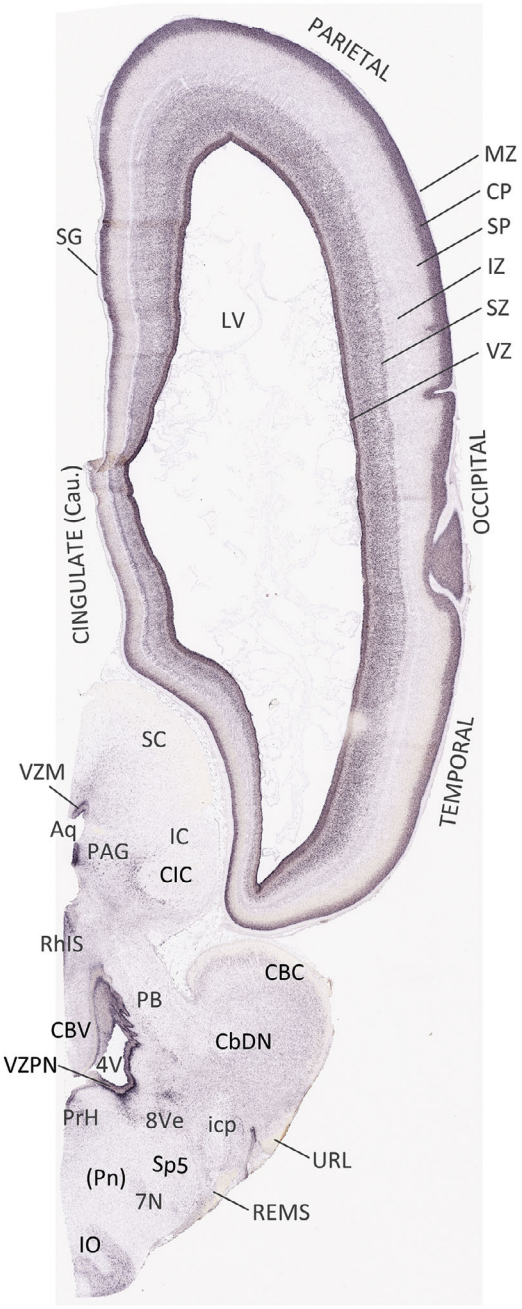

FABP7-02-335 (Level ~37-38)

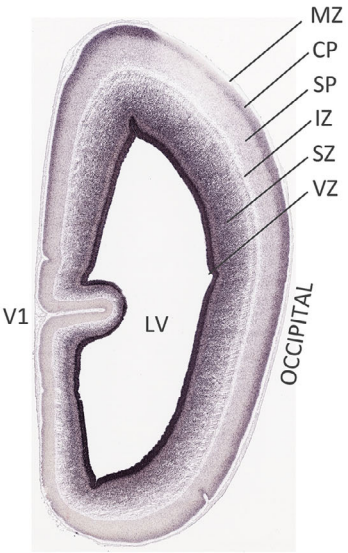

FABP7-02-543 (Level ~37-38)

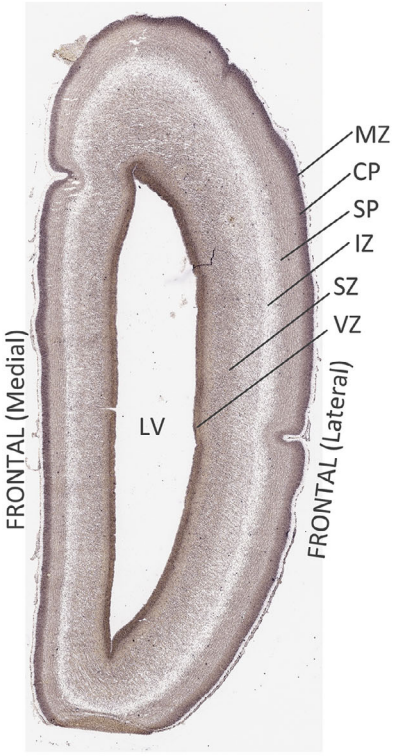

FADS2-01-076 (Level ~2-3)

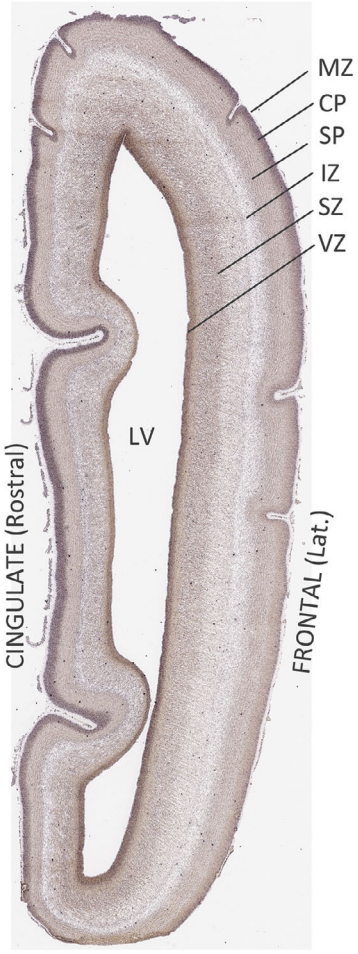

FADS2-01-180 (Level ~4-5)

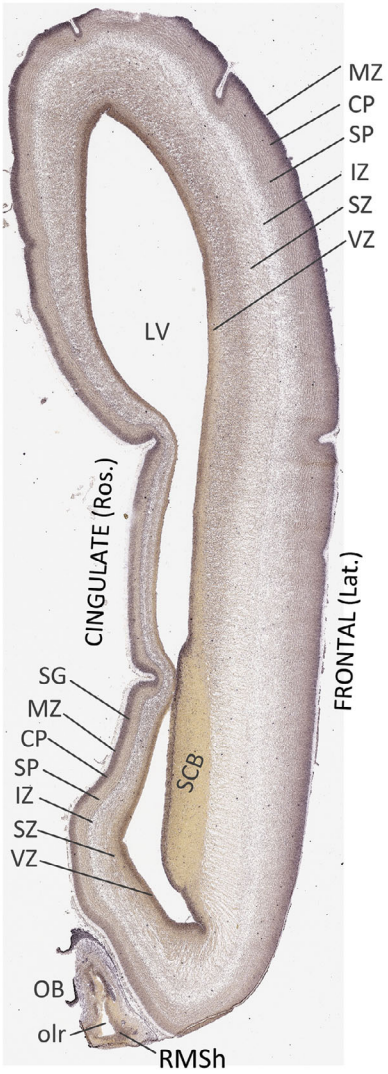

FADS2-01-336 (Level ~9)

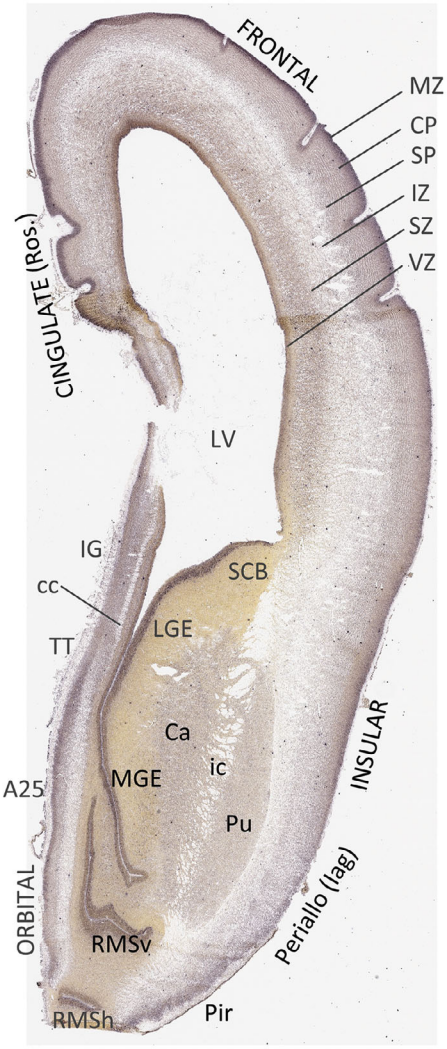

FADS2-01-440 (Level ~13)

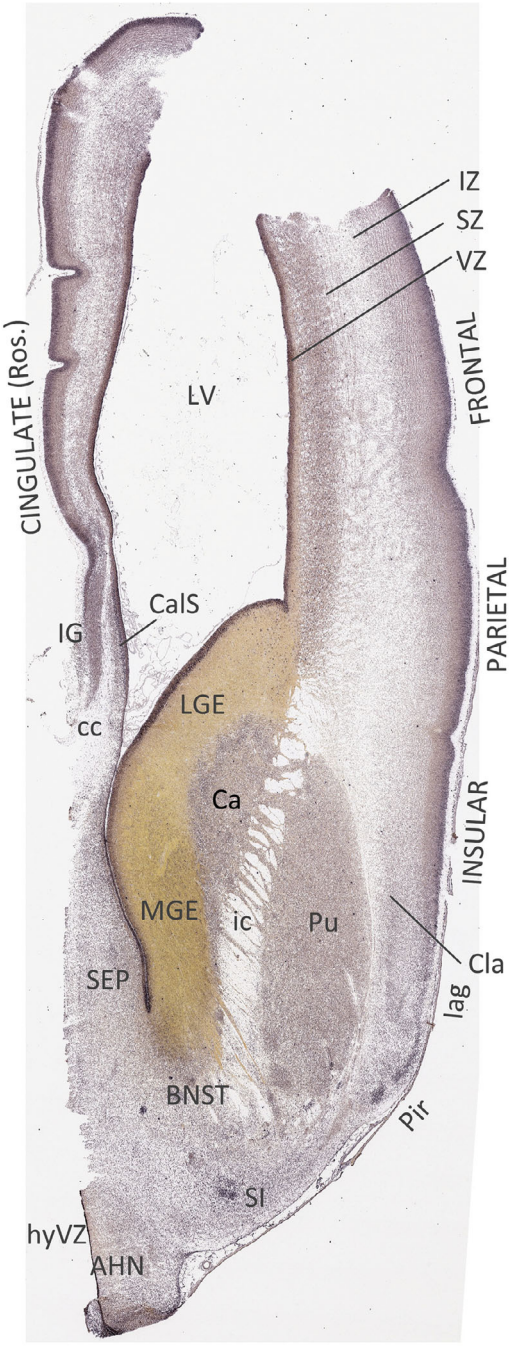

FADS2-01-544 (Level ~17)

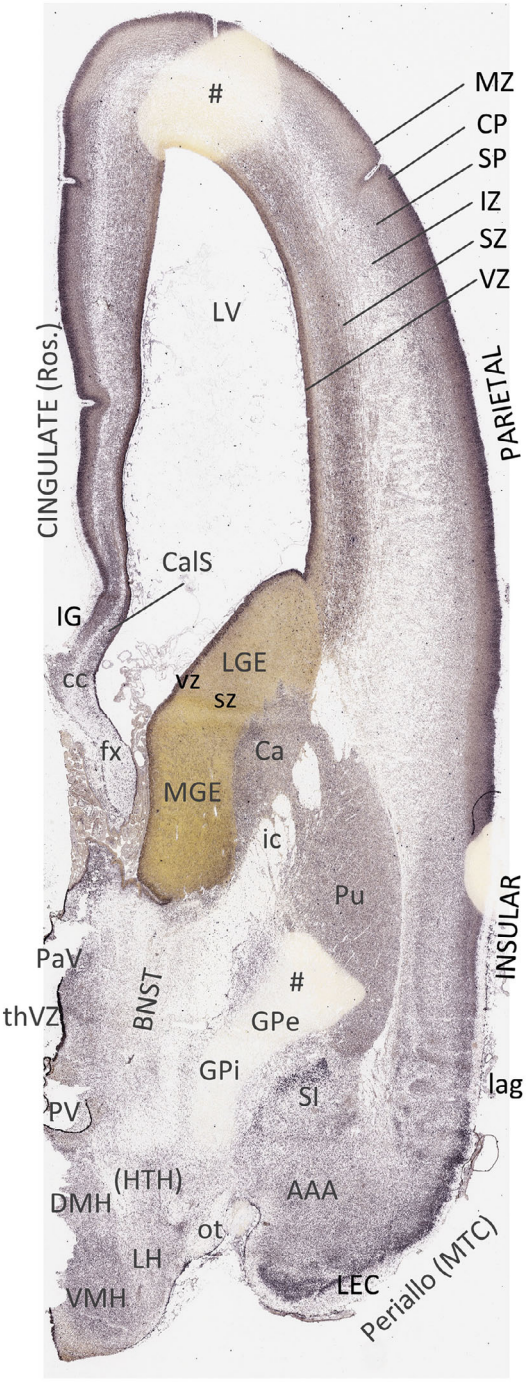

FADS2-01-648 (Level ~20)

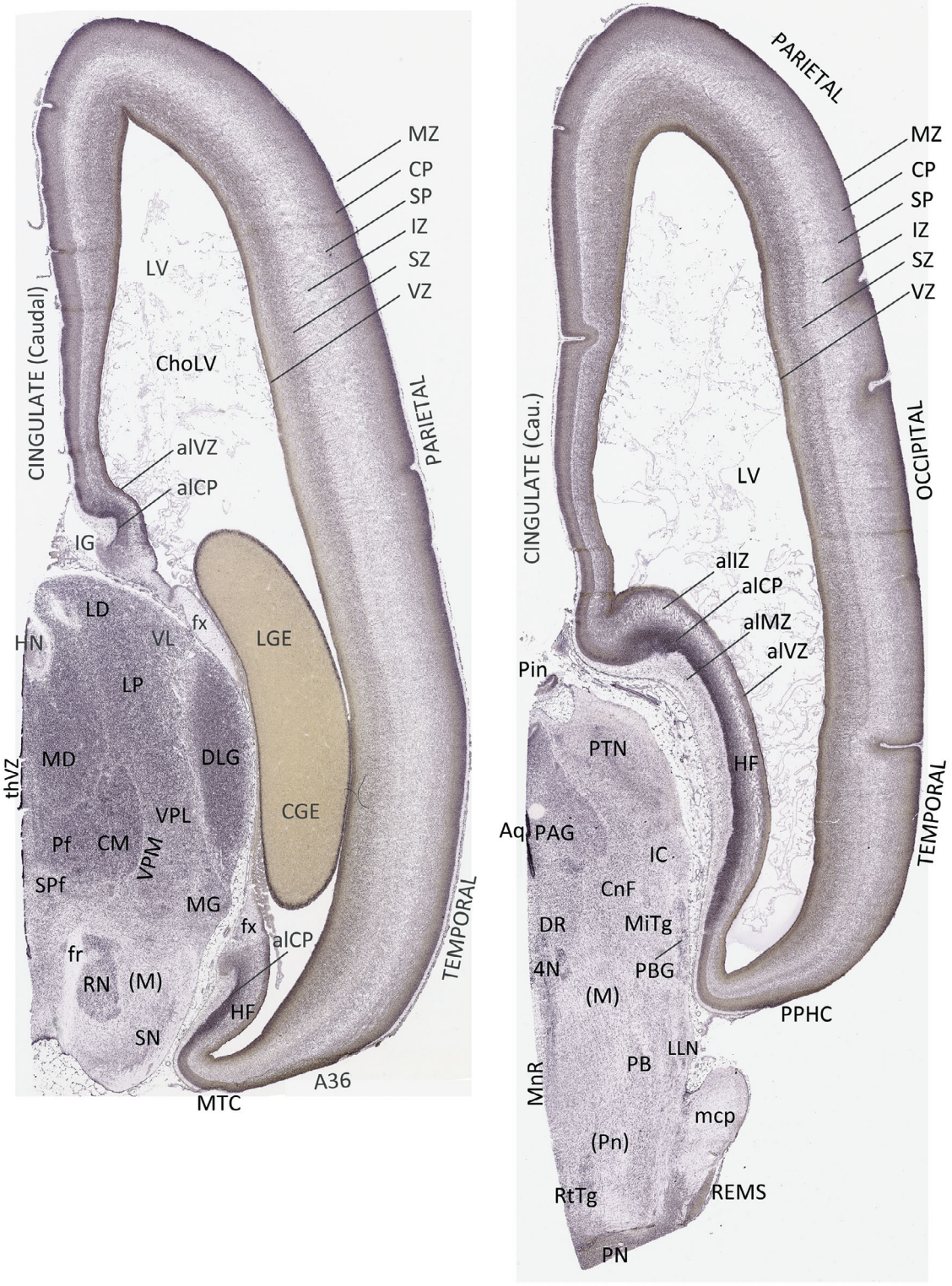

FADS2-02-076 (Level ~27)

FADS2-02-232 (Level ~33-34)

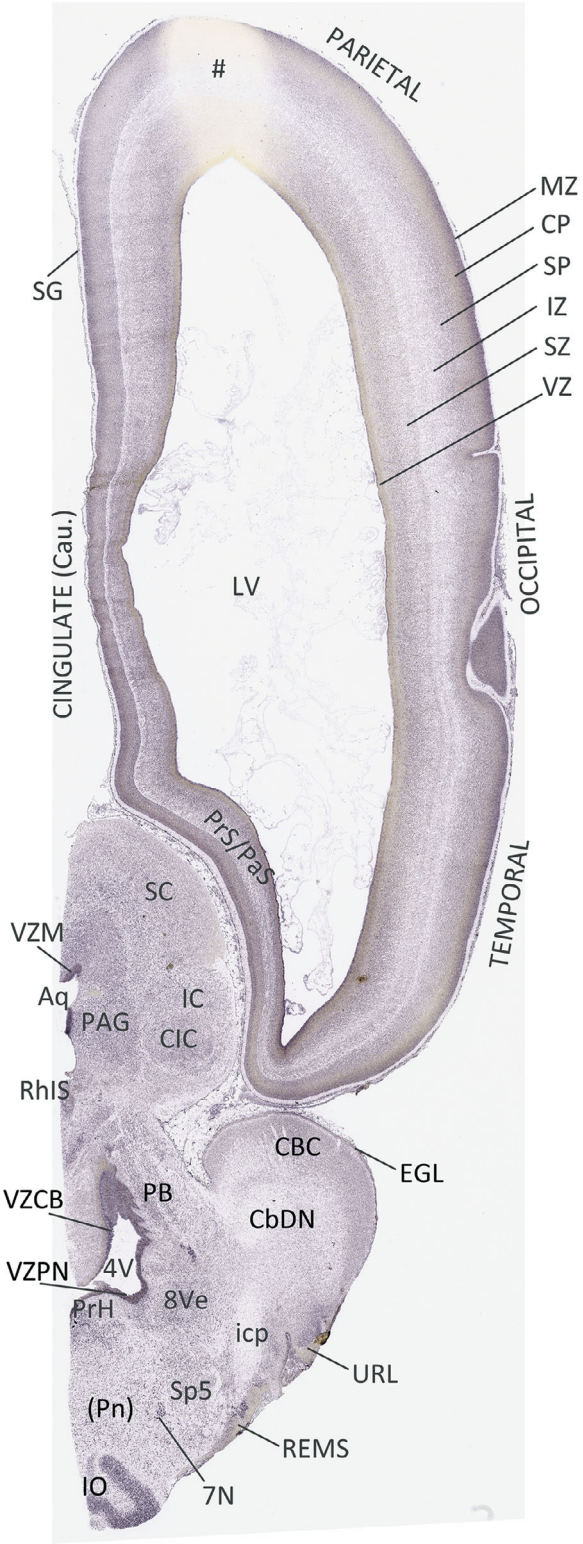

FADS2-02-336 (Level ~37-38)

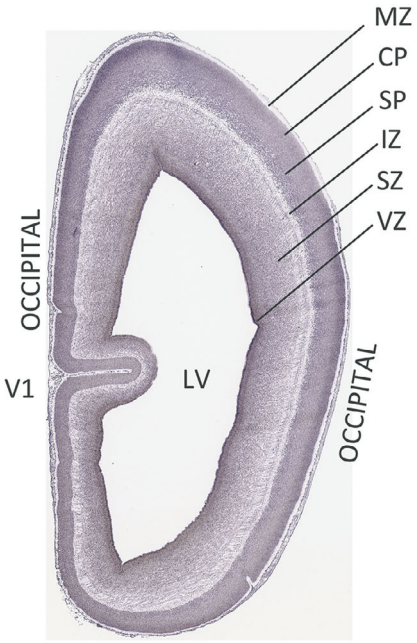

FADS2-02-544 (Level ~43)

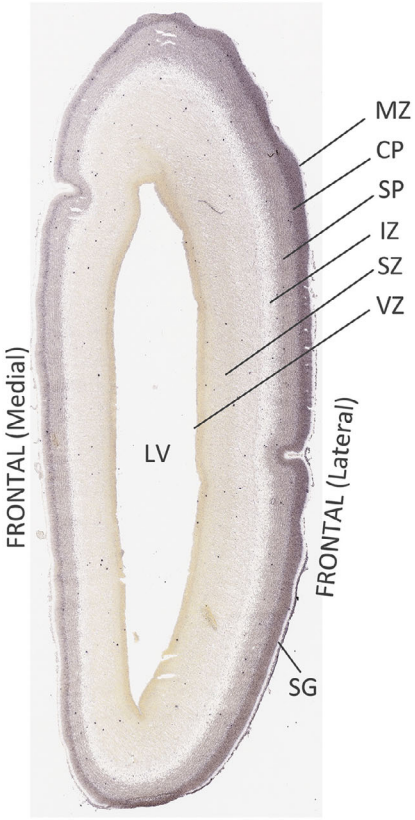

FEZF2-01-086 (Level ~3)

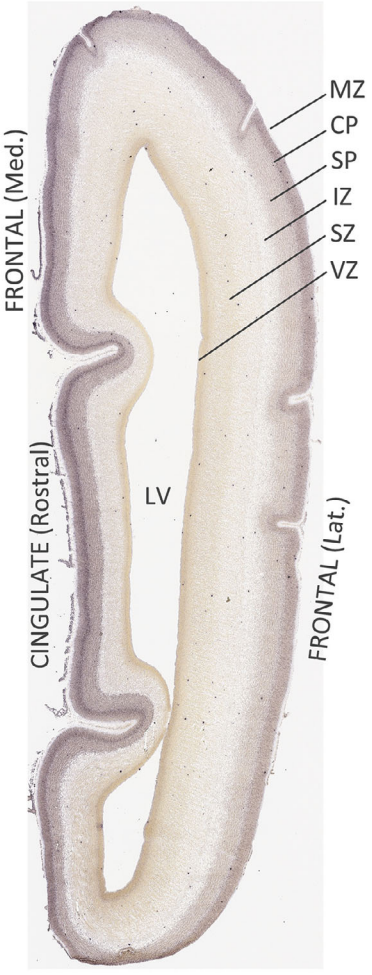

FEZF2-01-190 (Level ~5)

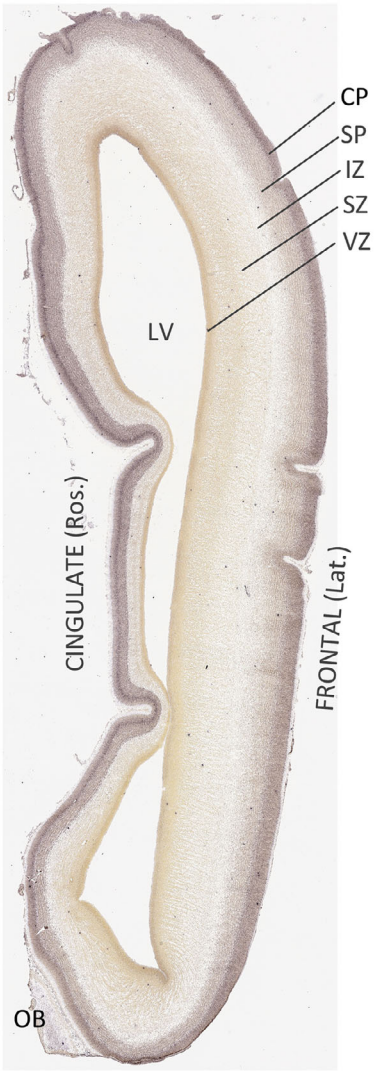

FEZF2-01-294 (Level ~7)

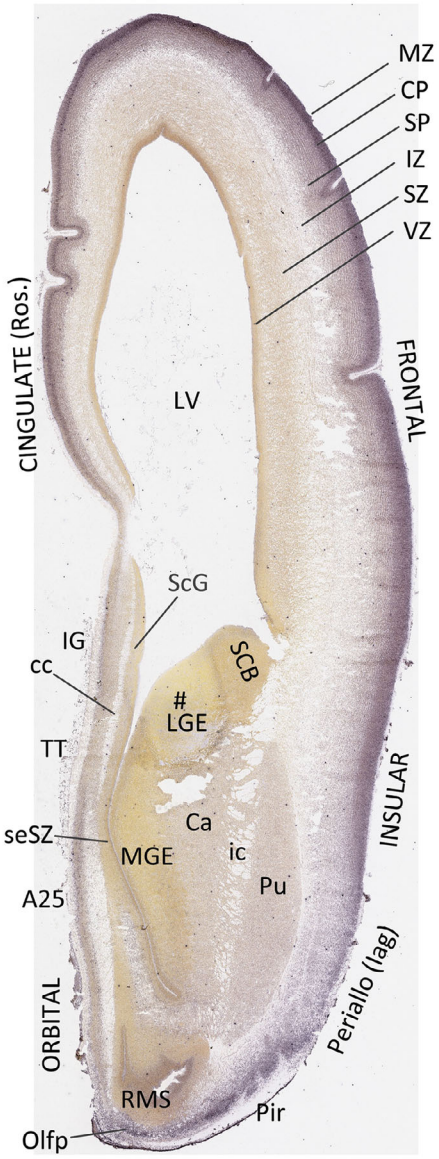

FEZF2-01-450 (Level ~13)

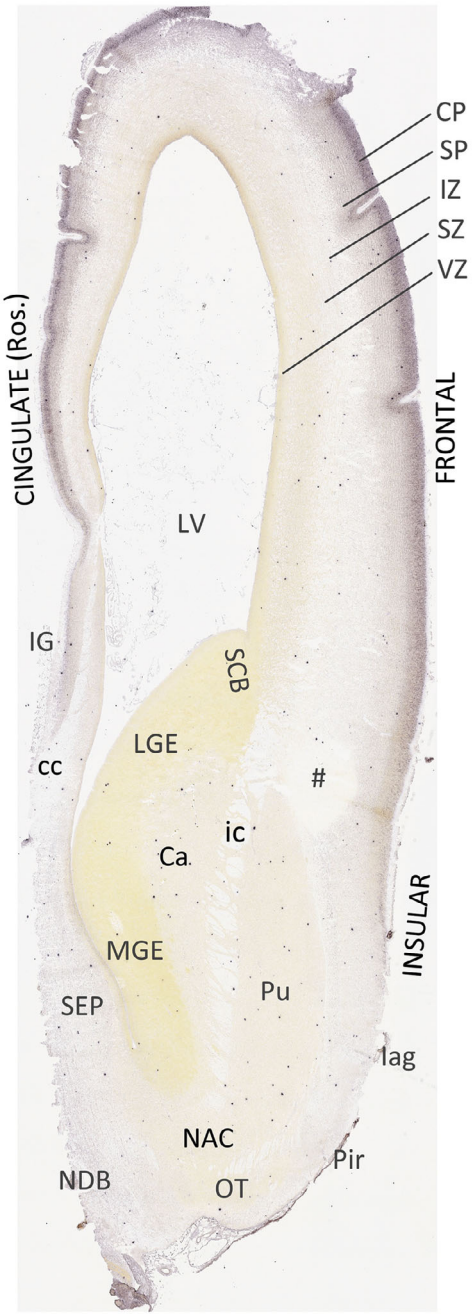

FEZF2-01-502 (Level ~15)

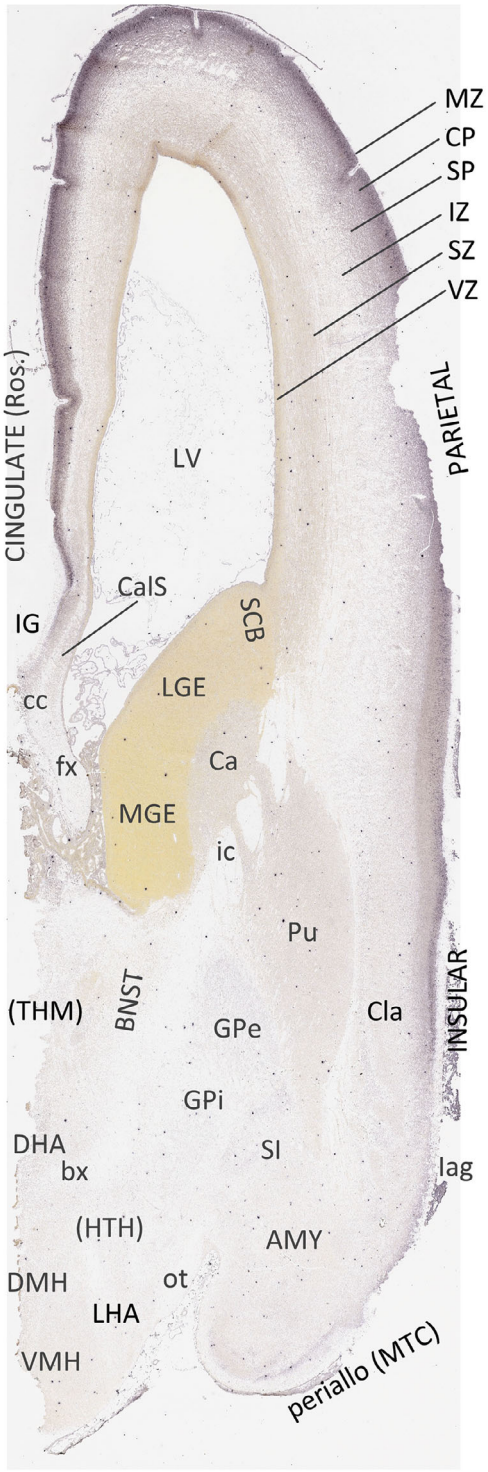

FEZF2-01-658 (Level ~20-21)

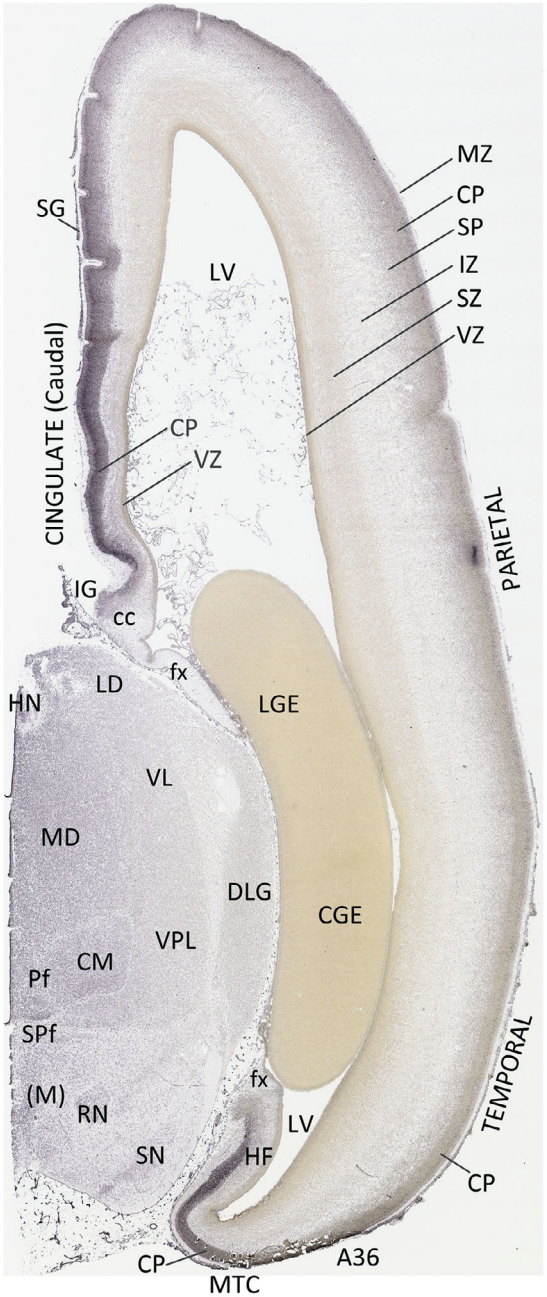

FEZF2-02-034 (Level ~25)

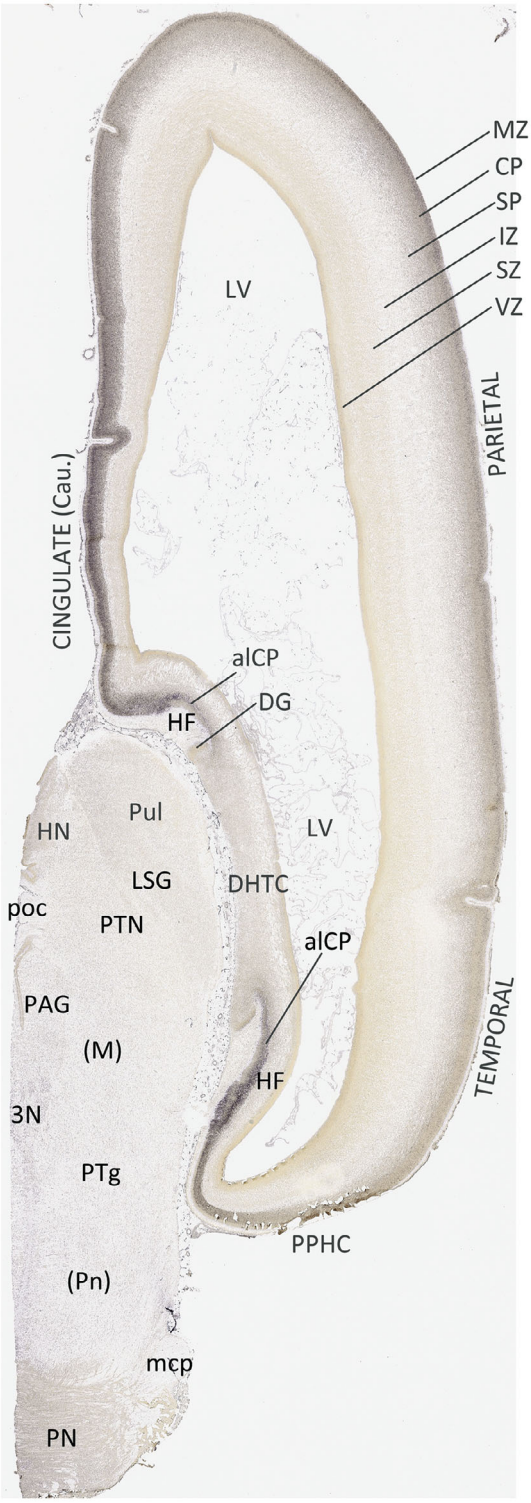

FEZF2-02-190 (Level ~32)

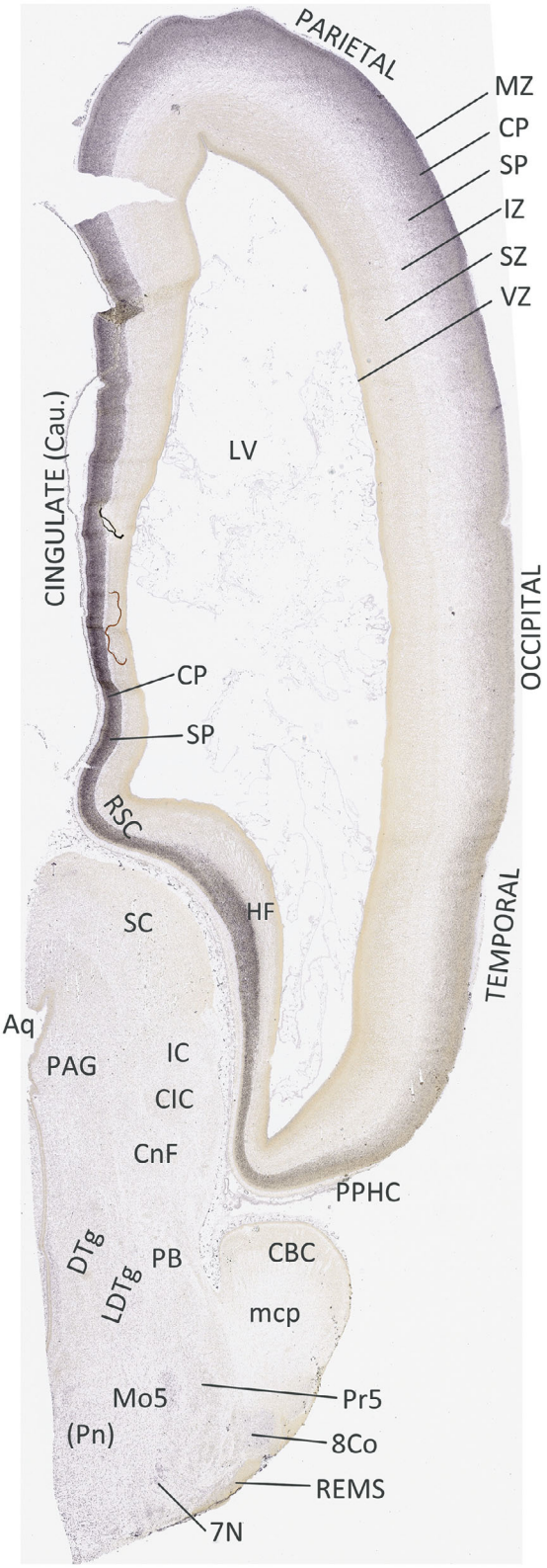

FEZF2-02-294 (Level ~36)

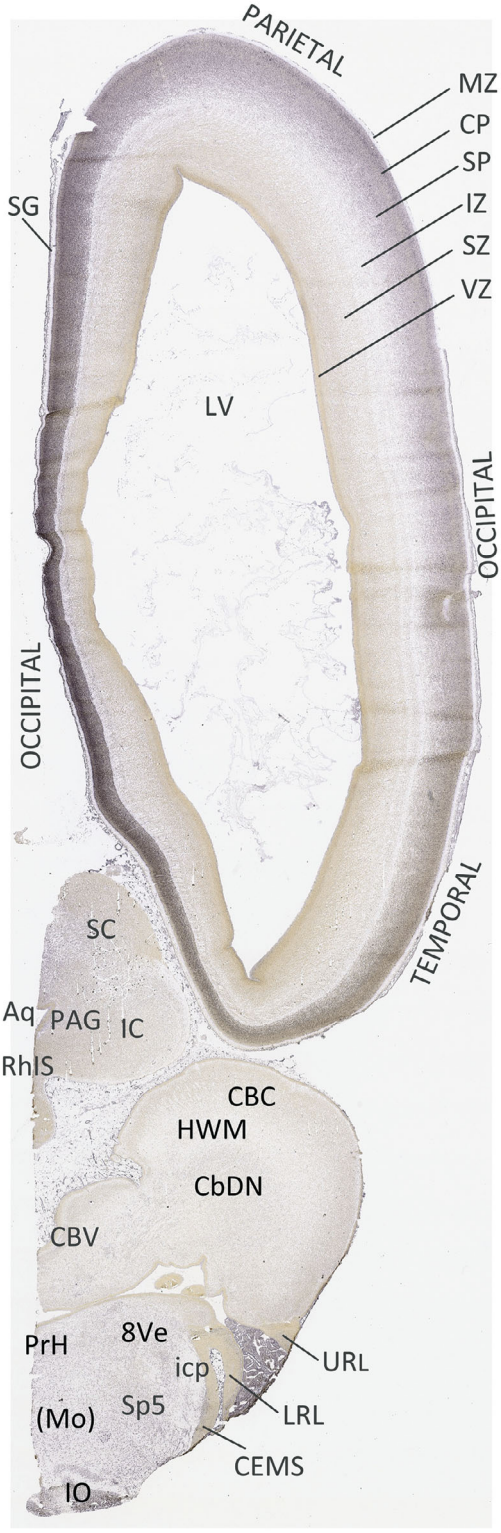

FEZF2-02-398 (Level ~40)

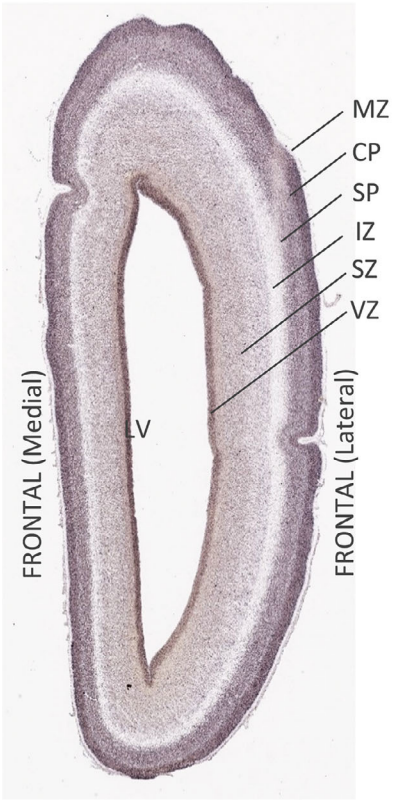

FOXG1-01-077 (Level ~2-3)

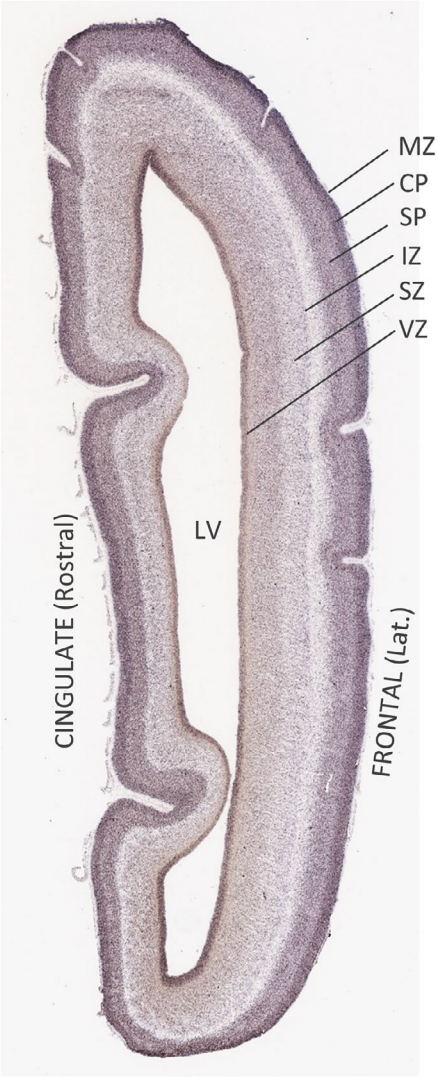

FOXG1-01-181 (Level ~4-5)

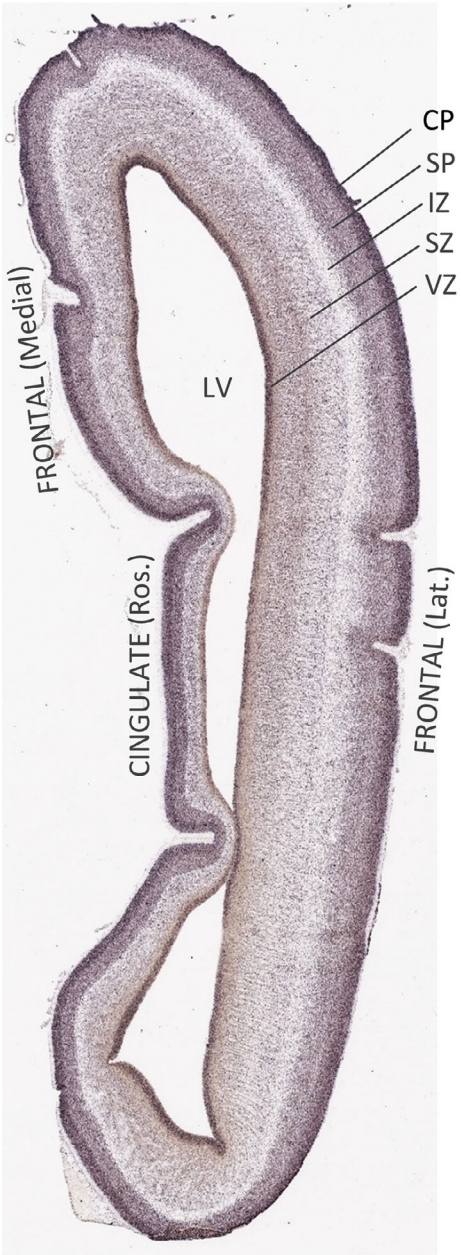

FOXG1-01-285 (Level ~7)

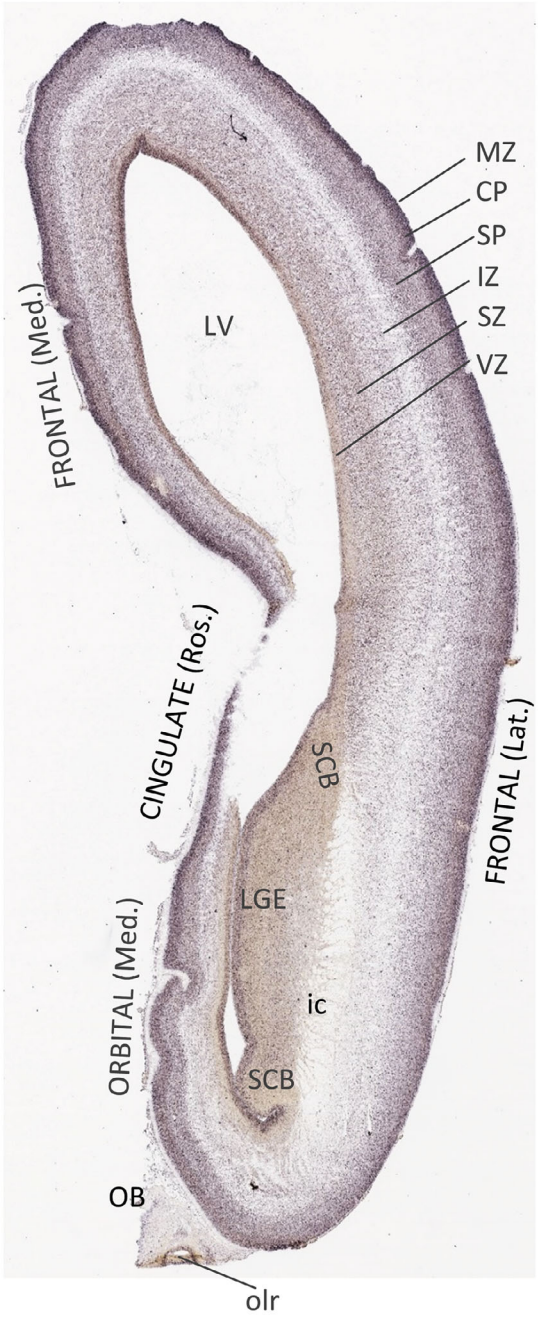

FOXG1-01-389 (Level ~11)

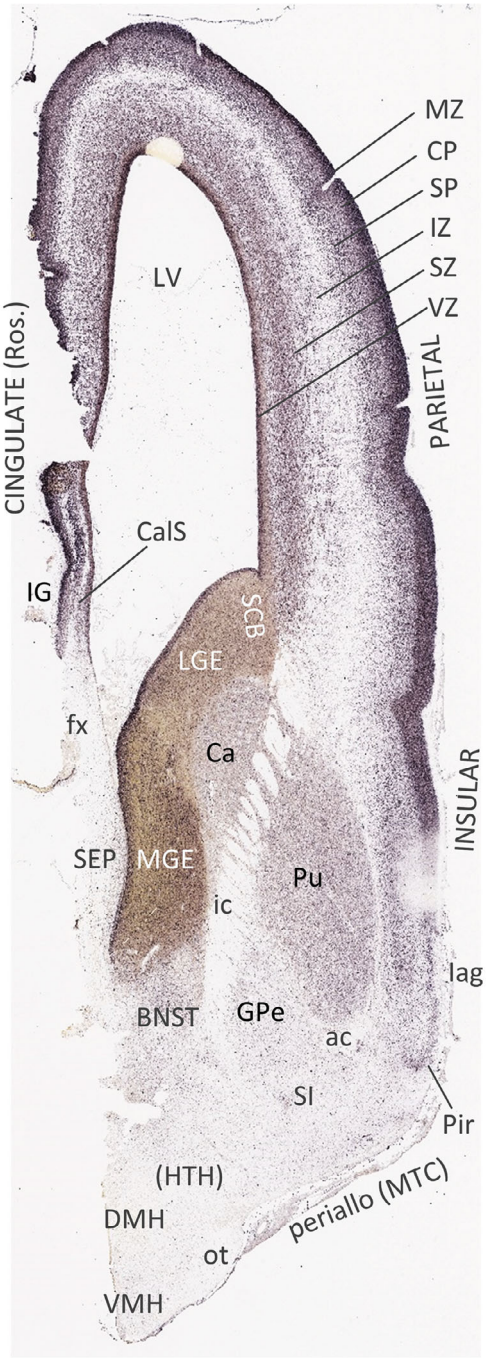

FOXG1-01-597 (Level ~18-19)

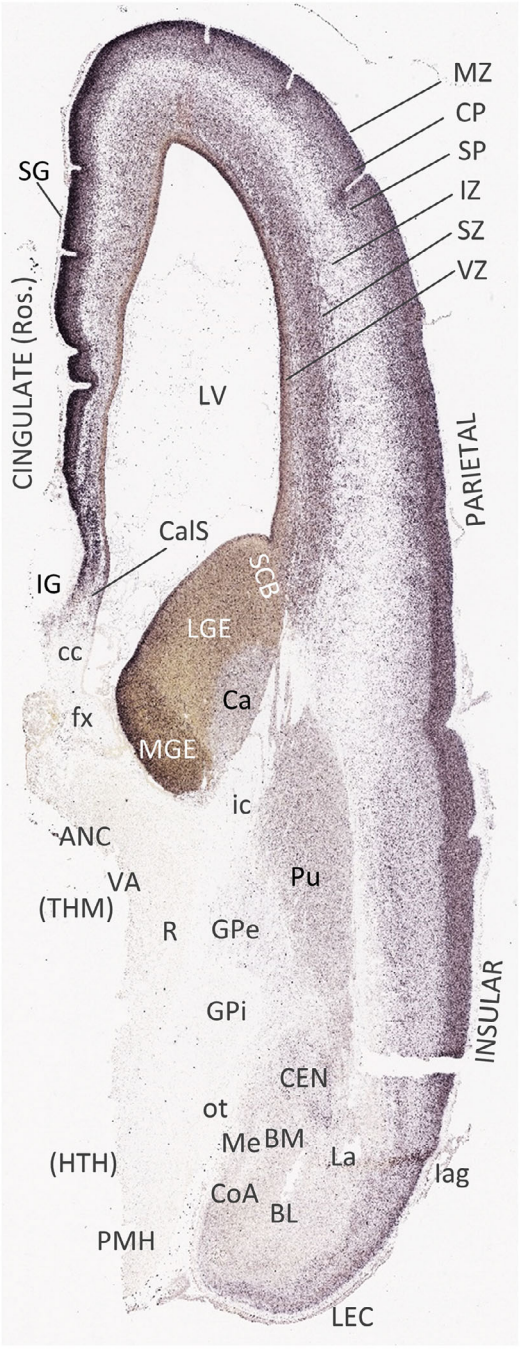

FOXG1-01-701 (Level ~22)

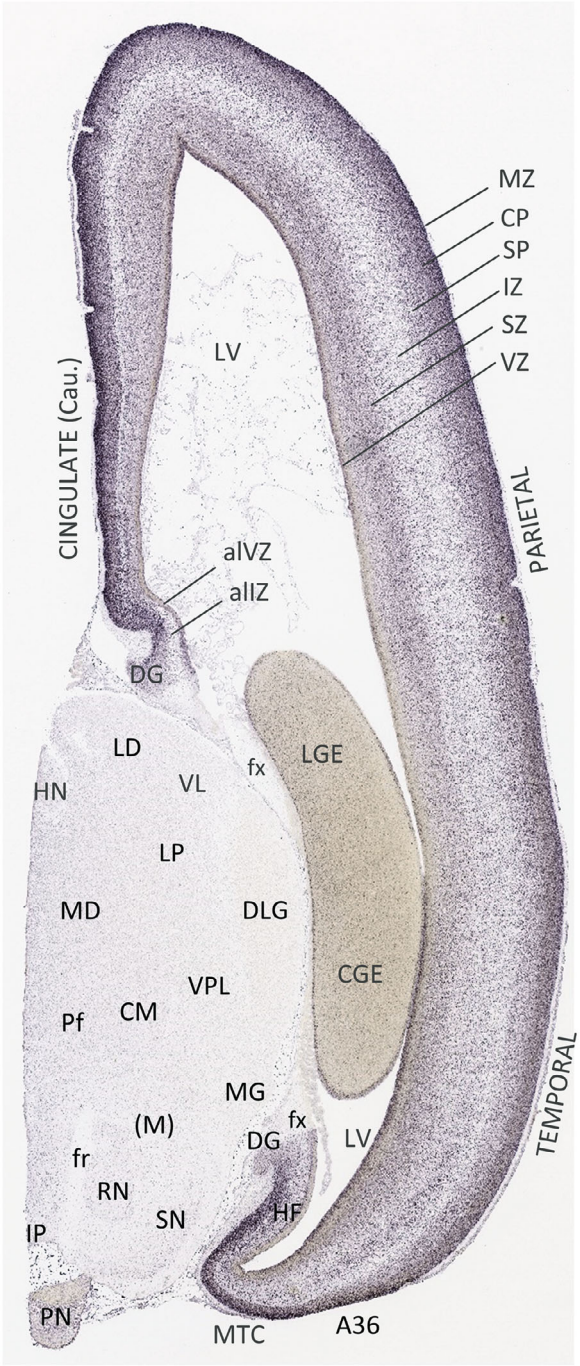

FOXG1-02-077 (Level ~27-28)

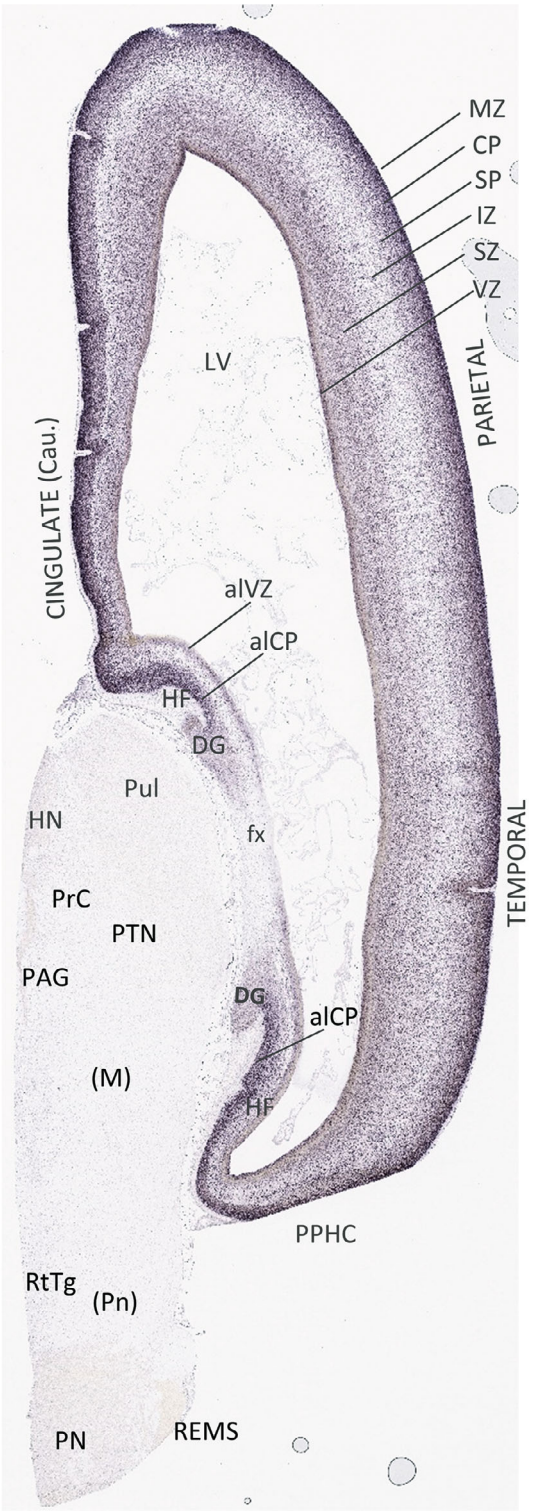

FOXG1-02-181 (Level ~31-32)

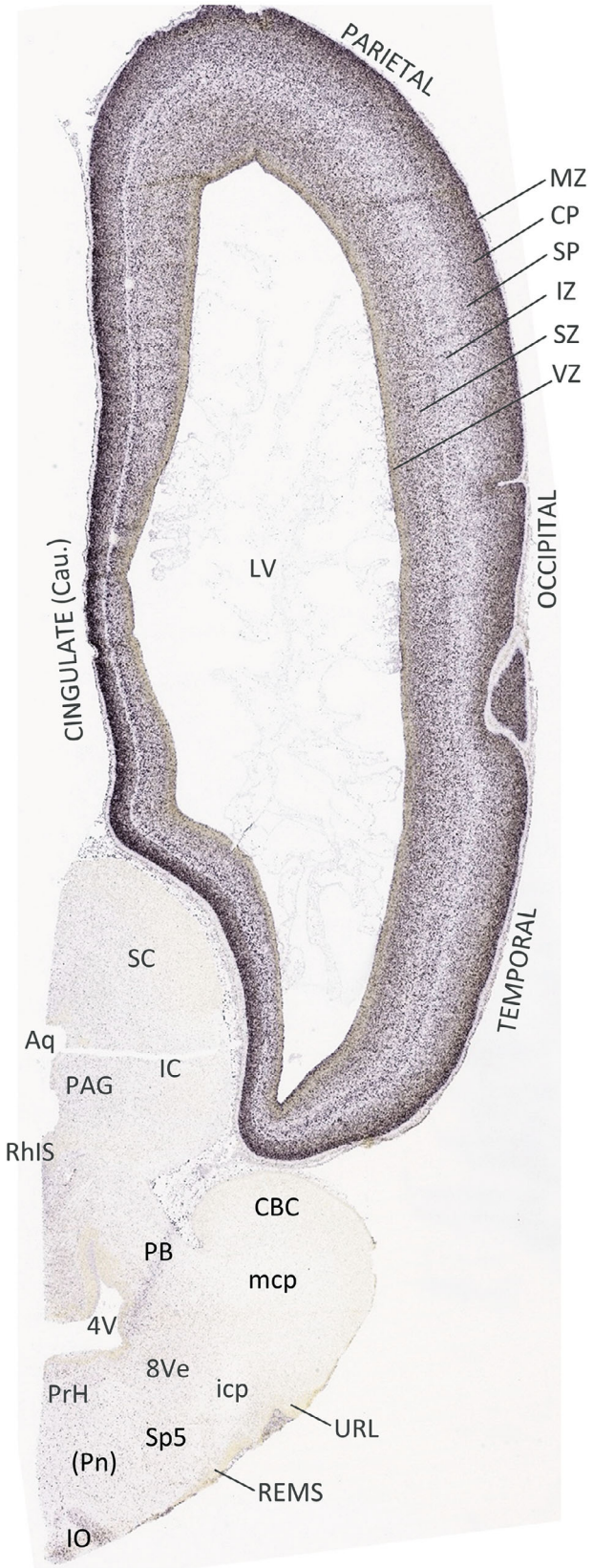

FOXG1-02-337 (Level ~37-38)

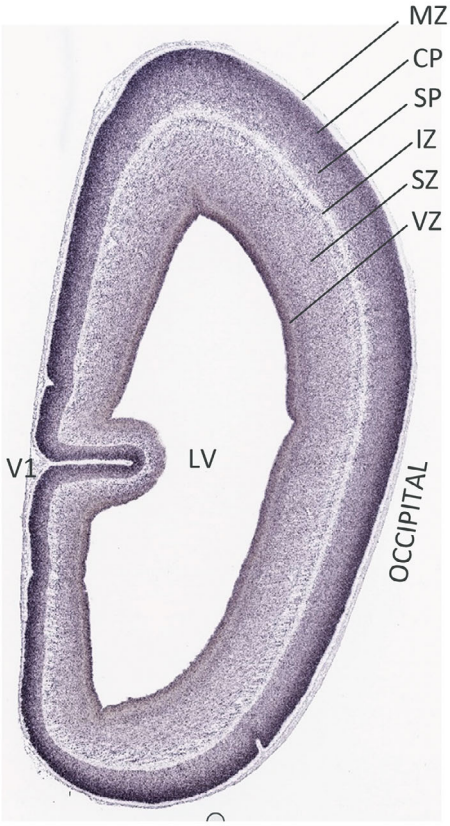

FOXG1-02-545 (Level ~43)

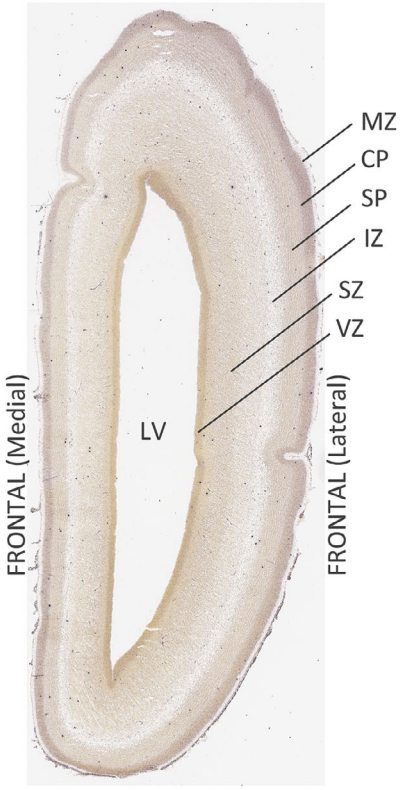

FOXP1-01-078 (Level ~3)

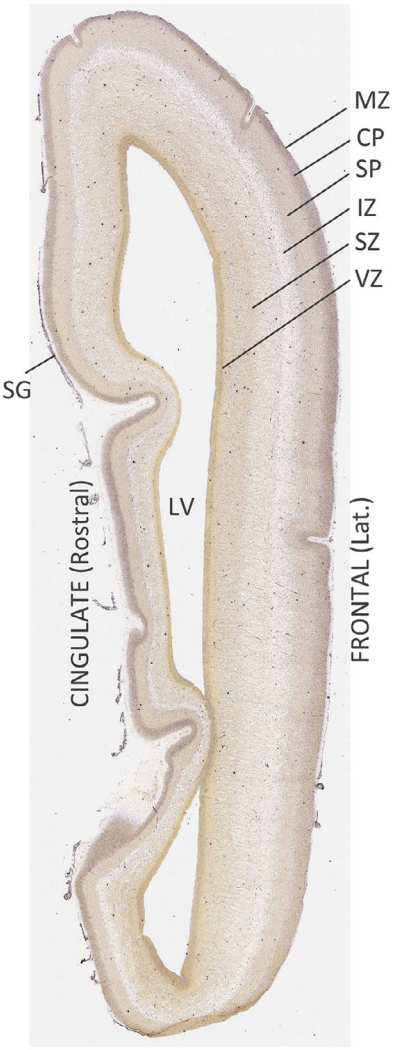

FOXP1-01-234 (Level ~6)

FOXP1-01-338 (Level ~9)

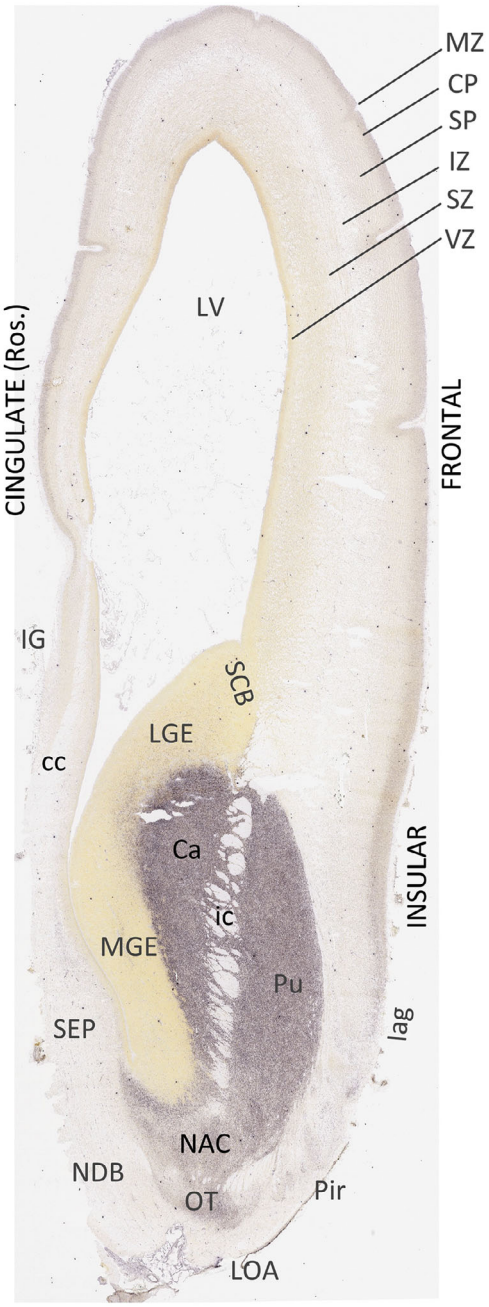

FOXP1-01-494 (Level ~15)

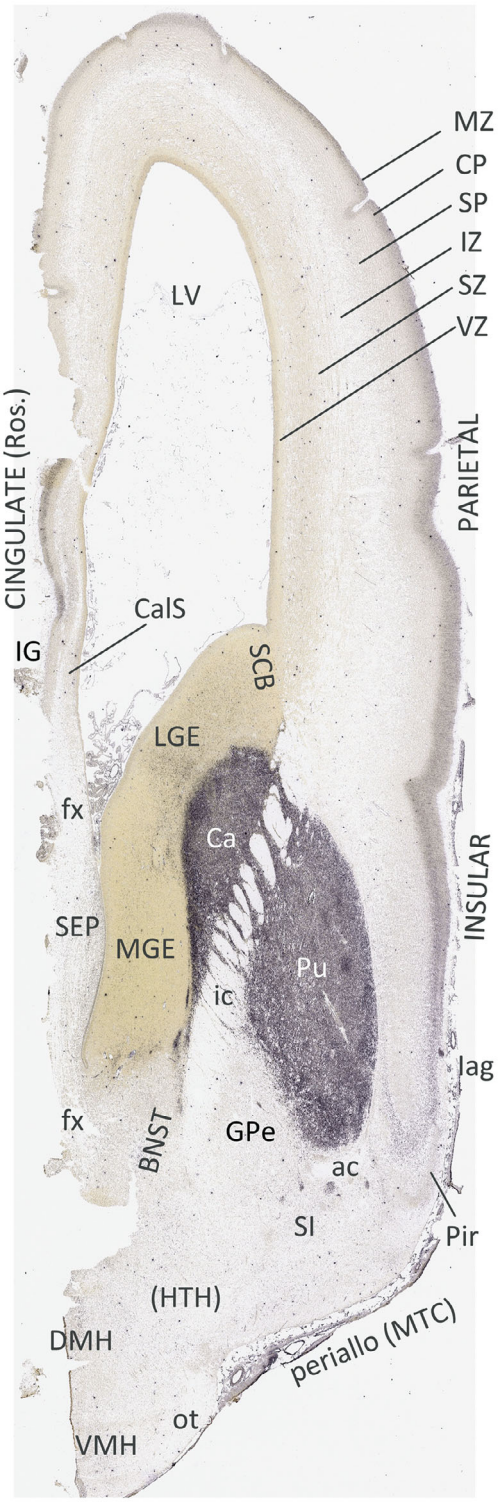

FOXP1-01-598 (Level ~19)

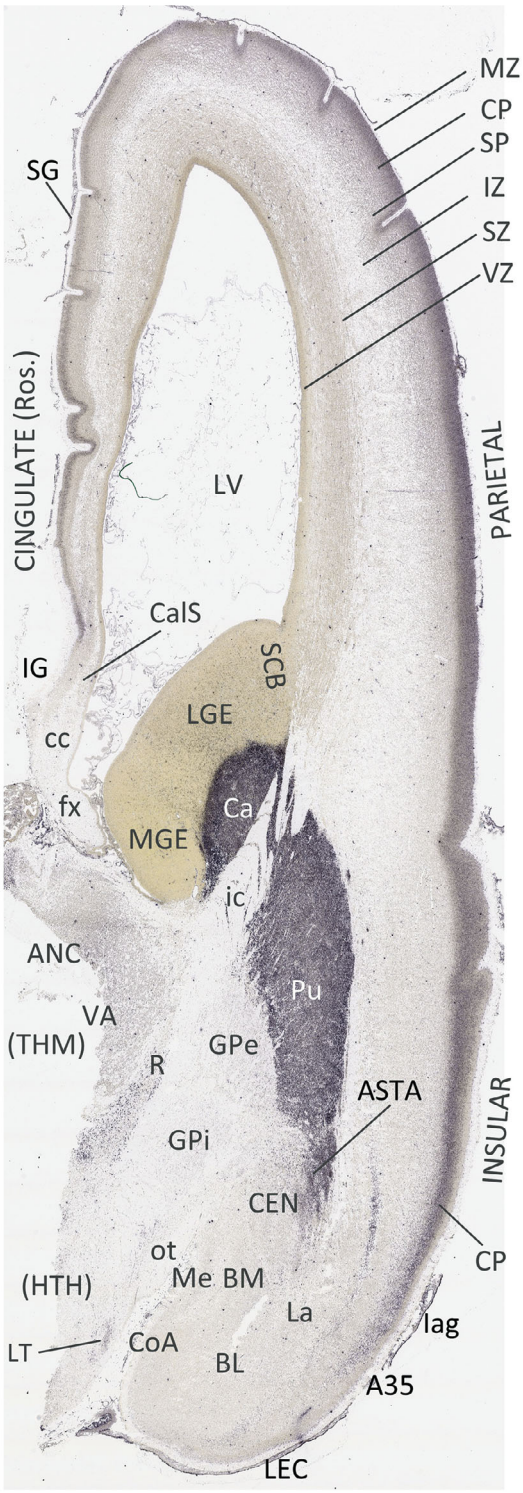

FOXP1-01-702 (Level ~22)

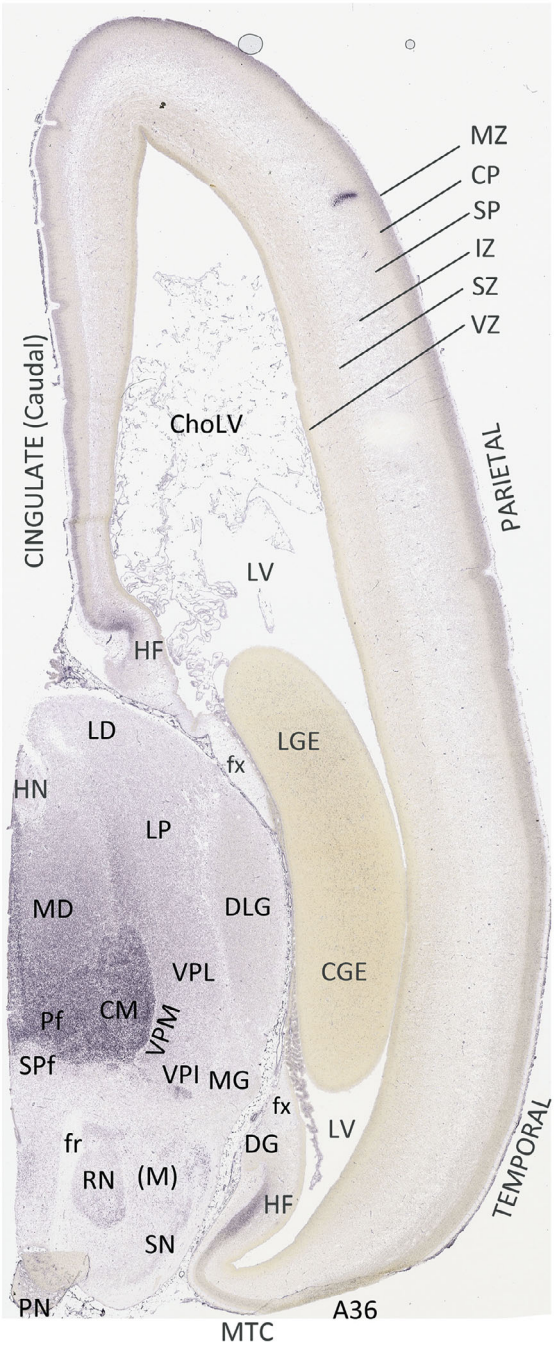

FOXP1-02-078 (Level ~27)

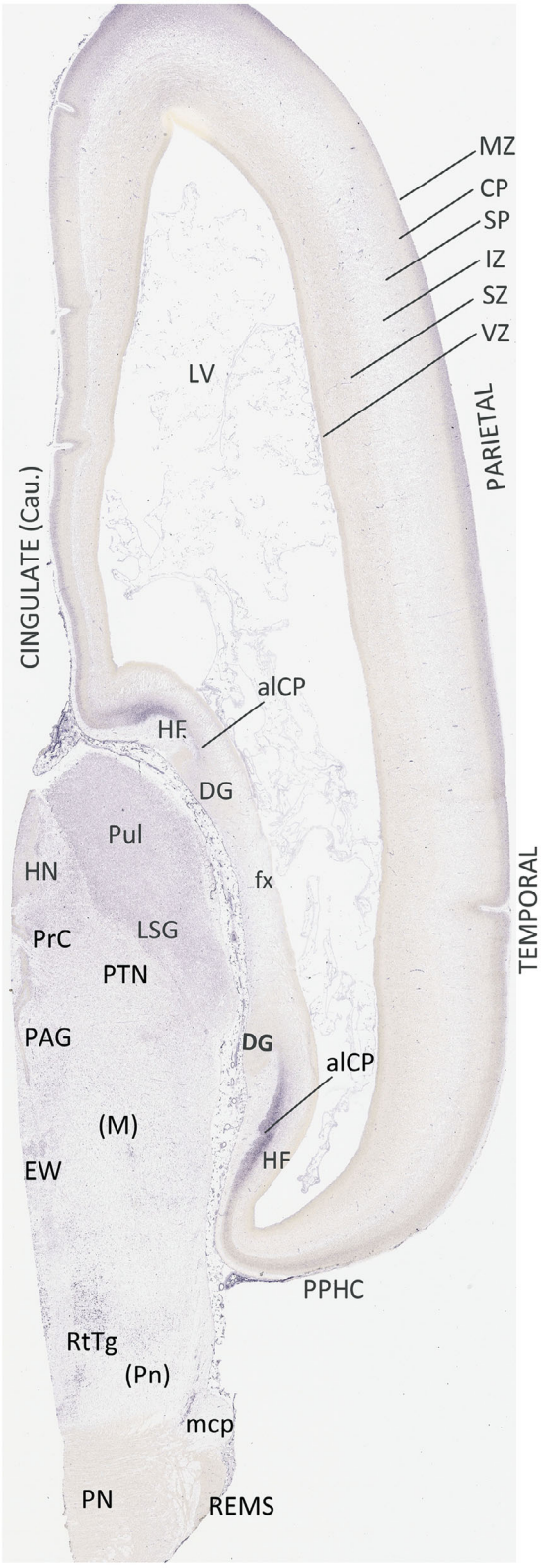

FOXP1-02-182 (Level ~31)

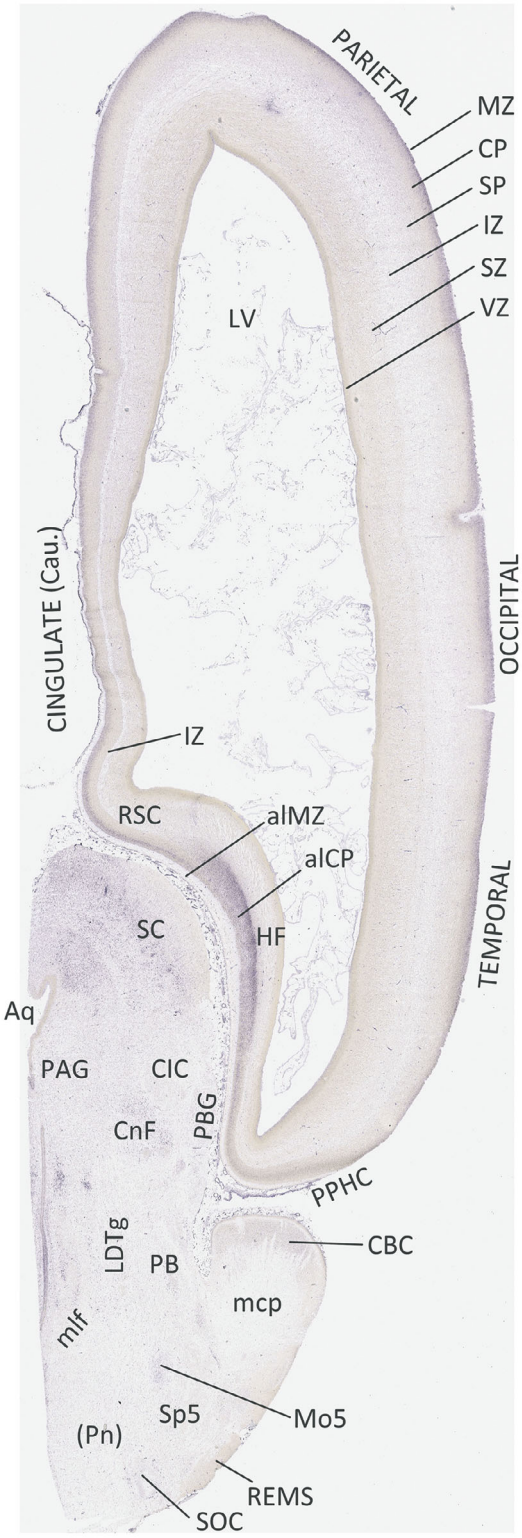

FOXP1-02-286 (Level ~35)

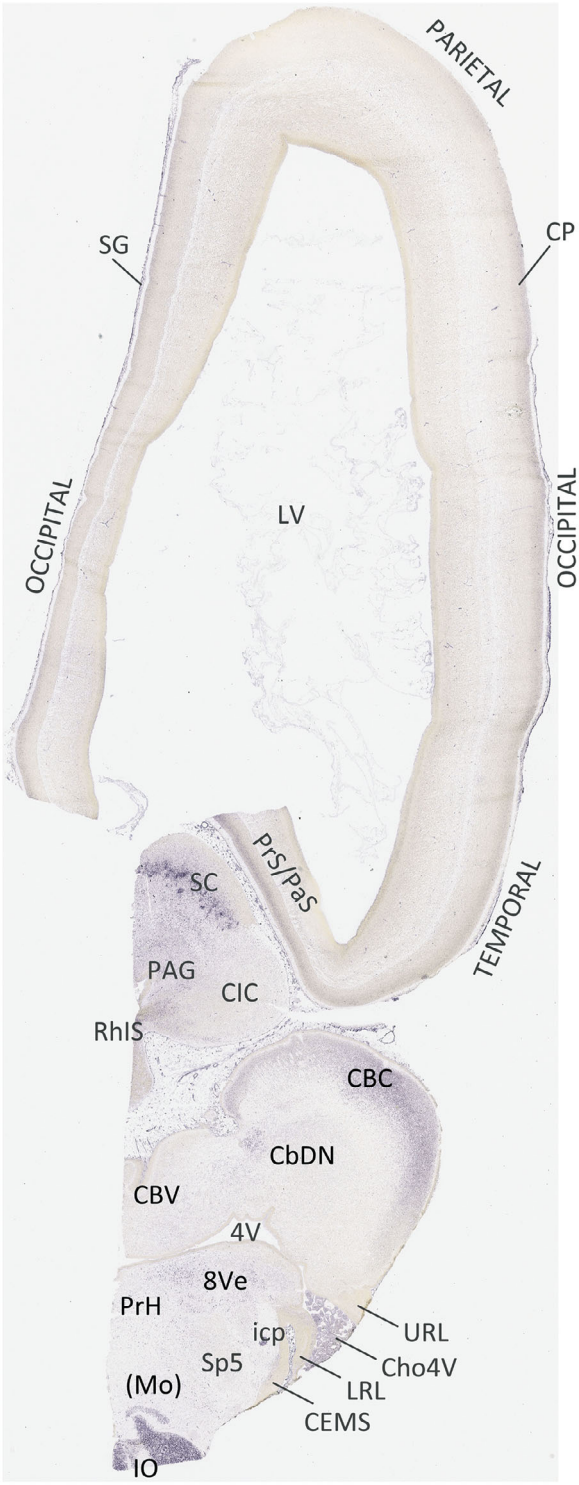

FOXP1-02-390 (Level ~40)

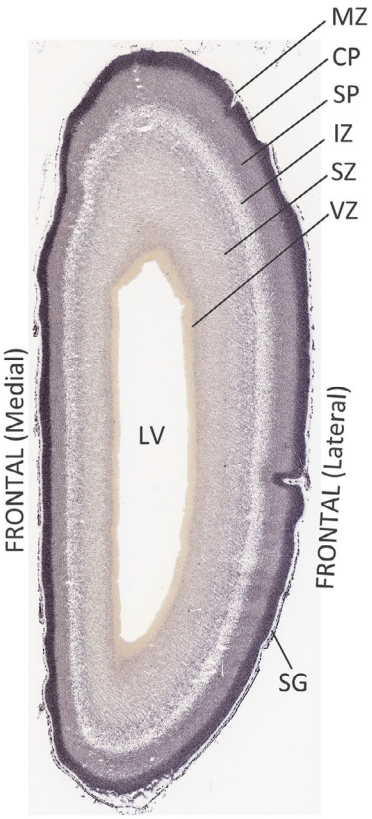

GAP43-01-055 (Level ~2)

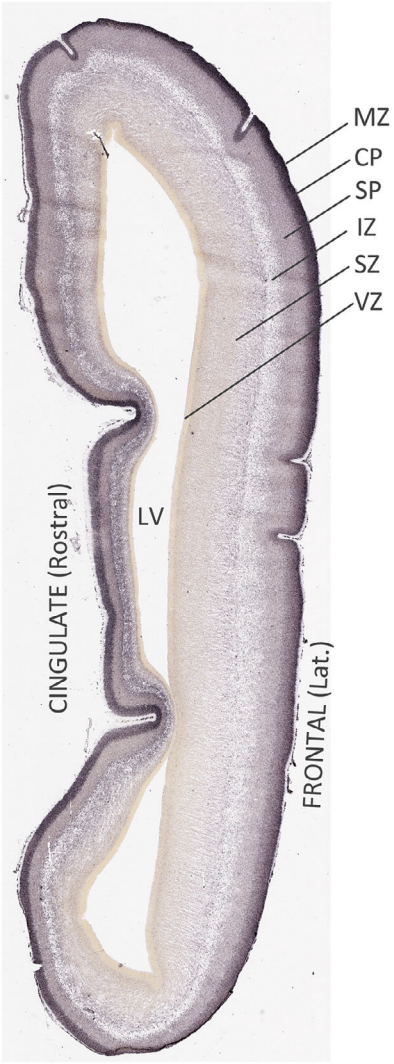

GAP43-01-263 (Level ~6)

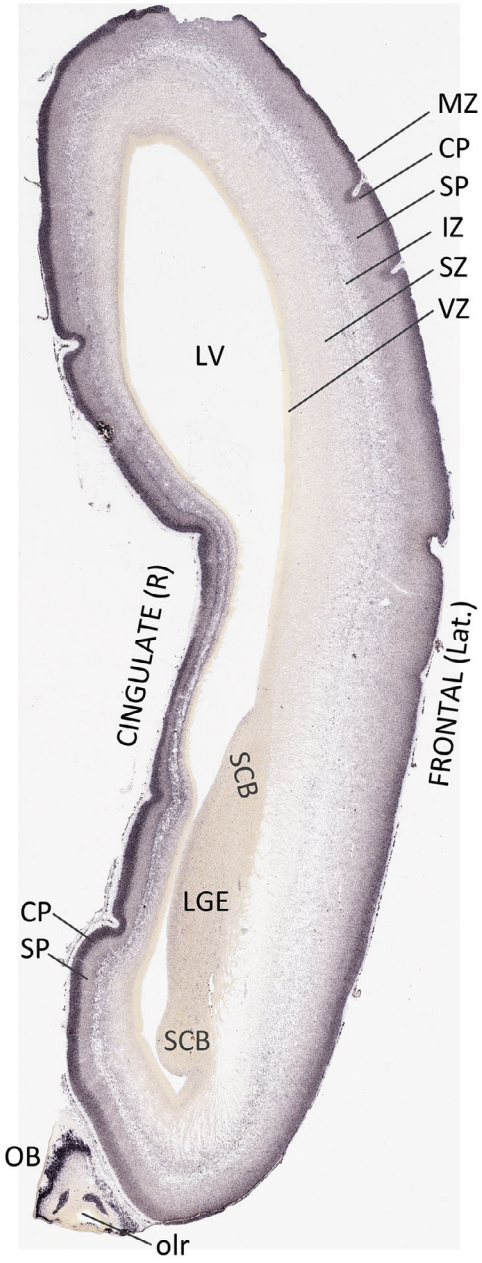

GAP43-01-367 (Level ~10)

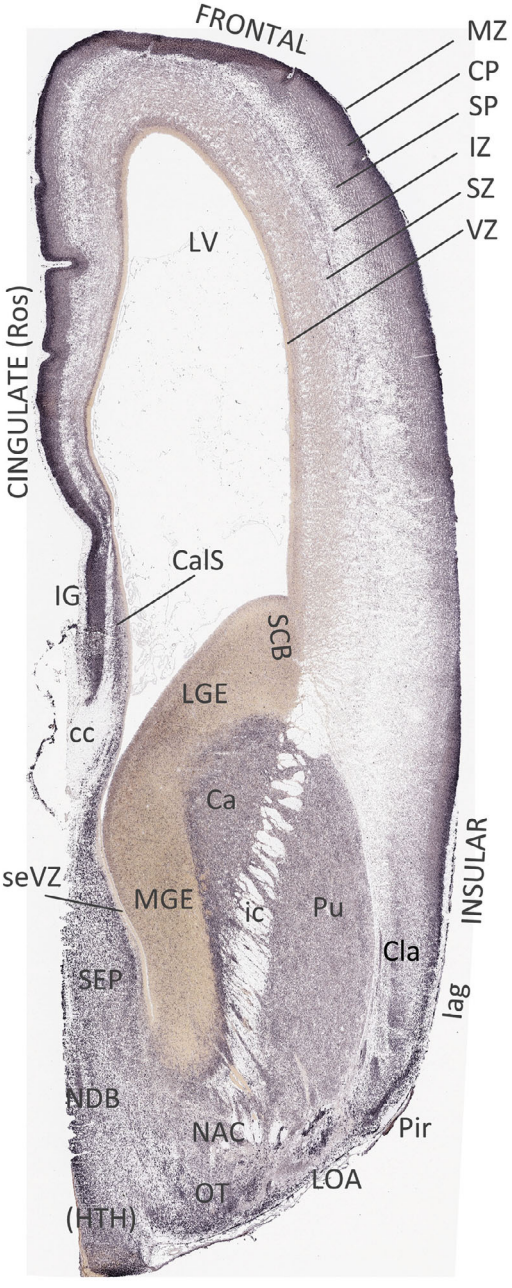

GAP43-01-523 (Level ~16)

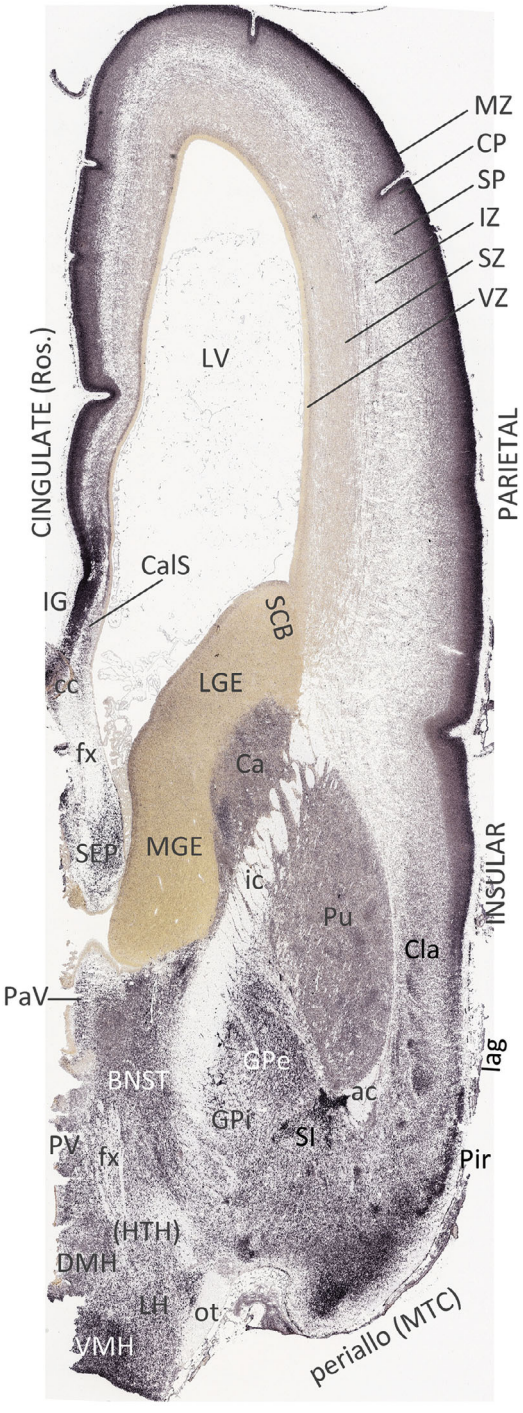

GAP43-01-627 (Level ~19-20)

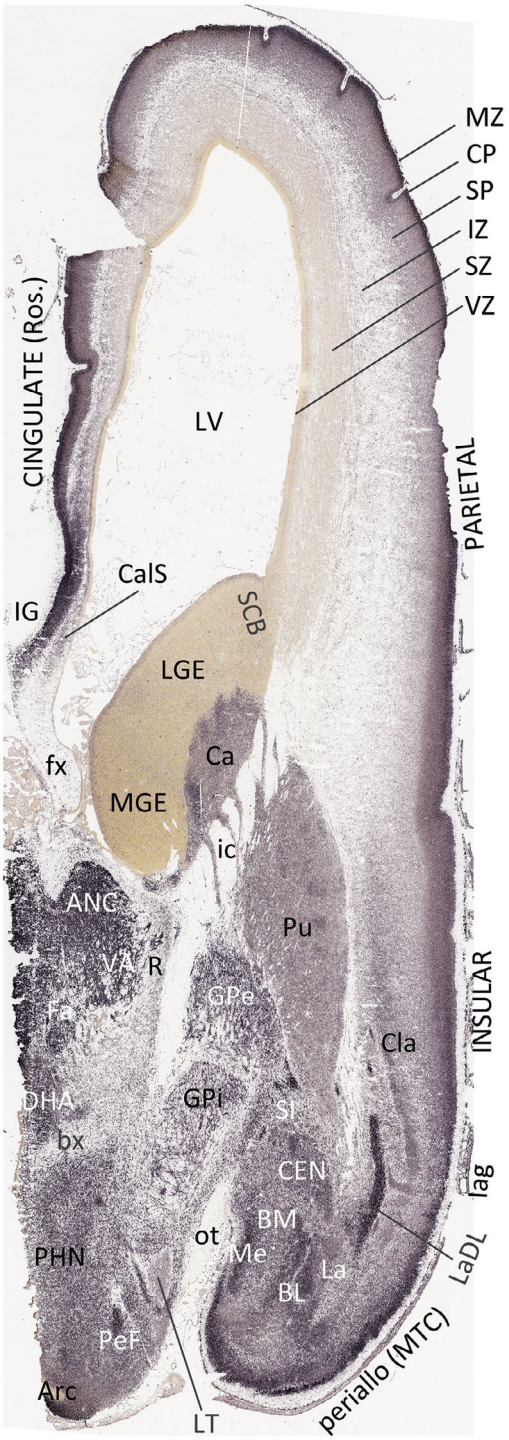

GAP43-01-679 (Level ~21)

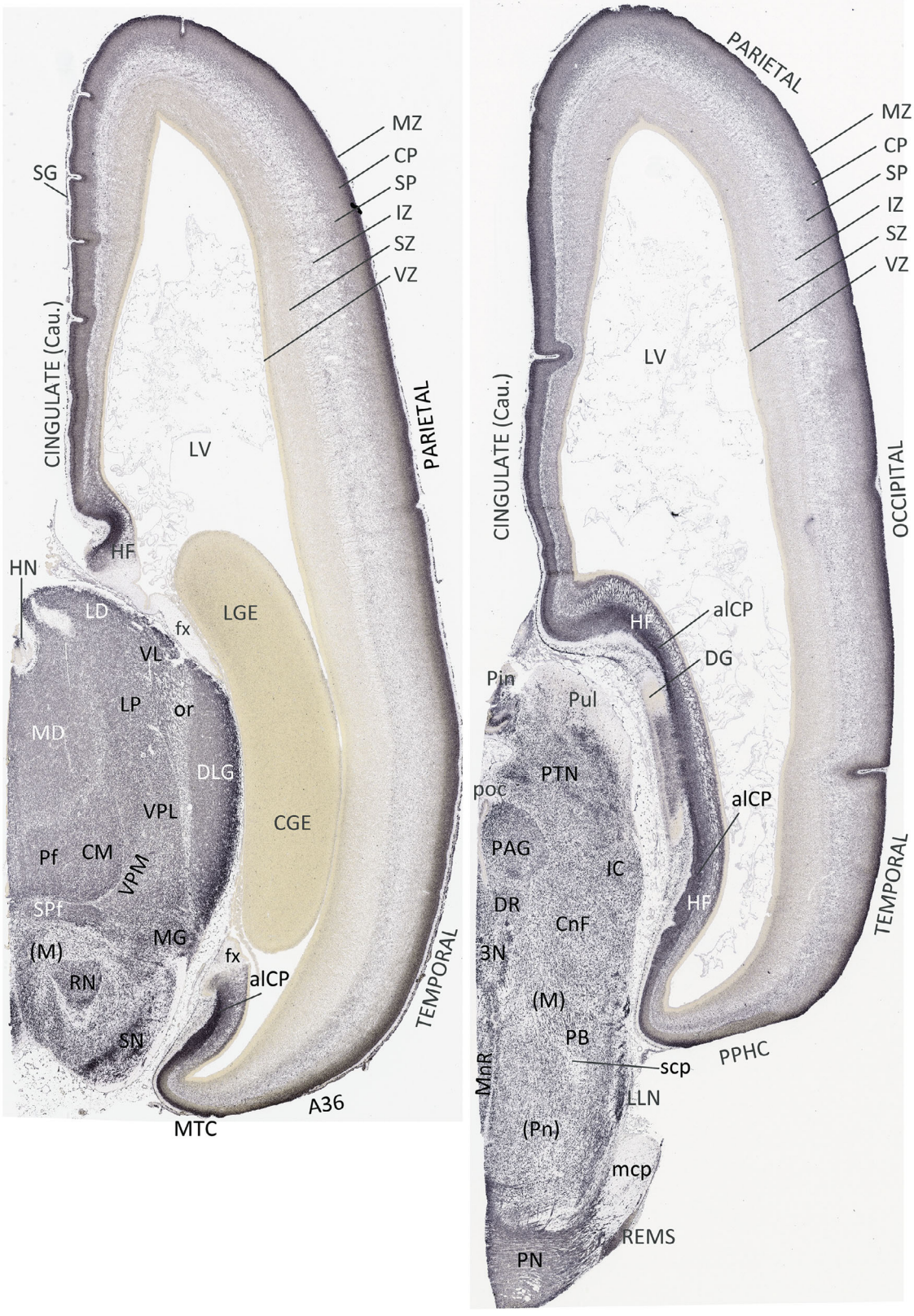

GAP43-02-055 (Level ~26-27)

GAP43-02-211 (Level ~33)

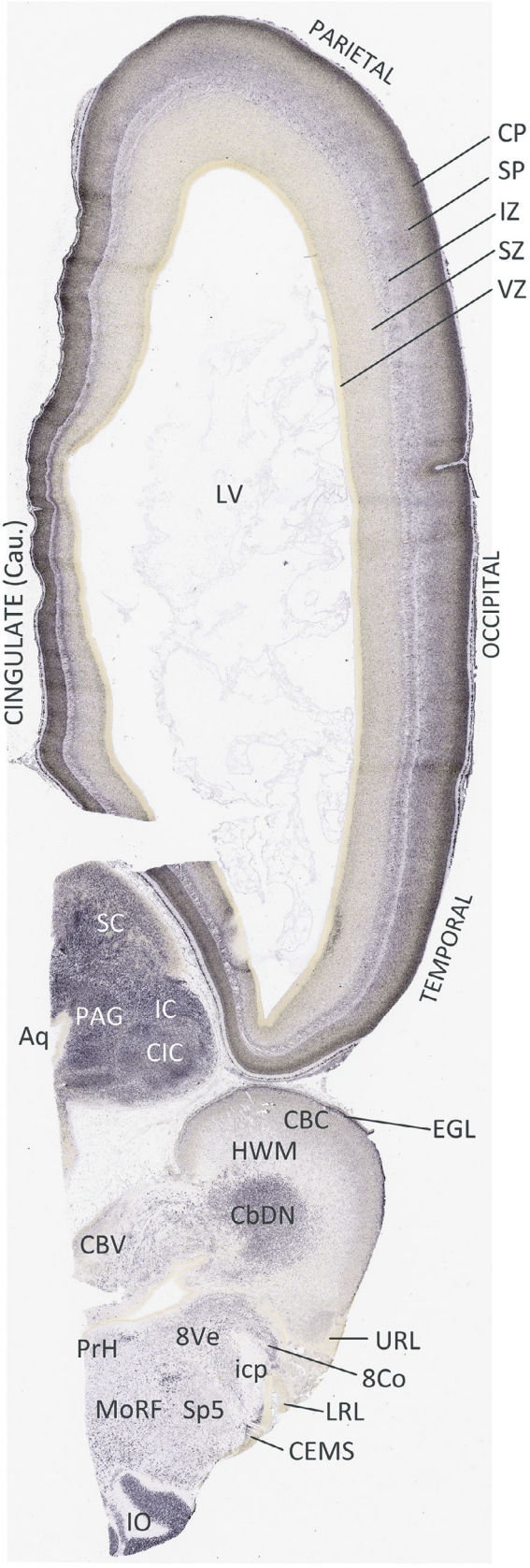

GAP43-02-367 (Level ~39)

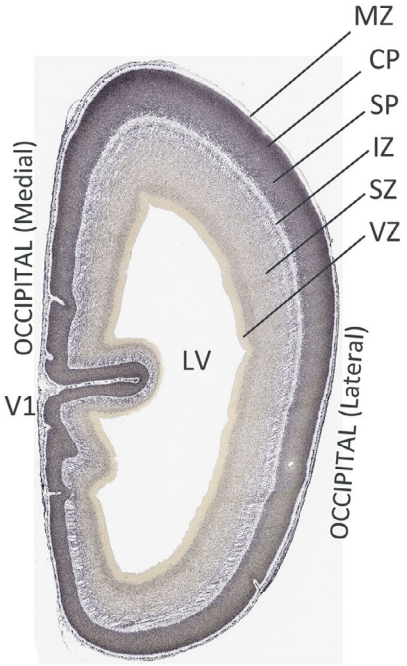

GAP43-02-575 (Level ~44)

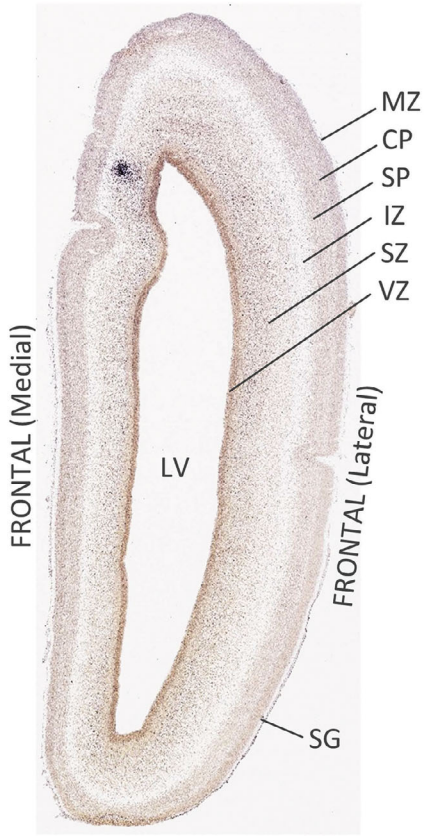

GFAP-01-115 (Level ~3)

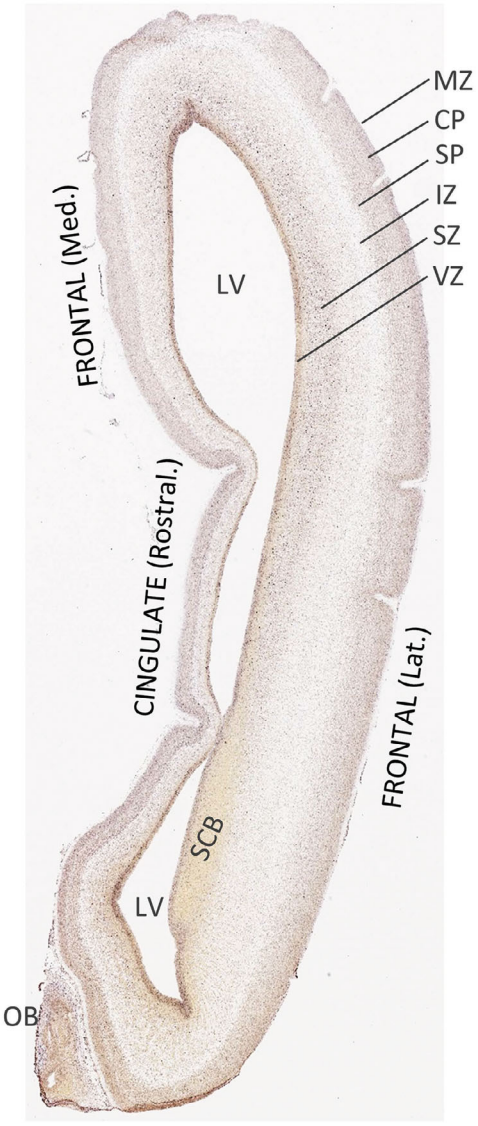

GFAP-01-323 (Level ~8)

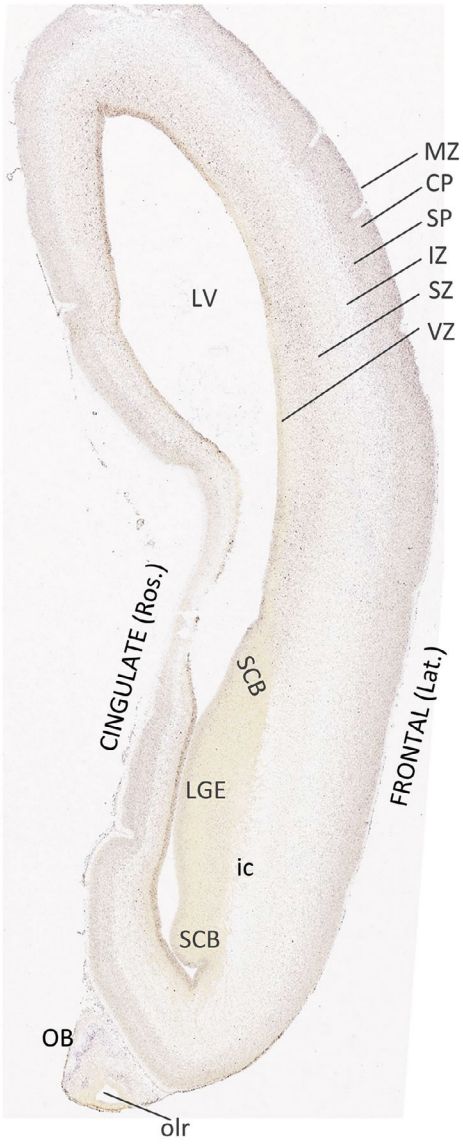

GFAP-01-375 (Level ~10-11)

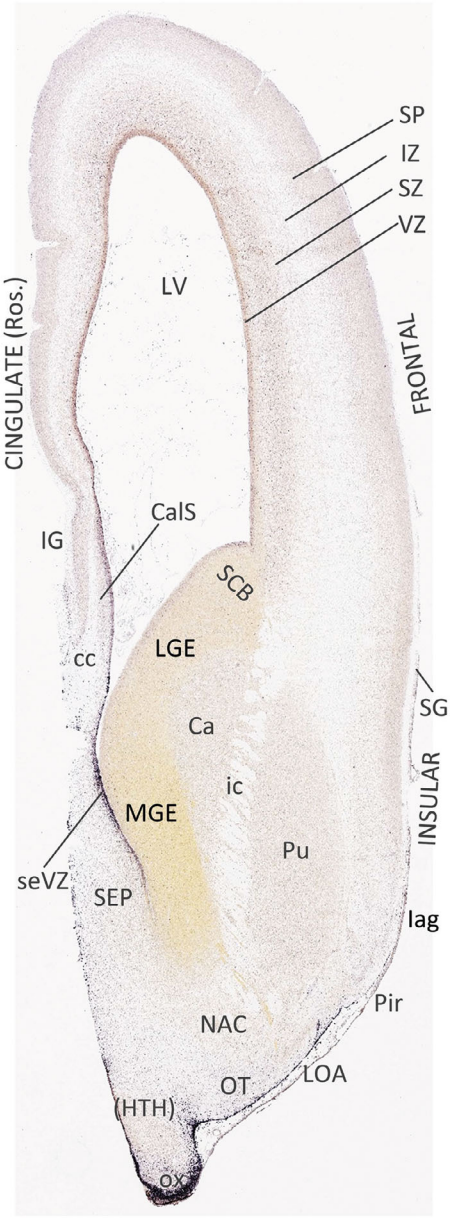

GFAP-01-531 (Level ~16-17)

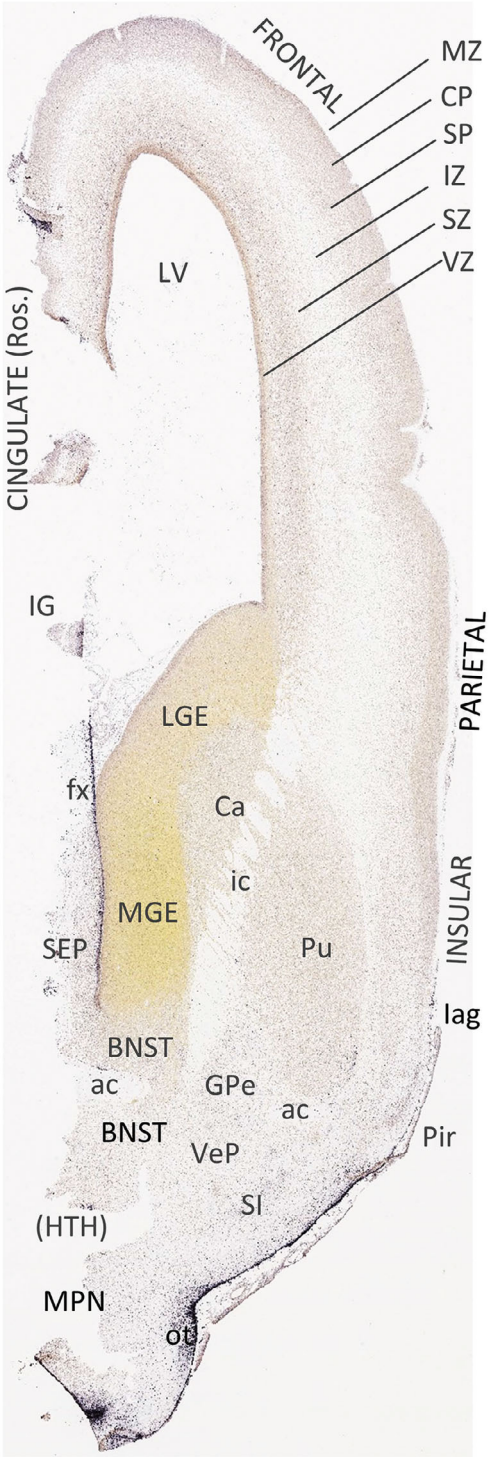

GFAP-01-583 (Level ~18)

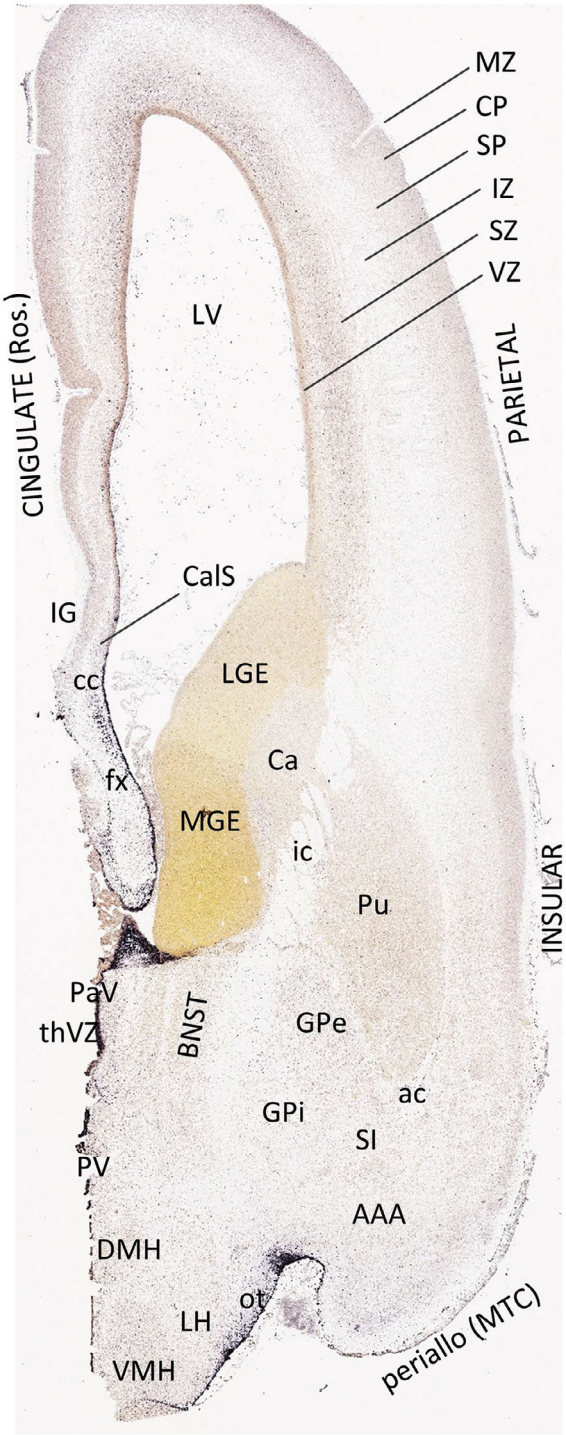

GFAP-01-635 (Level ~20)

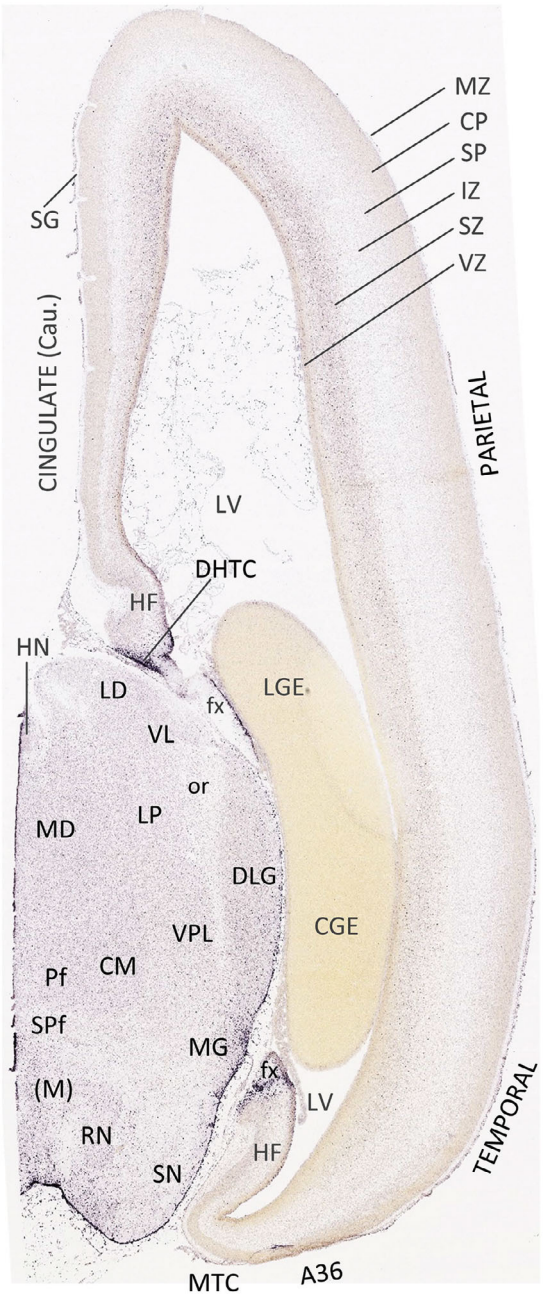

GFAP-02-063 (Level ~27)

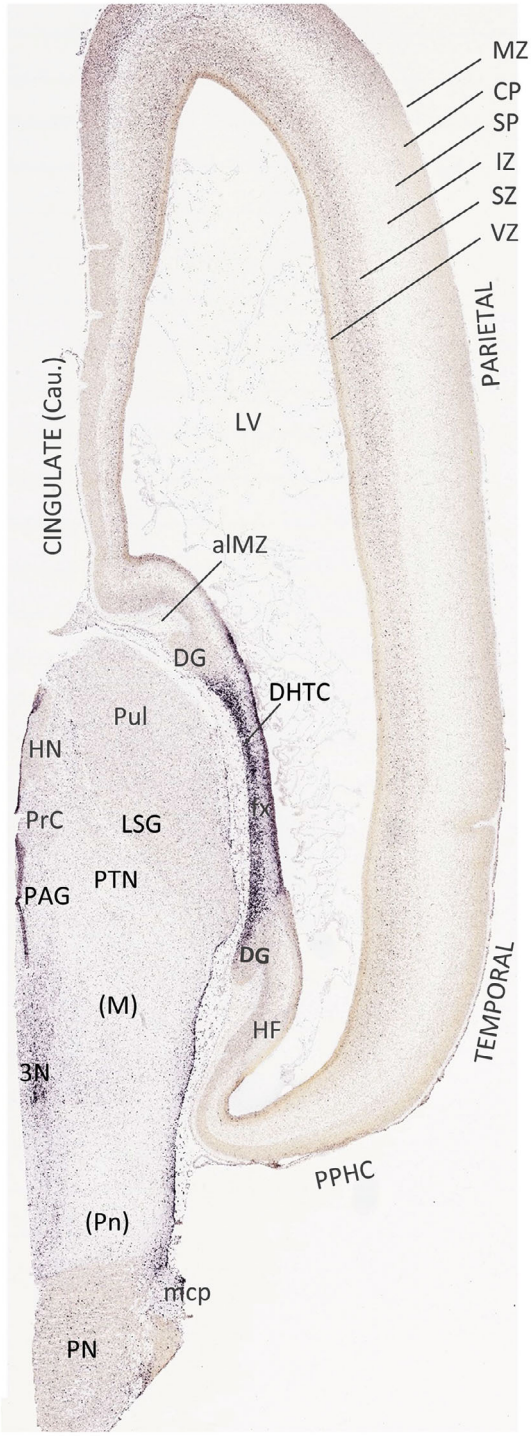

GFAP-02-167 (Level ~31)

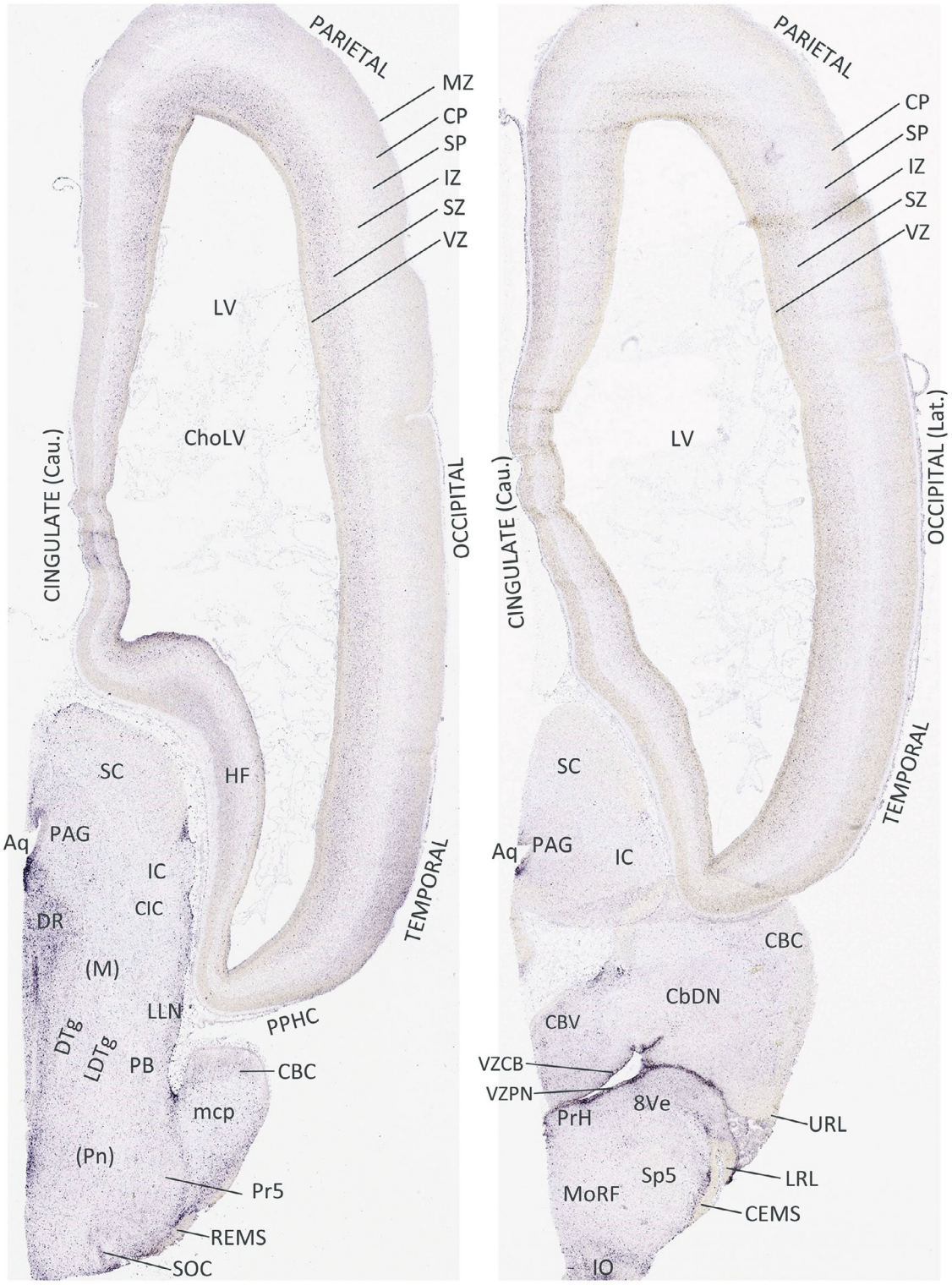

GFAP-02-271 (Level ~35) **GFAP-02-375 (Level ~39)**

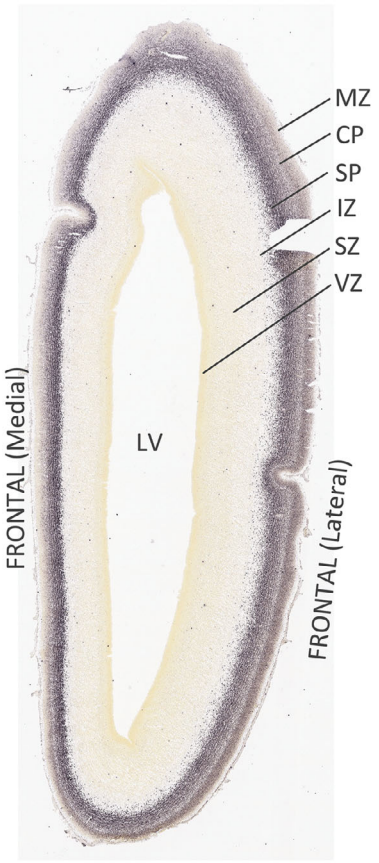

GRIK2-01-094 (Level ~3)

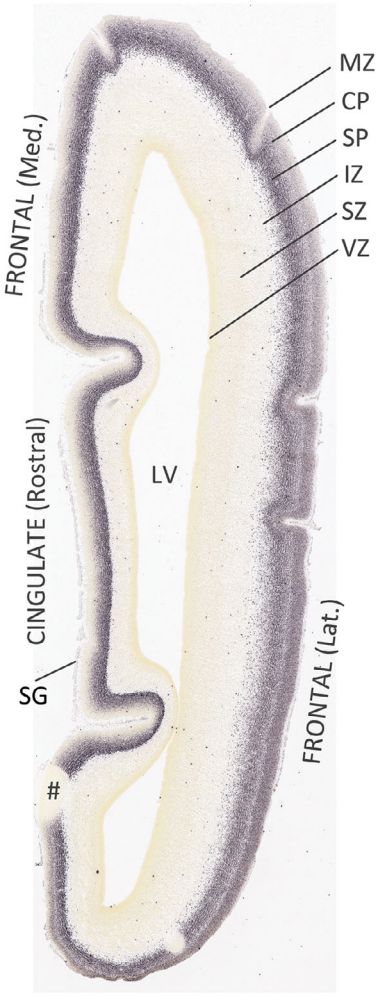

GRIK2-01-198 (Level ~5)

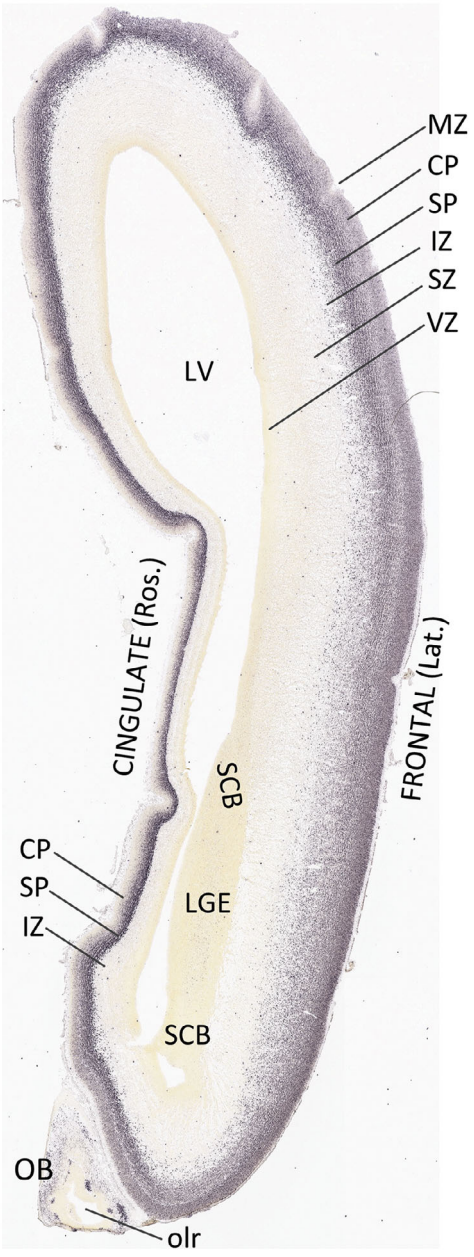

GRIK2-01-354 (Level ~10)

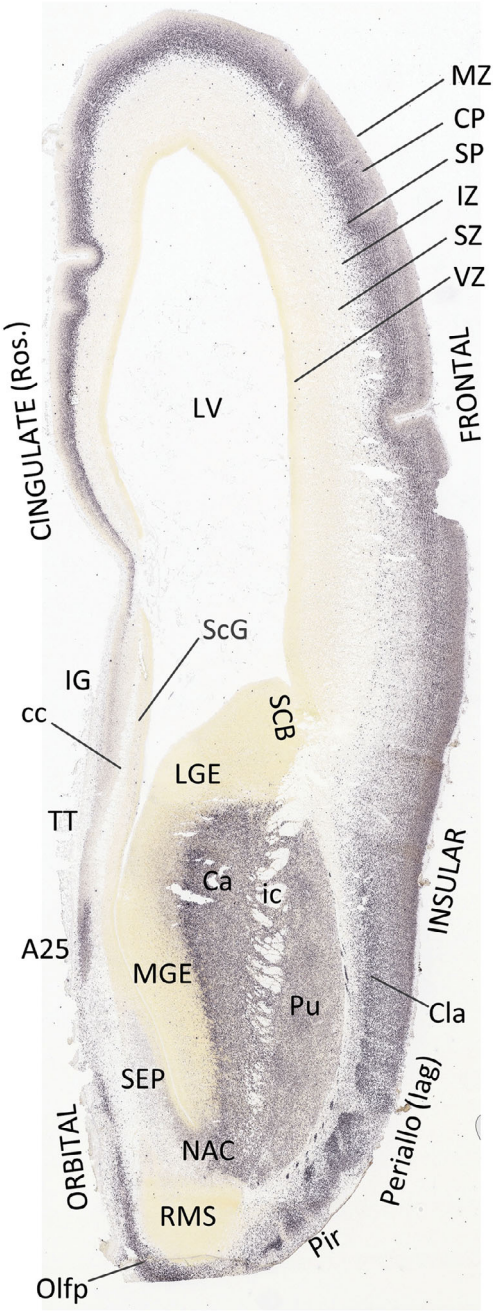

GRIK2-01-458 (Level ~14)

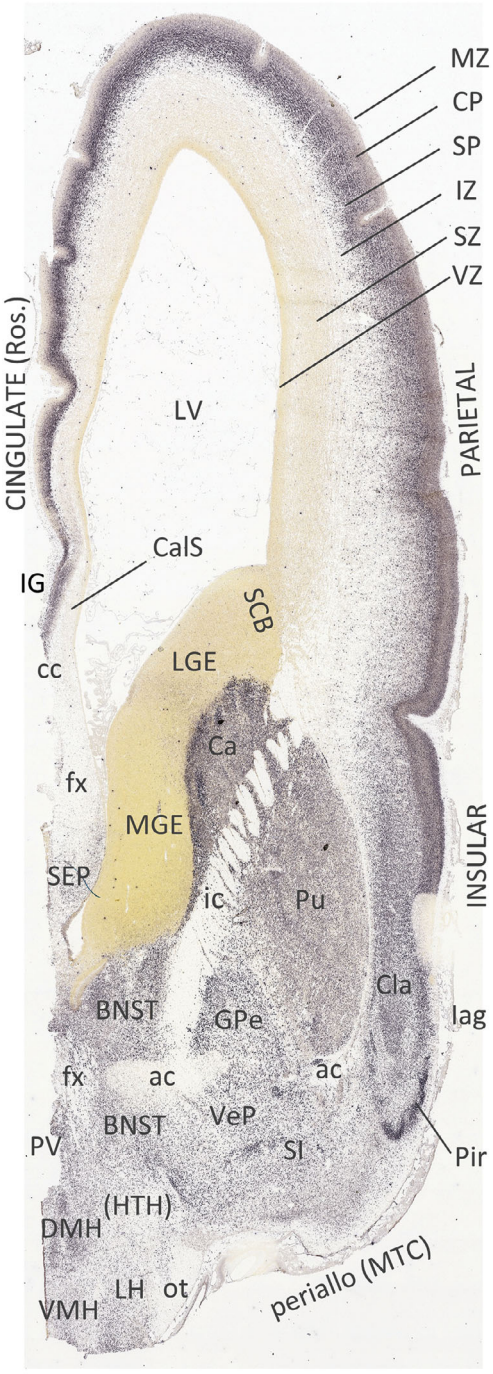

GRIK2-01-614 (Level ~19)

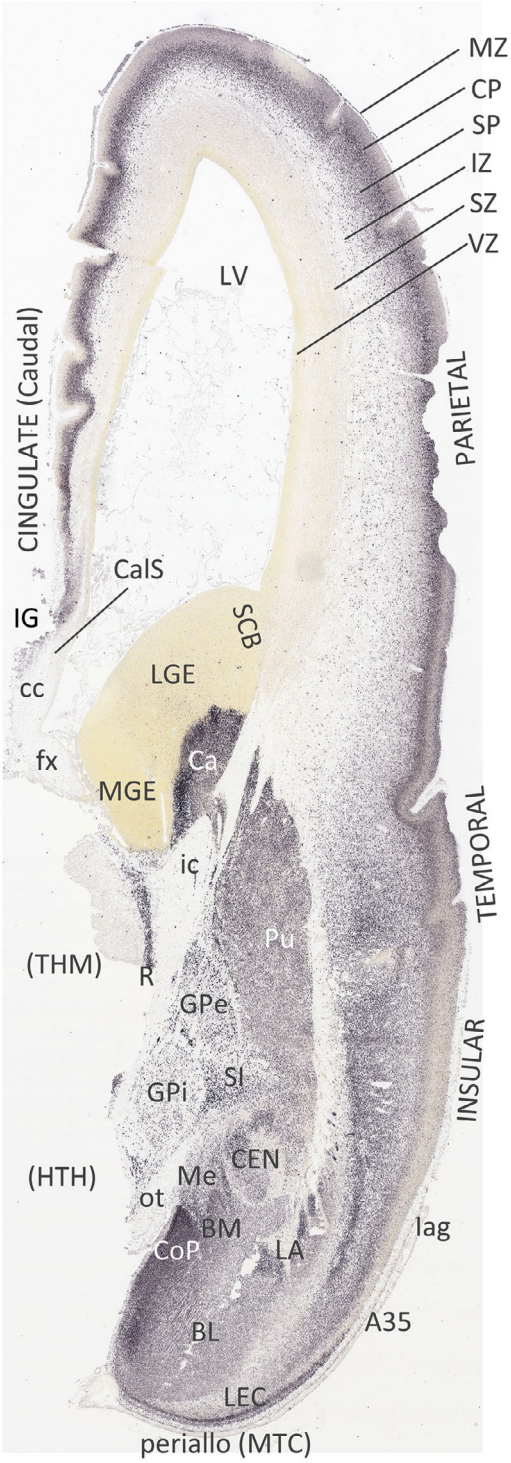

GRIK2-01-718 (Level ~22-23)

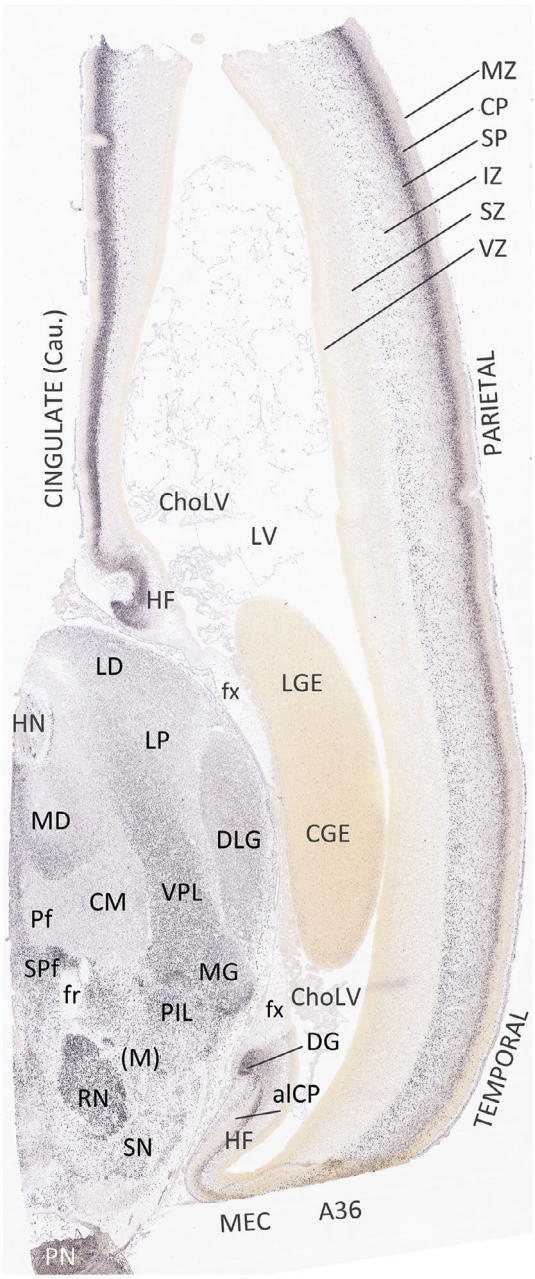

GRIK2-02-094 (Level ~28)

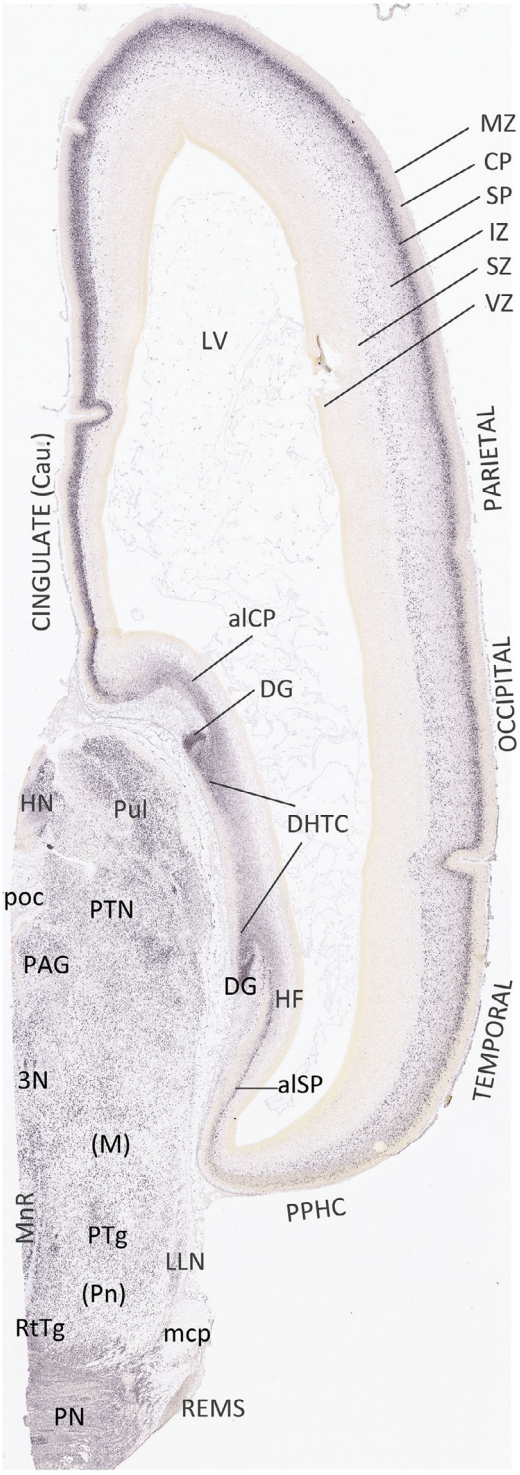

GRIK2-02-198 (Level ~32)

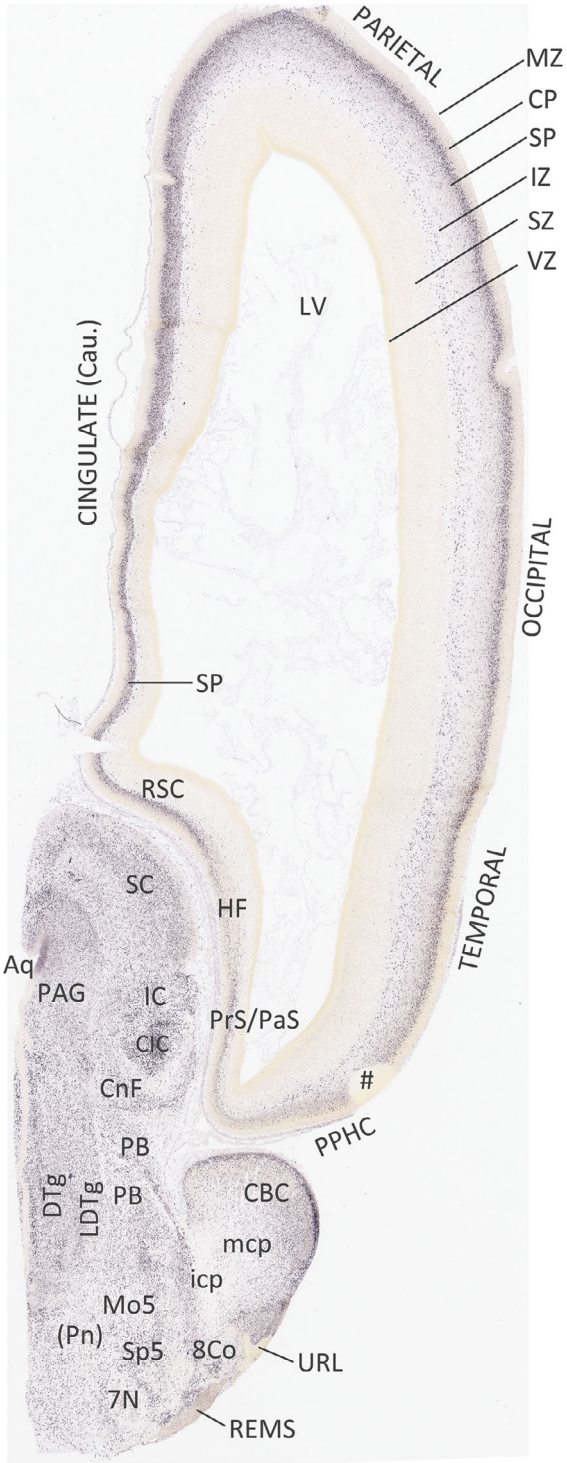

GRIK2-02-302 (Level ~36)

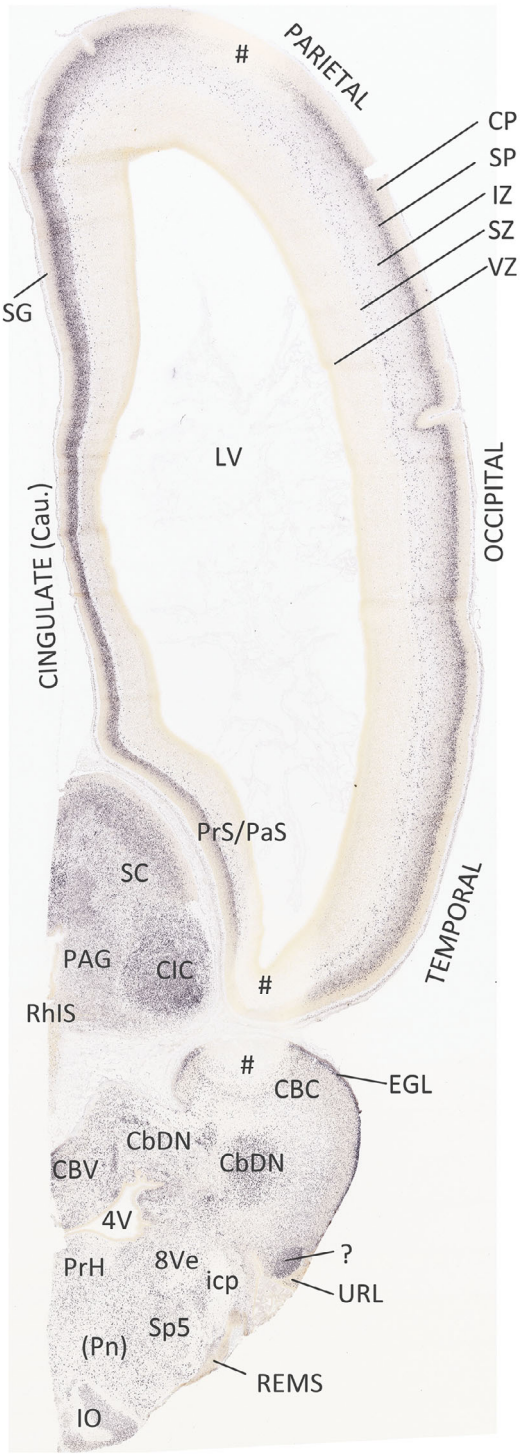

GRIK2-02-354 (Level ~38)

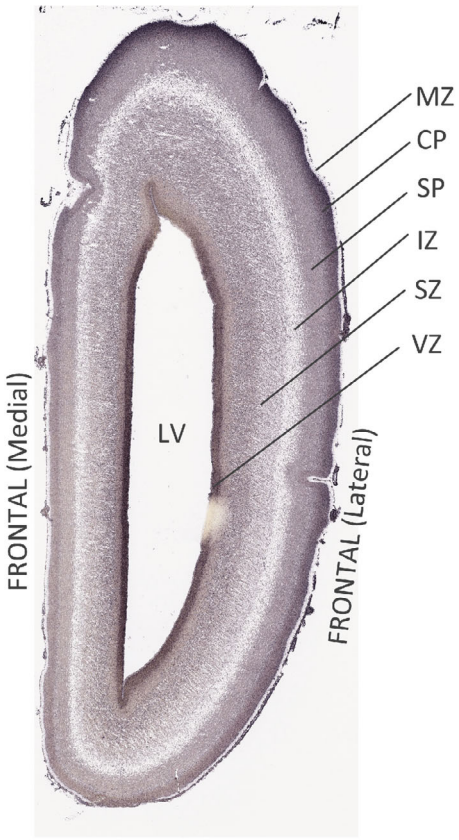

LHX2-01-068 (Level ~2-3)

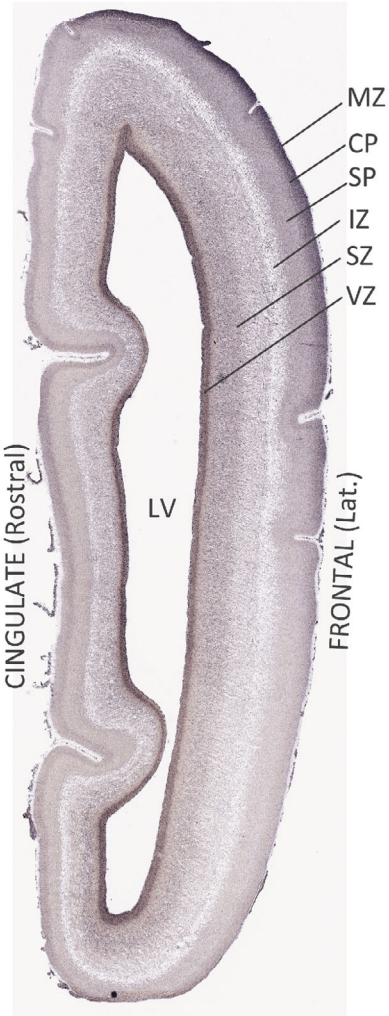

LHX2-01-172 (Level ~4-5)

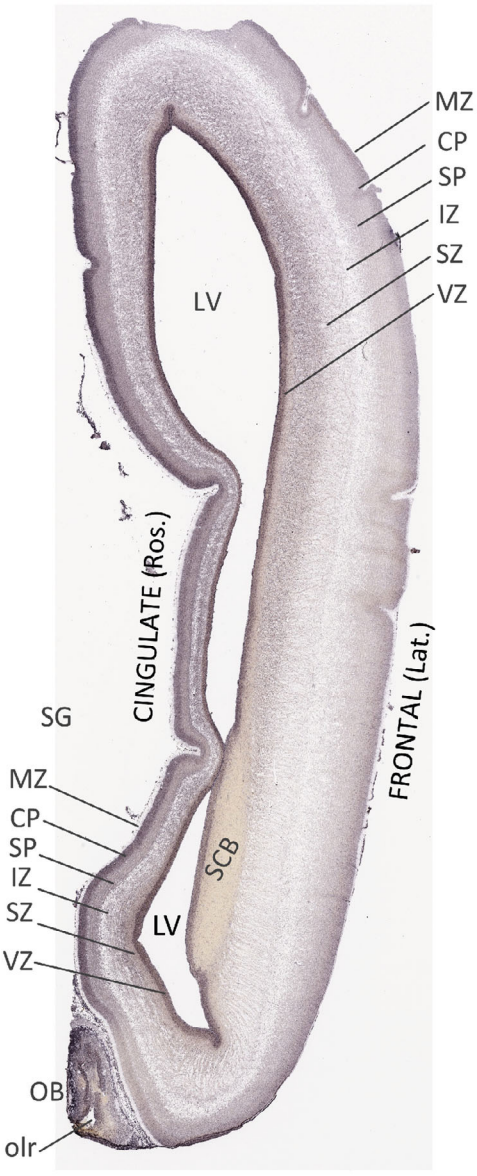

LHX2-01-328 (Level ~9)

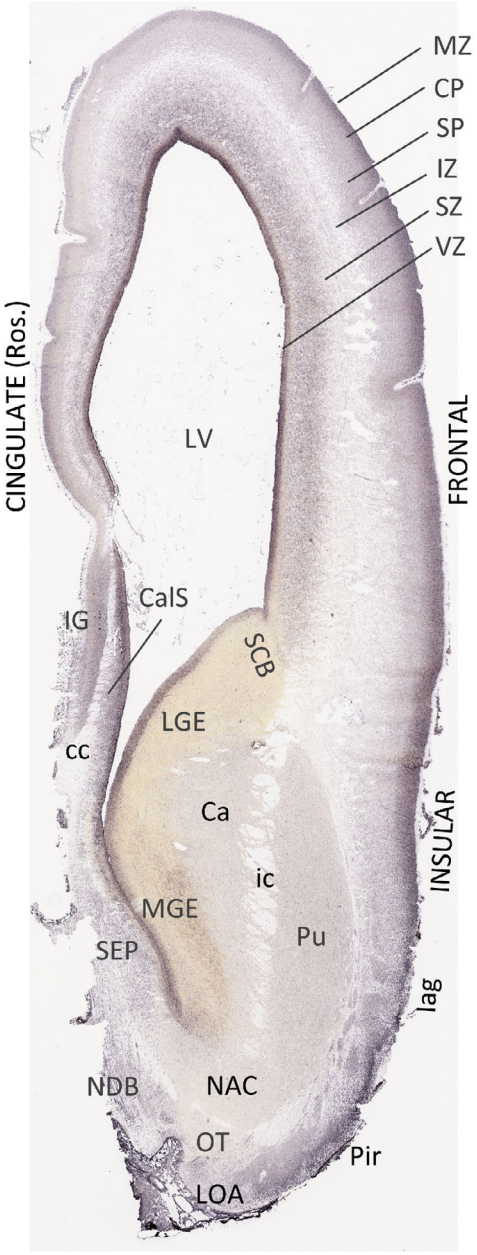

LHX2-01-484 (Level ~15)

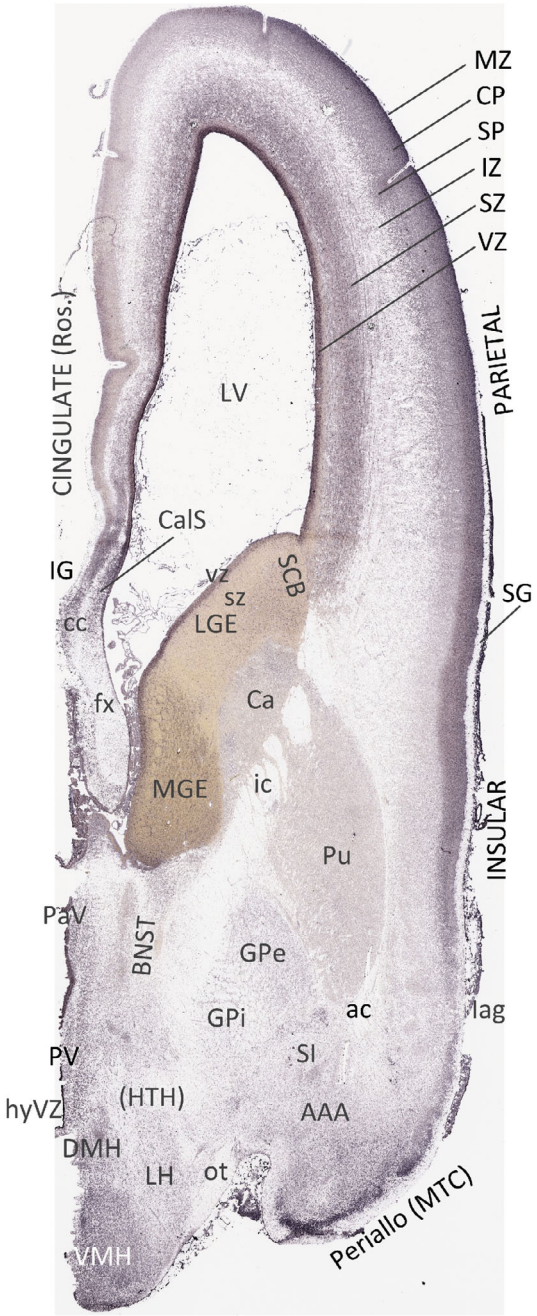

LHX2-01-640 (Level ~20)

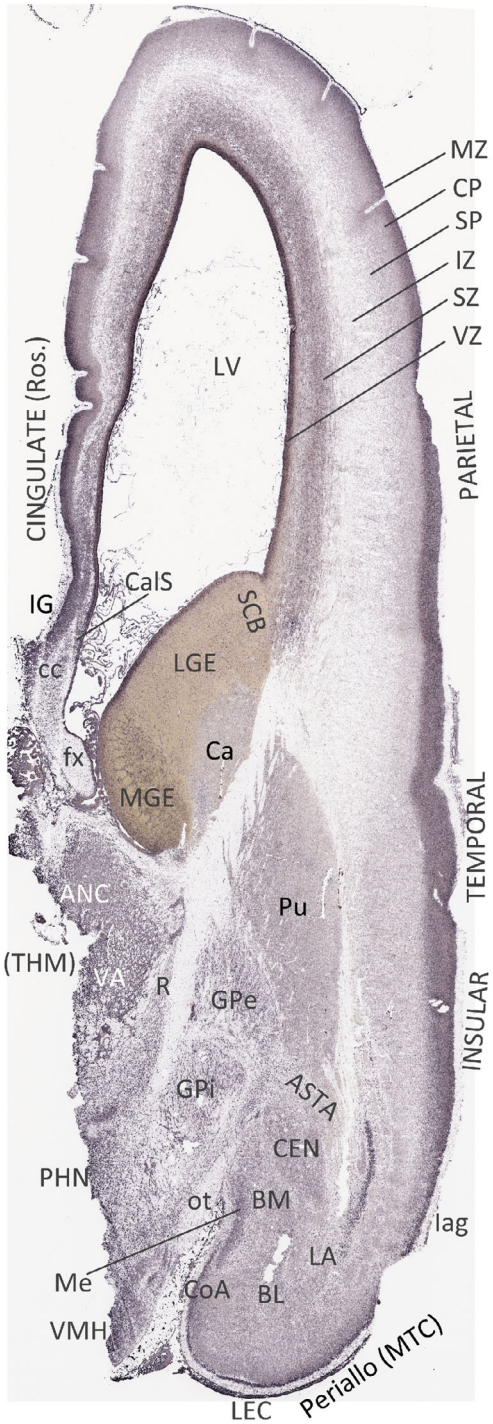

LHX2-01-692 (Level ~22)

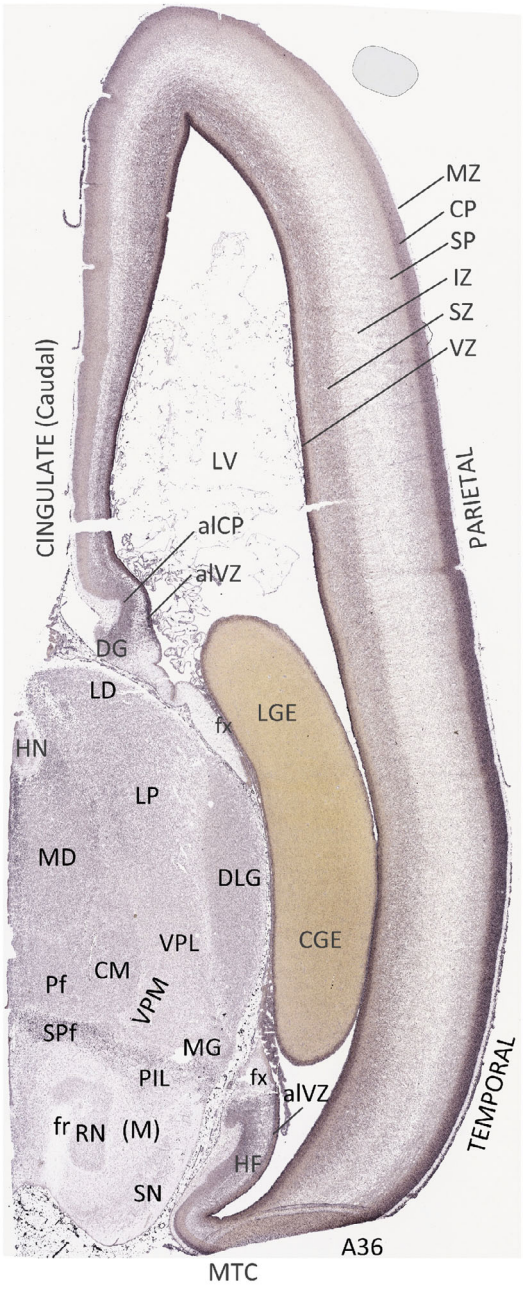

LHX2-02-068 (Level ~27)

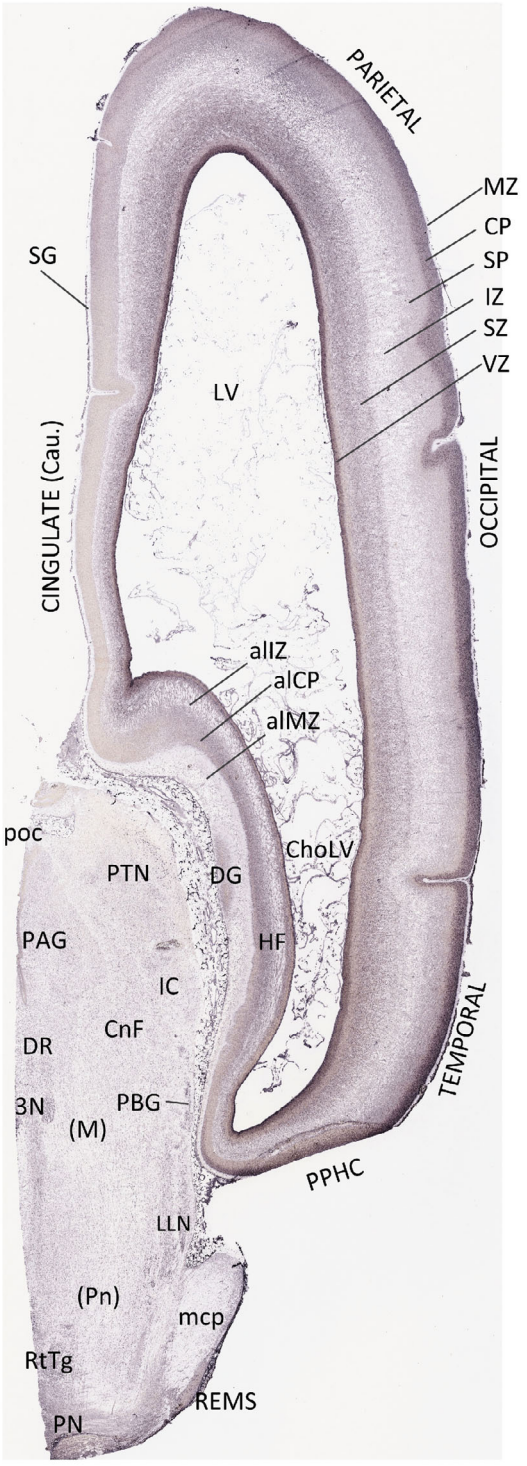

LHX2-02-224 (Level ~33)

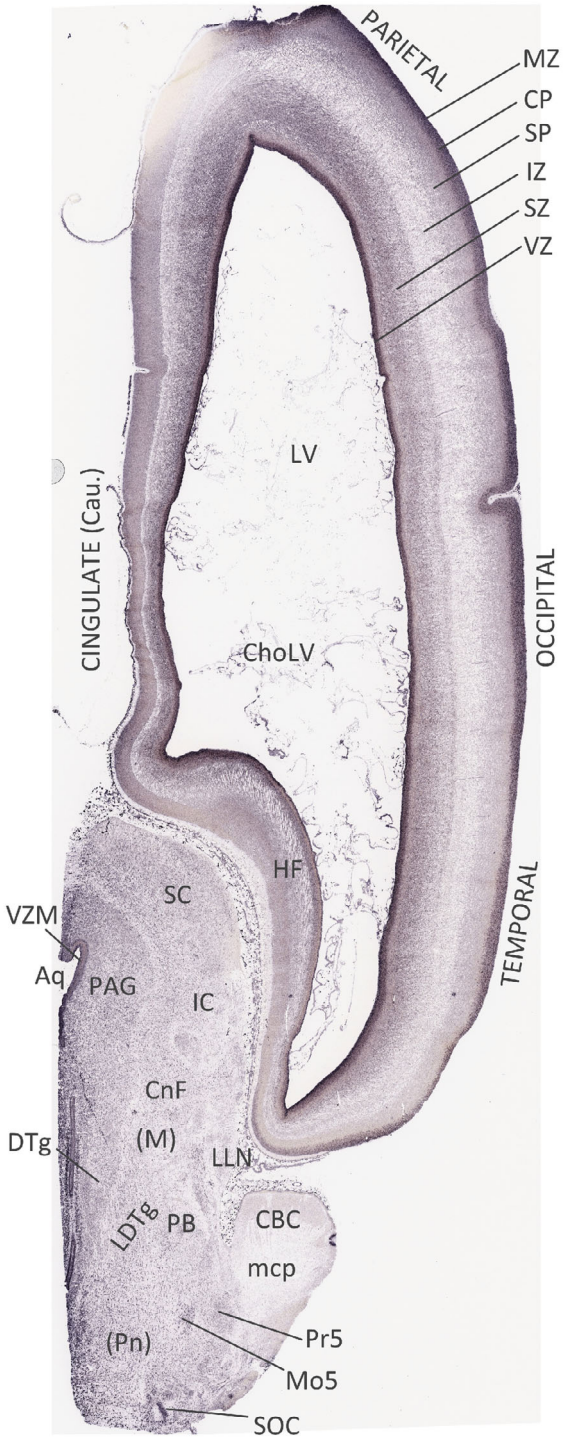

LHX2-02-276 (Level ~35)

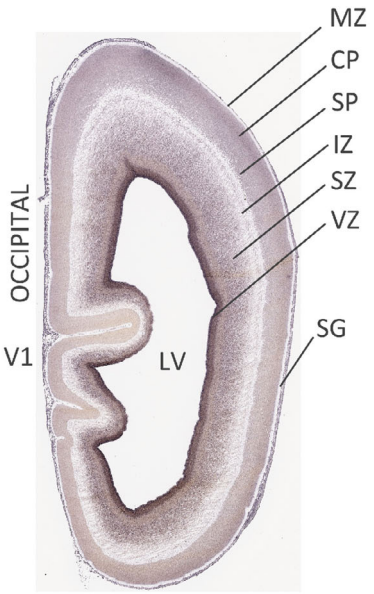

LHX2-02-588 (Level ~44)

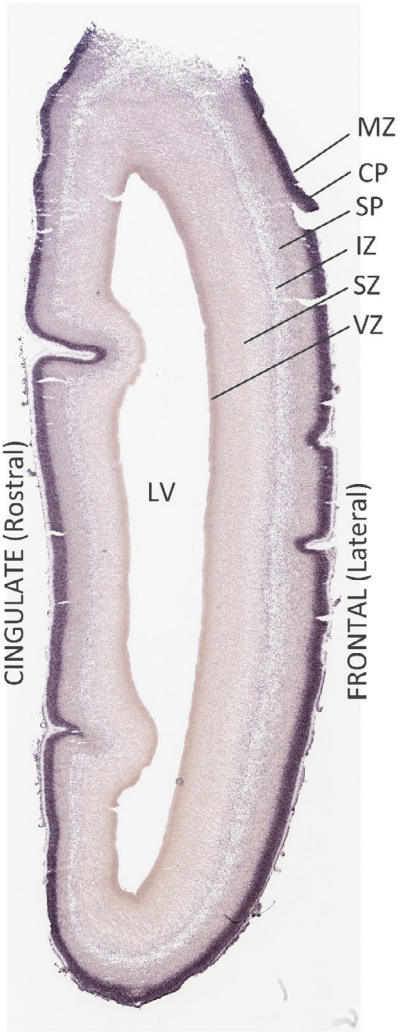

LMO4-01-155 (Level ~4)

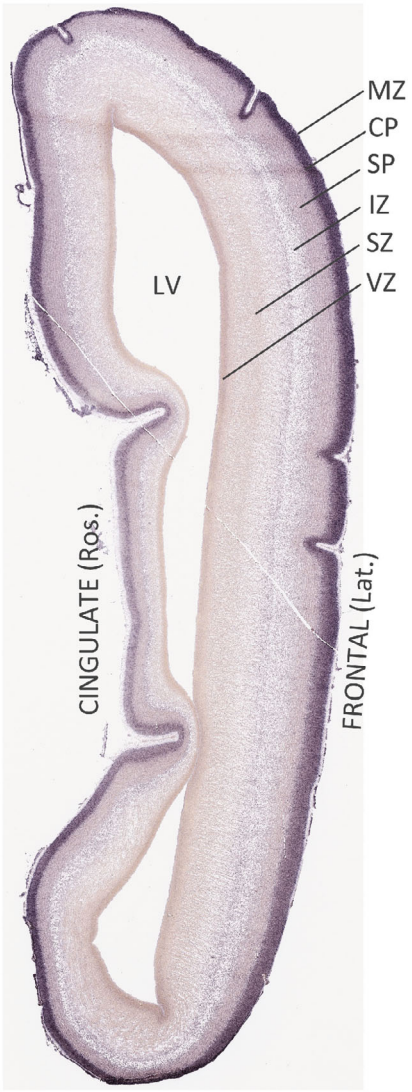

LMO4-01-259 (Level ~6)

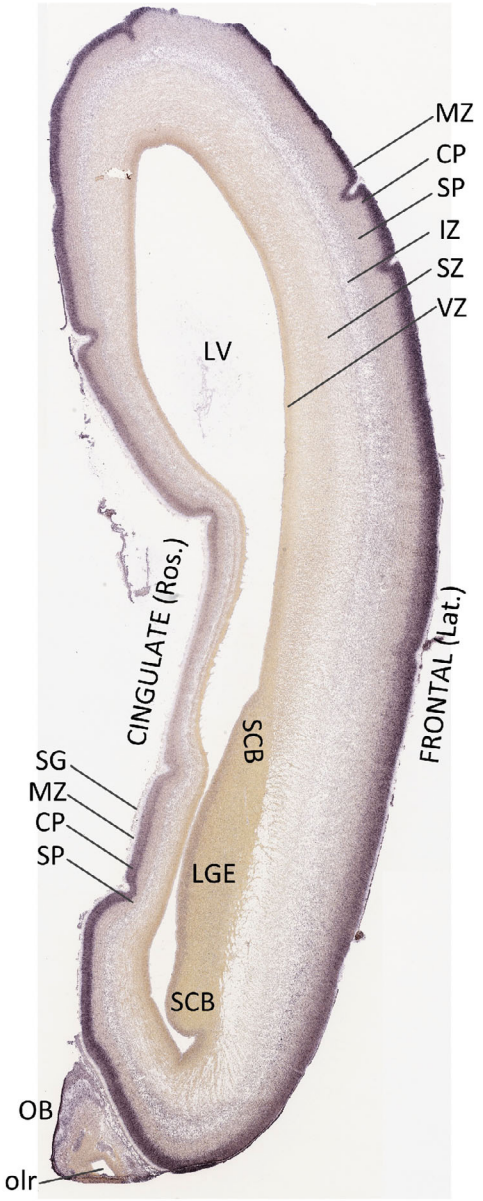

LMO4-01-363 (Level ~10)

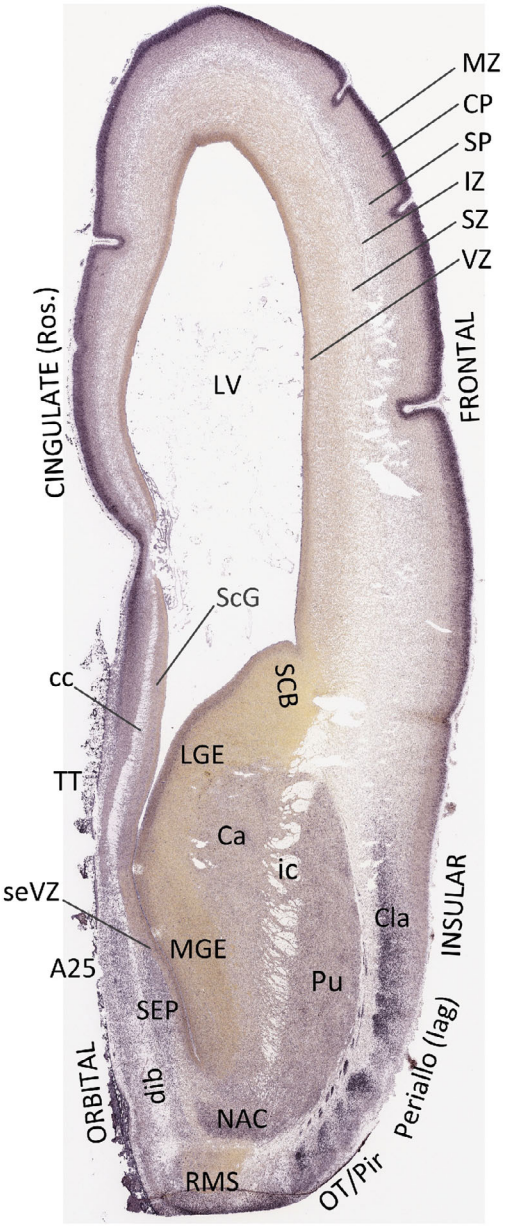

LMO4-01-467 (Level ~14)

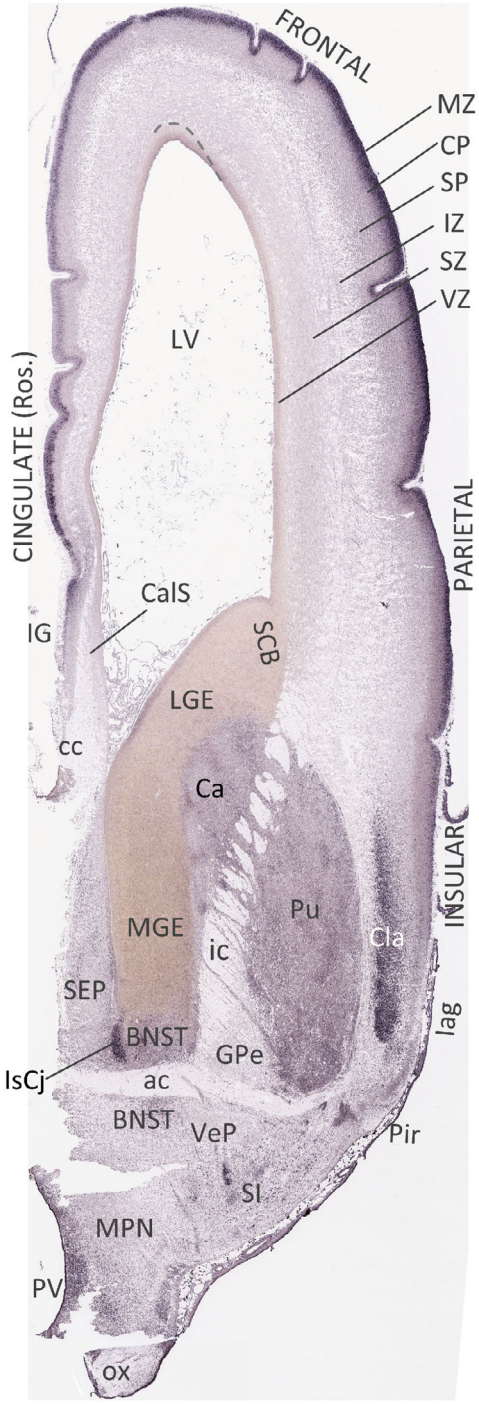

LMO4-01-571 (Level ~18)

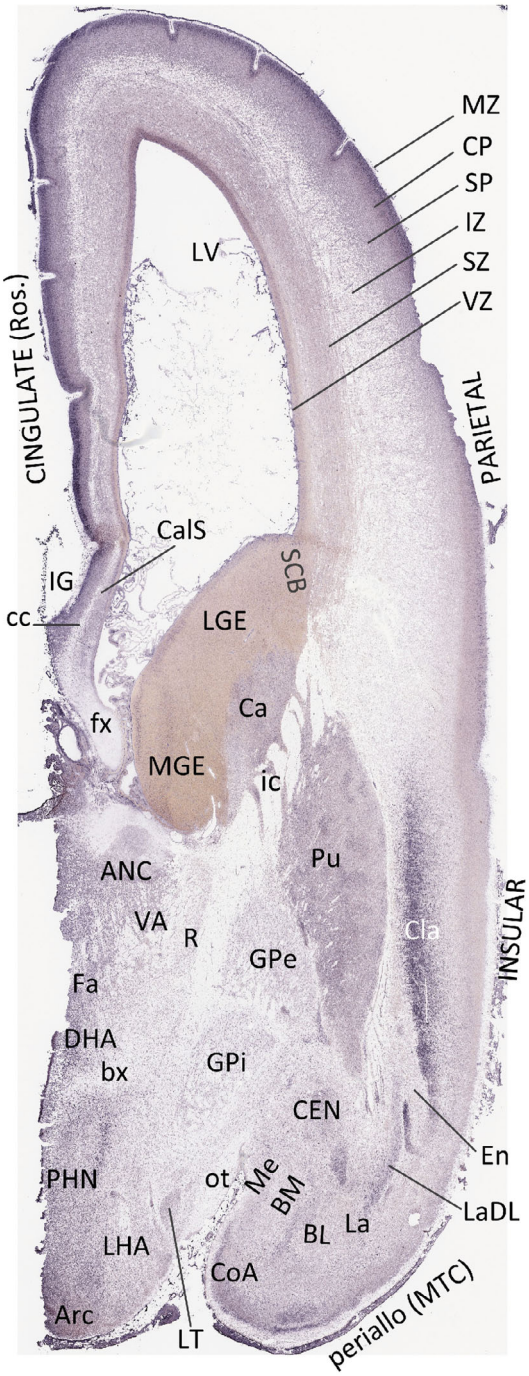

LMO4-01-675 (Level ~21)

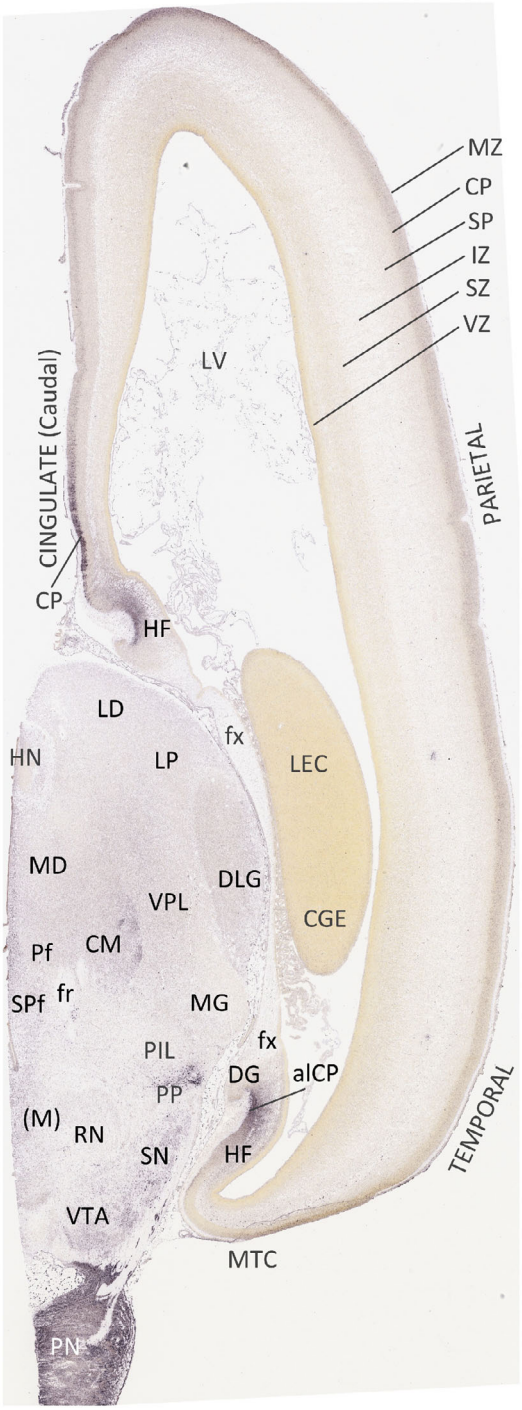

LMO4-02-103 (Level ~28-29)

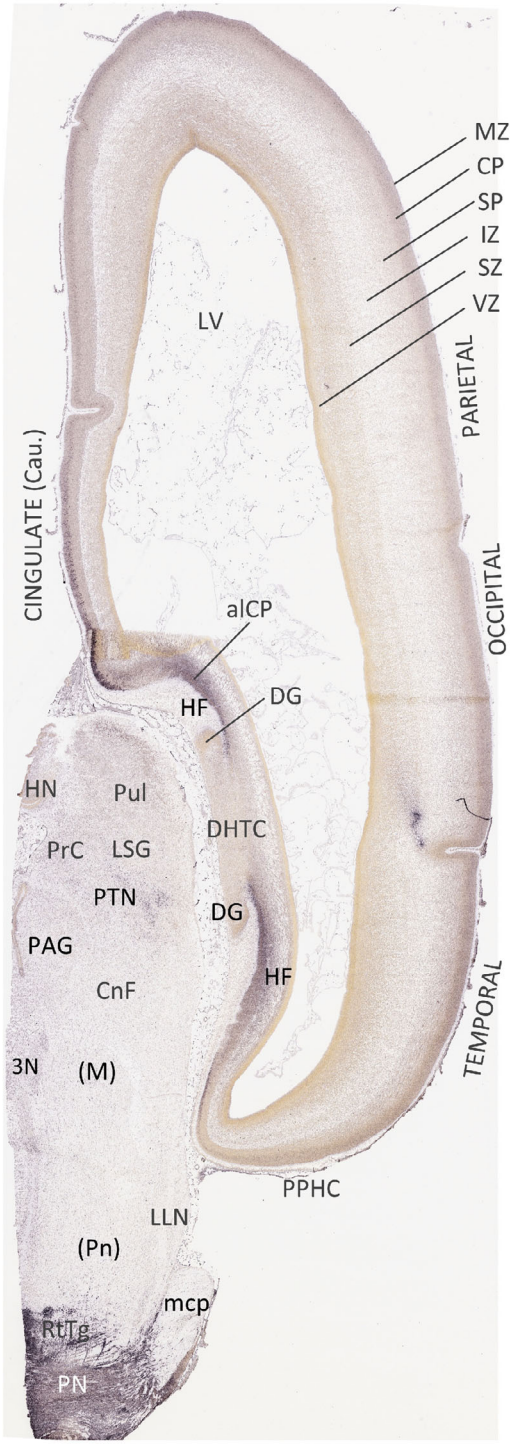

LMO4-02-207 (Level ~32-33)

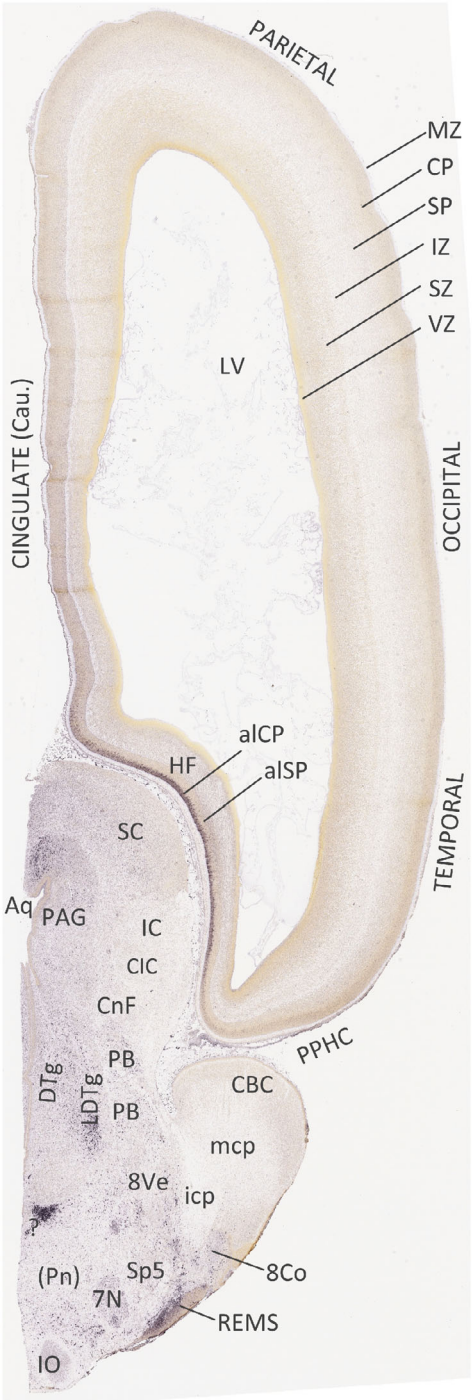

LMO4-02-311 (Level ~36-37)

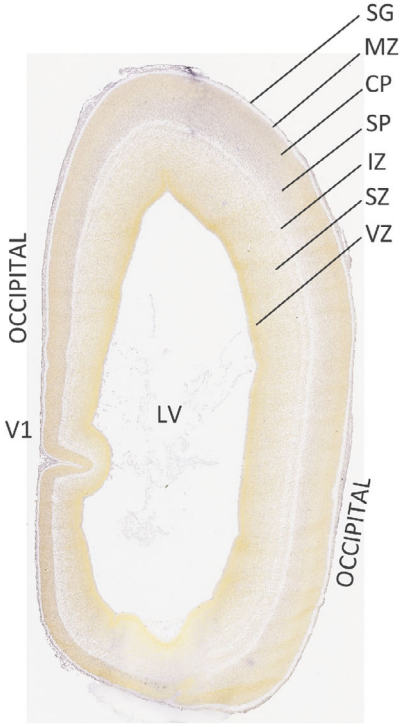

LMO4-02-467 (Level ~42)

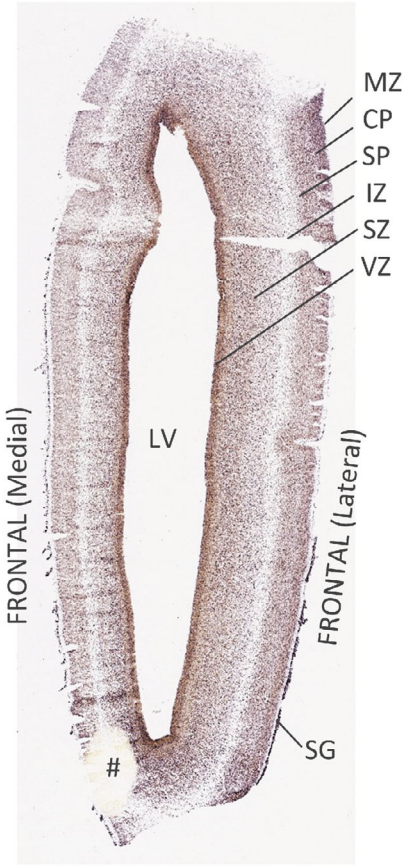

NES-01-109 (Level ~3)

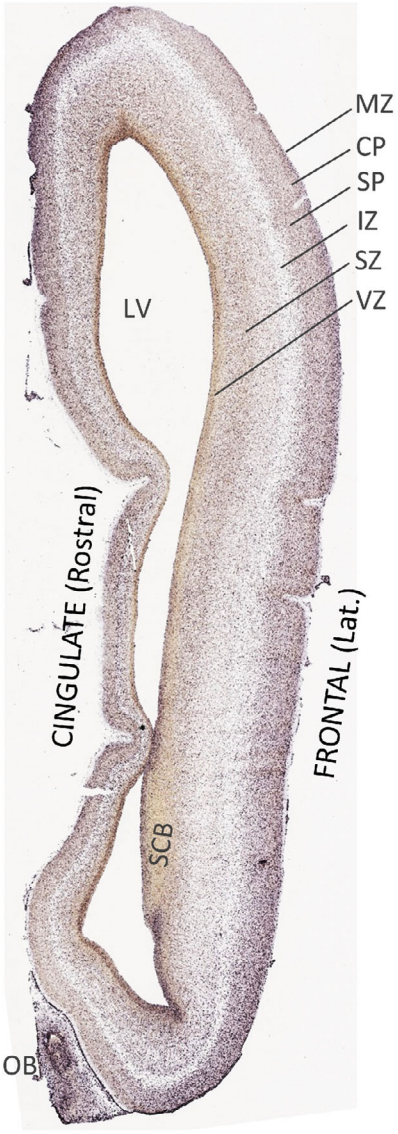

NES-01-317 (Level ~8)

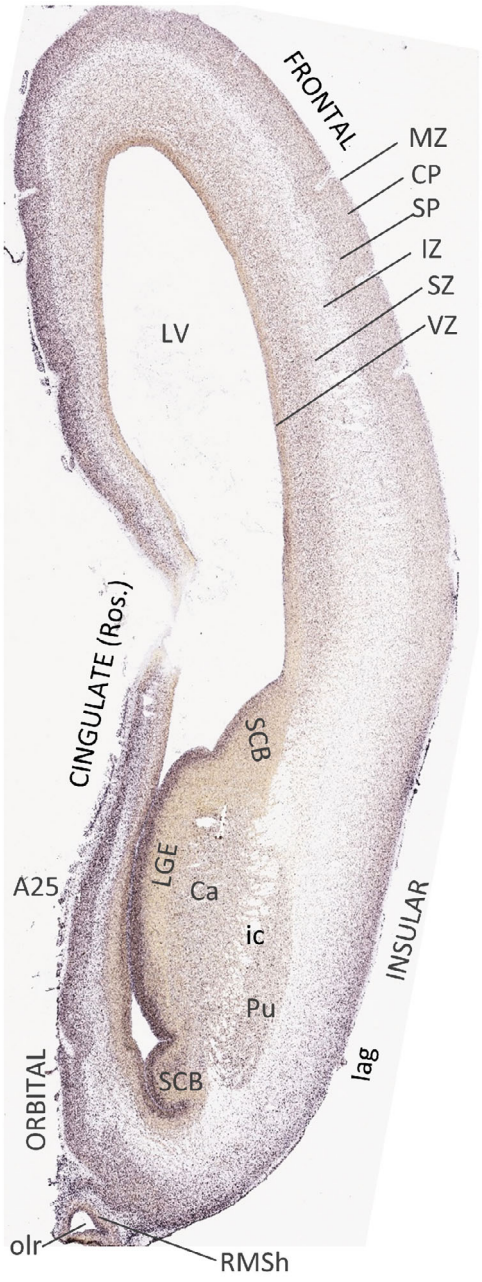

NES-01-421 (Level ~12)

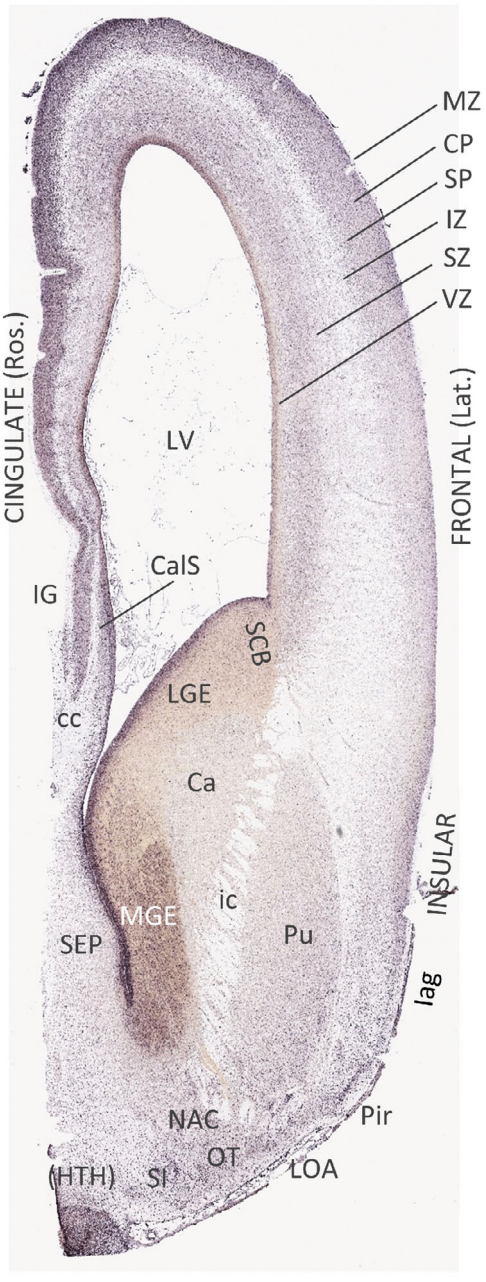

NES-01-421 (Level ~16)

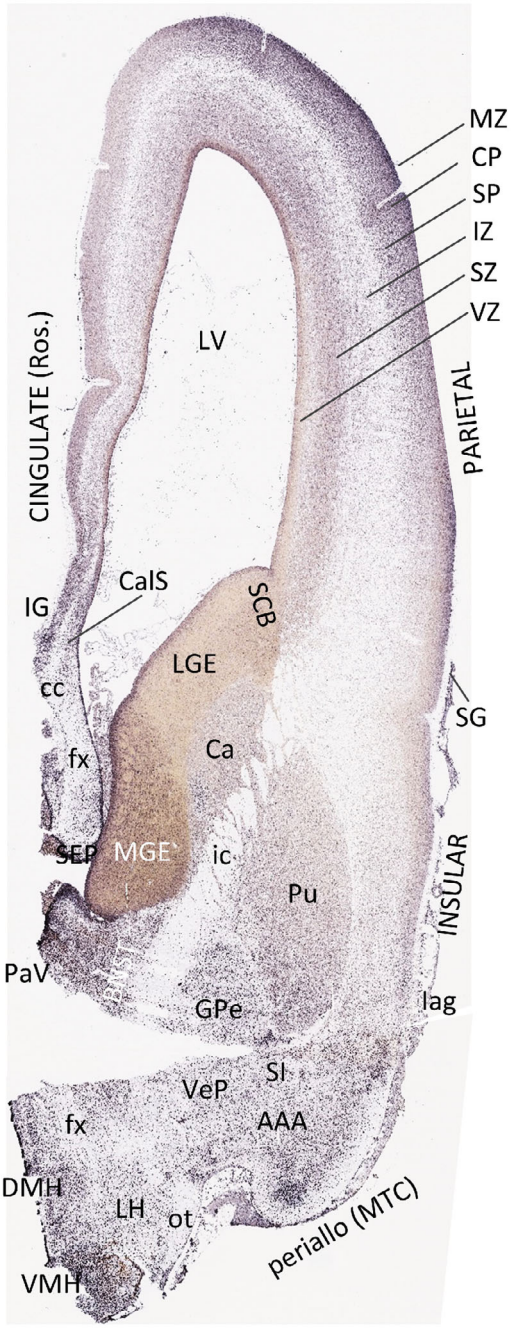

NES-01-629 (Level ~20)

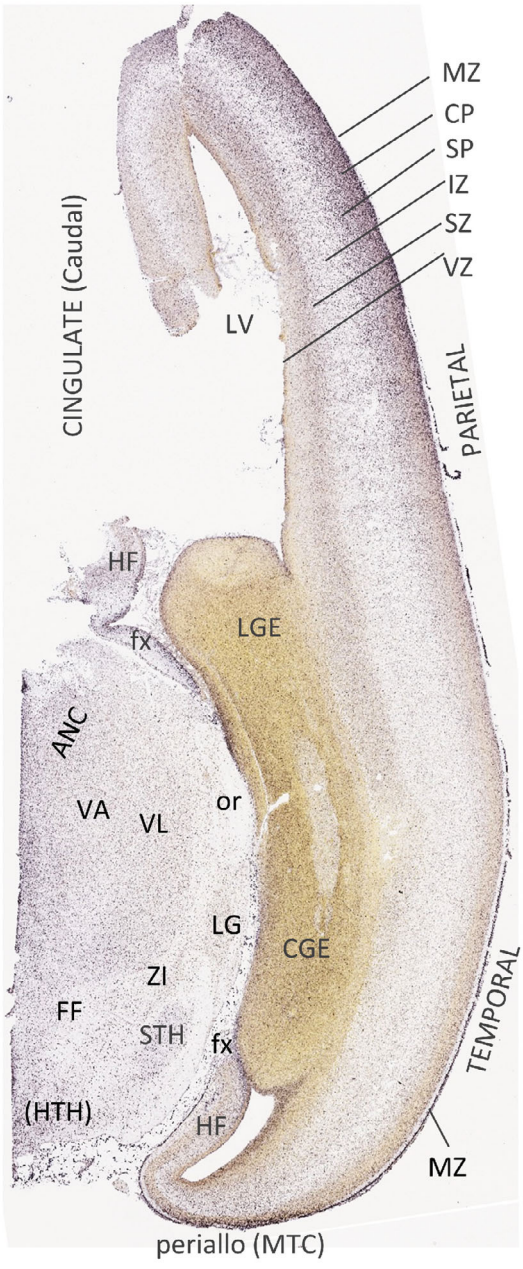

NES-01-005 (Level ~24)

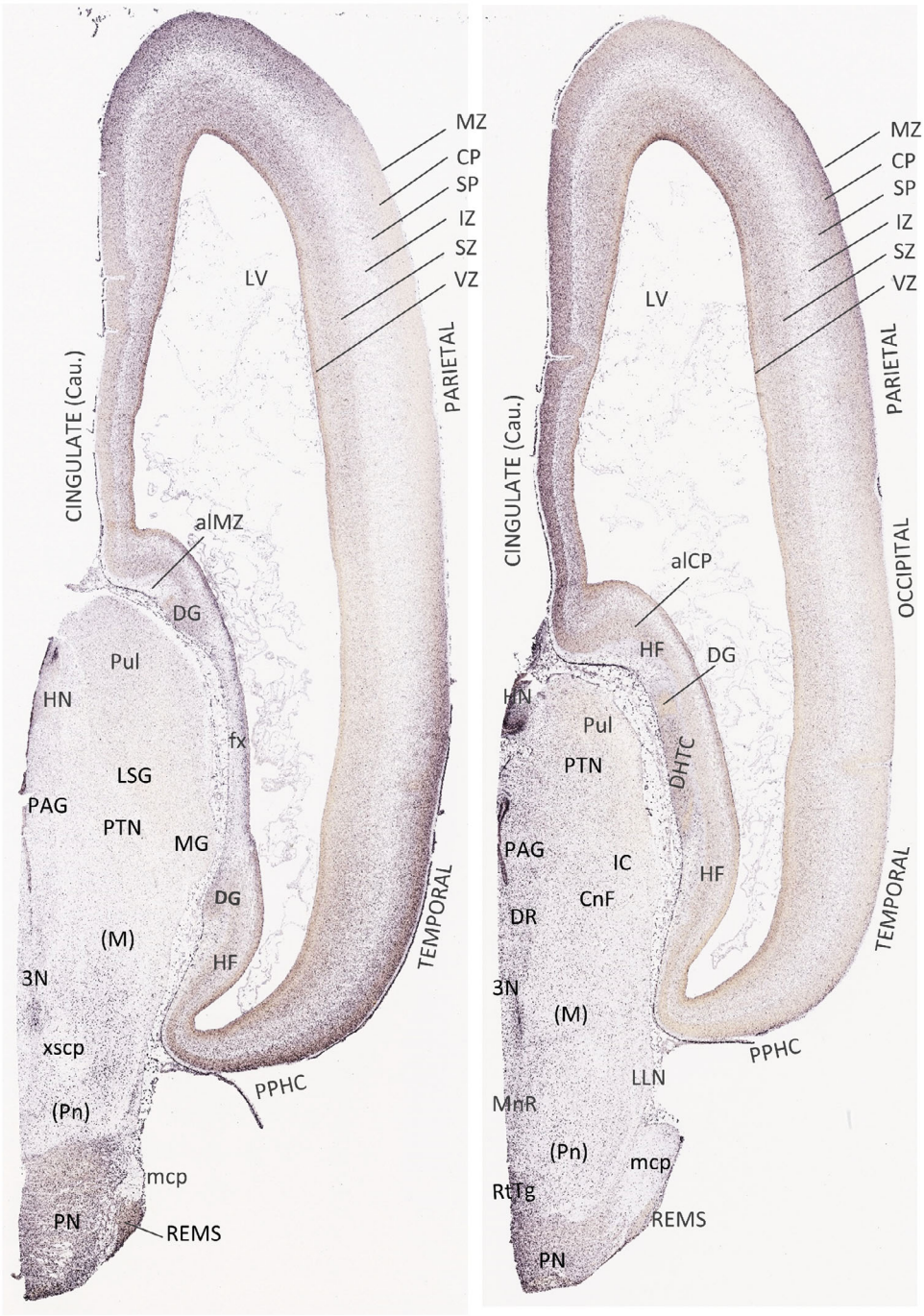

NES-02-161 (Level ~31) **NES-02-213 (Level ~33)**

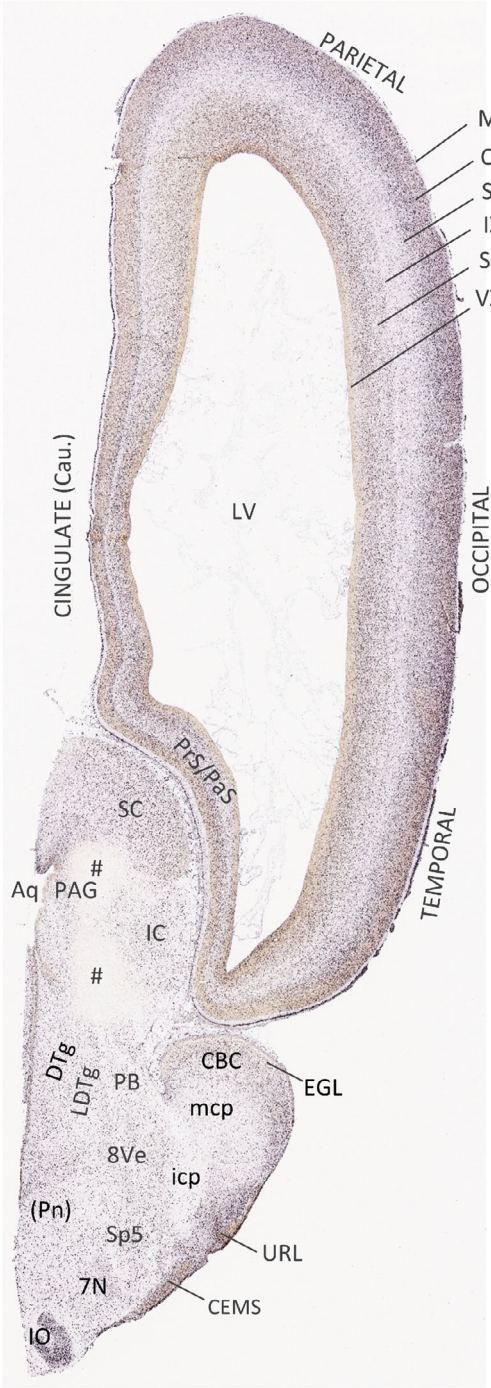

NES-02-317 (Level ~37)

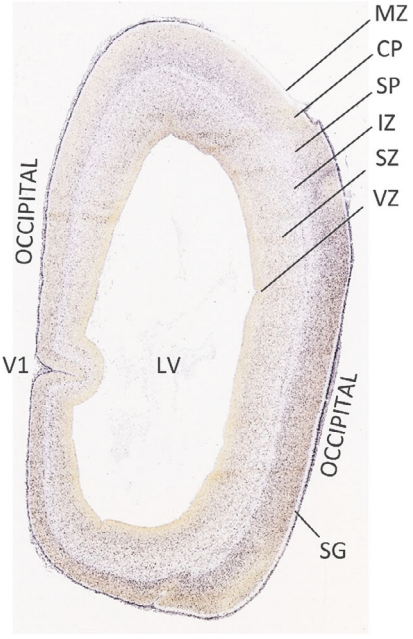

NES-02-473 (Level ~42)

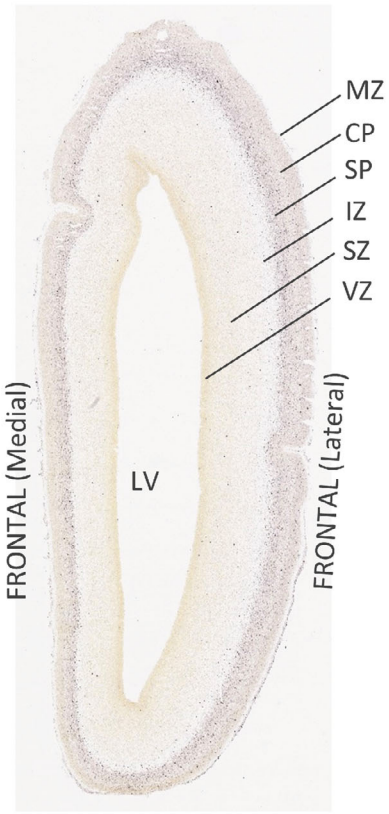

NKX2.1-01-097 (Level ~3)

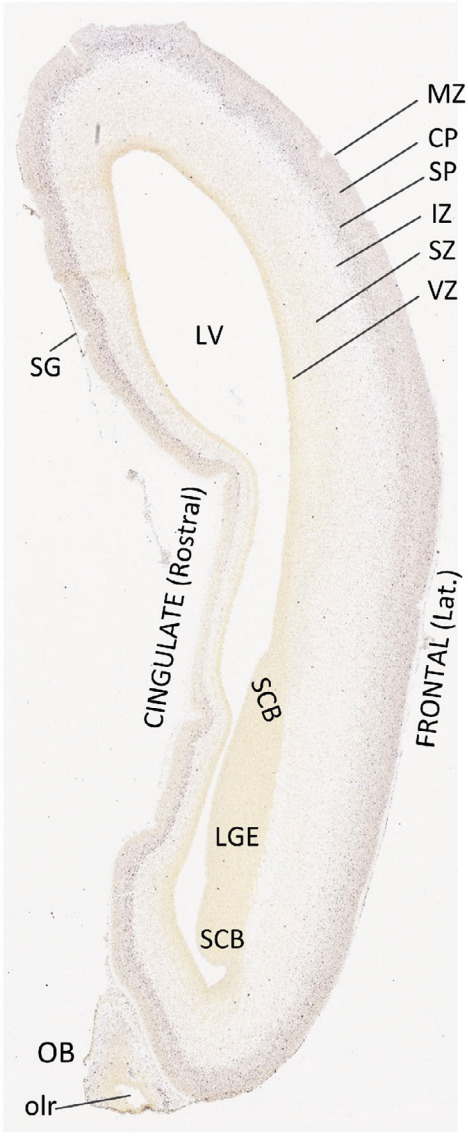

NKX2.1-01-357 (Level ~10)

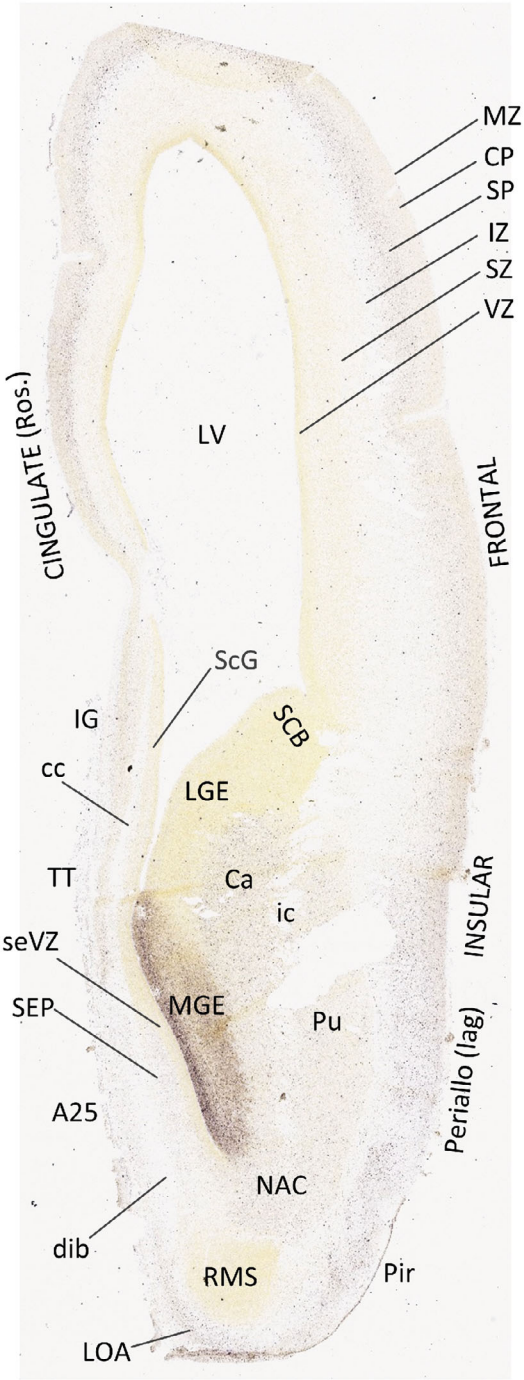

NKX2.1-01-461 (Level ~14)

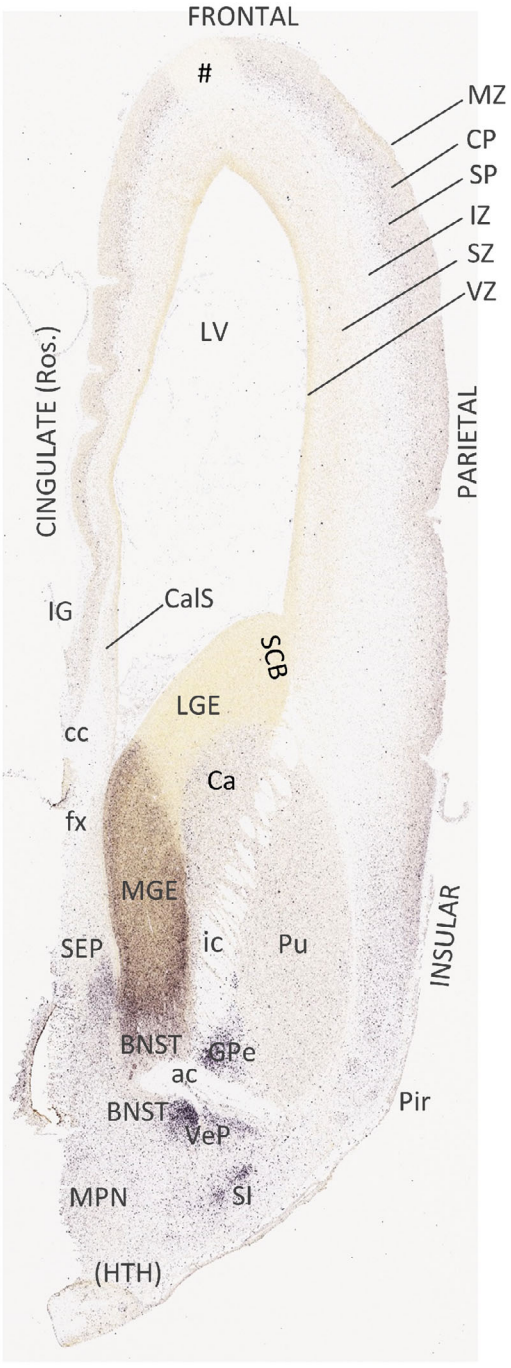

NKX2.1-01-565 (Level ~18)

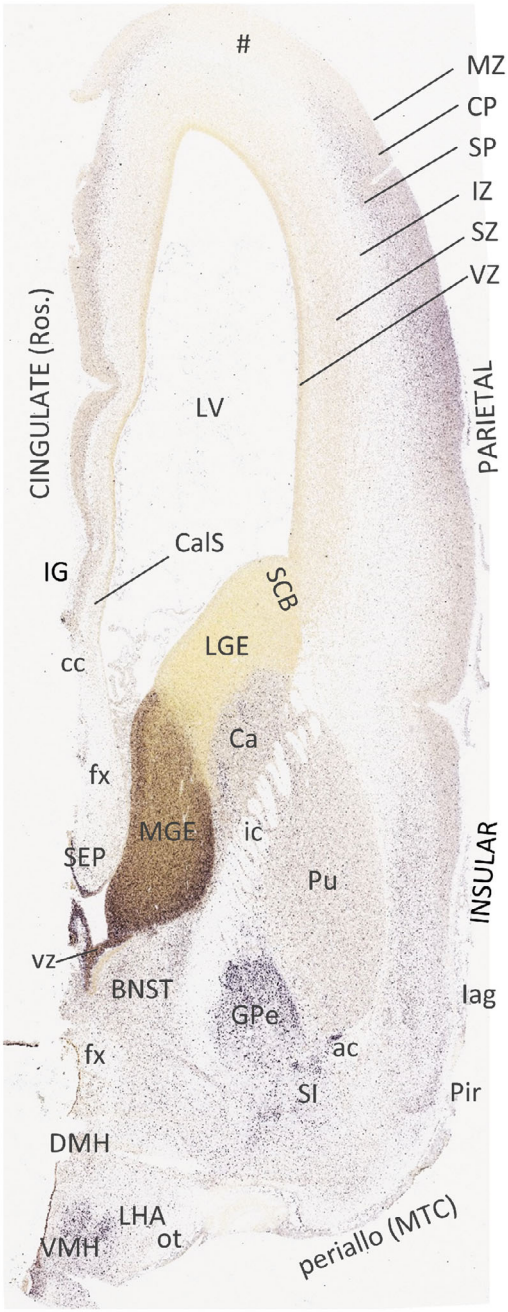

NKX2.1-01-617 (Level ~19)

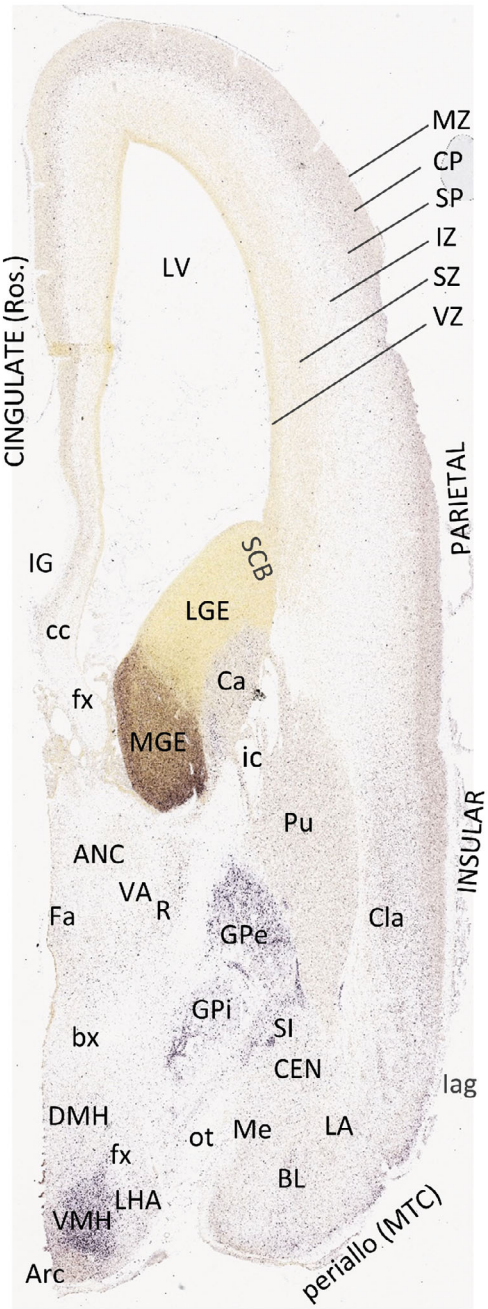

NKX2.1-01-669 (Level ~20-21)

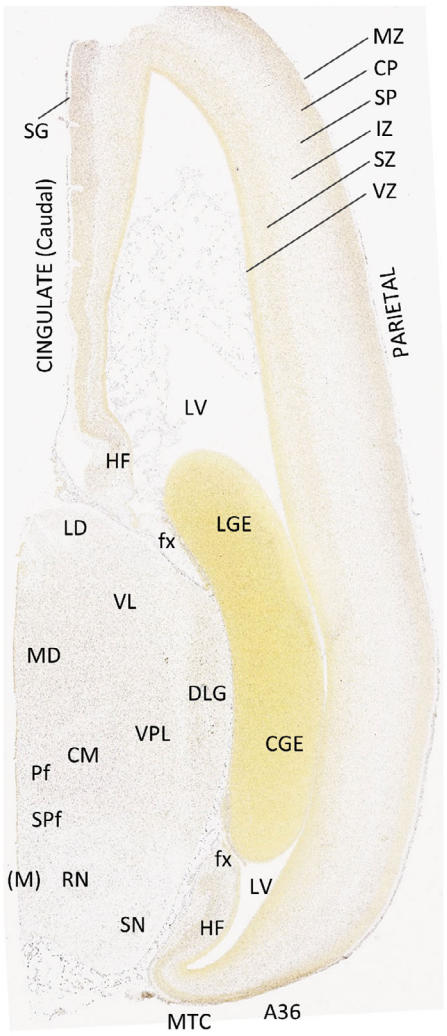

NKX2.1-02-045 (Level ~26)

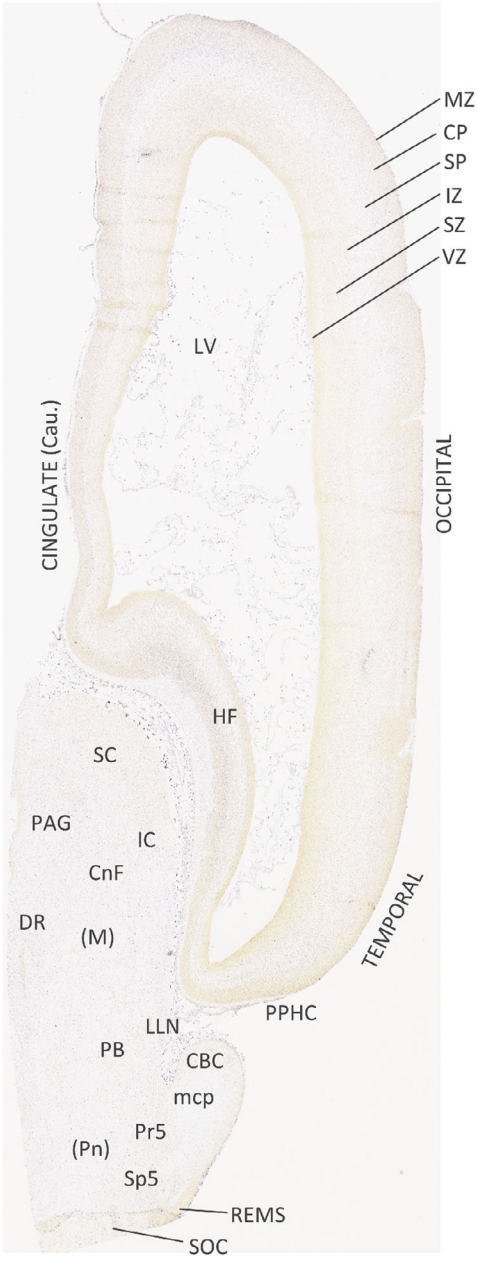

NKX2.1-02-253 (Level ~34)

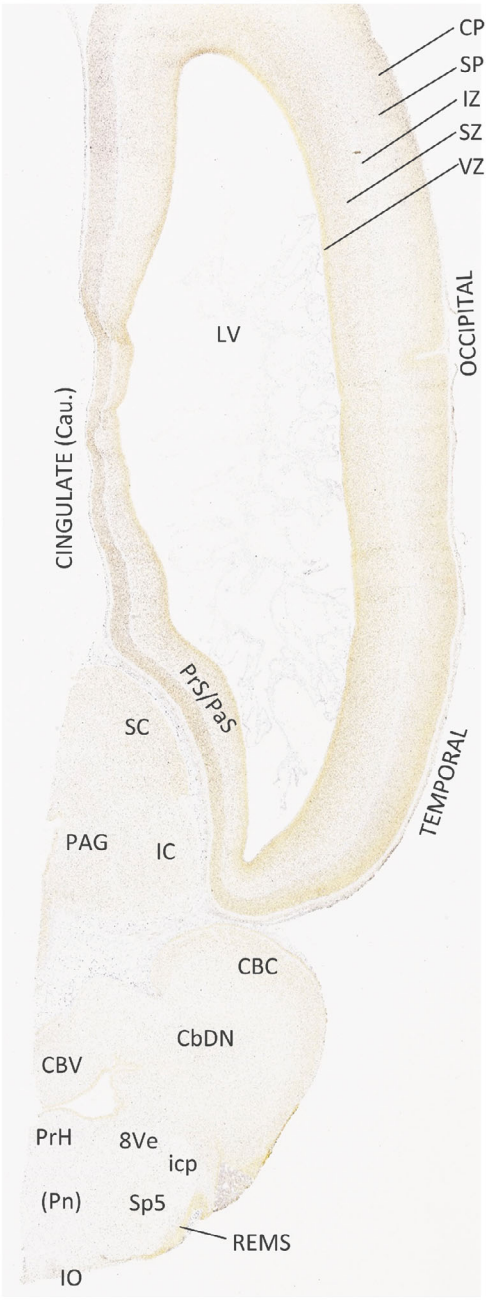

NKX2.1-02-357 (Level ~38)

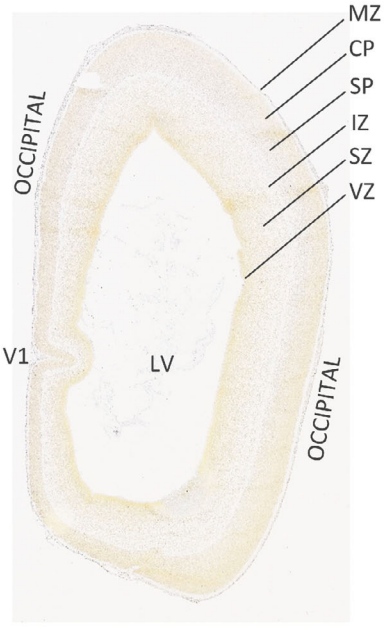

NKX2.1-02-461 (Level ~42)

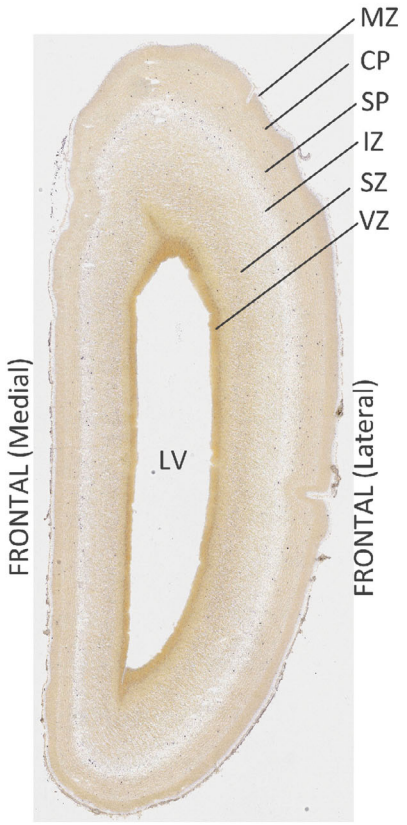

NPY-01-061 (Level ~2)

NPY-01-217 (Level ~5)

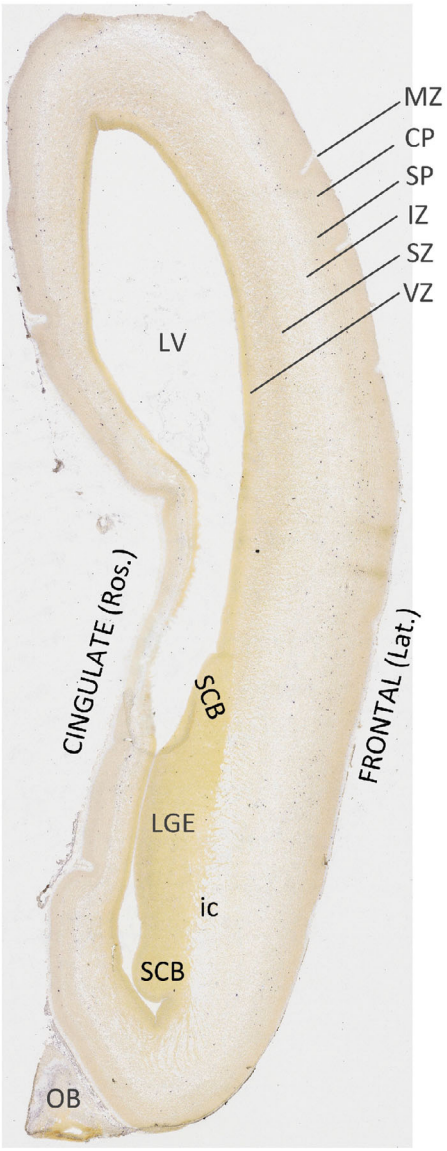

NPY-01-373 (Level ~10)

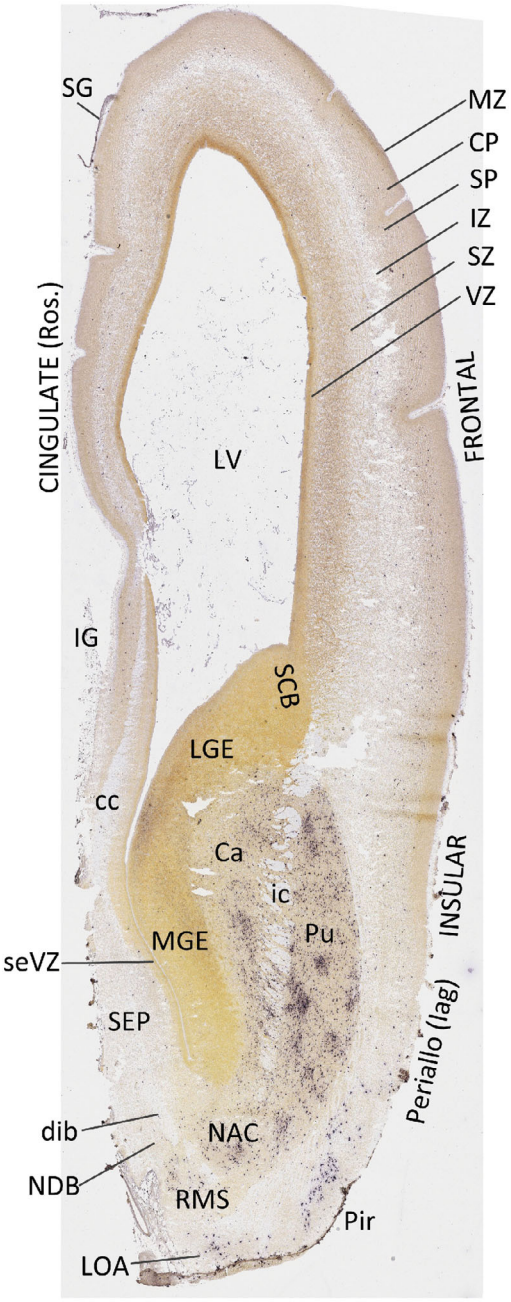

NPY-01-477 (Level ~14)

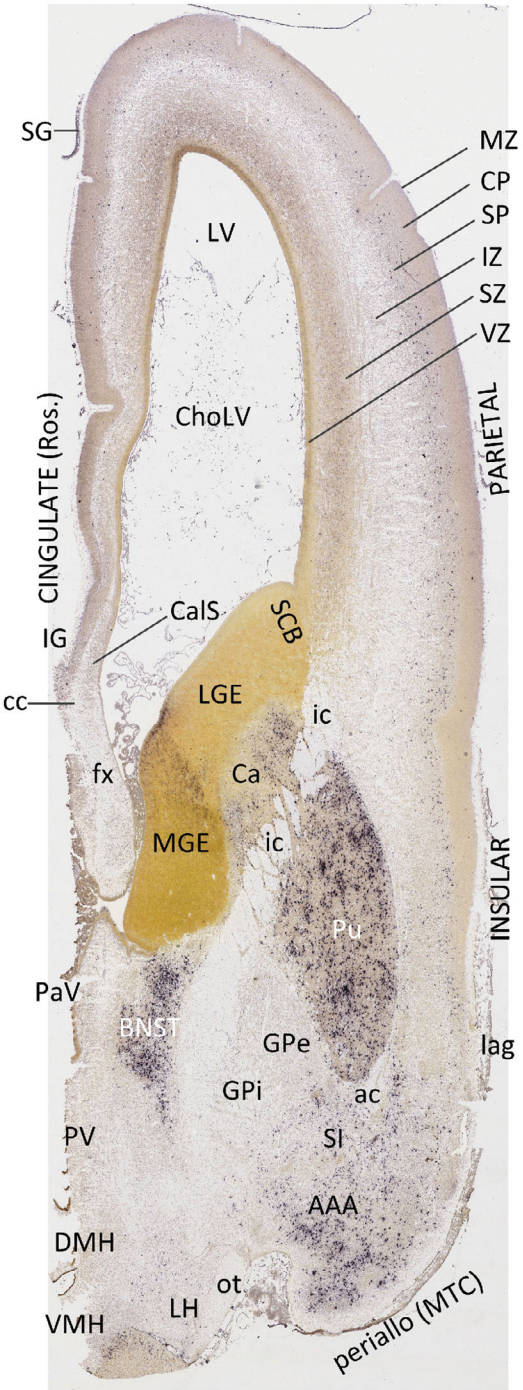

NPY-01-633 (Level ~20)

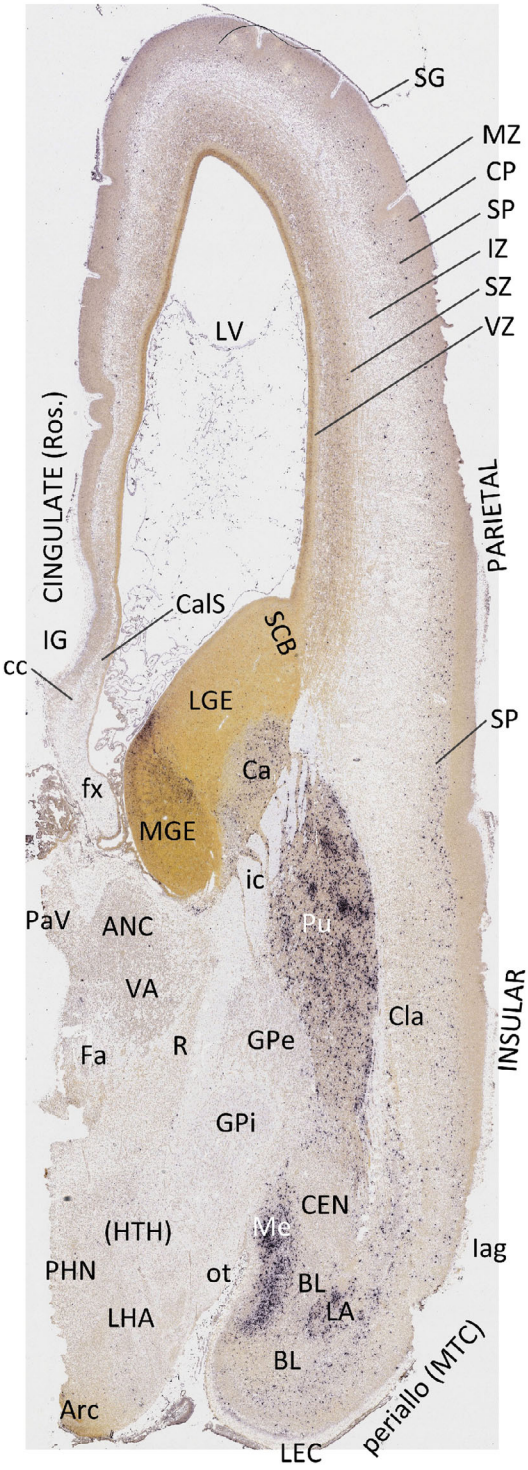

NPY-01-685 (Level ~21)

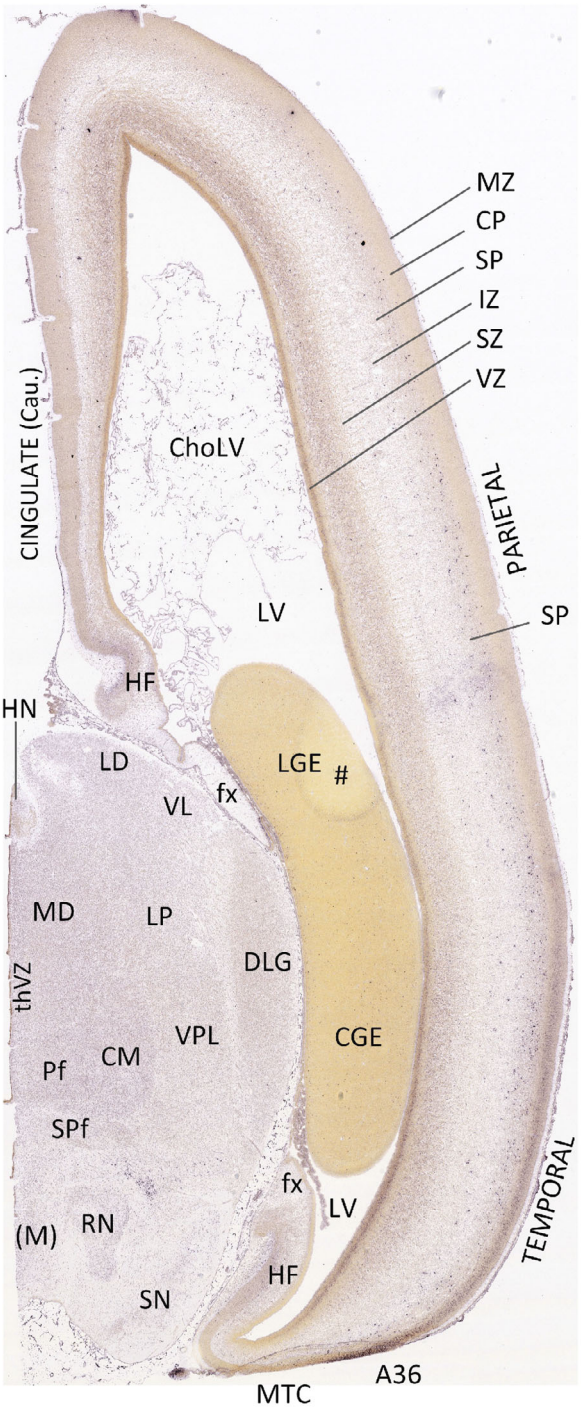

NPY-02-061 (Level ~27)

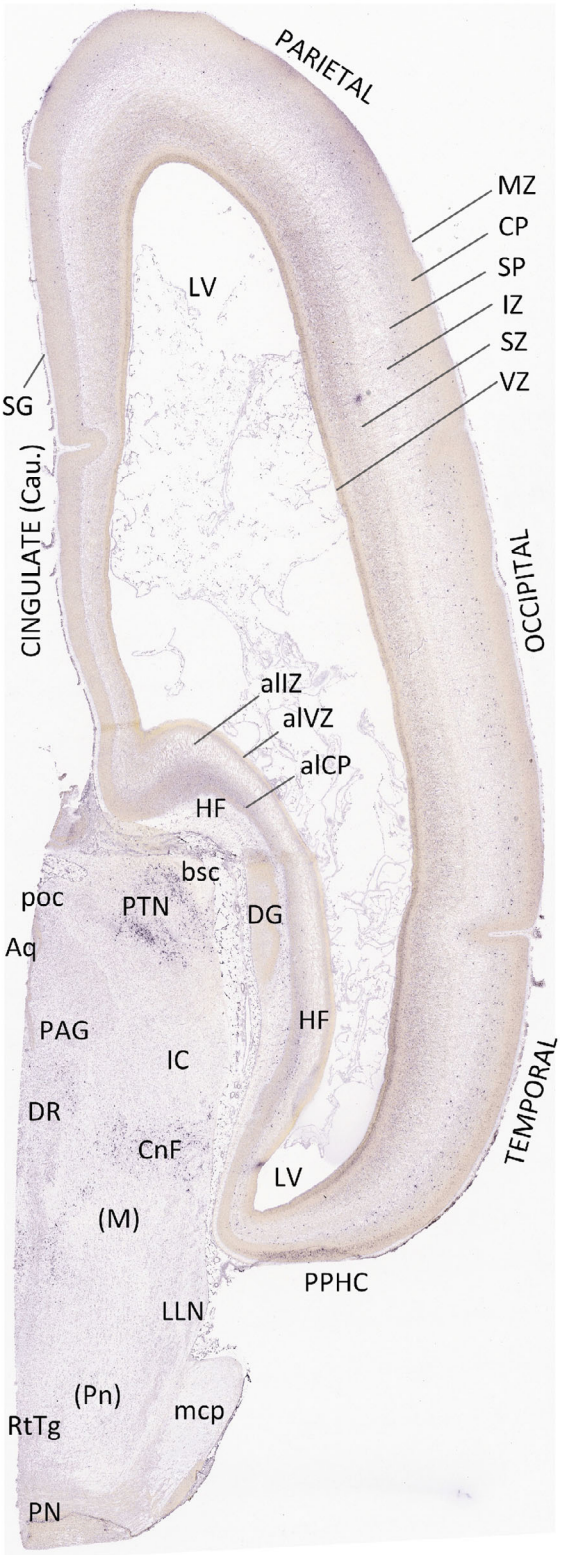

NPY-02-217 (Level ~33)

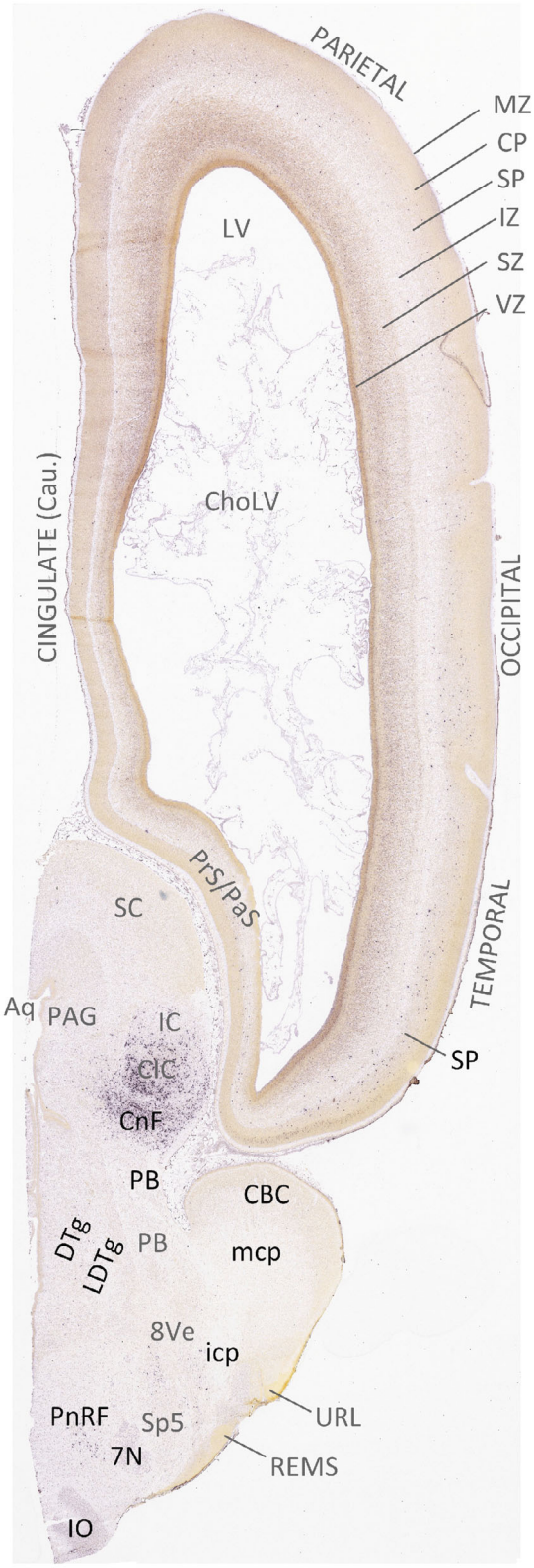

NPY-02-321 (Level ~37)

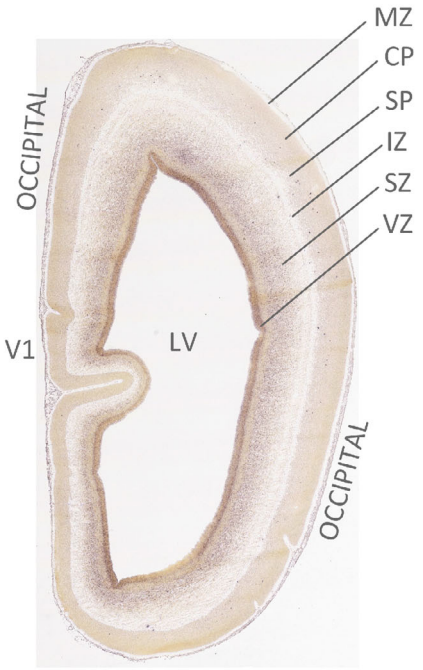

NPY-02-529 (Level ~43)

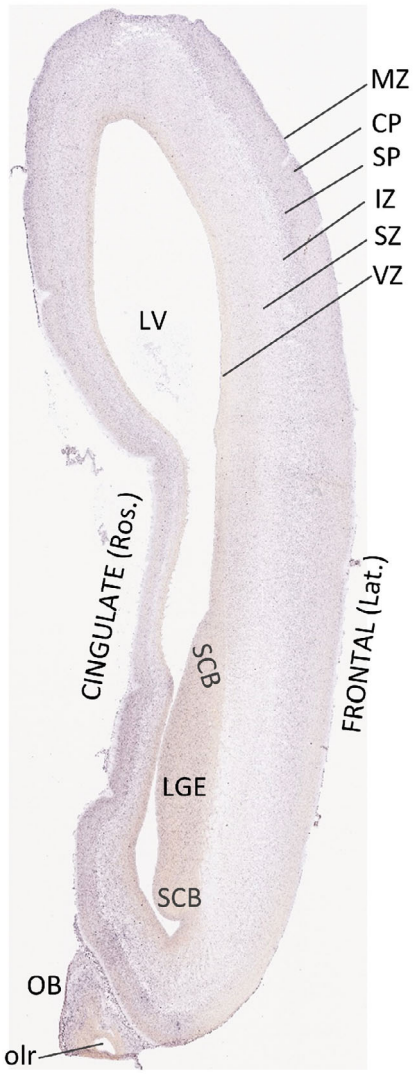

NRGN-01-362 (Level ~10)

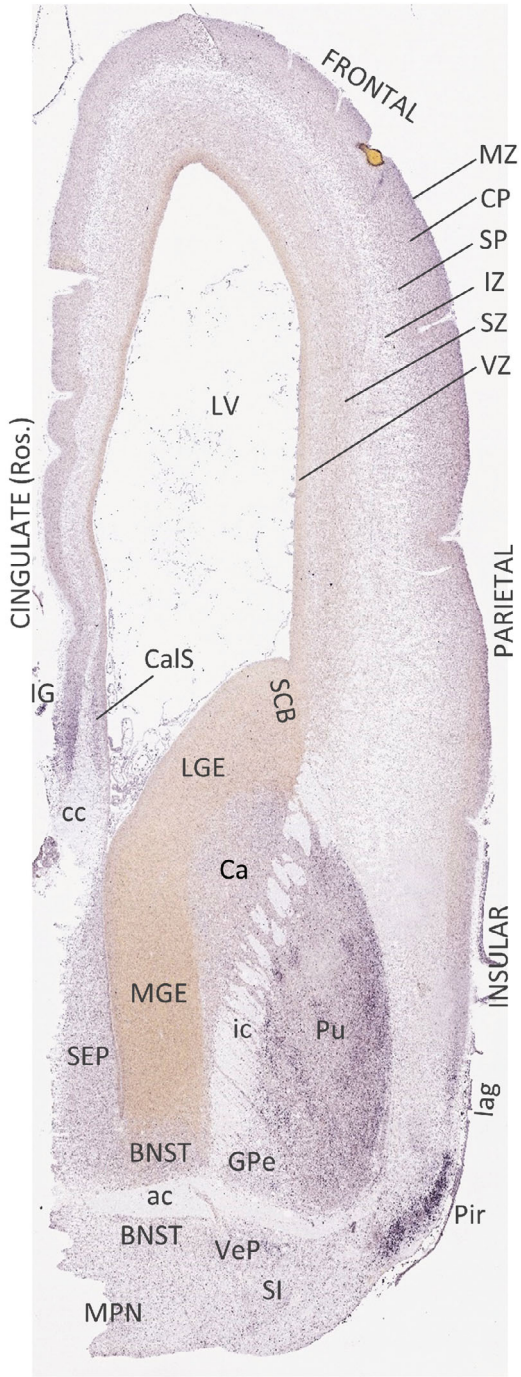

NRGN-01-570 (Level ~18)

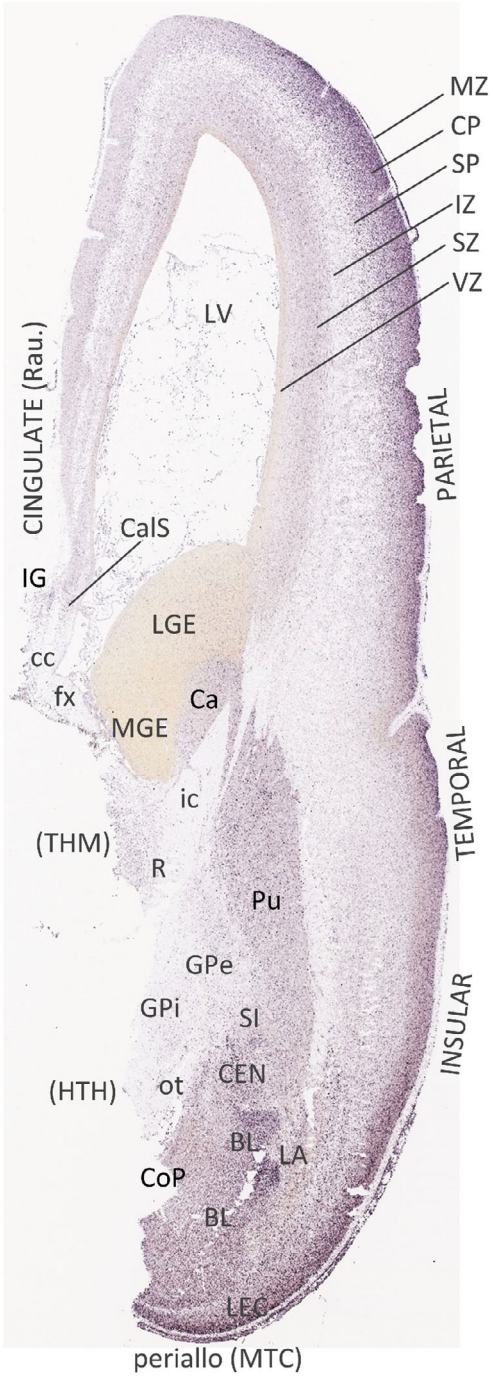

NRGN-01-726 (Level ~23)

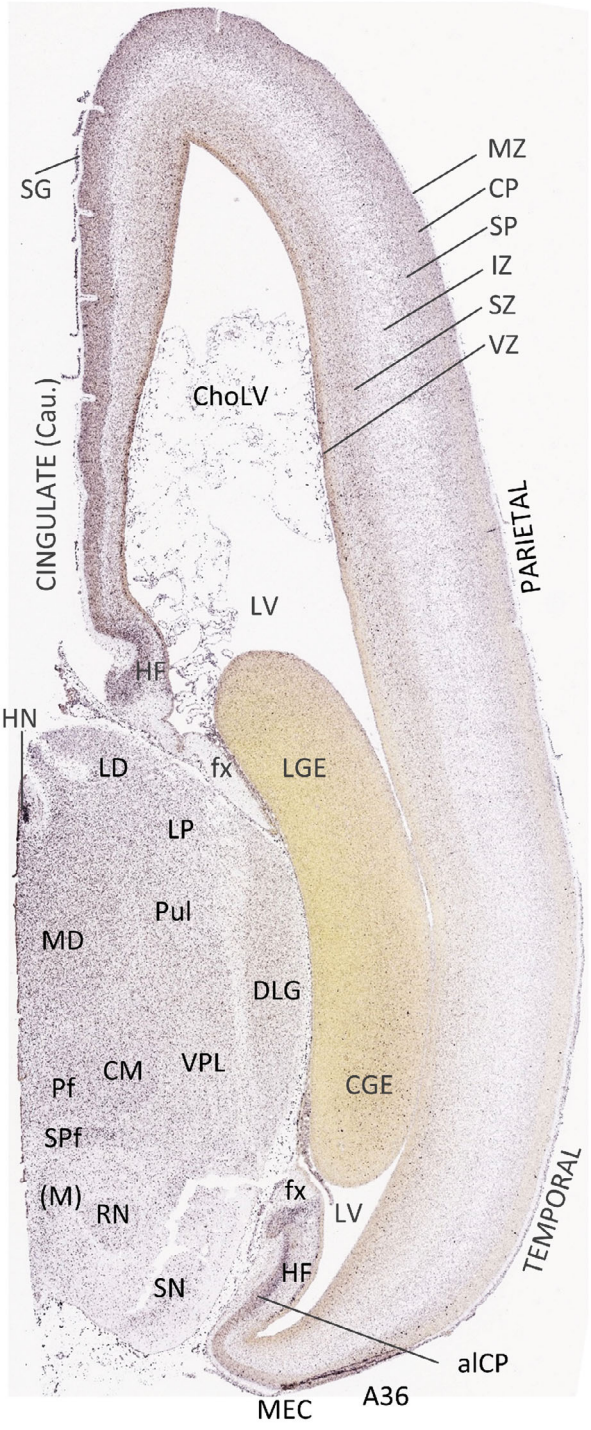

NRGN-02-050 (Level ~26)

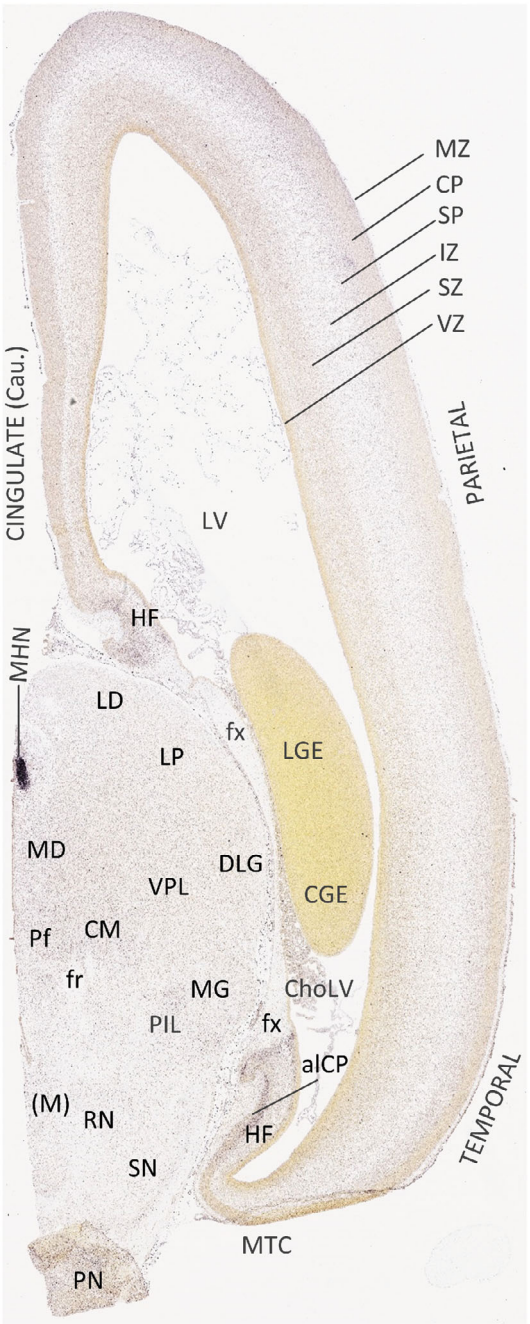

NRGN-02-102 (Level ~28)

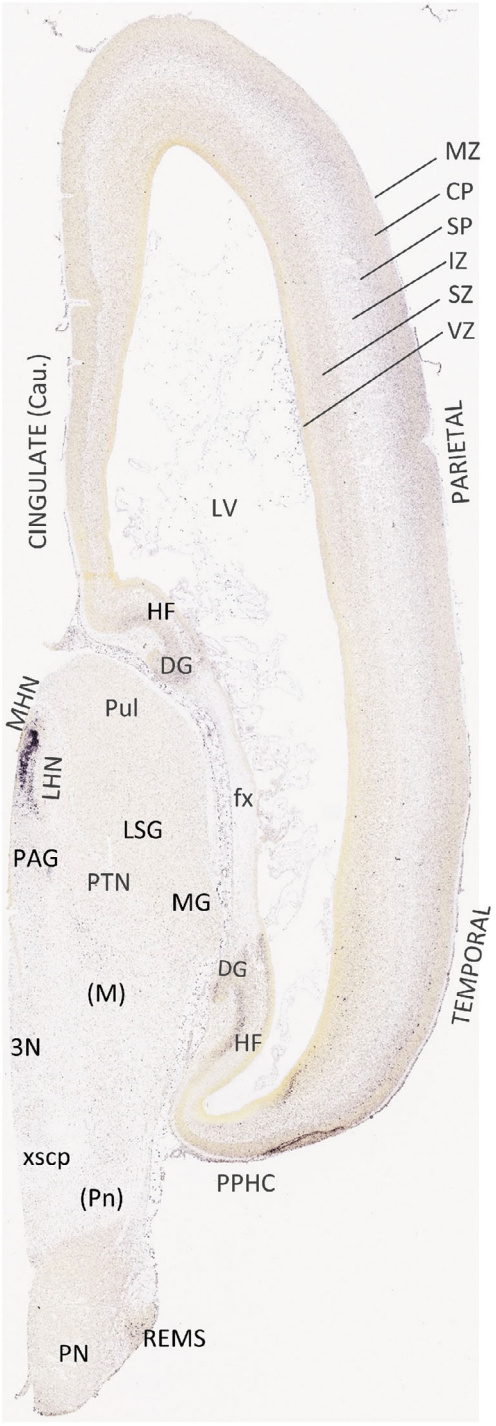

NRGN-02-154 (Level ~30)

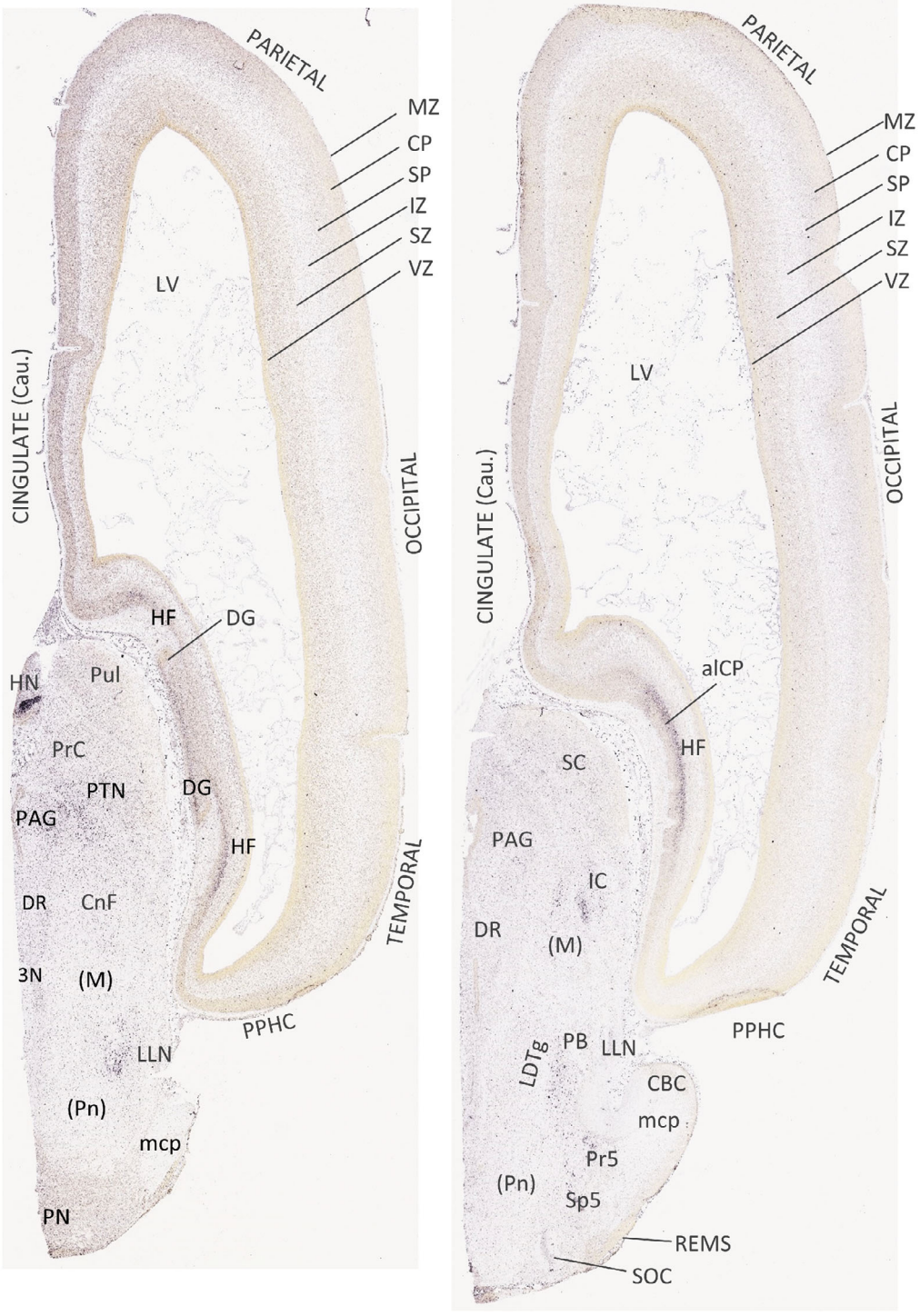

NRGN-02-206 (Level ~32) **NRGN-02-258 (Level ~34)**

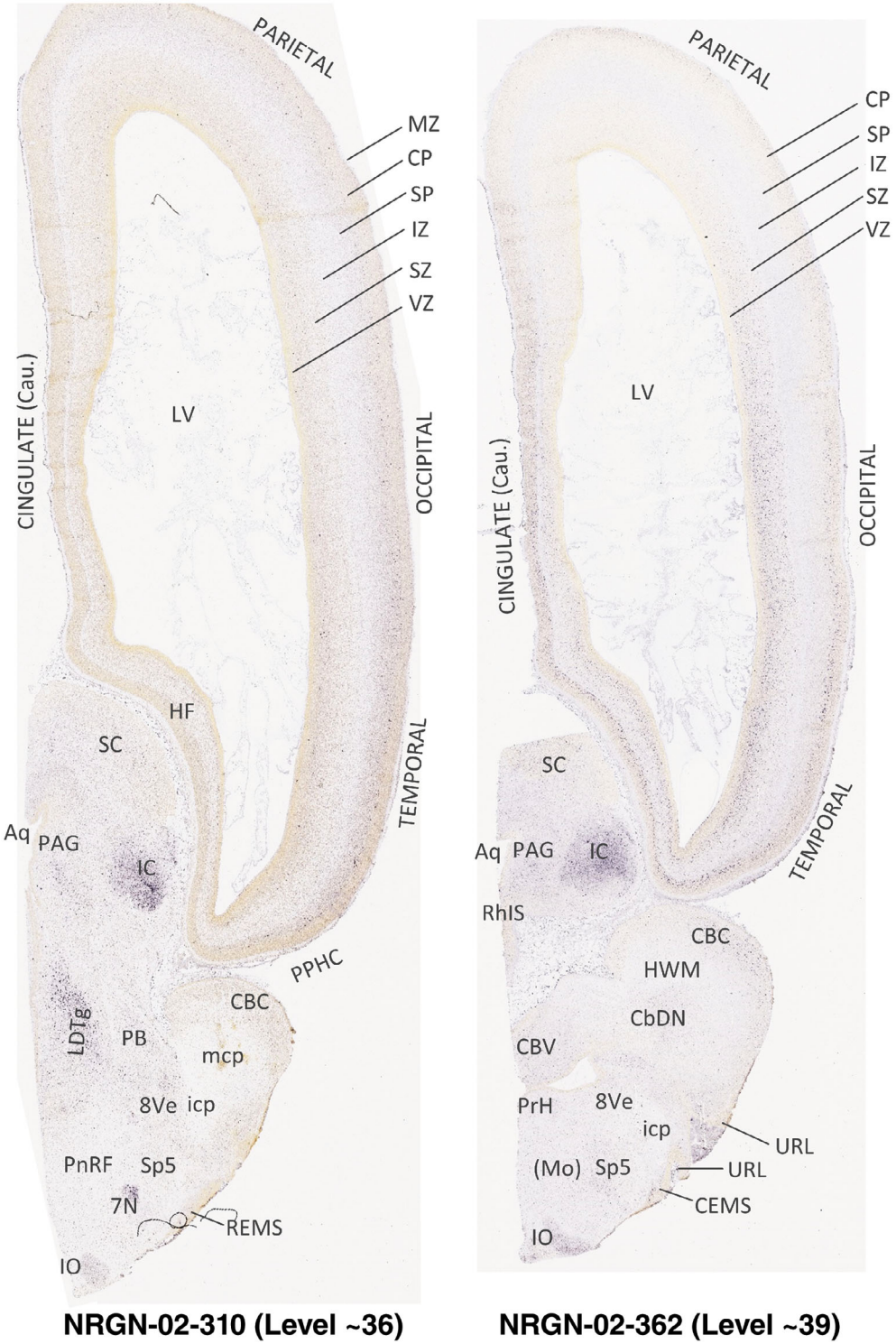

NRGN-02-310 (Level ~36)

NRGN-02-362 (Level ~39)

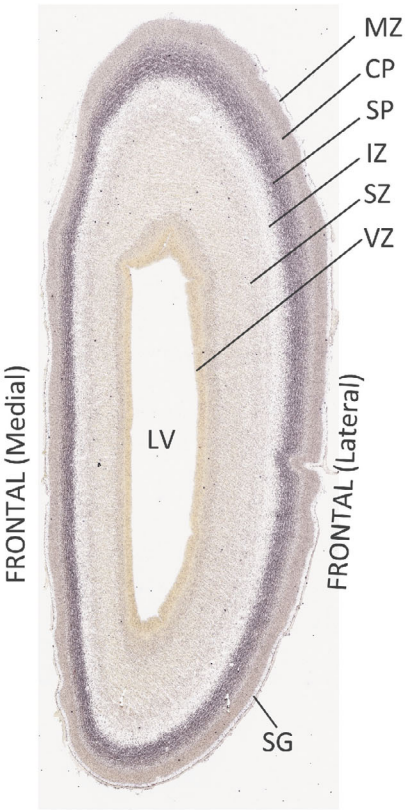

NRXN1-01-048 (Level ~2)

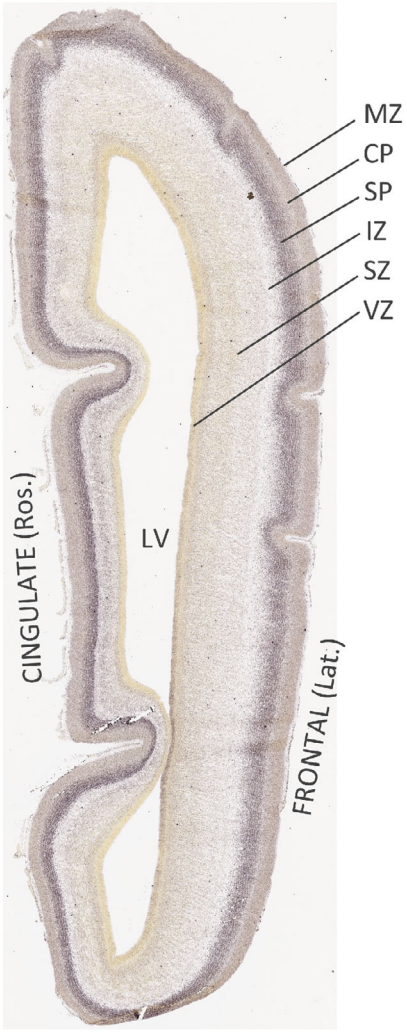

NRXN1-01-204 (Level ~5)

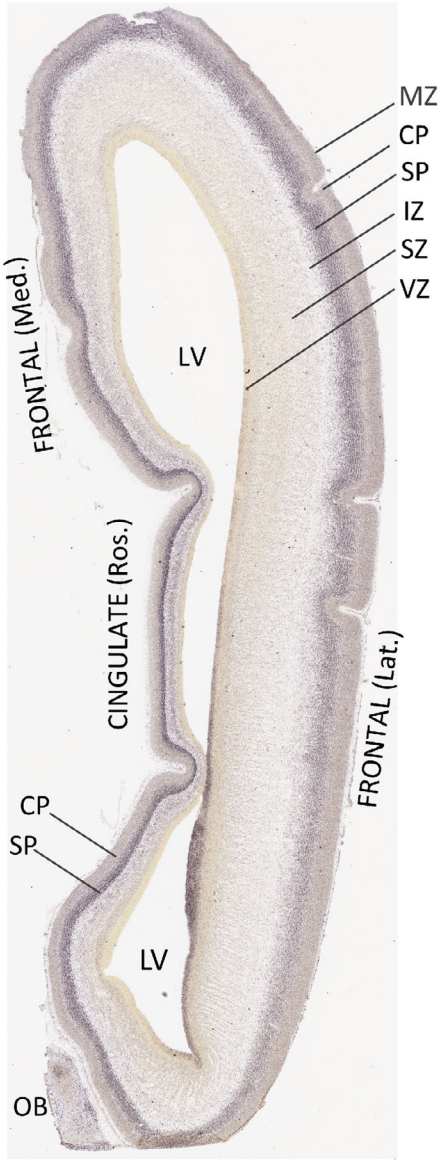

NRXN1-01-308 (Level ~7)

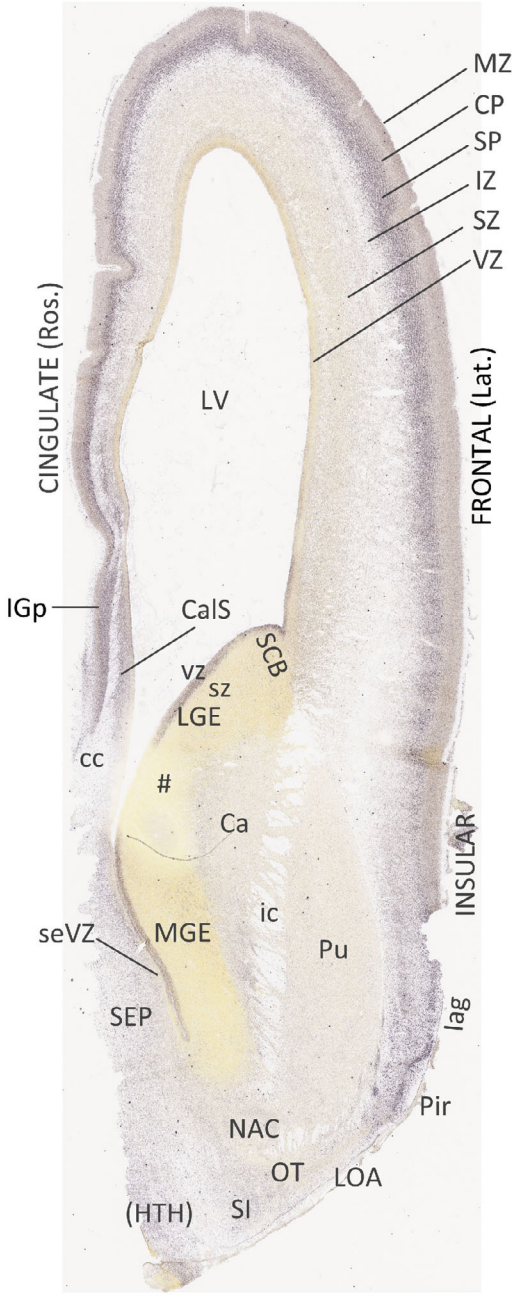

NRXN1-01-516 (Level ~16)

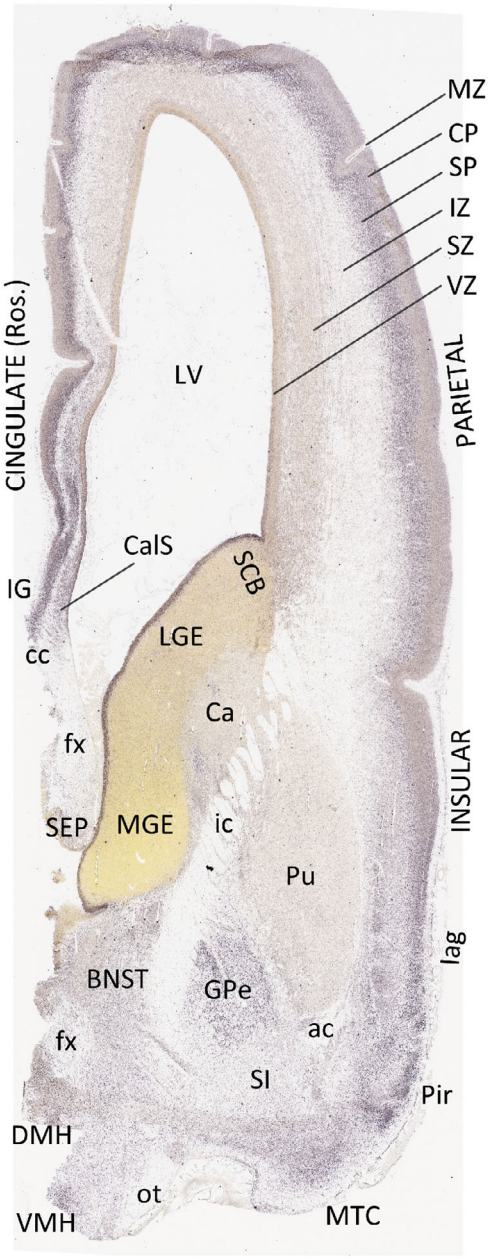

NRXN1-01-620 (Level ~19)

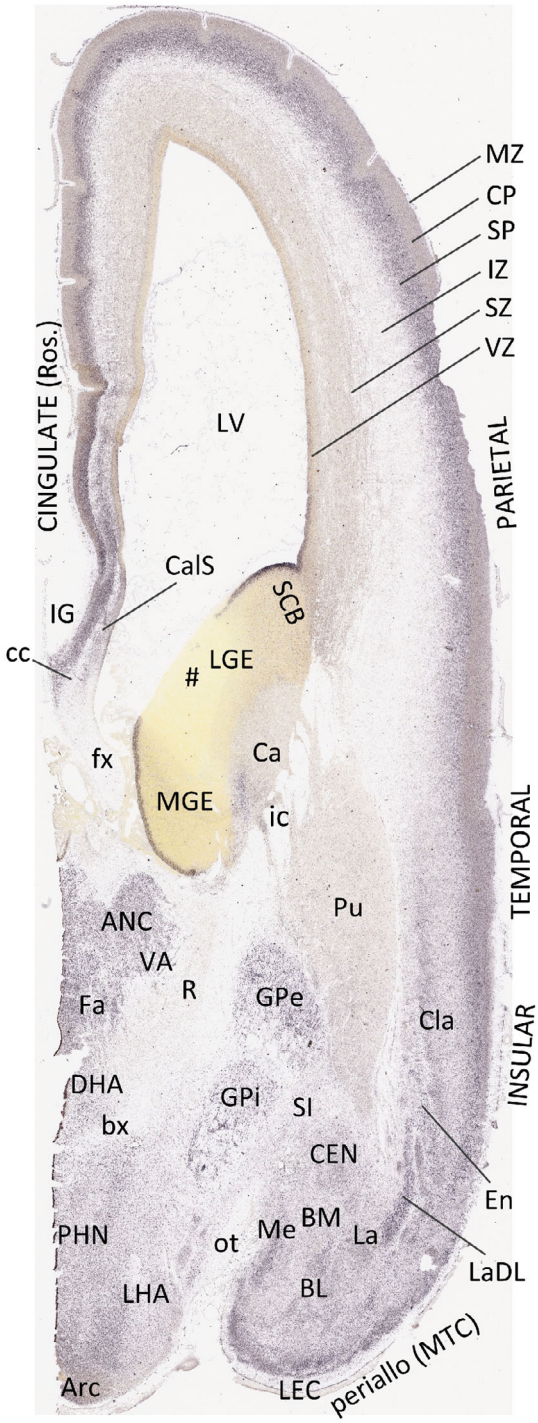

NRXN1-01-672 (Level ~21)

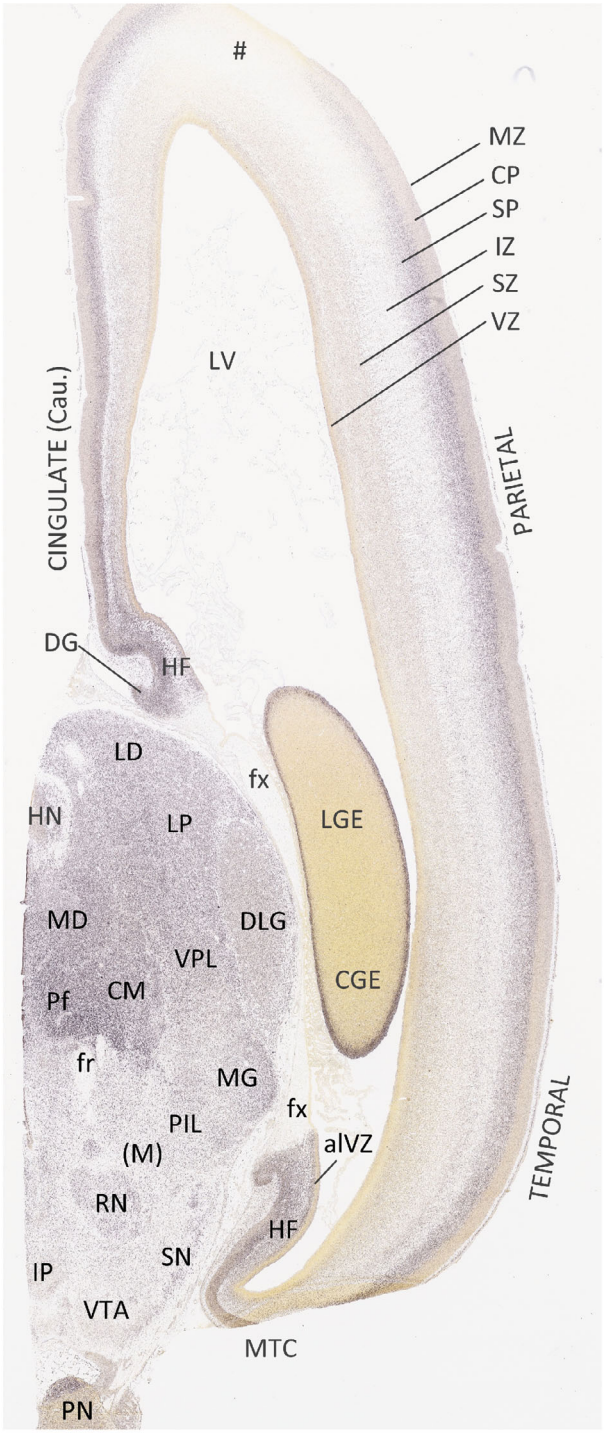

NRXN1-02-100 (Level ~28)

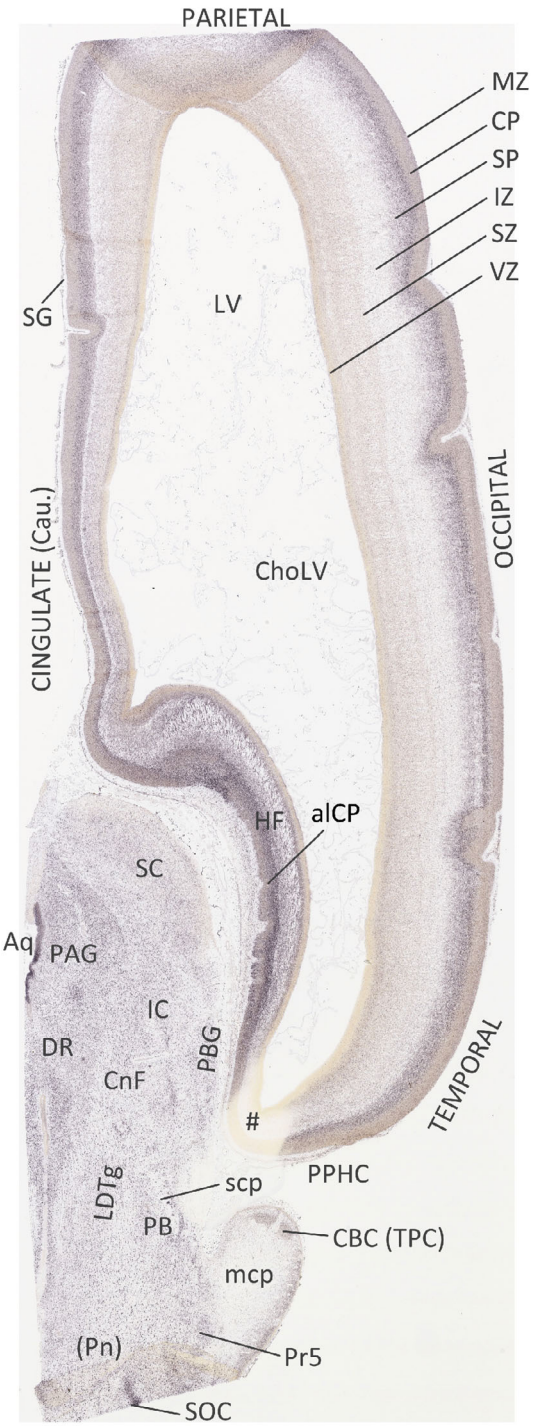

NRXN1-02-256 (Level ~34-35)

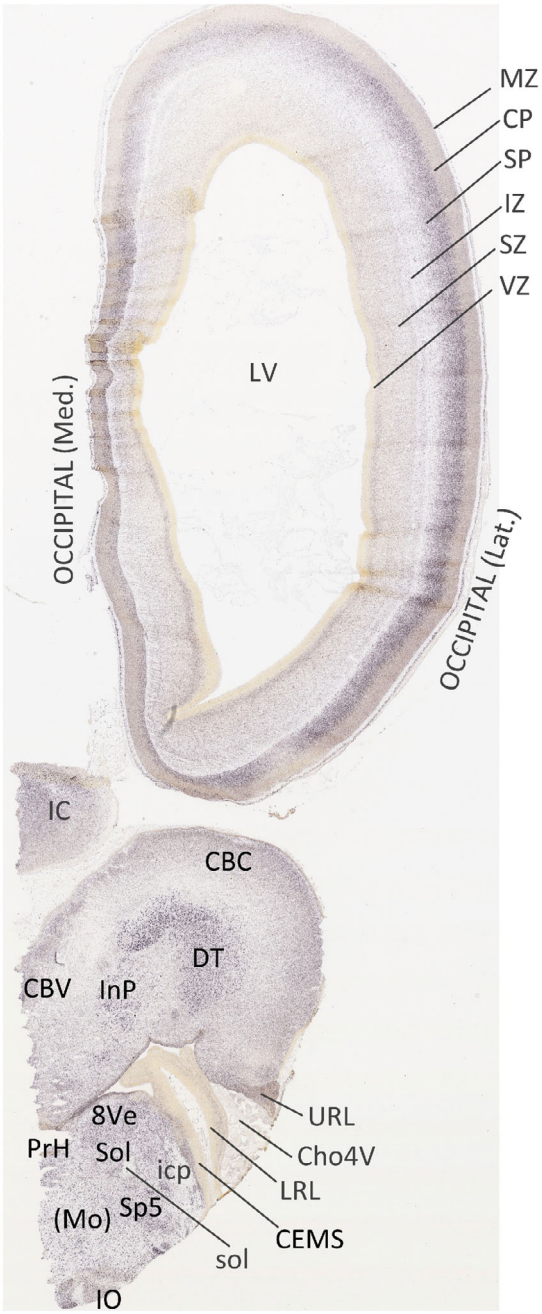

NRXN1-02-412 (Level ~40-41)

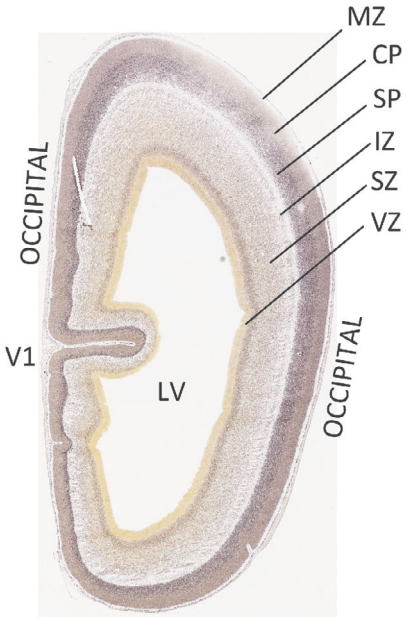

NRXN1-02-568 (Level ~44)

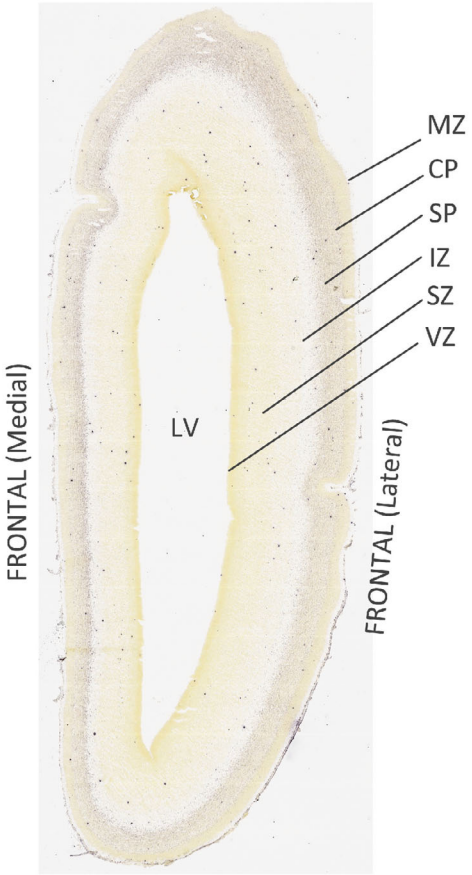

NTRK2-01-088 (Level ~3)

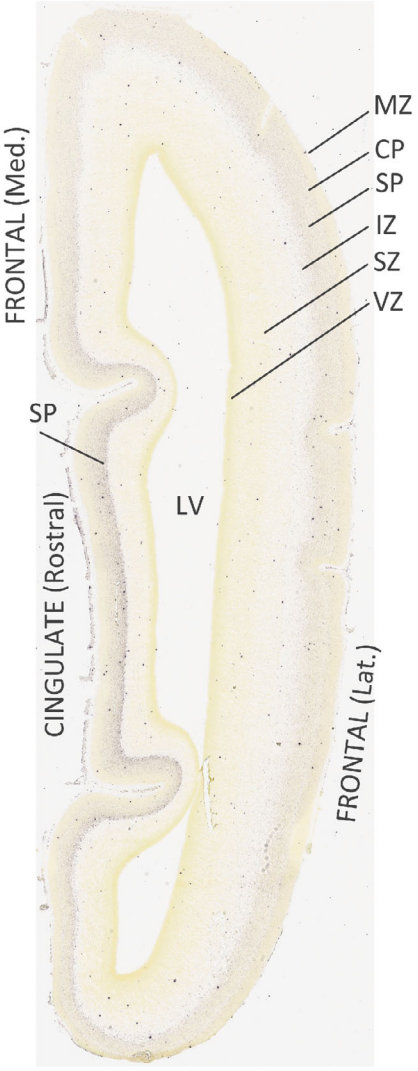

NTRK2-01-192 (Level ~5)

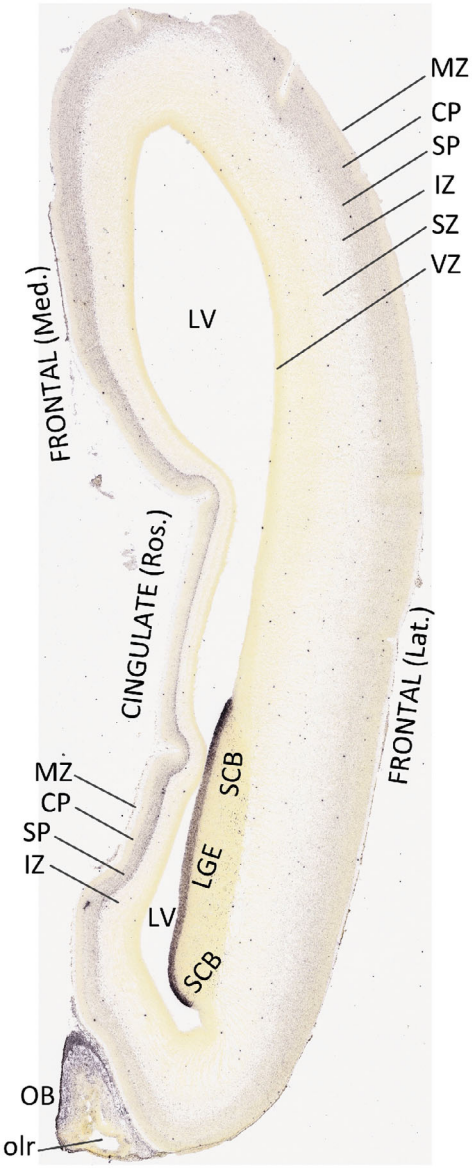

NTRK2-01-348 (Level ~9)

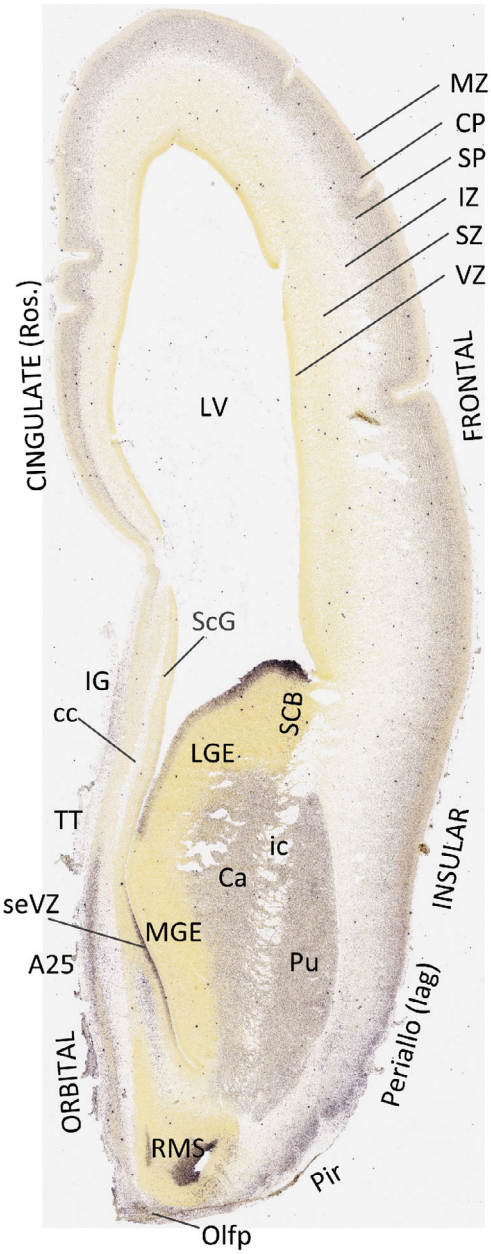

NTRK2-01-452 (Level ~13-14)

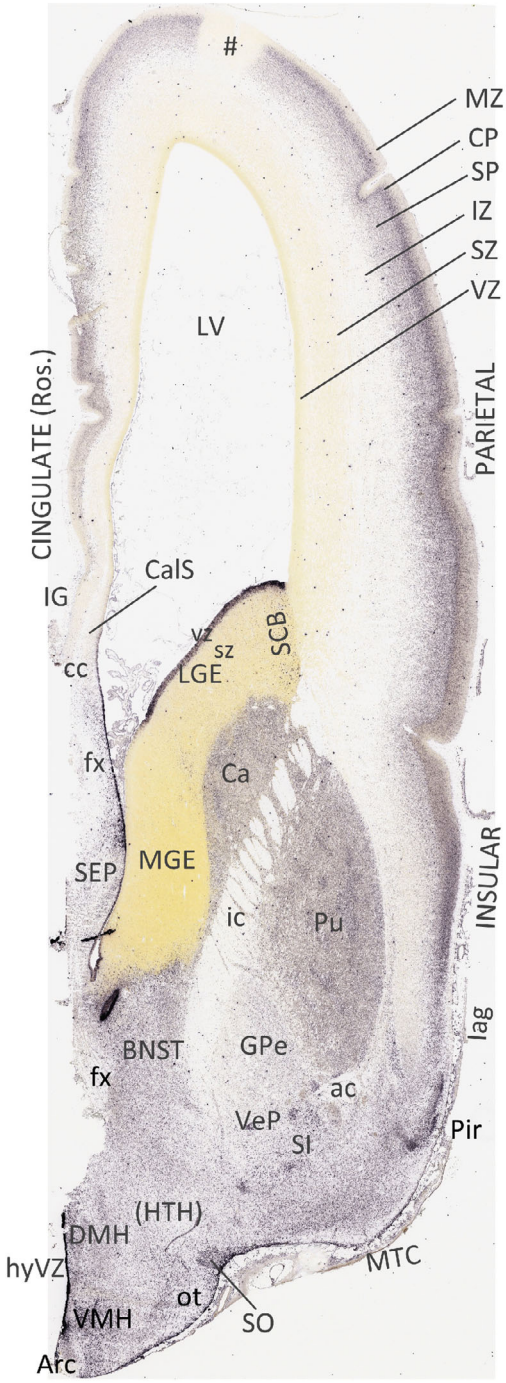

NTRK2-01-608 (Level ~19)

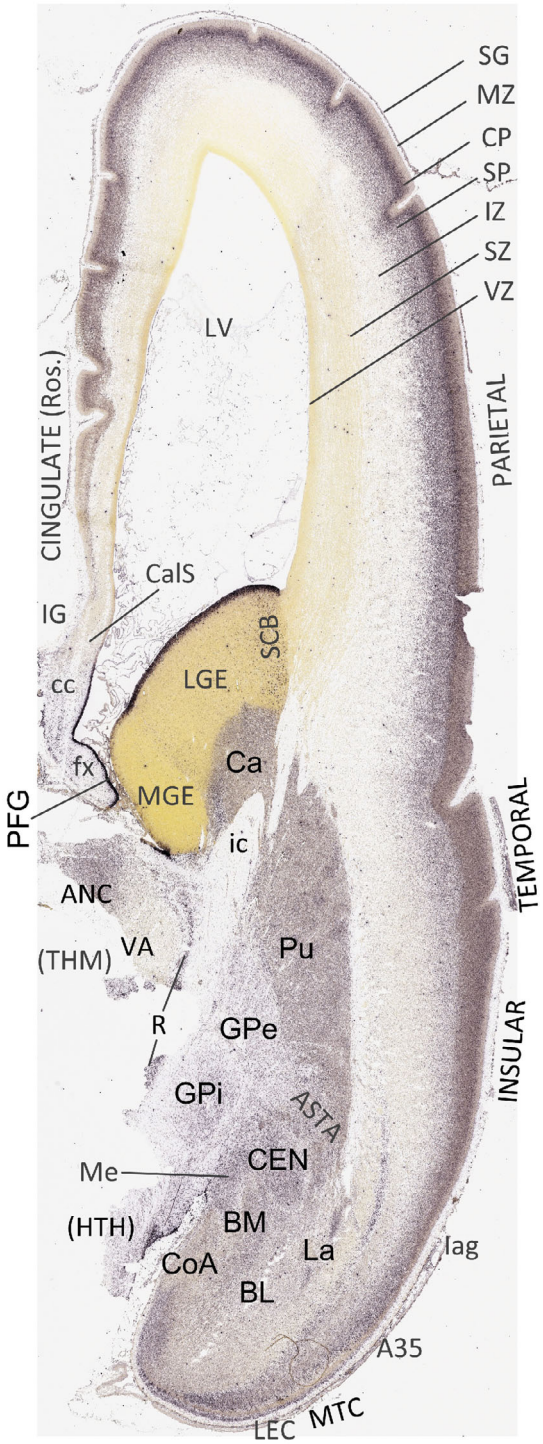

NTRK2-01-712 (Level ~22)

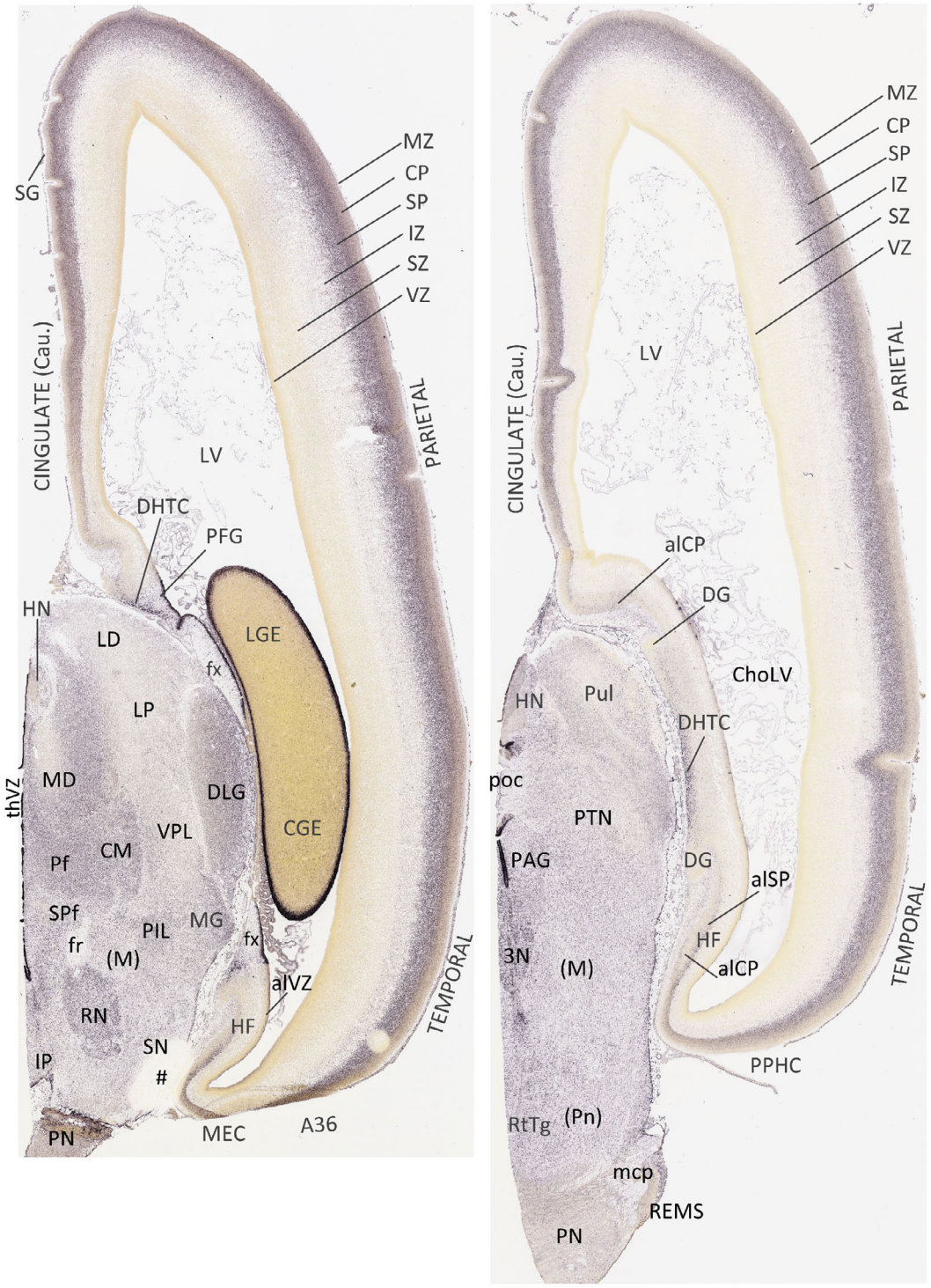

NTRK2-02-088 (Level ~28) **NTRK2-02-192 (Level ~32)**

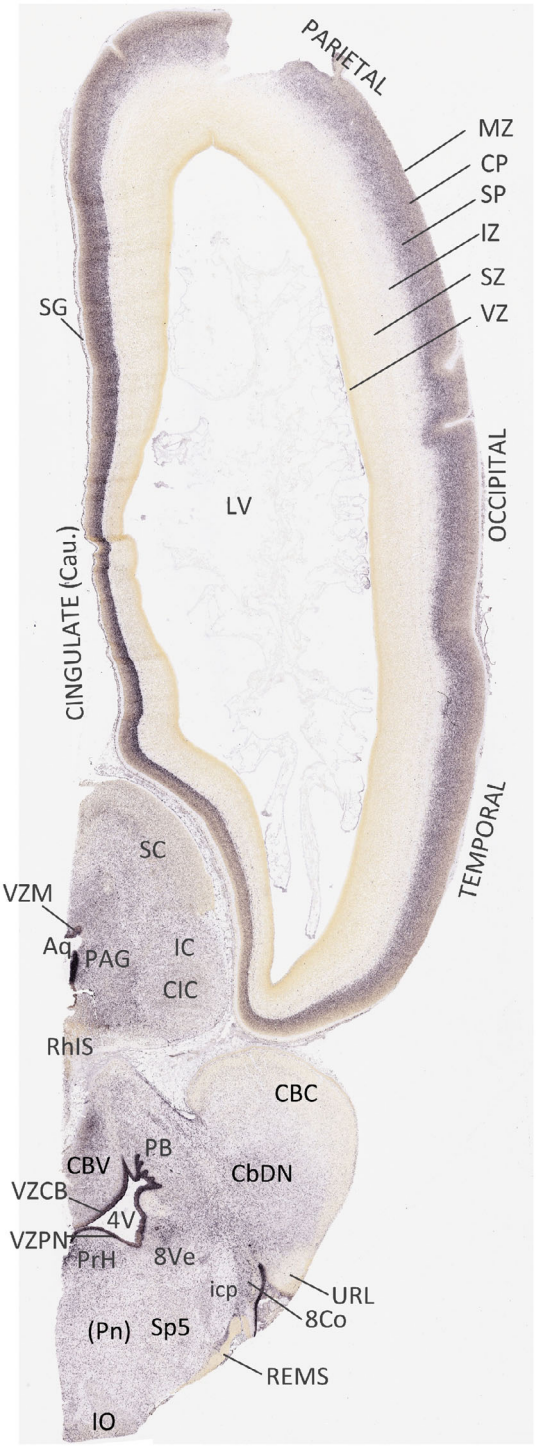

NTRK2-02-348 (Level ~38)

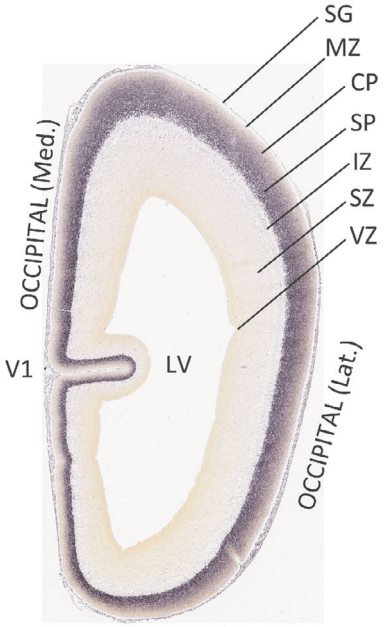

NTRK2-02-556 (Level ~43-44)

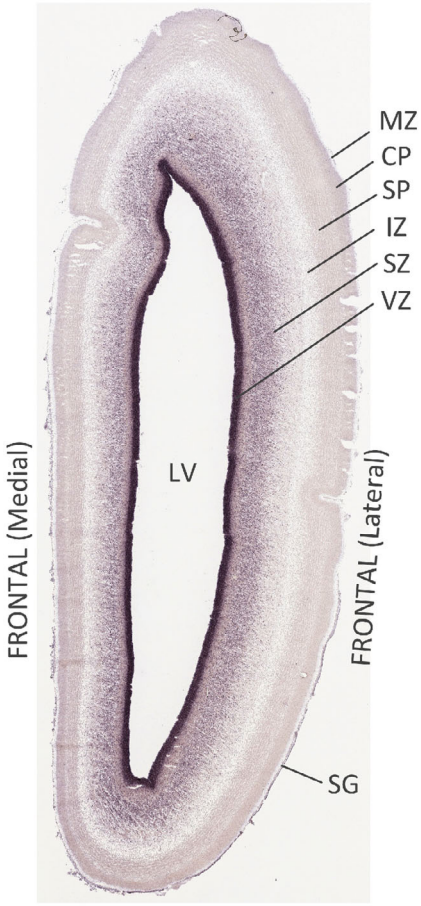

PAX6-01-101 (Level ~3)

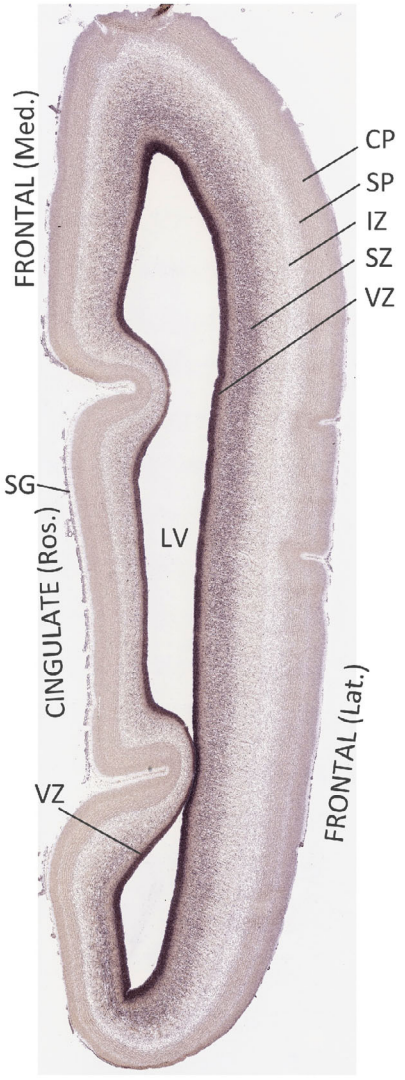

PAX6-01-205 (Level ~5)

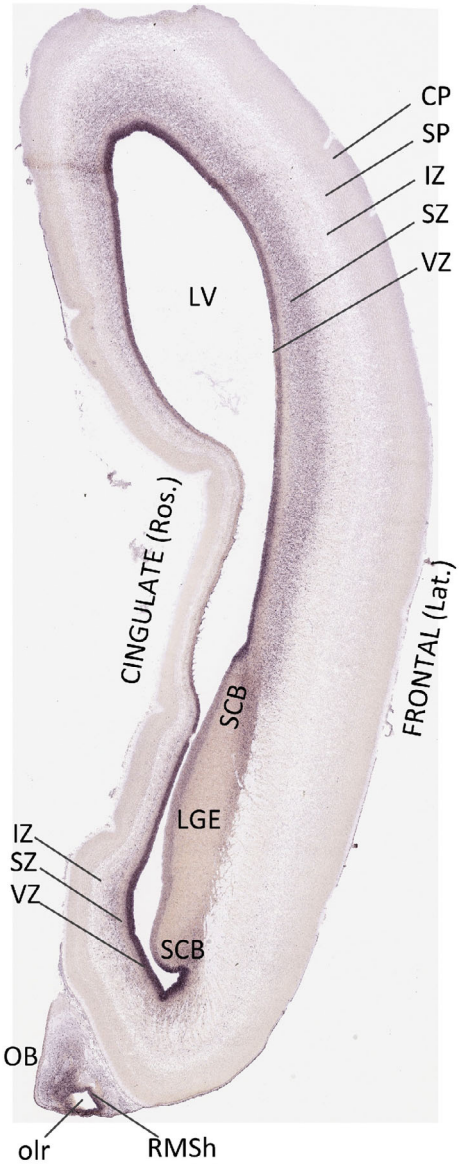

PAX6-01-361 (Level ~10)

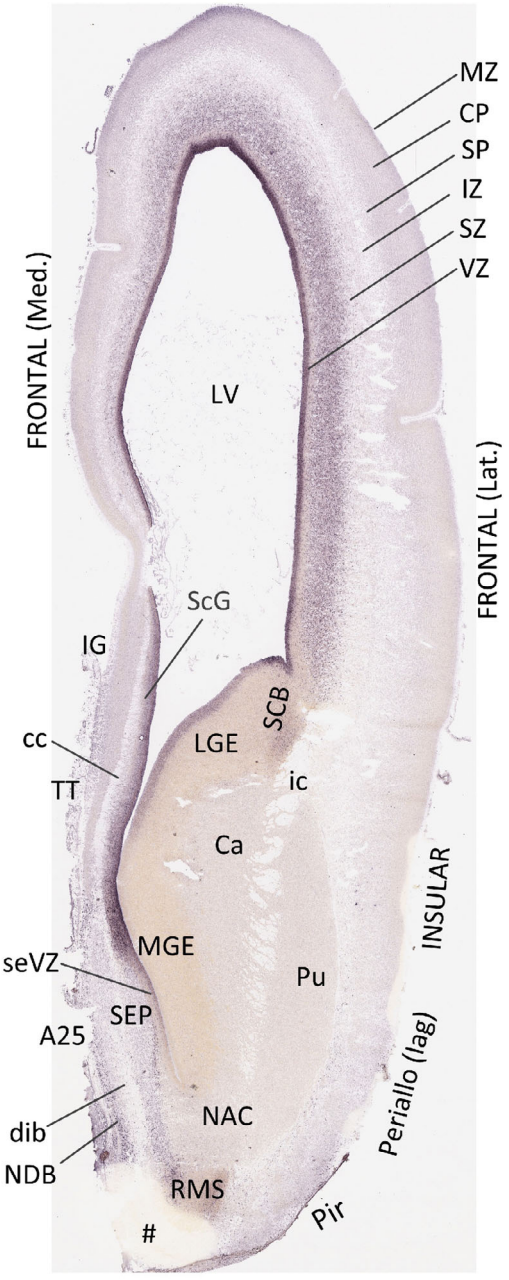

PAX6-01-465 (Level ~14)

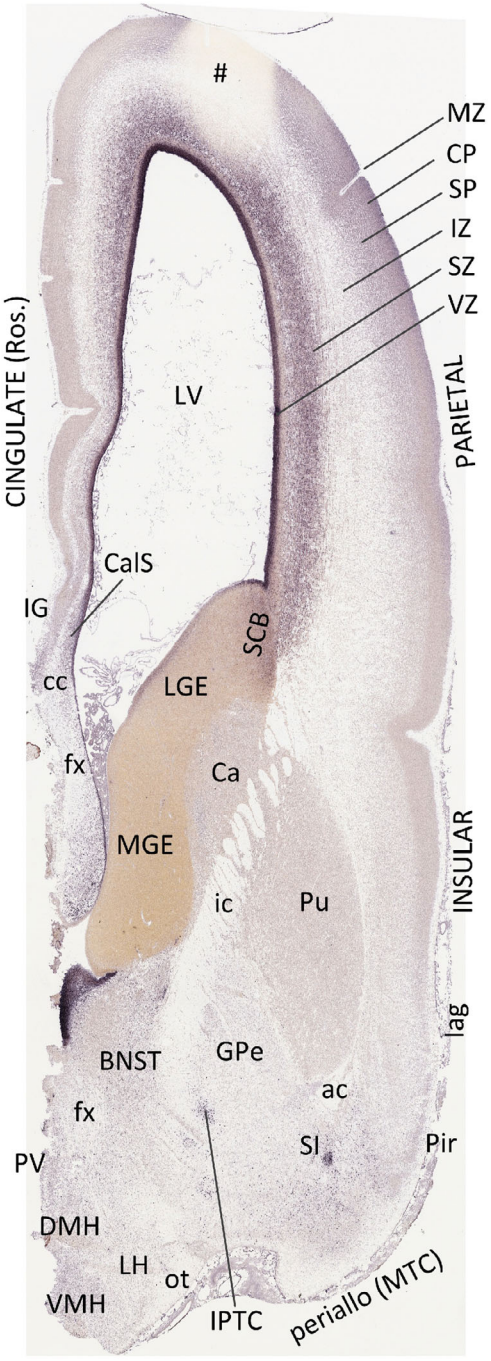

PAX6-01-621 (Level ~19)

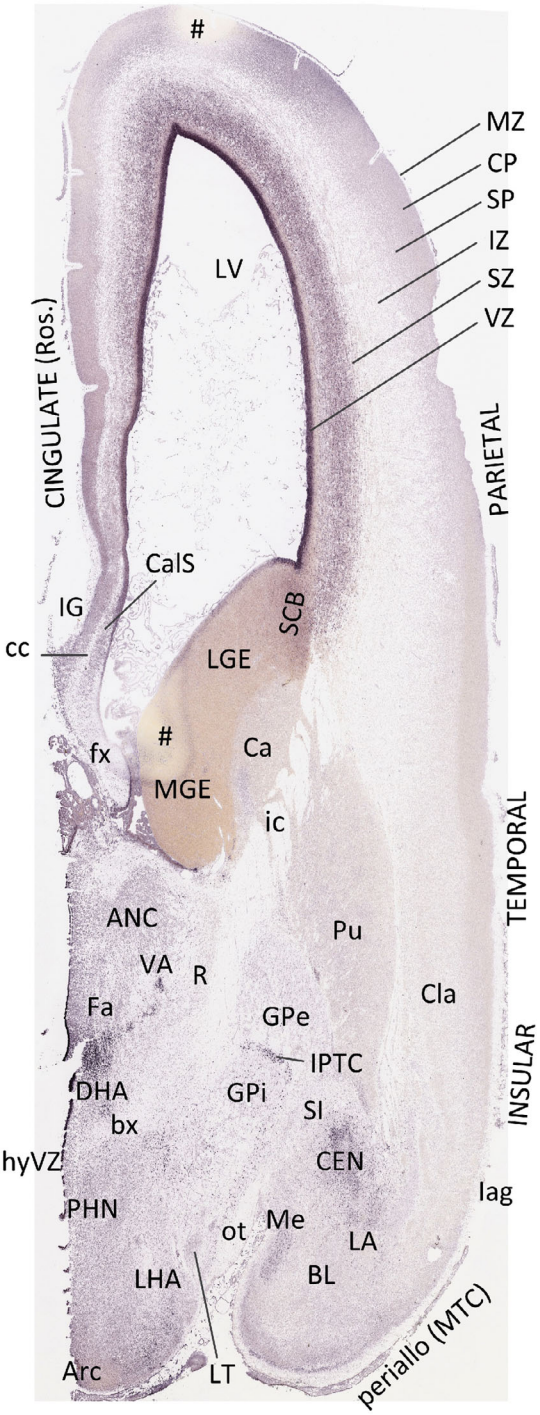

PAX6-01-673 (Level ~21)

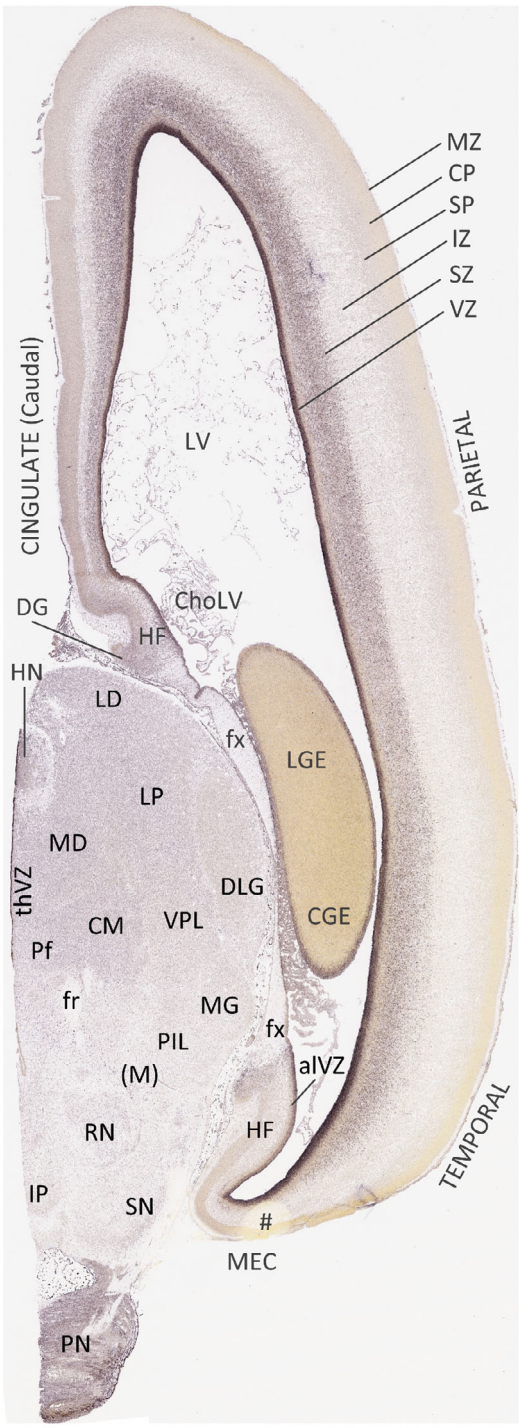

PAX6-02-101 (Level ~28)

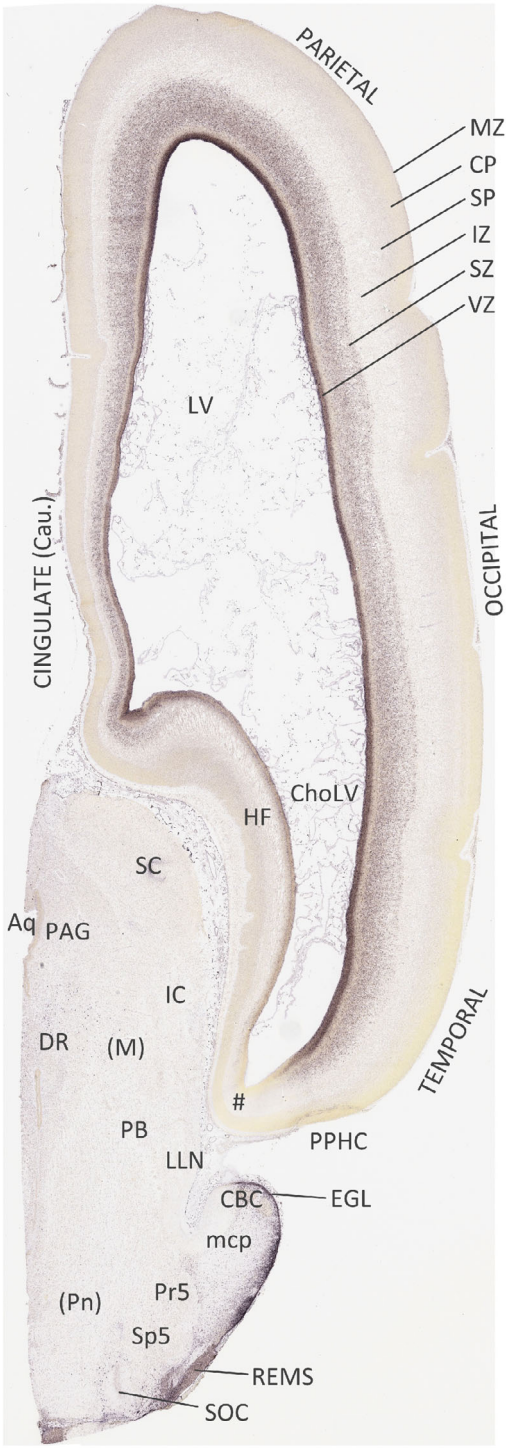

PAX6-02-257 (Level ~34)

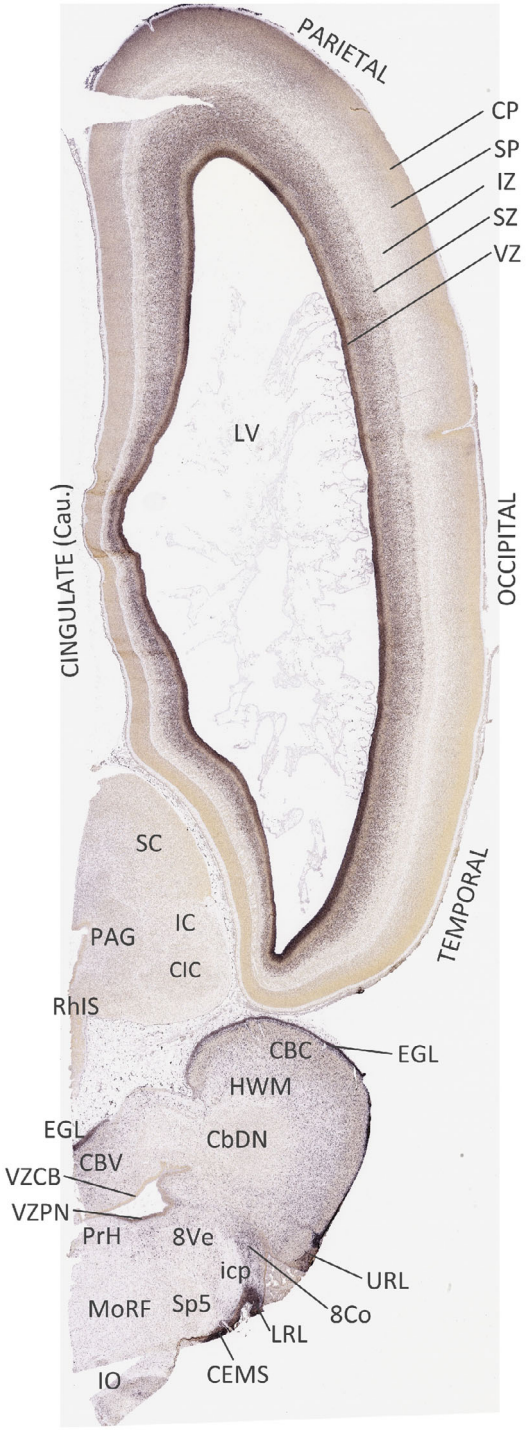

PAX6-02-361 (Level ~39)

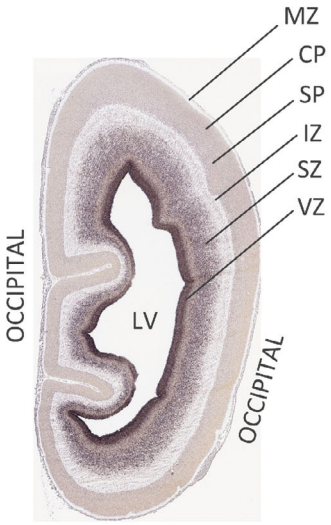

PAX6-02-621 (Level ~45)

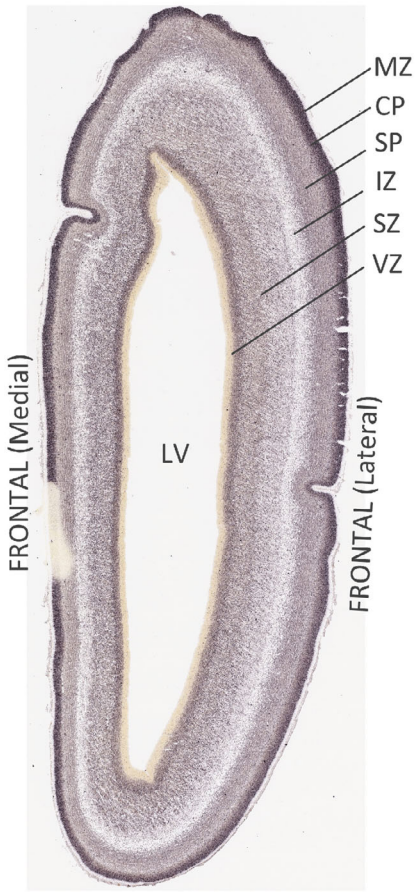

PLXNA2-01-098 (Level ~3)

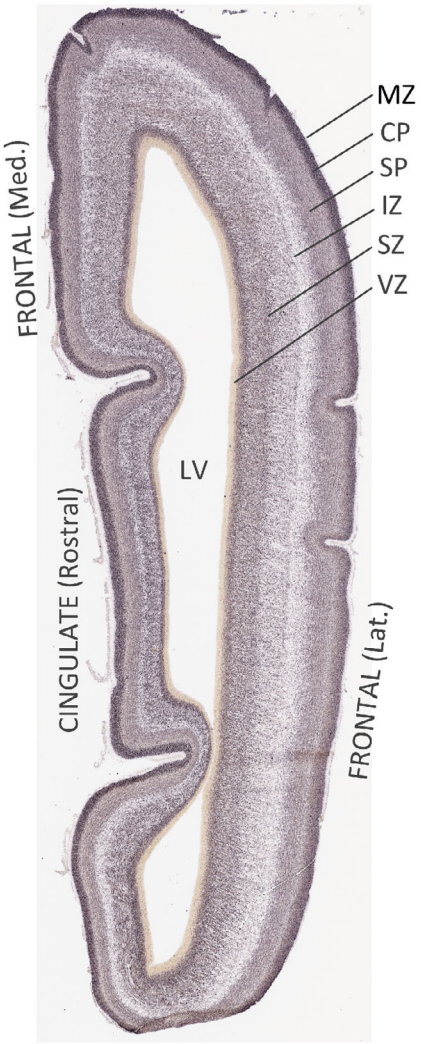

PLXNA2-01-202 (Level ~5)

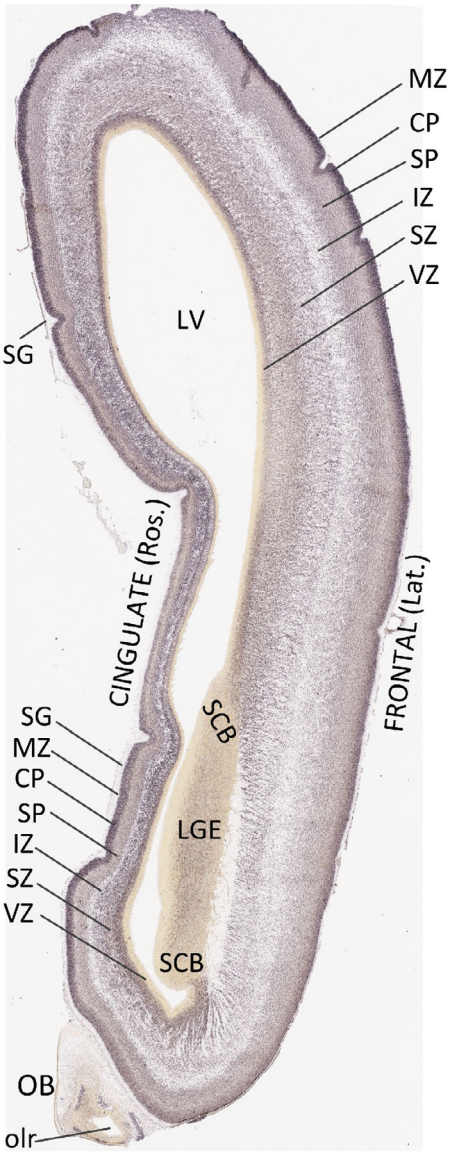

PLXNA2-01-358 (Level ~10)

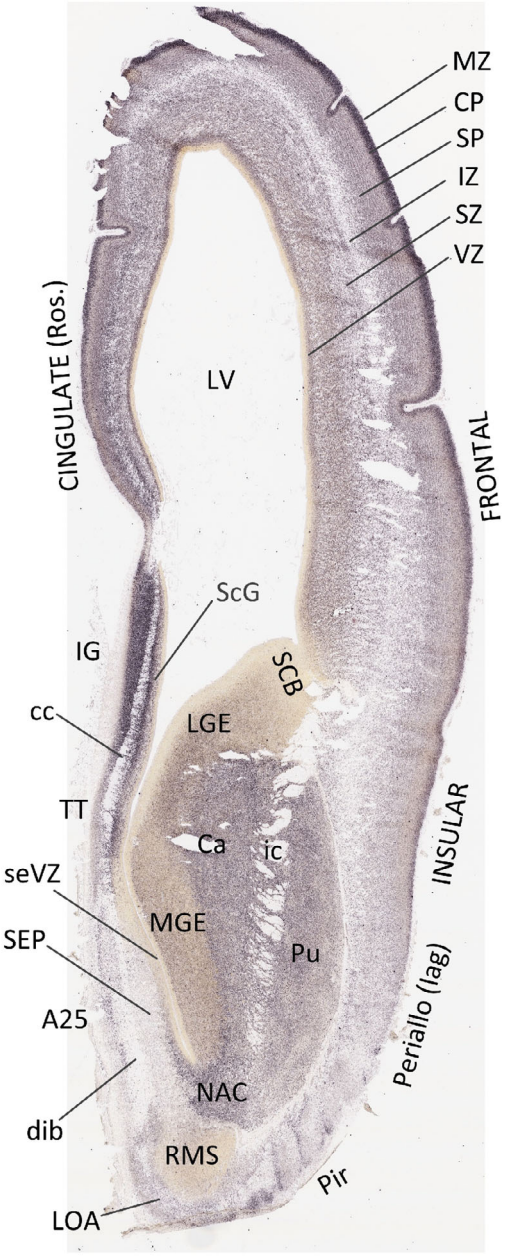

PLXNA2-01-462 (Level ~14)

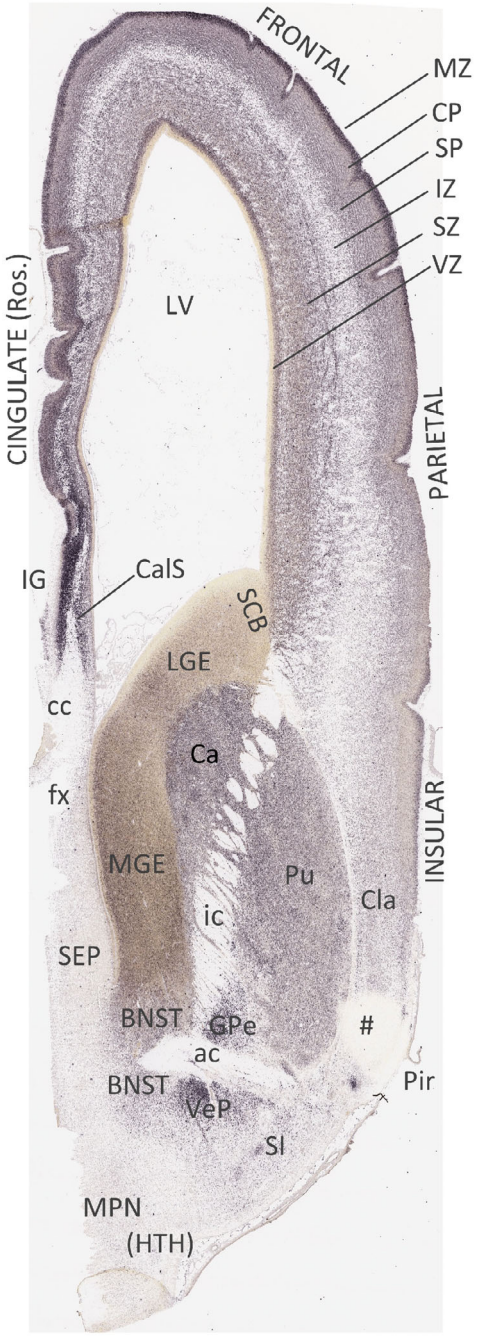

PLXNA2-01-566 (Level ~18)

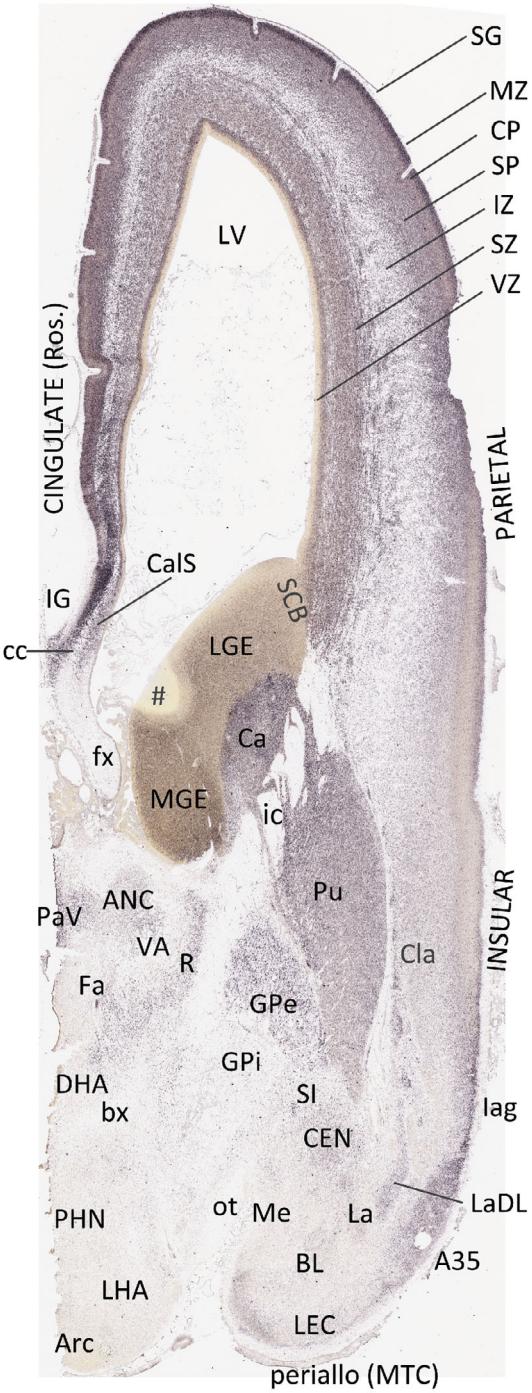

PLXNA2-01-670 (Level ~21)

PLXNA2-02-046 (Level ~26) **PLXNA2-02-202 (Level ~32)**

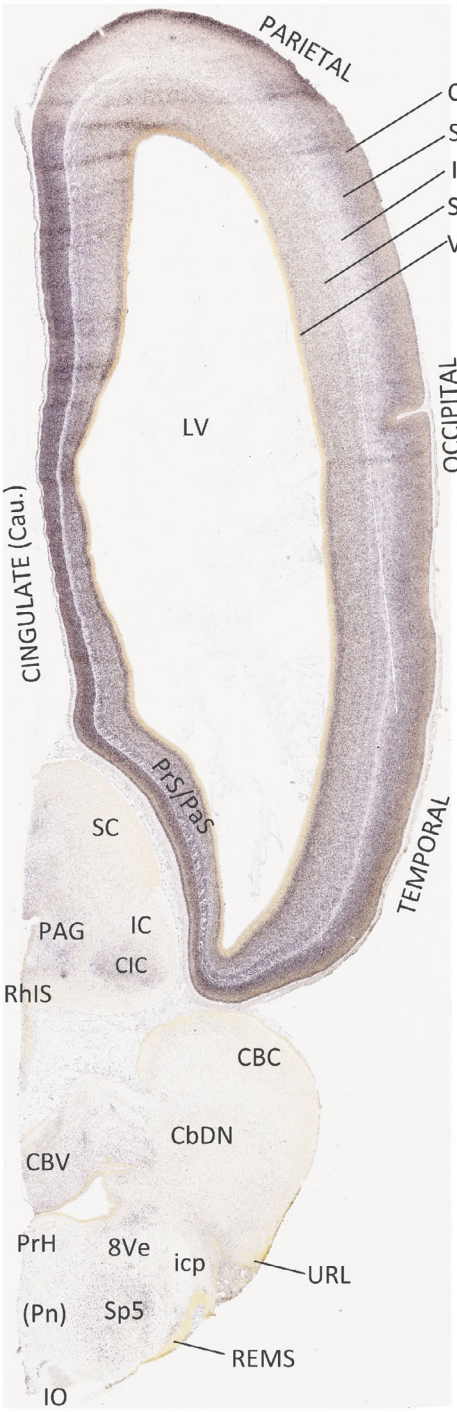

PLXNA2-02-358 (Level ~38)

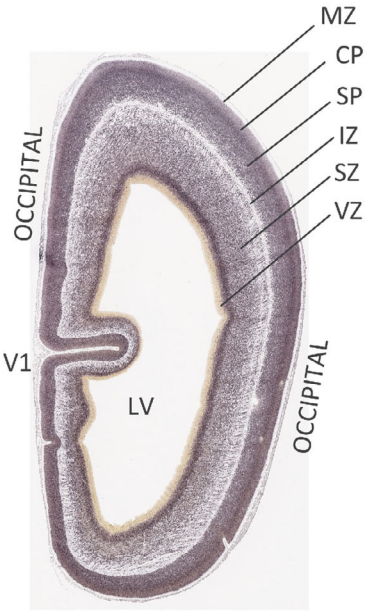

PLXNA2-02-566 (Level ~44)

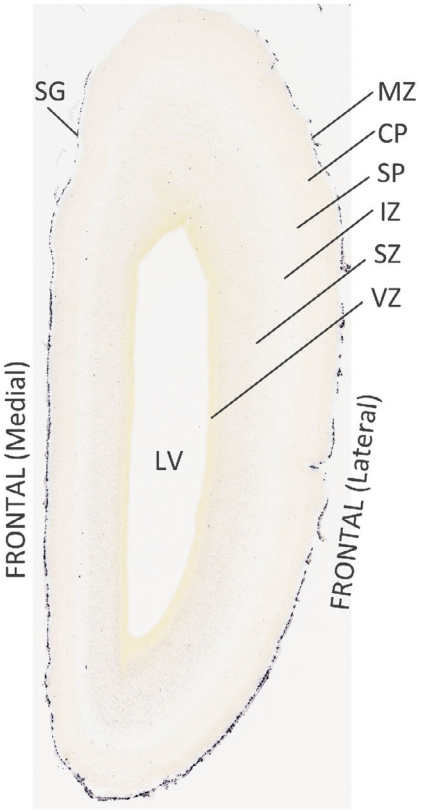

RELN-01-058 (Level ~2)

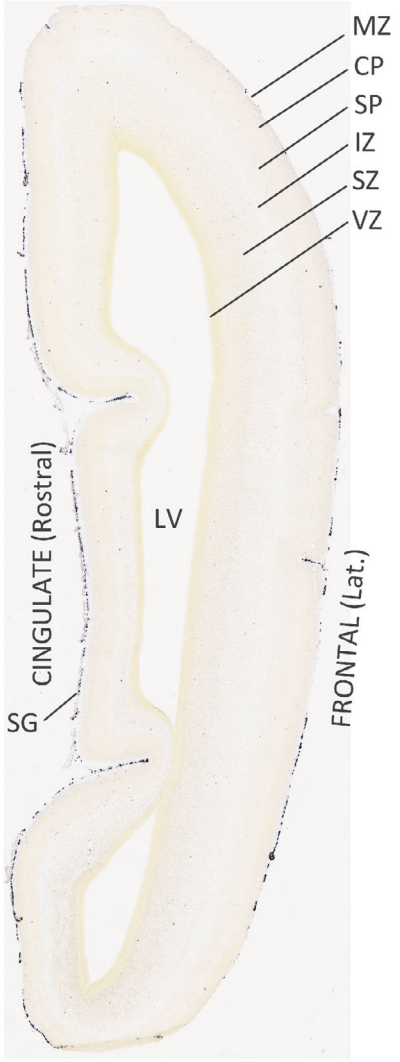

RELN-01-214 (Level ~5)

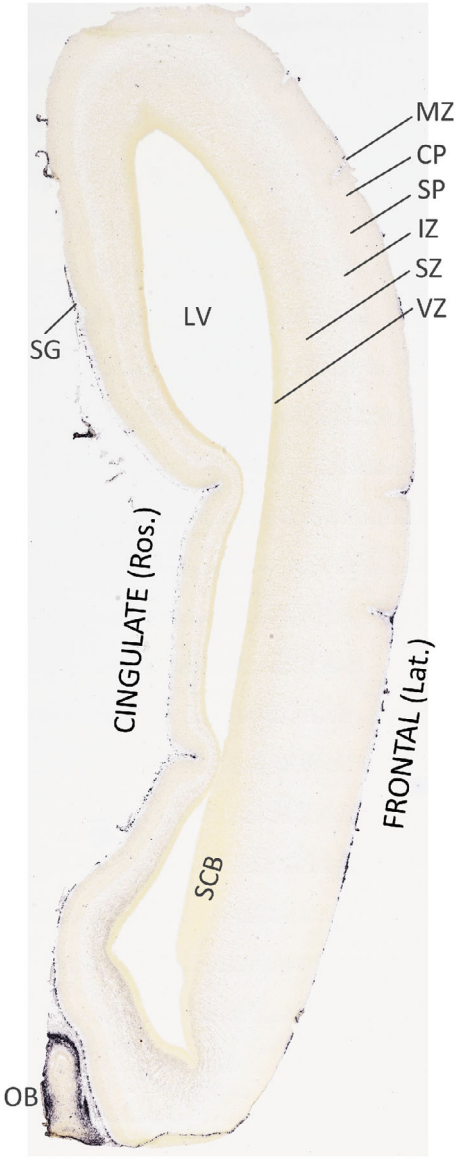

RELN-01-318 (Level ~8)

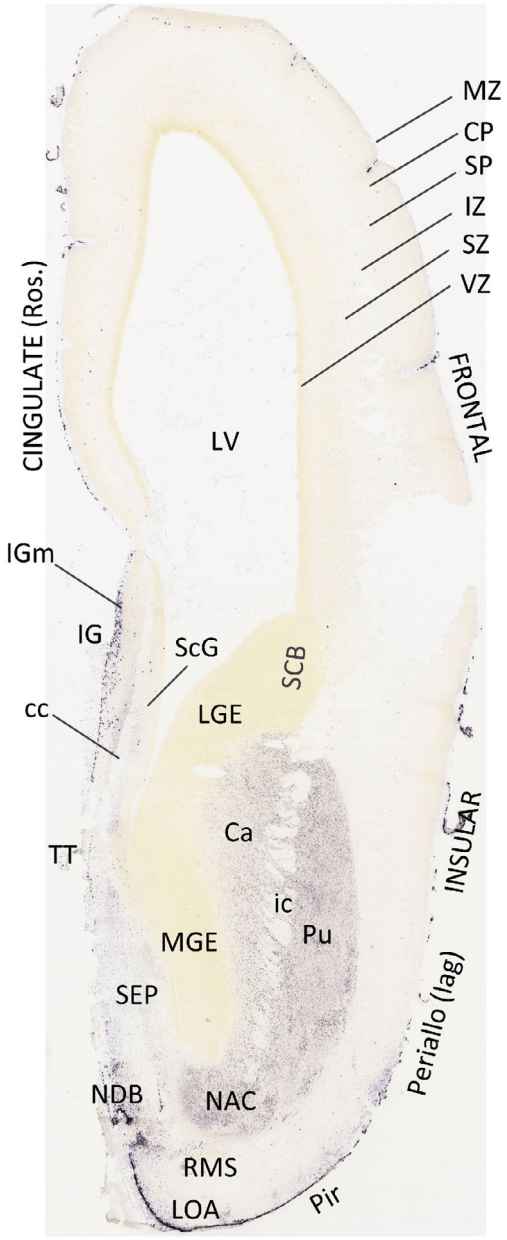

RELN-01-474 (Level ~14)

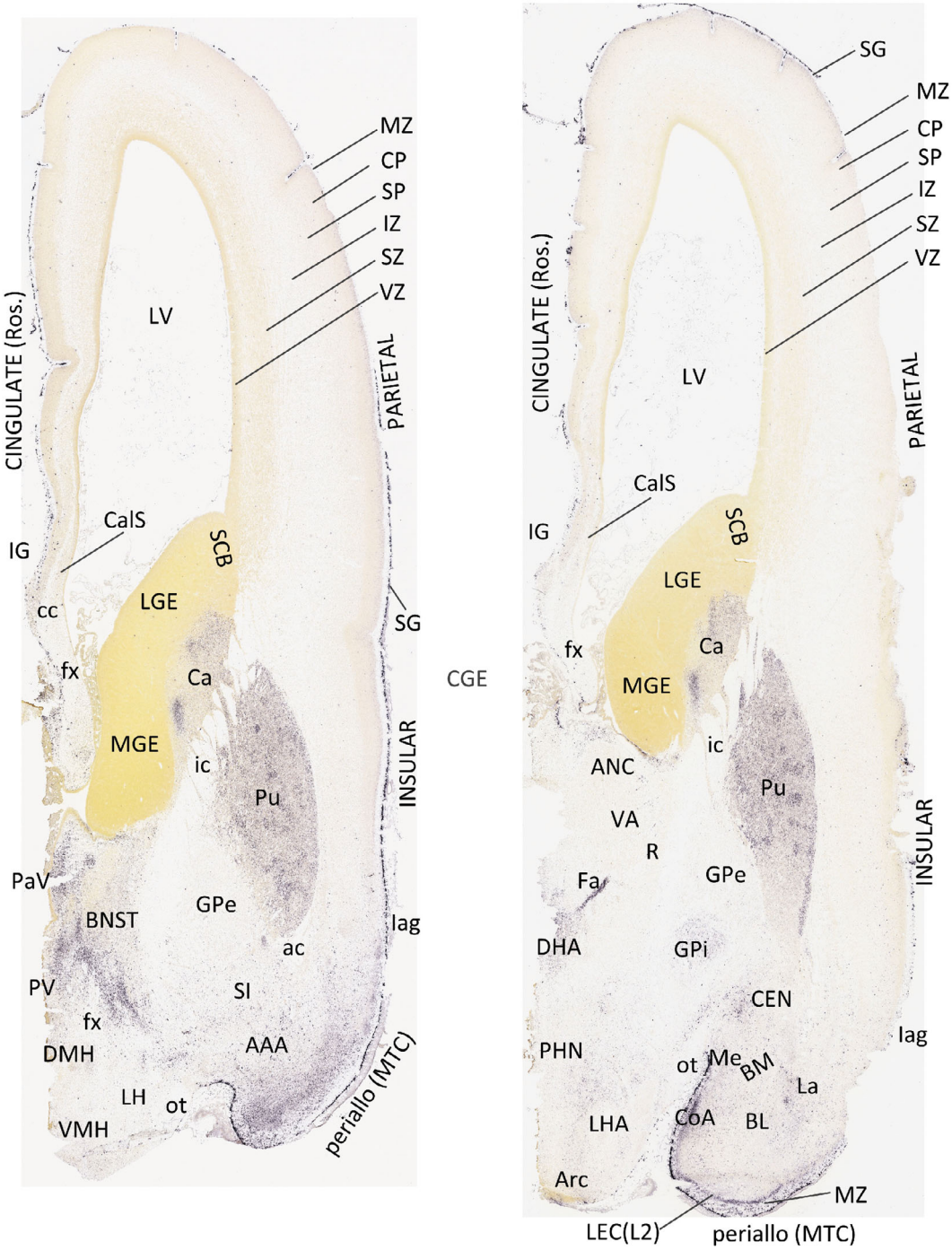

RELN-01-630 (Level ~20) **RELN-01-682 (Level ~21)**

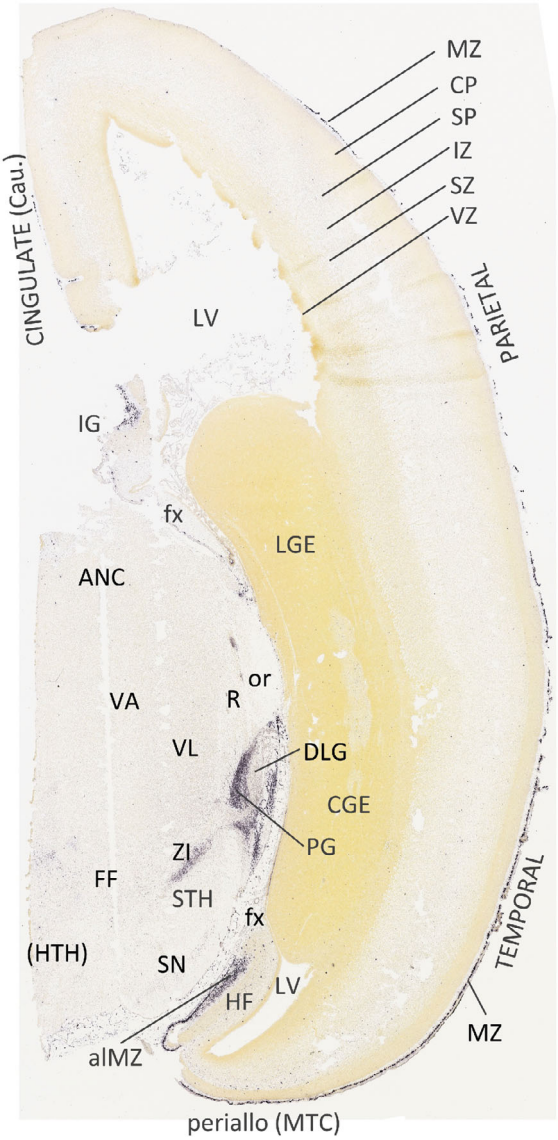

RELN-02-006 (Level ~24)

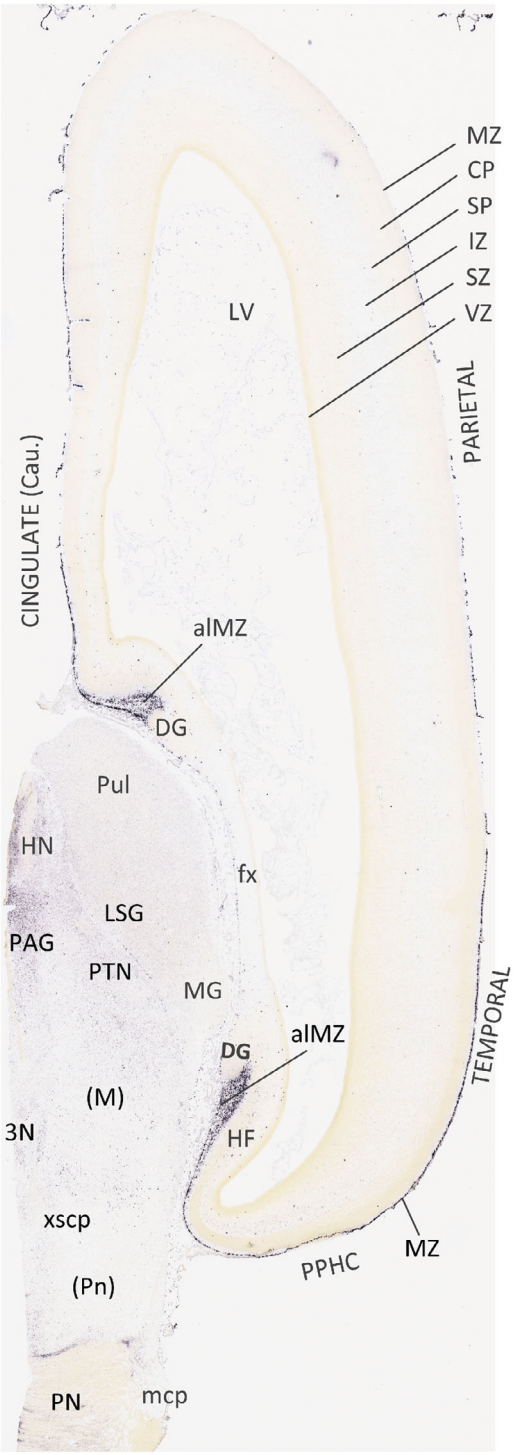

RELN-02-162 (Level ~30-31)

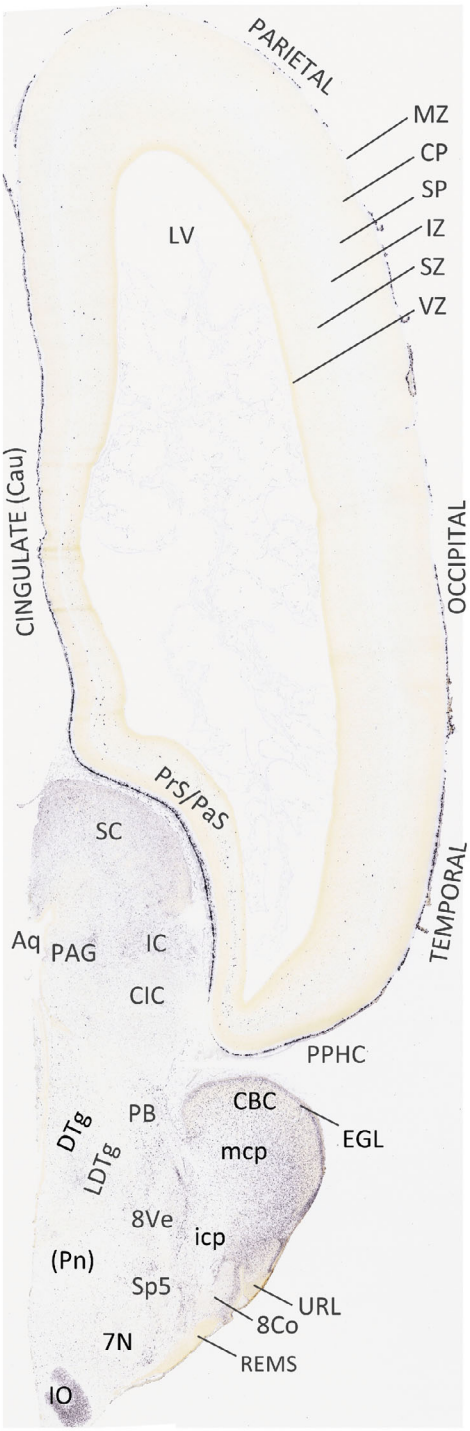

RELN-02-318 (Level ~37)

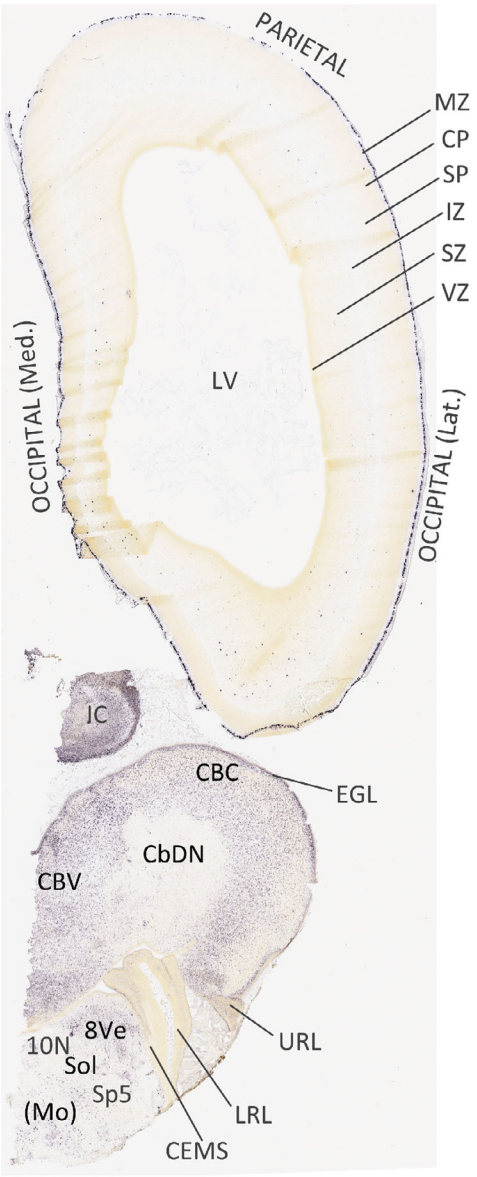

RELN-02-422 (Level ~41)

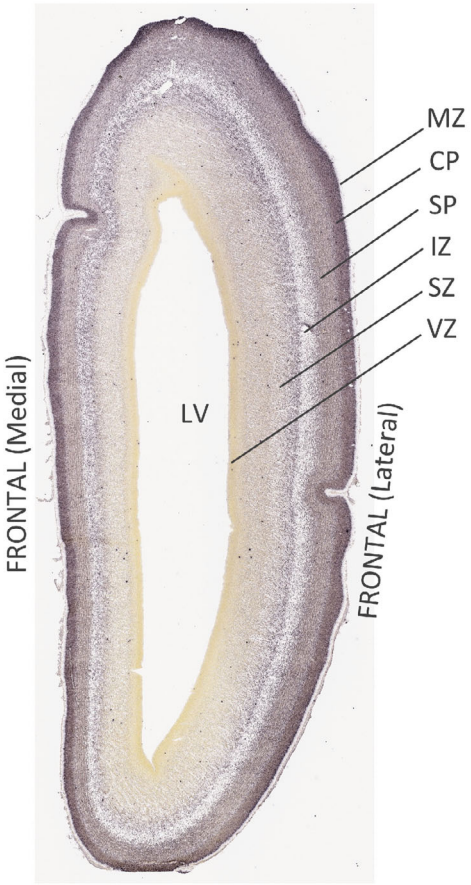

SATB2-01-089 (Level ~3)

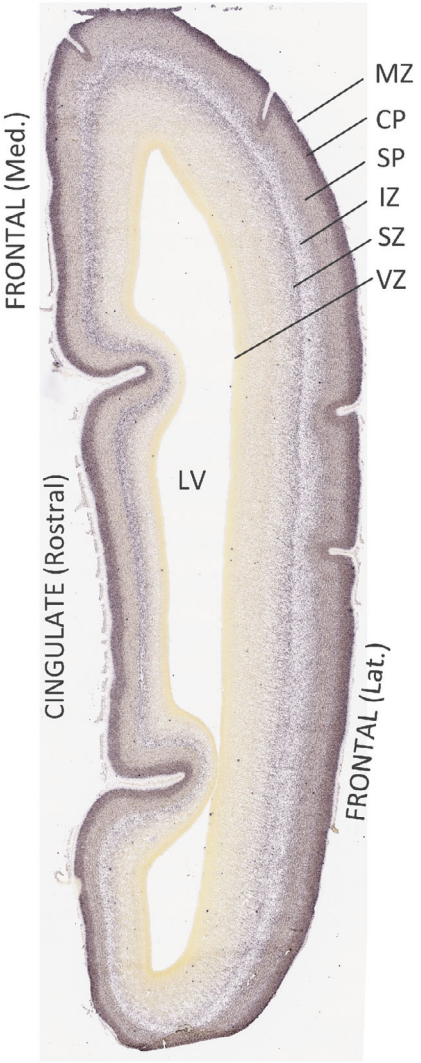

SATB2-01-193 (Level ~5)

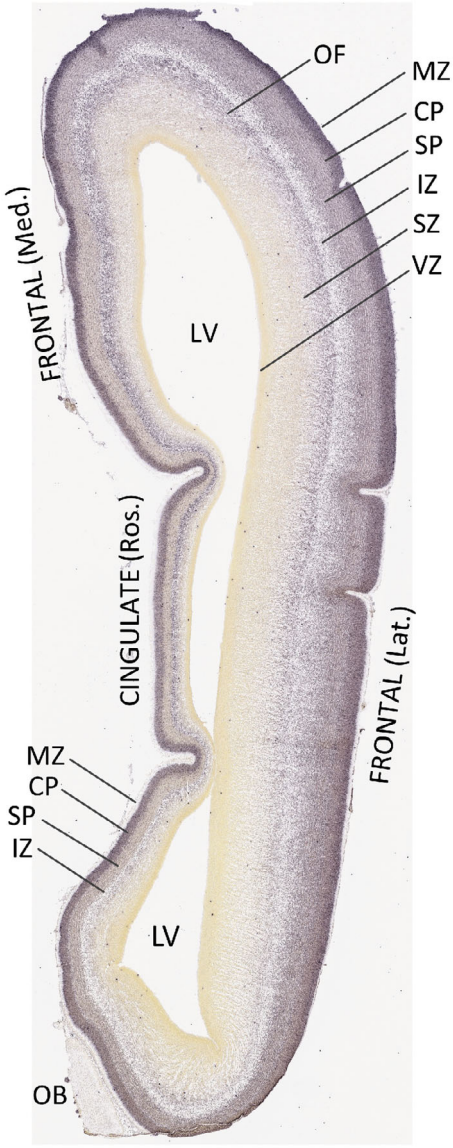

SATB2-01-297 (Level ~7)

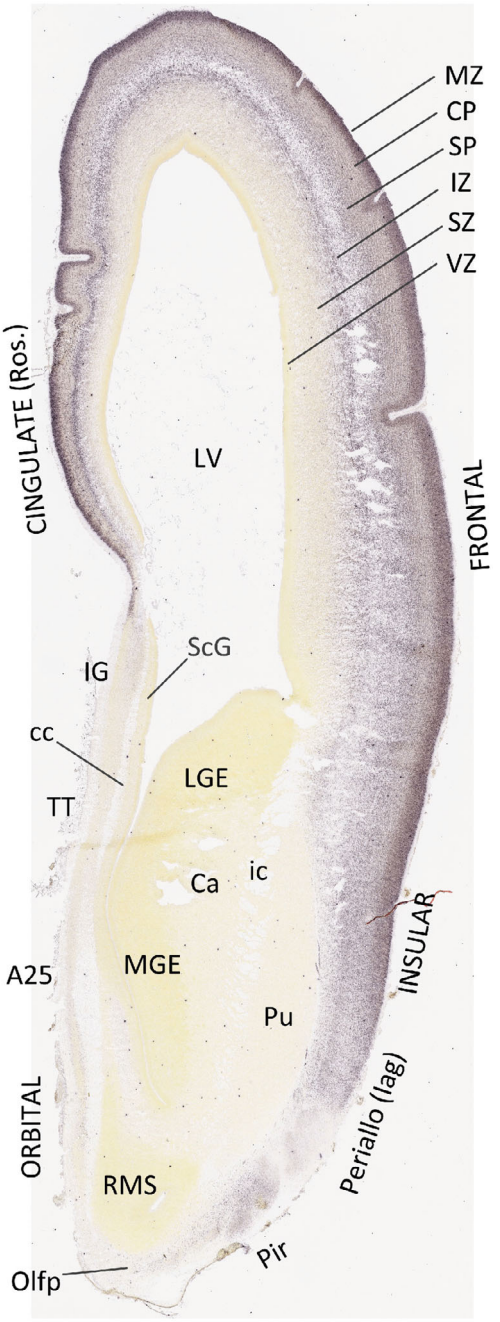

SATB2-01-453 (Level ~13)

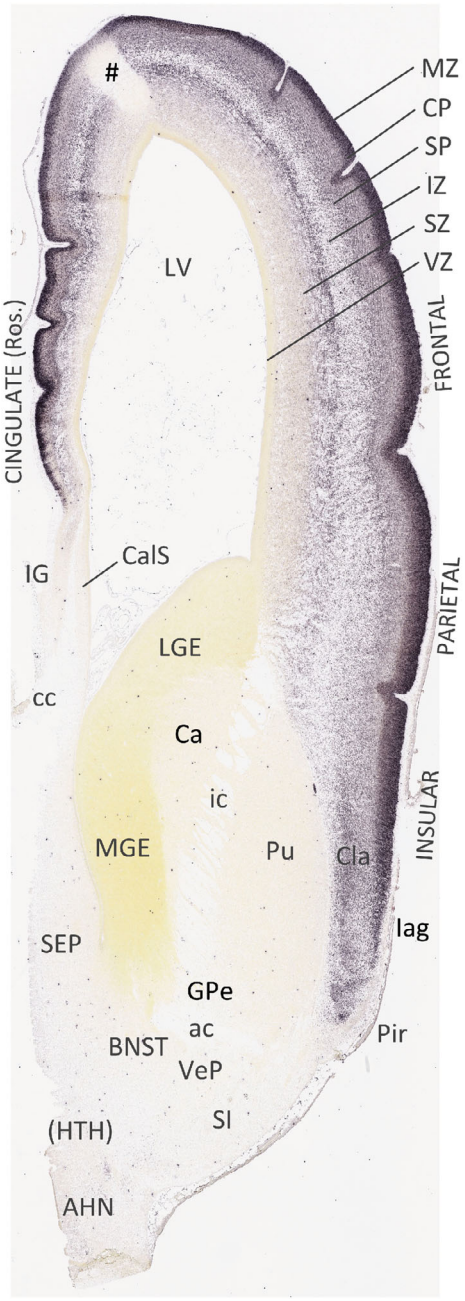

SATB2-01-557 (Level ~17)

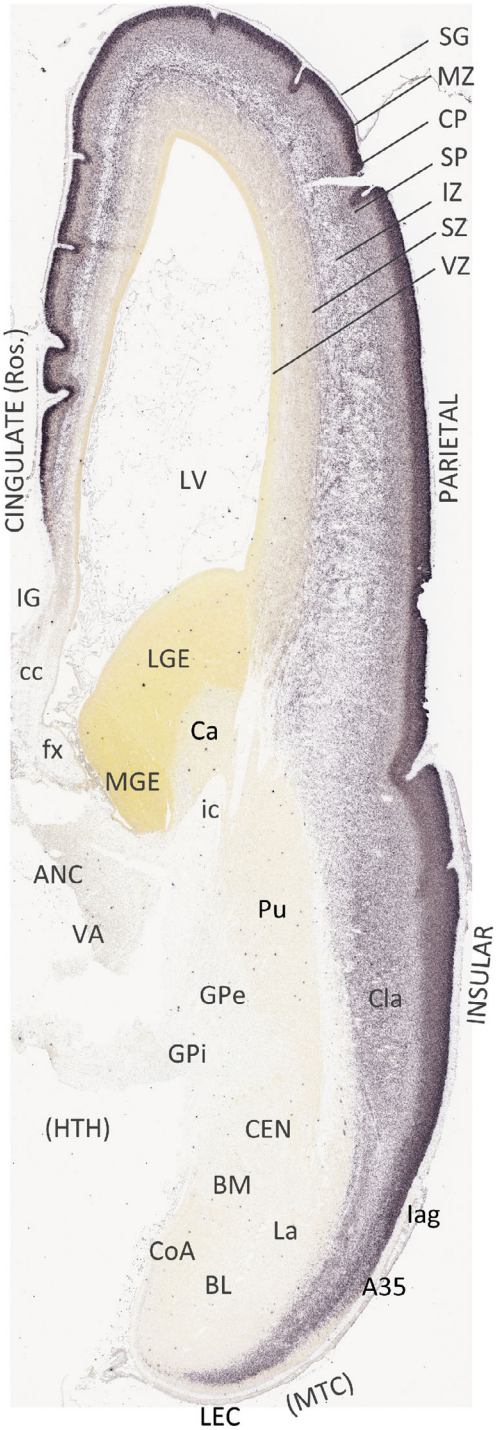

SATB2-01-713 (Level ~22)

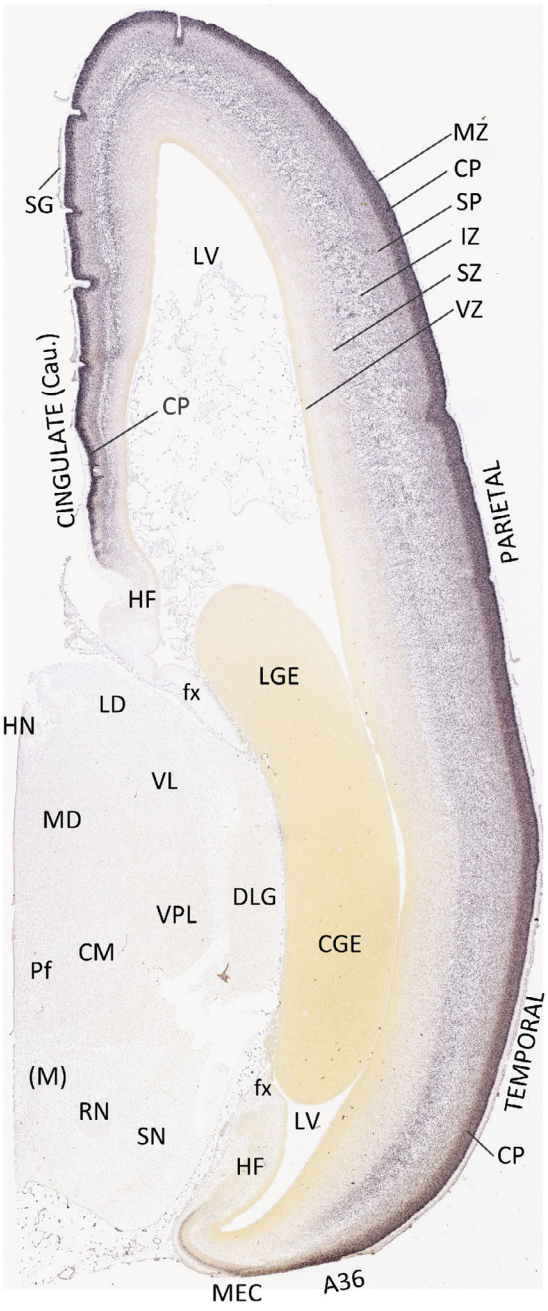

SATB2-02-037 (Level ~26)

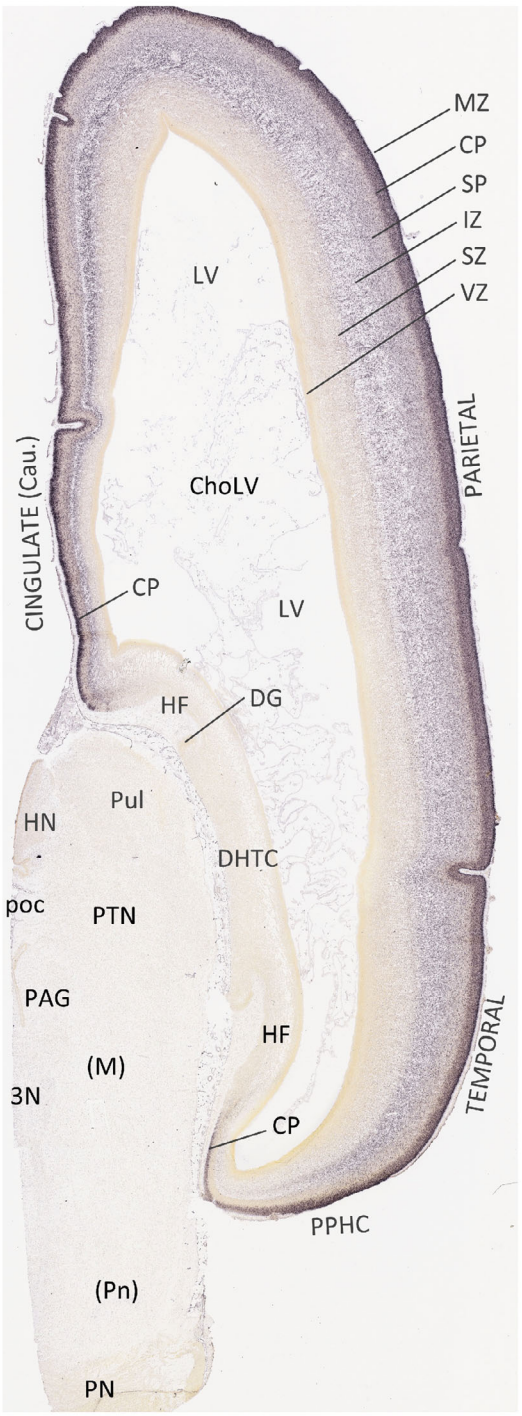

SATB2-02-193 (Level ~32)

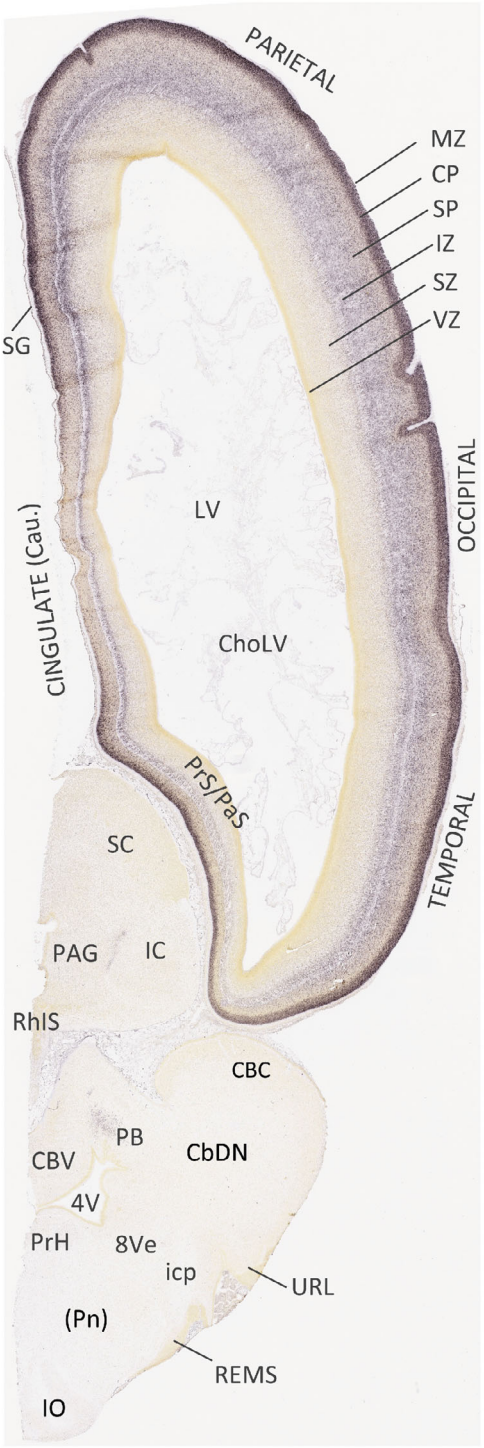

SATB2-02-349 (Level ~38)

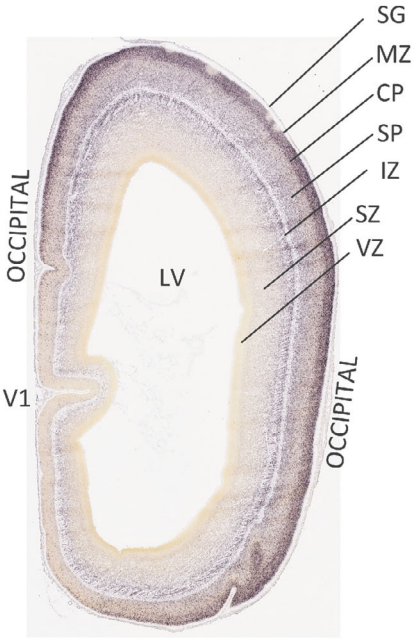

SATB2-02-505 (Level ~42)

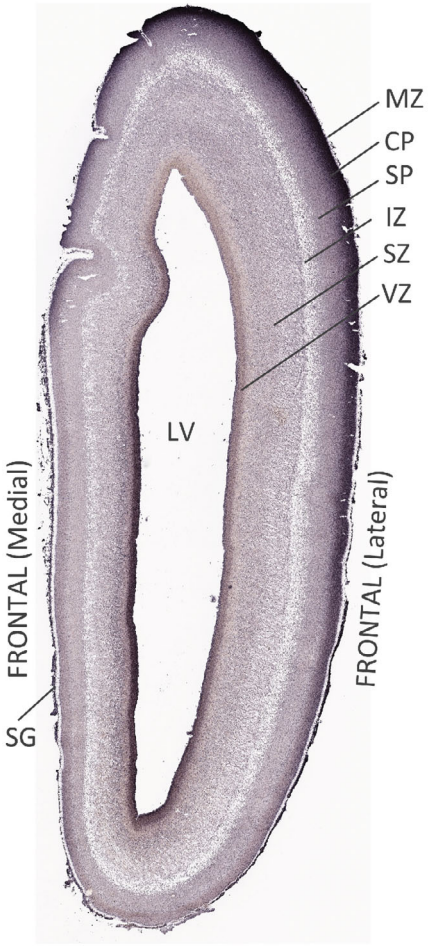

SOX2-01-122 (Level ~3-4)

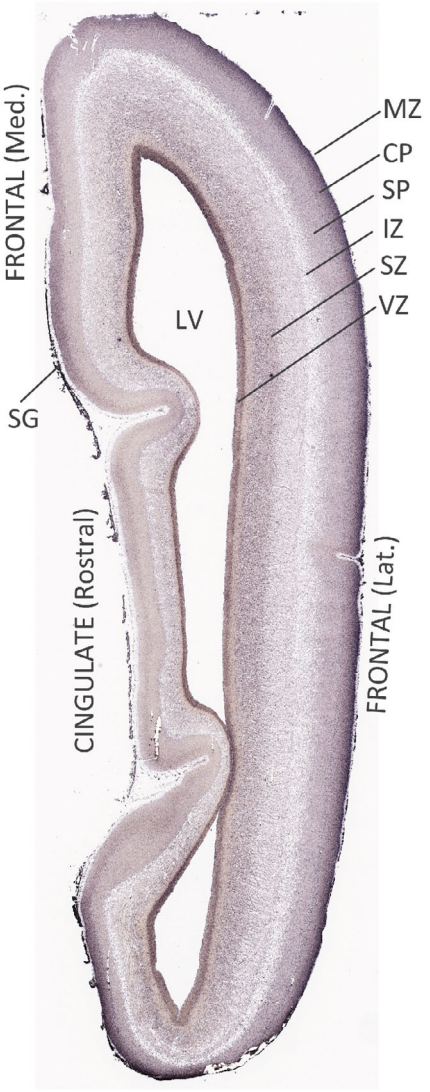

SOX2-01-226 (Level ~5-6)

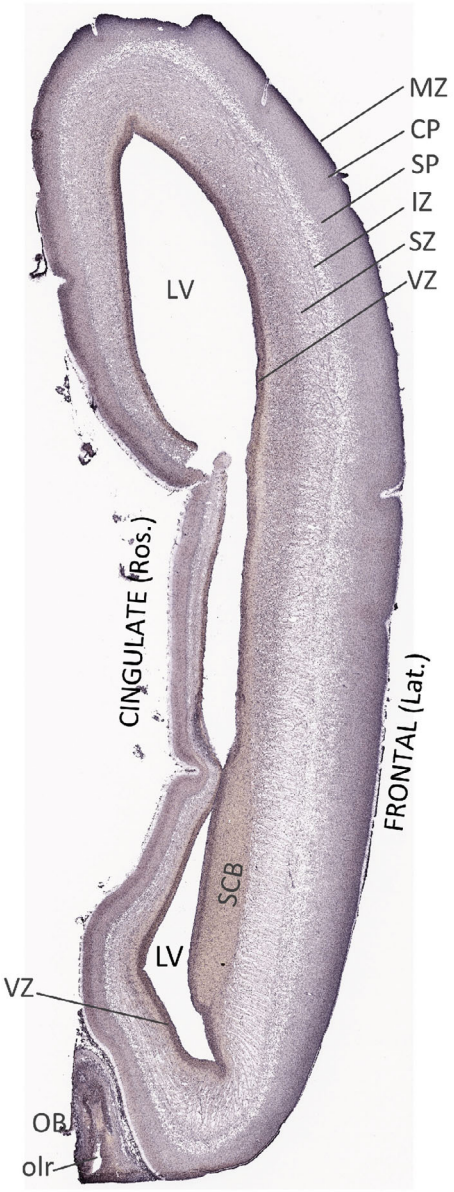

SOX2-01-330 (Level ~9)

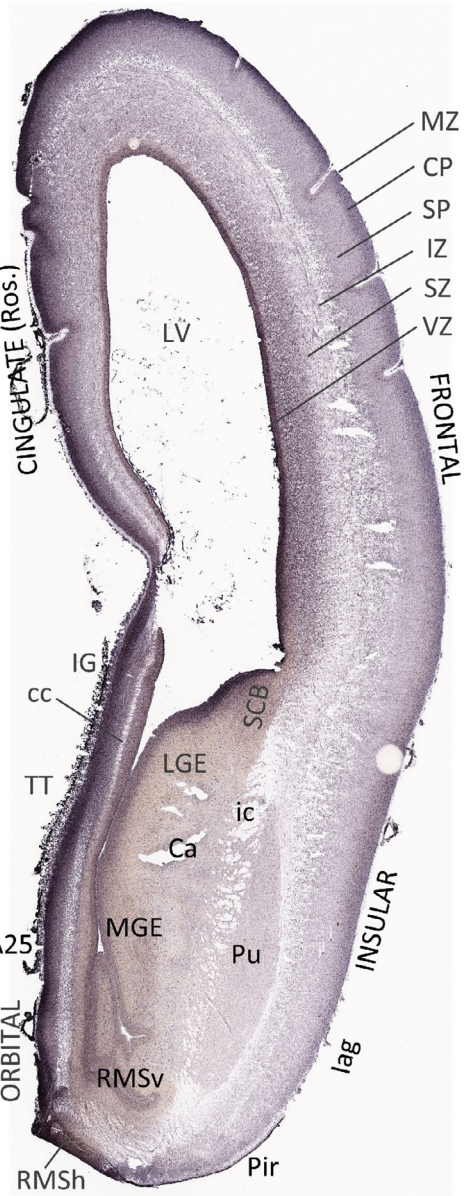

SOX2-01-434 (Level ~13)

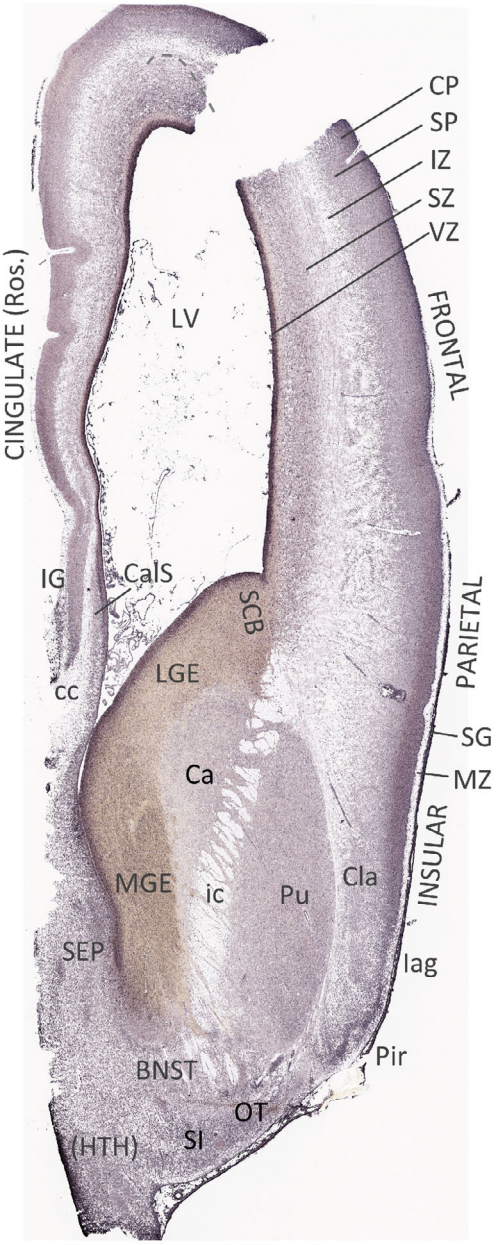

SOX2-01-538 (Level ~17)

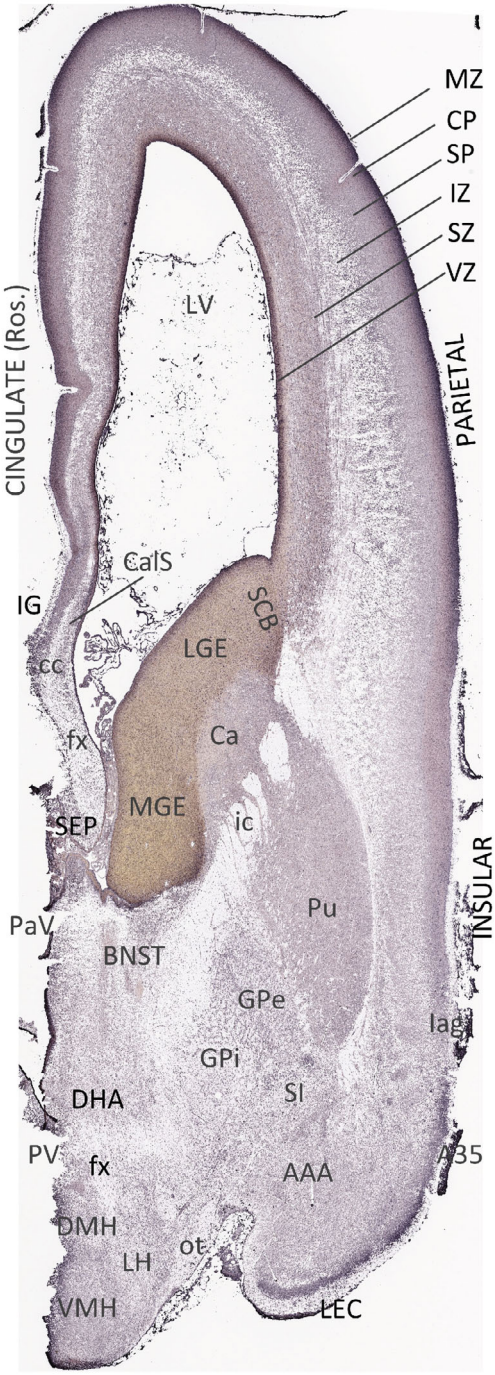

SOX2-01-642 (Level ~20)

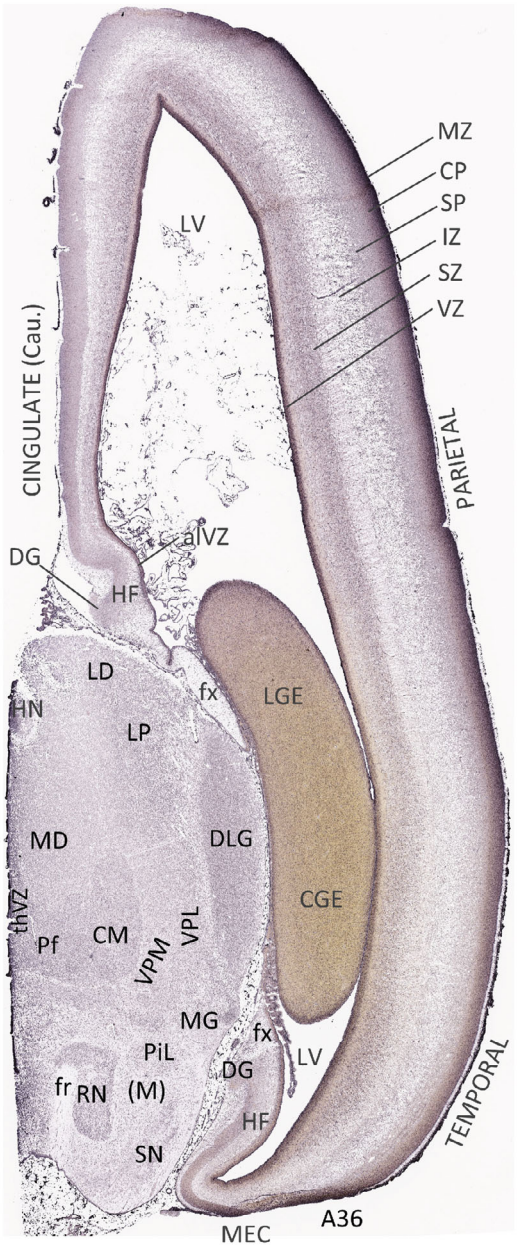

SOX2-02-070 (Level ~27)

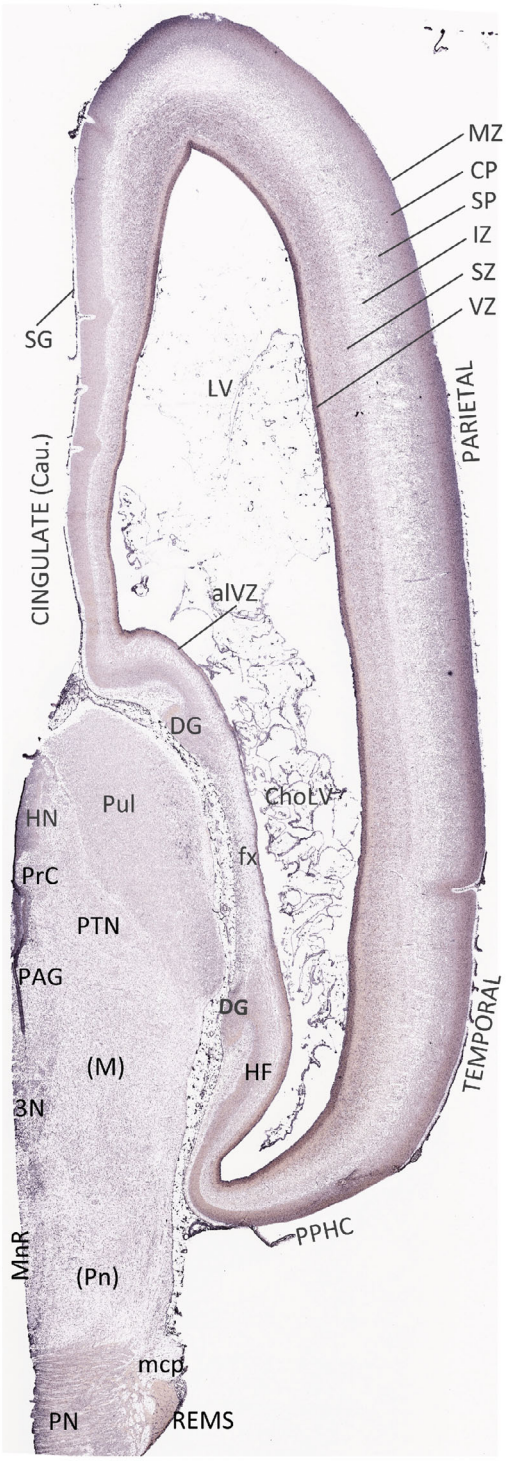

SOX2-02-174 (Level ~31)

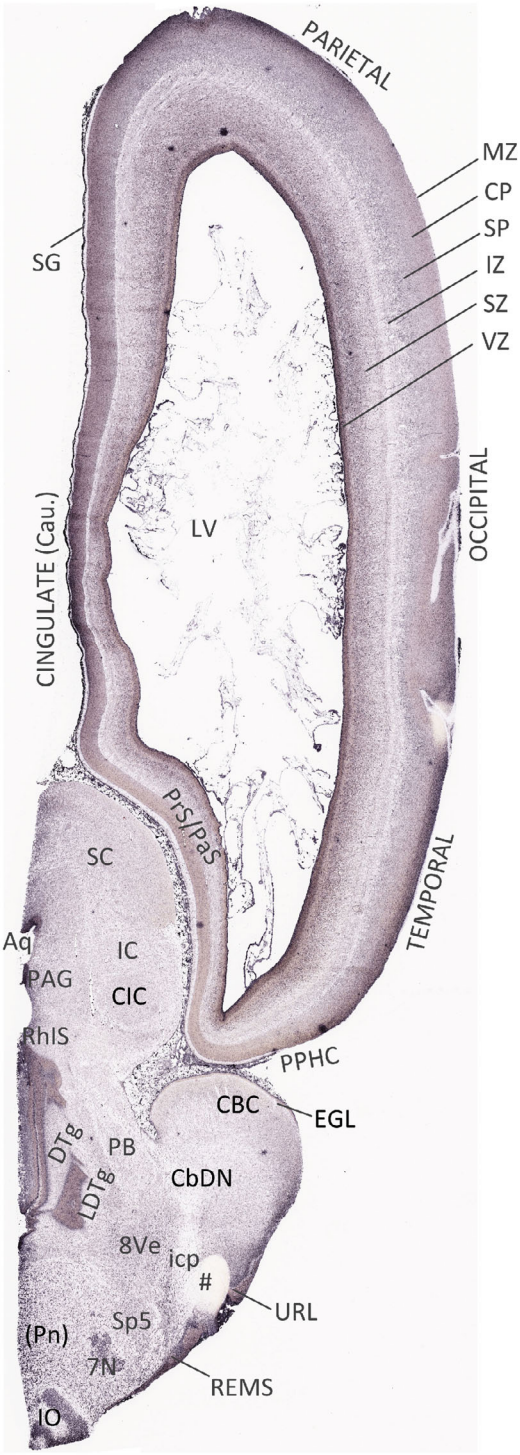

SOX2-02-330 (Level ~37)

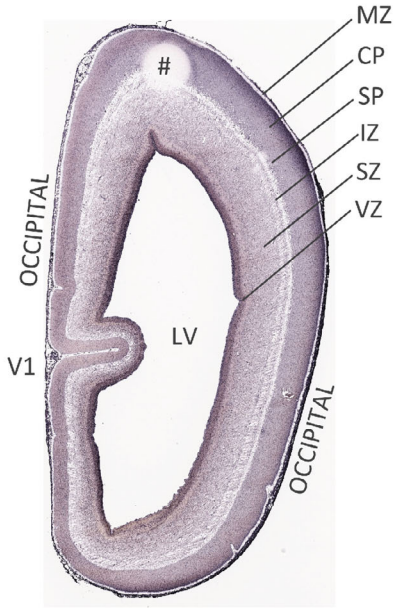

SOX2-02-538 (Level ~43)

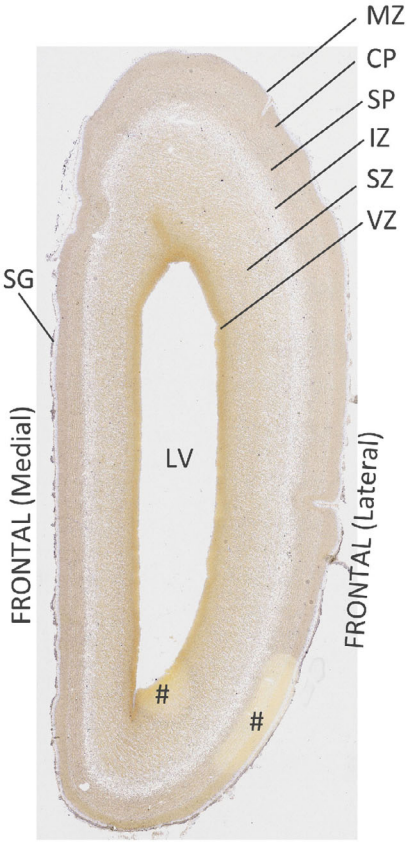

SST-01-062 (Level ~2)

SST-01-218 (Level ~5)

SST-01-374 (Level ~10-11)

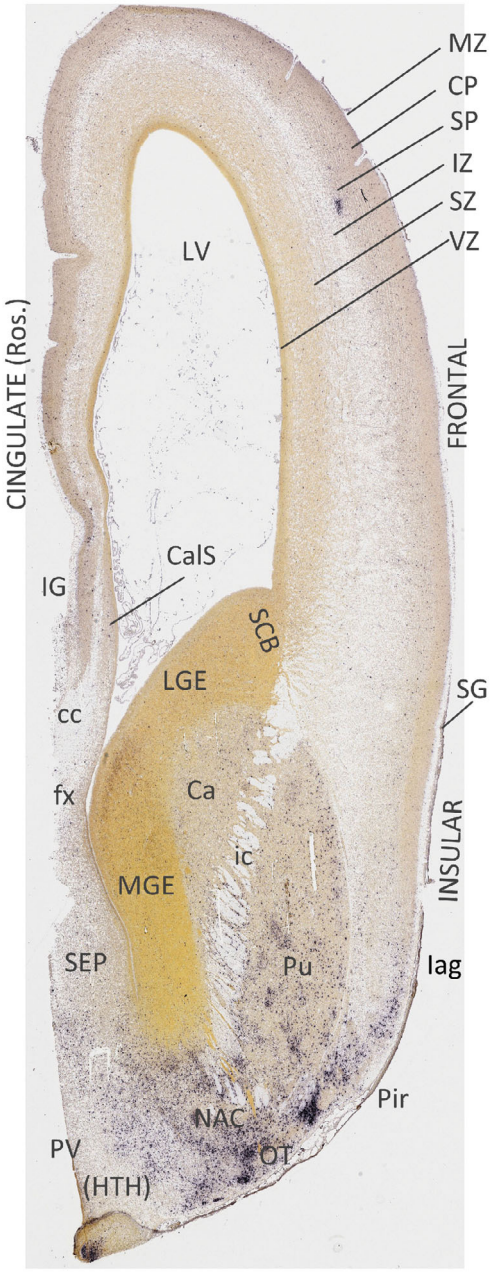

SST-01-530 (Level ~16-17)

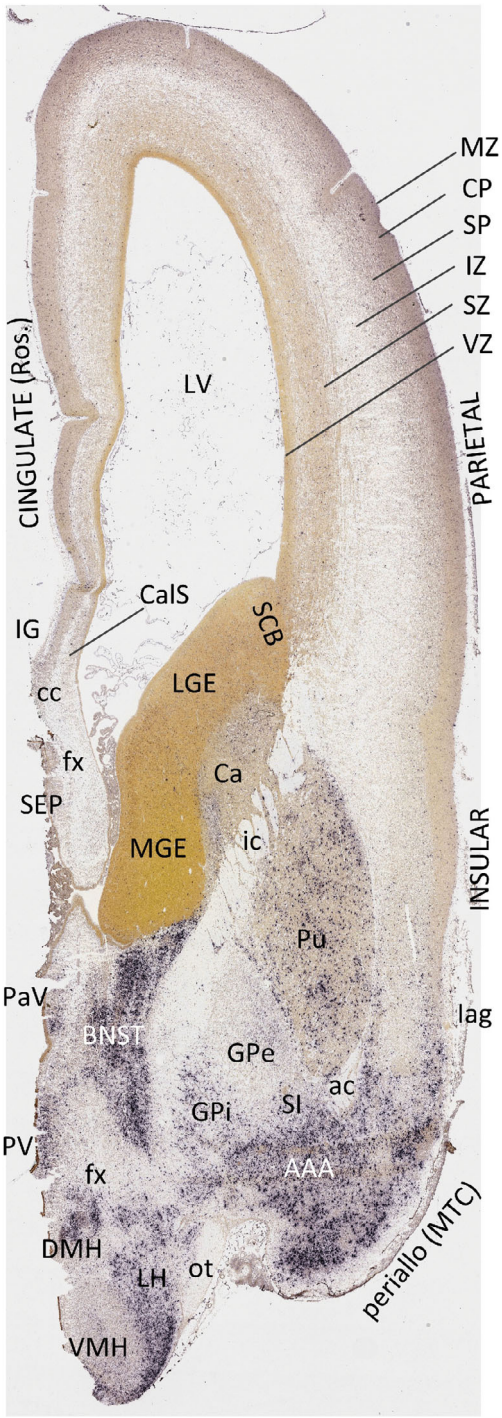

SST-01-634 (Level ~20)

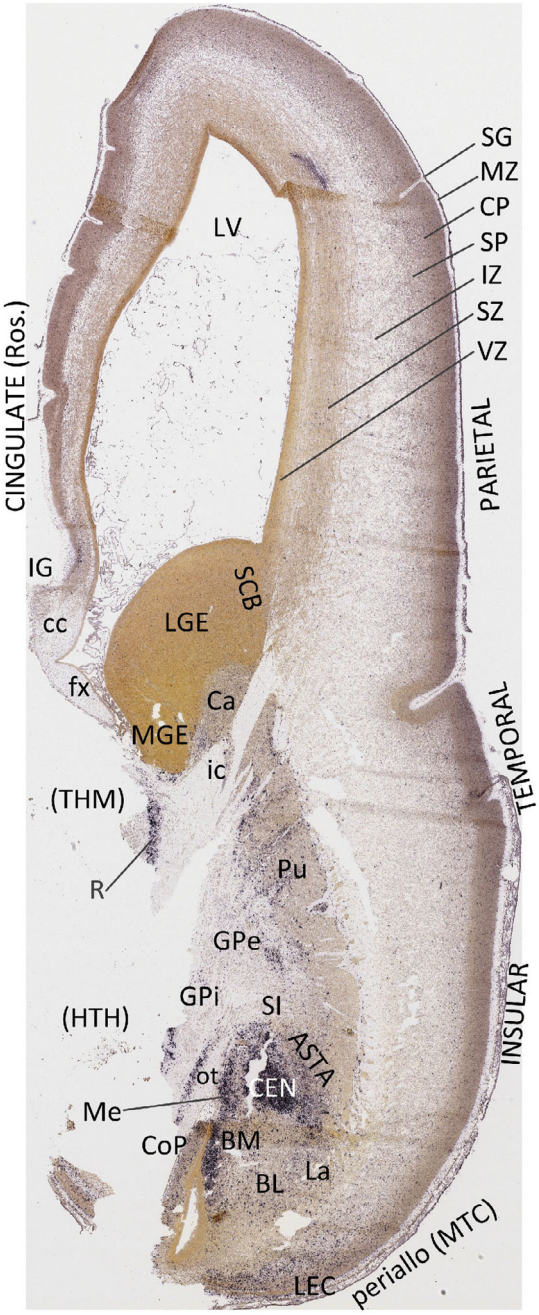

SST-01-738 (Level ~23)

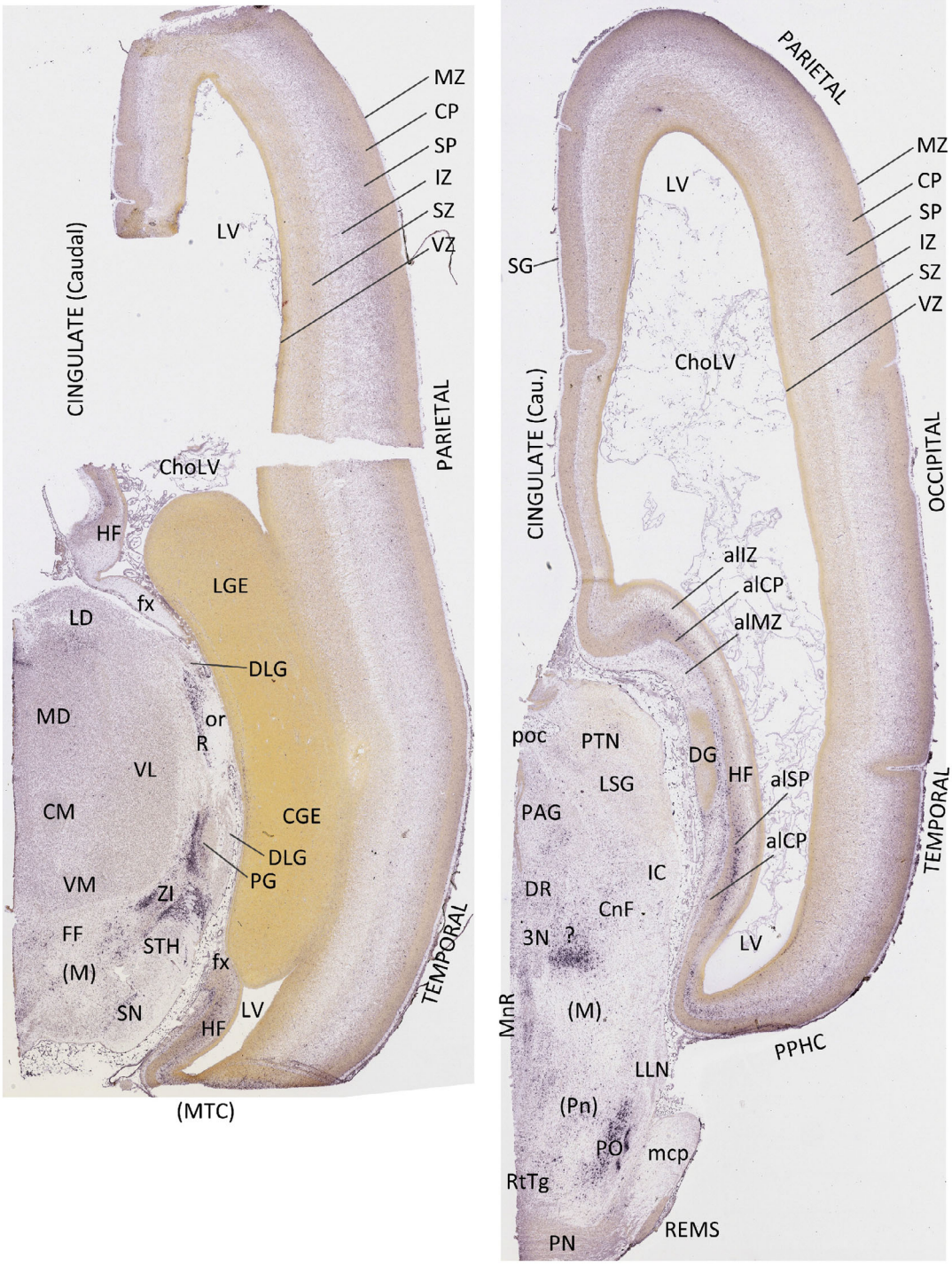

SST-02-010 (Level ~25) **SST-02-218 (Level ~33)**

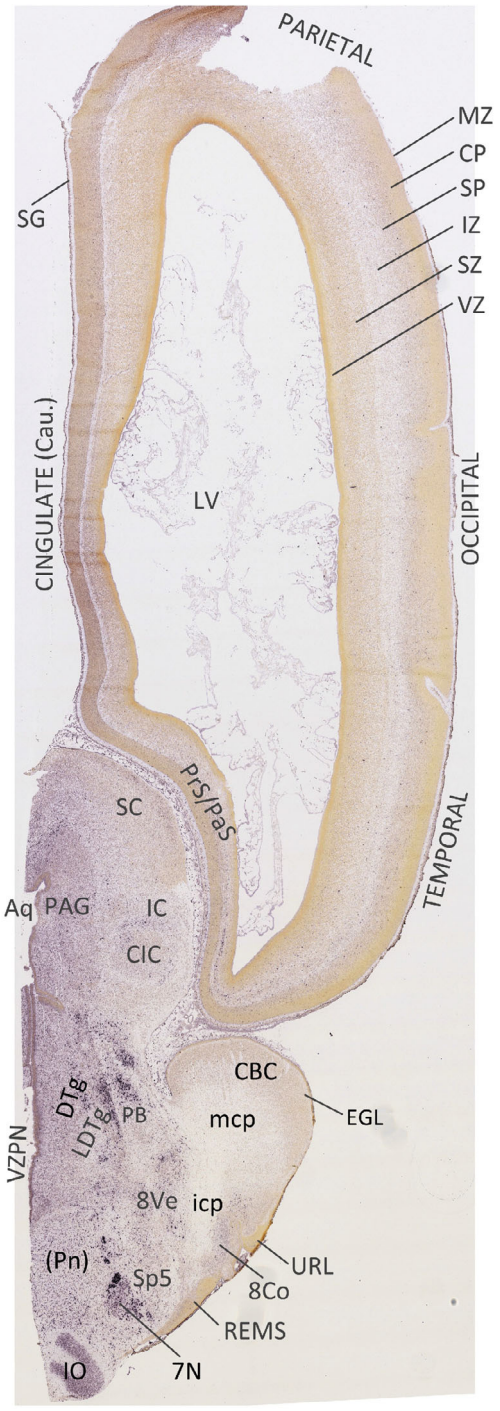

SST-02-322 (Level ~37)

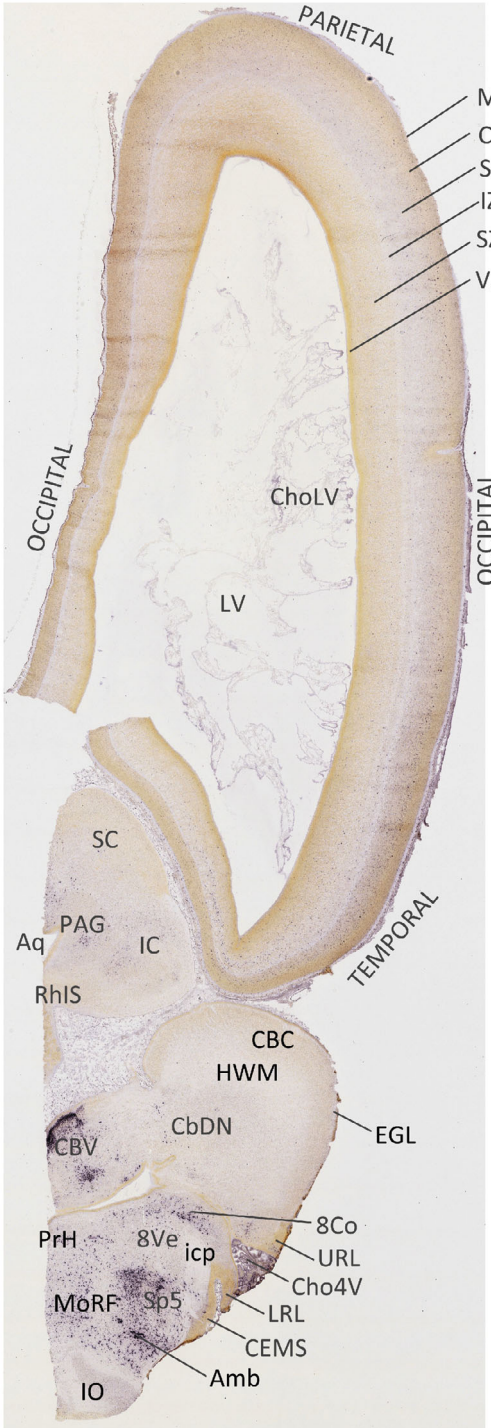

SST-02-374 (Level ~39-40)

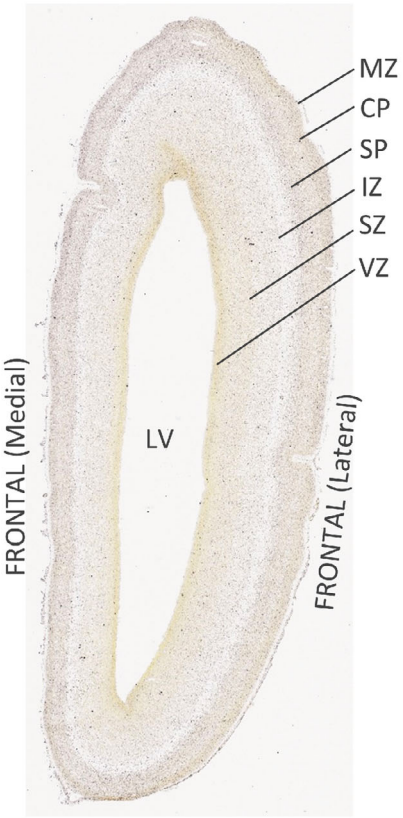

SYNGAP1-01-091 (Level ~3)

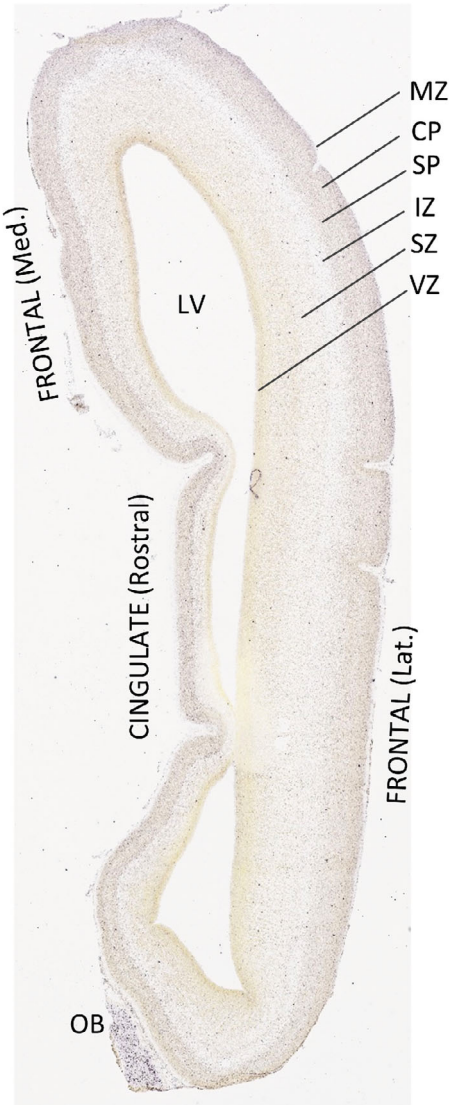

SYNGAP1-01-299 (Level ~7)

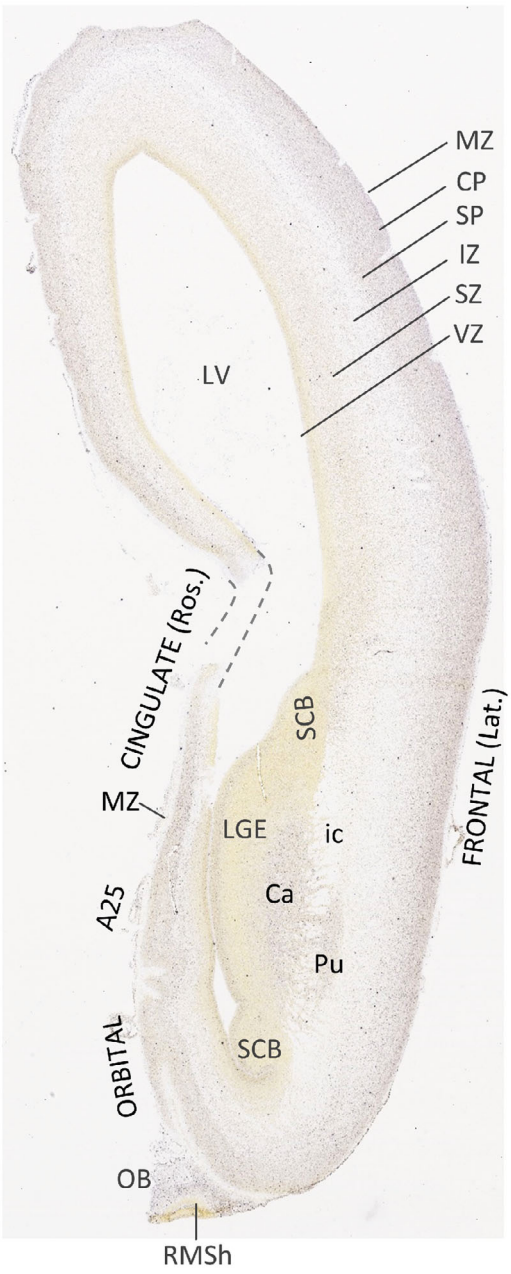

SYNGAP1-01-403 (Level ~11-12)

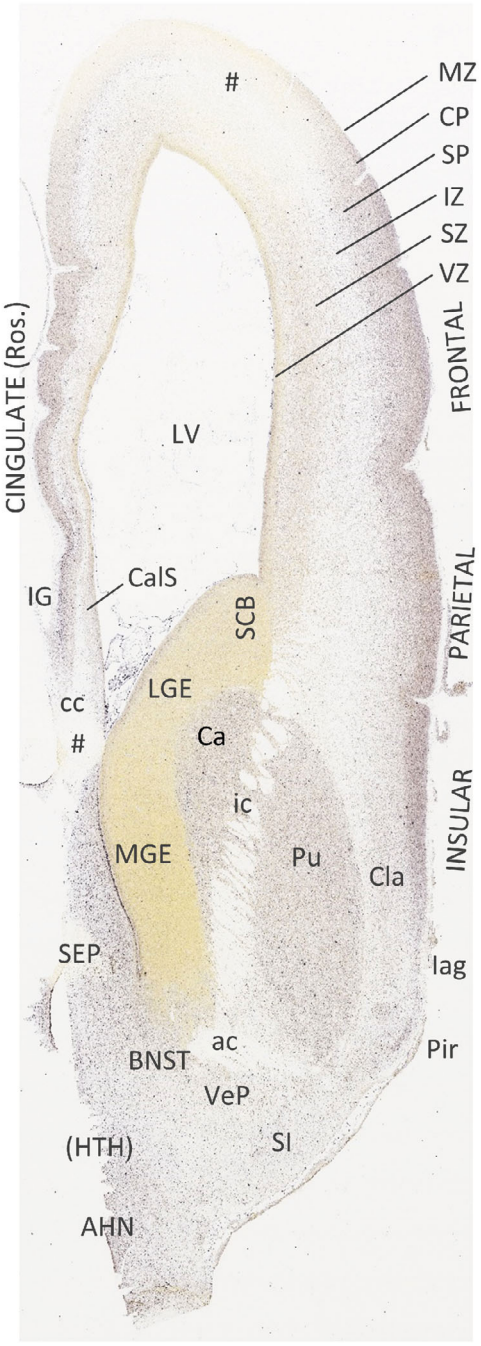

SYNGAP1-01-559 (Level ~17-18)

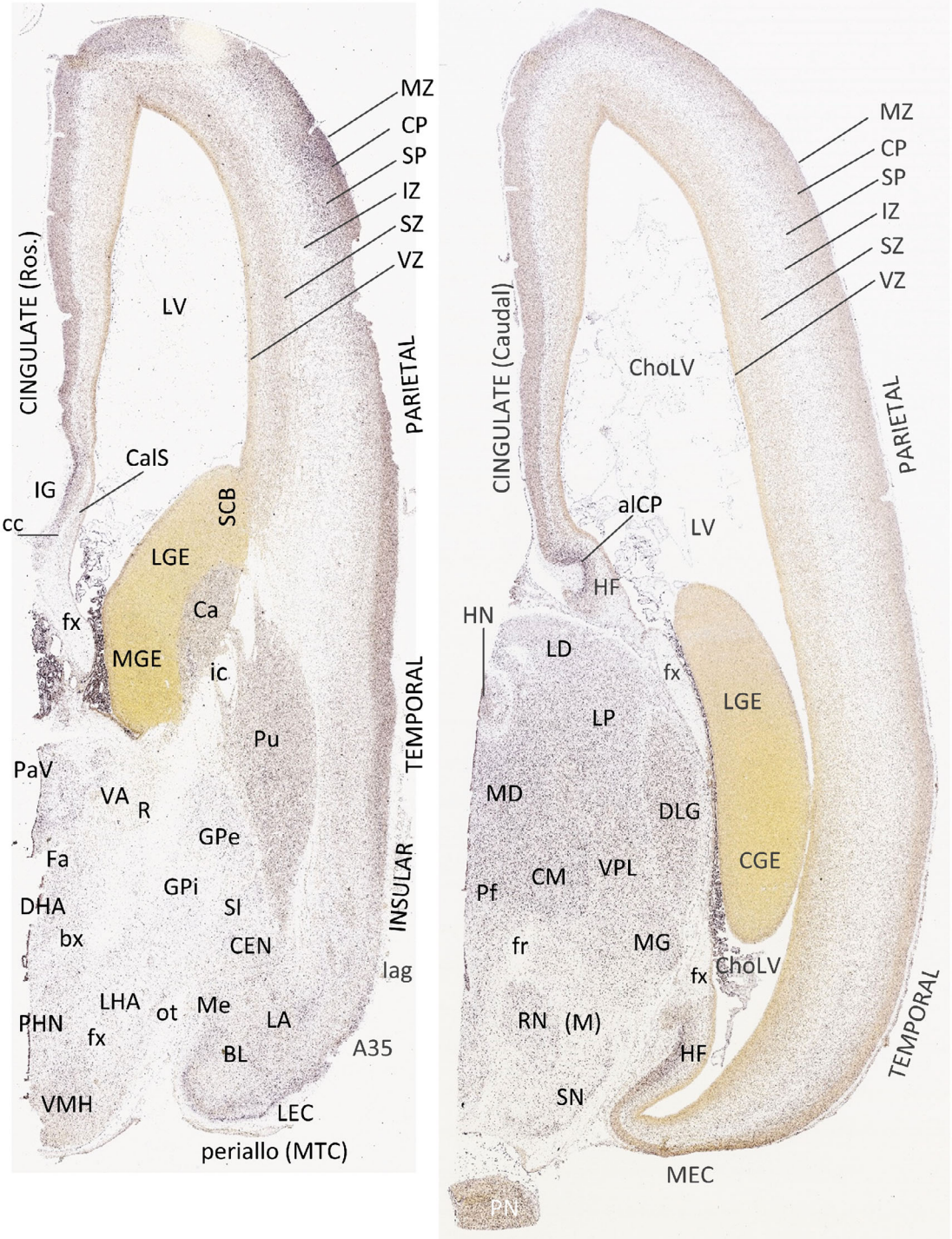

SYNGAP1-01-663 (Level ~22) **SYNGAP1-02-091 (Level ~28)**

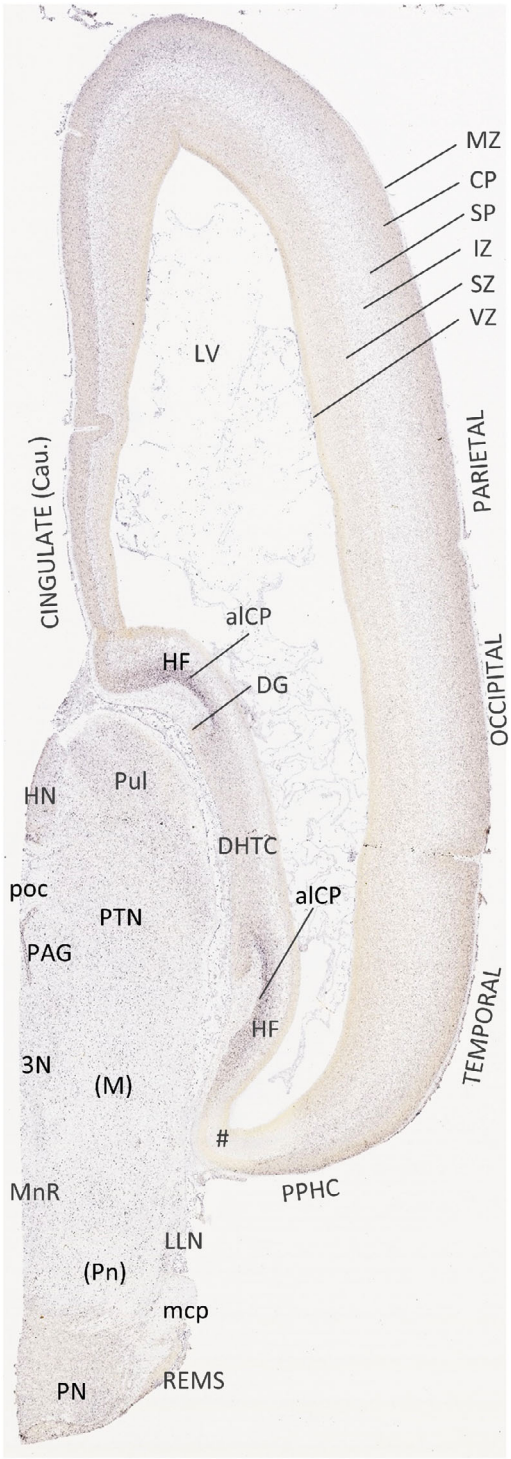

SYNGAP1-02-195 (Level ~32)

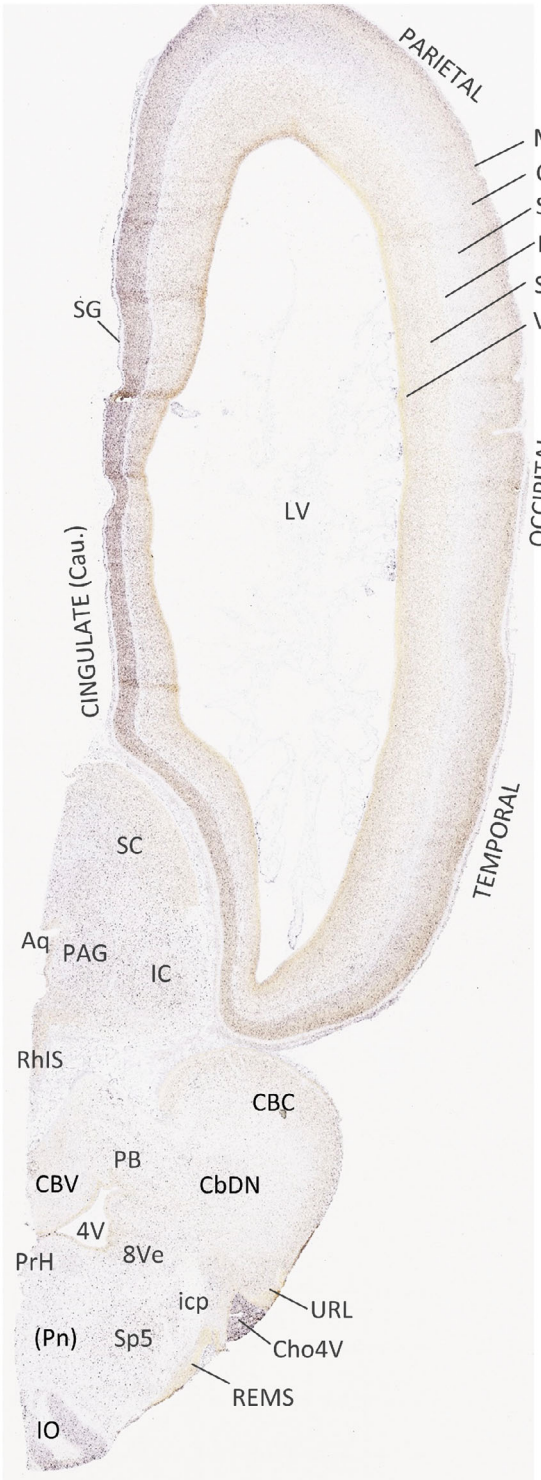

SYNGAP1-02-351 (Level ~38)

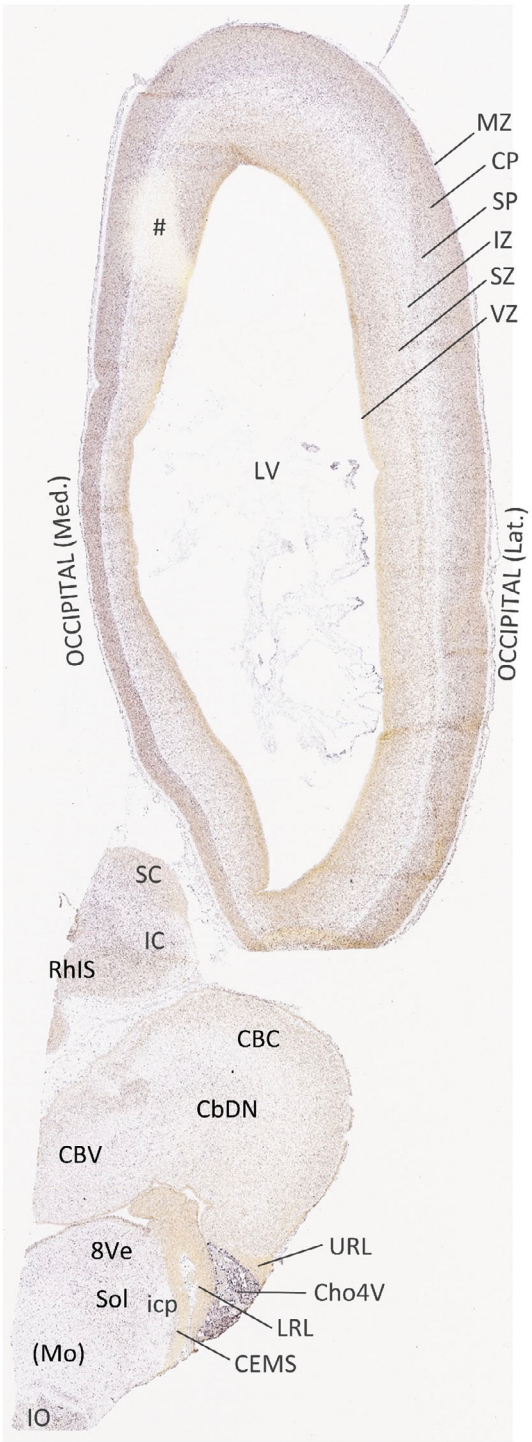

SYNGAP1-02-403 (Level ~40)

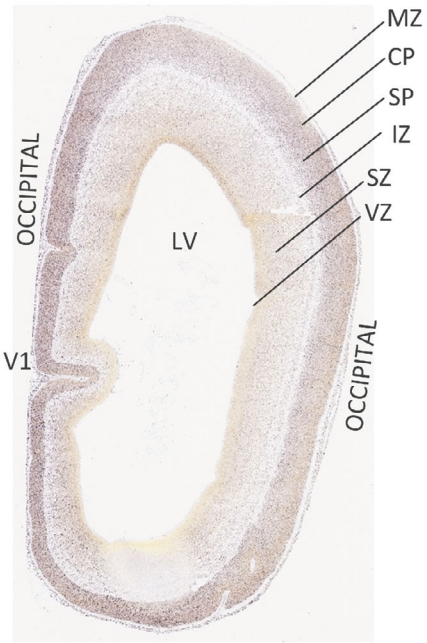

SYNGAP1-02-507 (Level ~42)

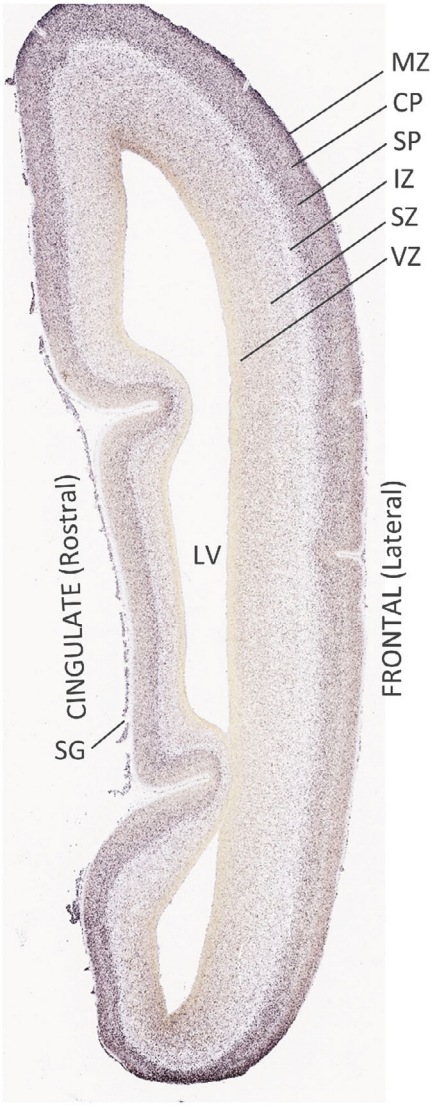

TBR1-01-215 (Level ~5)

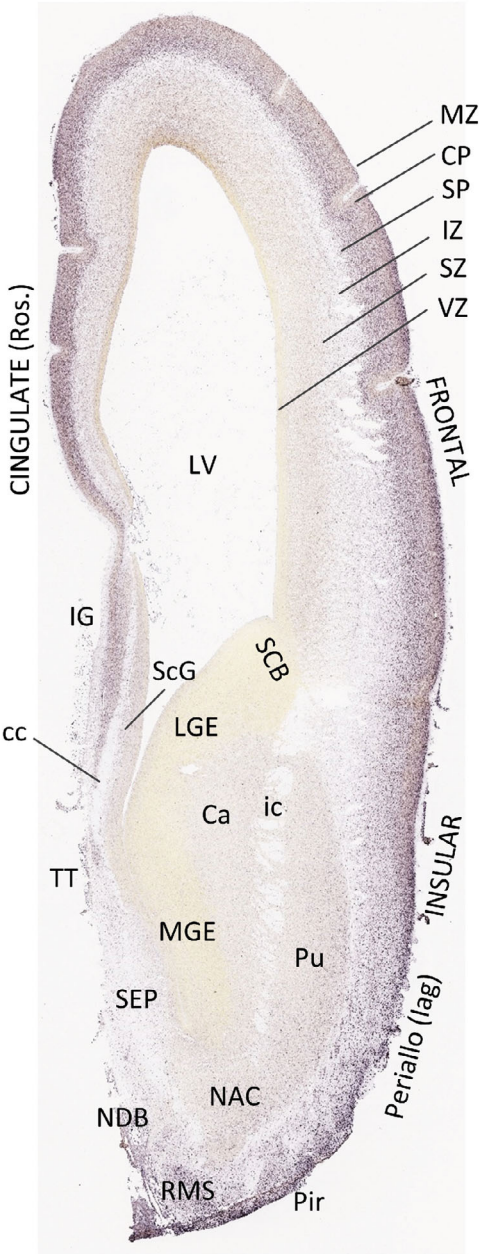

TBR1-01-475 (Level ~14)

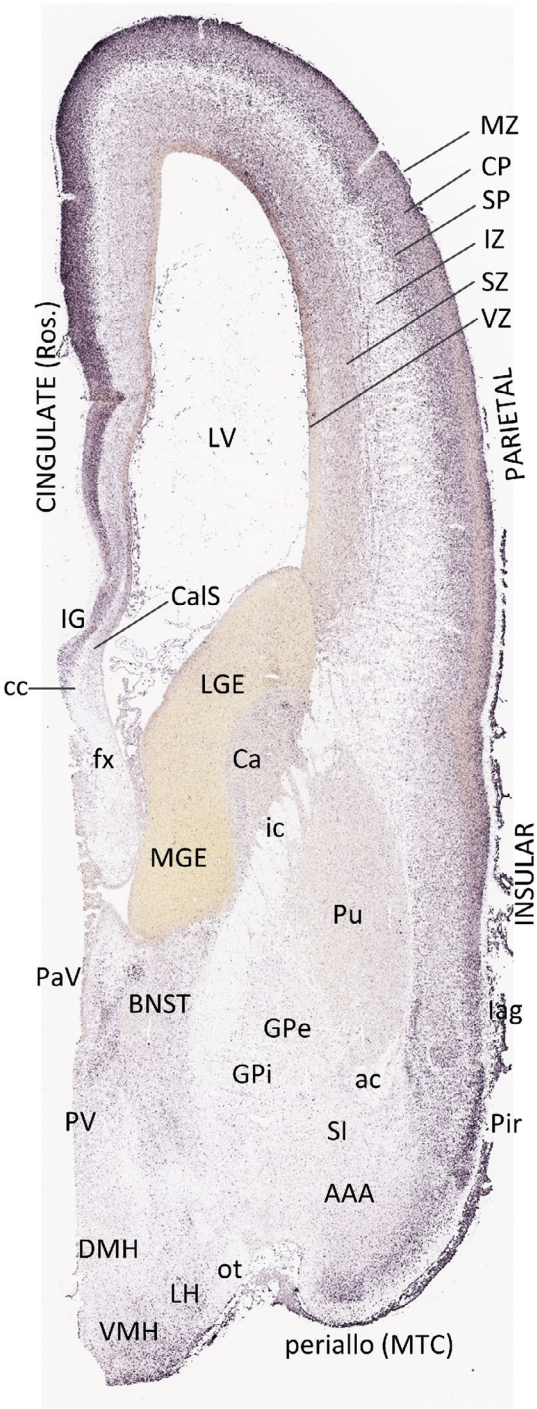

TBR1-01-631 (Level ~20)

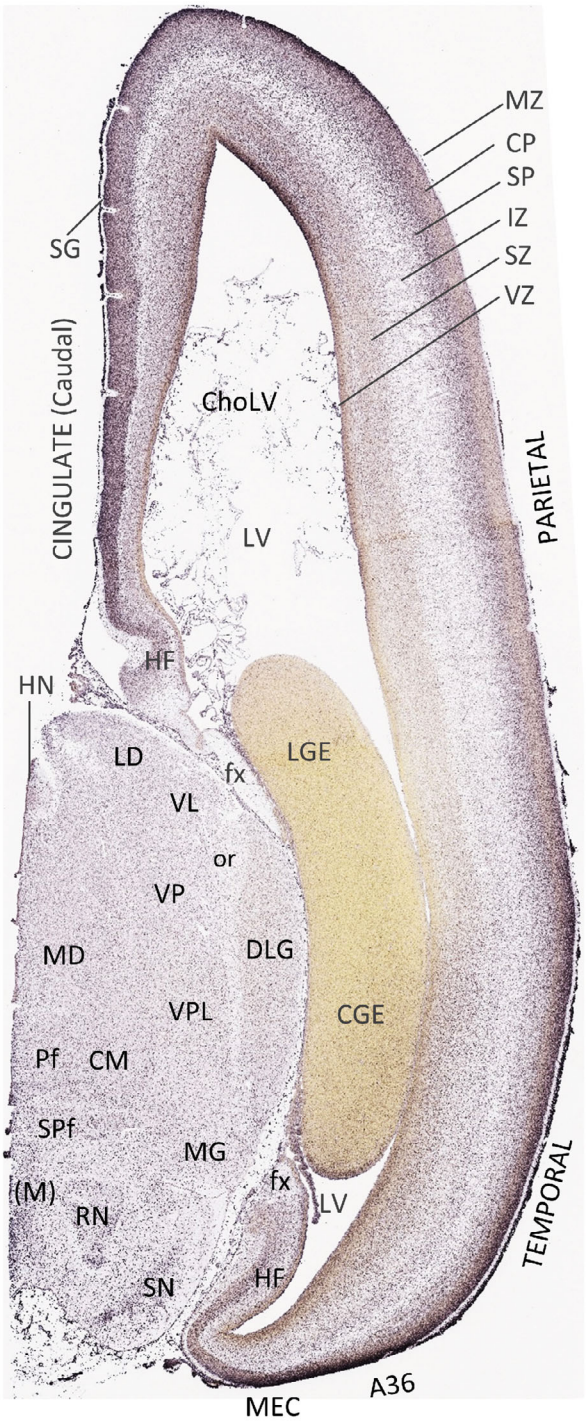

TBR1-02-059 (Level ~27)

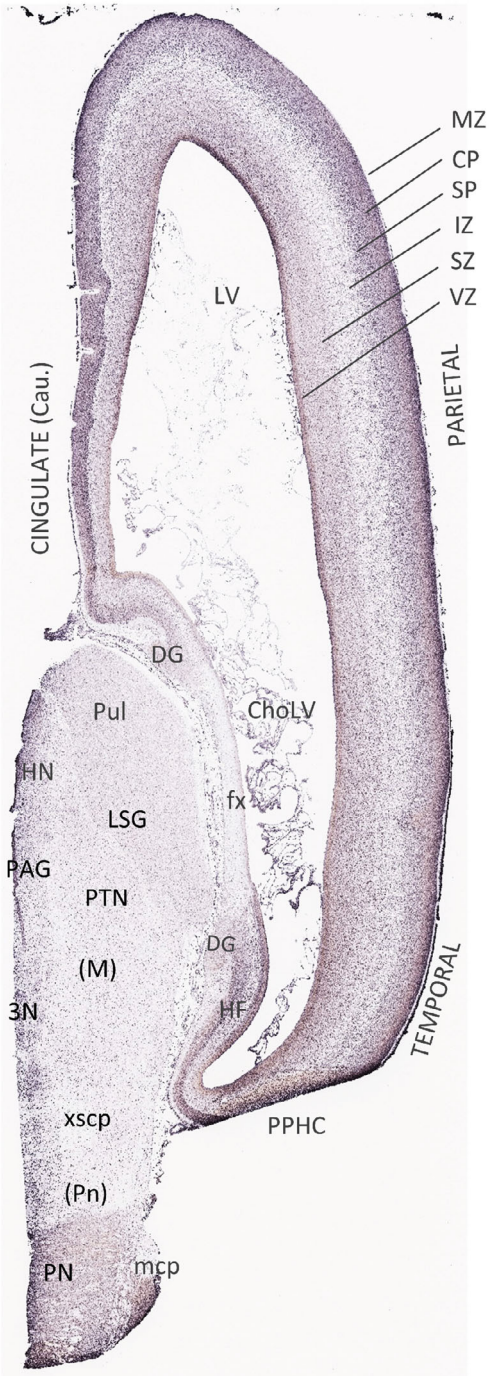

TBR1-02-163 (Level ~21)

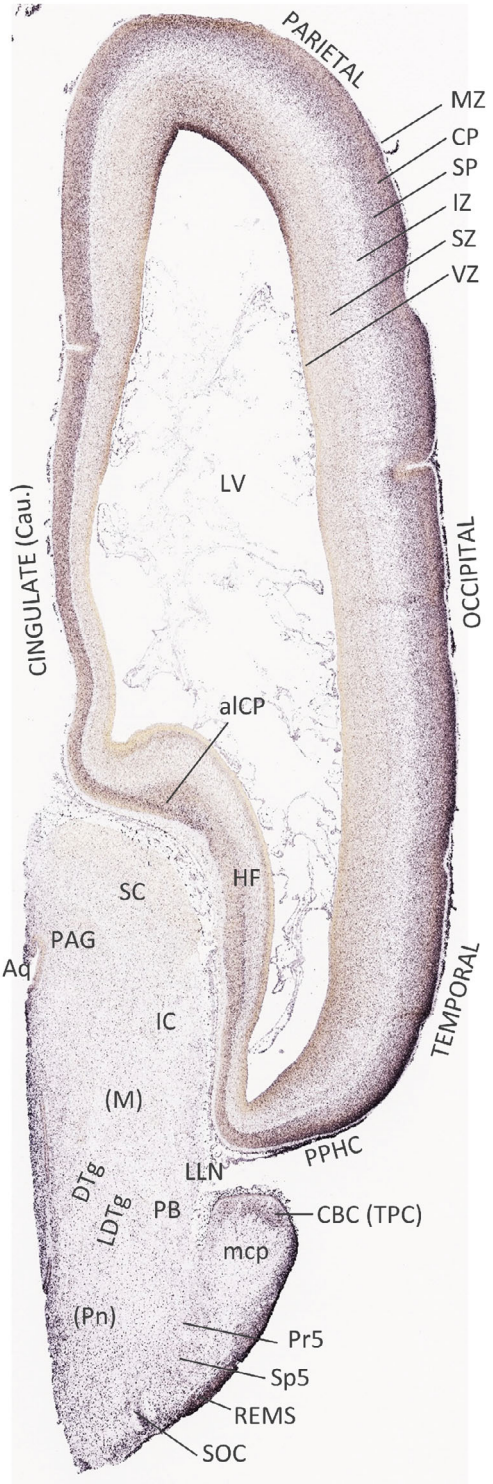

TBR1-02-267 (Level ~35)

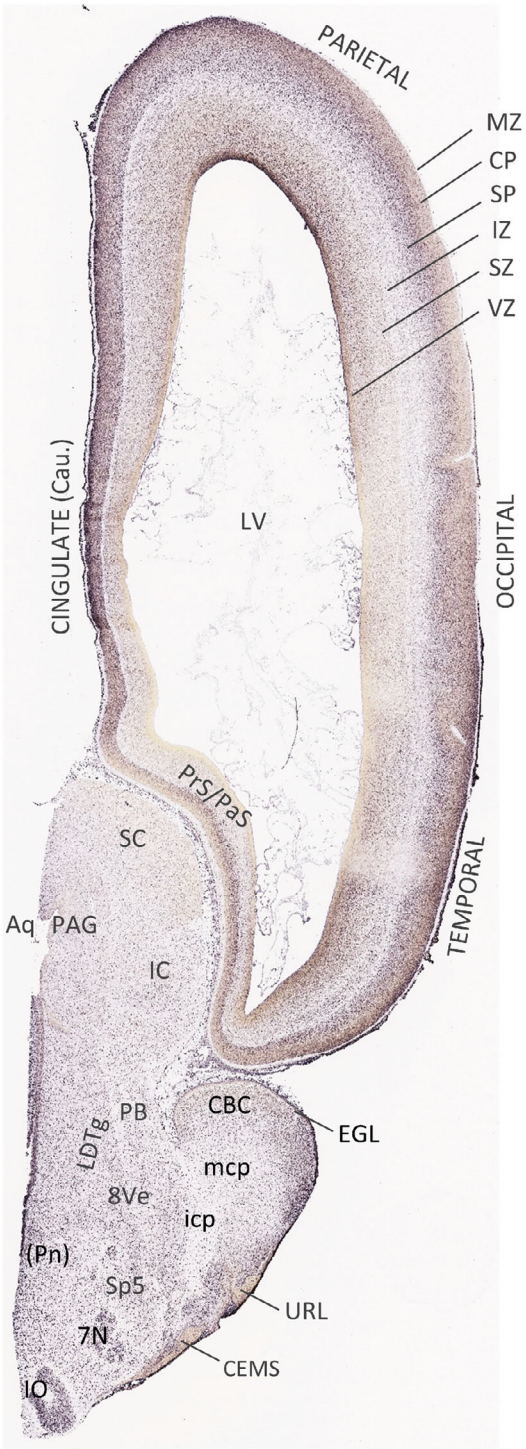

TBR1-02-319 (Level ~37)

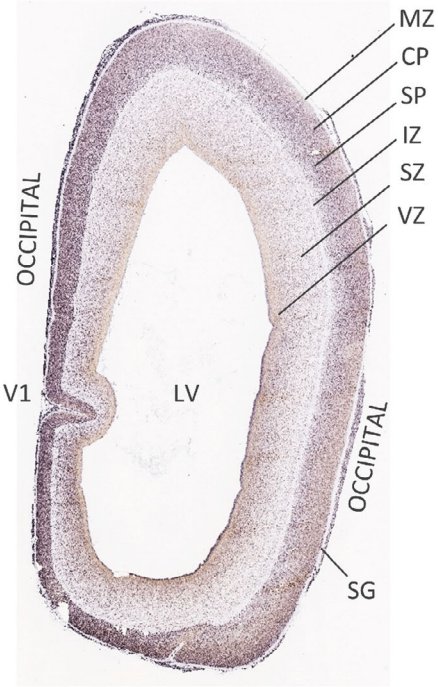

TBR1-02-475 (Level ~42)

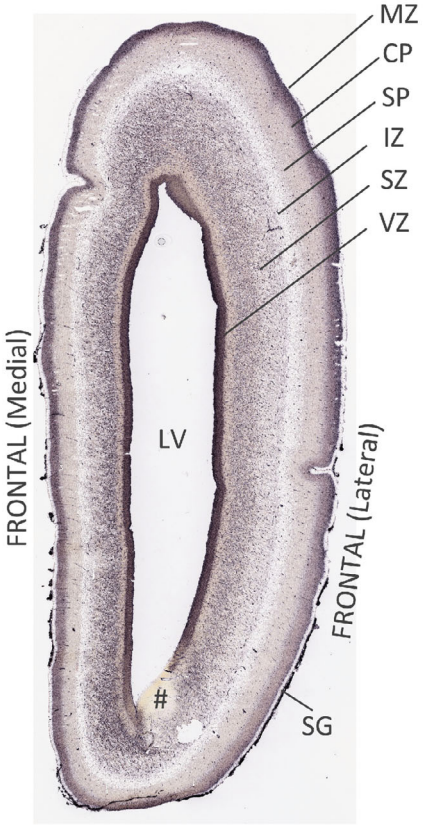

VIM-01-082 (Level ~3)

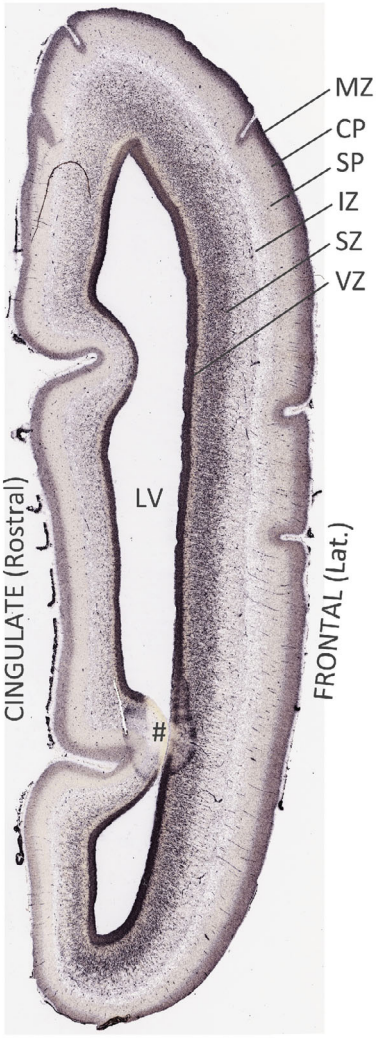

VIM-01-186 (Level ~5)

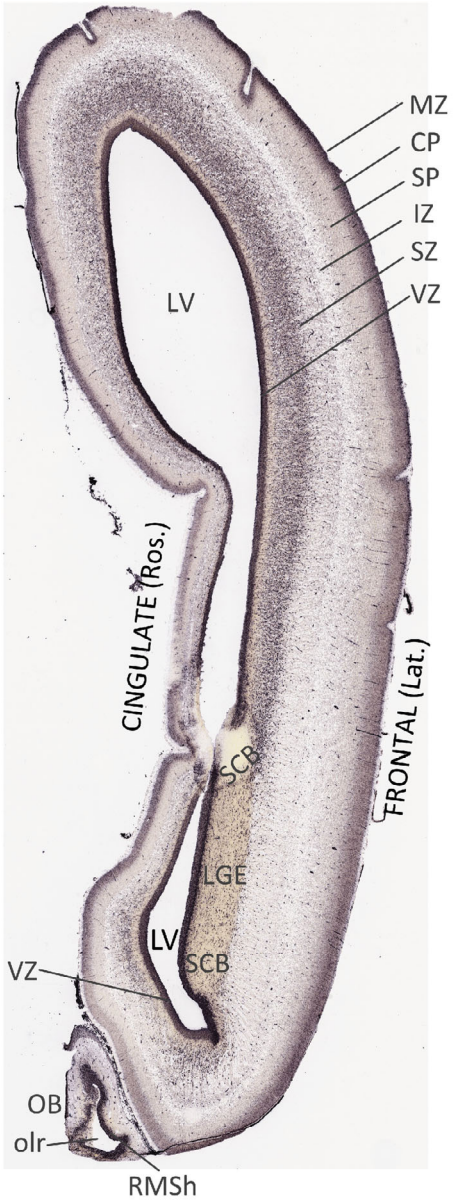

VIM-01-342 (Level ~9)

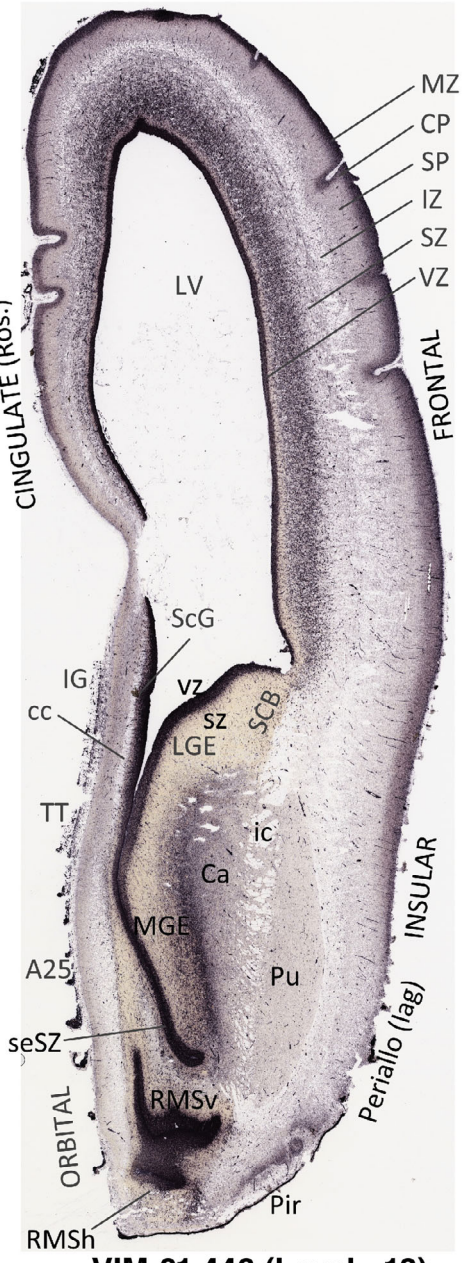

VIM-01-446 (Level ~13)

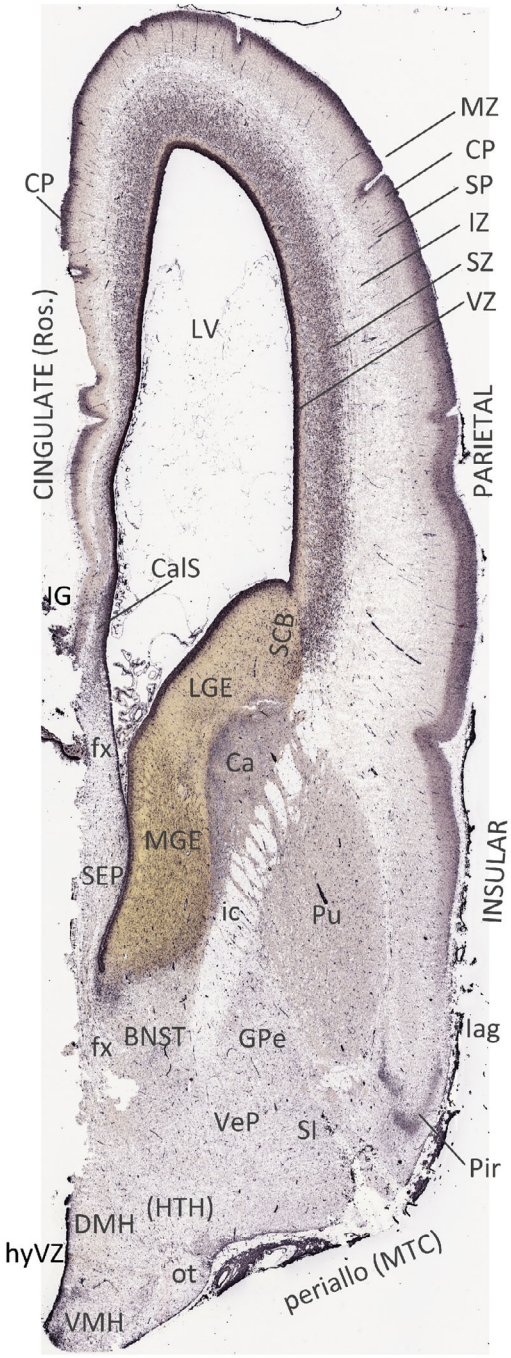

VIM-01-602 (Level ~19)

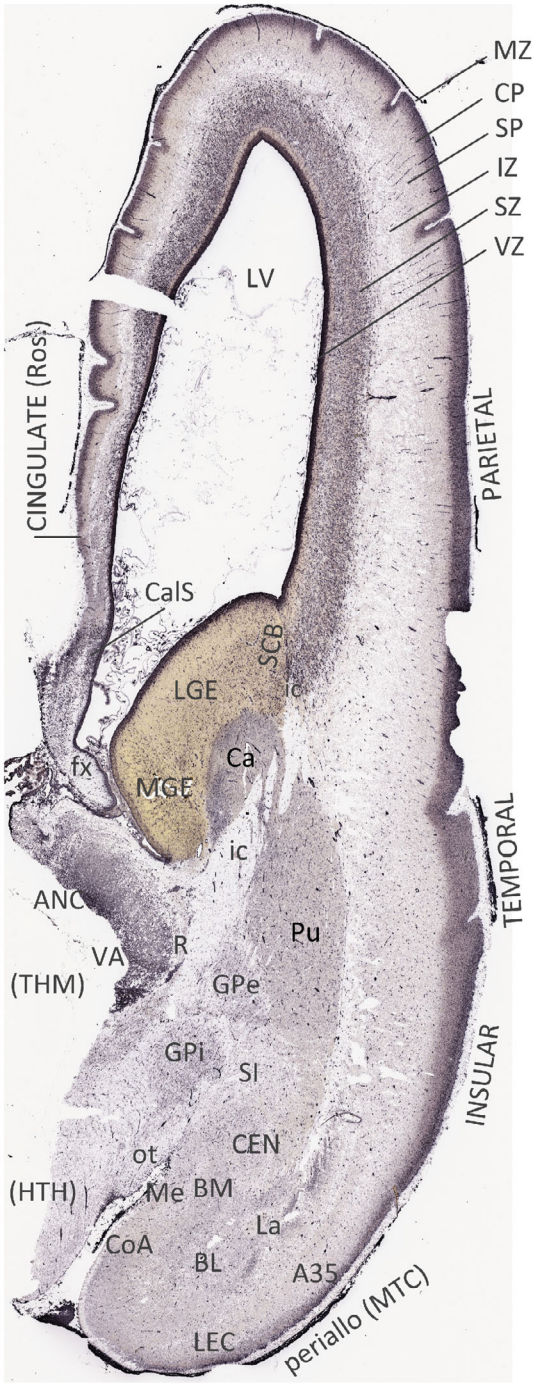

VIM-01-706 (Level ~22)

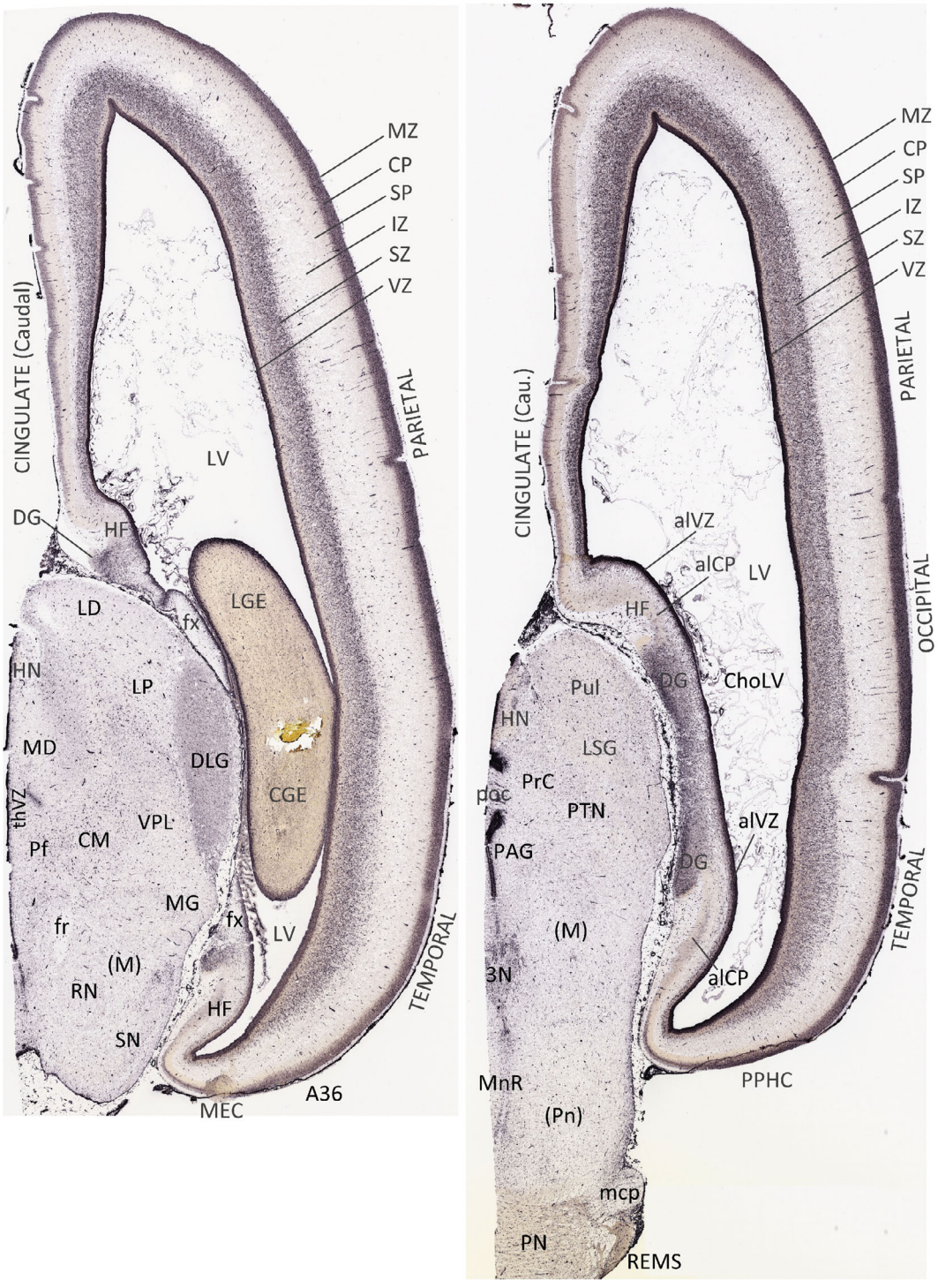

VIM-02-082 (Level ~28) **VIM-02-186 (Level ~31-32)**

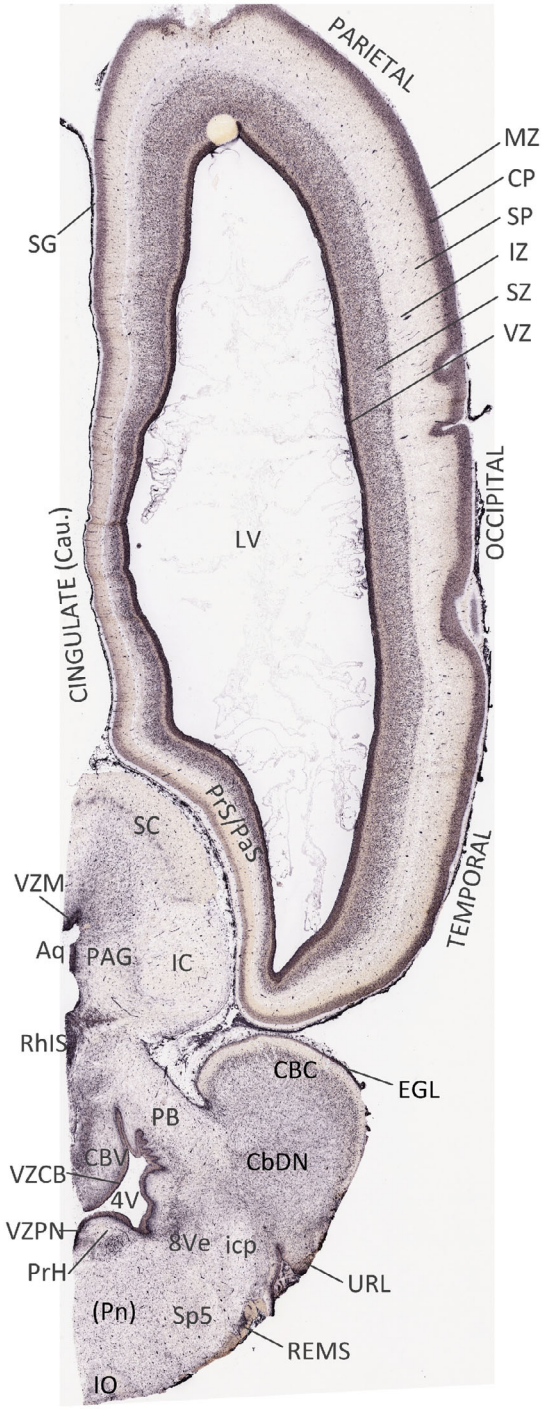

VIM-02-342 (Level ~37-38)

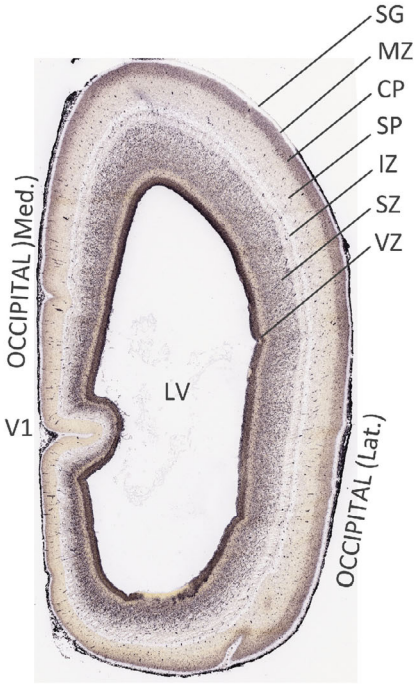

VIM-02-498 (Level ~42)

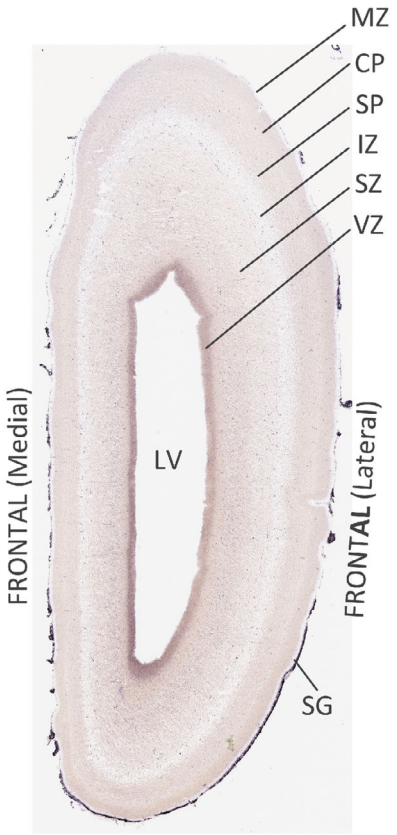

ZIC1-01-052 (Level ~2)

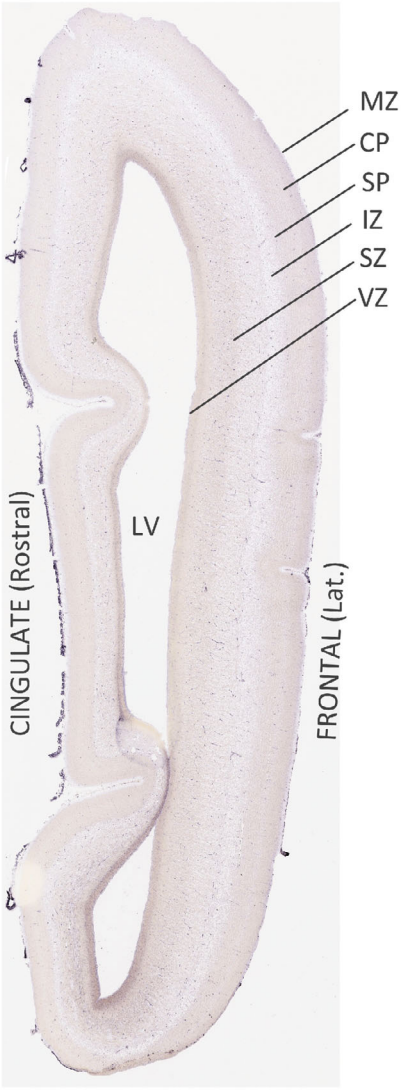

ZIC1-01-208 (Level ~5)

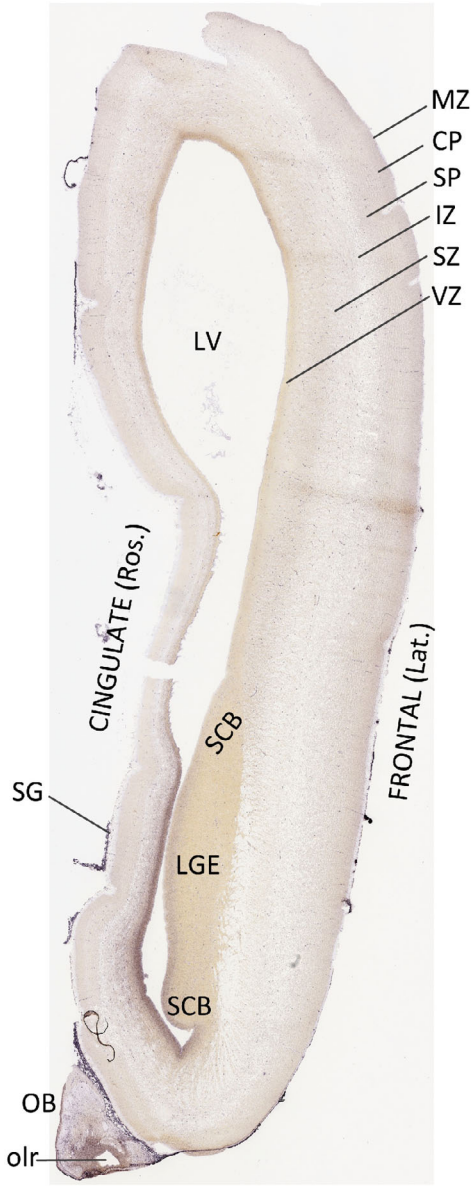

ZIC1-01-364 (Level ~10)

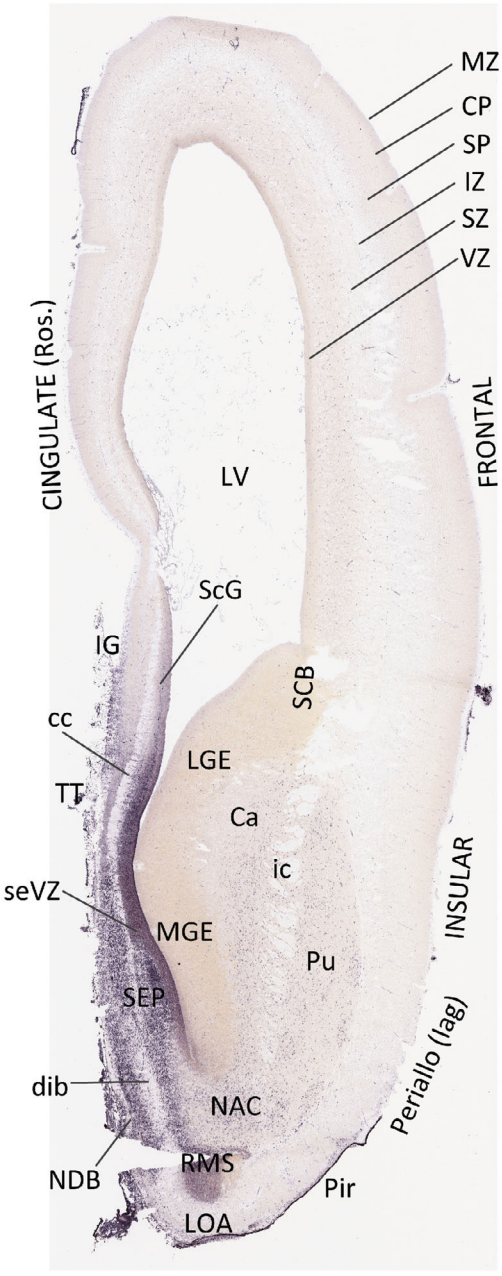

ZIC1-01-468 (Level ~14)

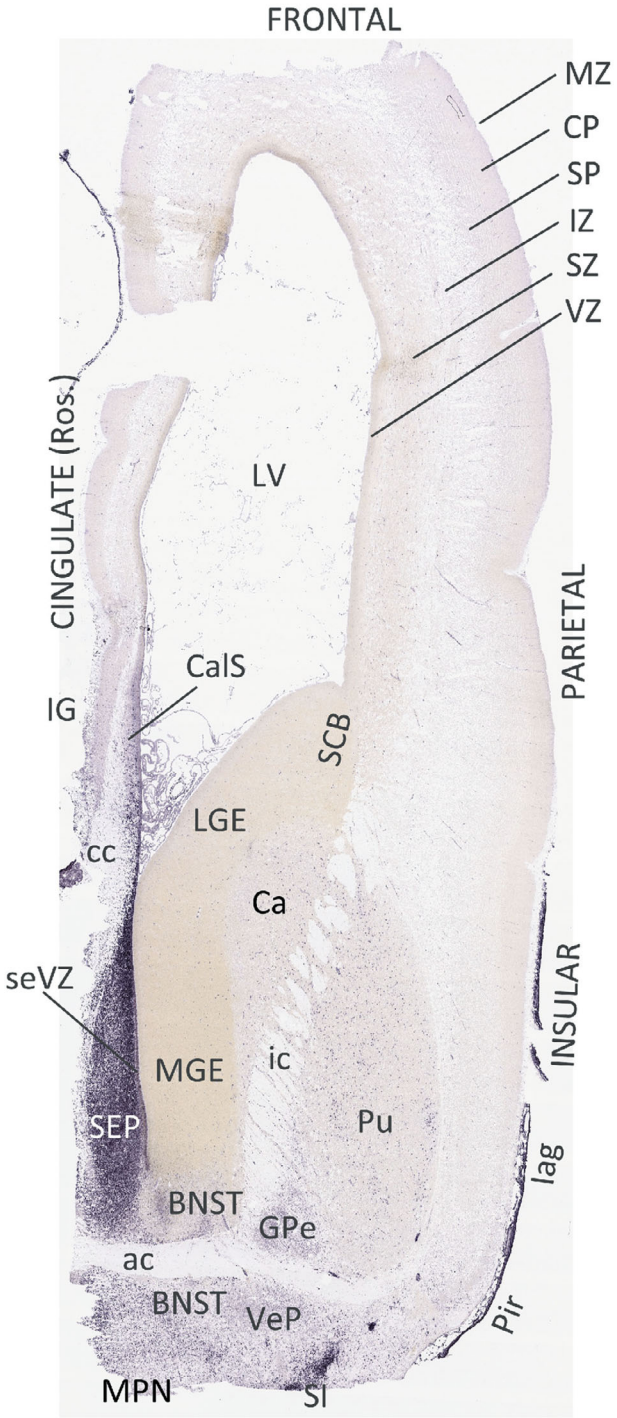

ZIC1-01-572 (Level ~18)

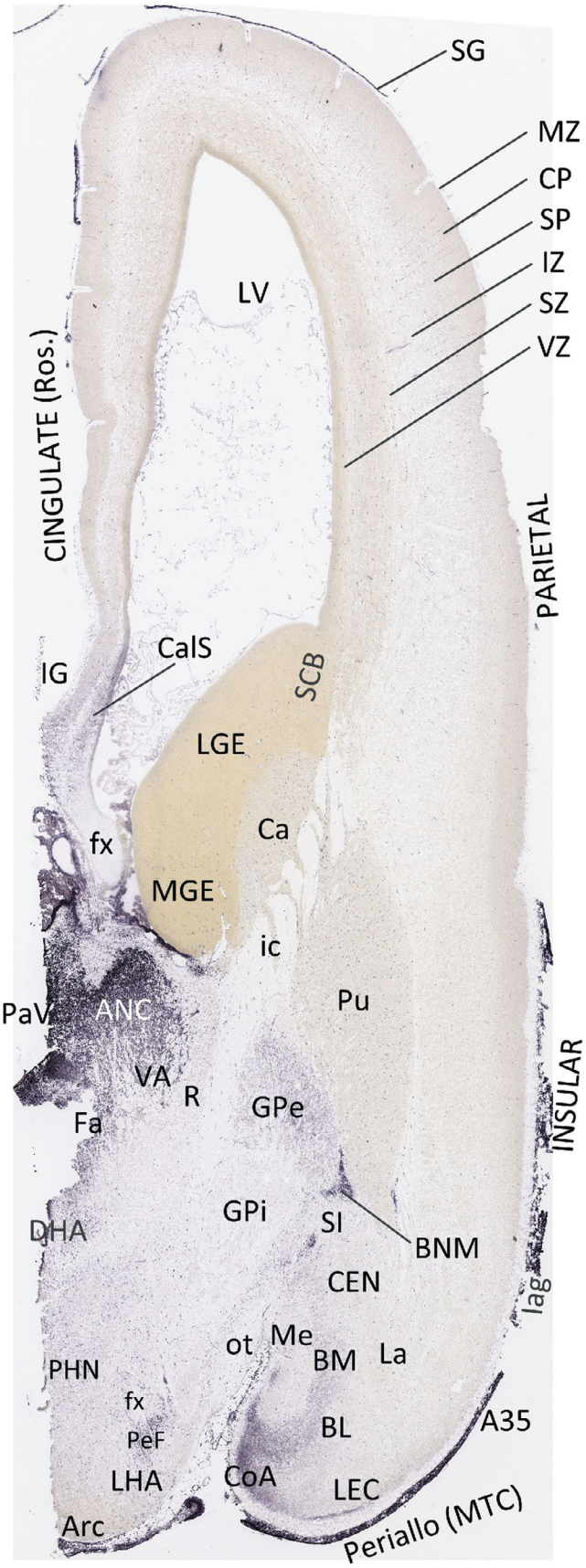

ZIC1-01-676 (Level ~21)

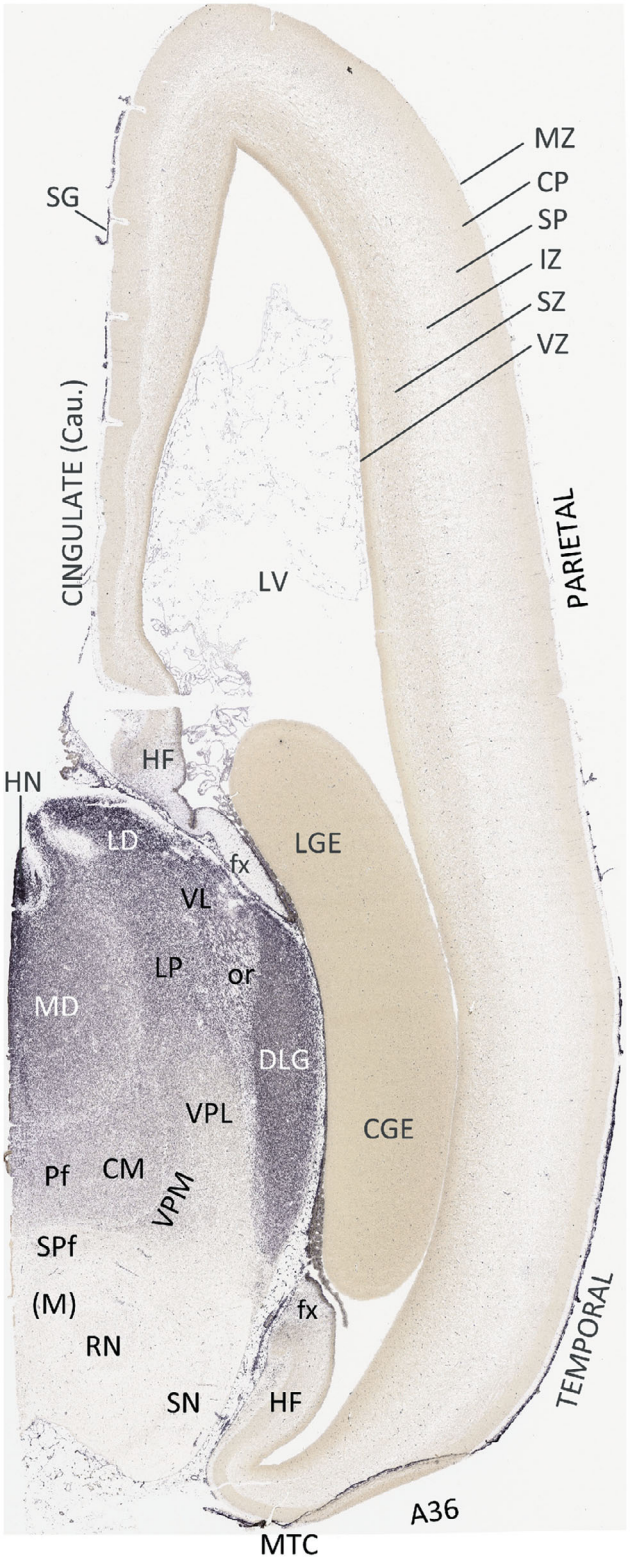

ZIC1-02-052 (Level ~26)

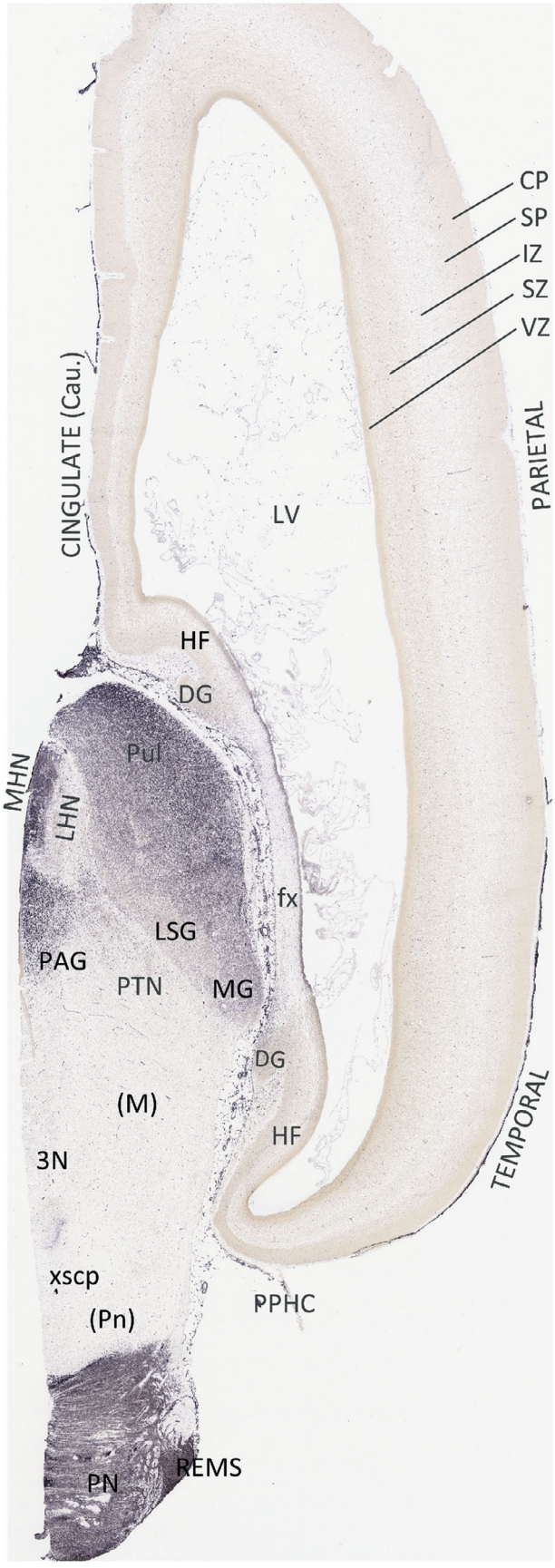

ZIC1-02-156 (Level ~30)

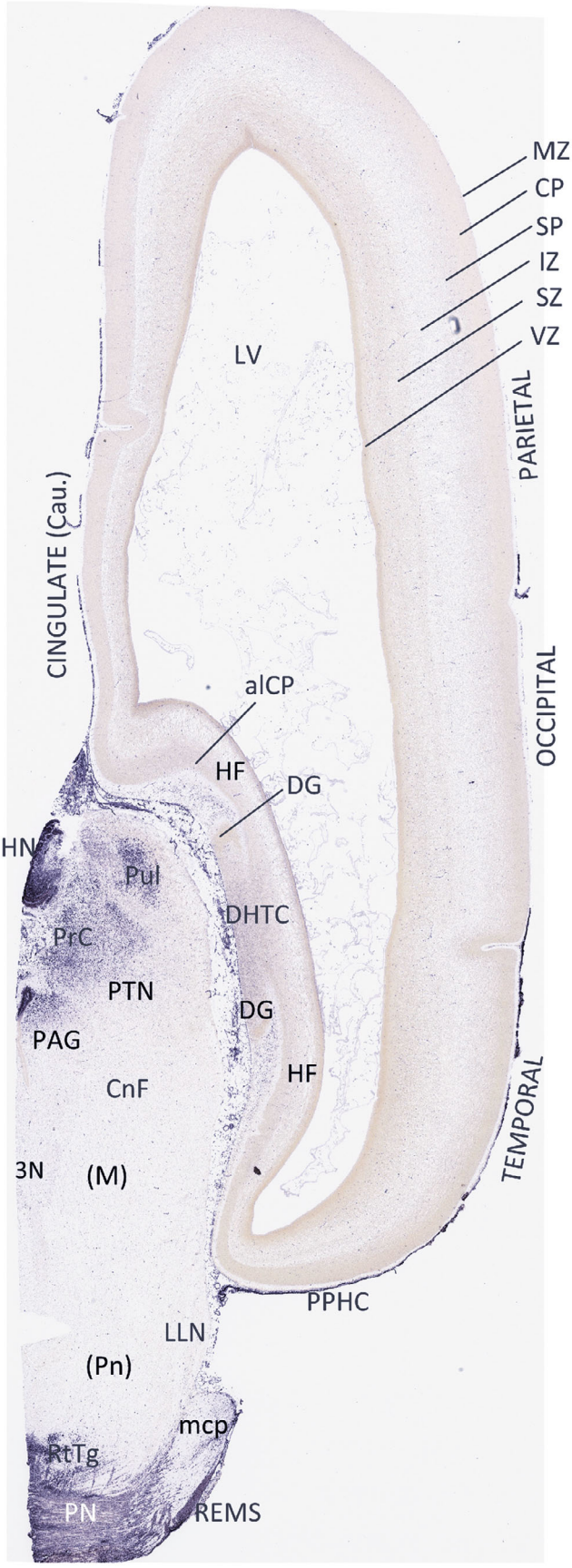

ZIC1-02-208 (Level ~33)

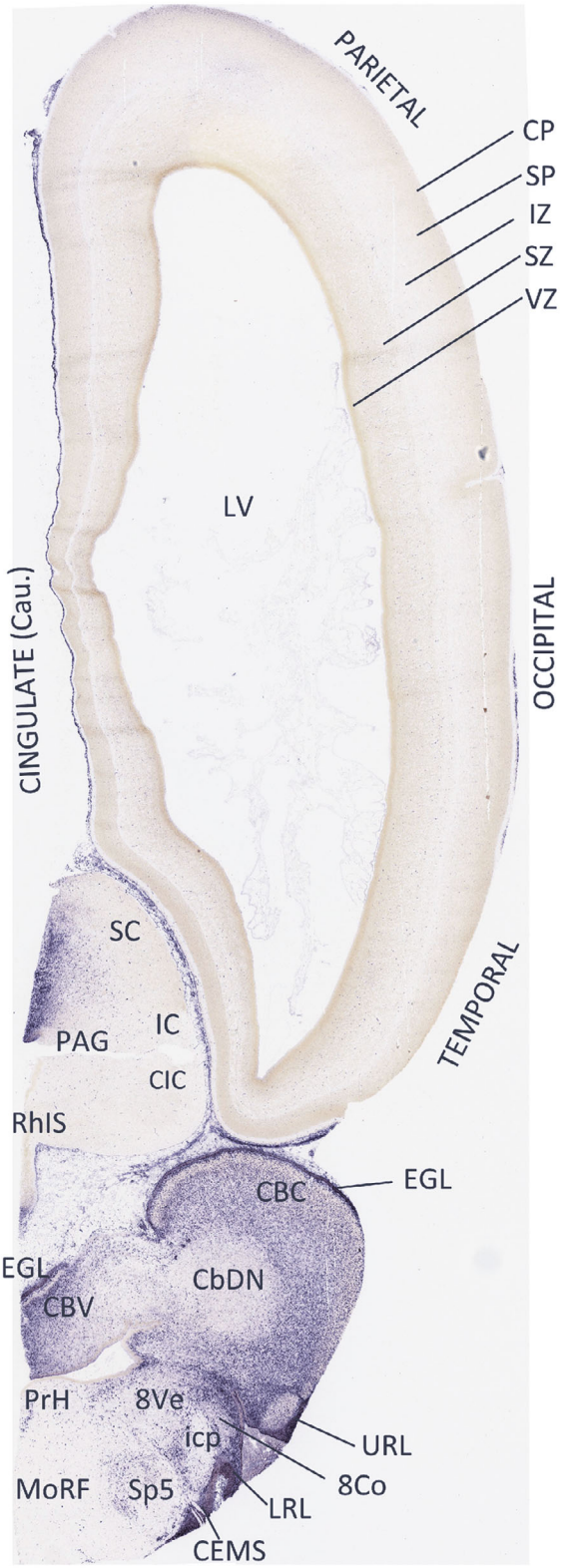

ZIC1-02-364 (Level ~39)

APPENDIX 3: Anatomical atlas plates for the prenatal human brain at PCW 21

Eighty-one plates with matching histological (Nissl-stained) sections are displayed in anterior-to-posterior (A-P) order. The A-P positions of 81 atlas plates (levels 1–81) and the locations of the four slabs and their starting and ending plate levels in each slab are indicated in the Inset of this Appendix (below). For each atlas plate, its A-P levels, slab, and section numbers are labeled in this style: Level number (slab number-sections number in the slabs). For example, Level 1 (01–026) represents the 26th section from slab 1, which is atlas plate 1 (i.e., Level 1). The matching Nissl-stained sections are labeled in this way: NISSL-slab section number in the slabs. For example, NISSL-01–026 represents the 26th section from slab 1, on which the annotation of atlas plate 1 (Level 1) was performed. In addition, one series of sequential AChE-stained sections from the same brain hemisphere is also available and linked online here (https://www.brainspan.org/ish/experiment/show?id=100134984). The parcellation and subdivisions of different brain regions as well as the parent–daughter relationship and abbreviation of each structure are detailed in Table 1 (for transient structures) and in our adult human brain atlas (Ding et al., 2016; for permanent structures). Note that all annotated brain structures and their abbreviation in this atlas can be searched in the interactive window of the online version of this atlas (www.brainspan.org or http://brainspan.org/static/atlas).

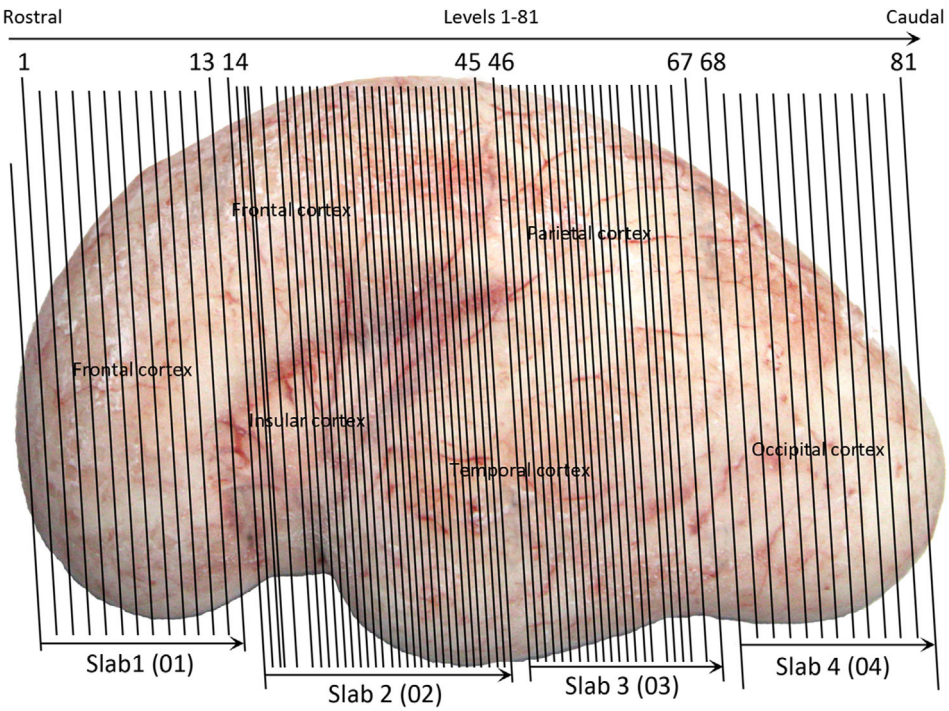

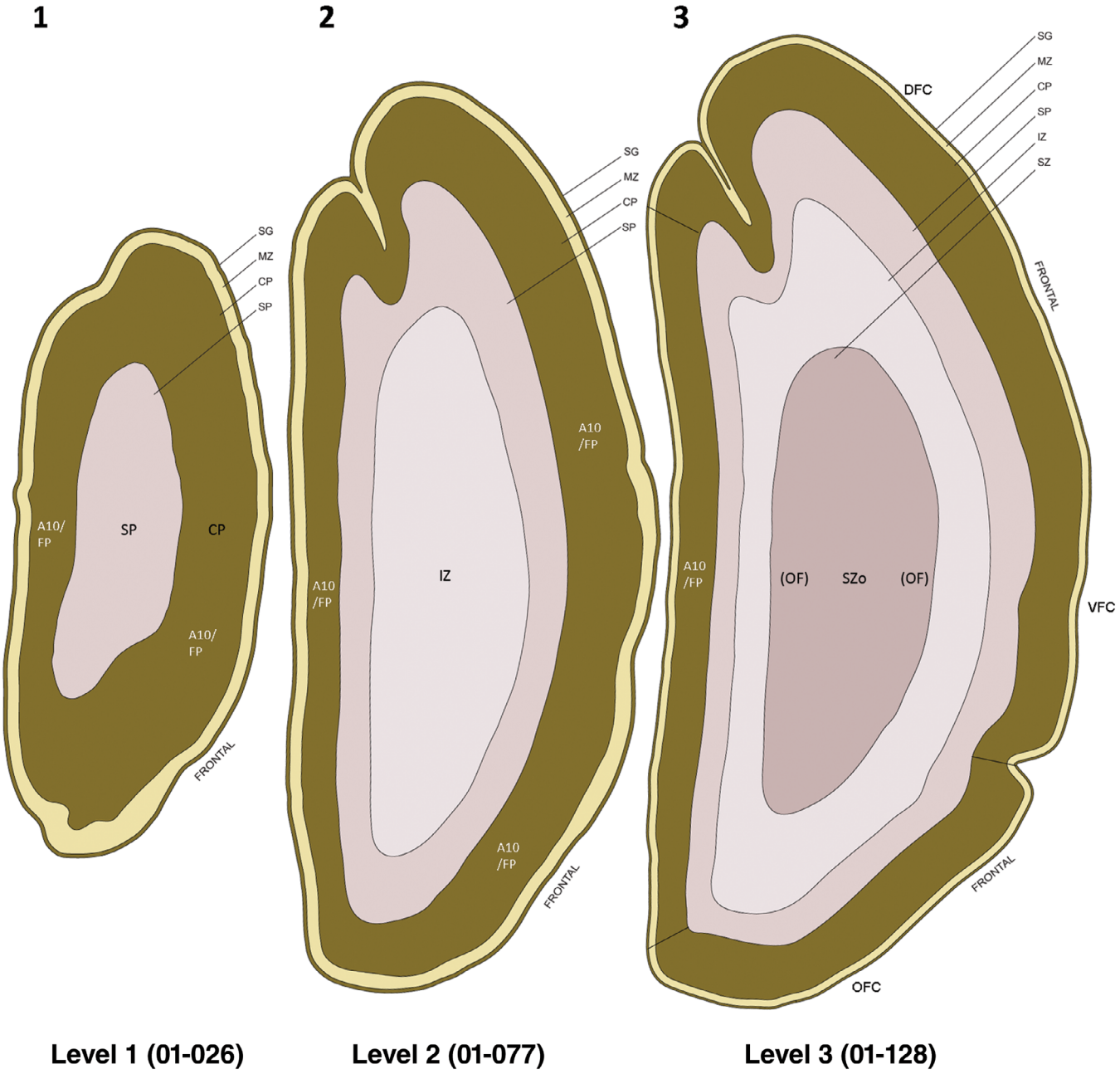
1
2
3
SG
MZ
CP
SP
A10/
FP
SP
CP
A10/
FP
FRONTAL
IZ
A10
/FP
FRONTAL
DFC
IZ
SZ
(OF)
SZo
(OF)
VFC
OFC
Level 1 (01-026)
Level 2 (01-077)
Level 3 (01-128)

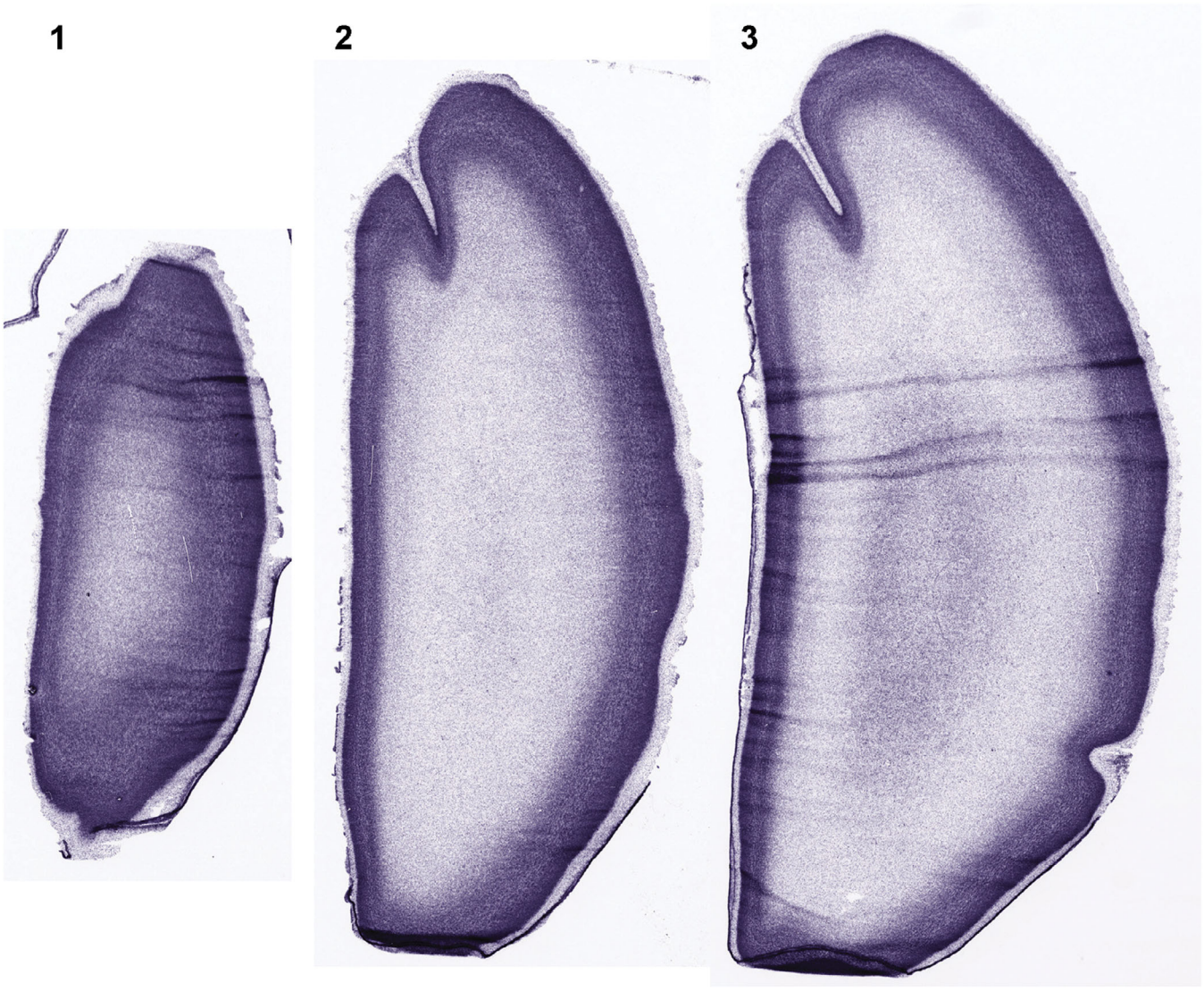
1
2
3
NISSL-01-026
NISSL-01-077
NISSL-01-128

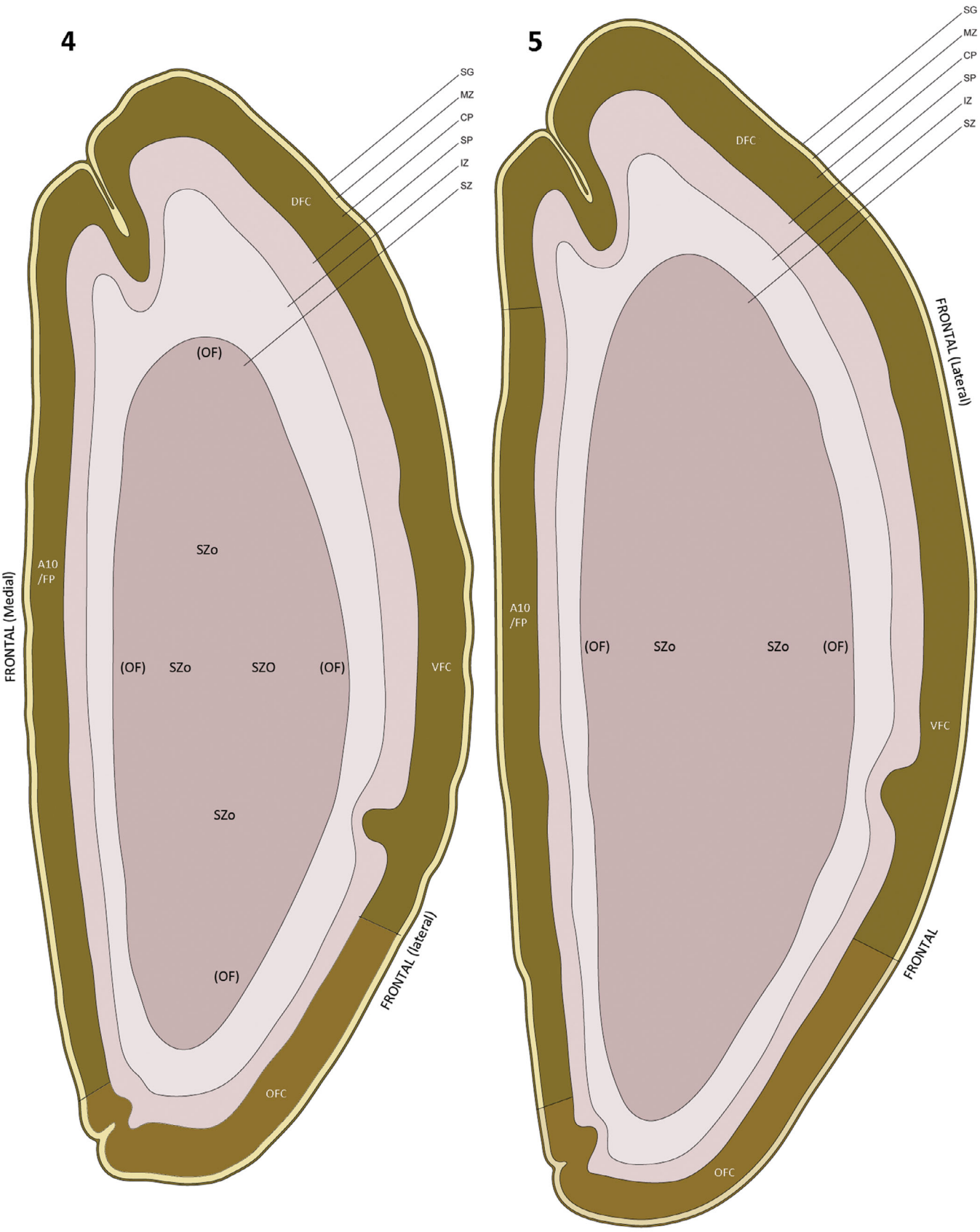

Level 4 (01-204) **Level 5 (01-255)**

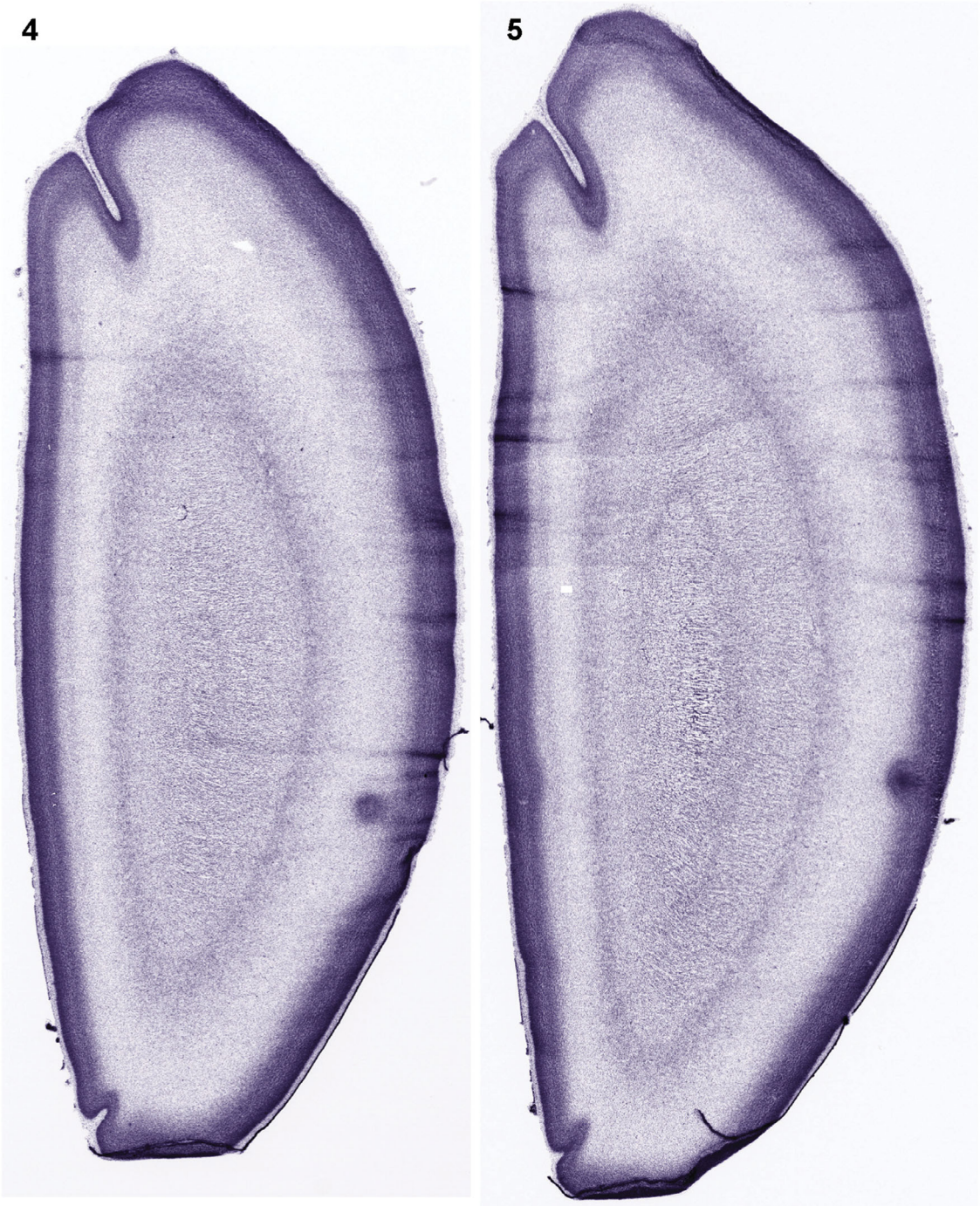

NISSL-01-204 NISSL-01-255

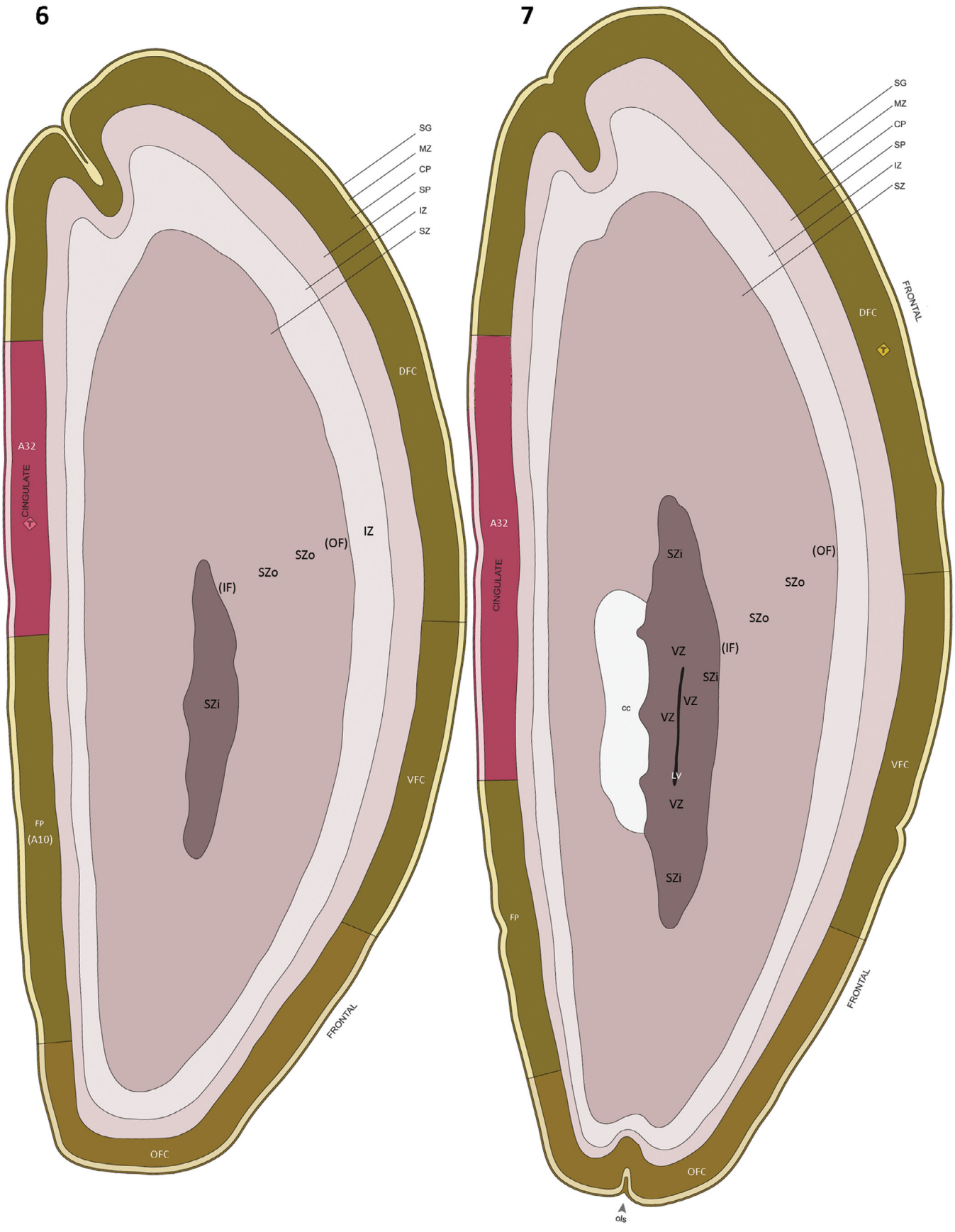

Level 6 (01-306)

Level 7 (01-357)

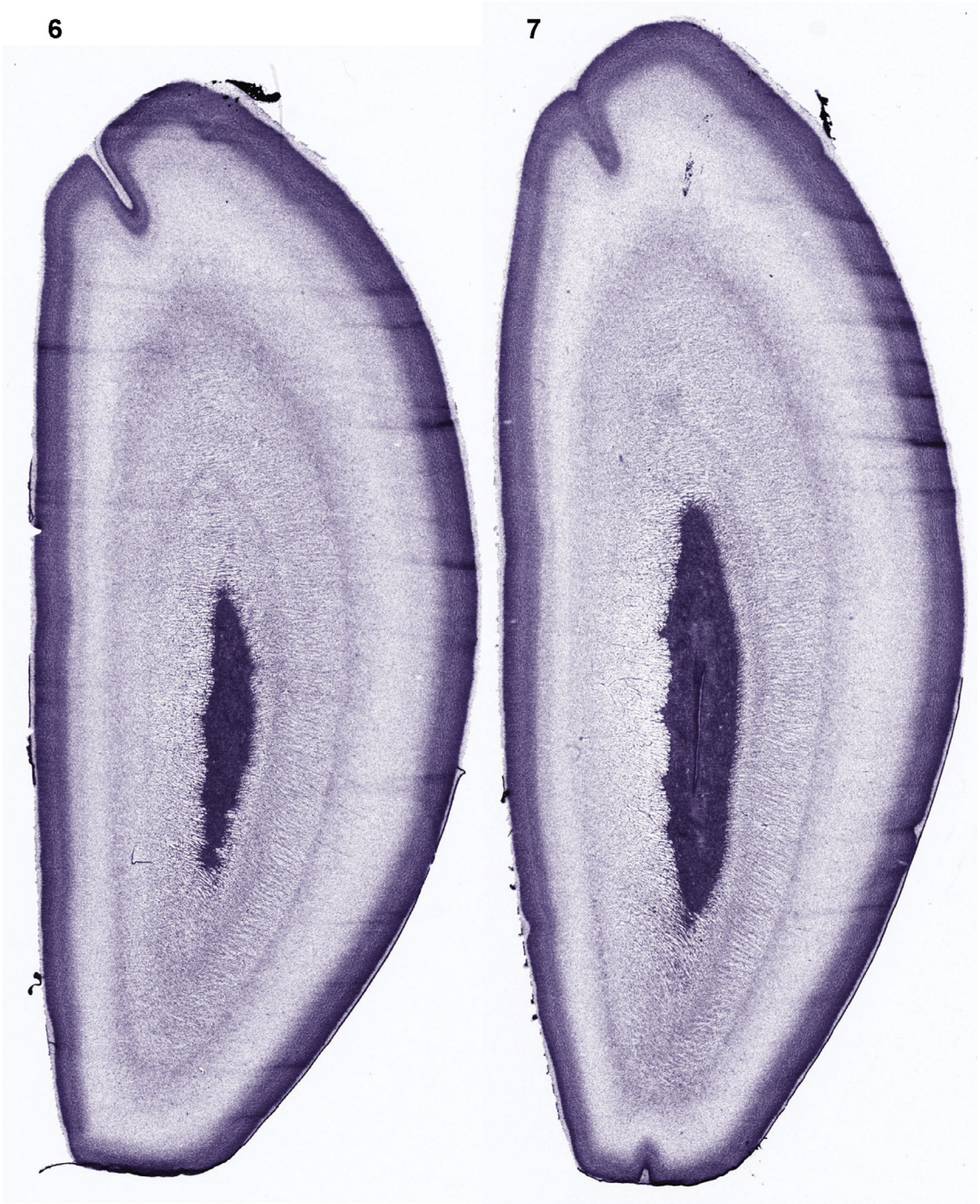
6
7
NISSL-01-306
NISSL-01-357

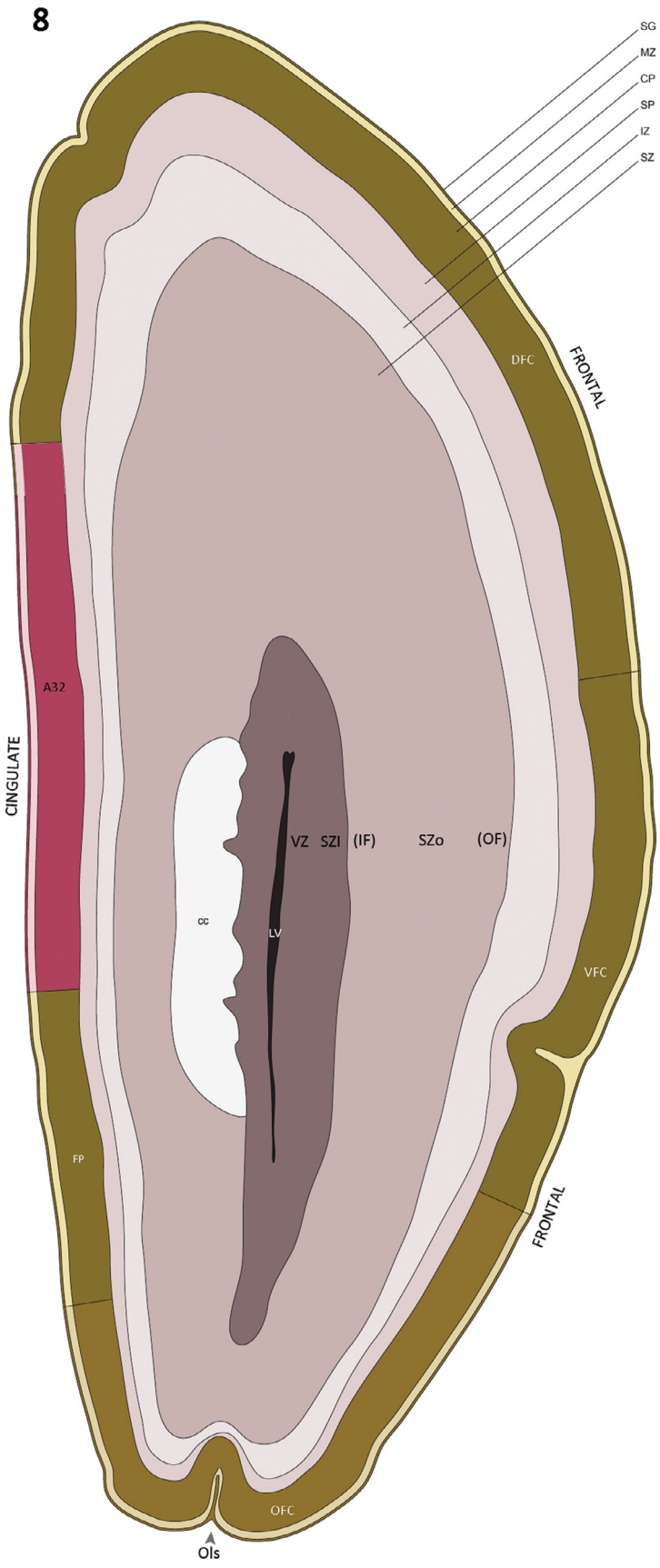

Level 8 (01-408)

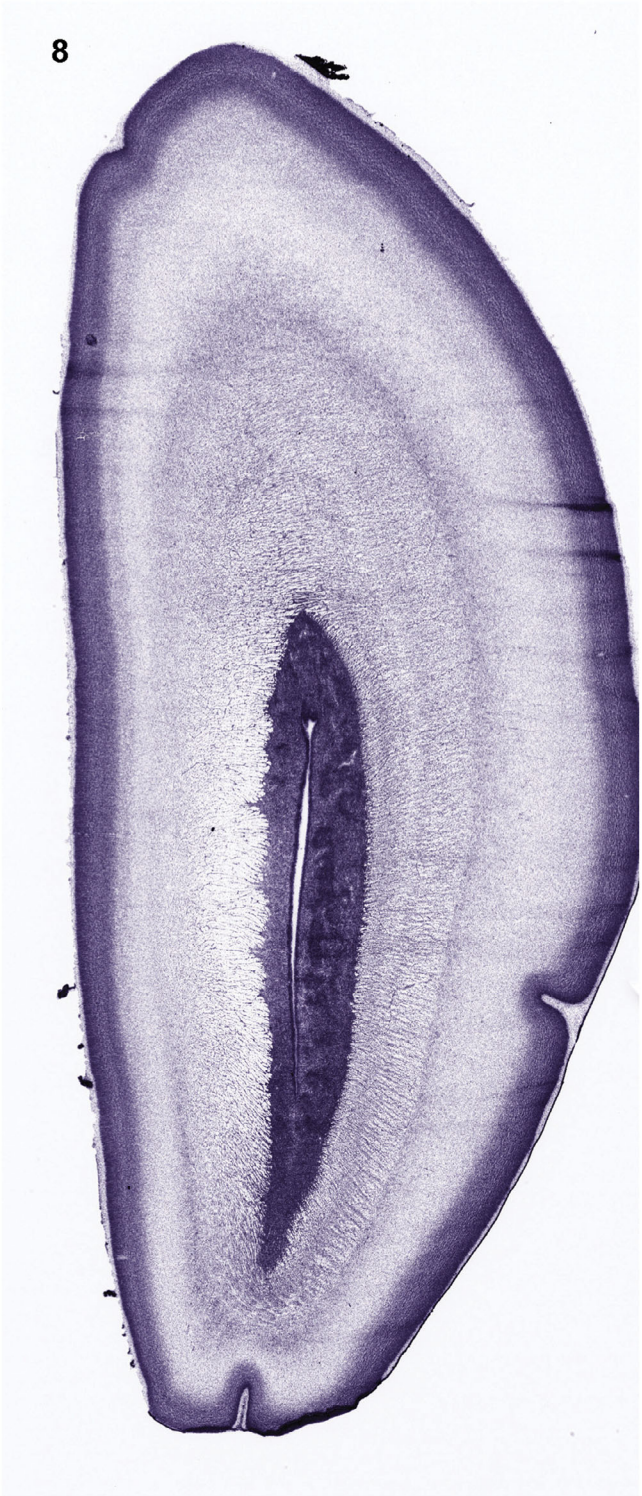

NISSL-01-408

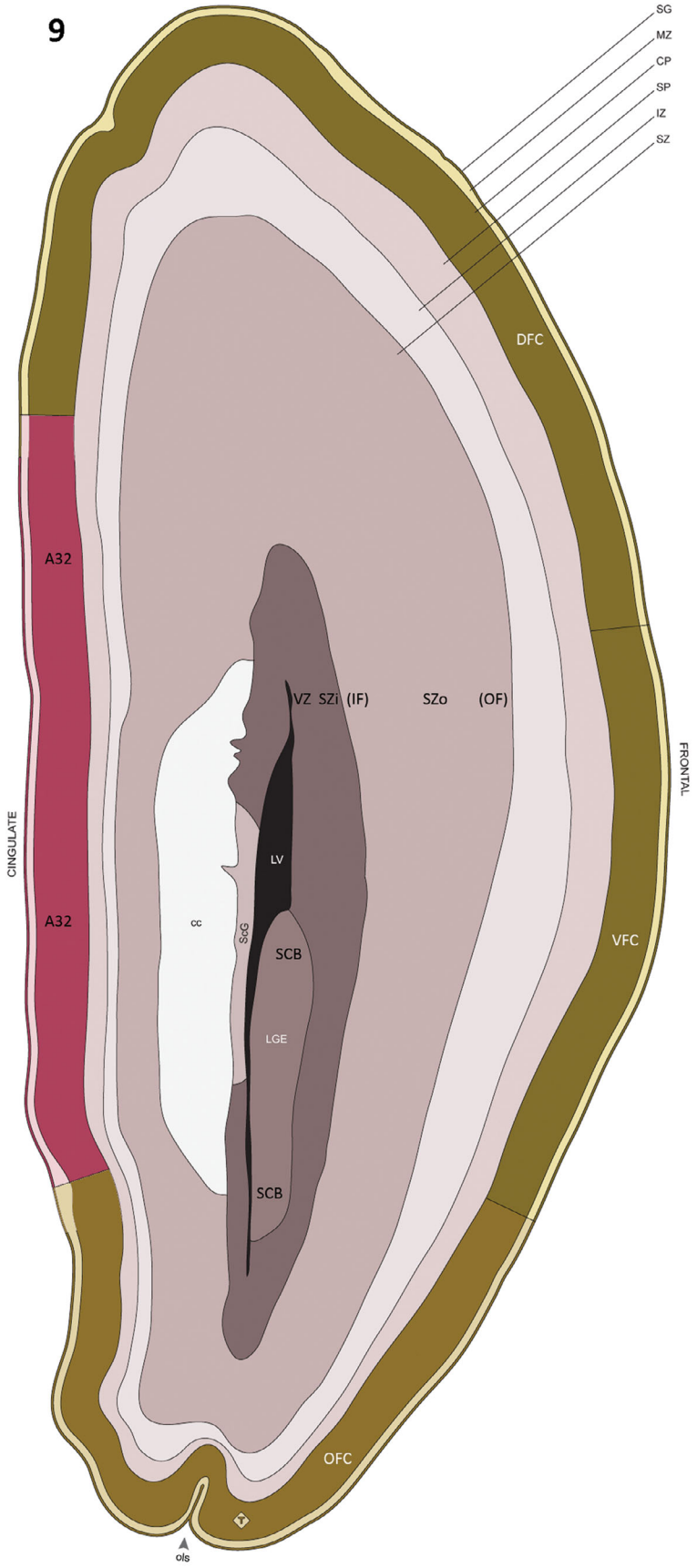

Level 9 (01-459)

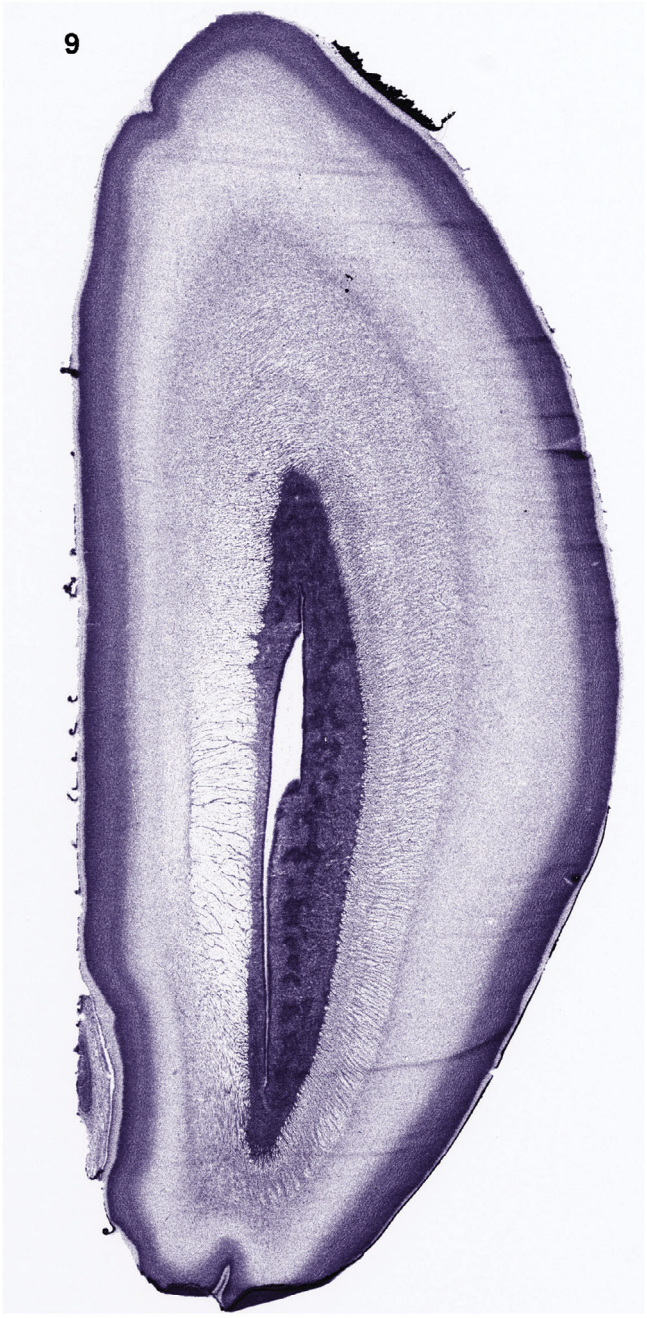

NISSL-01-459

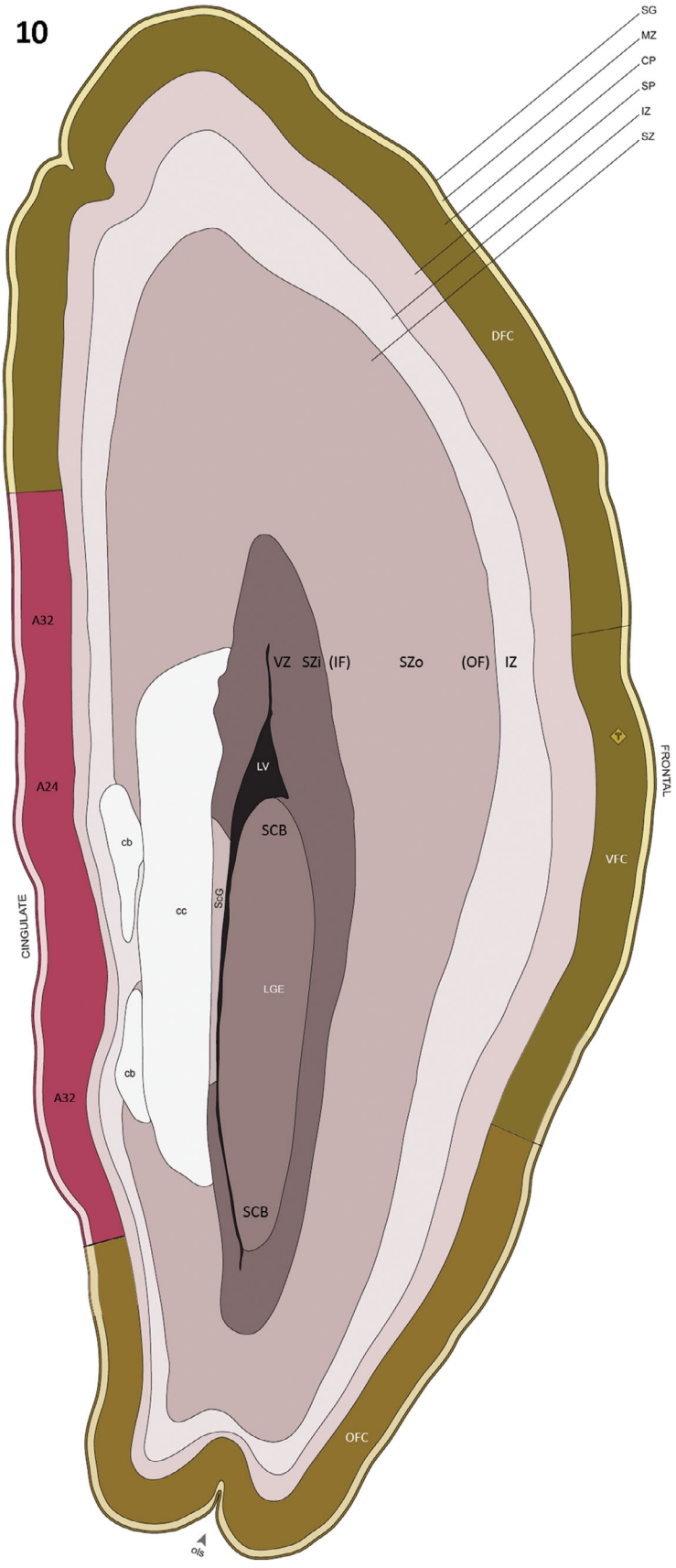

Level 10 (01-510)

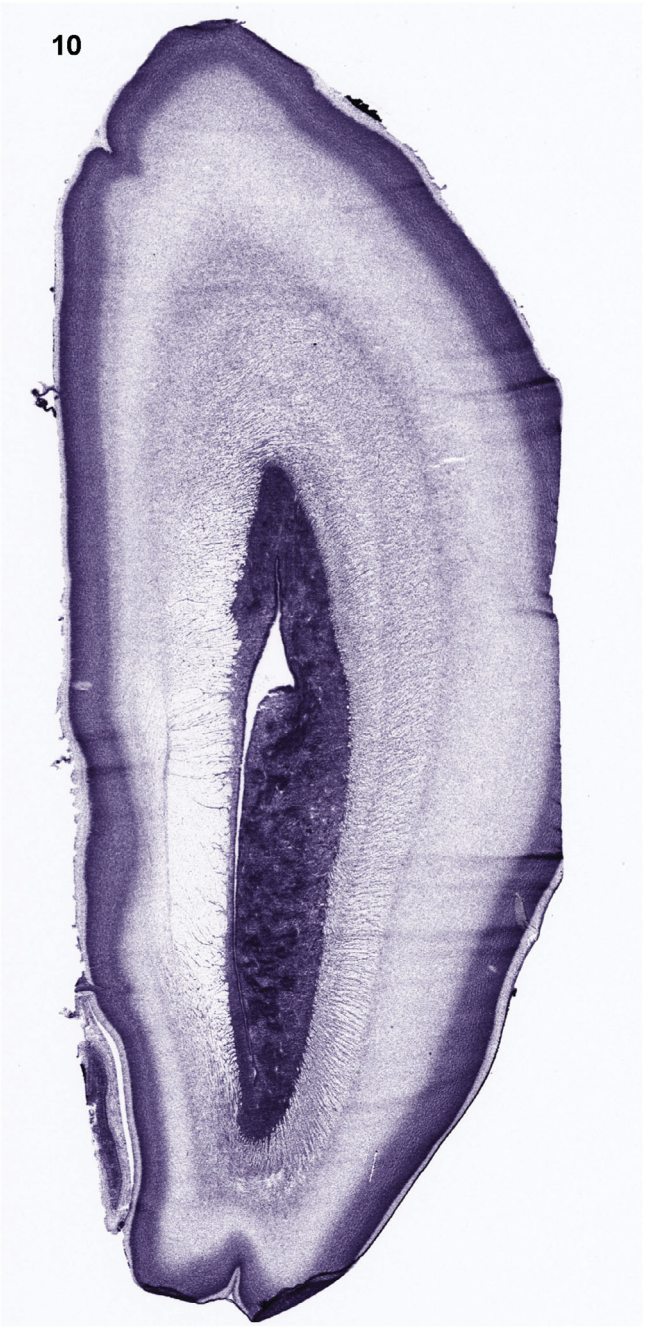

NISSL-01-510

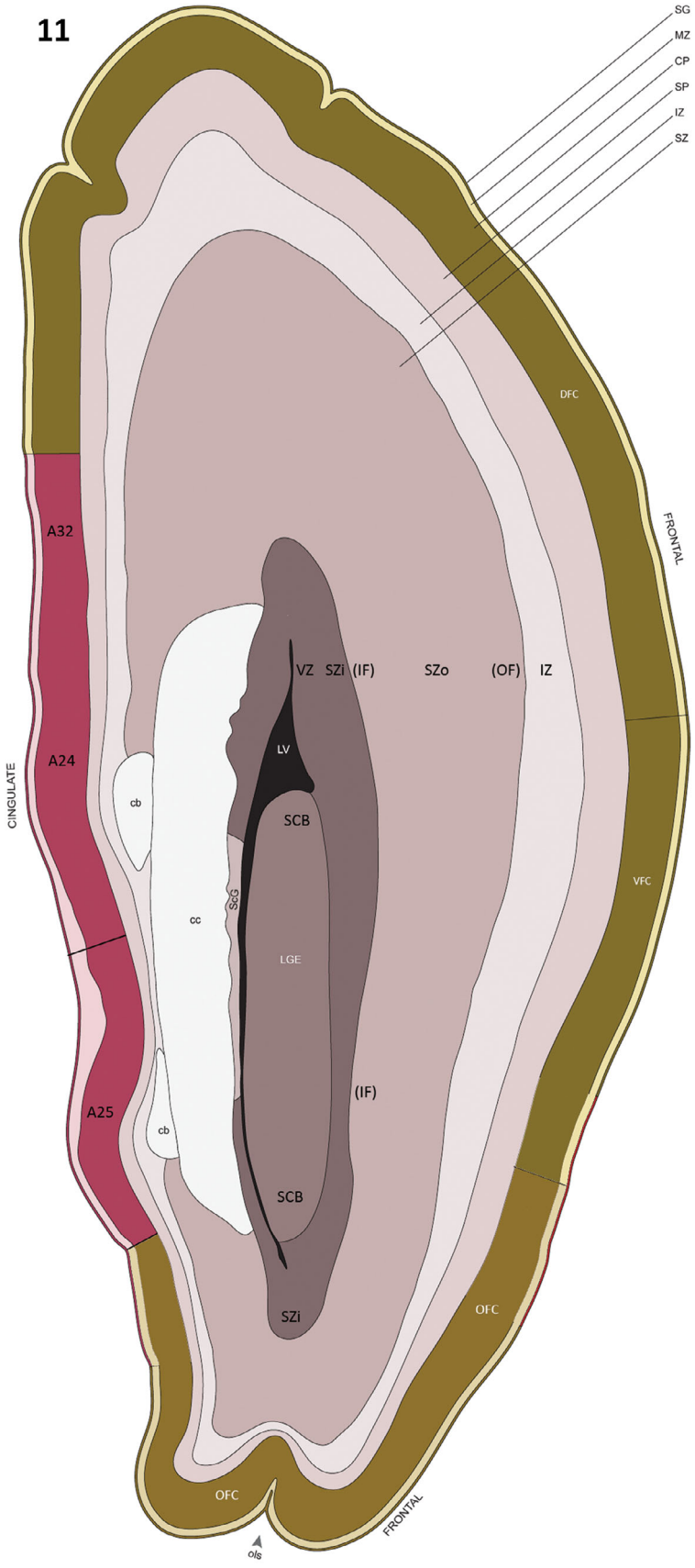

Level 11 (01-536)

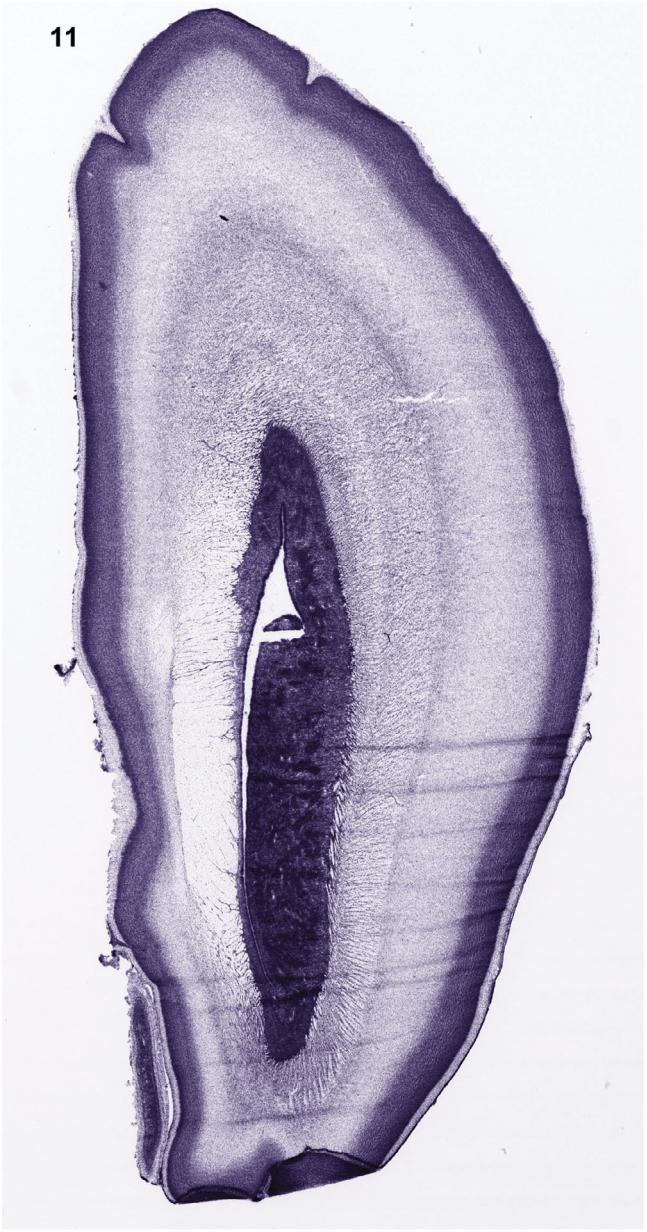

NISSL-01-536

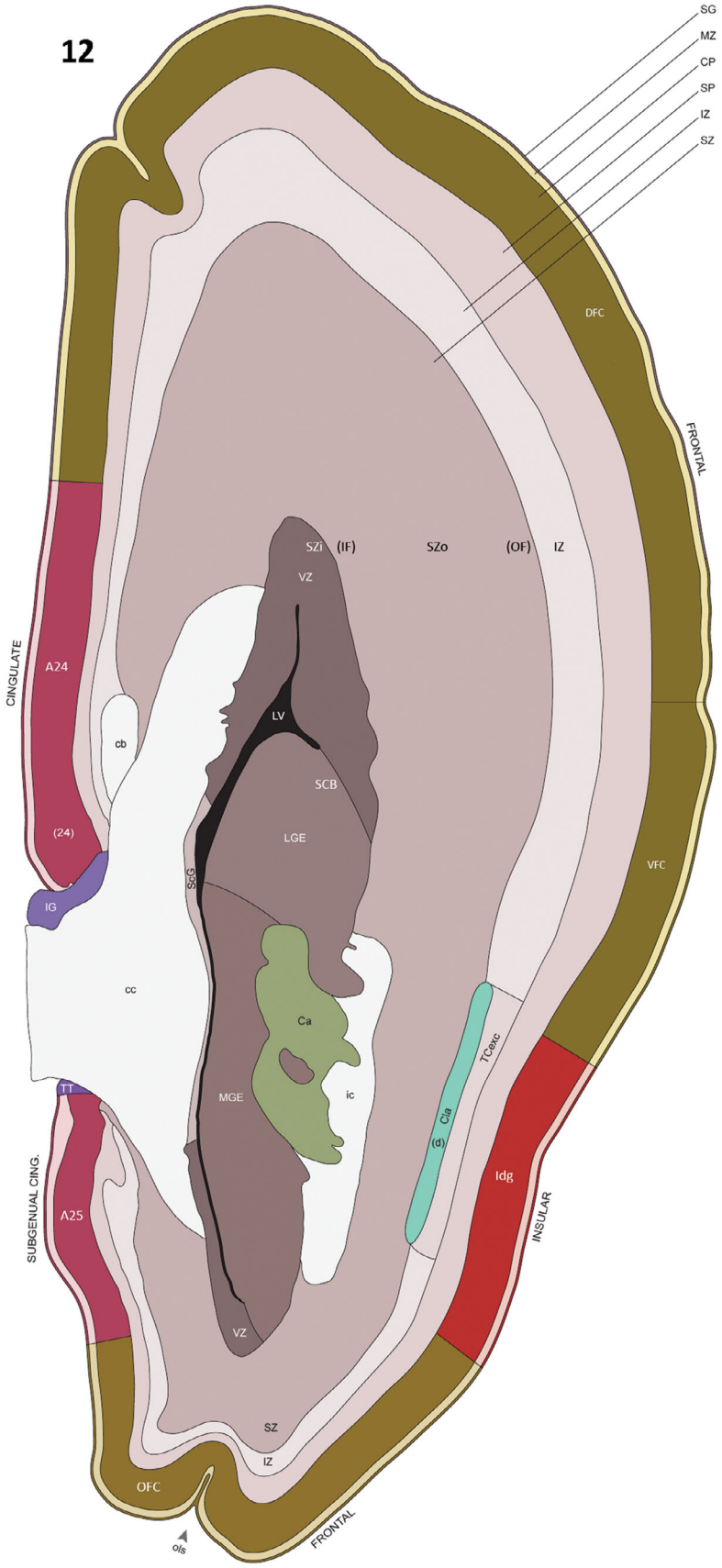

Level 12 (01-612)

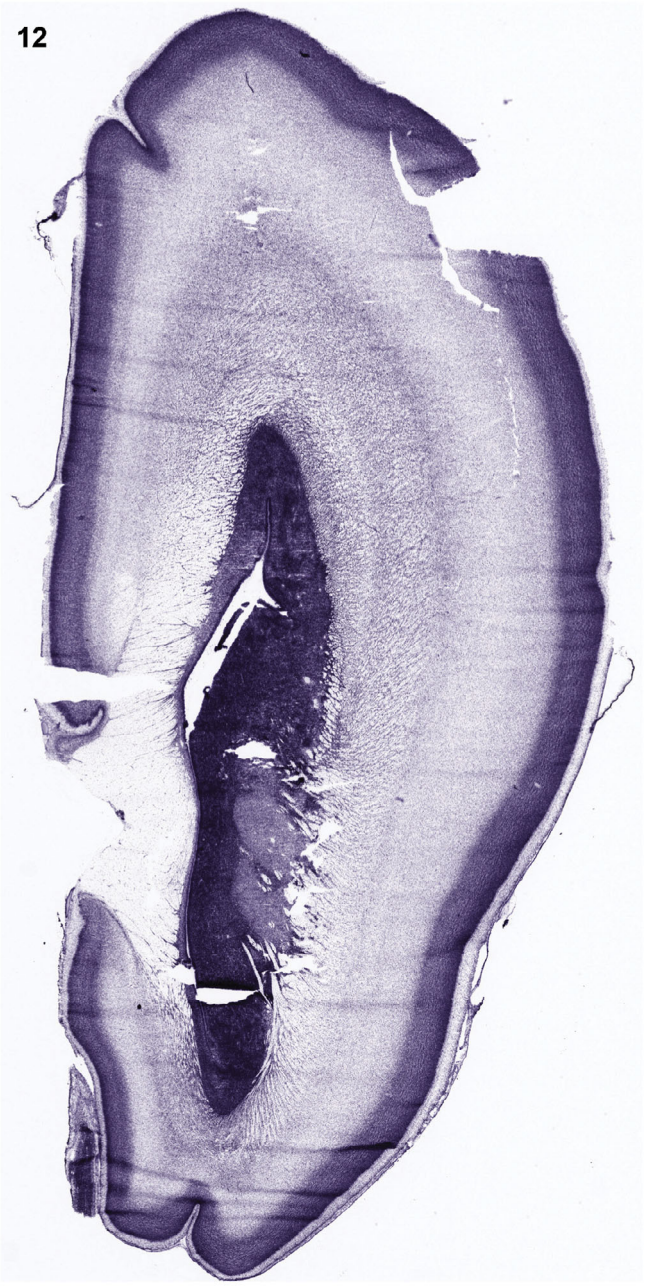

NISSL-01-612

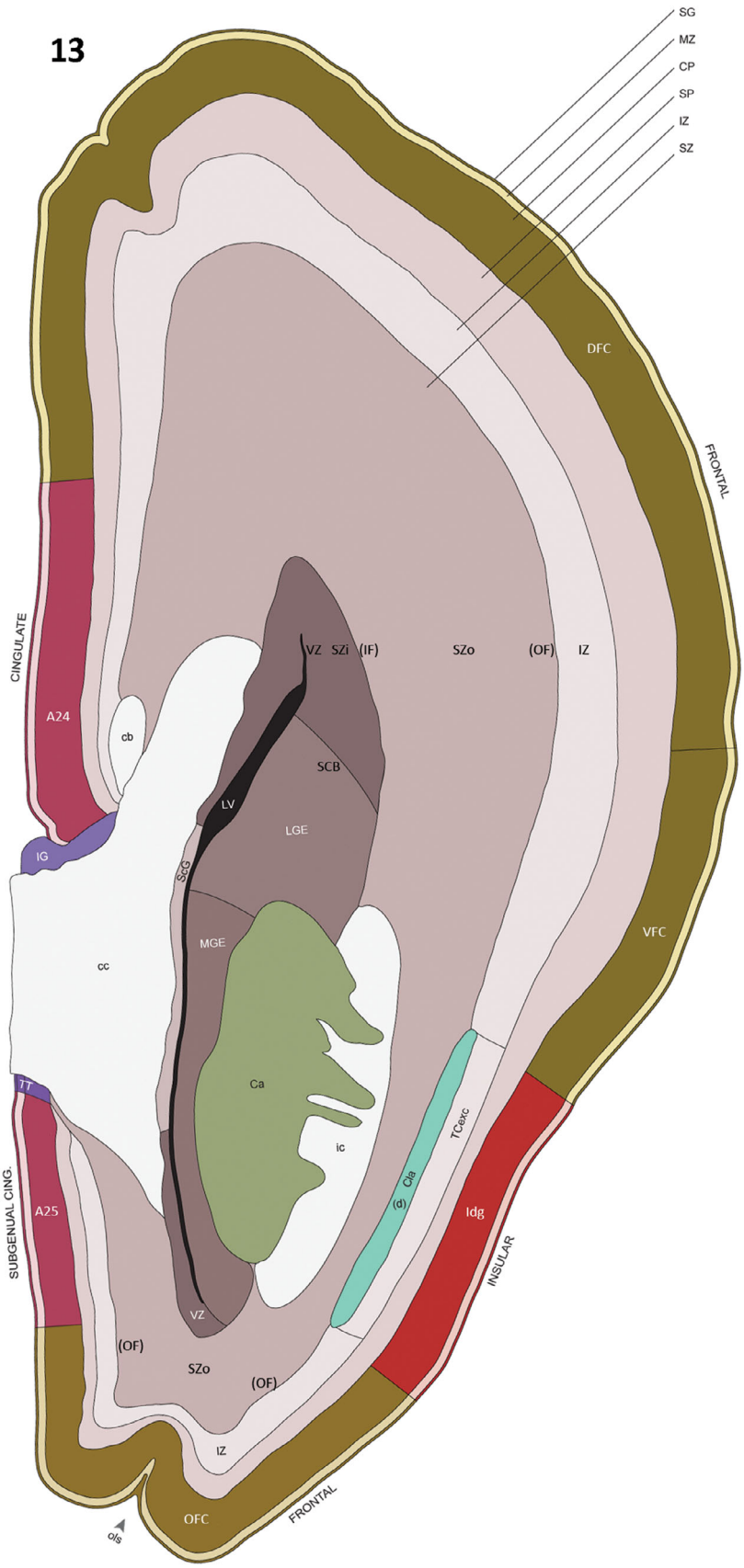

Level 13 (01-638)

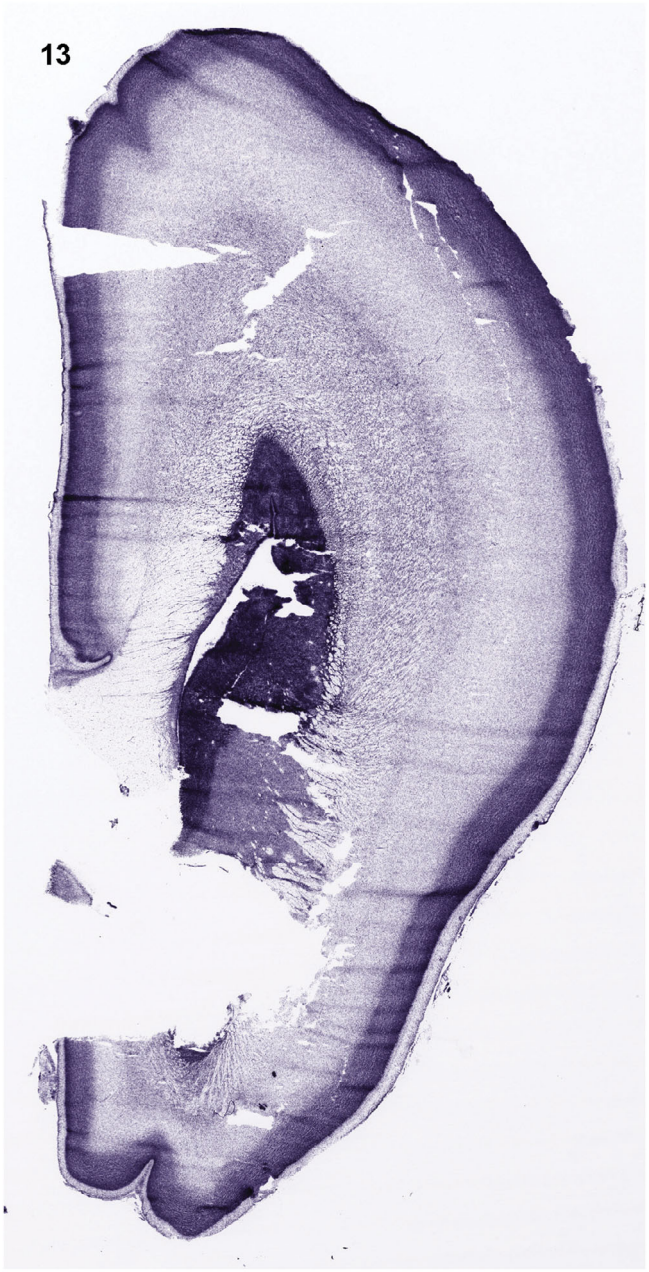

NISSL-01-638

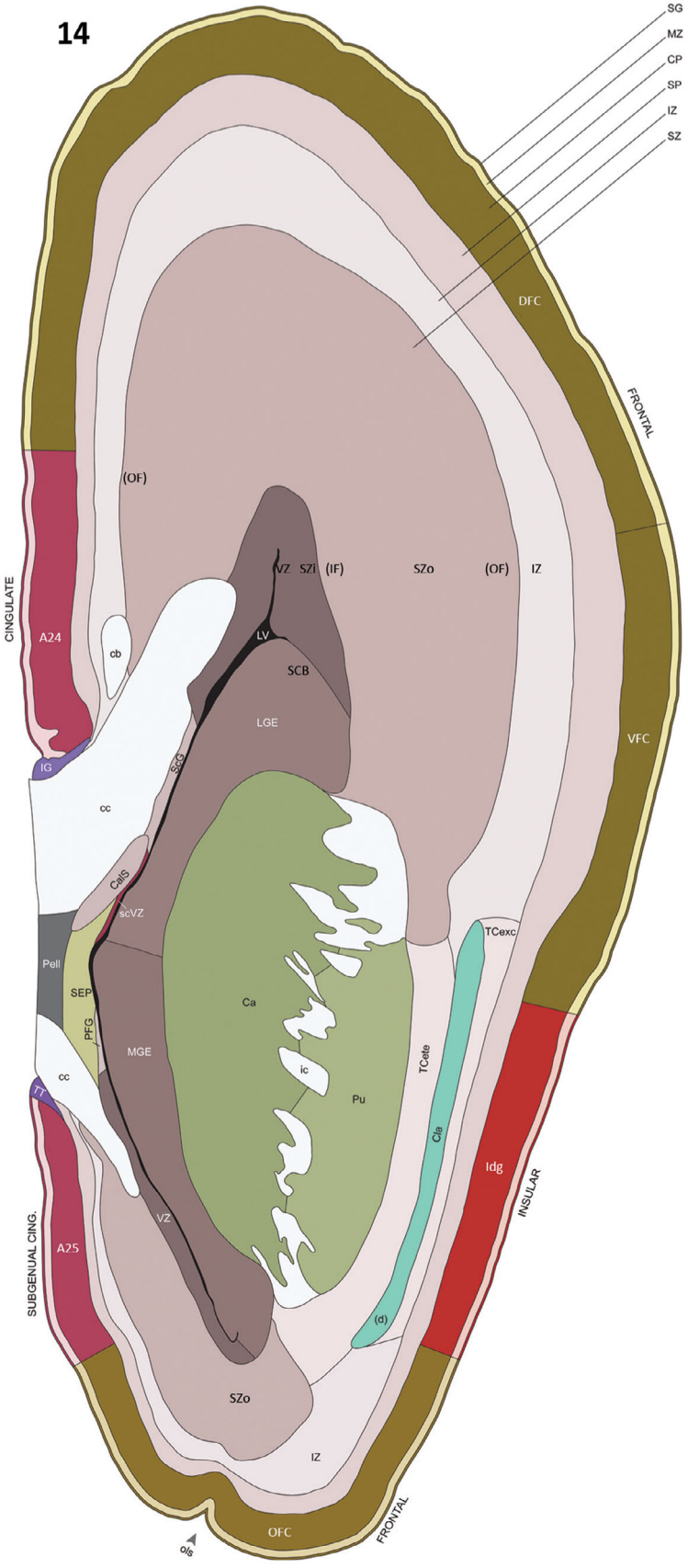

Level 14 (02-001)

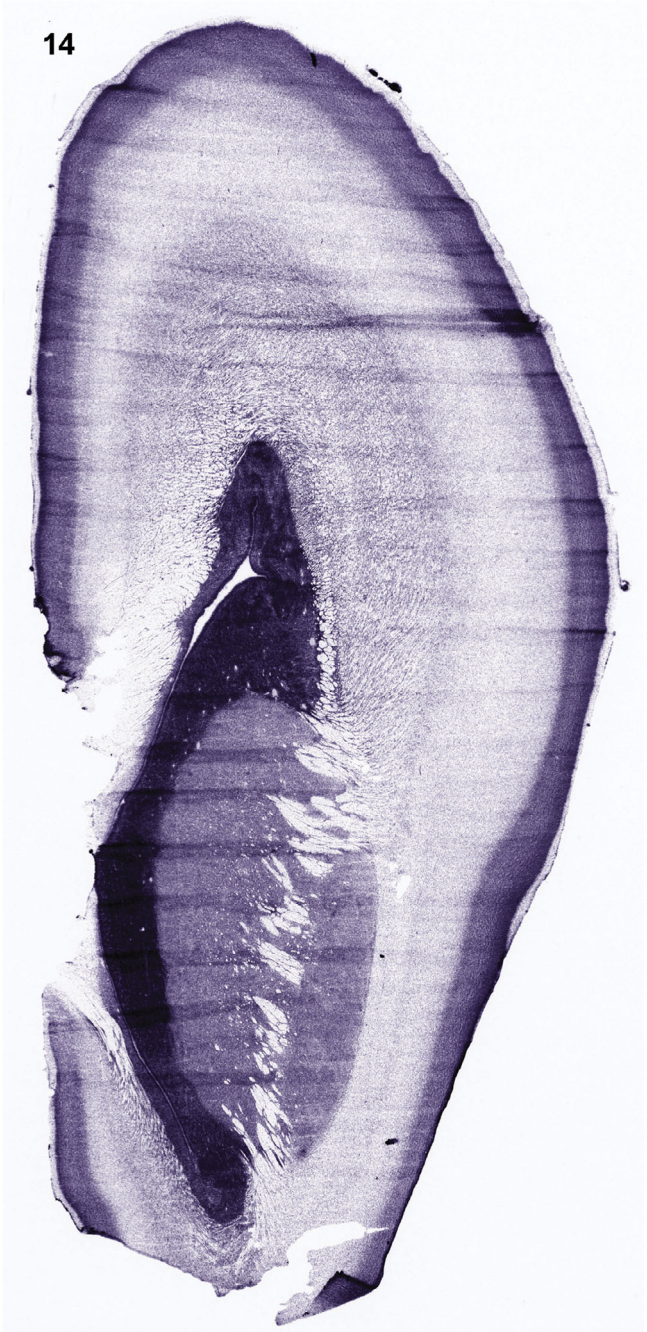

NISSL-02-001

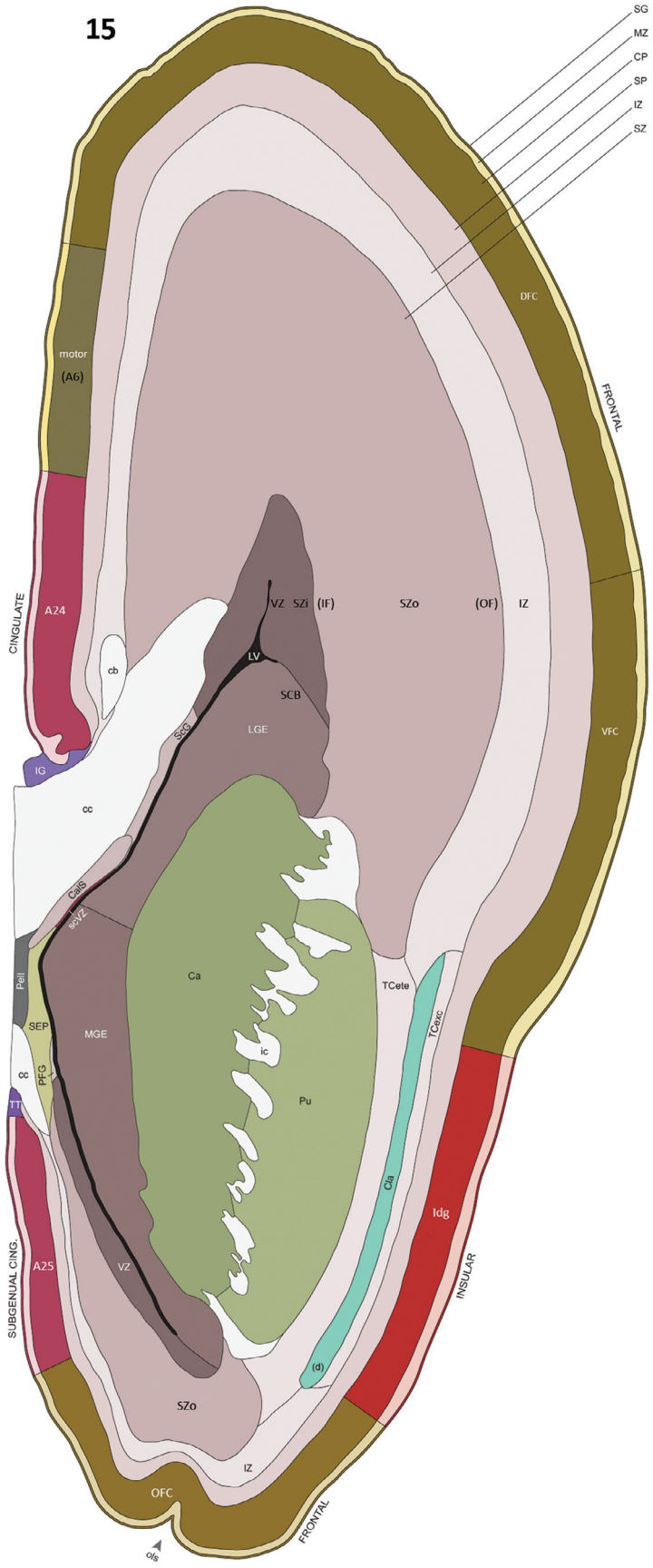

Level 15 (02-026)

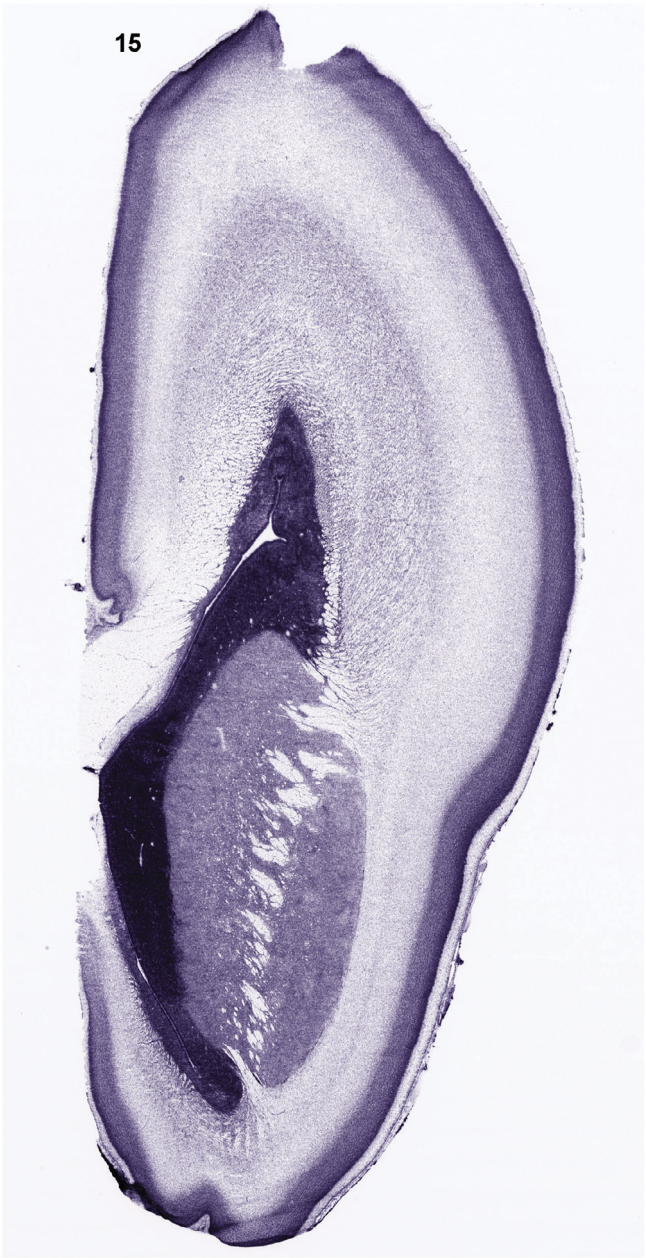

NISSL-02-026

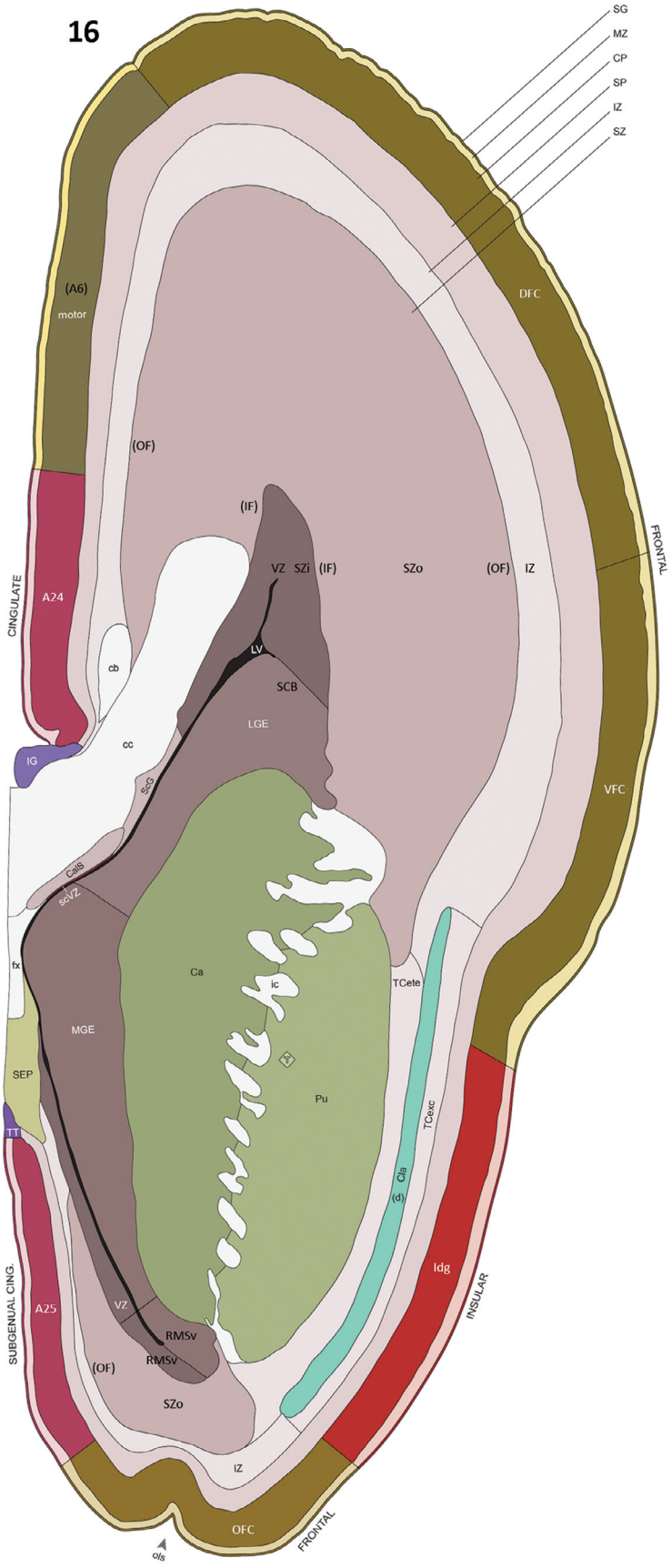

Level 16 (02-051)

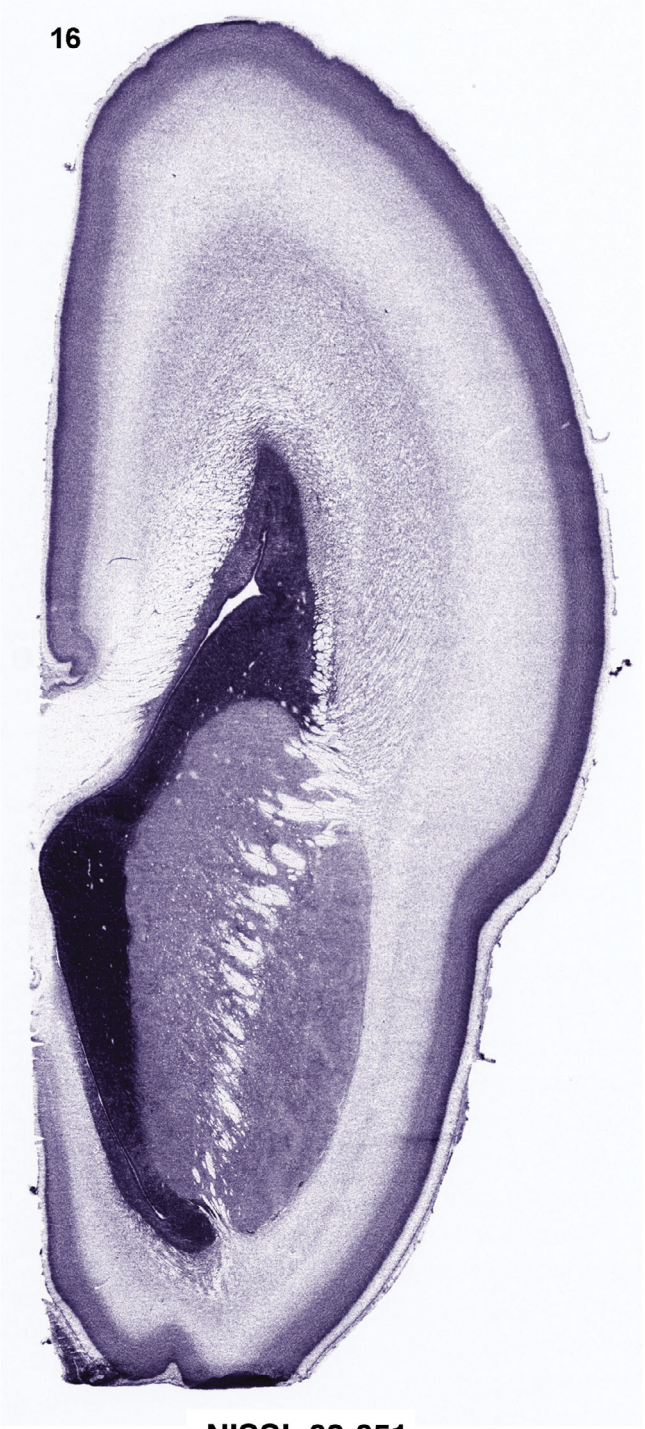

NISSL-02-051

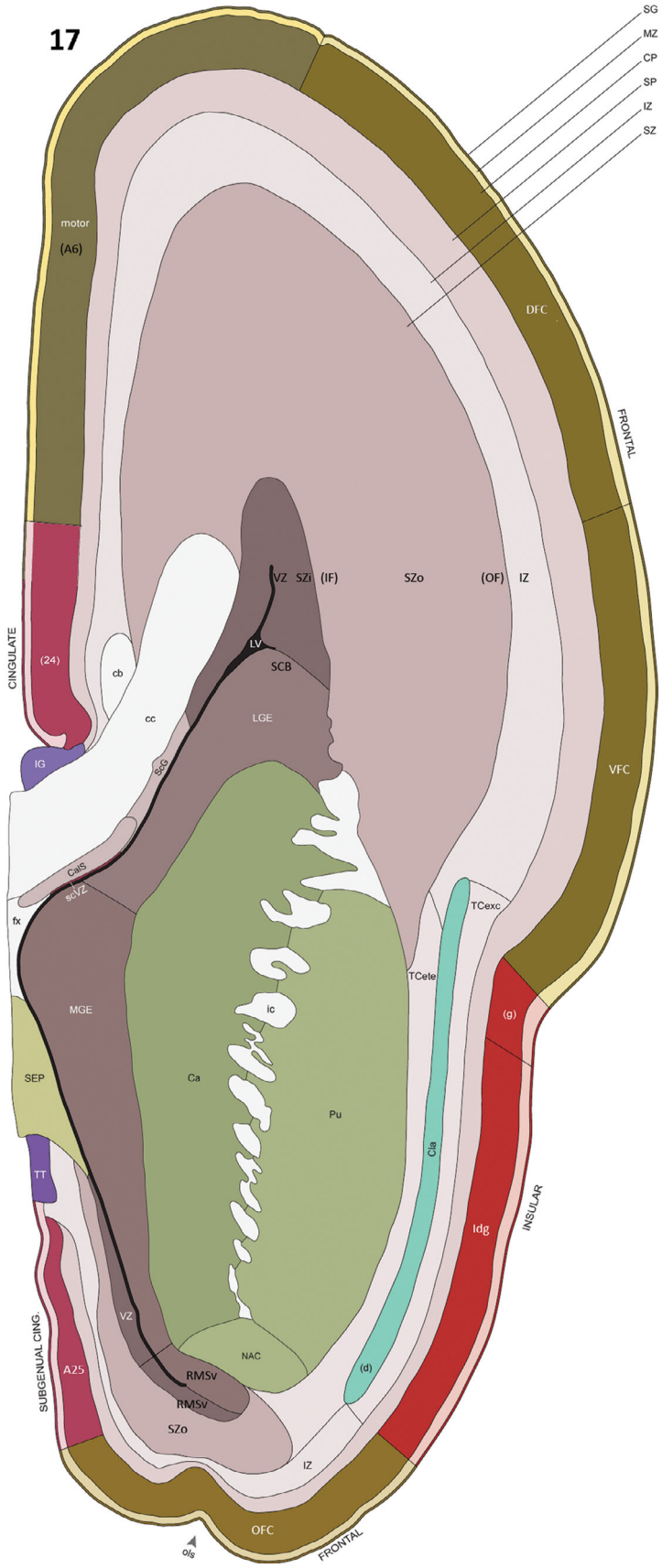

Level 17 (02-057)

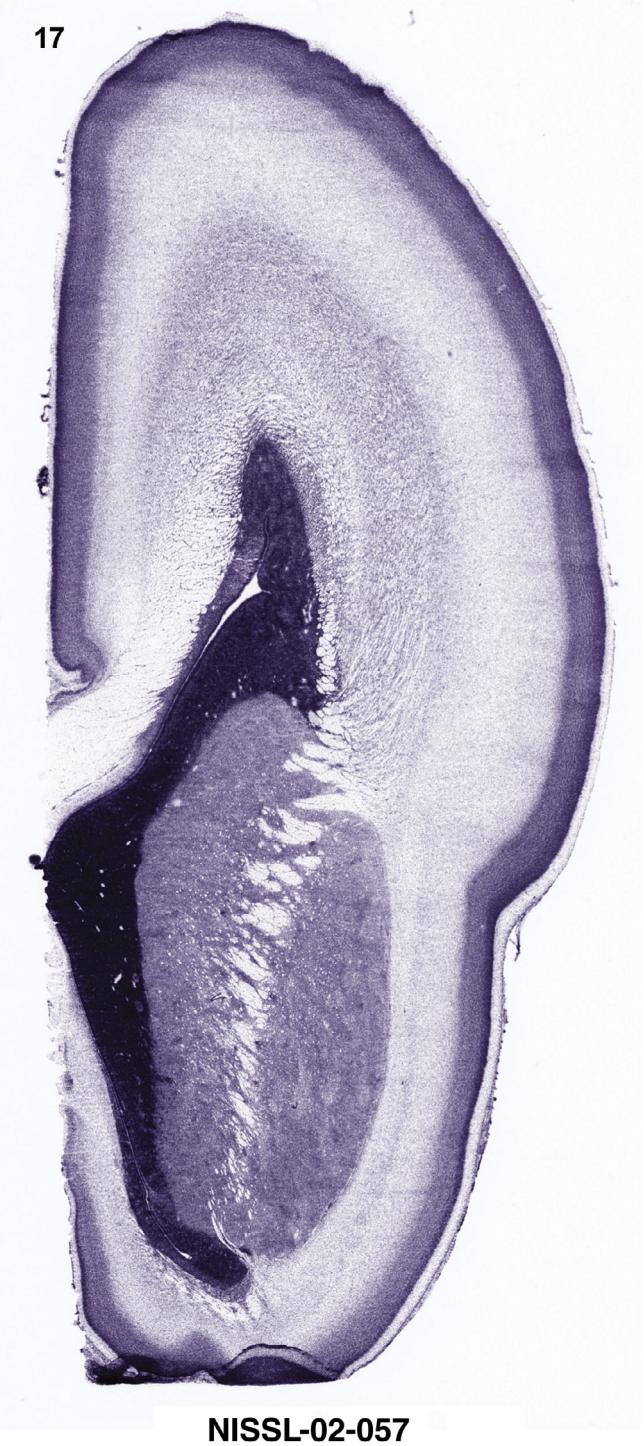
17
NISSL-02-057

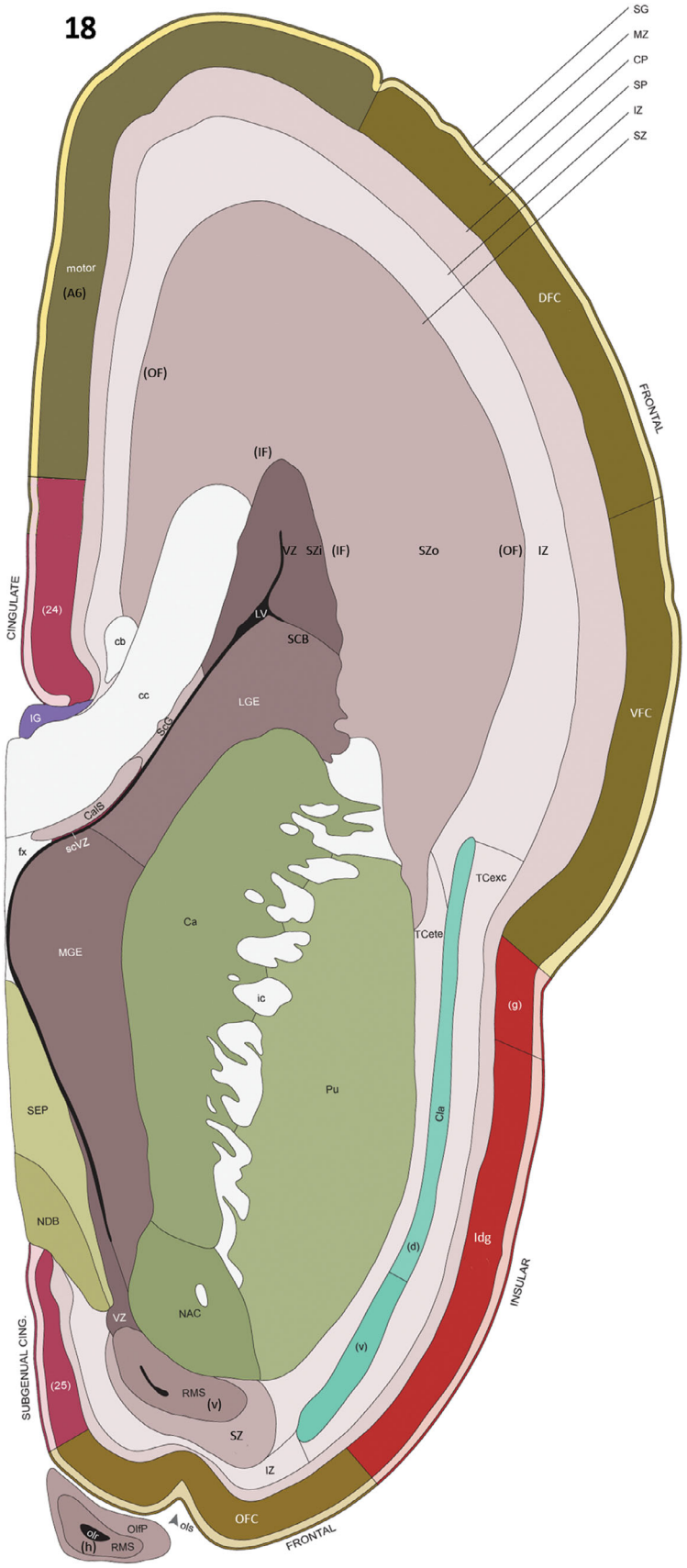

Level 18 (02-103)

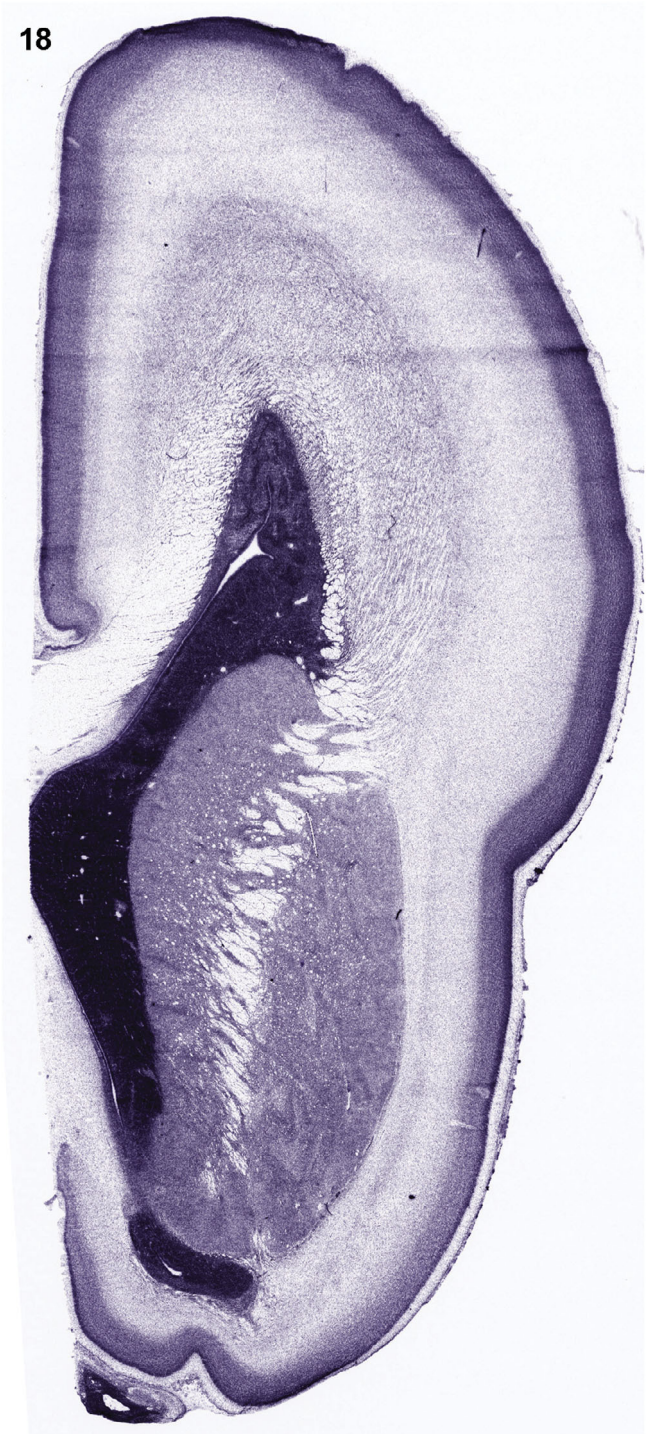
18
NISSL-02-103

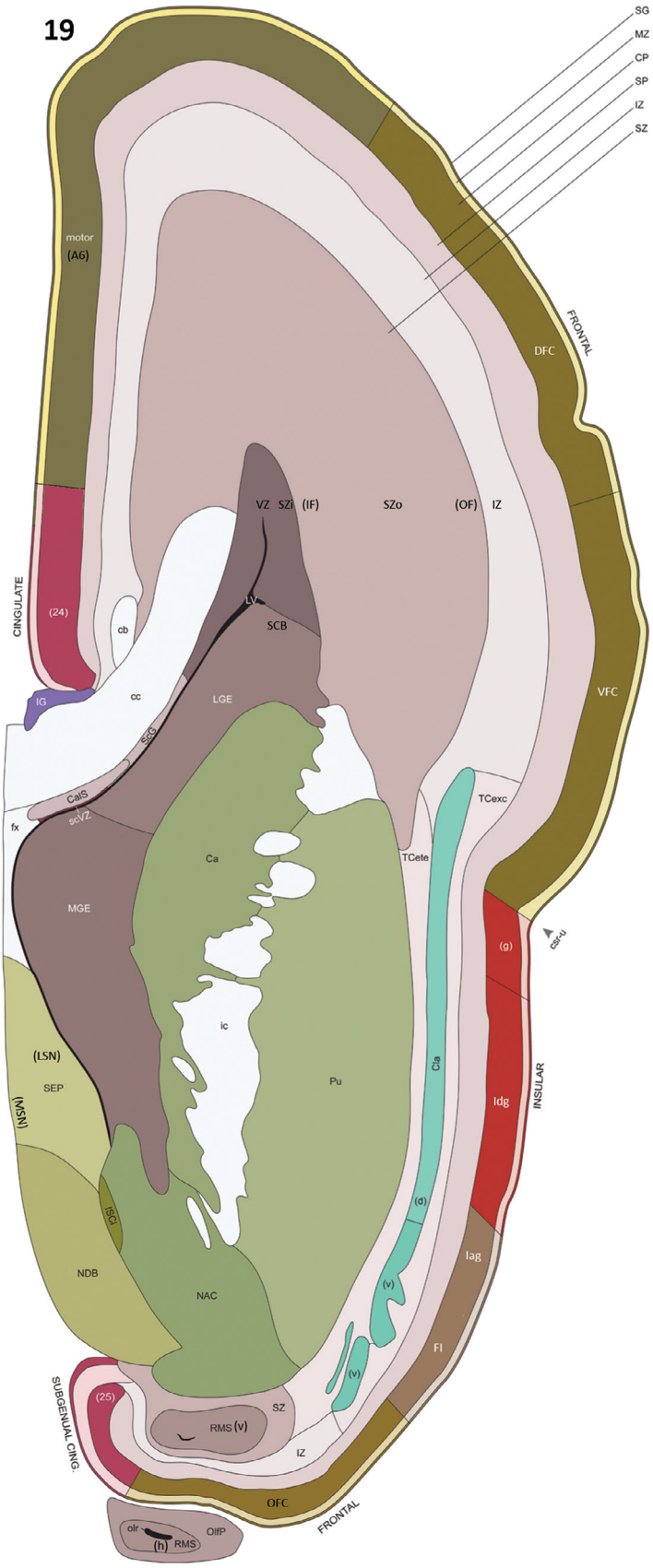

Level 19 (02-154)

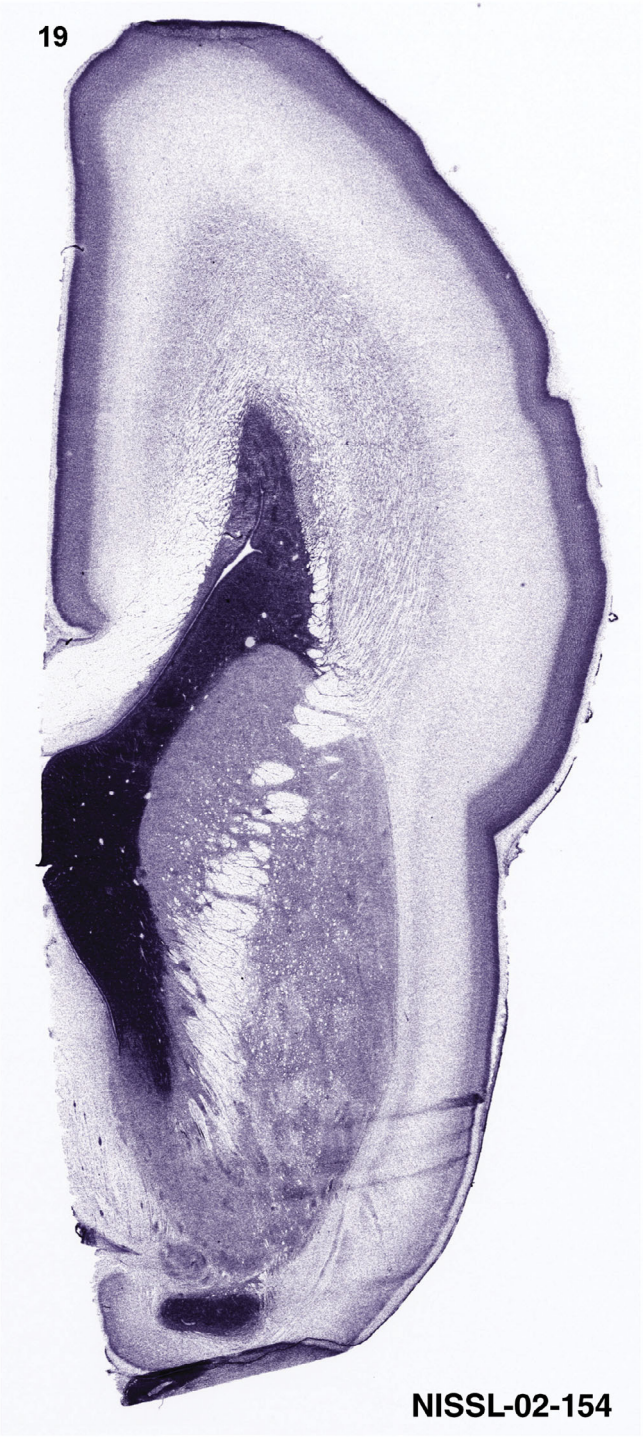
19
NISSL-02-154

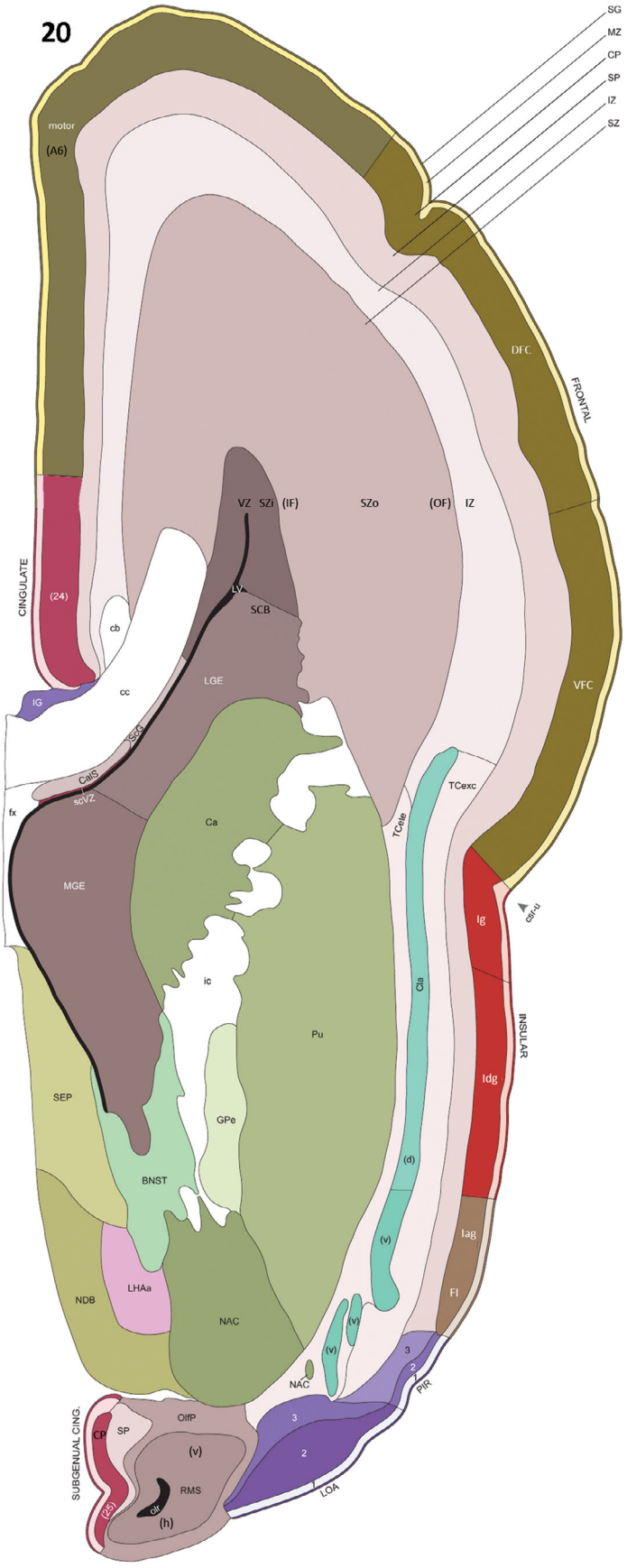

Level 20 (02-179)

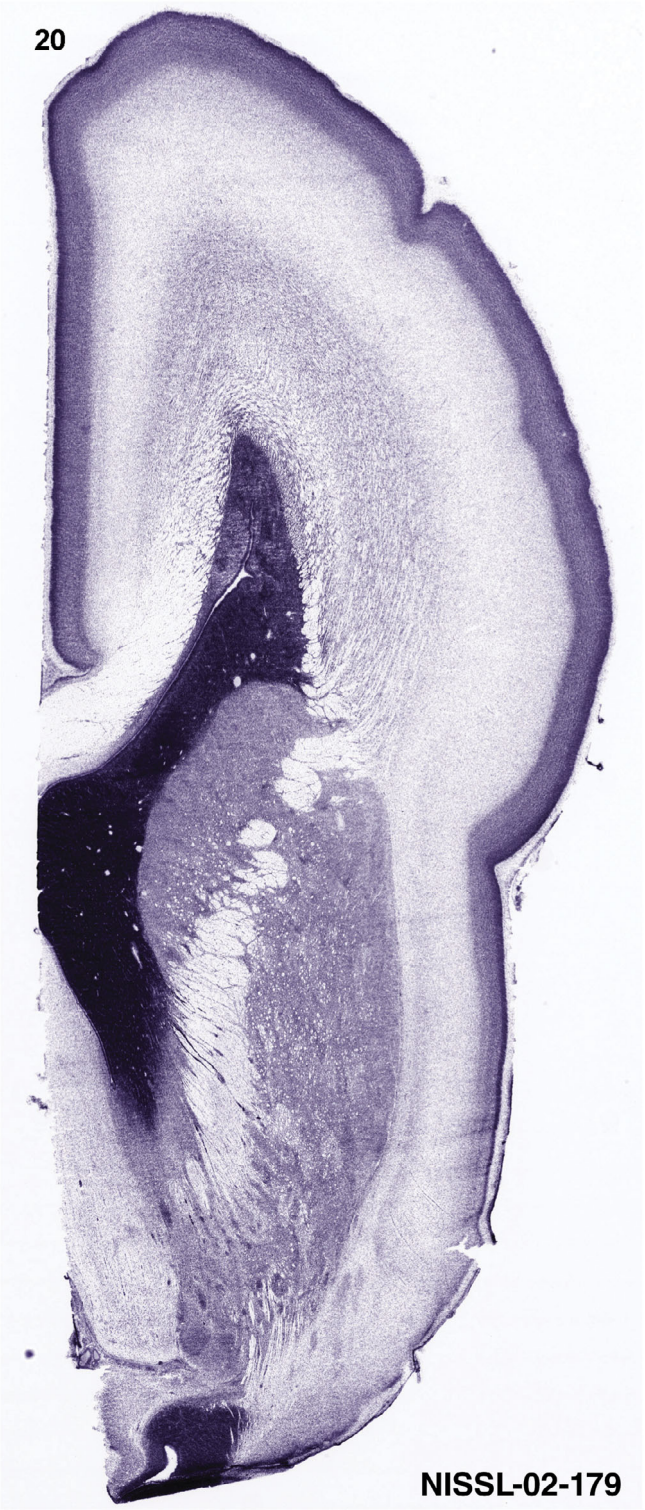
20
NISSL-02-179

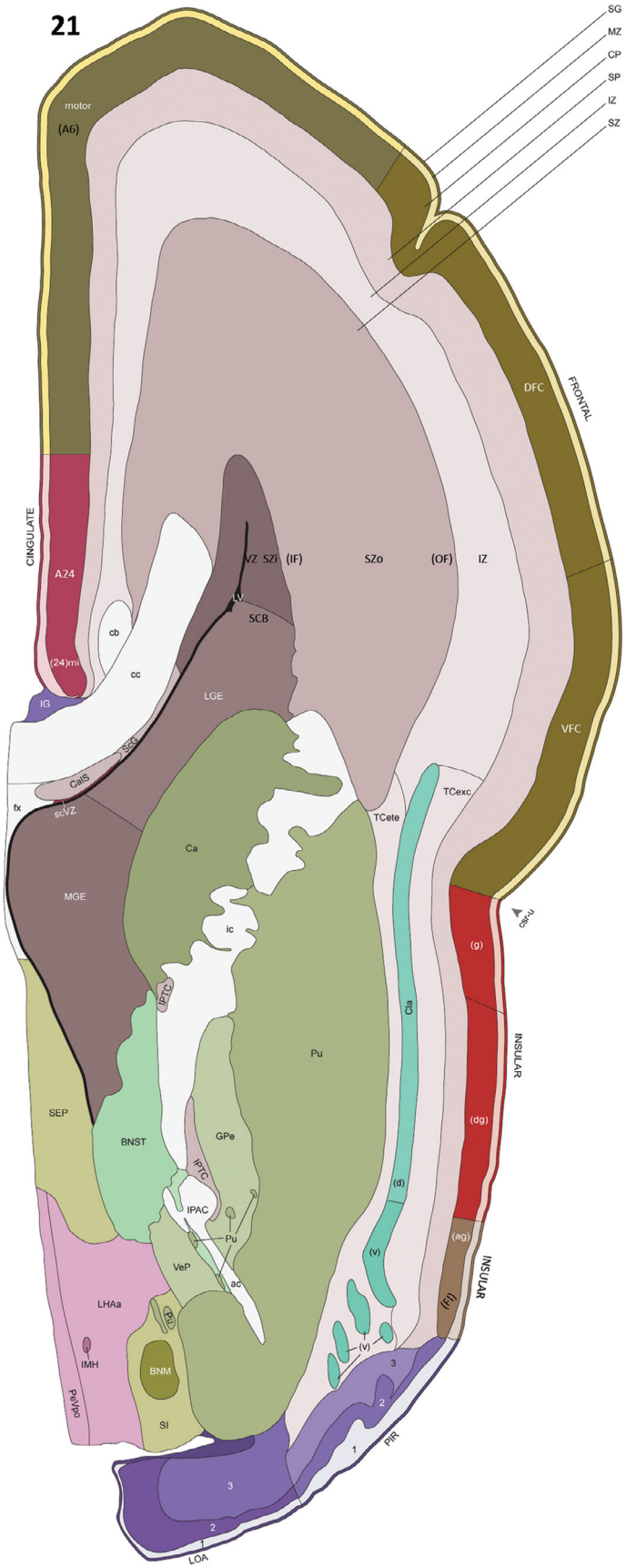

Level 21 (02-204)

21
NISSL-02-204

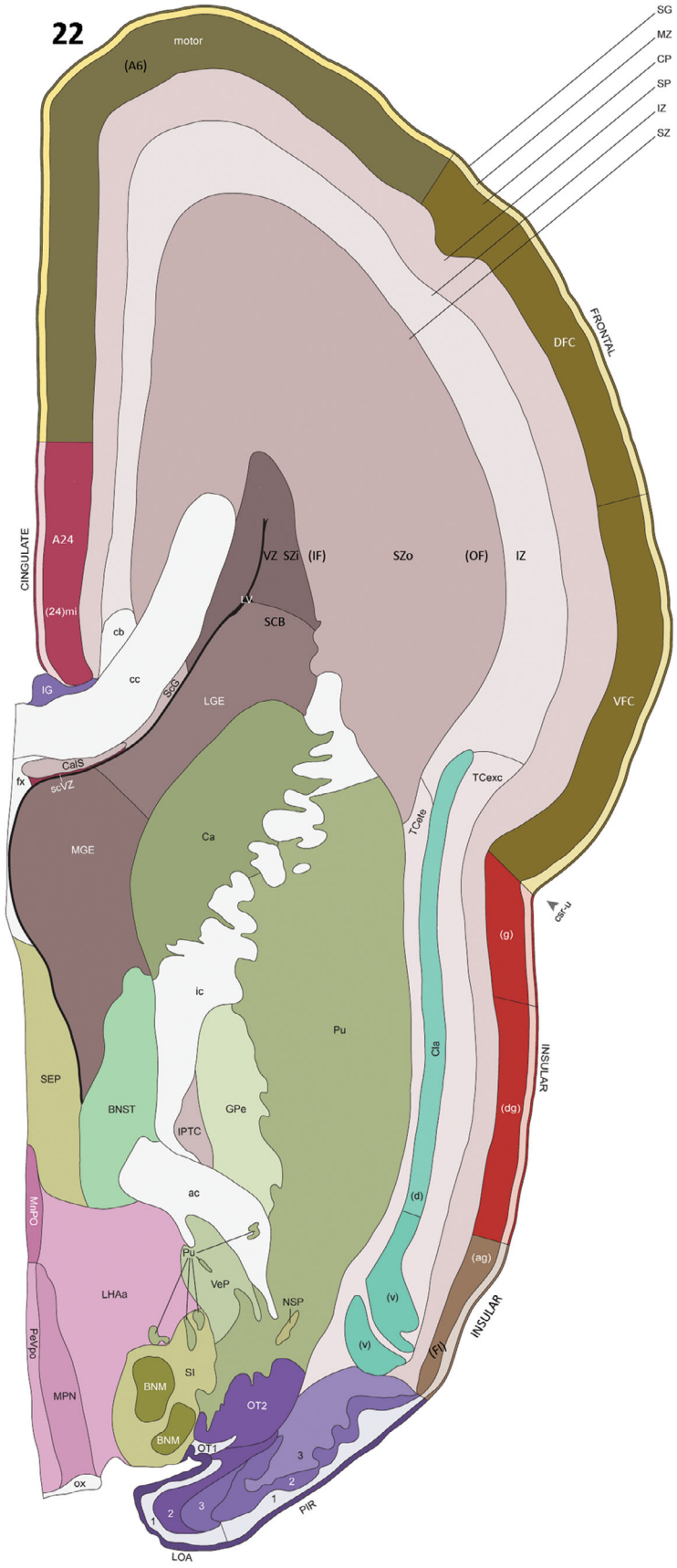

Level 22 (02-230)

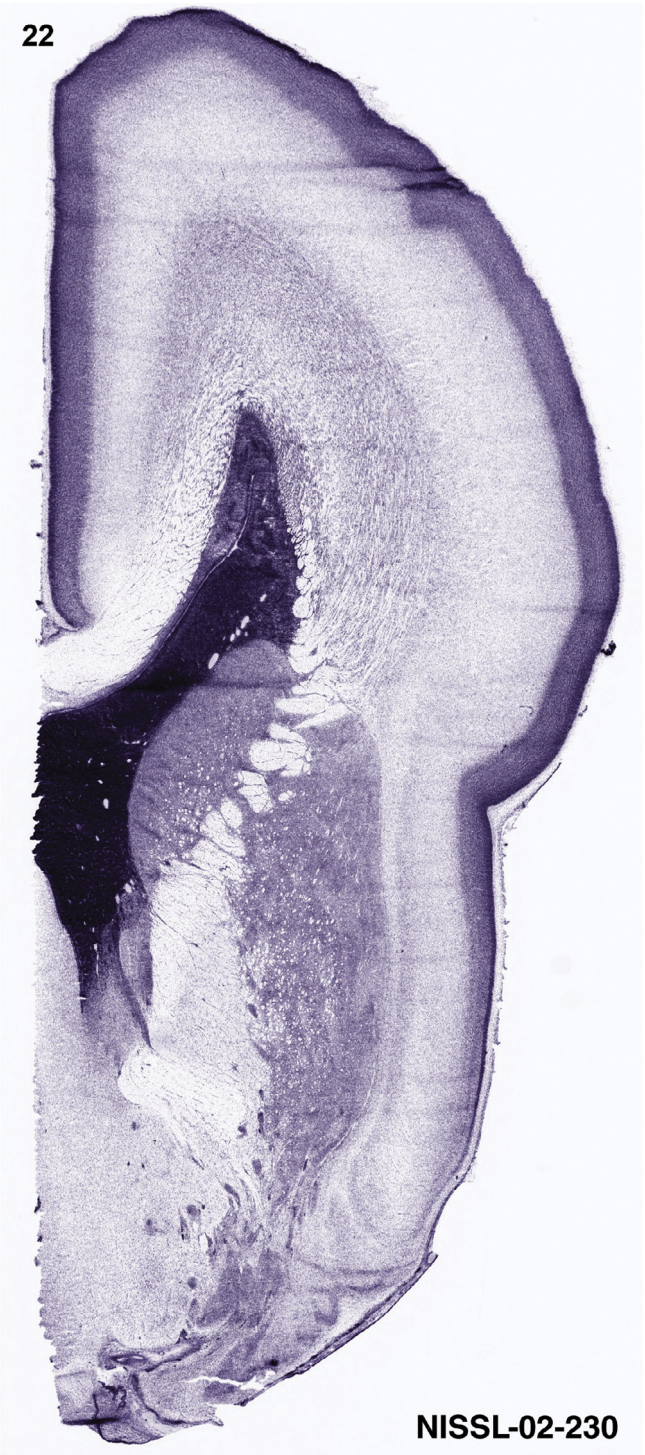
22
NISSL-02-230

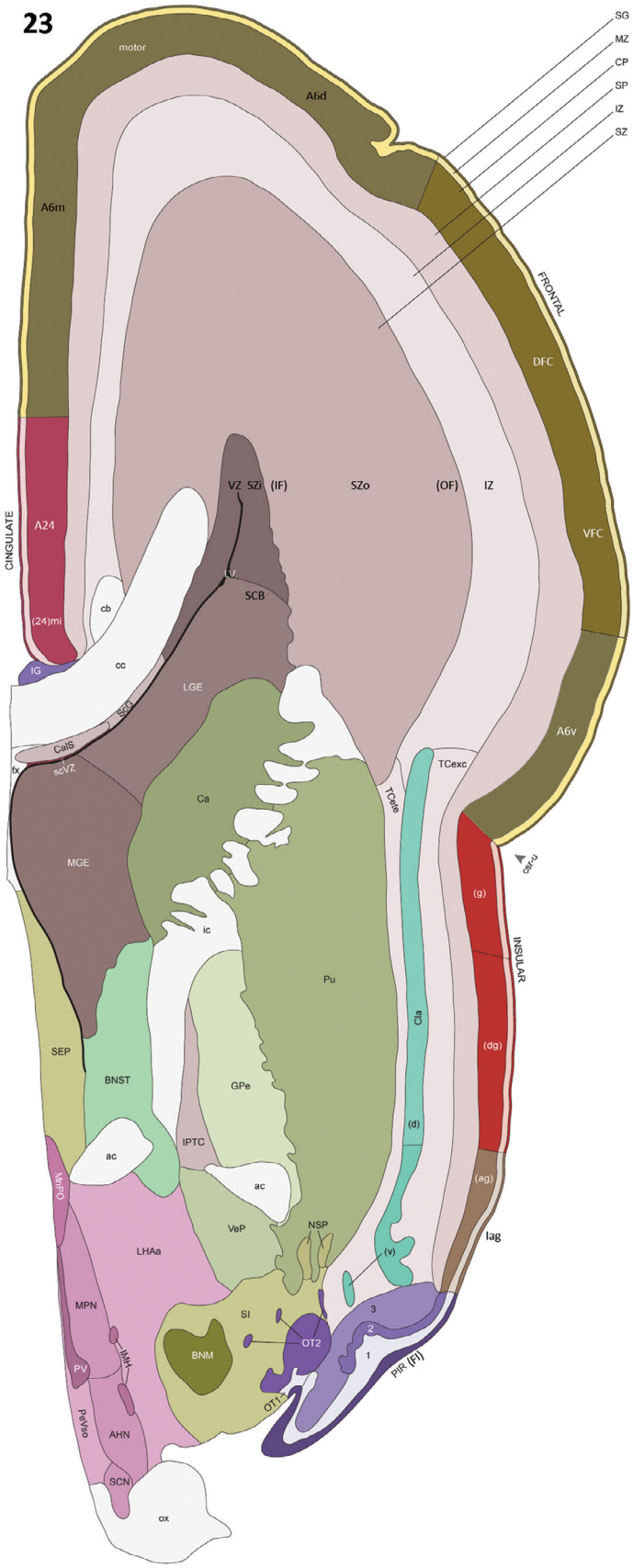

Level 23 (02-255)

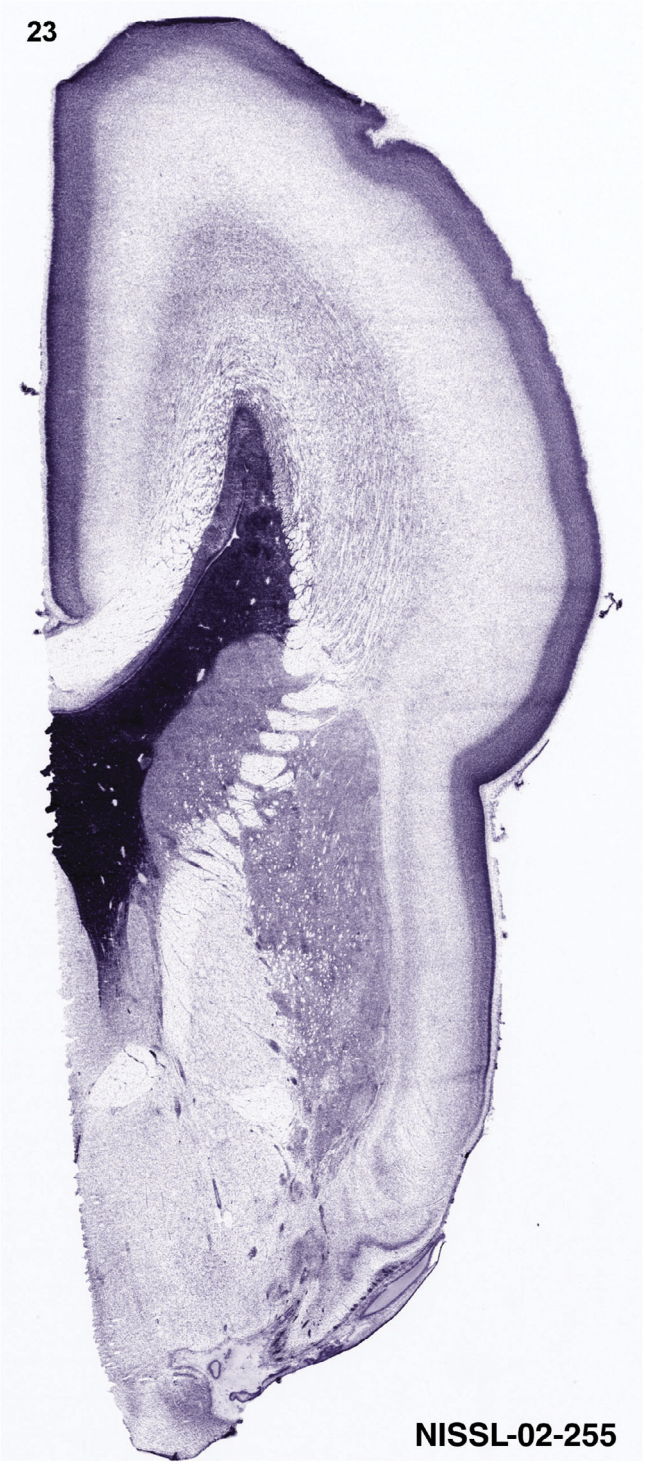
23
NISSL-02-255

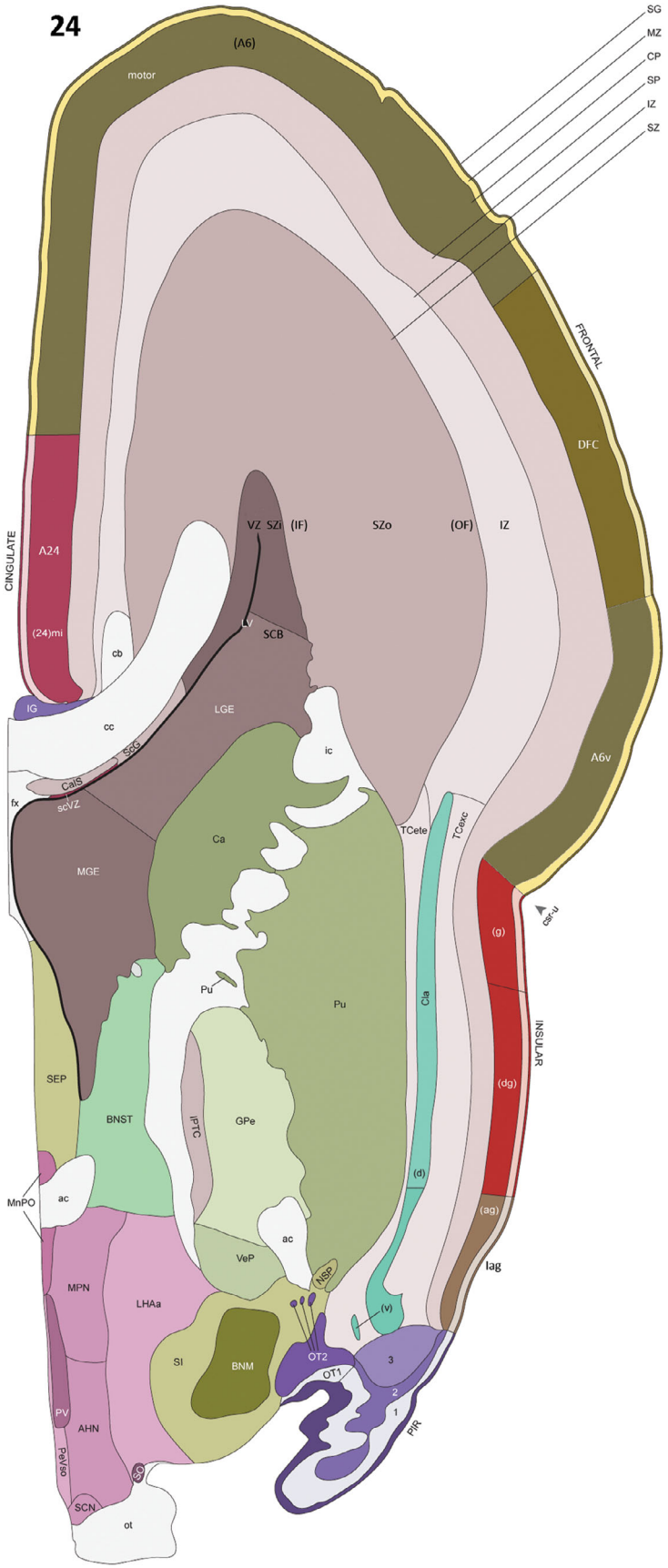

Level 24 (02-281)

24
NISSL-02-281

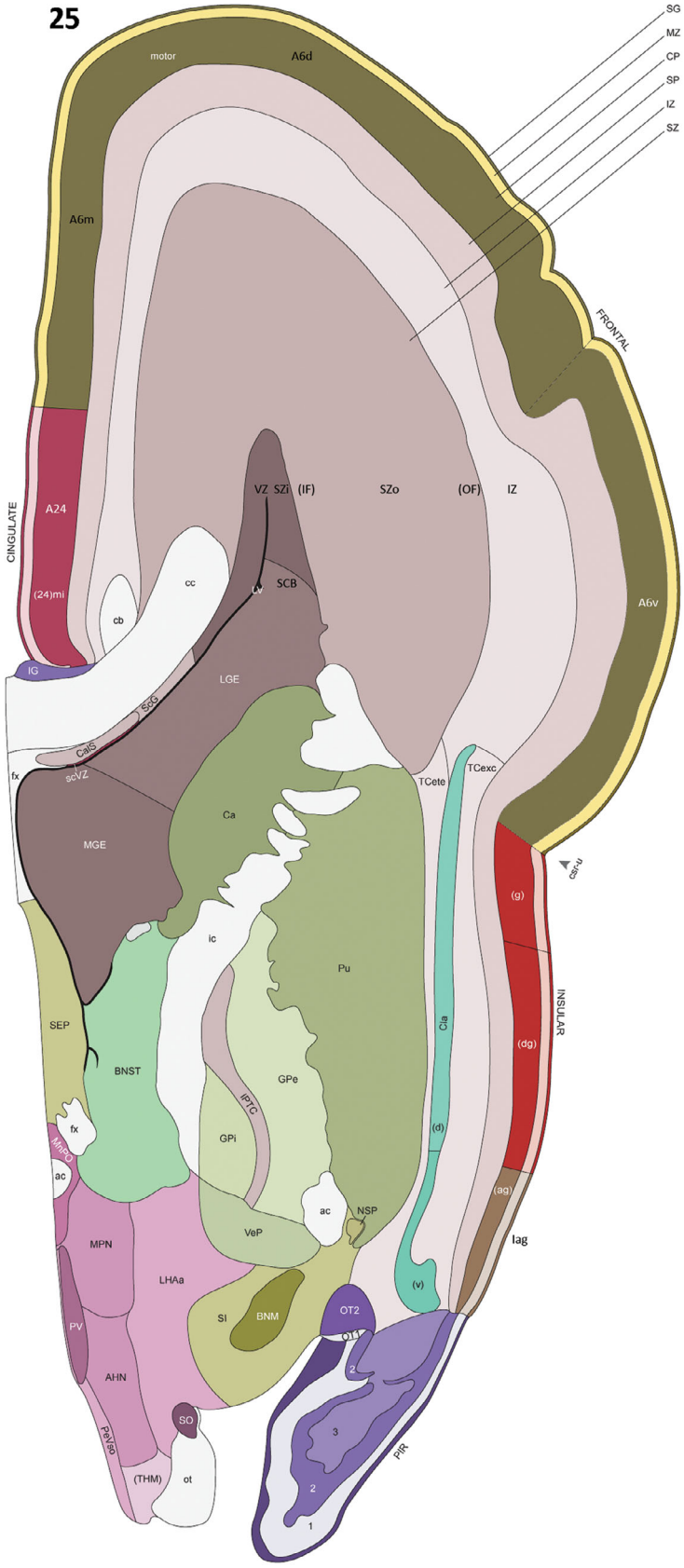

Level 25 (02-306)

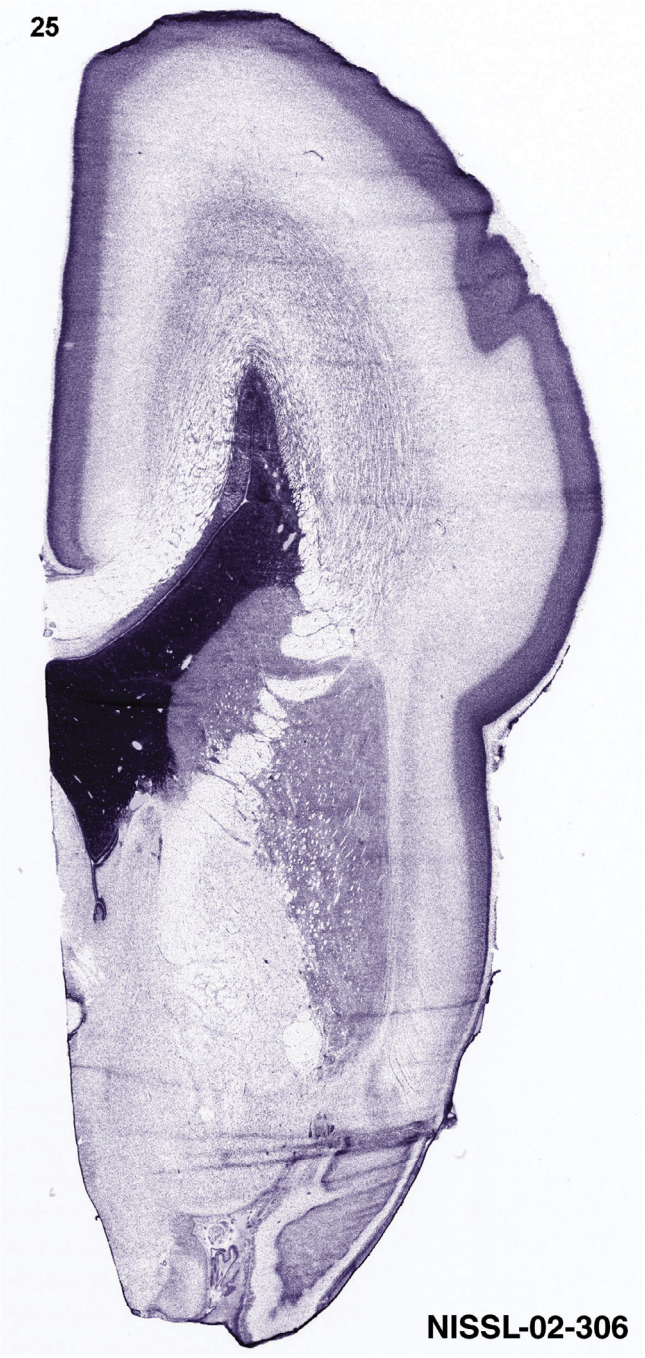
25
NISSL-02-306

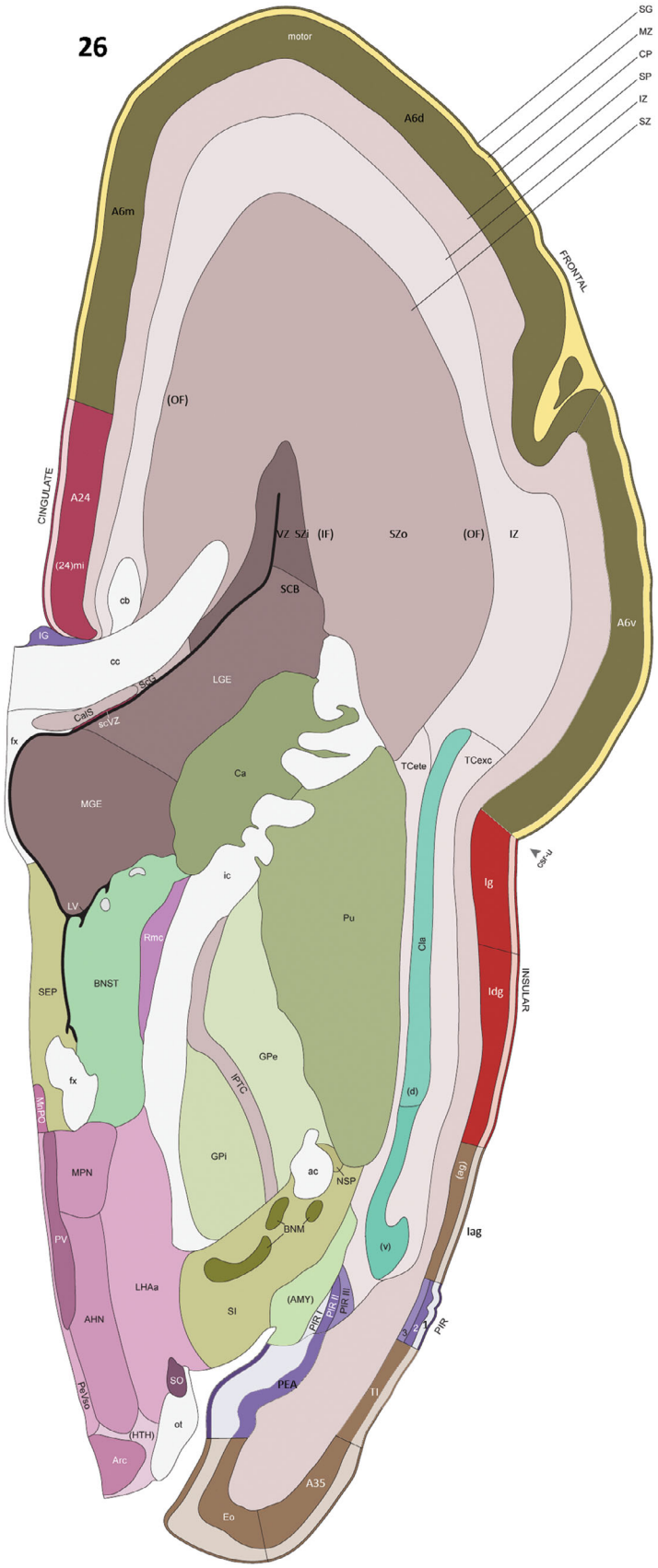

Level 26 (02-332)

26
NISSL-02-332

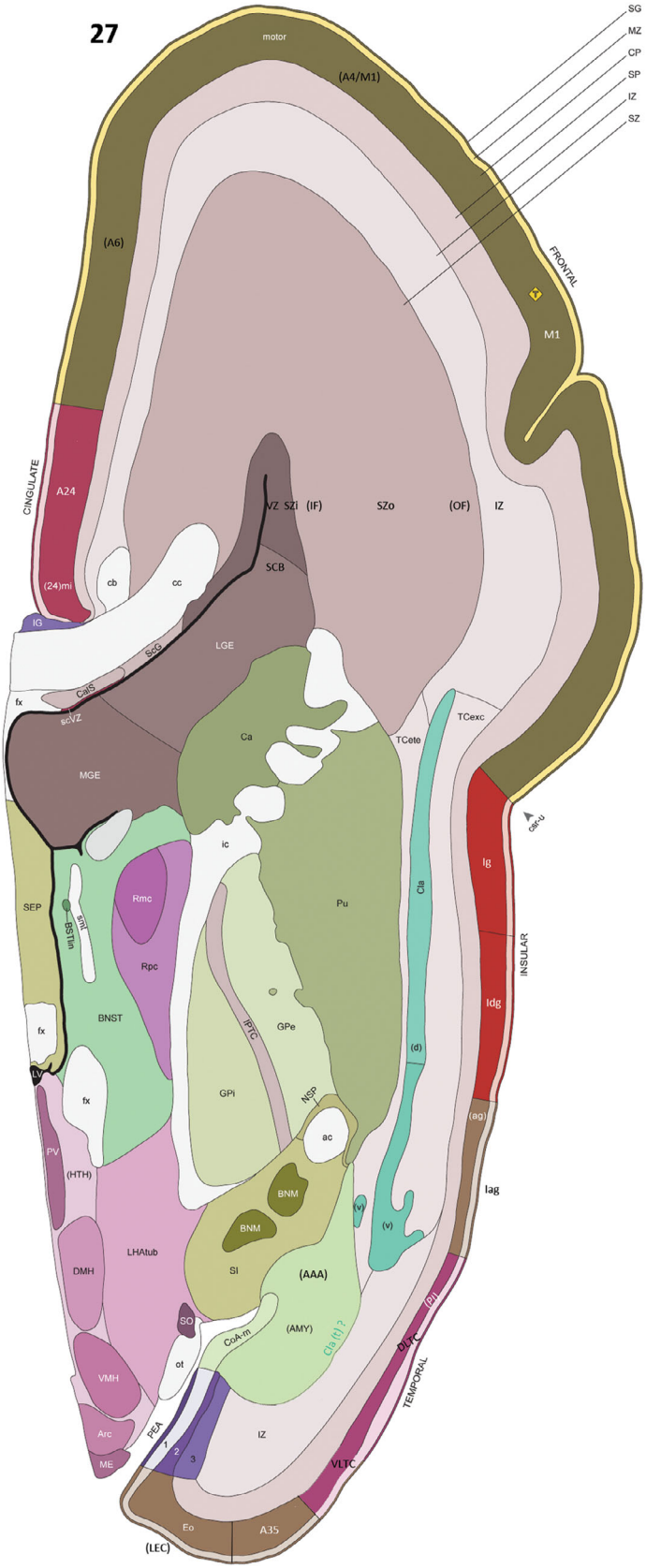

Level 27 (02-357)

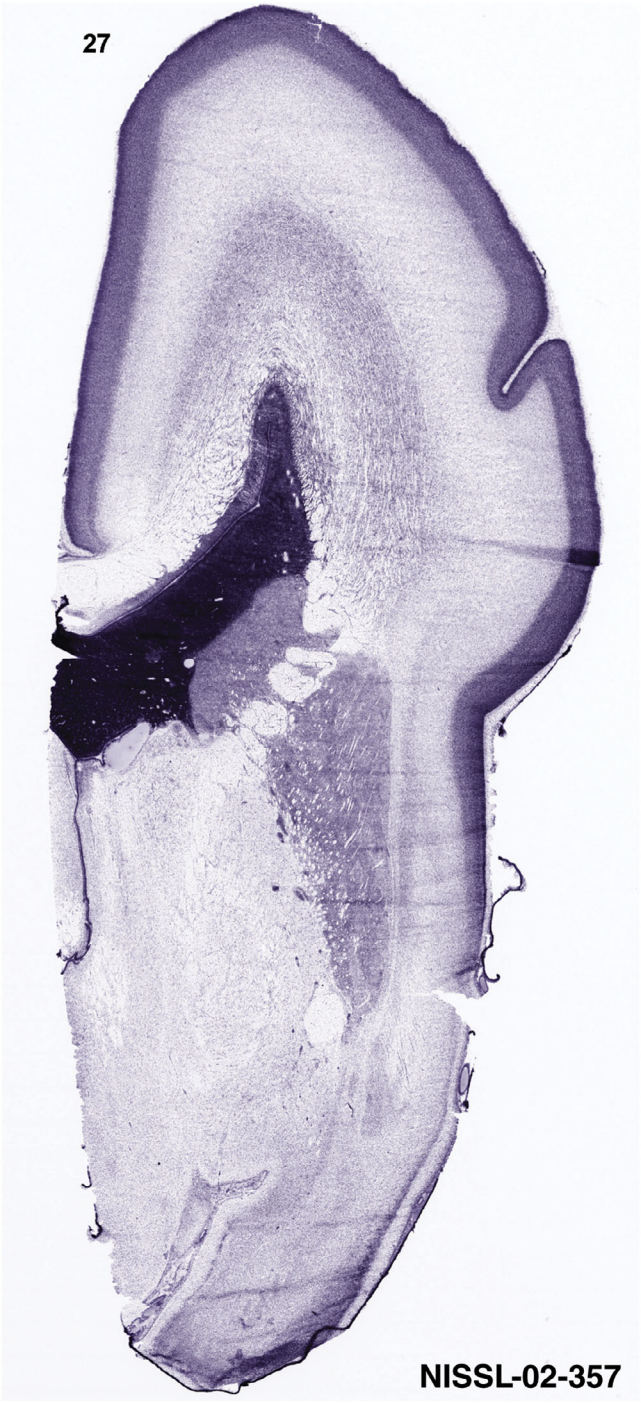
27
NISSL-02-357

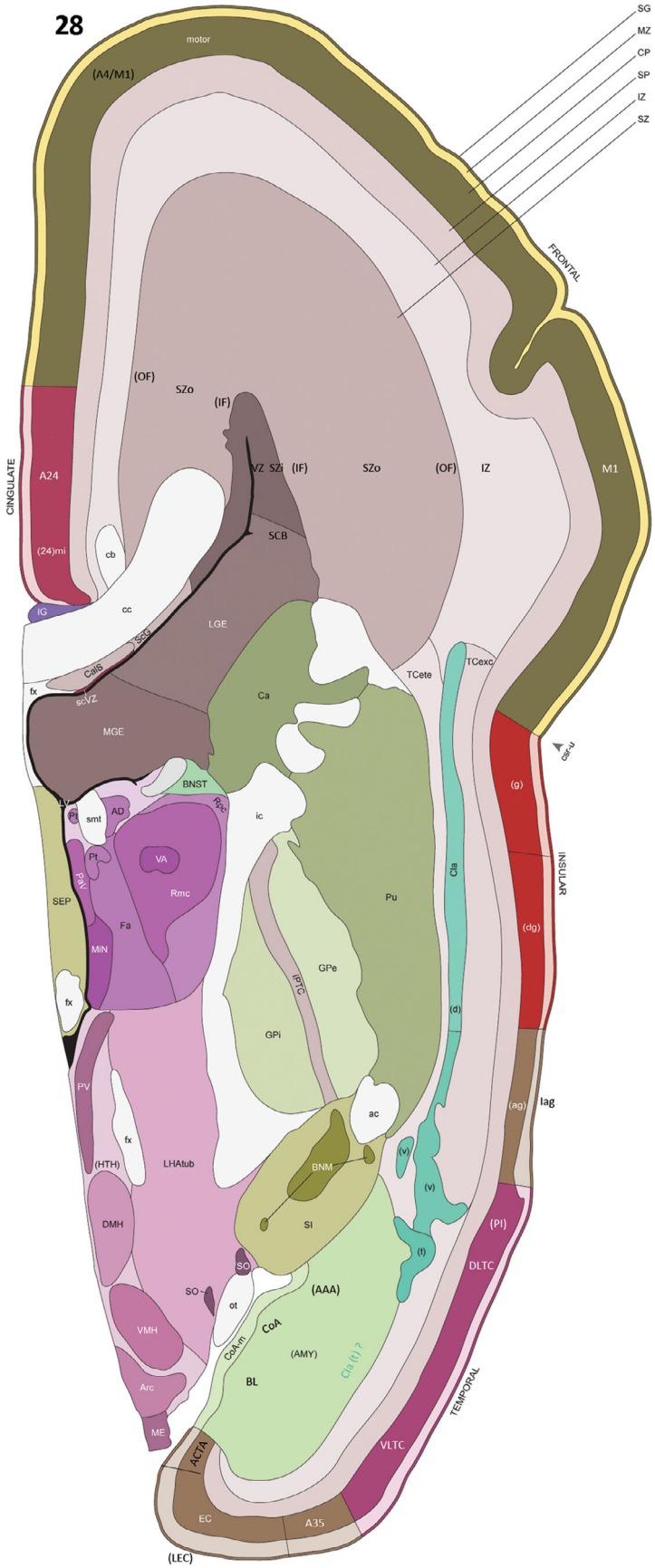

Level 28 (02-383)

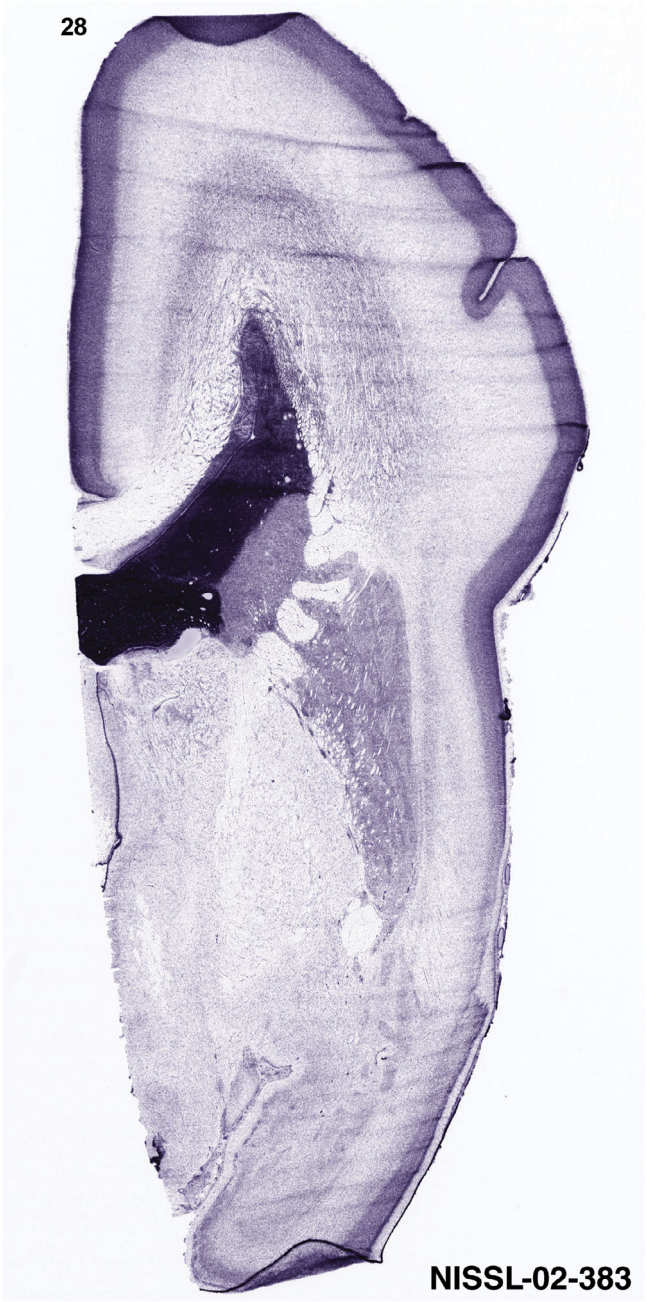
28
NISSL-02-383

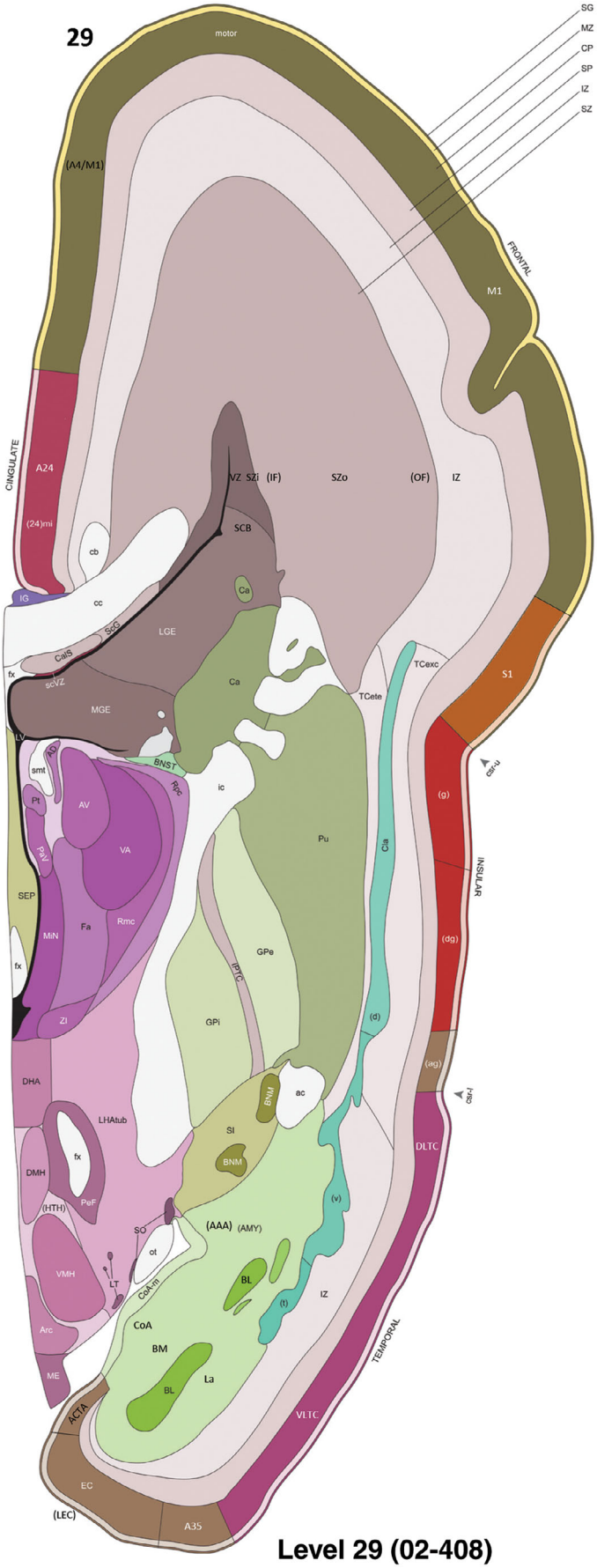

Level 29 (02-408)

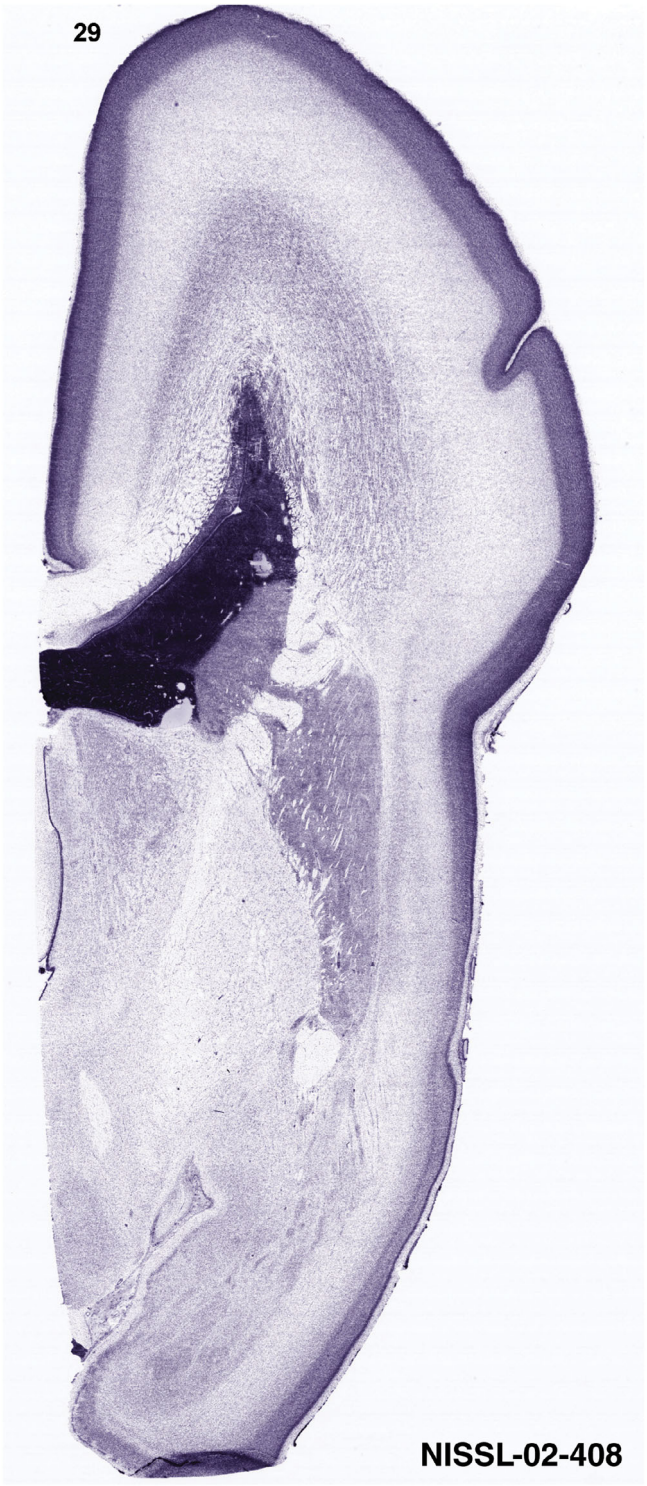
29
NISSL-02-408

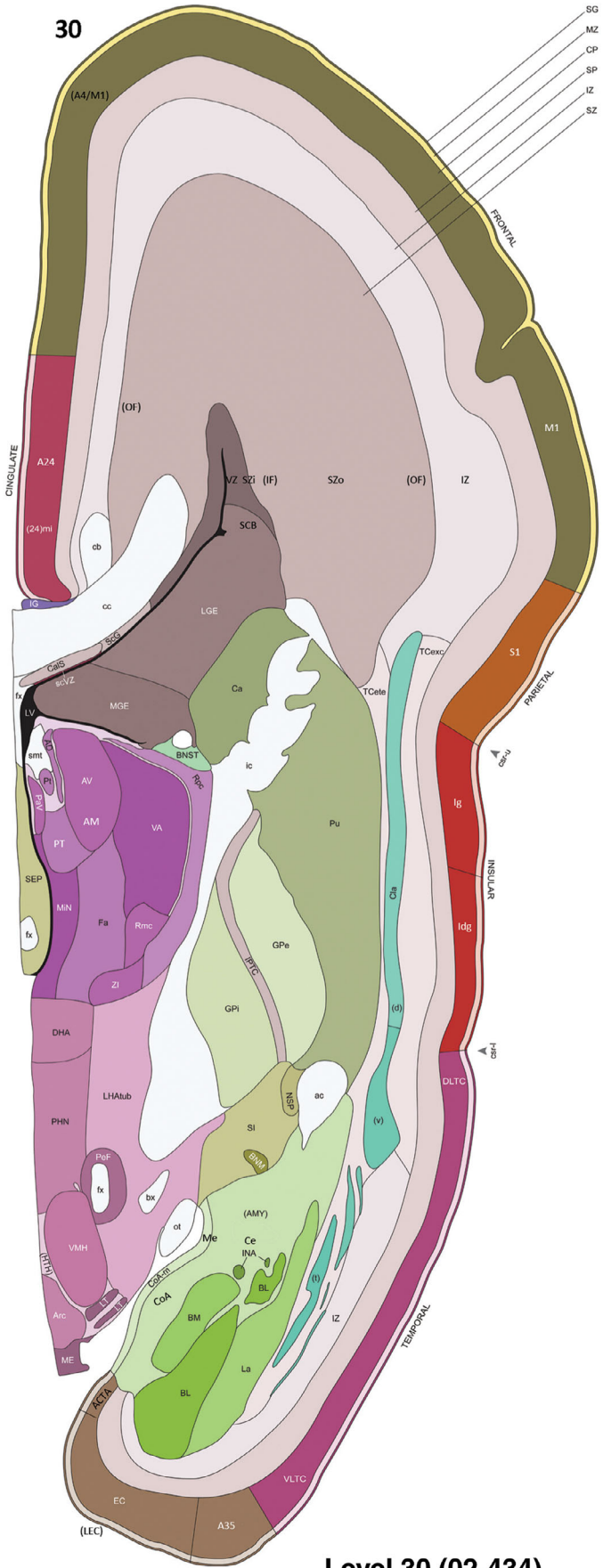

Level 30 (02-434)

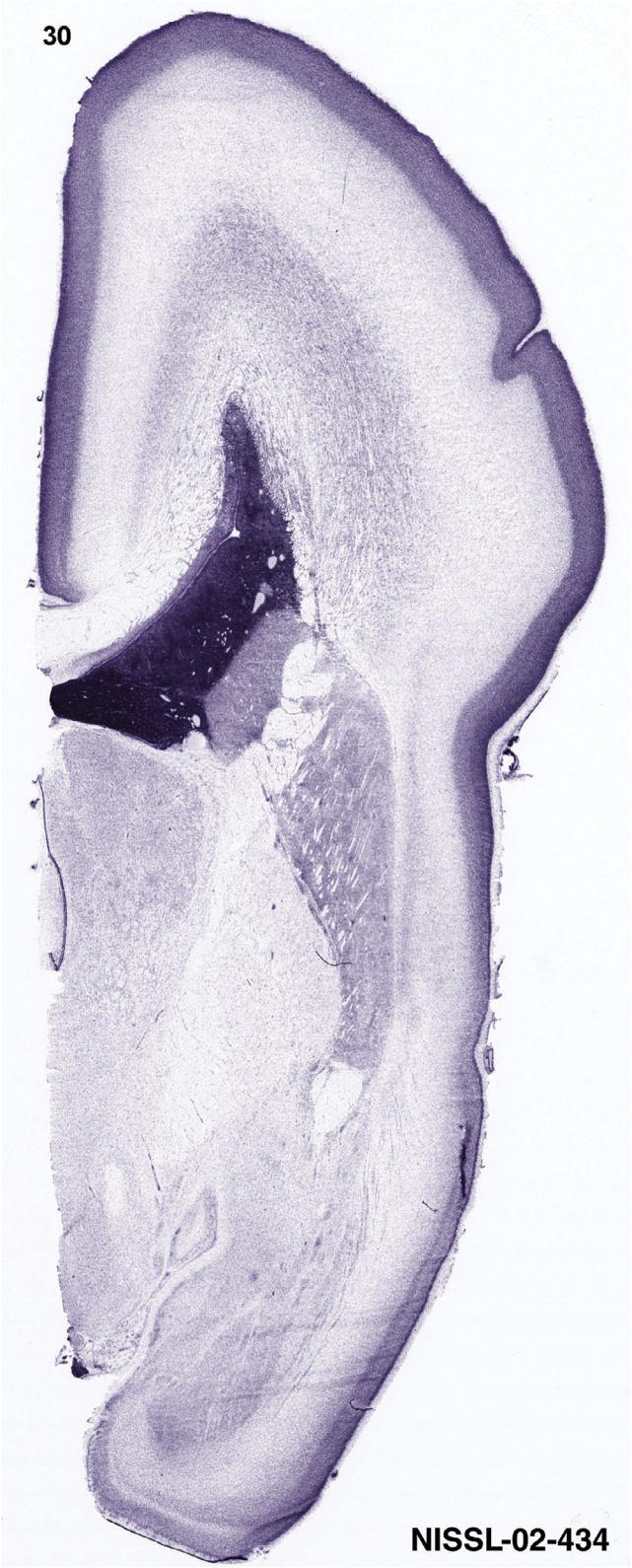
30
NISSL-02-434

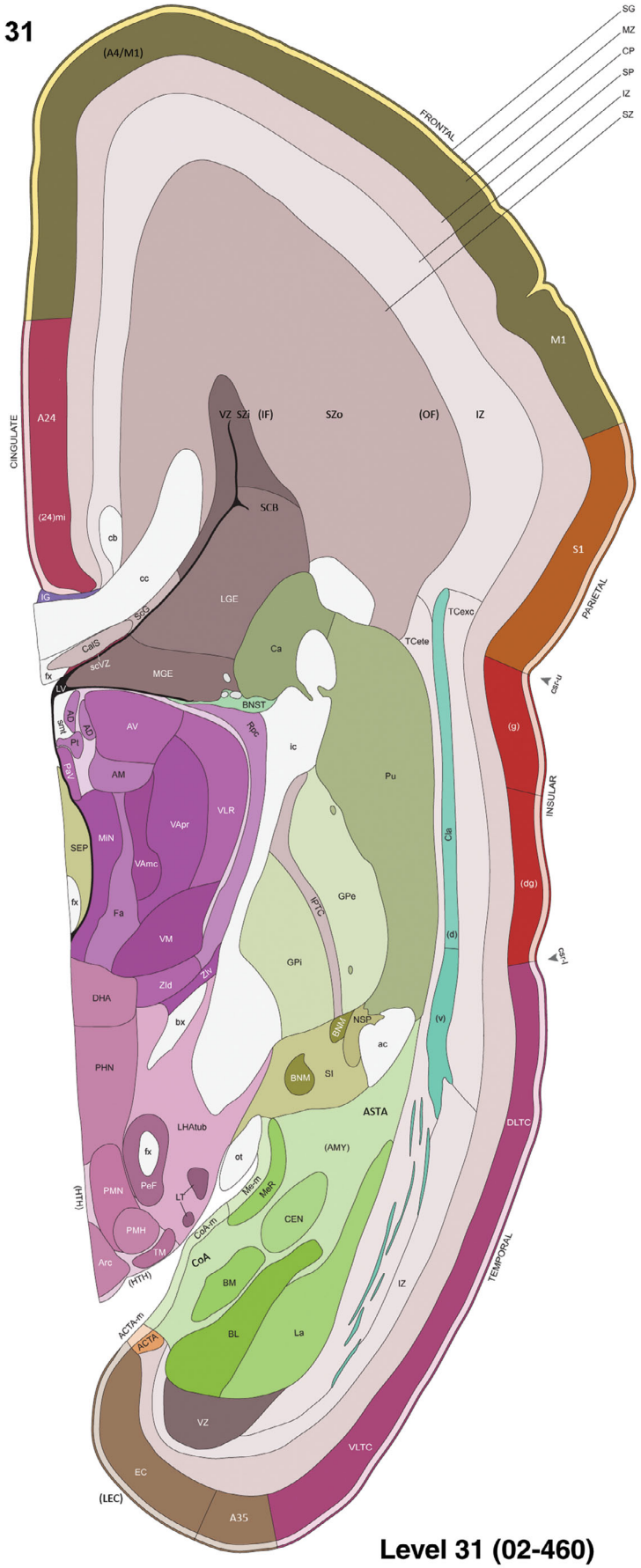

Level 31 (02-460)

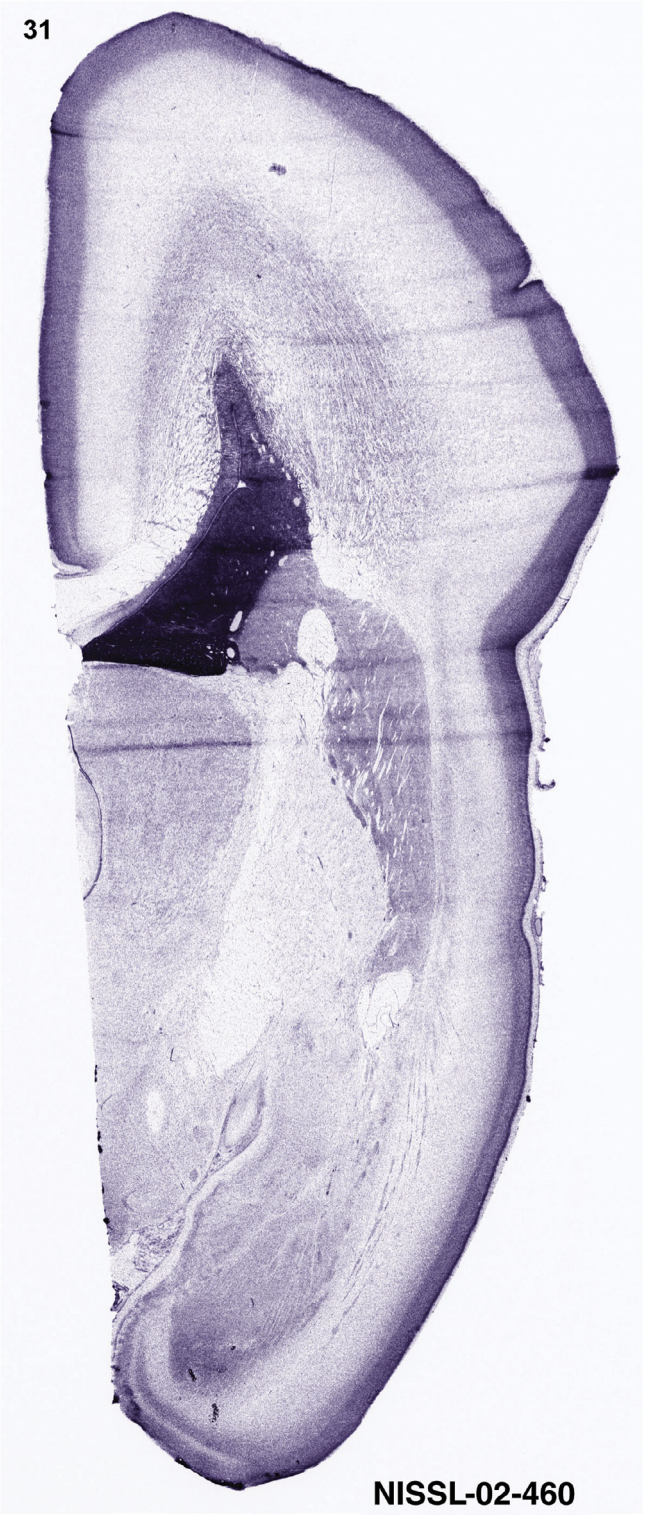
31
NISSL-02-460

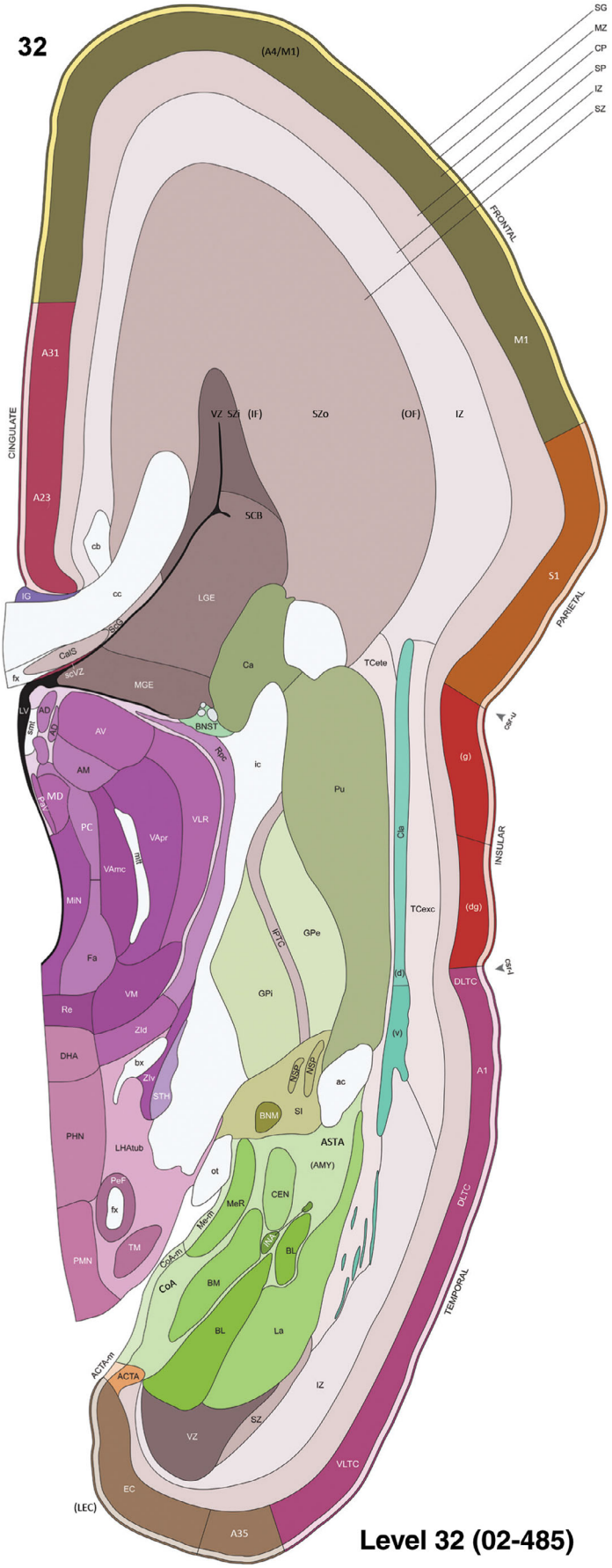
32
(A4/M1)
SG
MZ
CP
SP
IZ
SZ
FRONTAL
M1
A31
CINGULATE
A23
VZ SZi (IF)
SZo
(OF)
IZ
SCB
cb
cc
IG
LGE
S1
PARIETAL
CalS
scVZ
fx
MGE
Ca
TCete
BNST
LV
AD
AV
AM
MD
PC
VApr
VLR
VAmc
mt
MIN
Fa
VM
Re
Zld
DHA
bx
Zlv
STH
PHN
LHAtub
PeF
fx
TM
PMN
Rpc
ic
Pu
Cla
TCexc
(g)
(dg)
INSULAR
GPe
IPTG
GPi
(d)
(v)
DLTC
A1
NSP
ac
BNM
SI
ASTA
(AMY)
ot
CEN
MeR
Me.m
BL
CoA.m
CoA
BM
BL
La
ACTA.m
ACTA
IZ
SZ
VZ
VLTC
TEMPORAL
EC
(LEC)
A35
Level 32 (02-485)

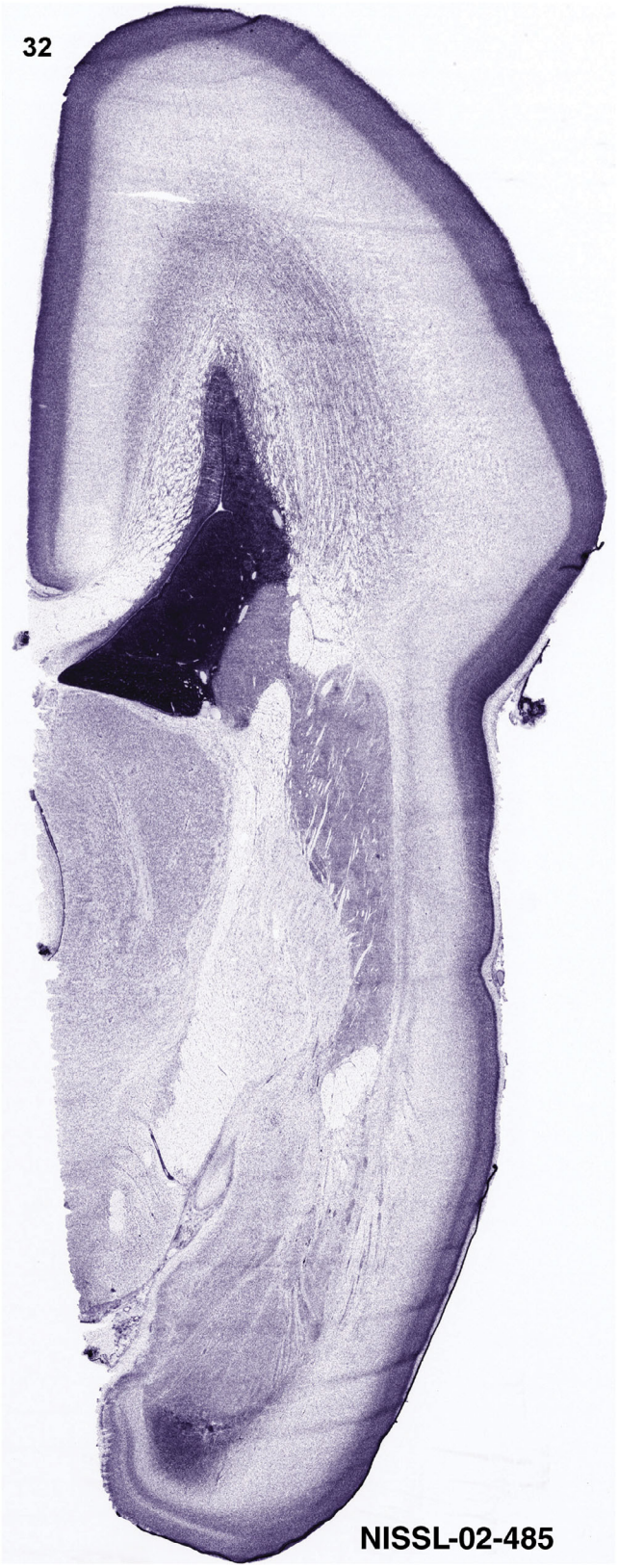
32
NISSL-02-485

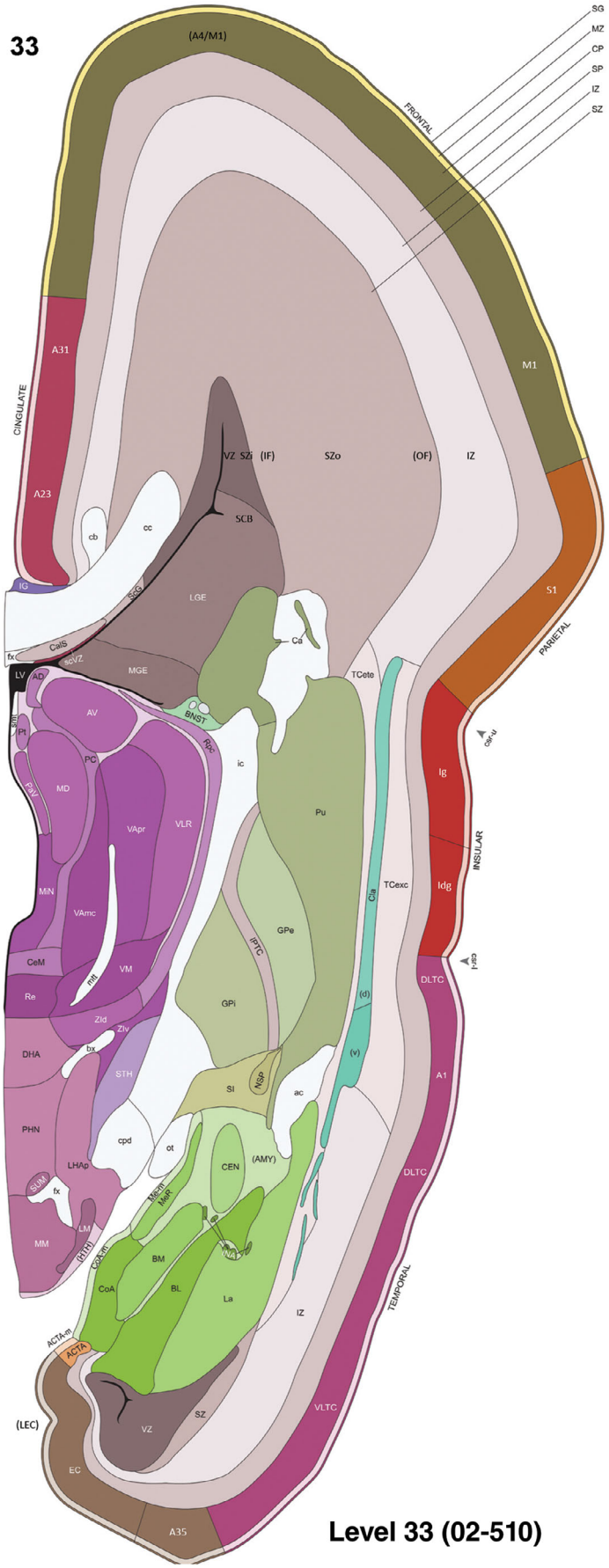
33
(A4/M1)
SG
MZ
CP
SP
IZ
SZ
FRONTAL
M1
A31
CINGULATE
A23
VZ SZi (IF)
SZo
(OF)
IZ
SCB
cb
cc
IG
fxg
LGE
S1
PARIETAL
fx
CaIS
acVZ
MGE
Ca
LV
AD
TCete
AV
BNST
sm
PI
Rpc
ic
PC
MD
Pu
VApr
VLR
lg
INSULAR
MiN
VAmc
TCexc
ldg
GPe
CeM
VM
mtt
IPTC
Re
GPi
DLTC
Zld
Zlv
(d)
DHA
bx
STH
(v)
A1
SI
NsP
ac
PHN
cpd
ot
LHAp
CEN
(AMY)
SUM
fx
Mam
MaR
DLTC
LM
MM
(mtt)
cxx.in
BM
CoA
BL
La
IZ
TEMPORAL
ACTAvp
ACTA
(LEC)
VZ
SZ
VLTC
EC
A35
Level 33 (02-510)

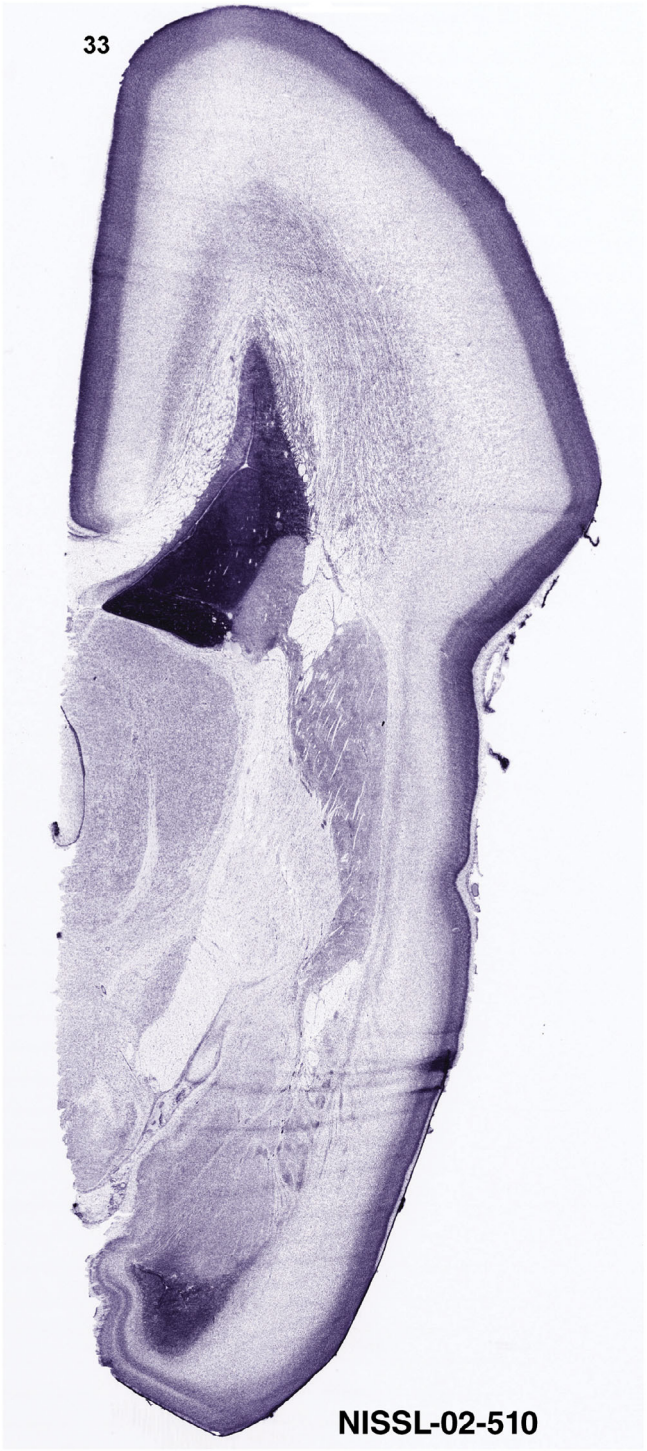
33
NISSL-02-510

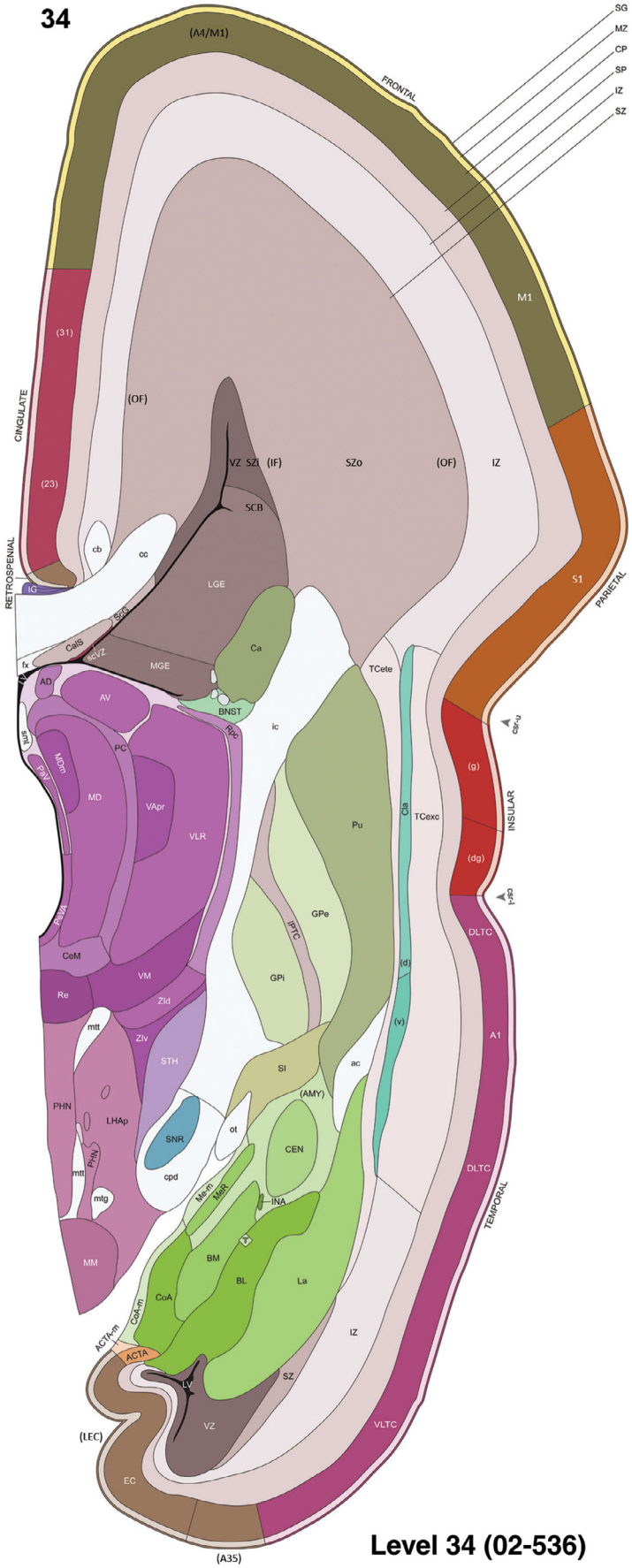

Level 34 (02-536)

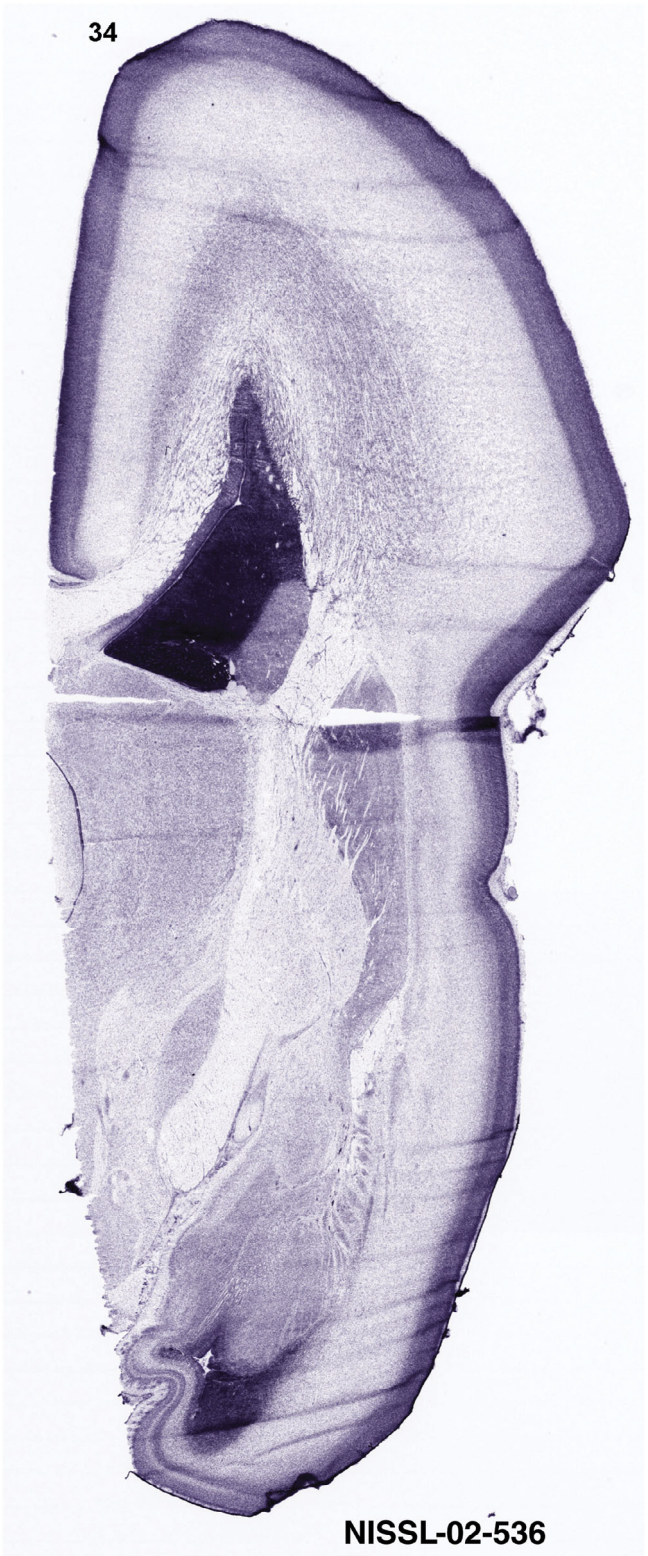
34
NISSL-02-536

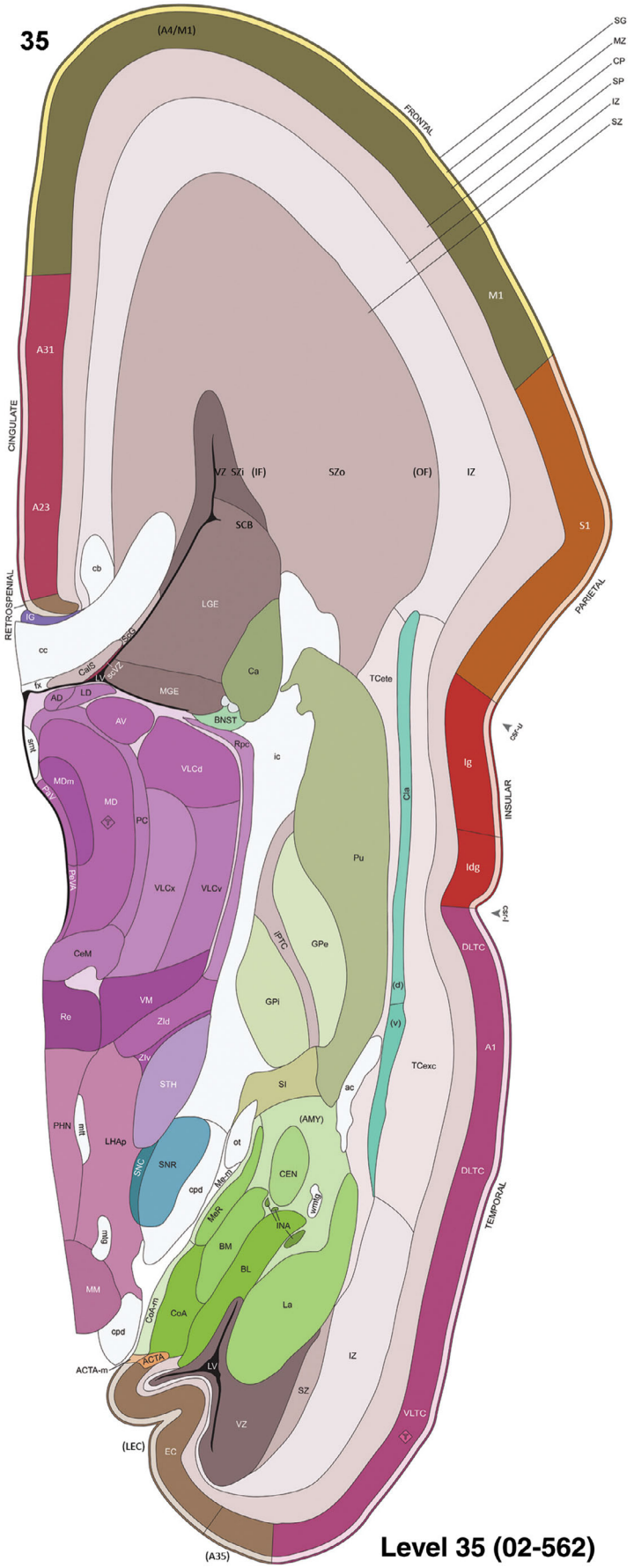
35
(A4/M1)
SG
MZ
CP
SP
IZ
SZ
FRONTAL
M1
A31
CINGULATE
A23
RETROSPENIAL
VZ SZi (IF)
SZo
(OF)
IZ
SCB
S1
PARIETAL
cb
LGE
IG
cc
CaIS
sSS
LV
sVZ
lx
MGE
Ca
TCete
AD
LD
AV
BNST
sm
Rpc
ic
lg
INSULAR
MDm
VLCd
MD
PC
PVT
VLCx
VLCv
Pu
Cla
ldg
PFM
CeM
GPe
iPTC
DLTC
VM
Re
Zld
GPi
(d)
(v)
A1
Zlv
STH
SI
ac
TCexc
PHN
mt
LHAp
(AMY)
ot
SNR
SNC
cpd
MenD
CEN
vmg
MeR
INA
mtg
BM
BL
MM
CoA-m
CoA
La
cpd
ACTA-m
ACTA
LV
IZ
SZ
VZ
VLTC
(LEC)
EC
(A35)
Level 35 (02-562)

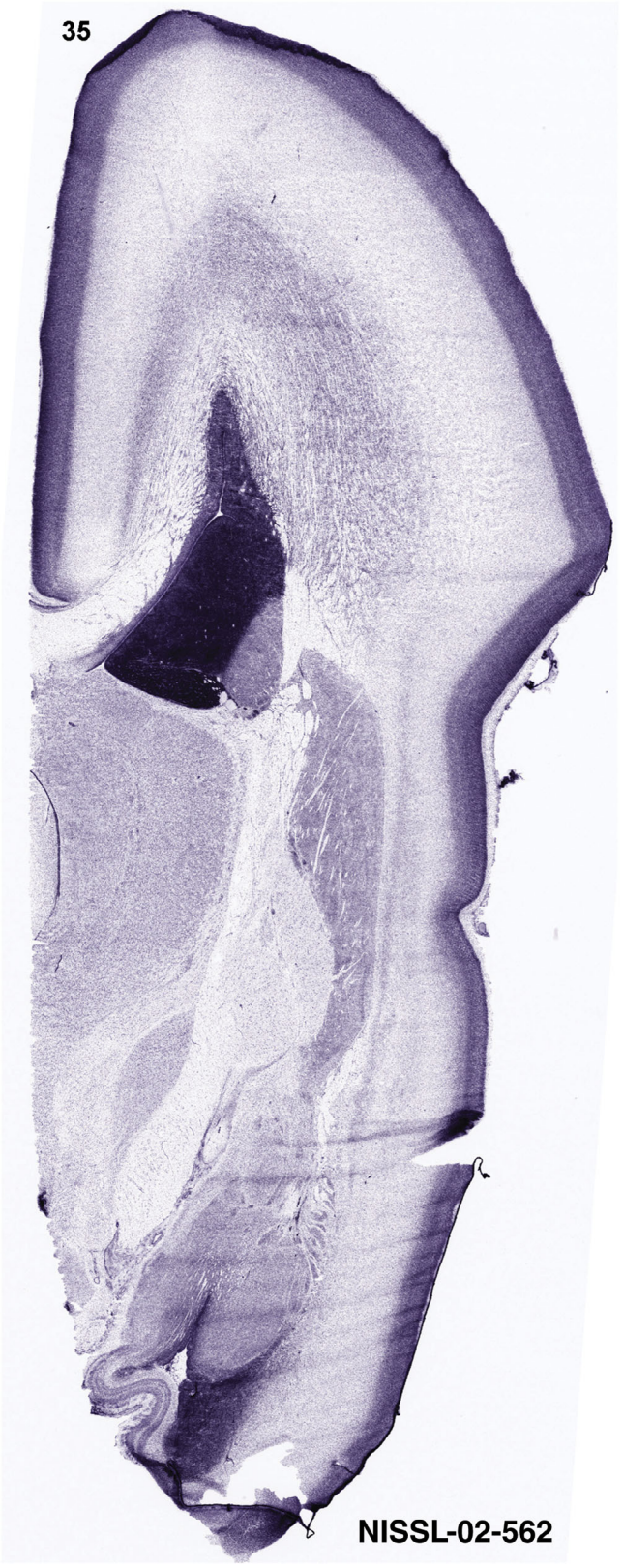
35
NISSL-02-562

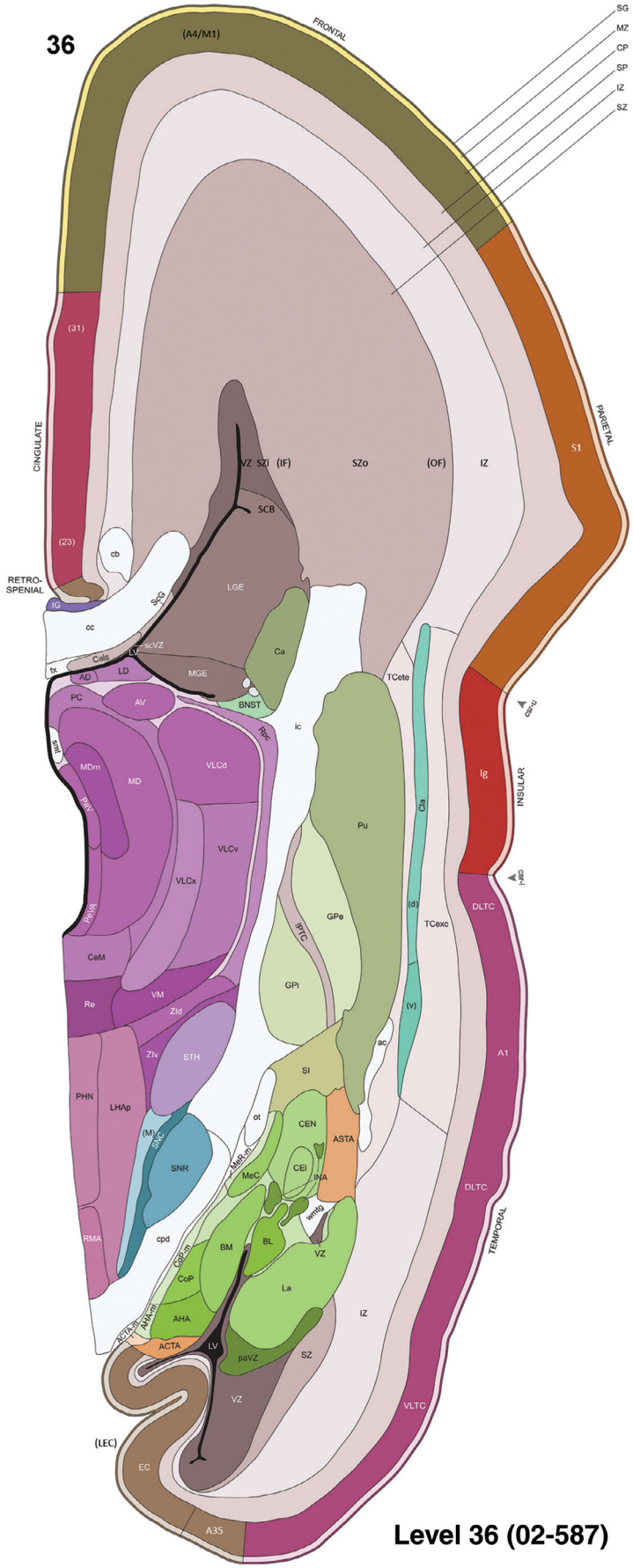
36
(A4/M1)
FRONTAL
SG
MZ
CP
SP
IZ
SZ
(31)
CINGULATE
(23)
RETRO-
SPENIAL
VZ SZI (IF)
SZo
(OF)
IZ
PARIETAL
S1
SCB
cb
LGE
IG
ScG
cc
scVZ
LV
Cals
fx
AD
LD
MGE
Ca
PC
AV
BNST
ic
TCete
csl-u
Rpc
sml
MDm
MD
VLCd
Cla
Ig
INSULAR
Pu
VLCv
VLCx
csl-l
GPe
(d)
TCexc
DLTC
IPTC
CeM
GPi
Re
VM
Zld
(v)
ac
Zlv
STH
A1
SI
PHN
LHAp
(M)
SNC
ot
CEN
ASTA
SNR
MeC
CEl
INA
DLTC
wmtg
RMA
cpd
BM
BL
VZ
CoP
La
IZ
AHA
ACTA
LV
paVZ
SZ
VZ
VLTC
(LEC)
EC
A35
Level 36 (02-587)

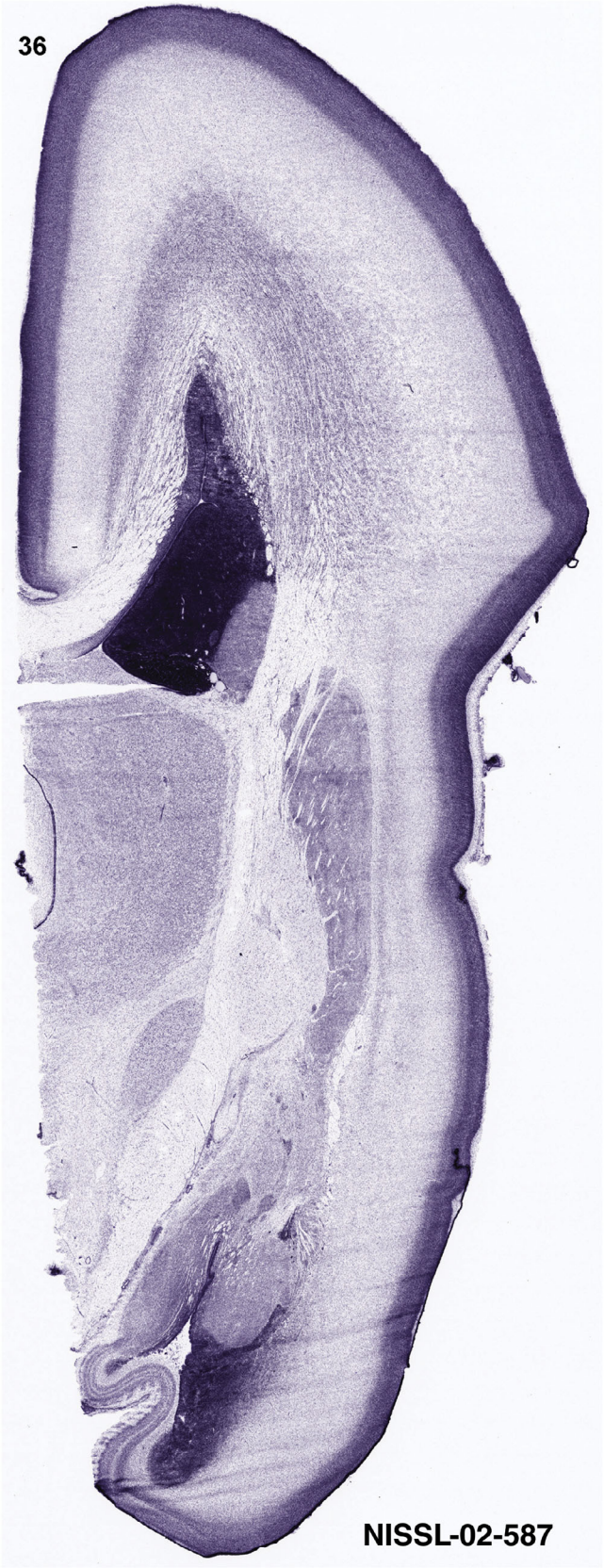
36
NISSL-02-587

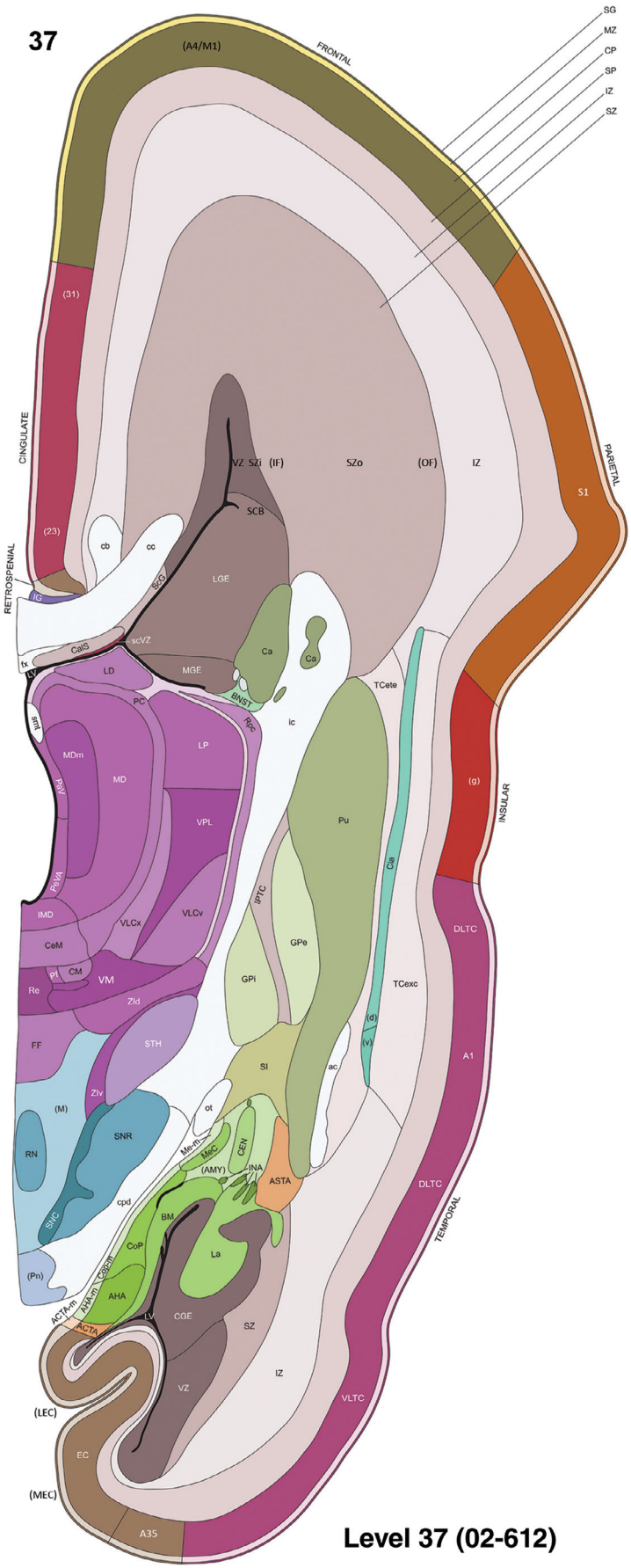

Level 37 (02-612)

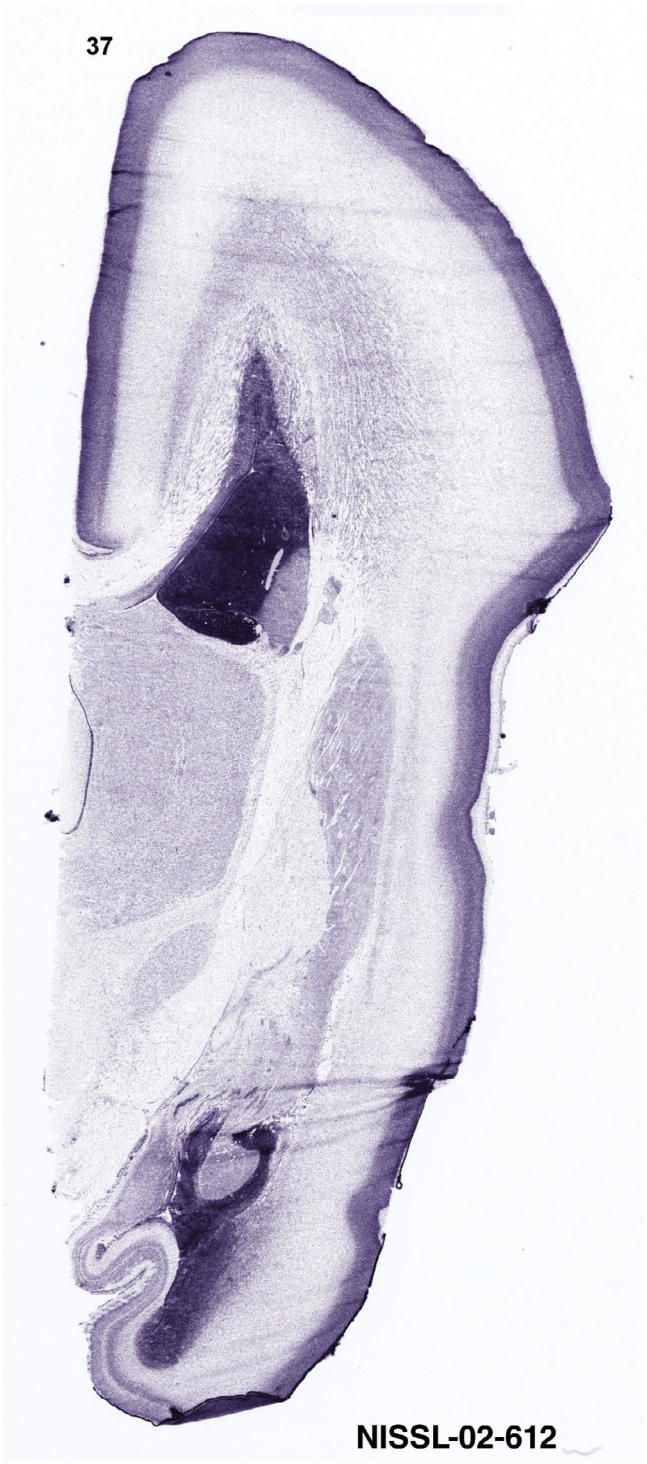
37
NISSL-02-612

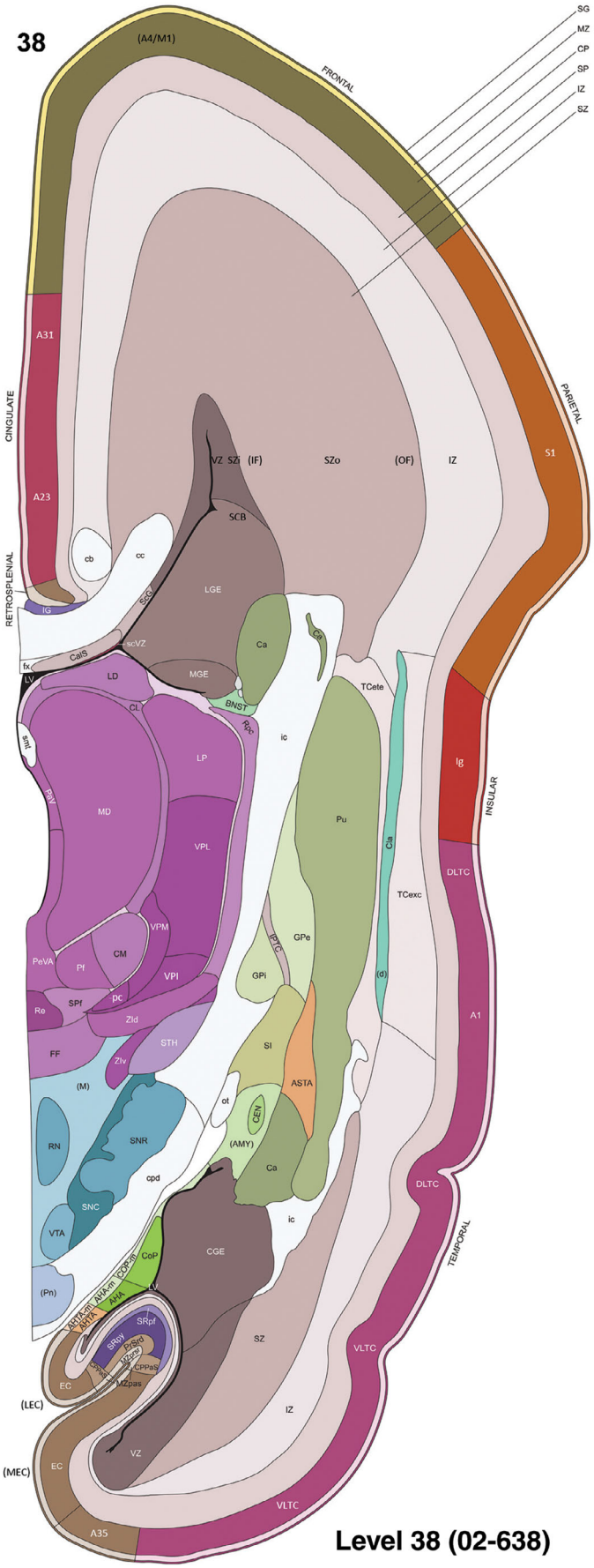

Level 38 (02-638)

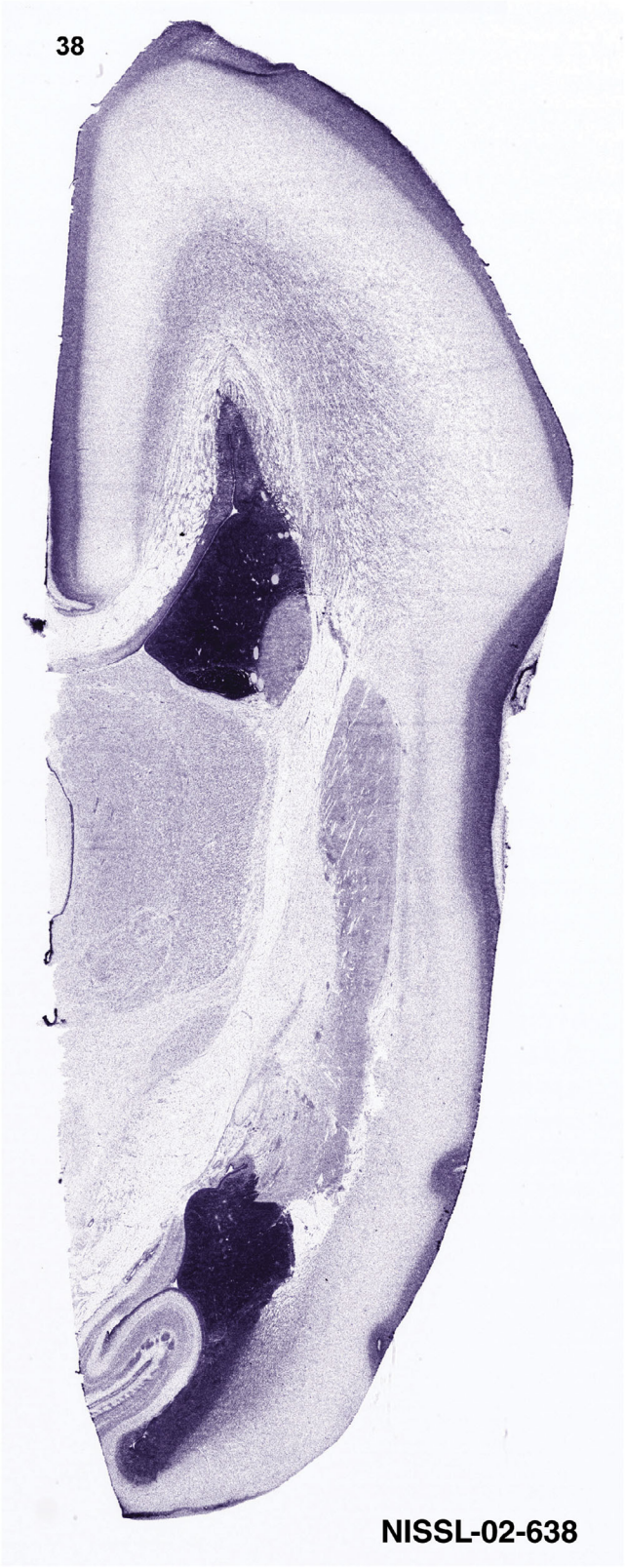
38
NISSL-02-638

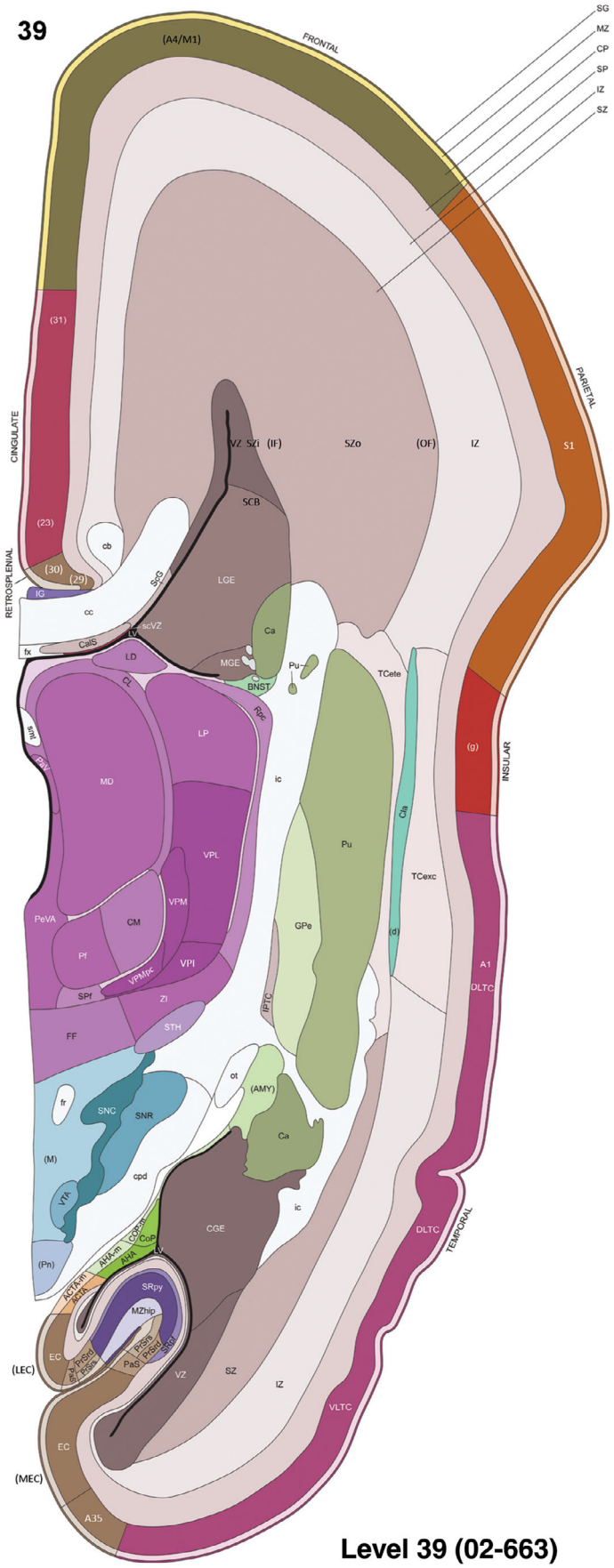

Level 39 (02-663)

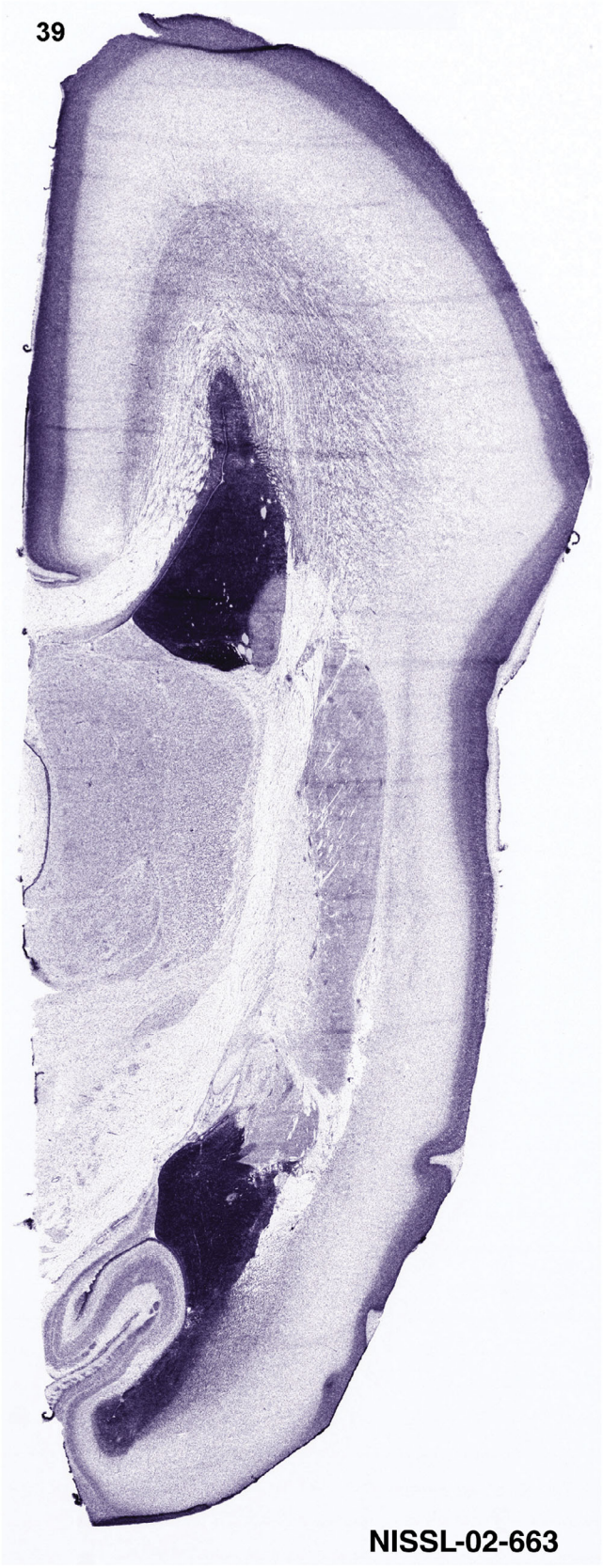
39
NISSL-02-663

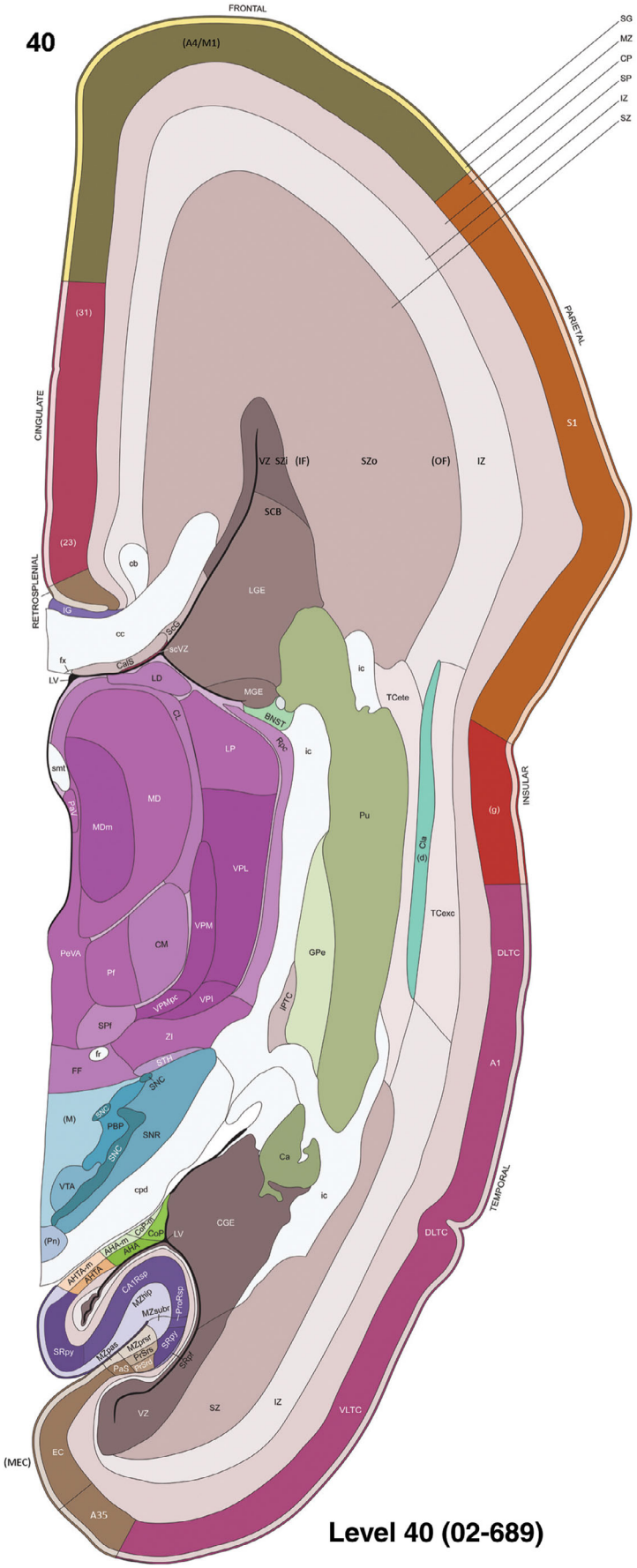

Level 40 (02-689)

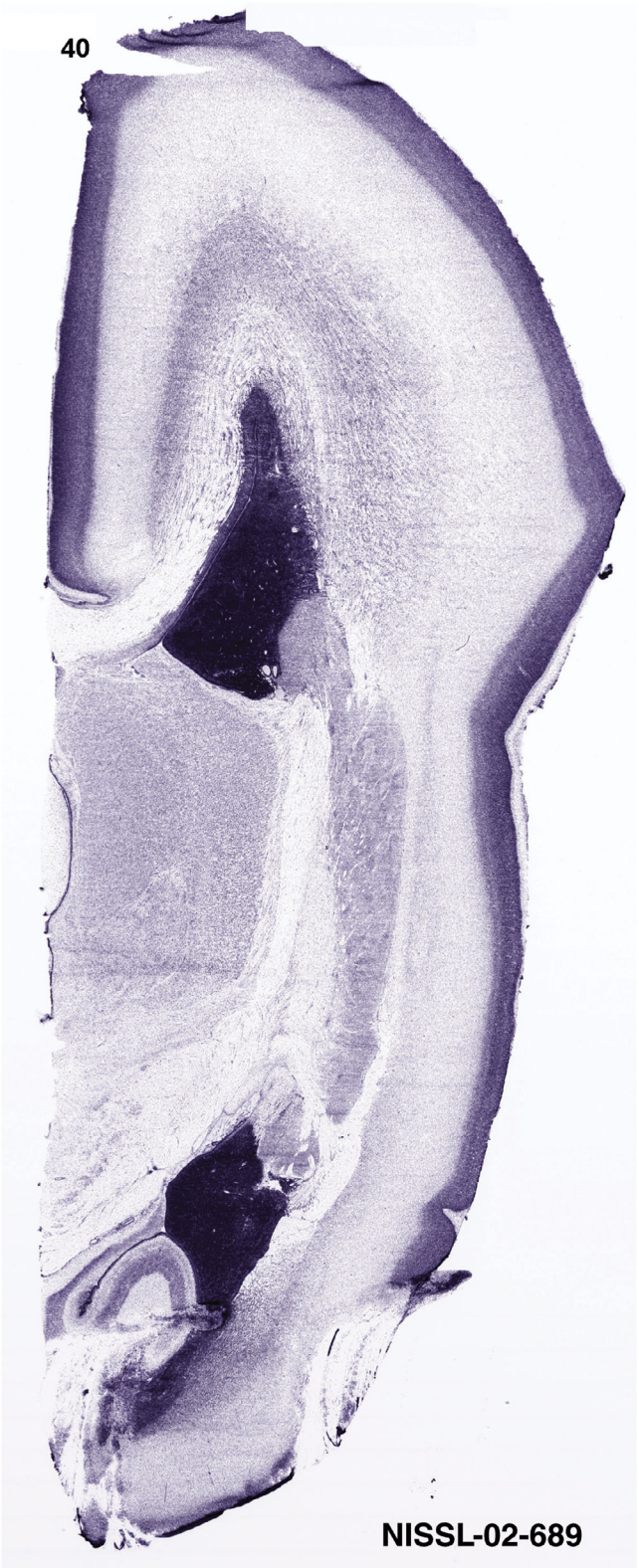
40
NISSL-02-689

Level 41 (02-715)

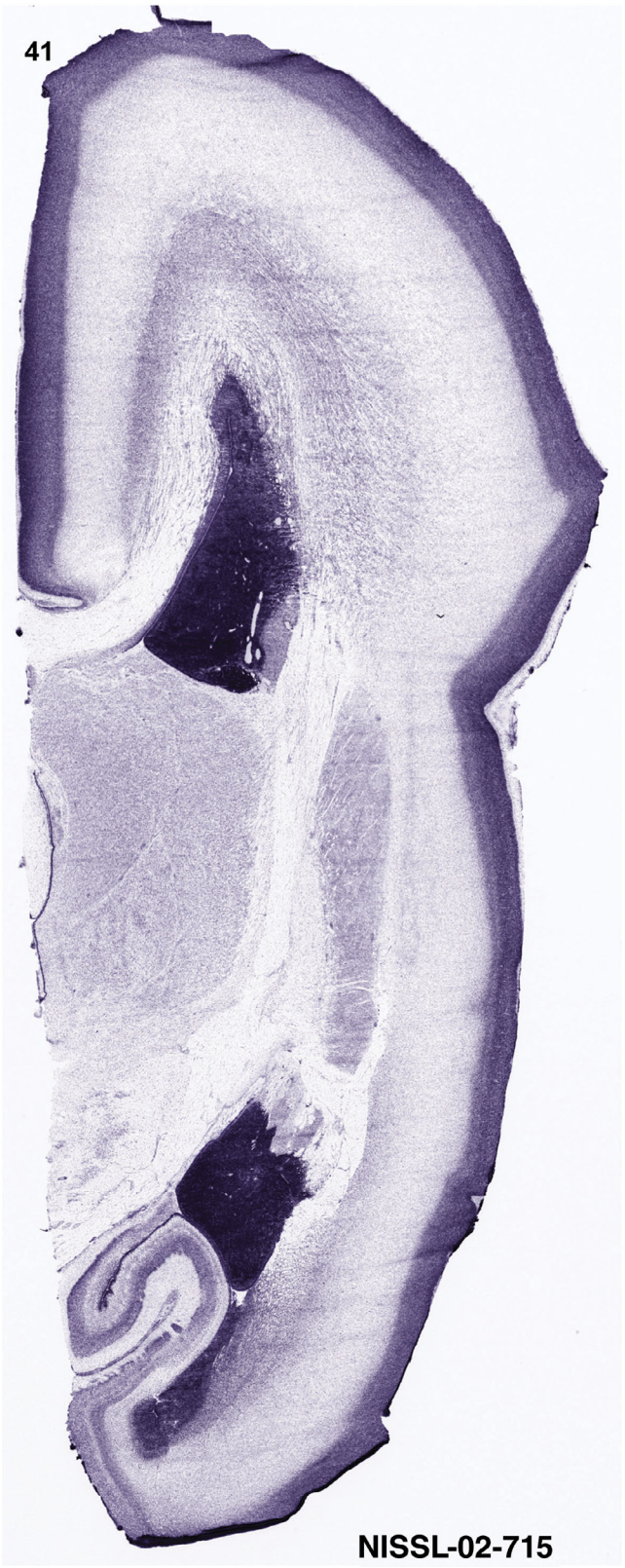
41
NISSL-02-715

Level 42 (02-740)

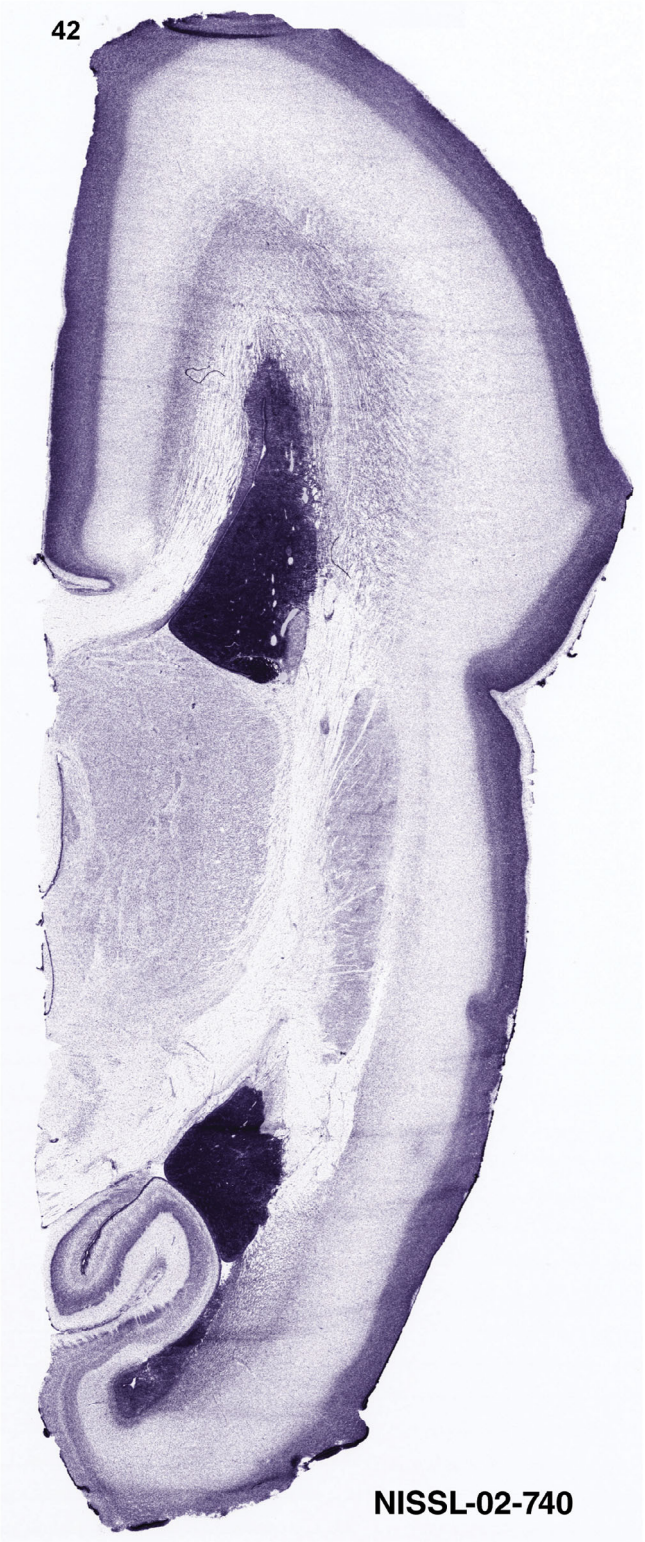
42
NISSL-02-740

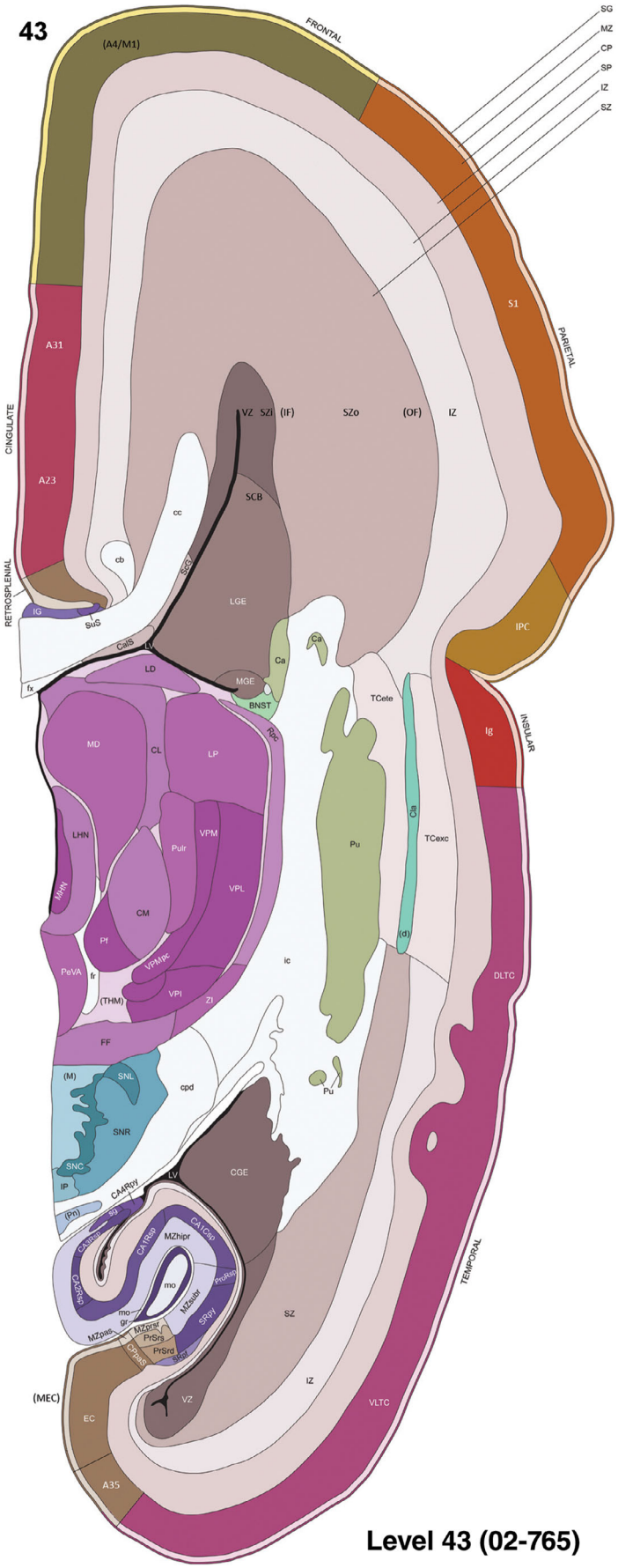

Level 43 (02-765)

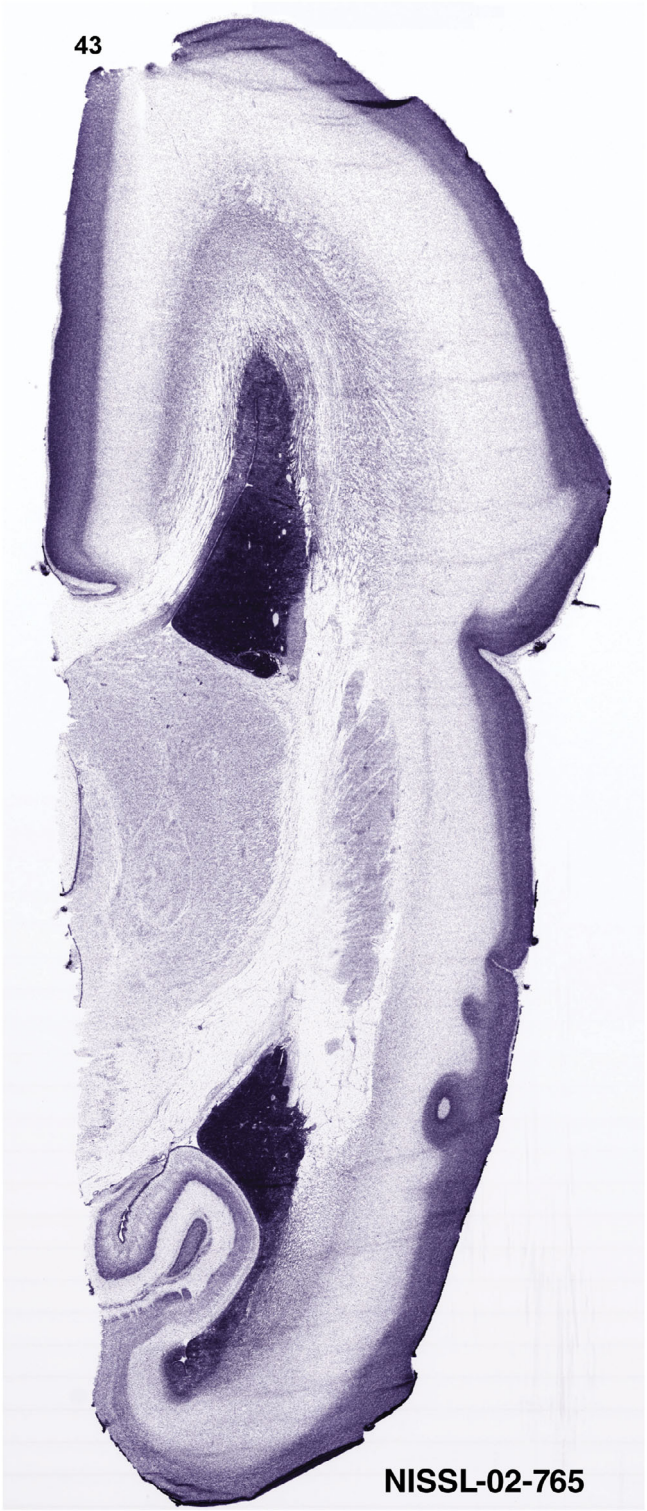
43
NISSL-02-765

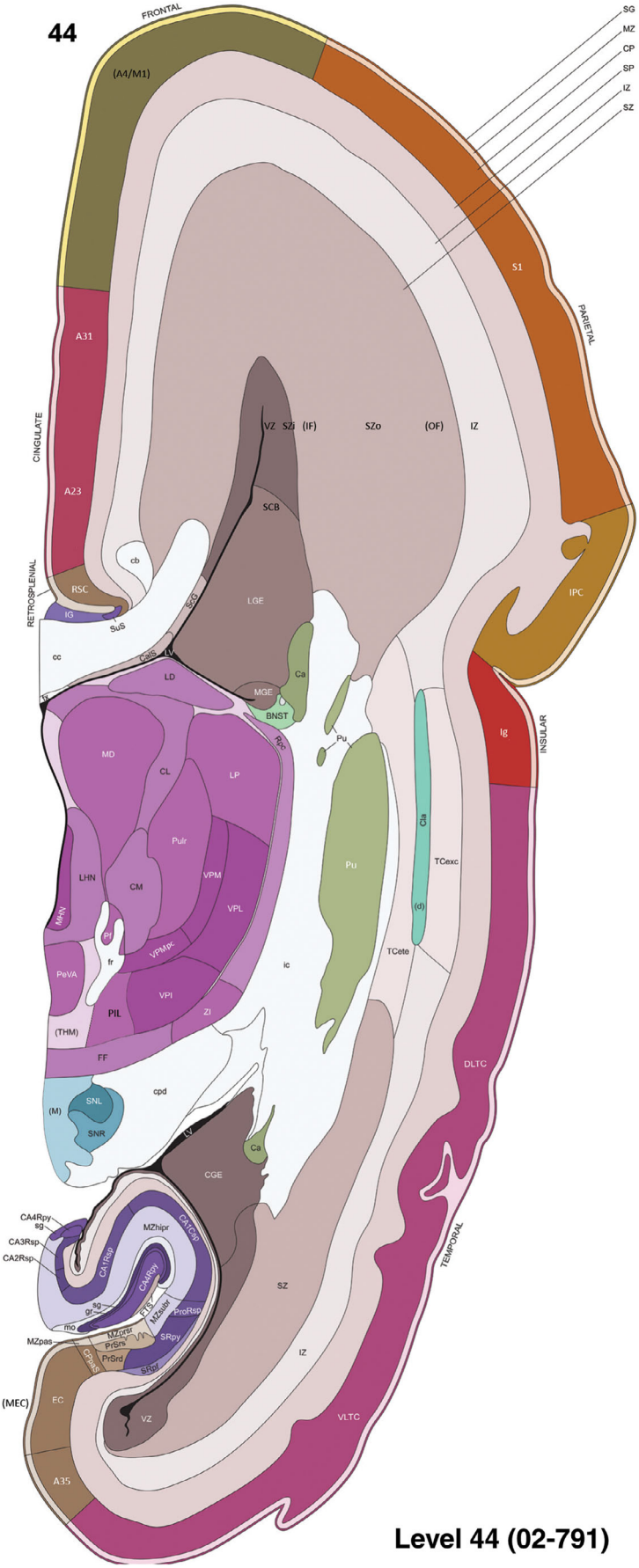

Level 44 (02-791)

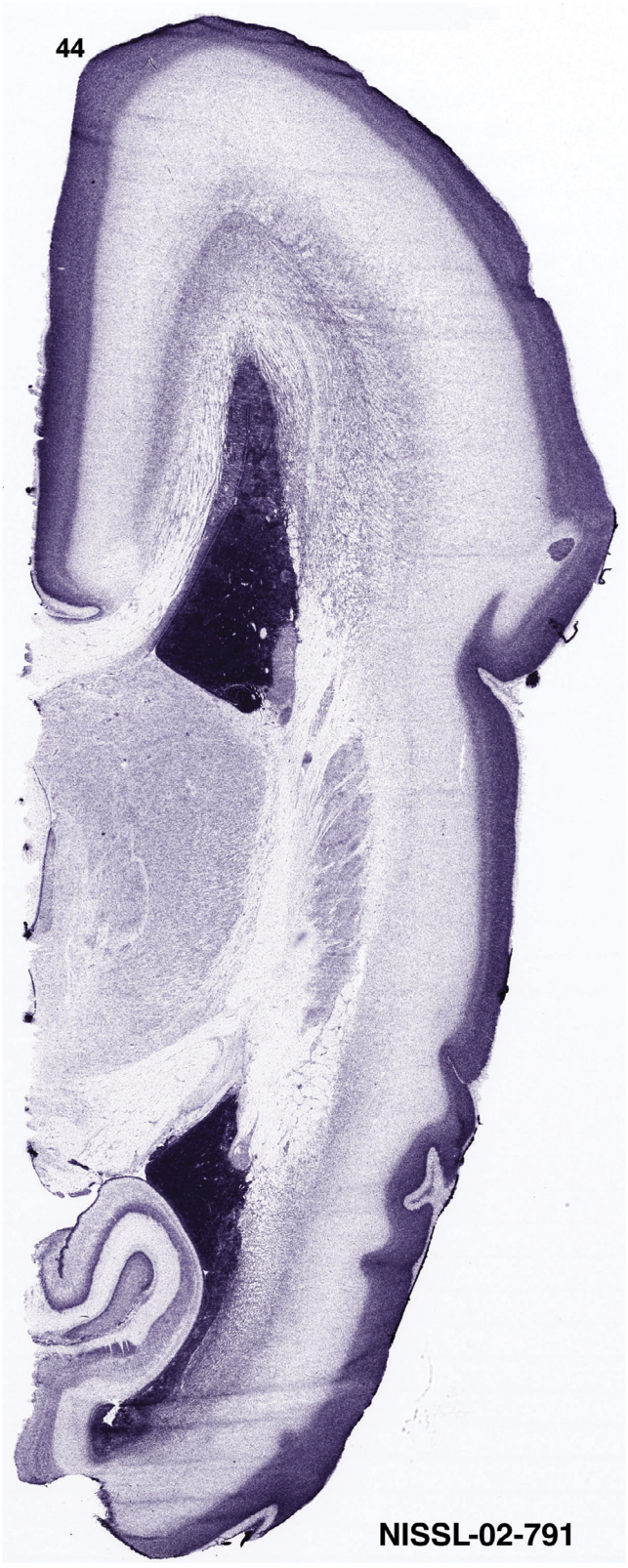
44
NISSL-02-791

Level 45 (02-816)

NISSL-02-816

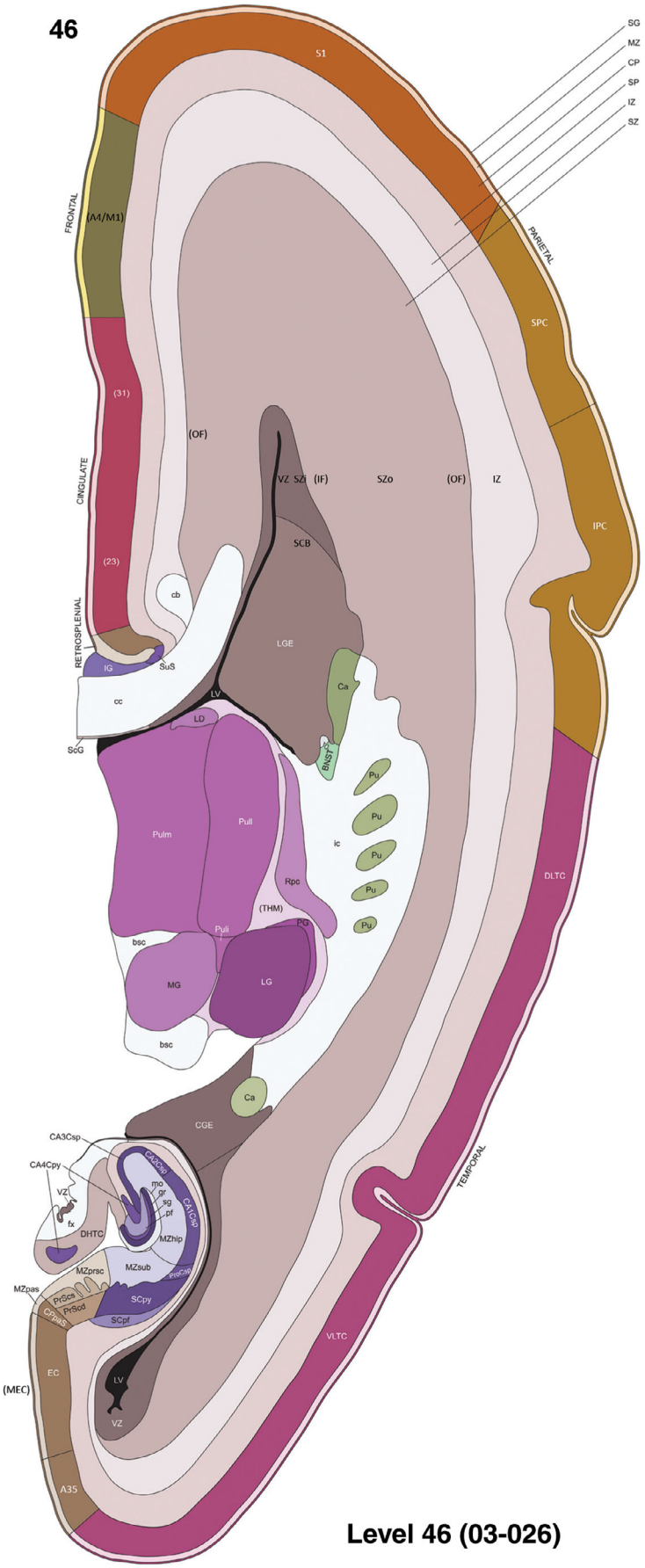

Level 46 (03-026)

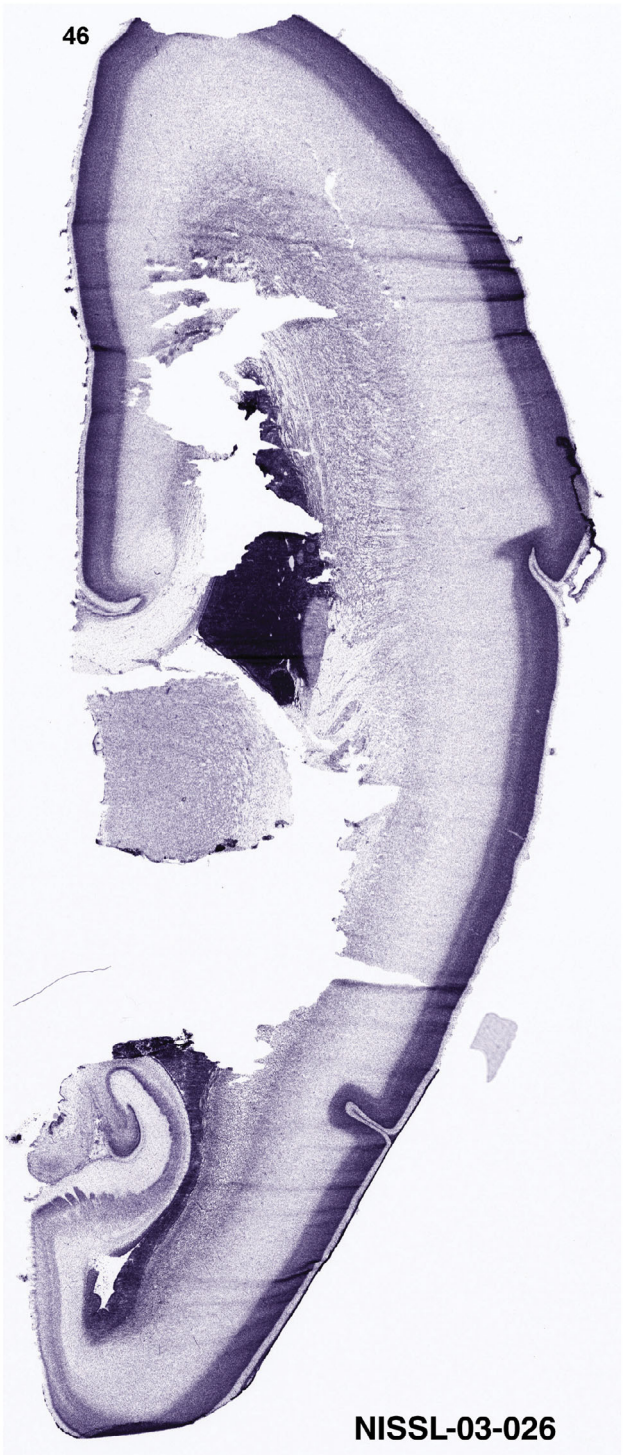
46
NISSL-03-026

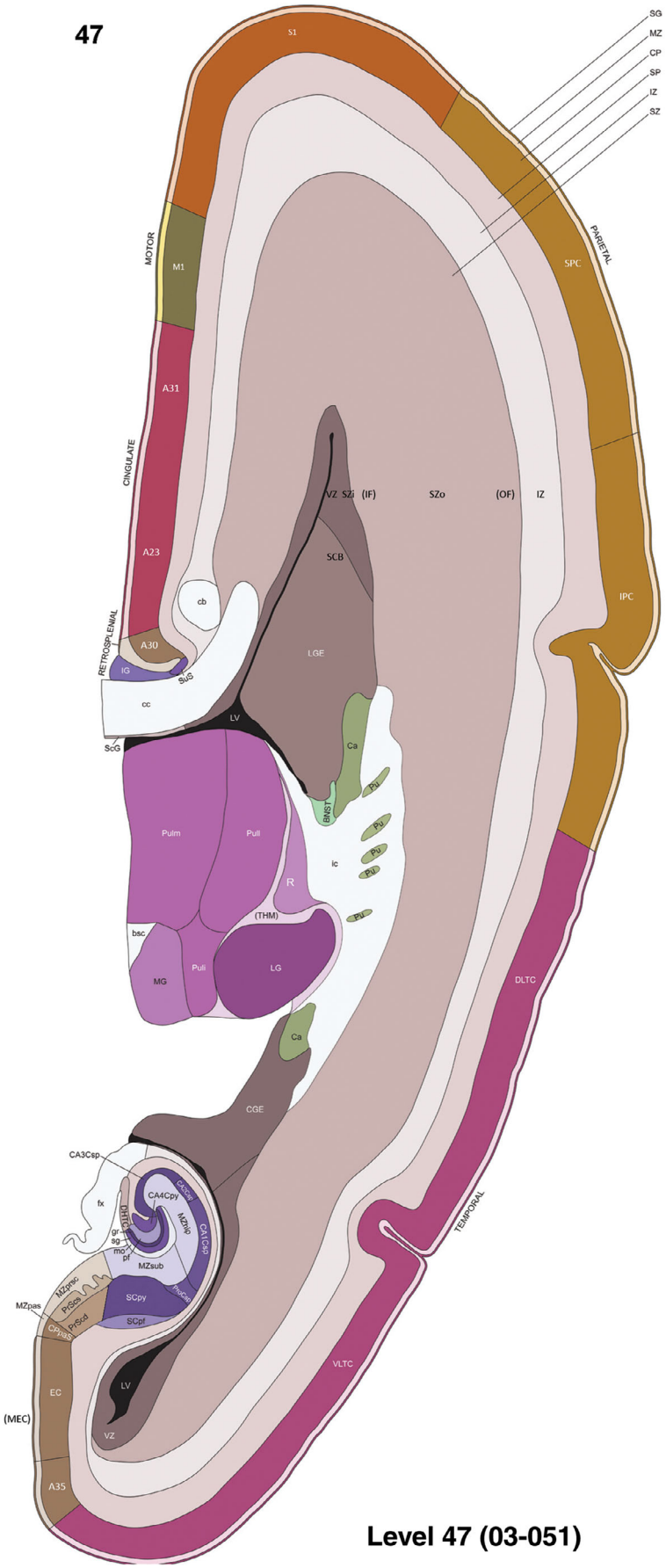

Level 47 (03-051)

47
NISSL-03-051

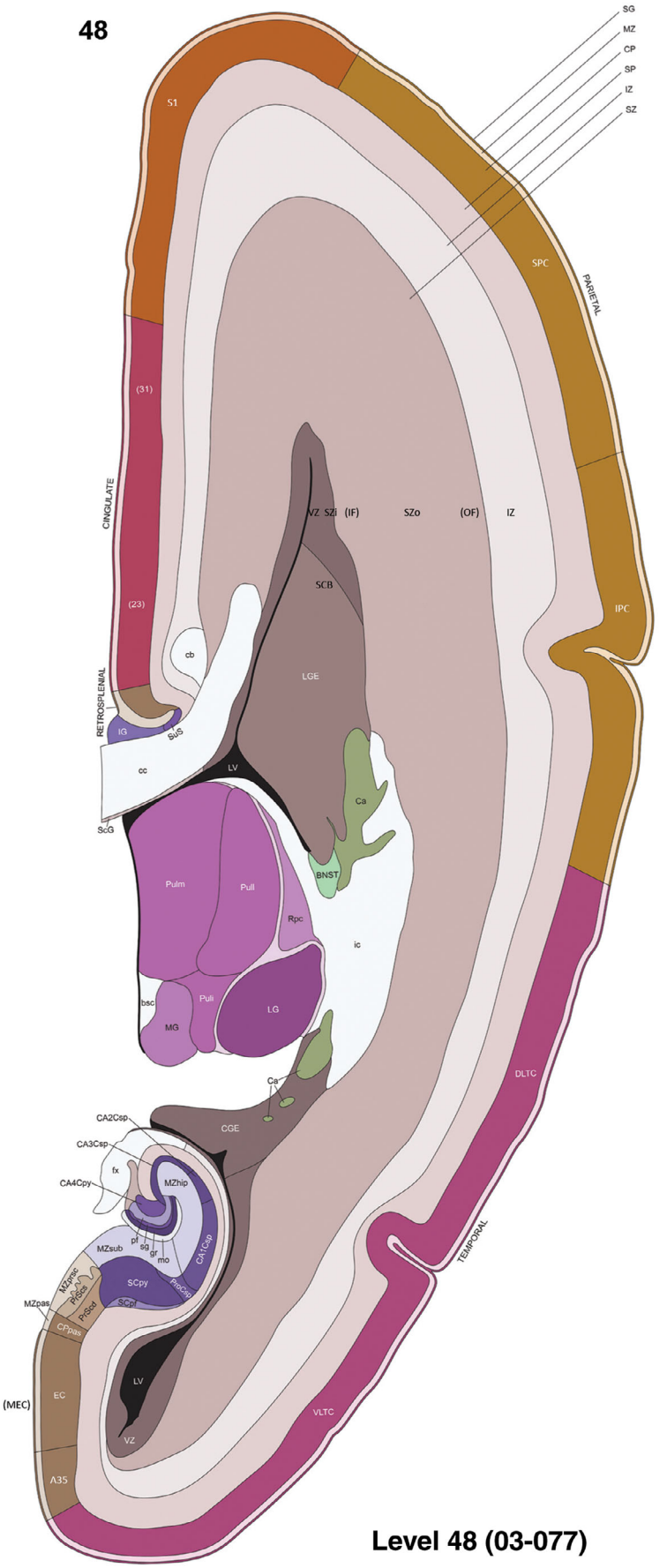

Level 48 (03-077)

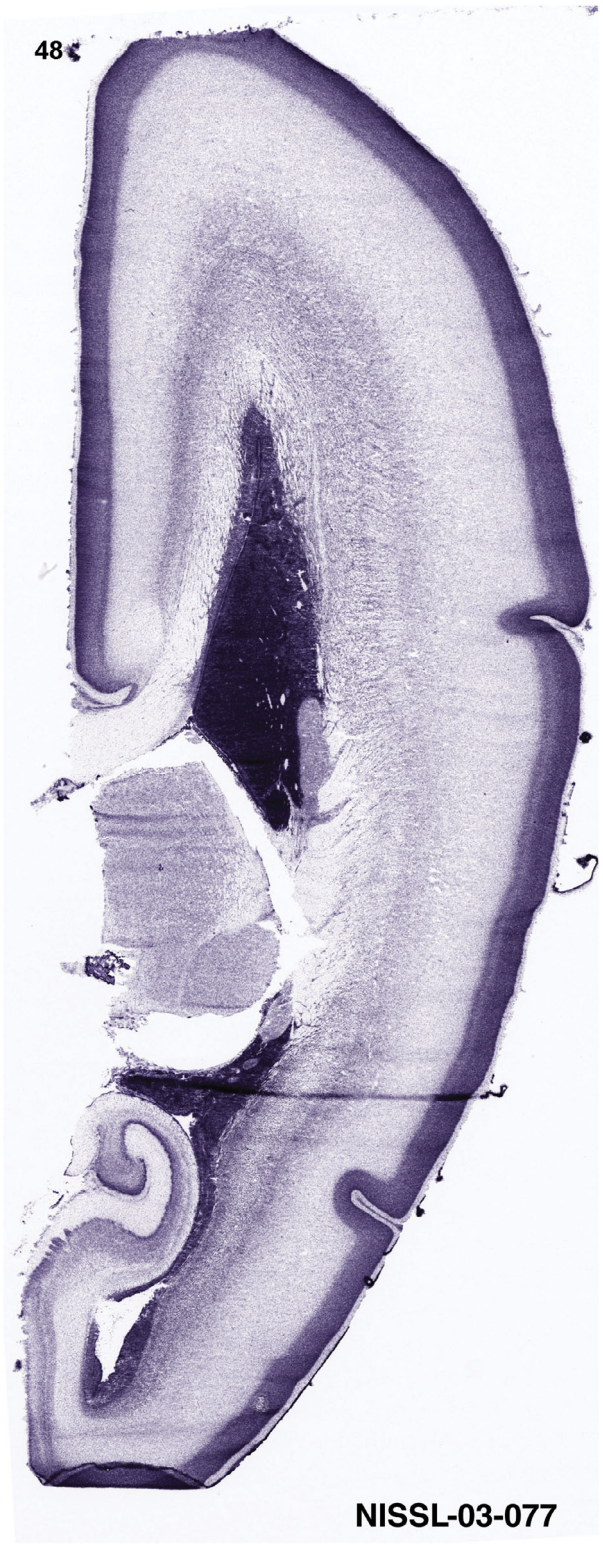
48
NISSL-03-077

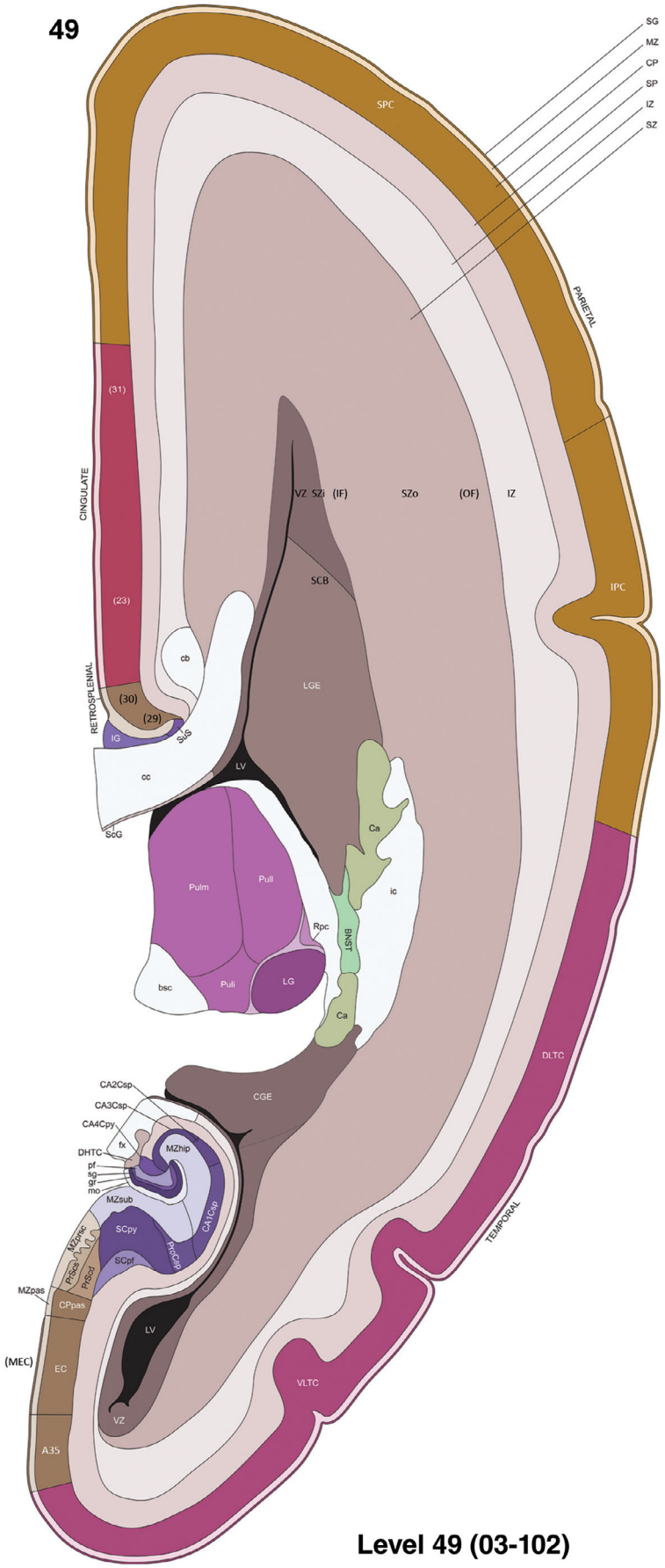

Level 49 (03-102)

49
NISSL-03-102

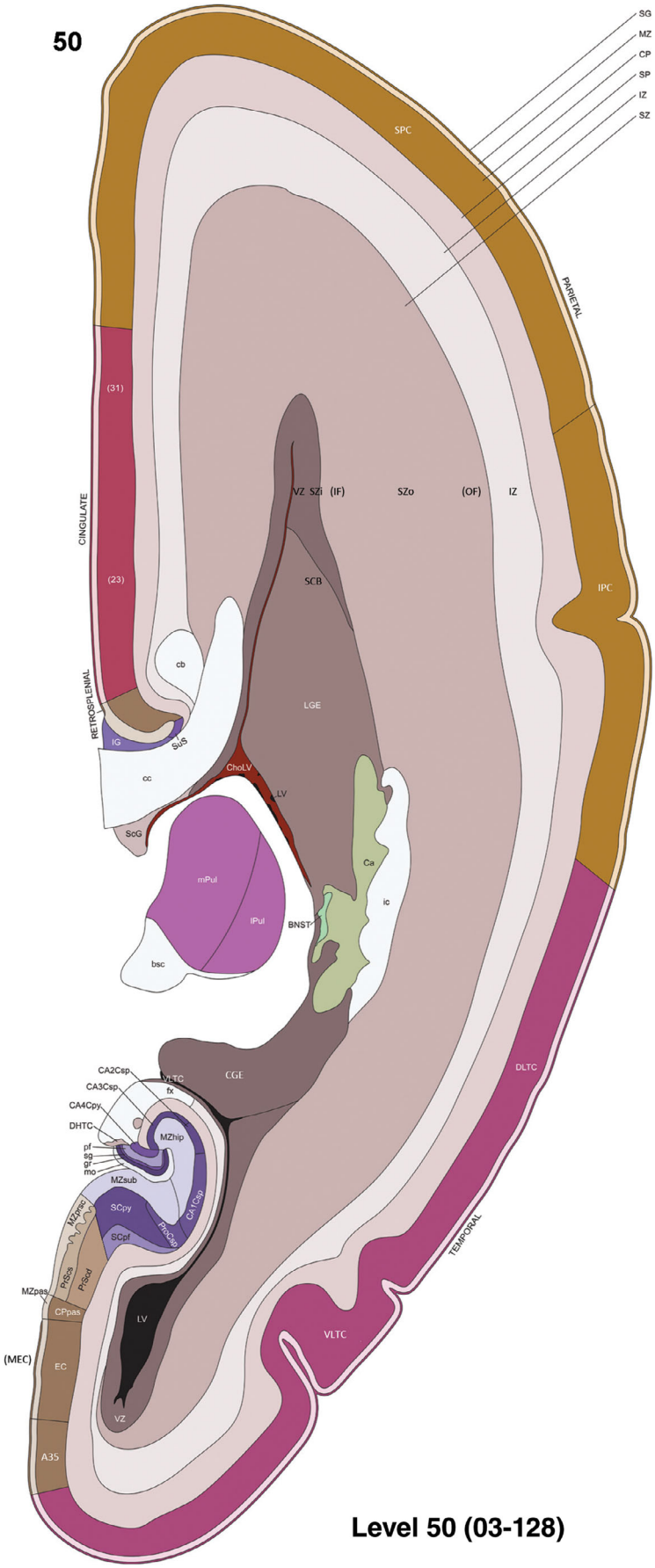

Level 50 (03-128)

50
NISSL-03-128

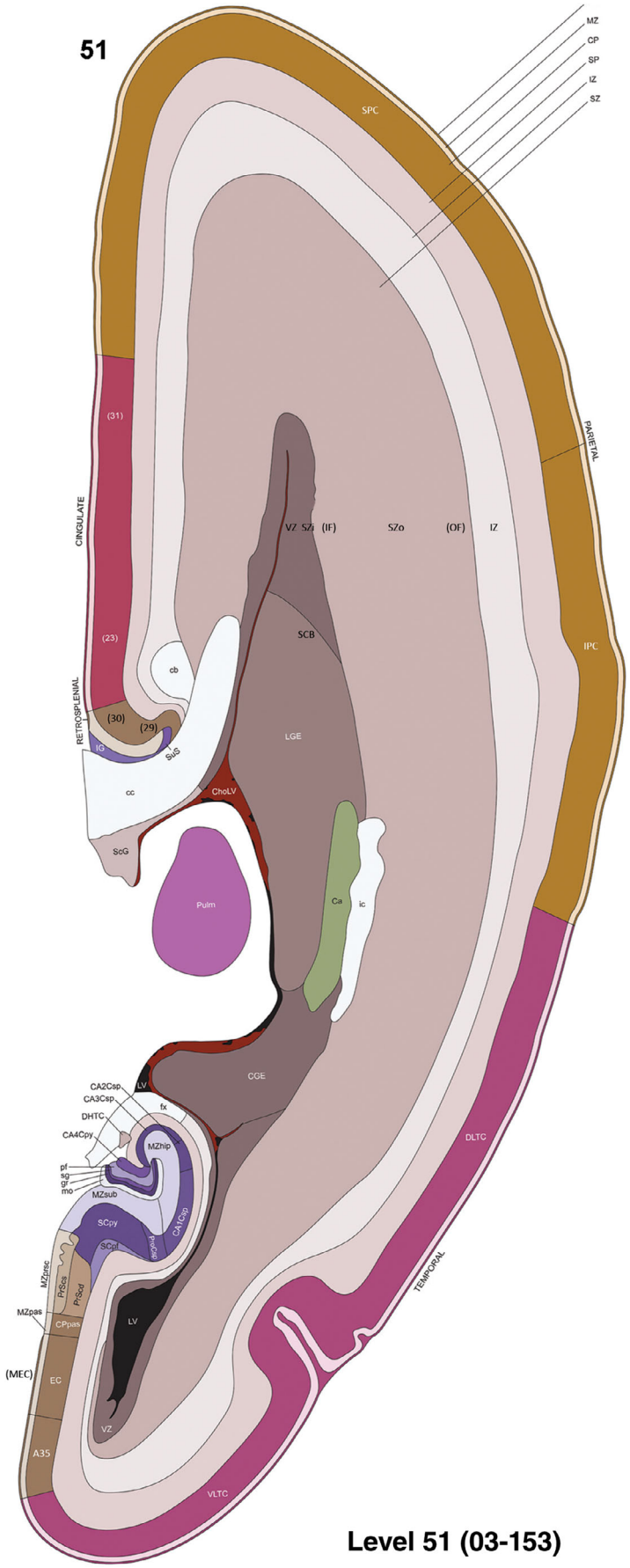

Level 51 (03-153)

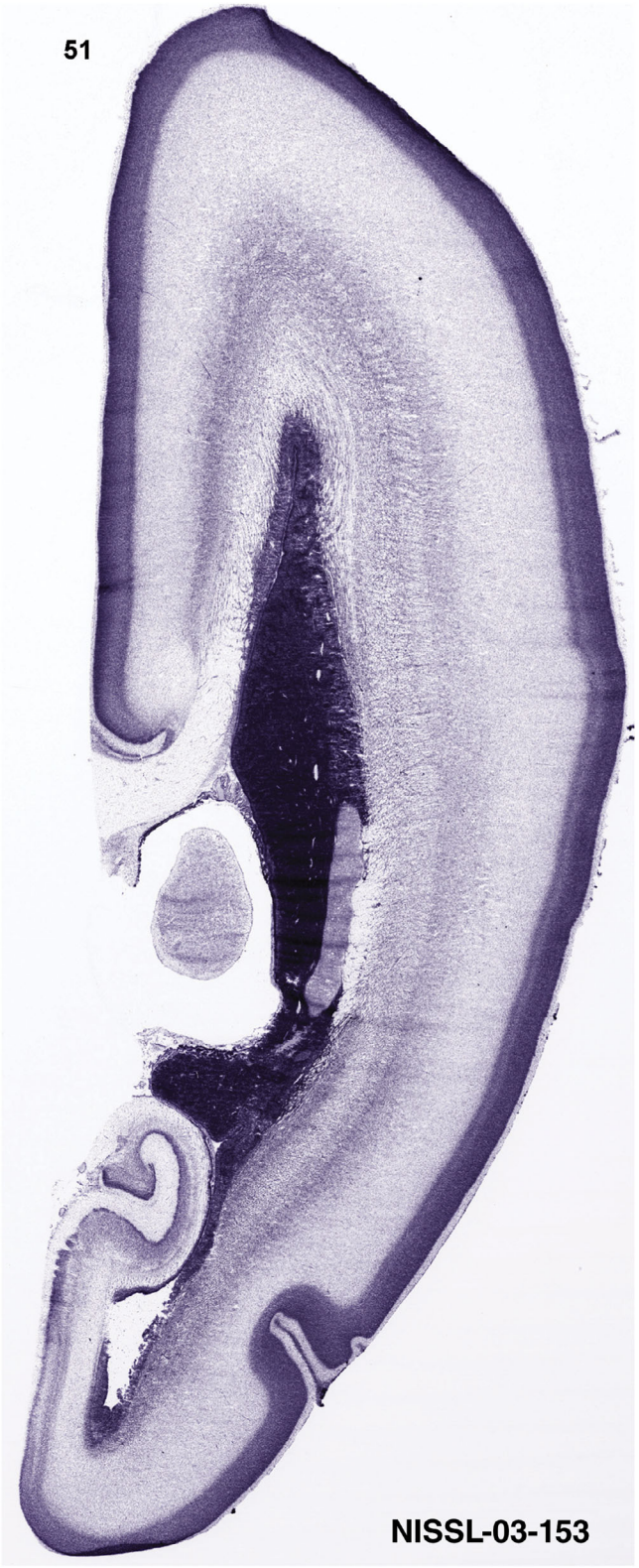
51
NISSL-03-153

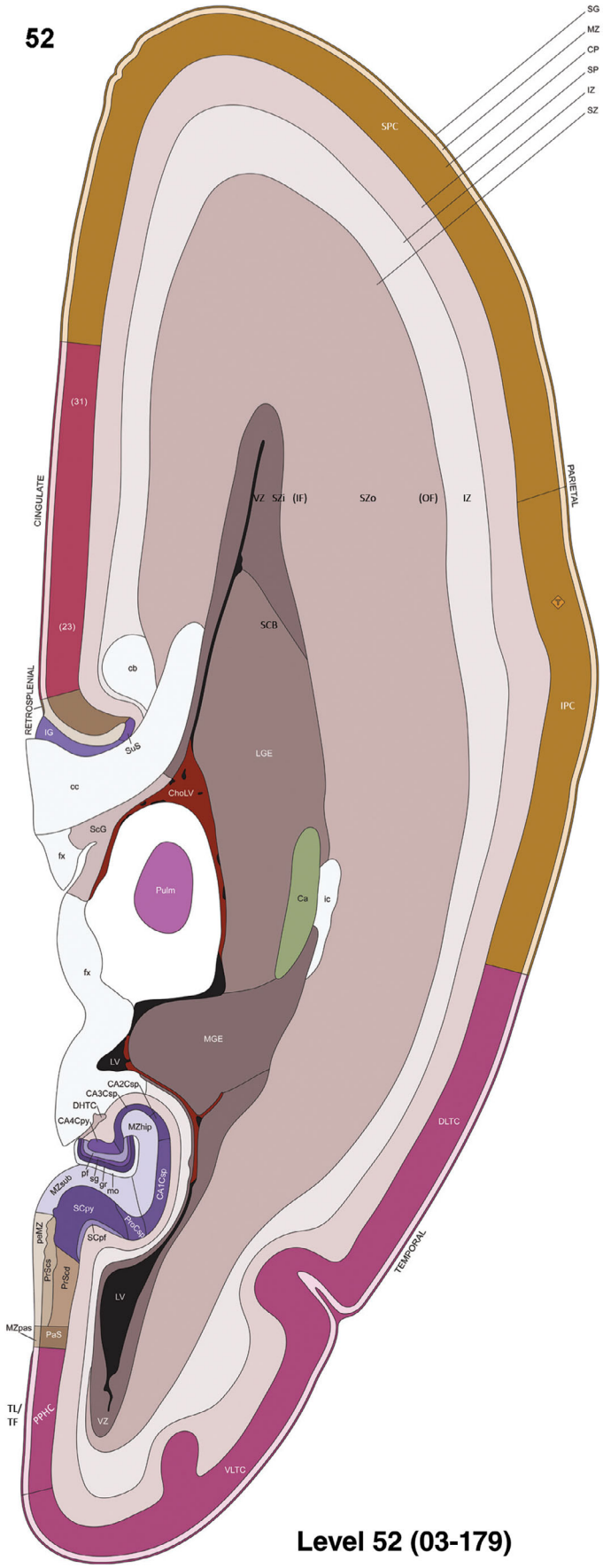

Level 52 (03-179)

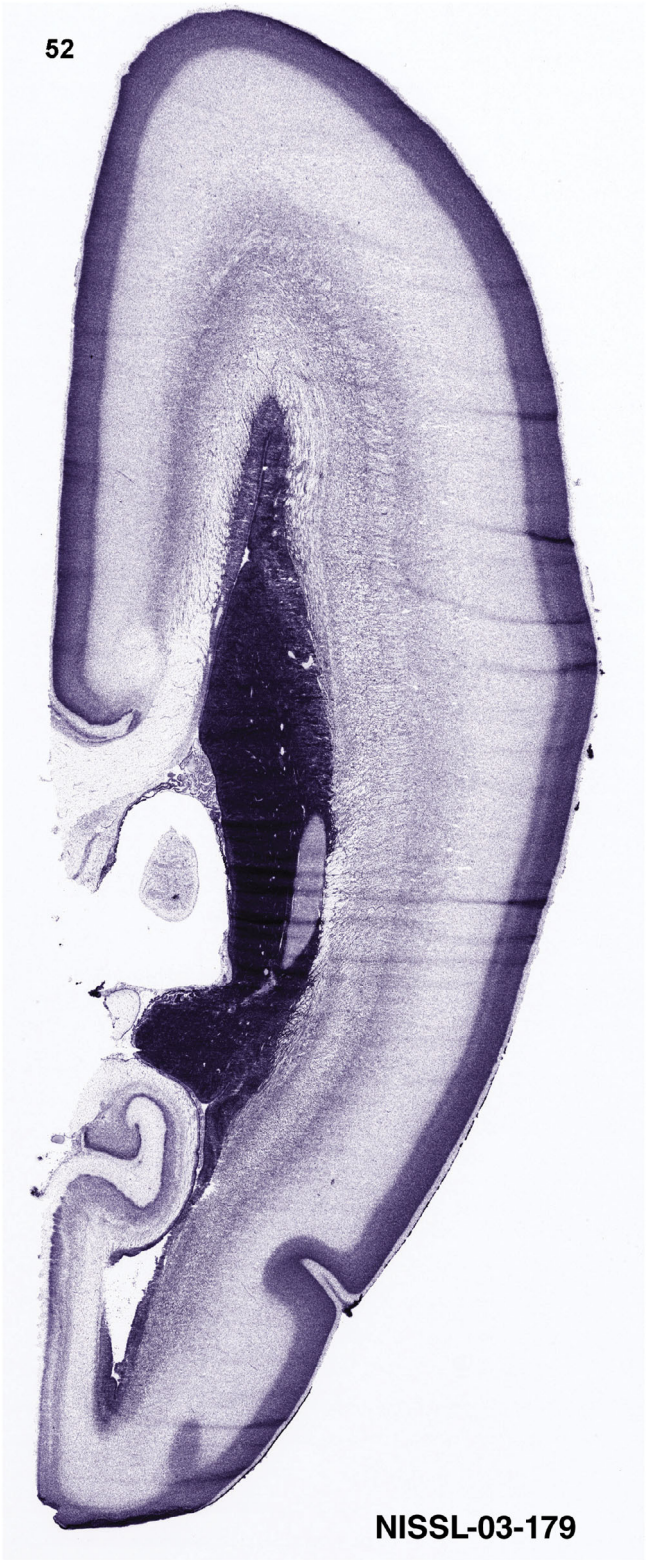
52
NISSL-03-179

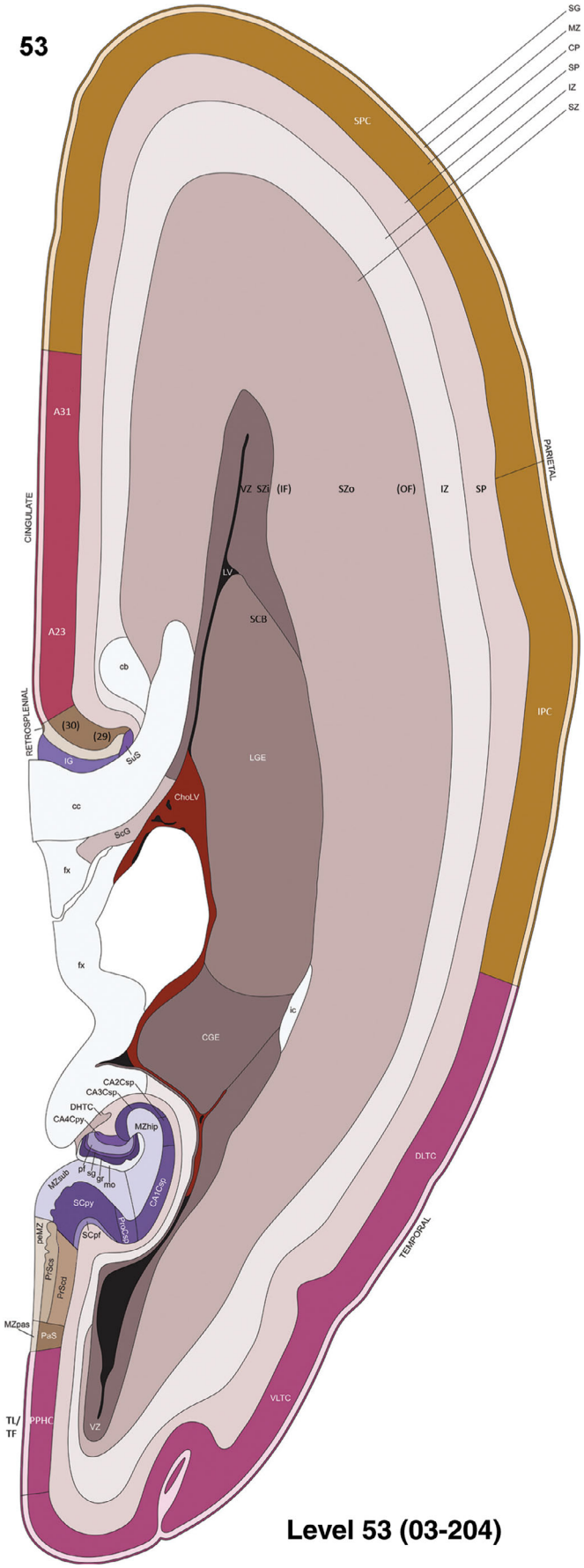

Level 53 (03-204)

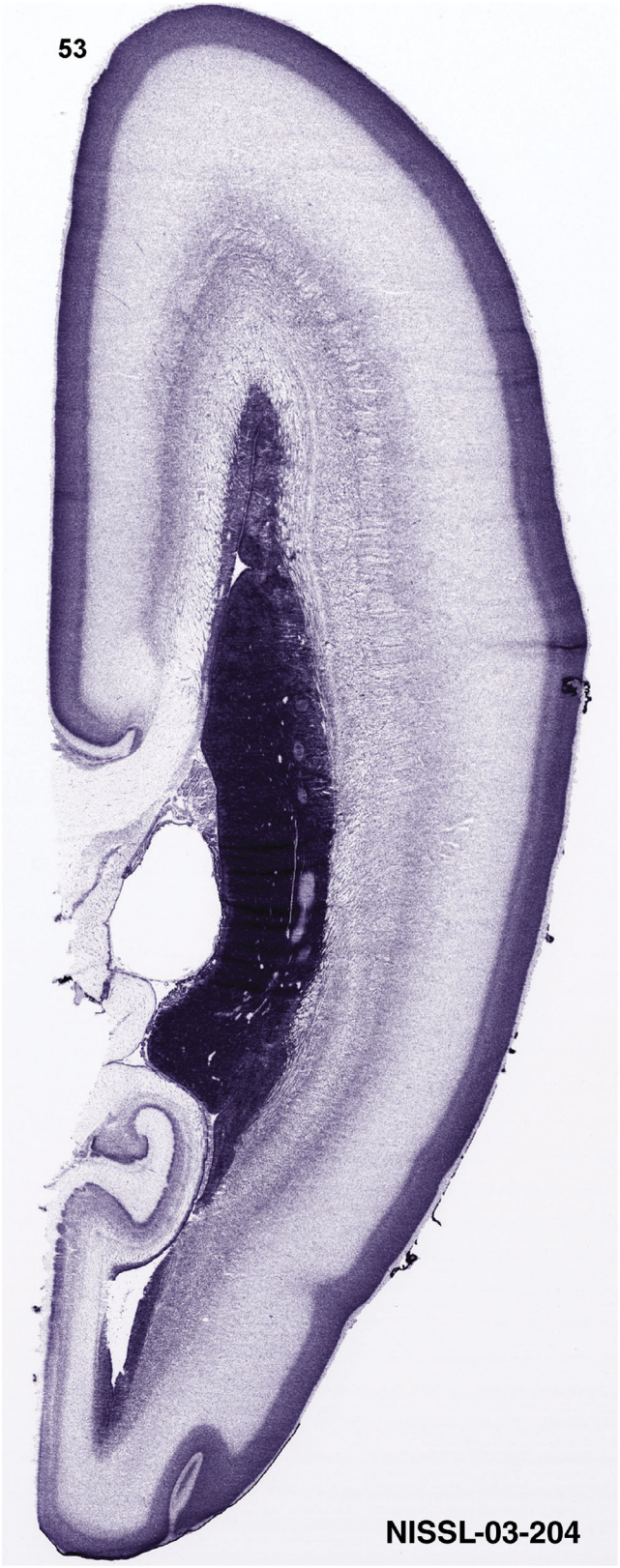
53
NISSL-03-204

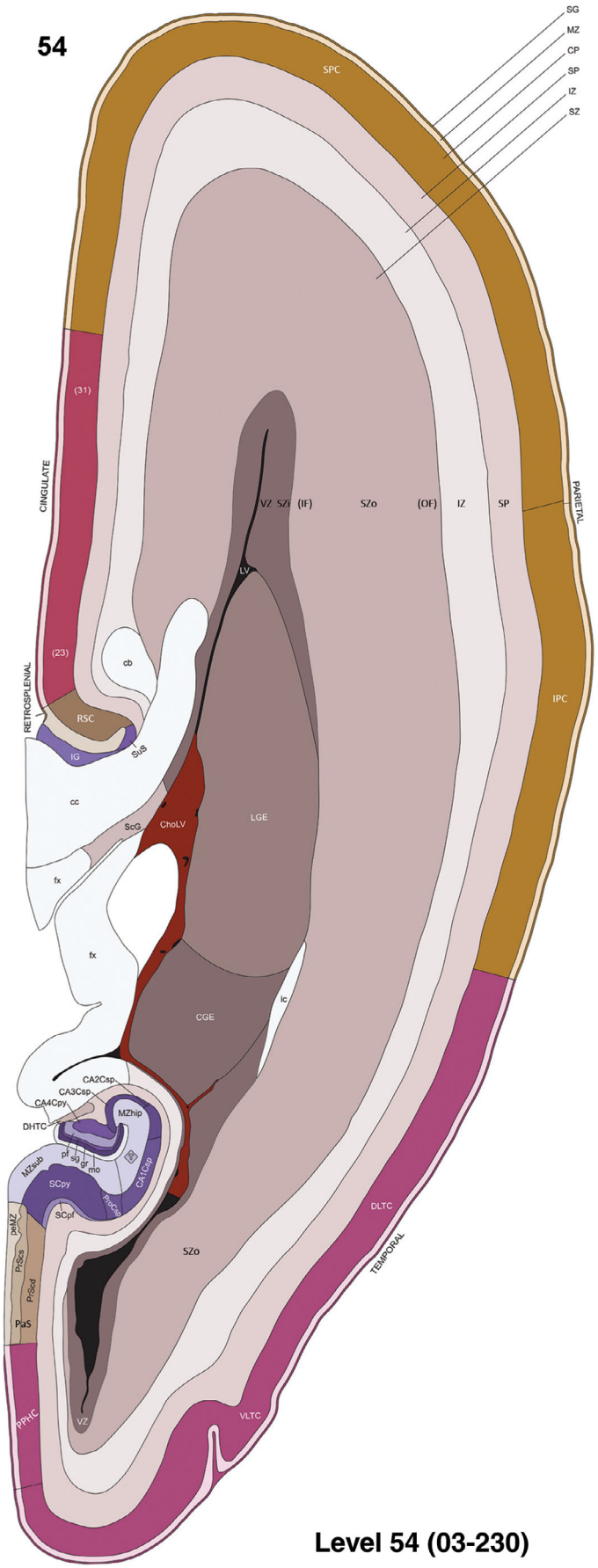

Level 54 (03-230)

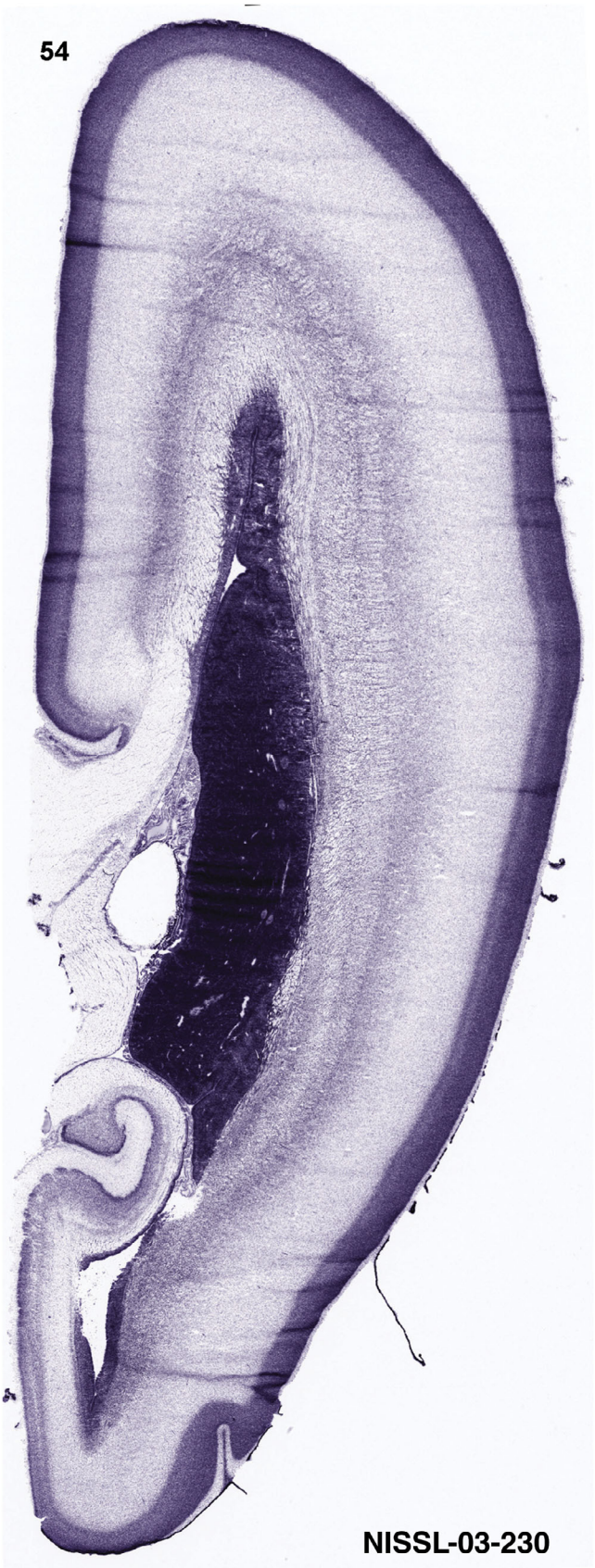
54
NISSL-03-230

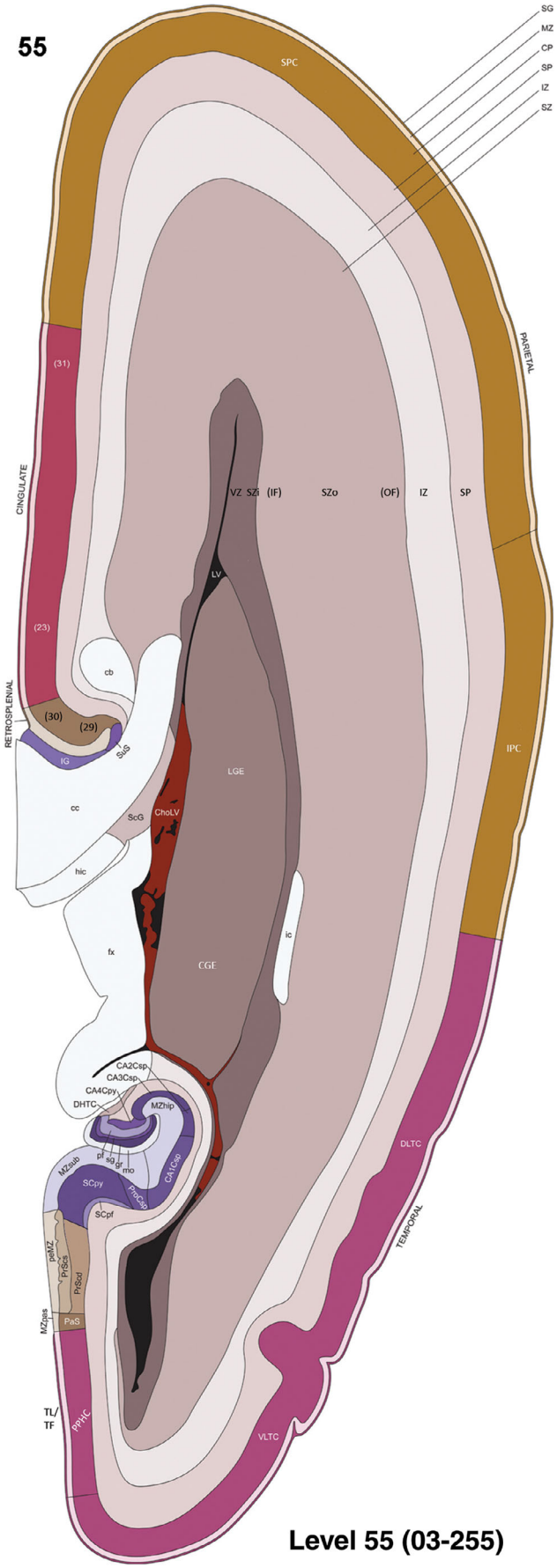

Level 55 (03-255)

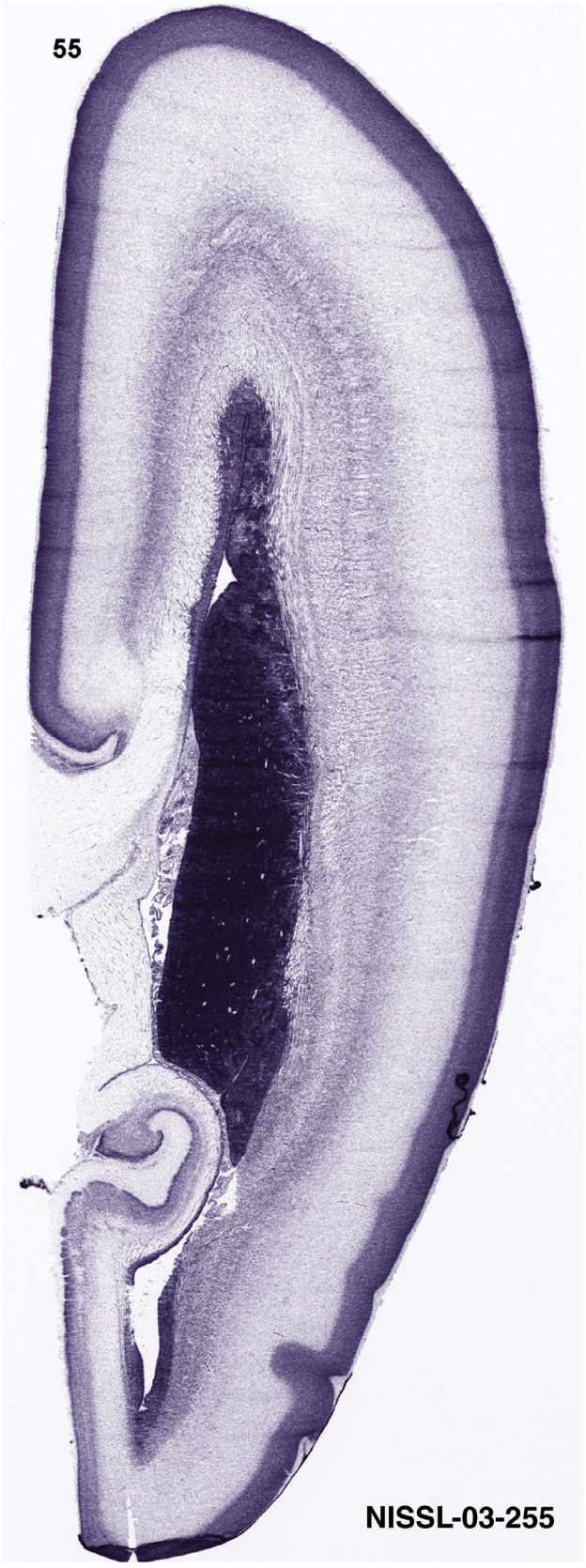
55
NISSL-03-255

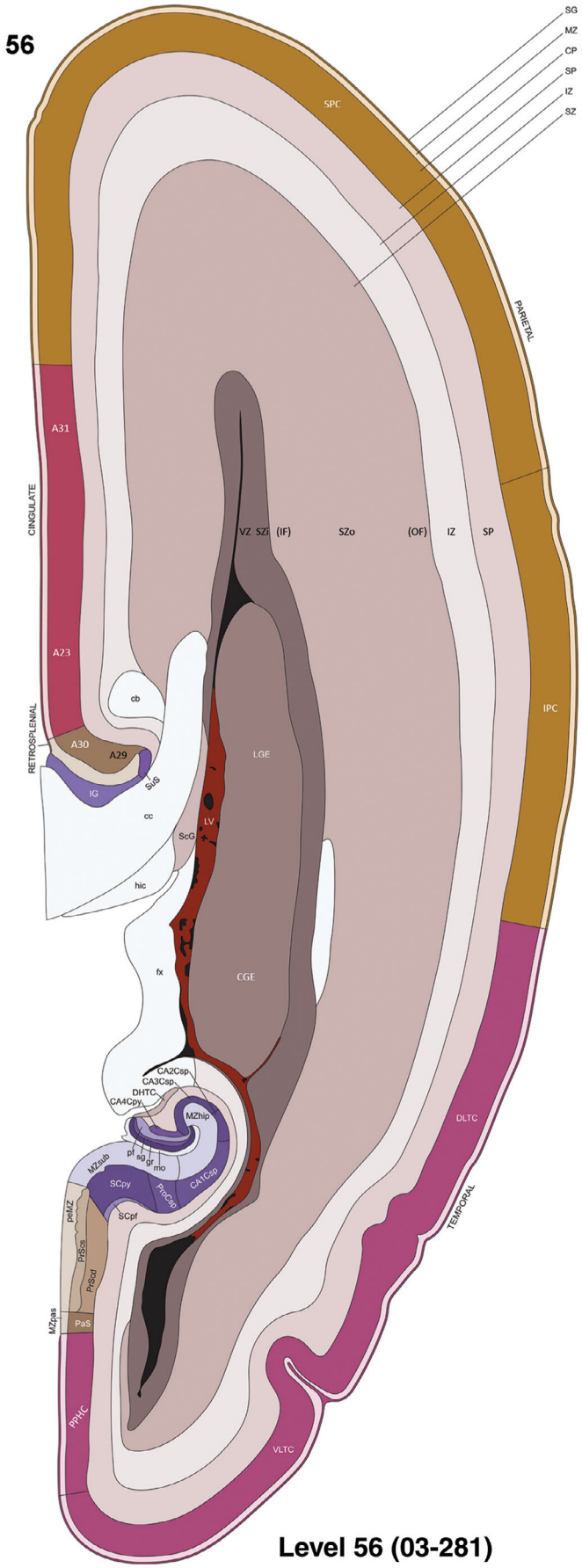

Level 56 (03-281)

56
NISSL-03-281

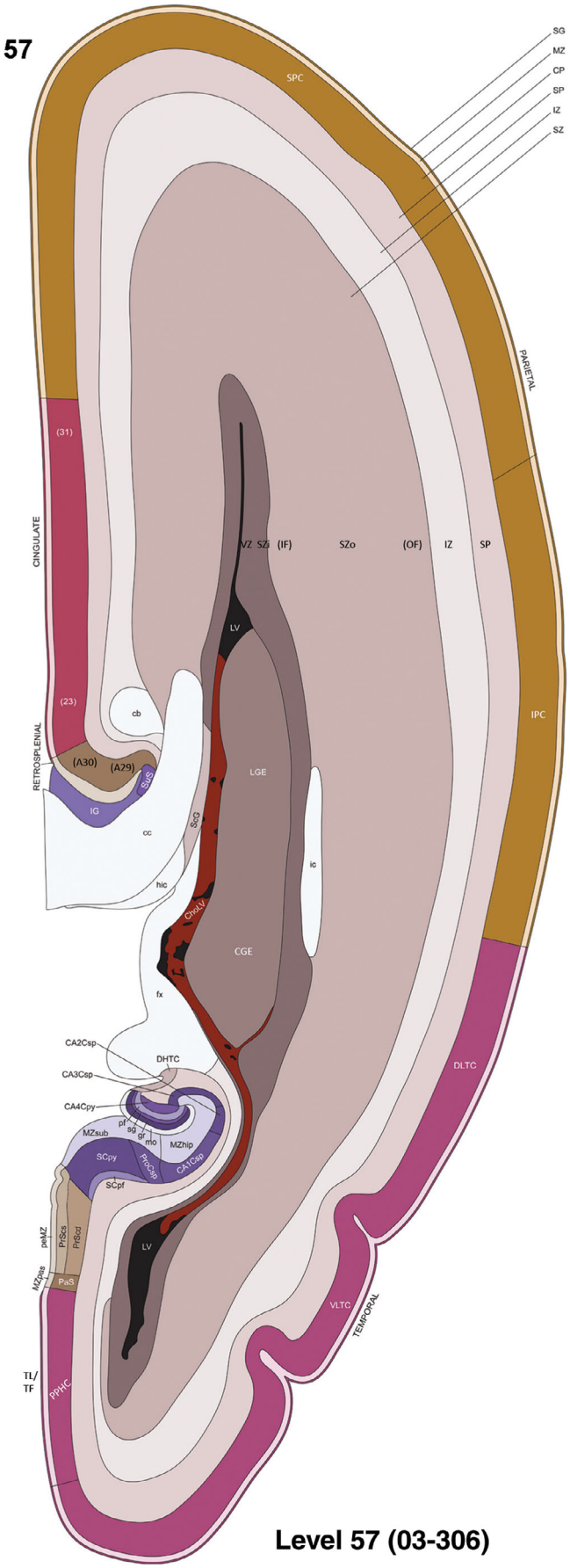

Level 57 (03-306)

57
NISSL-03-306

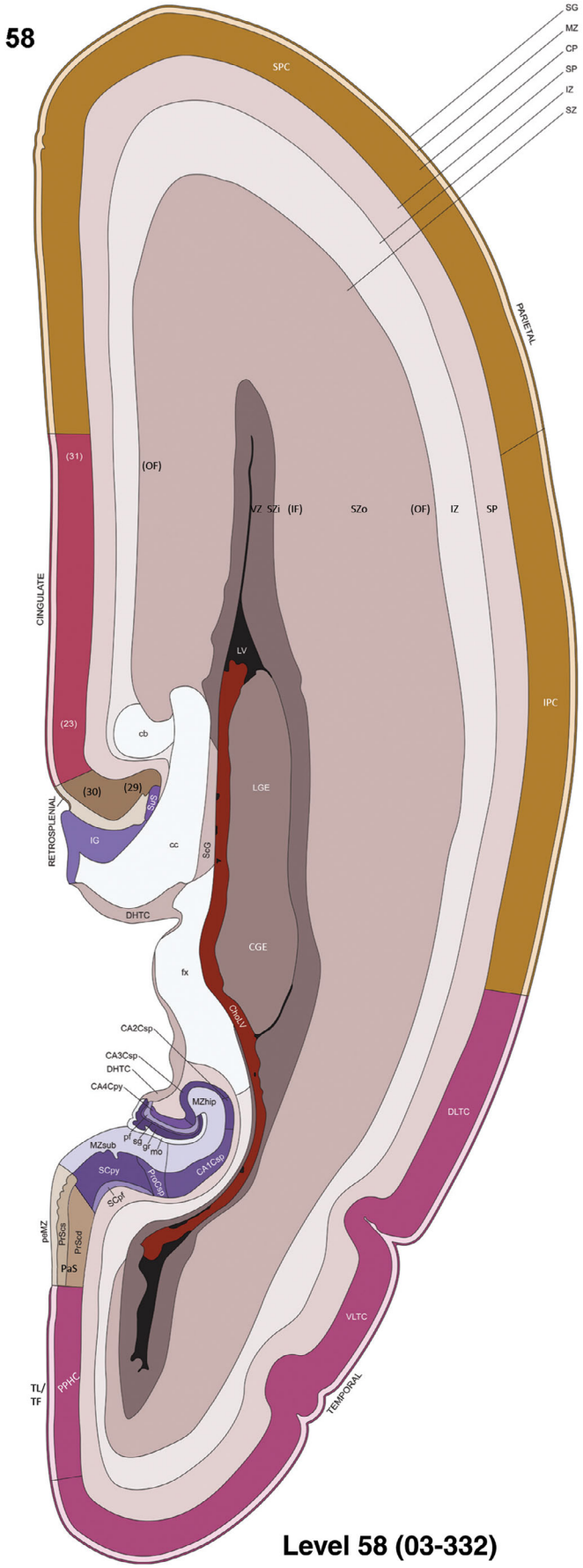

Level 58 (03-332)

58
NISSL-03-332

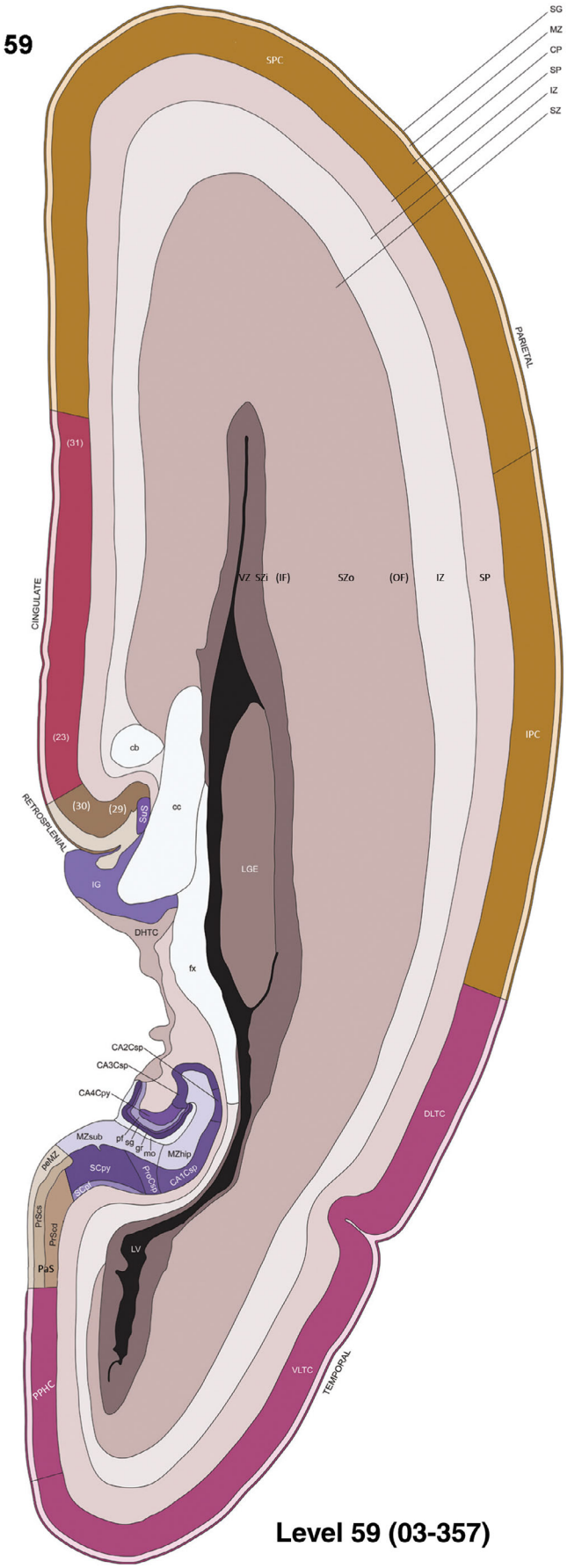

Level 59 (03-357)

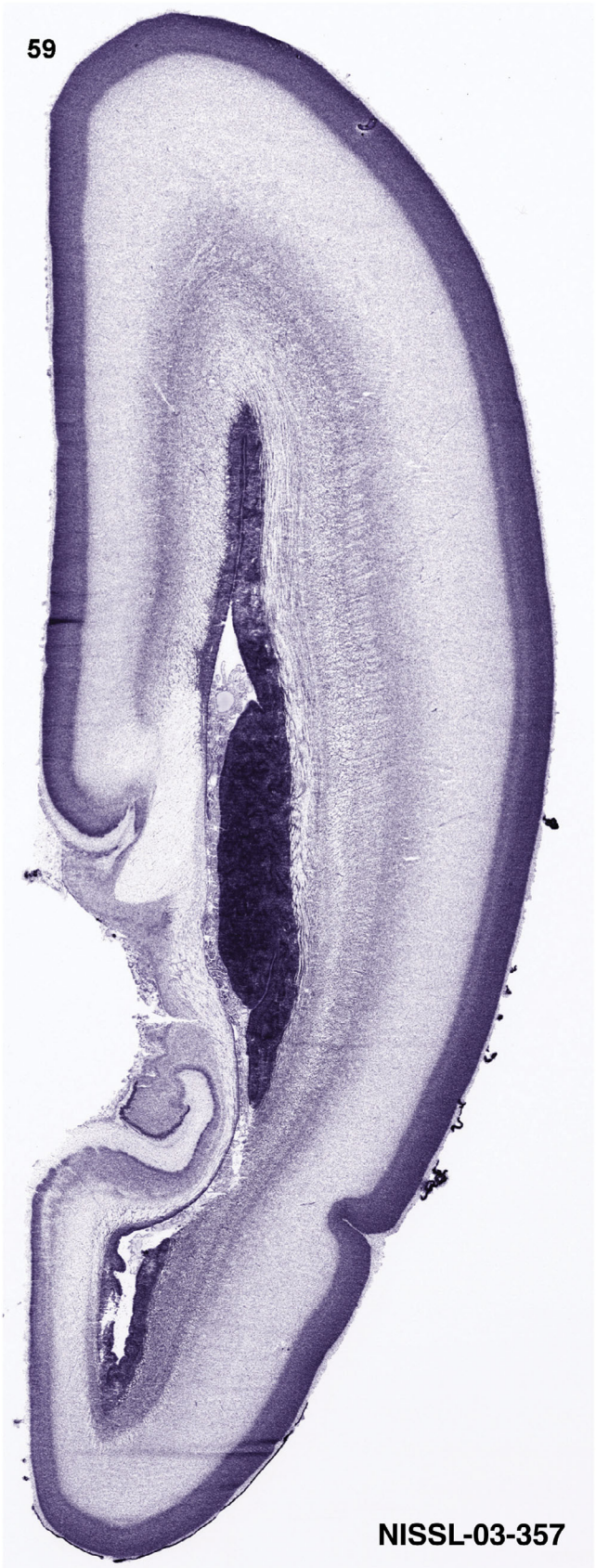
59
NISSL-03-357

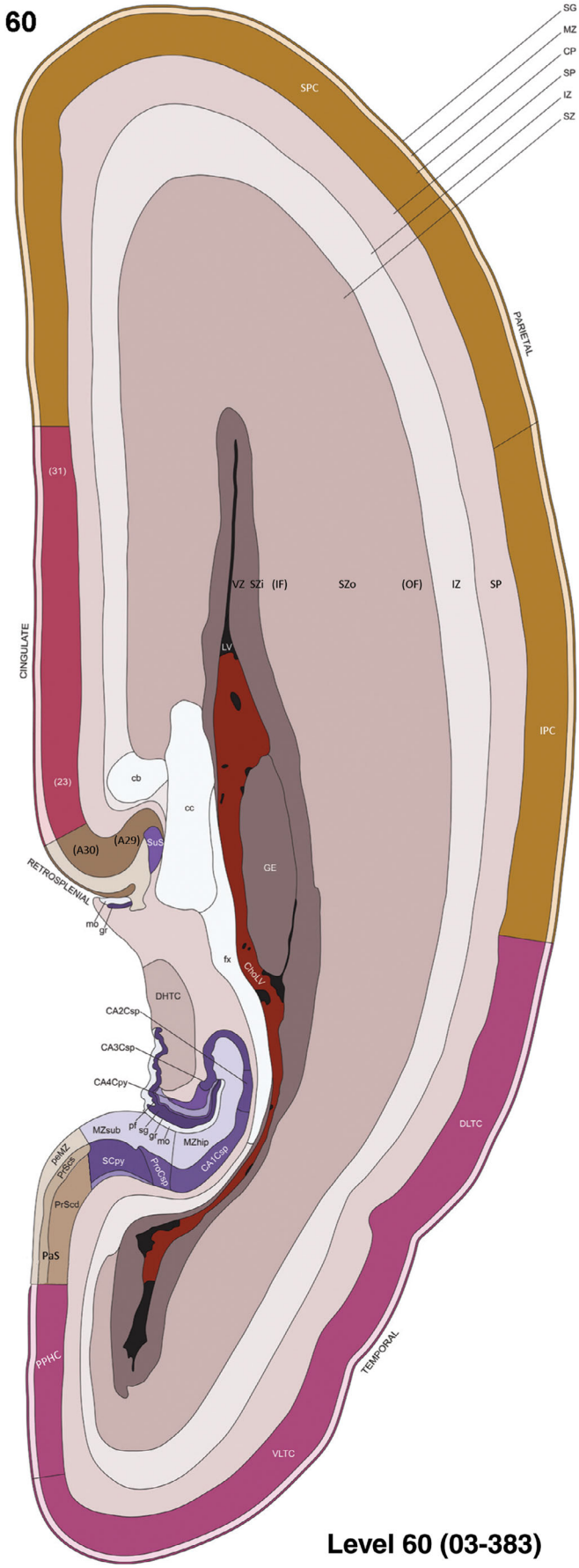

Level 60 (03-383)

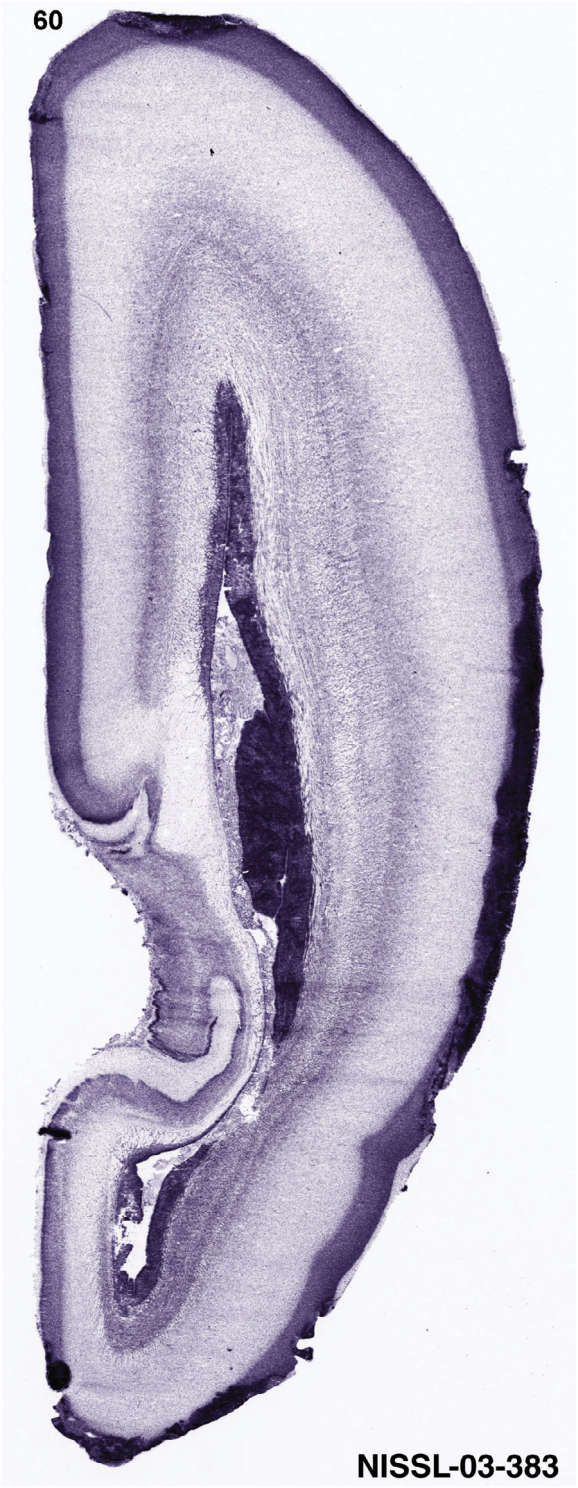
60
NISSL-03-383

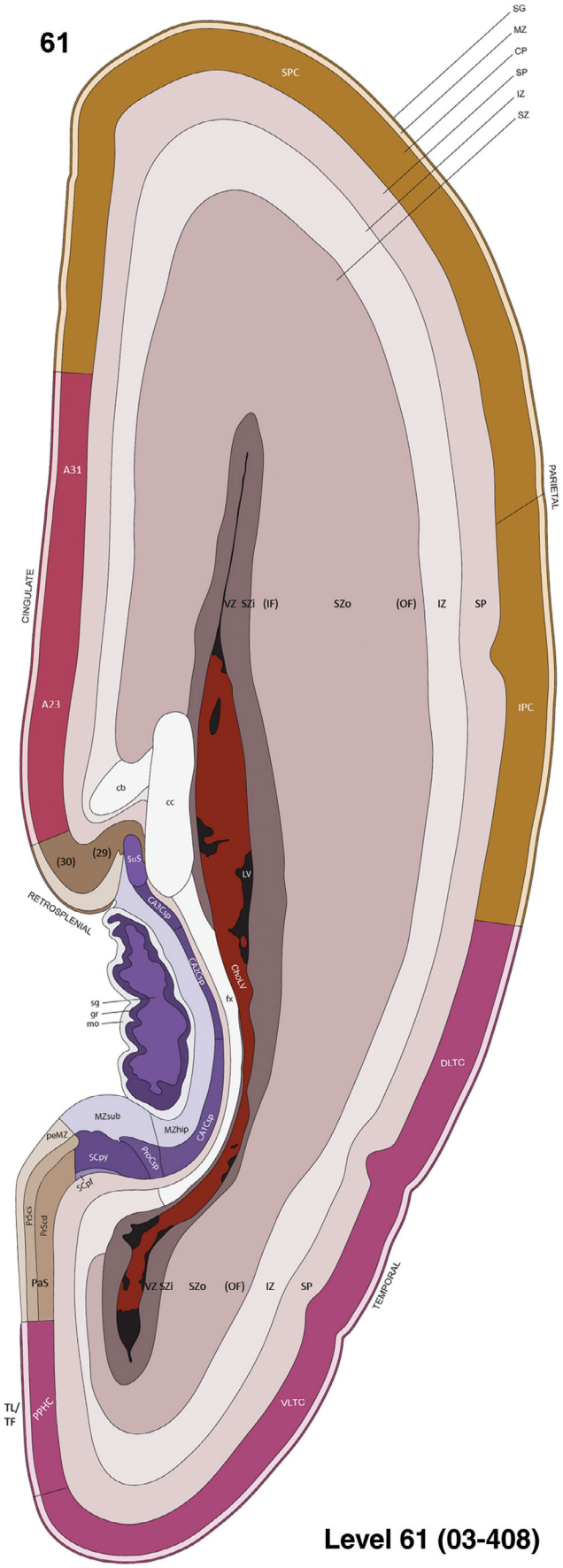

Level 61 (03-408)

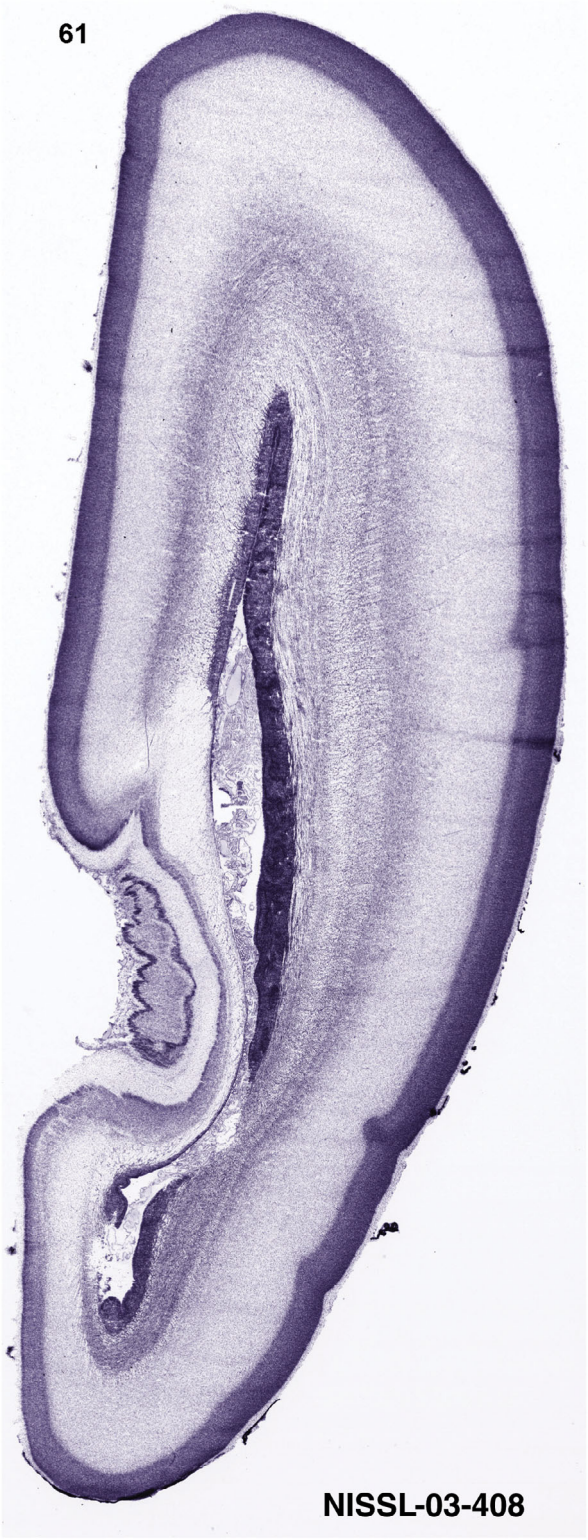
61
NISSL-03-408

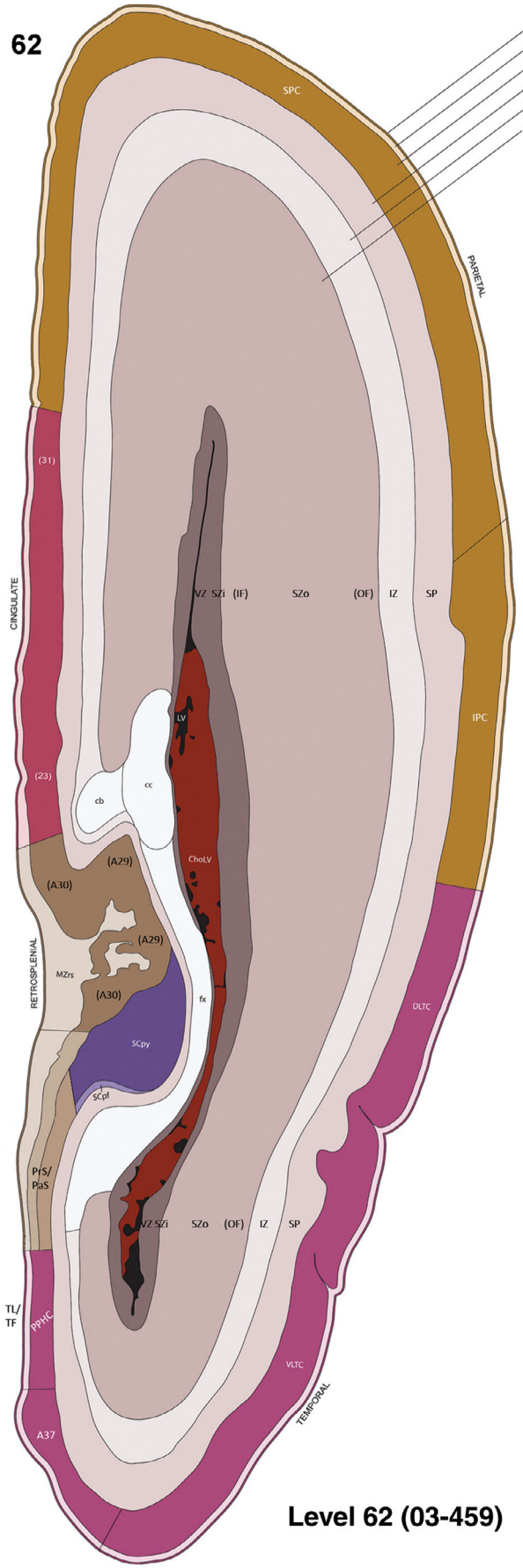

Level 62 (03-459)

62
NISSL-03-459

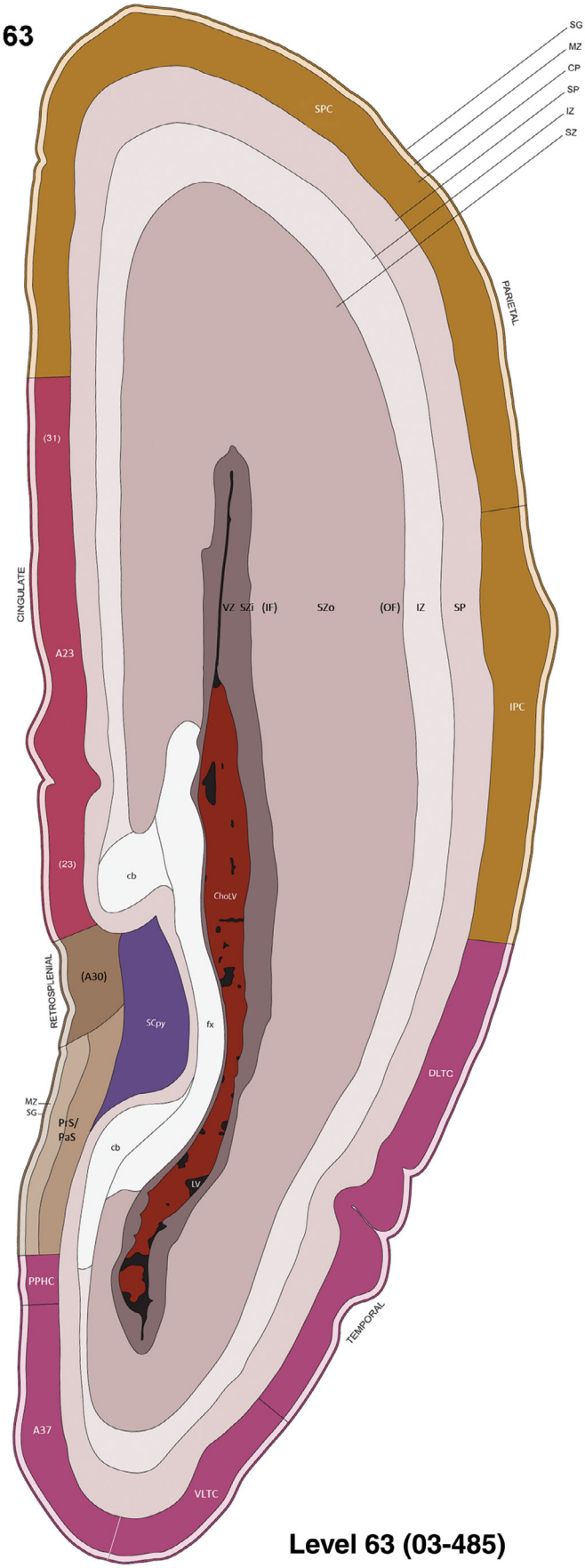

Level 63 (03-485)

63
NISSL-03-485

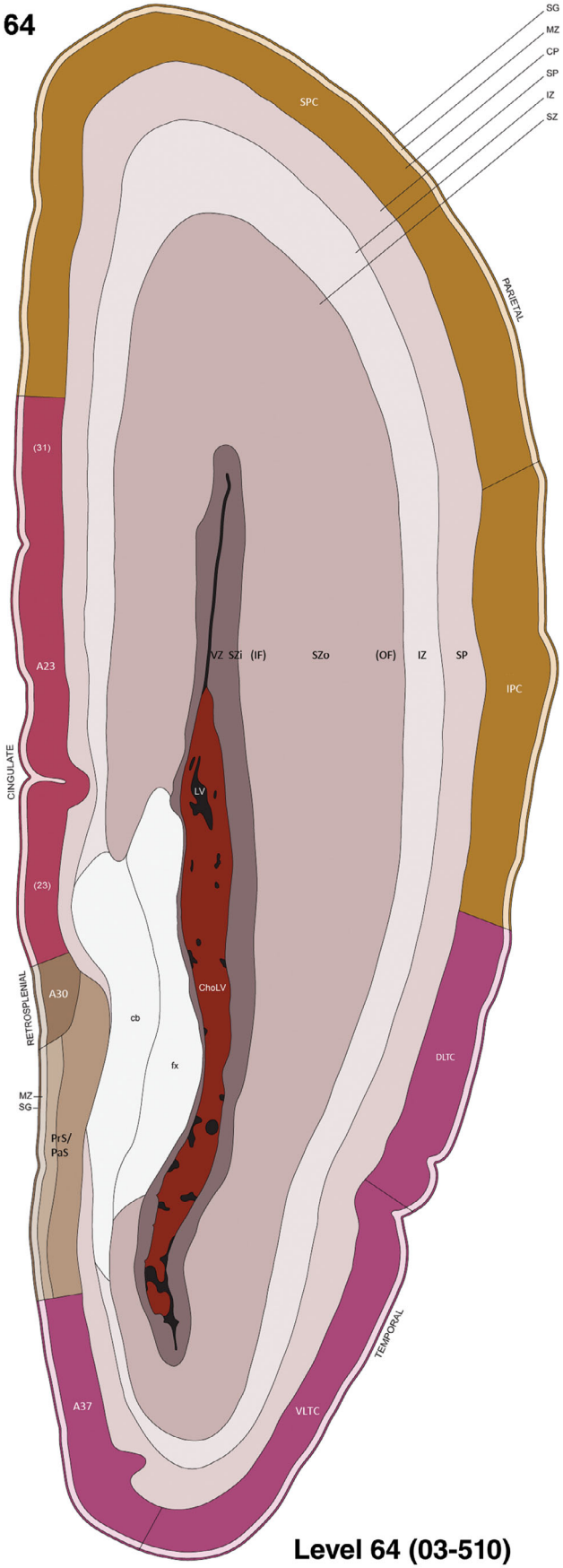

Level 64 (03-510)

64
NISSL-03-510

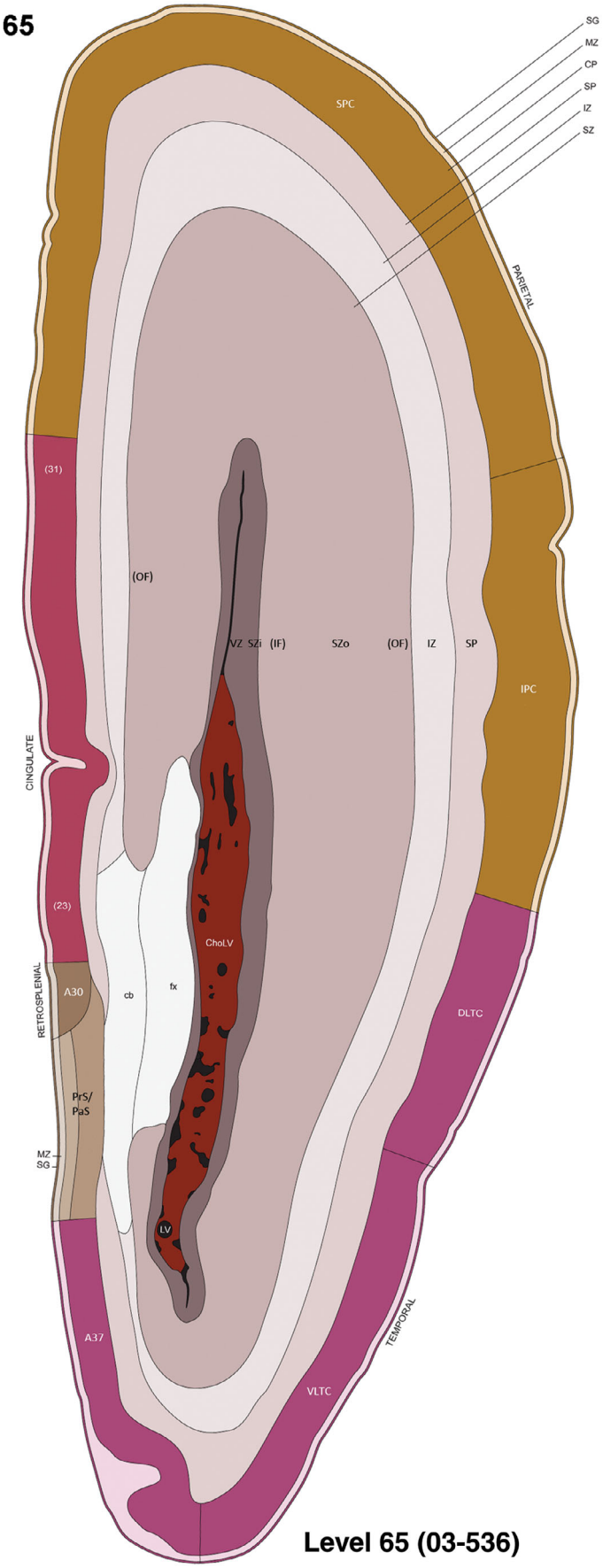

Level 65 (03-536)

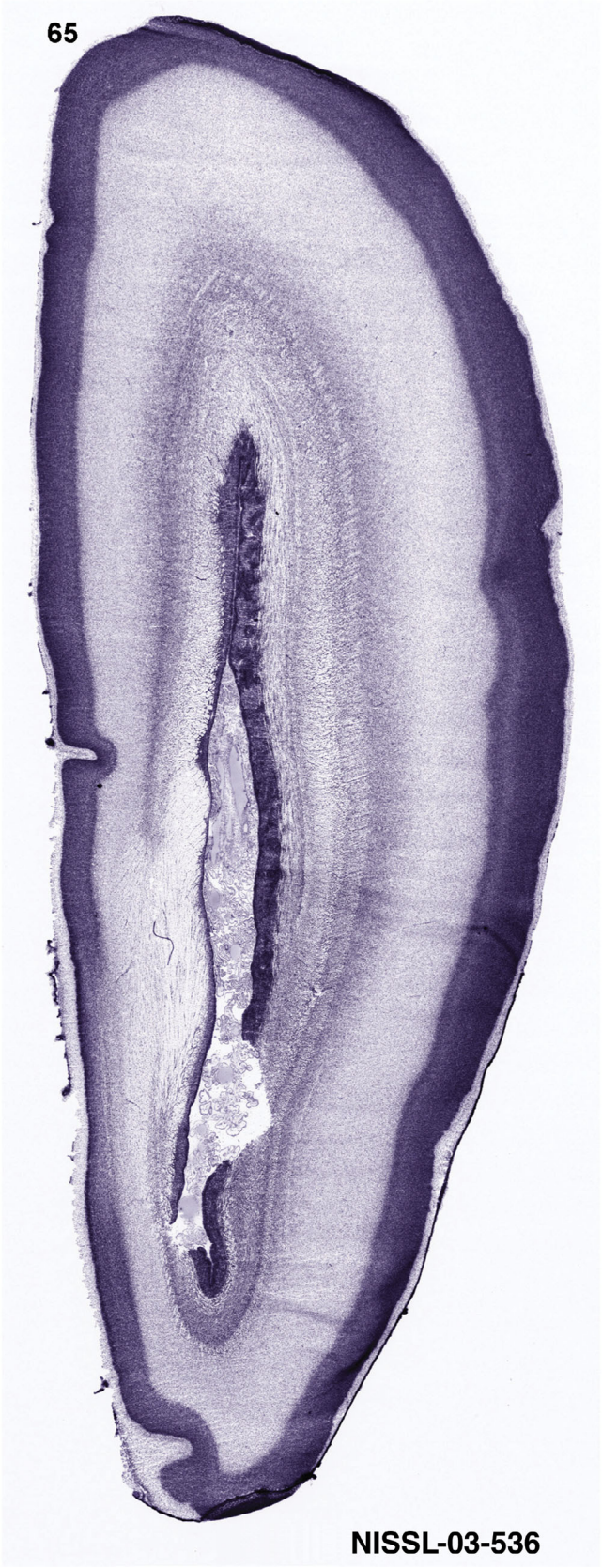
65
NISSL-03-536

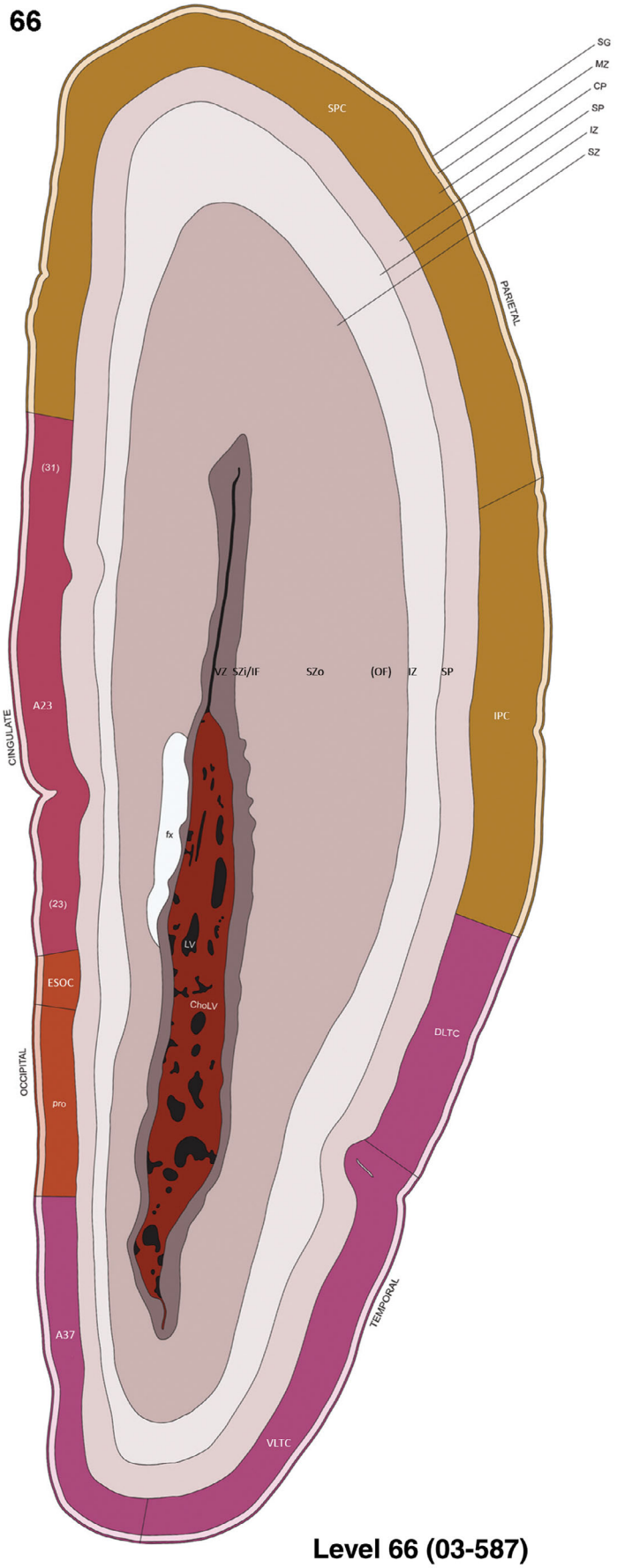

Level 66 (03-587)

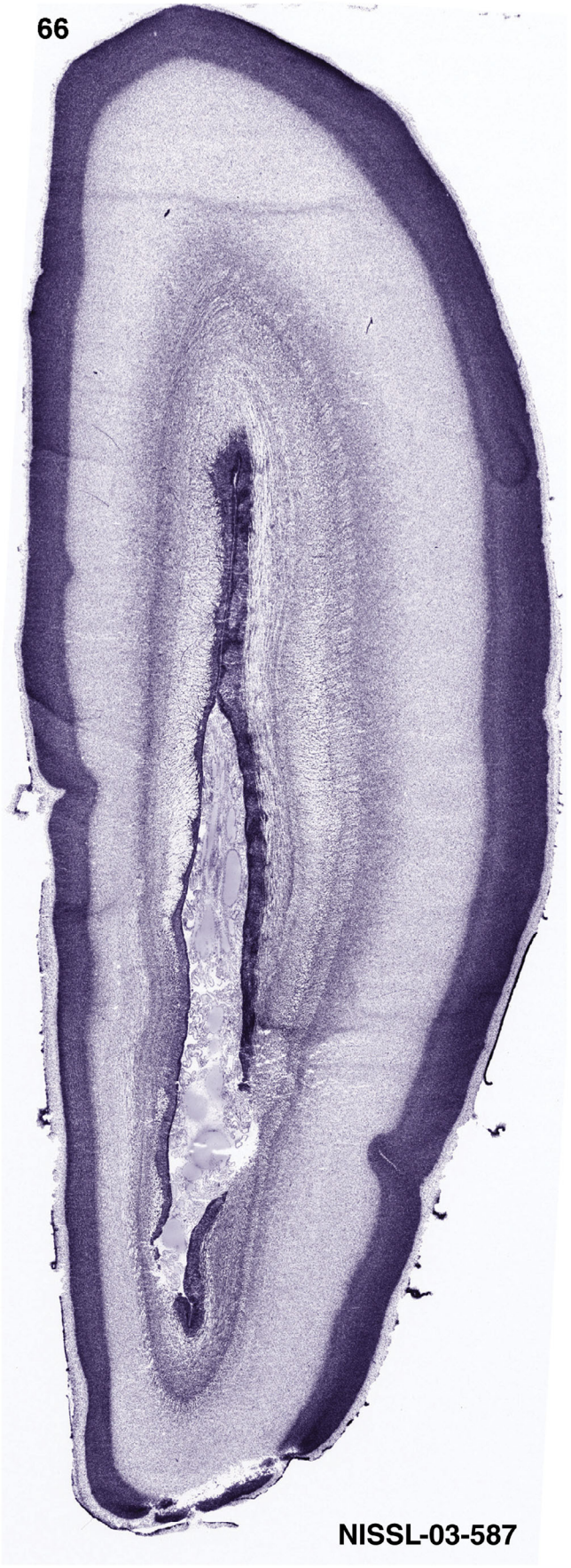
66
NISSL-03-587

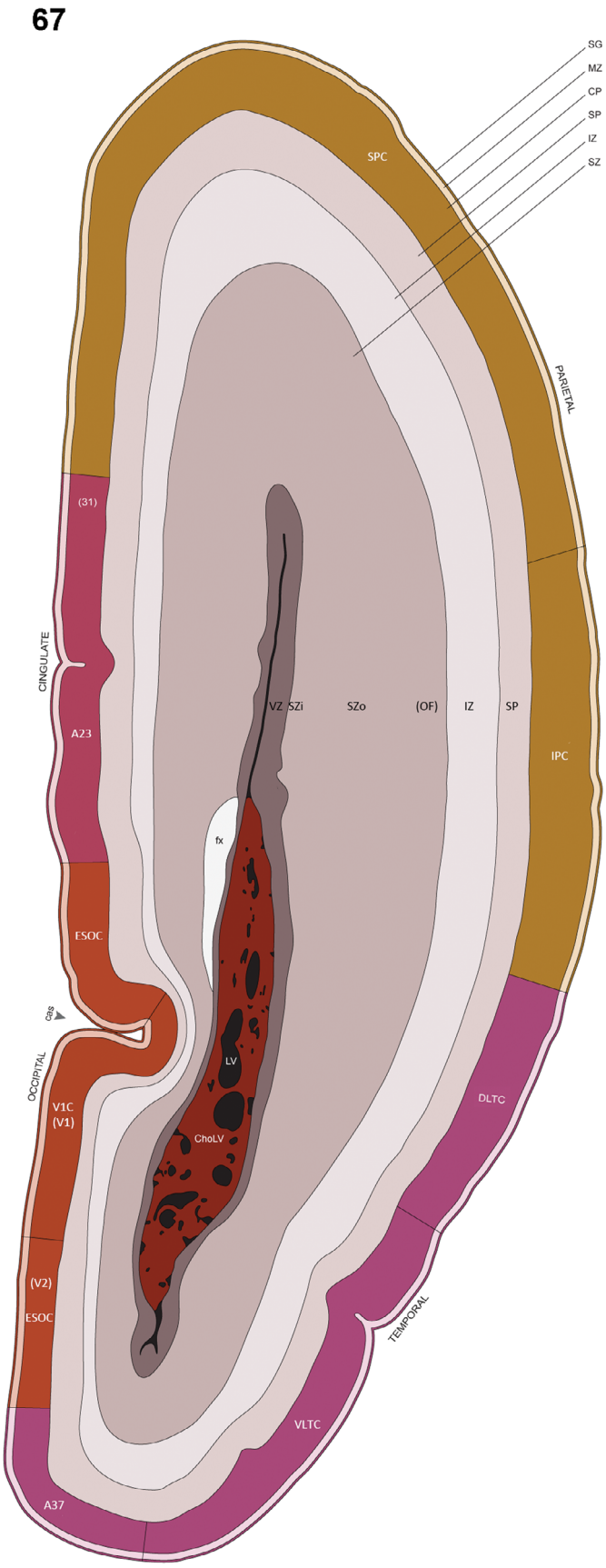

Level 67 (03-638)

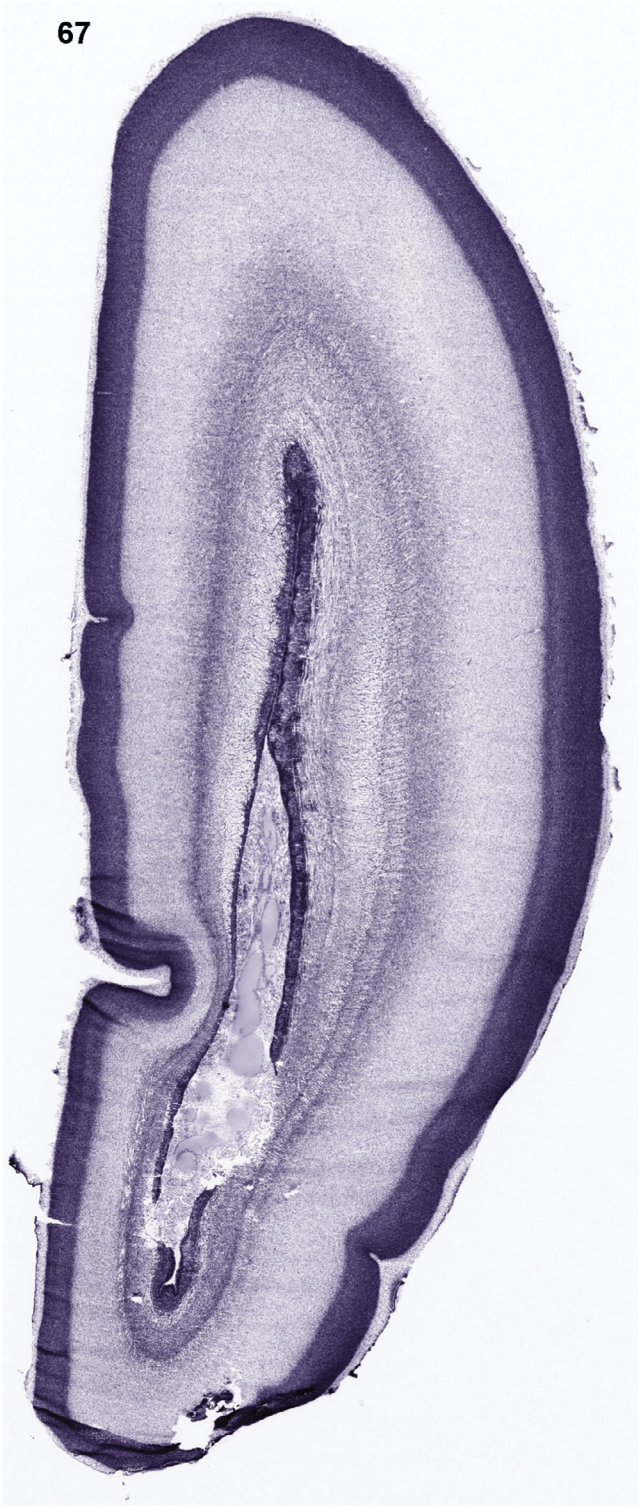

NISSL-03-638

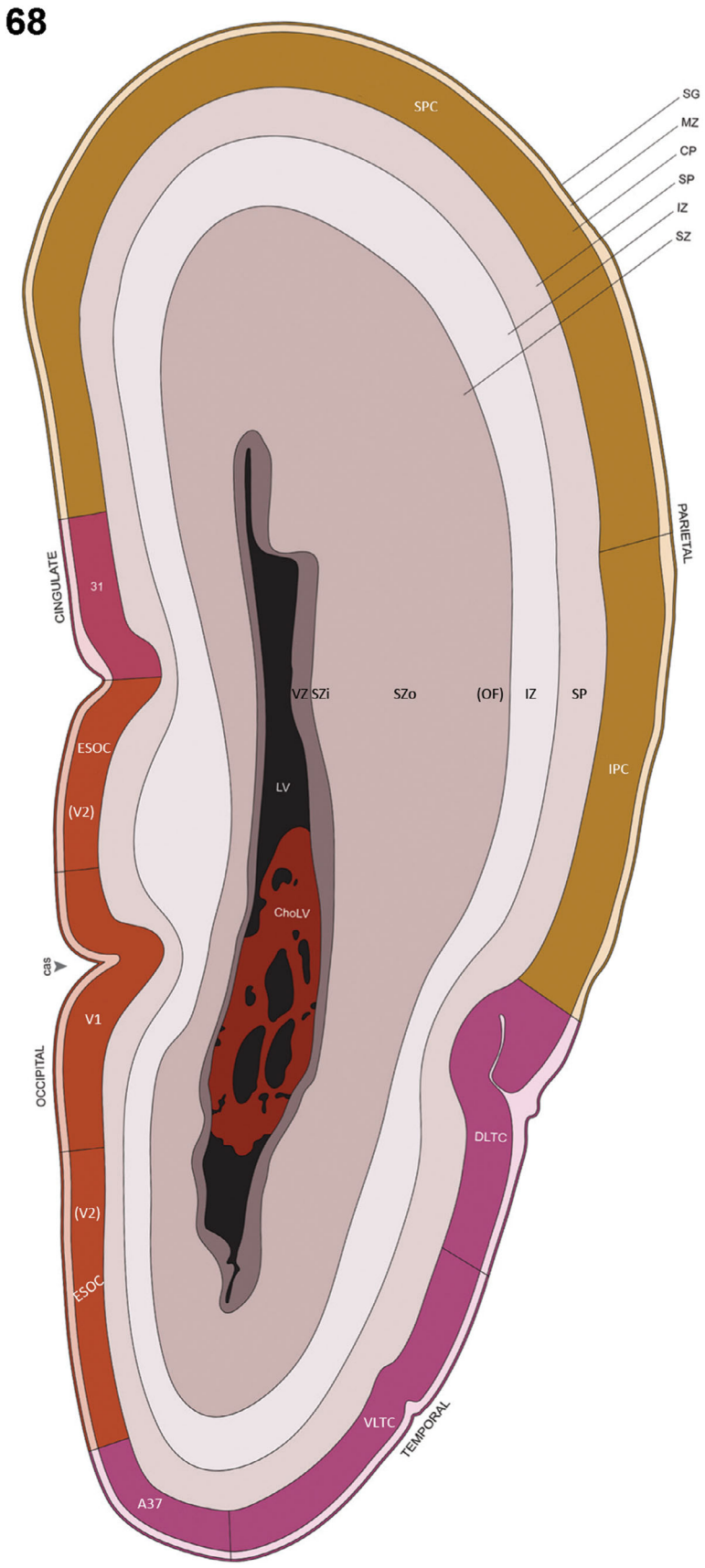

Level 68 (04-026)

68

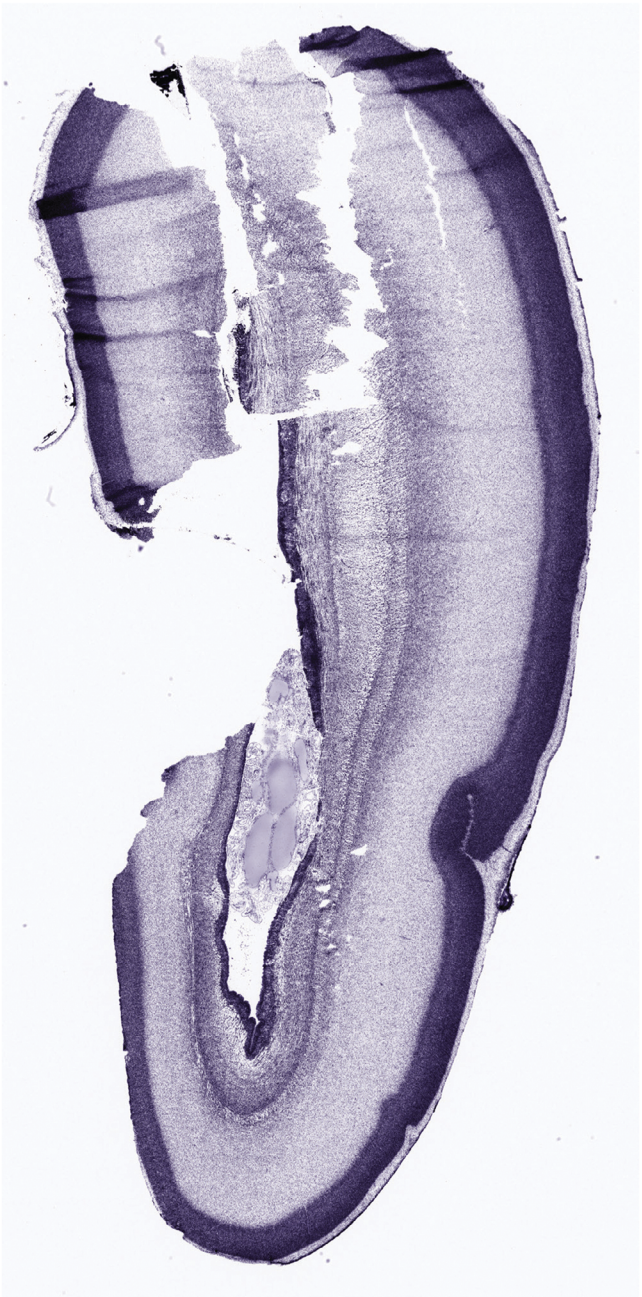

NISSL-04-026

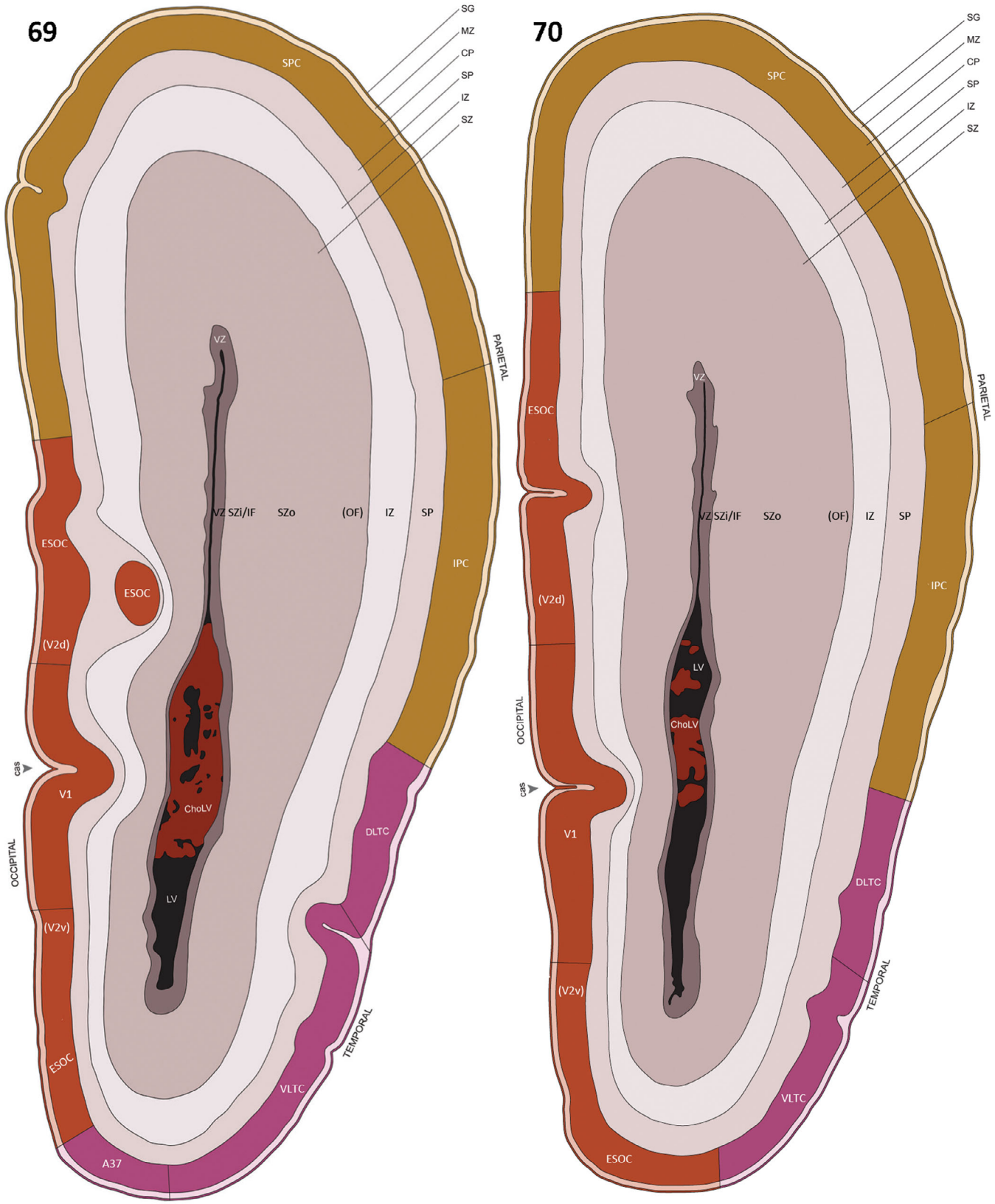

Level 71 (04-077) **Level 72 (04-128)**

69
70
NISSL-04-077
NISSL-04-128

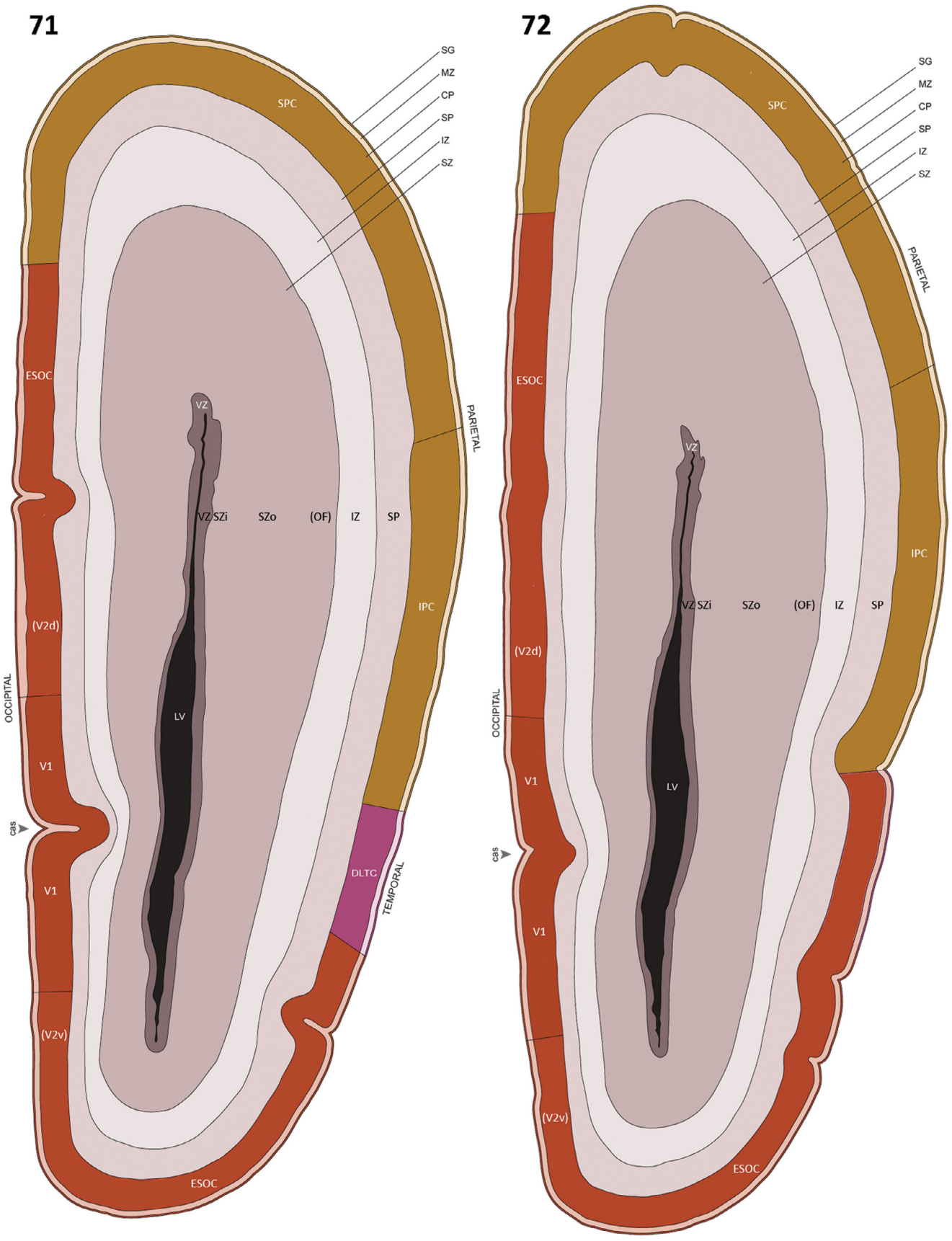

Level 71 (04-179)

Level 72 (04-230)

NISSL-04-179 NISSL-04-230

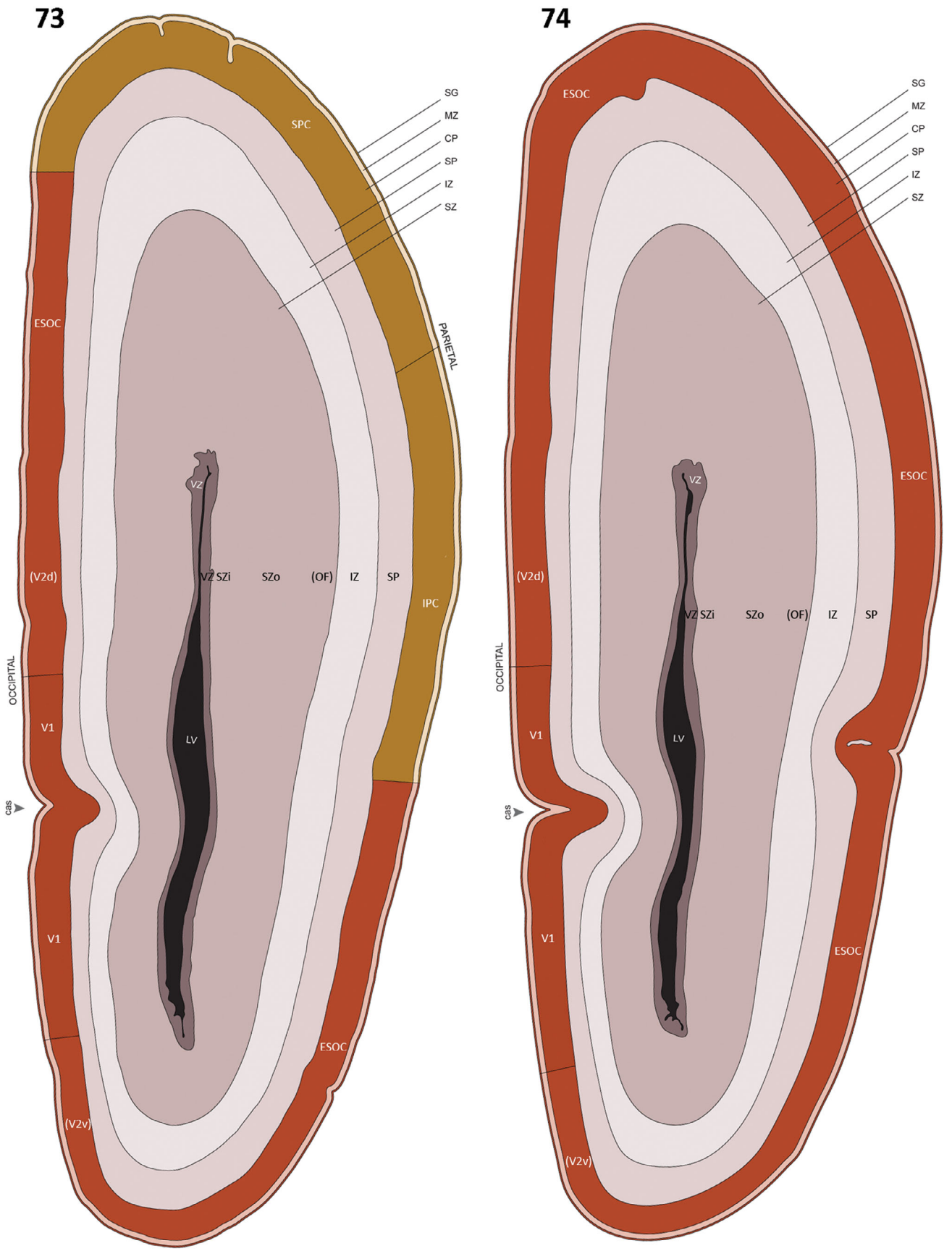

Level 73 (04-281)

Level 74 (04-306)

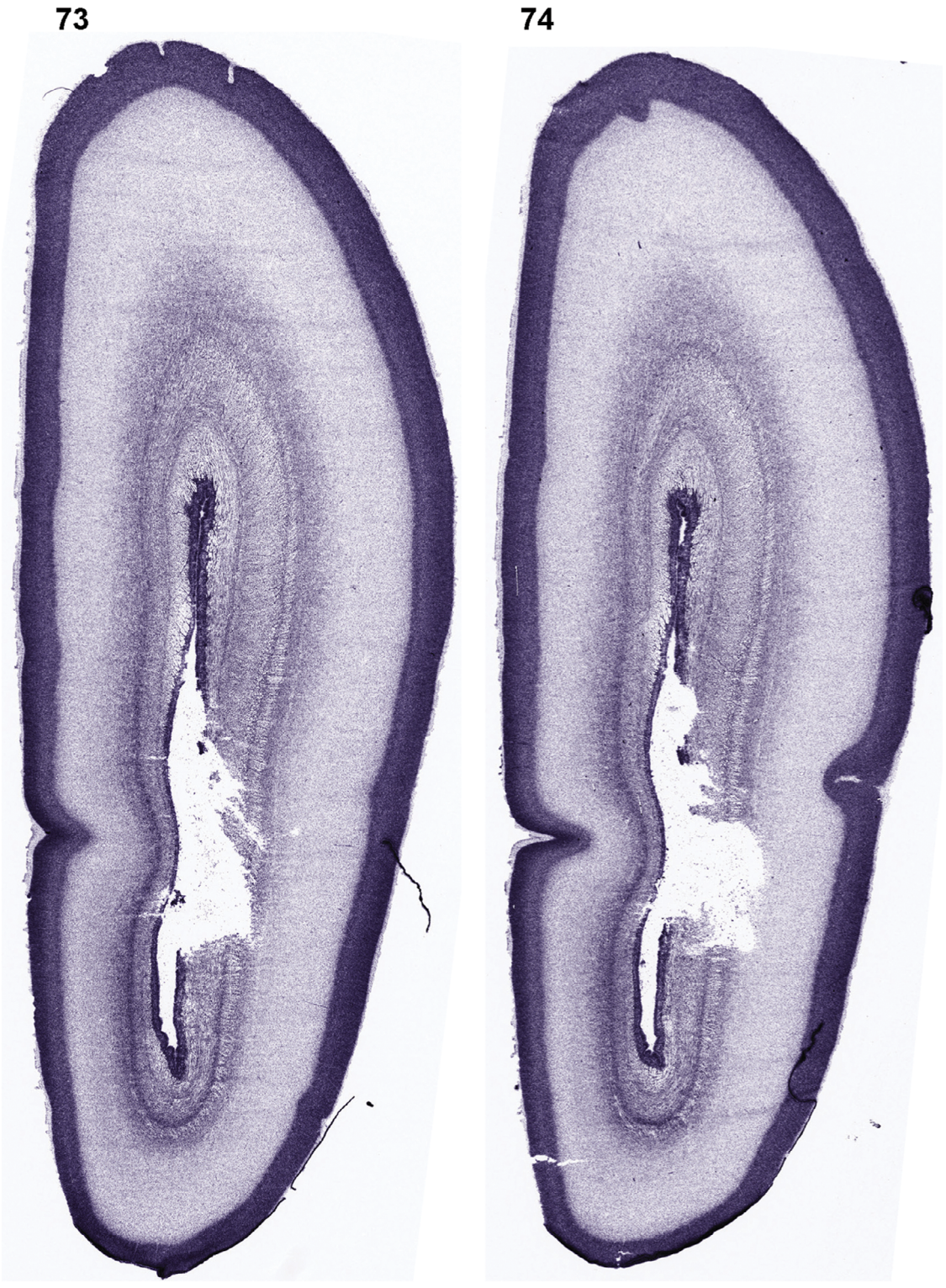
73
74
NISSL-04-281
NISSL-04-306

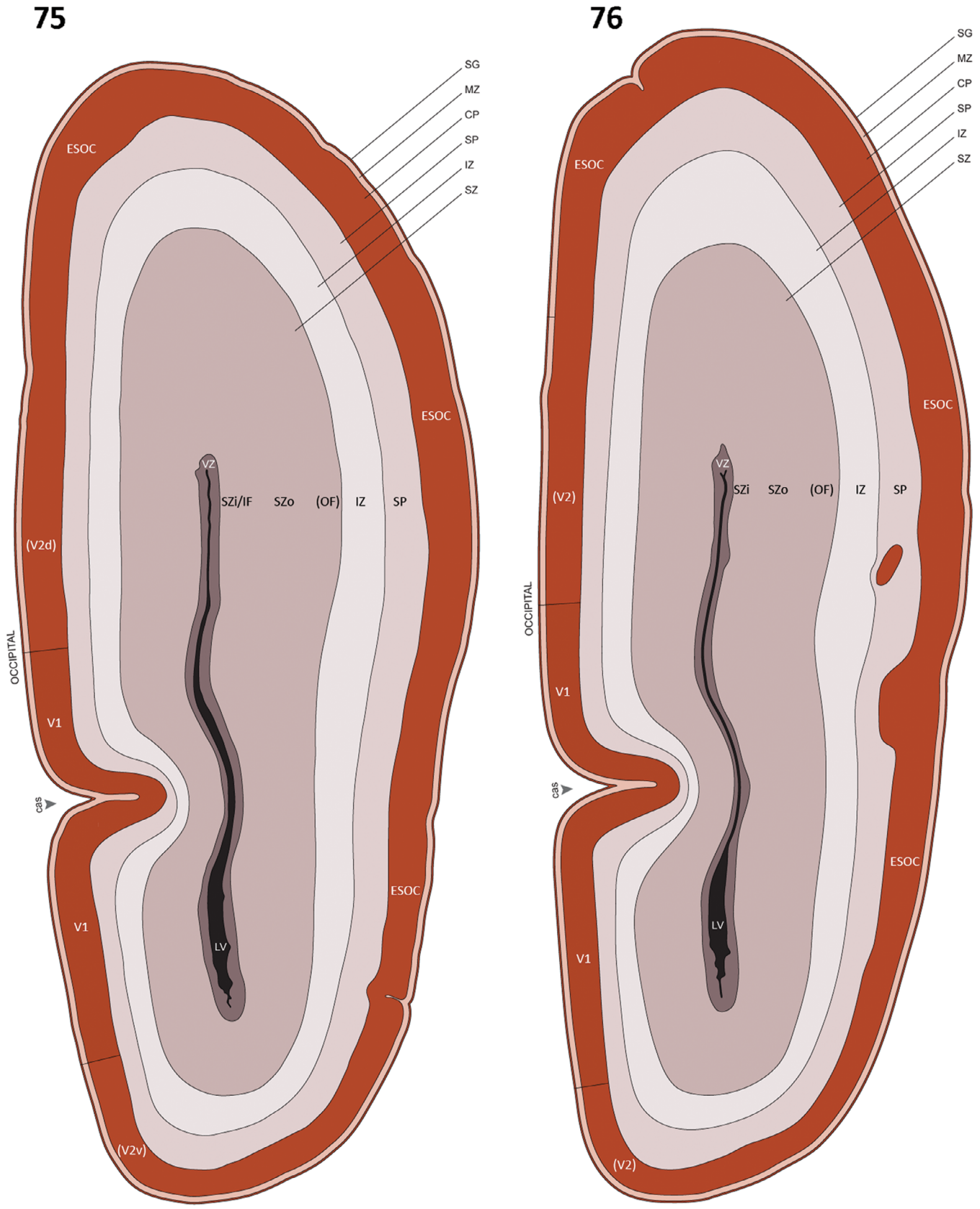

Level 75 (04-357)

Level 76 (04-408)

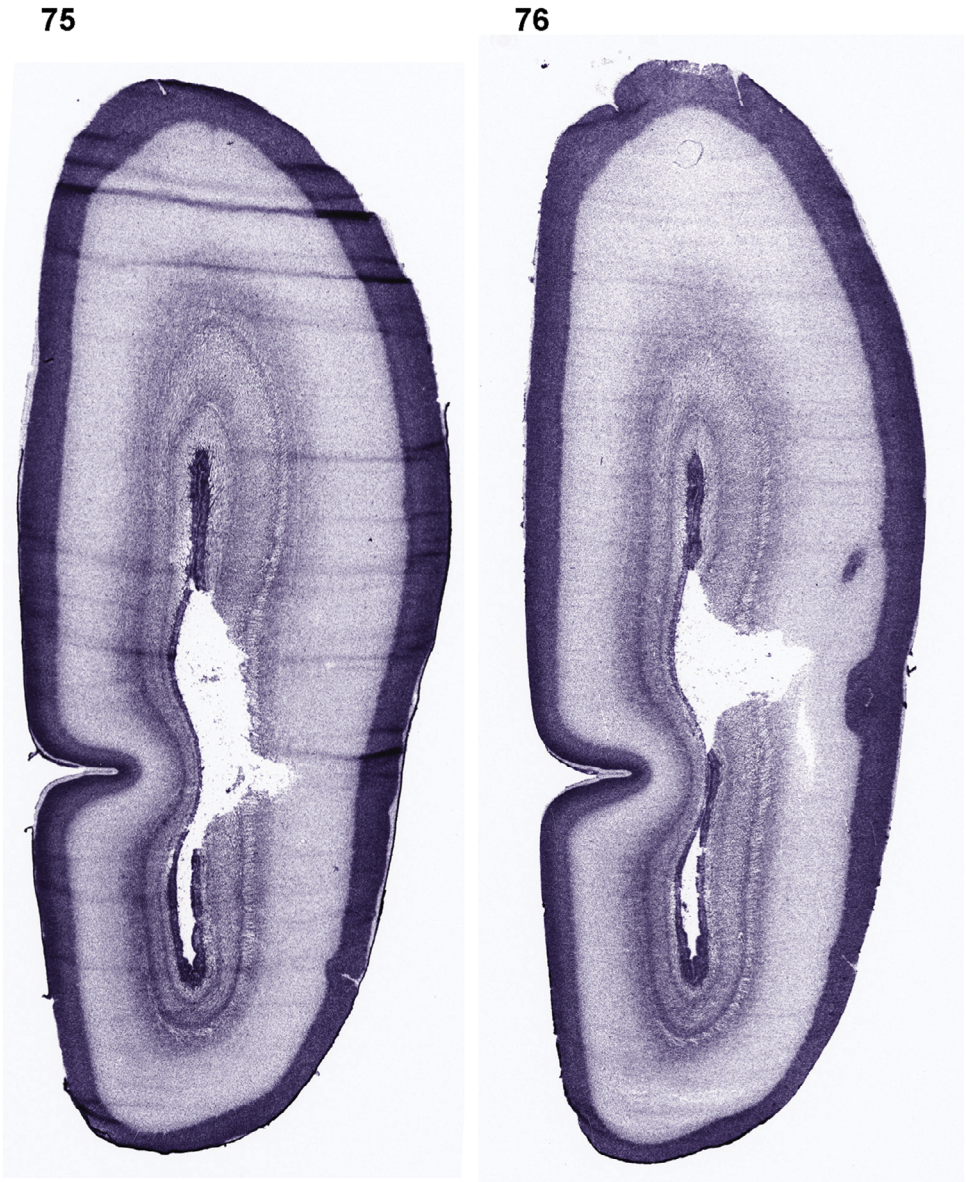
75
76
NISSL-04-357
NISSL-04-408

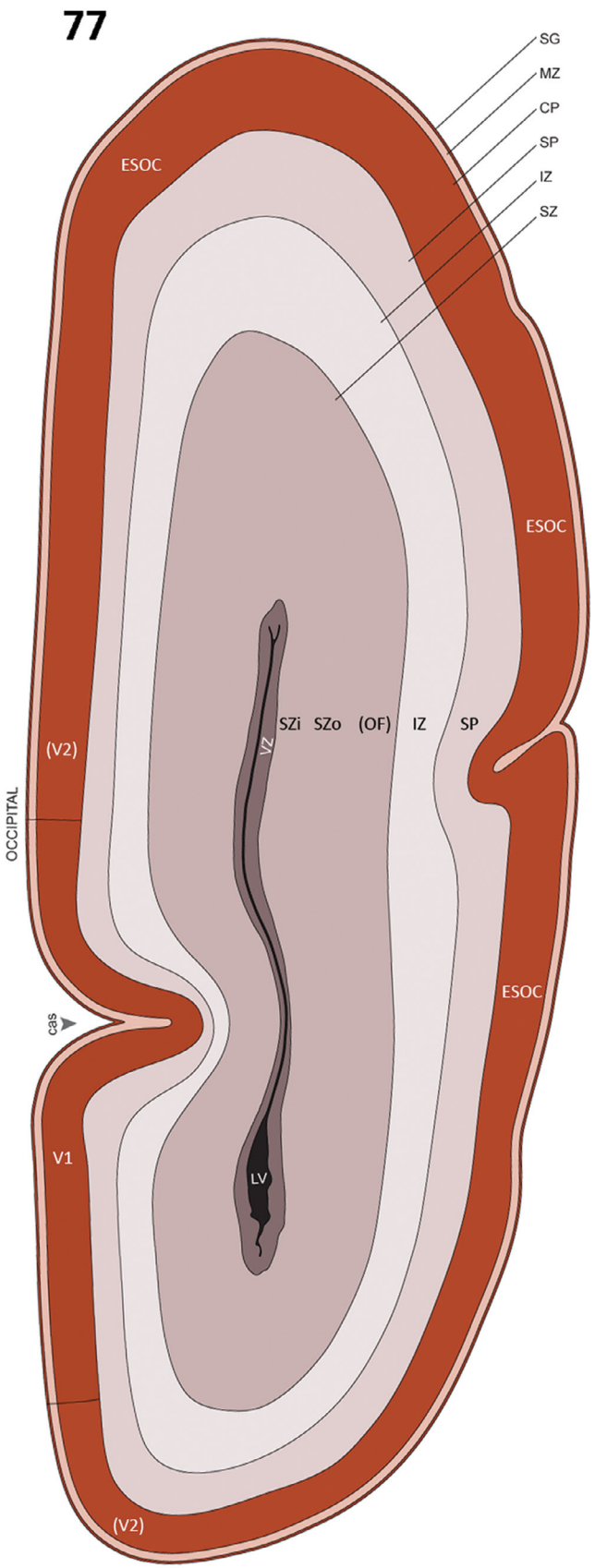

Level 77 (04-459)

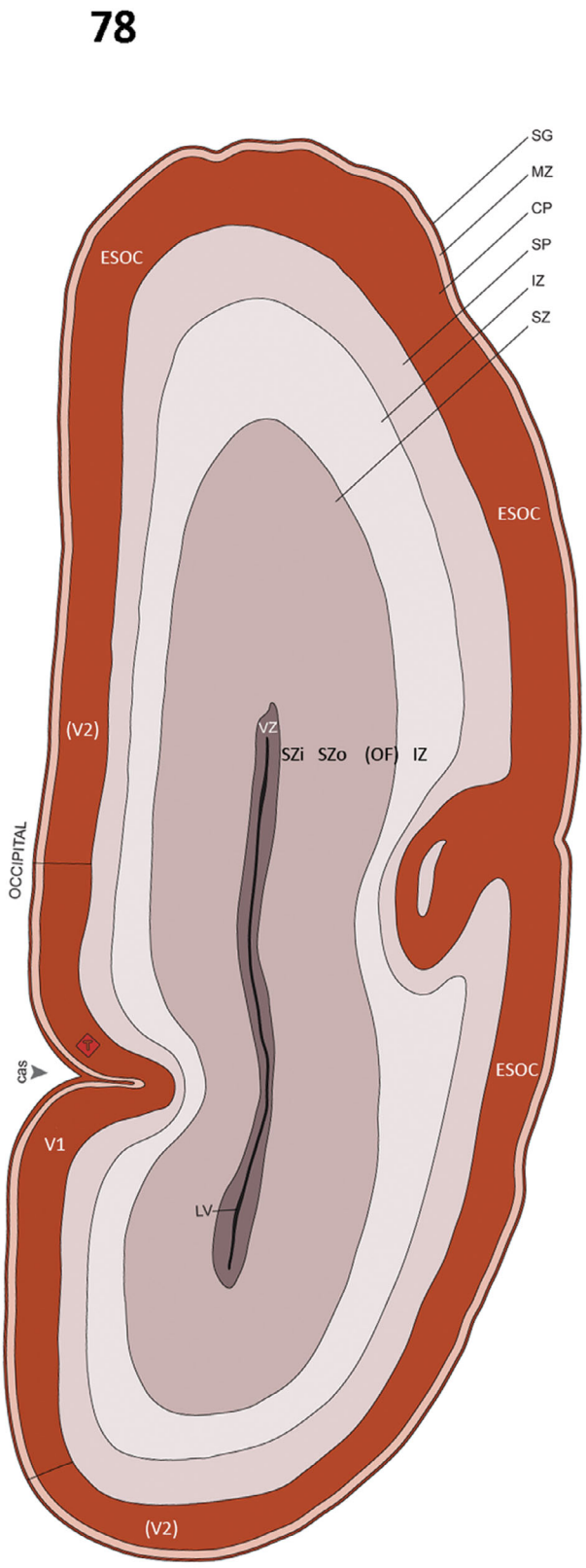

Level 78 (04-511)

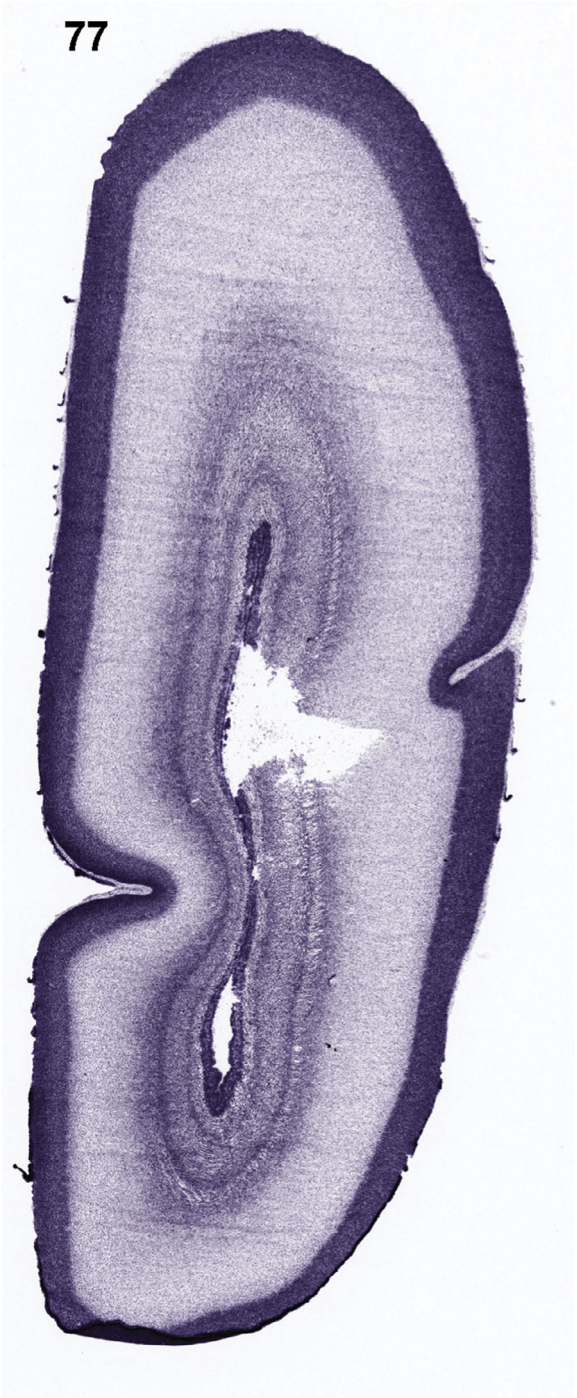

NISSL-04-459

NISSL-04-511

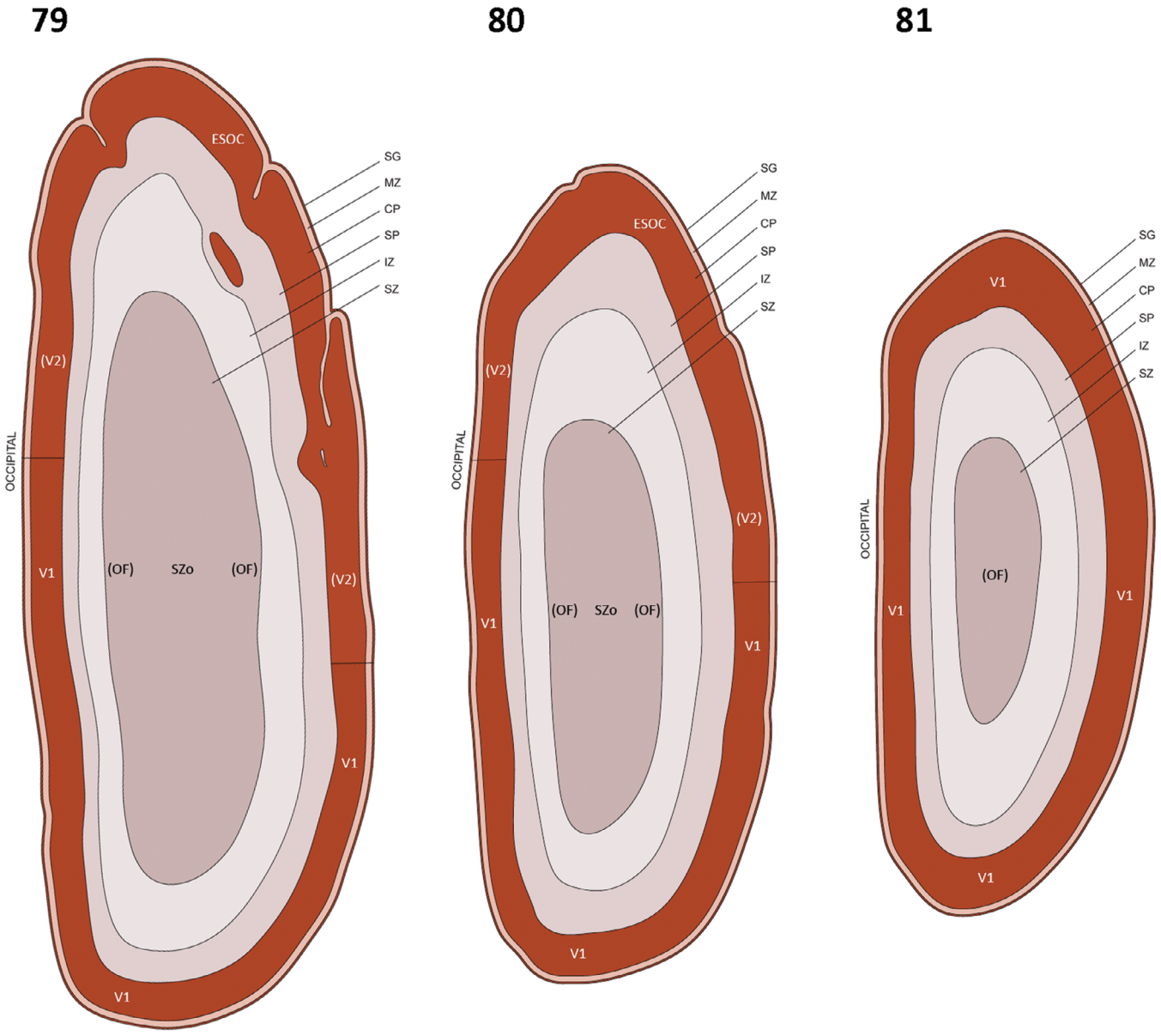

Level 79 (04-612) **Level 80 (04-664)** **Level 81 (04-714)**

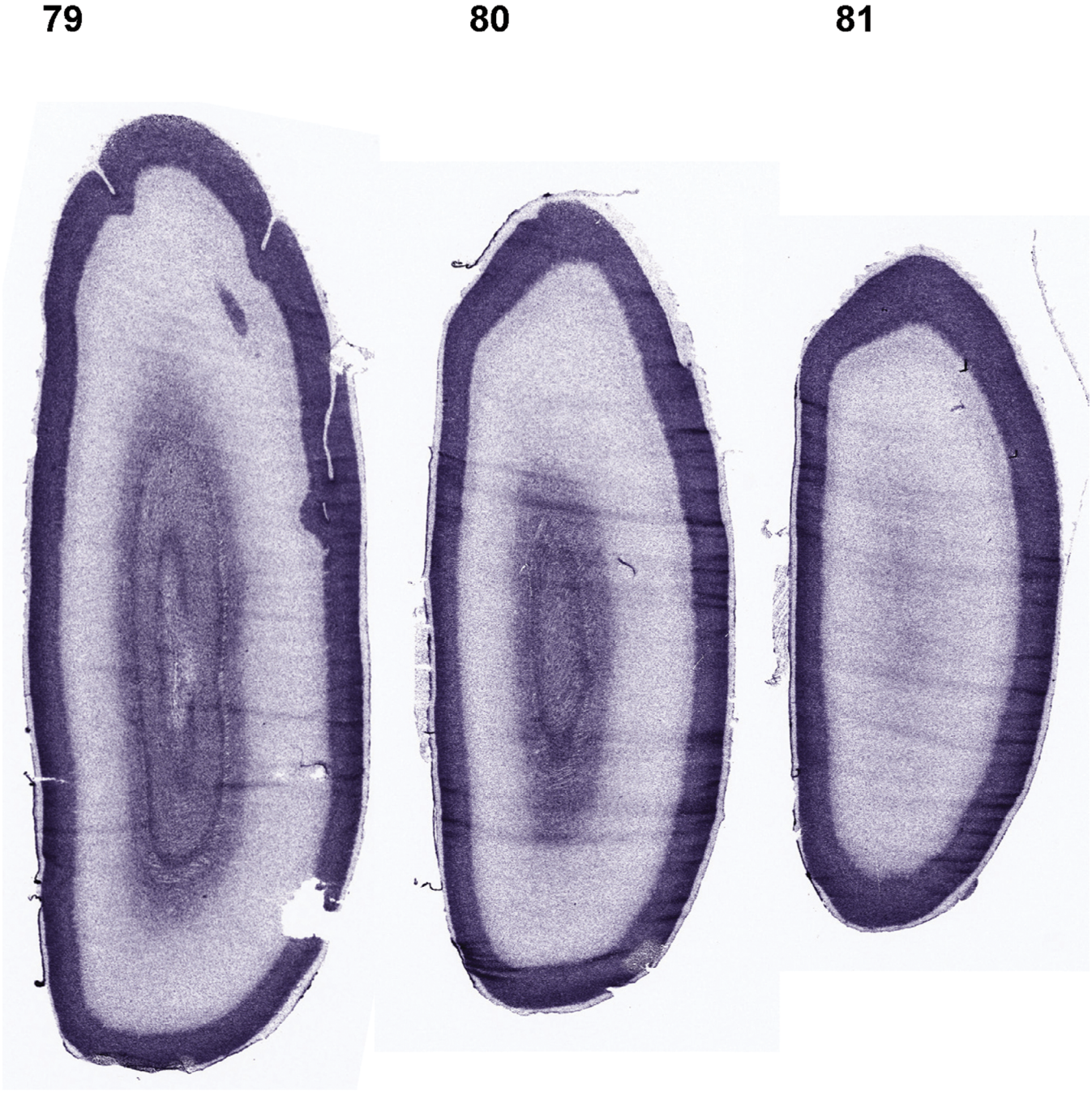
79
80
81
NISSL-04-612
NISSL-04-664
NISSL-04-714

APPENDIX 4: Spatial expression of five representative genes in the brain at PCW 21

Anatomical localizations of the gene expression are based on the anatomical brain atlas (Appendix 3) which is derived from the same brain hemisphere. Note that some artifacts like the blank (white) round or oval regions usually caused by air bulbs during ISH staining are indicated by (#). The spatial expression of the other 38 genes was not annotated because of limited length of this article but the sequential ISH images of these genes are linked online in this appendix. The spatial locations of their expression can be easily determined using our anatomical brain atlas (Appendix 3) as a guide, as demonstrated for the five genes displayed here.

a. **List of five genes and their spatial expression in the brain**

ENC1 [ectodermal-neural cortex (with BTB-like domain)] 423
(link to online high-resolution sequential ISH images)
GRIK2 (glutamate receptor, ionotropic, kainate 2): 449
(link to online high-resolution sequential ISH images)
NRGN neurogranin (protein kinase C substrate, RC3): 464
(link to online high-resolution sequential ISH images)
PLXNA2 (plexin A2): 475
(link to online high-resolution sequential ISH images)
SST (somatostatin): 491
(link to online high-resolution sequential ISH images)

b. **List of other 38 genes and their spatial expression in the brain (online link only)**

CALB2 (calbindin 2): link to online ISH images.

CDH4 [cadherin 4, type 1, R-cadherin (retinal)]: link to online ISH images.

CNTNAP2 (contactin associated protein-like 2): link to online ISH images.

DCX (doublecortin): link to online ISH images.

DLX1 (distal-less homeobox 1): link to online ISH images.

DLX2 (distal-less homeobox 2): link to online ISH images.

DLX5 (distal-less homeobox 5): link to online ISH images.

EOMES (eomesodermin) or TBR2 (T-box brain transcription factor 2): link to online ISH images.

ERBB4 [v-erb-a erythroblastic leukemia viral oncogene homolog 4 (avian)]: link to online ISH images.

ETV1 (ets variant 1): link to online ISH images.

FABP7 (fatty acid-binding protein 7, brain): link to online ISH images.

FADS2 (fatty acid desaturase 2): link to online ISH images.

FEZF2 (FEZ family zinc finger 2): link to online ISH images.

FOXG1 (forkhead box G1): link to online ISH images.

FOXP1 (forkhead box P1): link to online ISH images.

GAP43 (growth-associated protein 43): link to online ISH images.

GFAP (glial fibrillary acidic protein): link to online ISH images.

HOXA4 (homeobox A4): link to online ISH images.

LBX1 (ladybird homeobox 1): link to online ISH images.

LHX2 (LIM homeobox 2): link to online ISH images.

LMO4 (LIM domain only 4): link to online ISH images.

MECP2 (methyl CpG binding protein 2 [Rett syndrome]): link to online ISH images

NES (nestin): link to online ISH images.

NKX2.1 (NK2 homeobox 1): link to online ISH images.

NPY (neuropeptide Y): link to online ISH images.

NRXN1 (neurexin 1): link to online ISH images.

NTRK2 (neurotrophic tyrosine kinase, receptor, type 2): link to online ISH images.

PAX6 (paired box 6): link to online ISH images.

PLXNA2 (plexin A2): link to online ISH images.

RELN (reelin): link to online ISH images.

SATB2 (SATB homeobox 2): link to online ISH images.

SHANK3 (SH3 and multiple ankyrin repeat domains 3): link to online ISH images.

SOX2 [SRY (sex determining region Y)-box 2]: link to online ISH images.

SOX10 [SRY (sex determining region Y)-box 10]: link to online ISH images.

SYNGAP1 [synaptic Ras GTPase activating protein 1 homolog (rat)]: link to online ISH images.

TBR1 (T-box brain transcription factor 1): link to online ISH images.

TPP1 (tripeptidyl peptidase I): link to online ISH images.

VIM (tripeptidyl peptidase I): link to online ISH images.

ZIC1 [Zic family member 1 (odd-paired homolog, Drosophila)]: link to online ISH images.

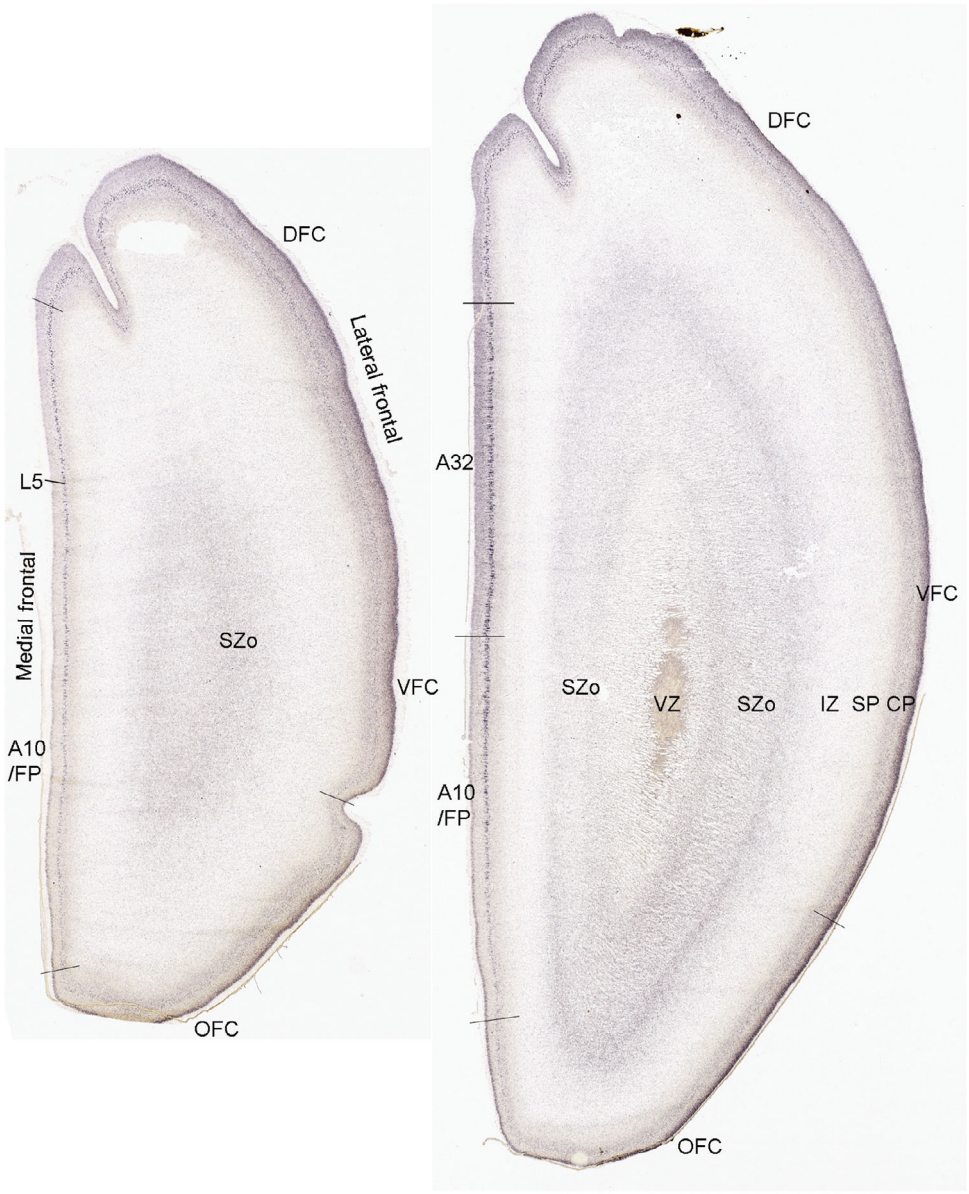

ENC1-01-130 (Level ~3) **ENC1-01-283 (Level ~5-6)**

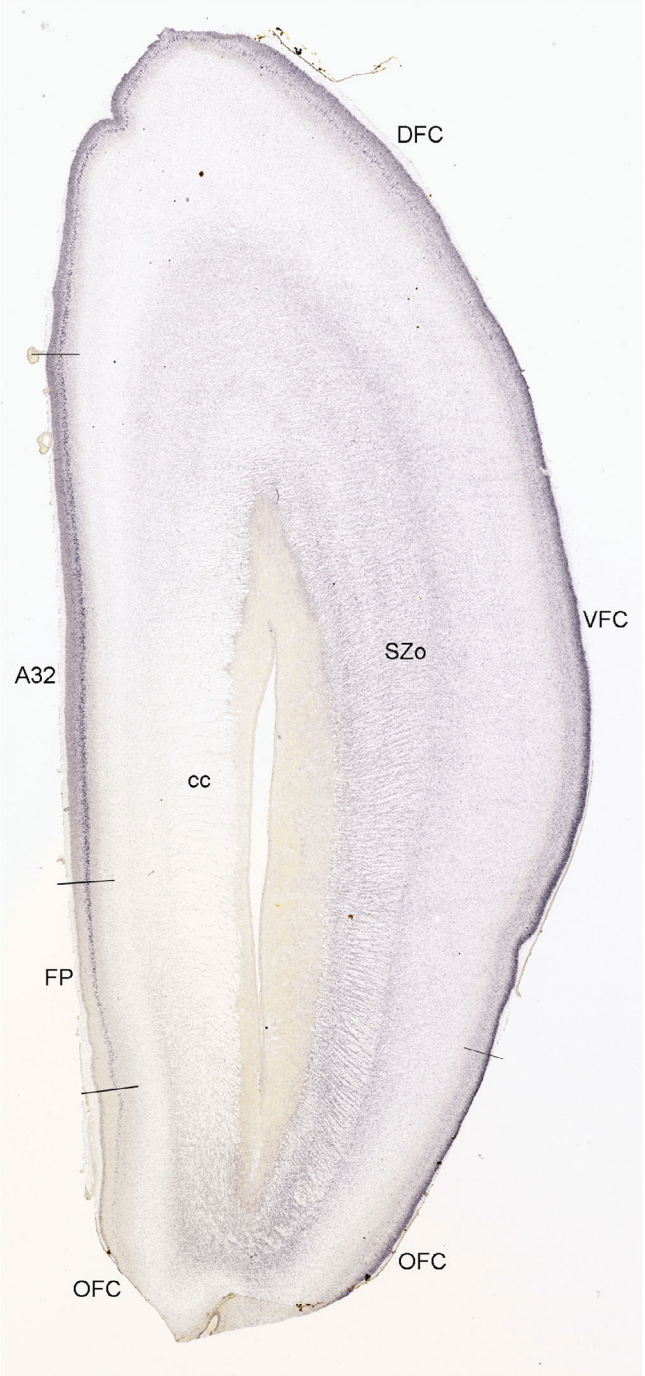

ENC1-01-436 (Level ~8-9)

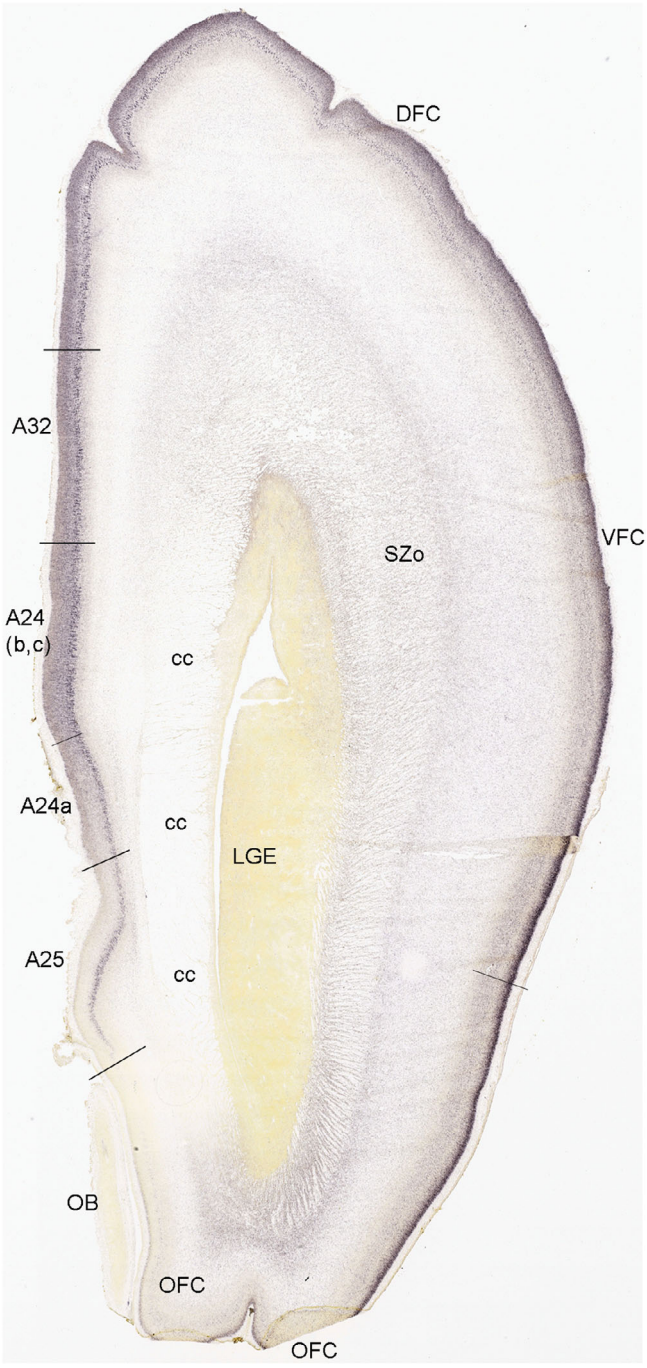

ENC1-01-538 (Level ~11)

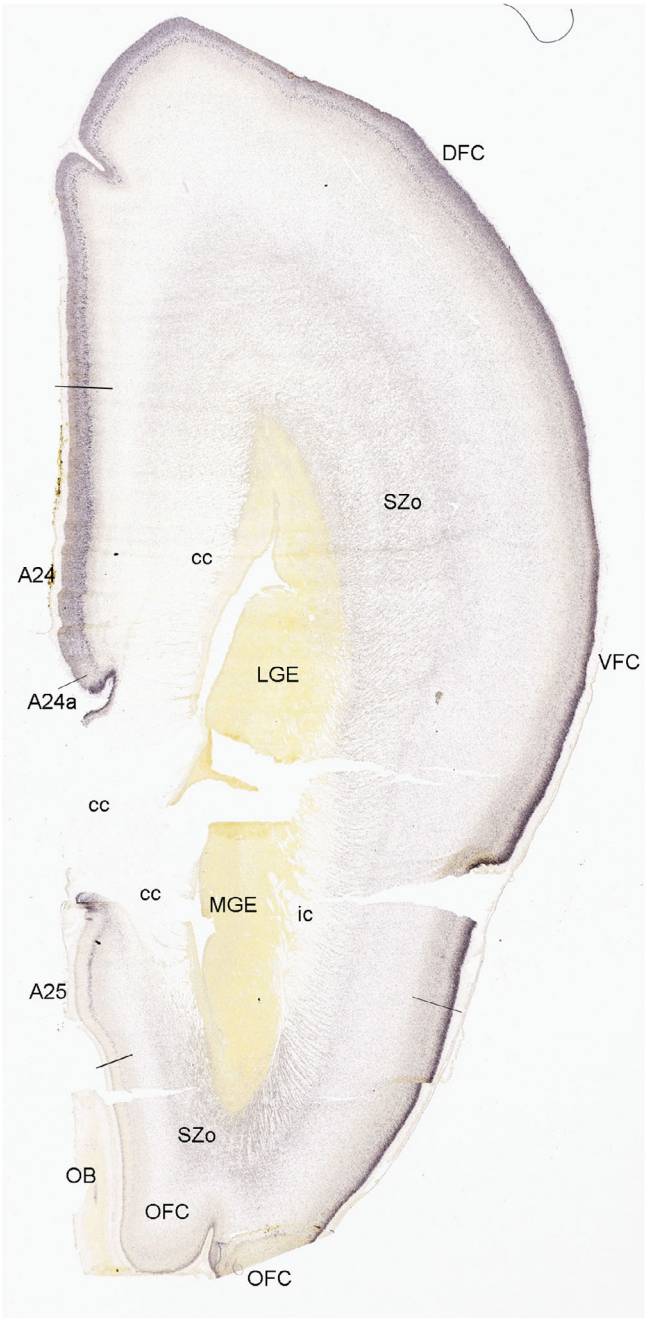

ENC1-01-589 (Level ~11-12)

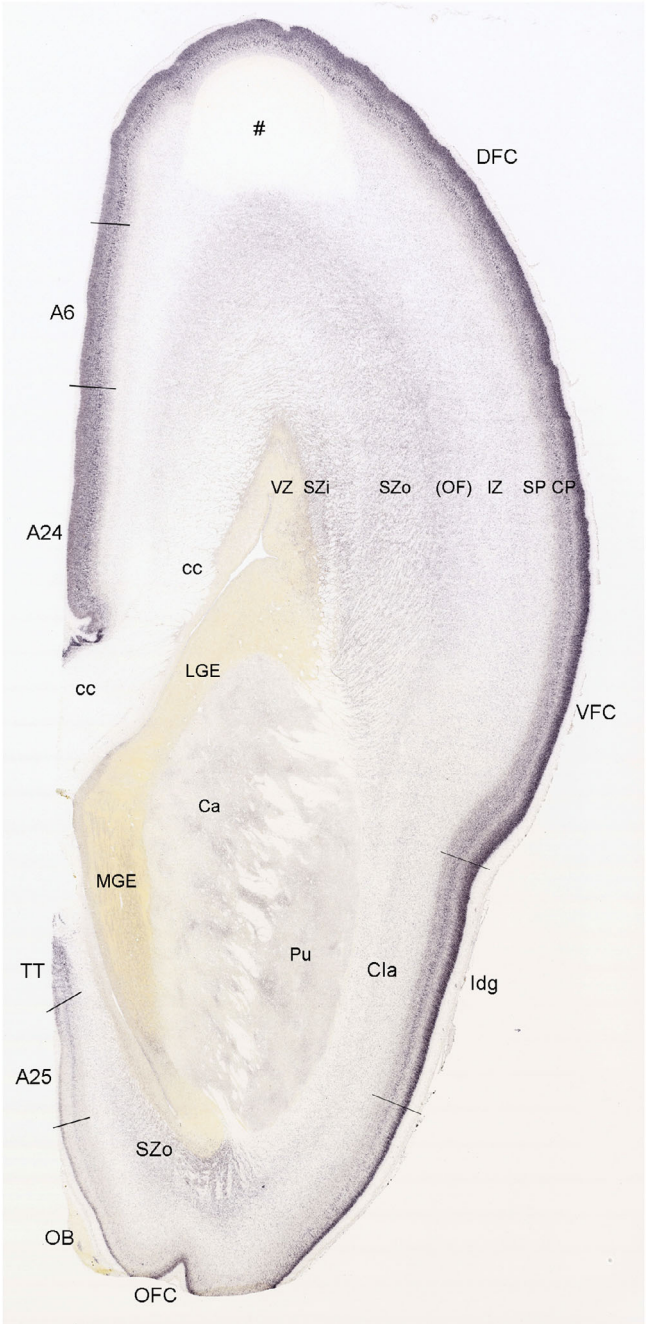

ENC1-02-028 (Level ~15)

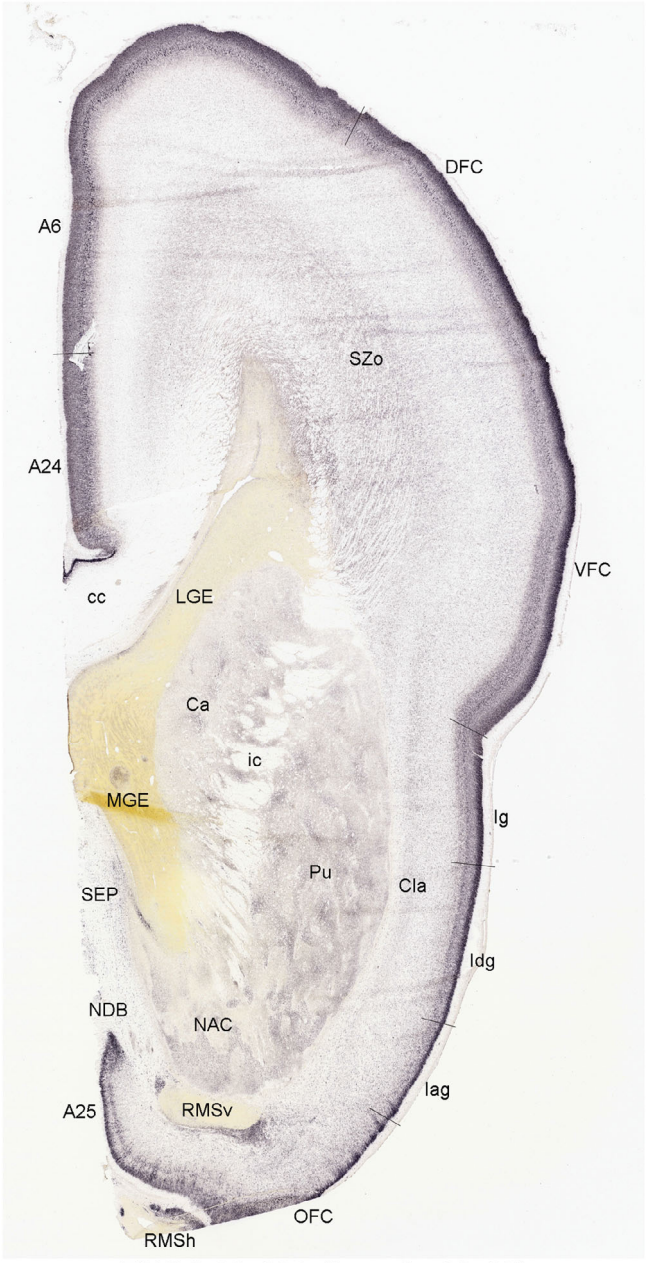

ENC1-02-130 (Level ~18-19)

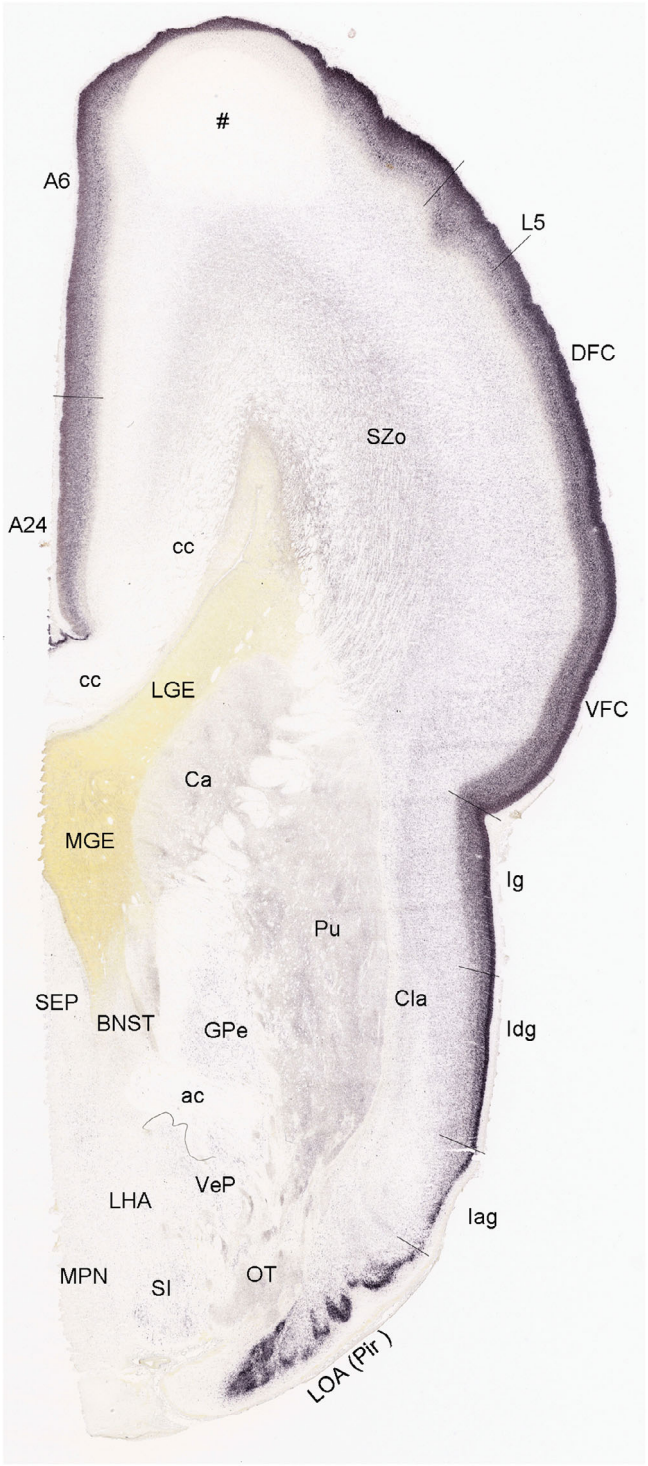

ENC1-02-232 (Level ~22)

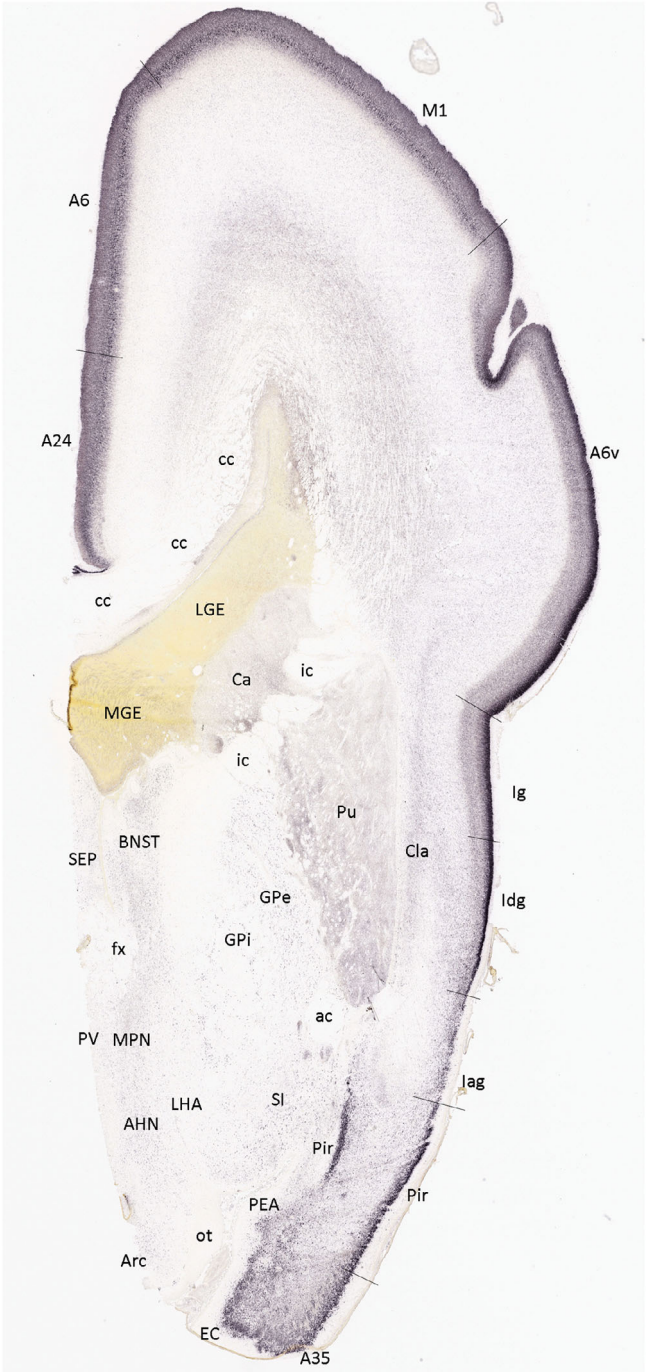

ENC1-02-334 (Level ~26)

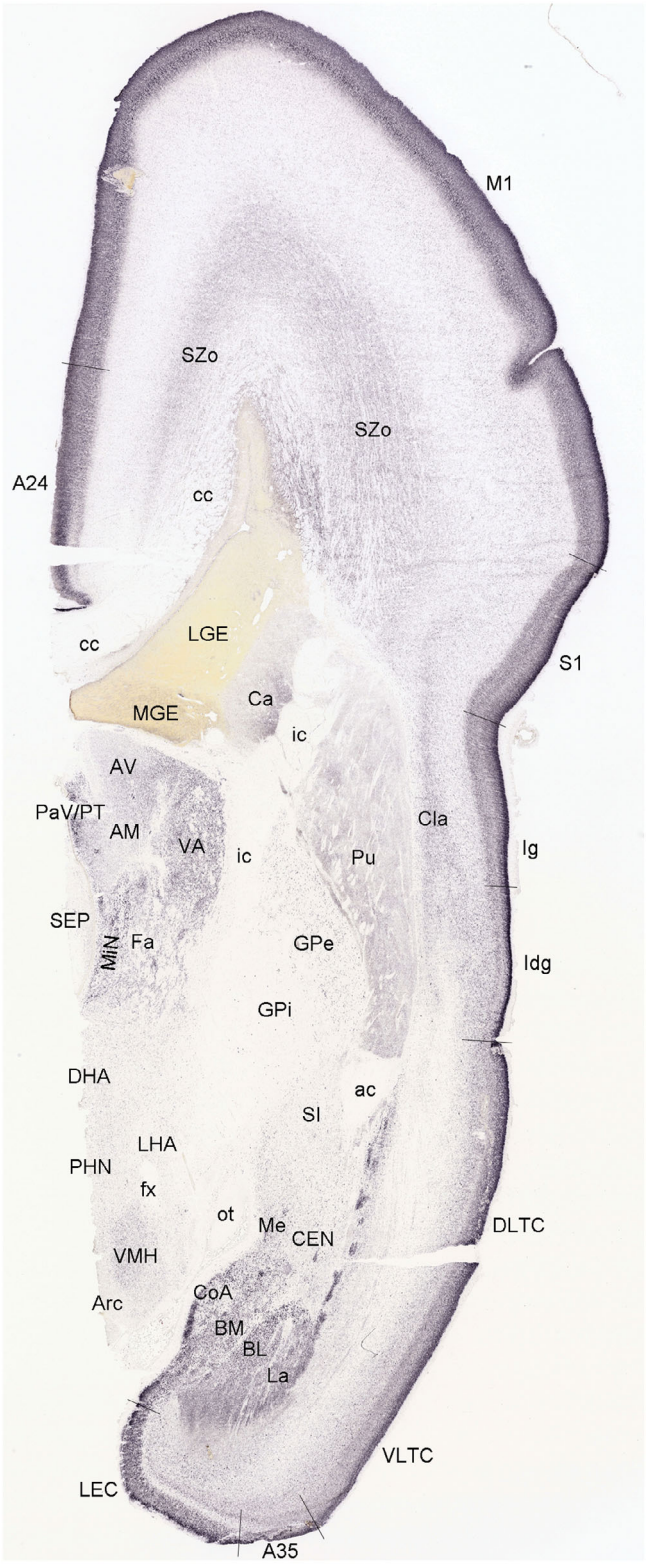

ENC1-02-436 (Level ~30)

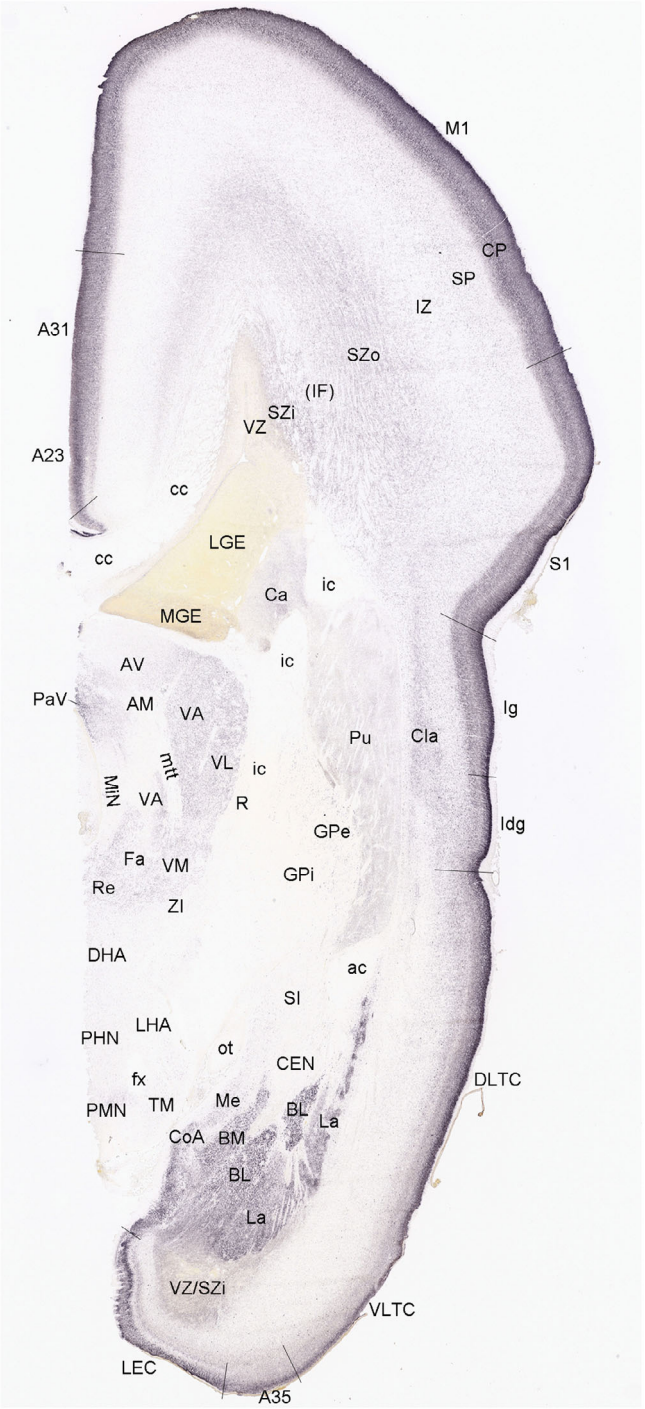

ENC1-02-487 (Level ~32)

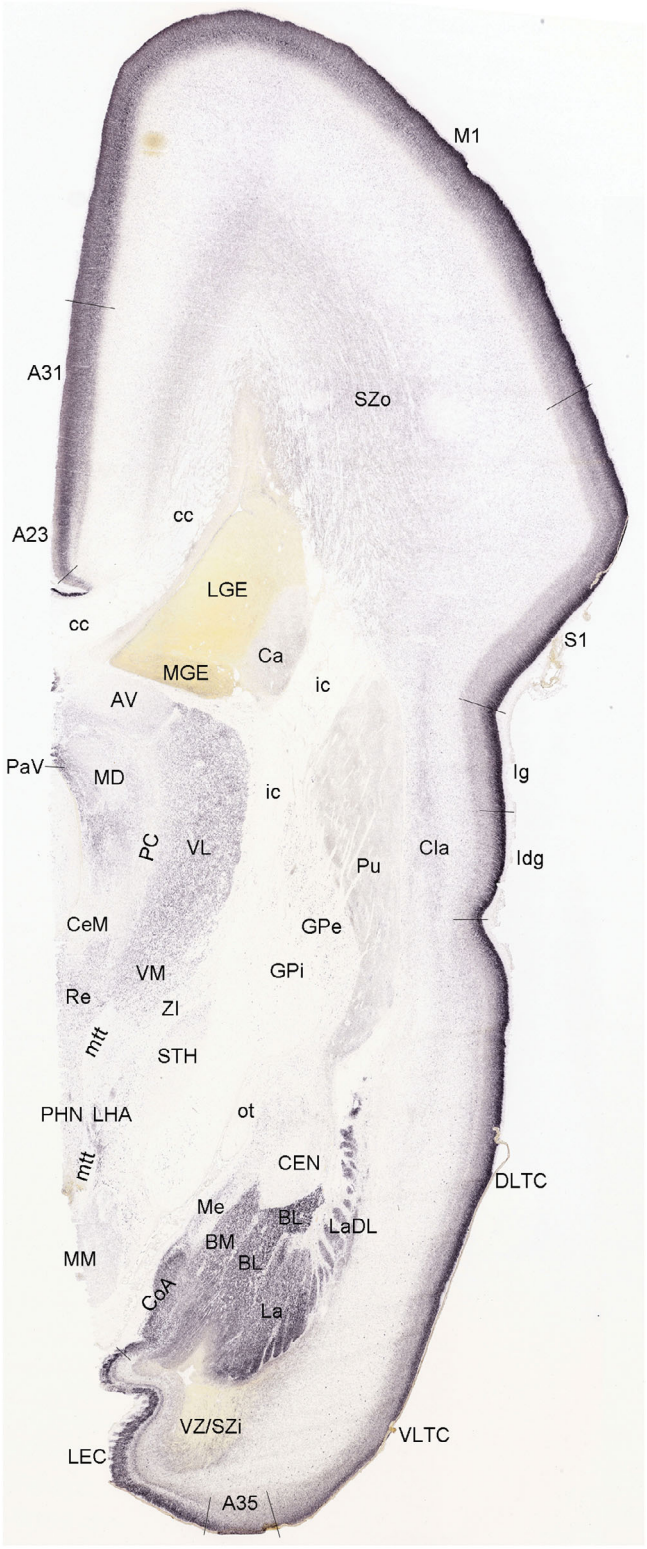

ENC1-02-538 (Level ~34)

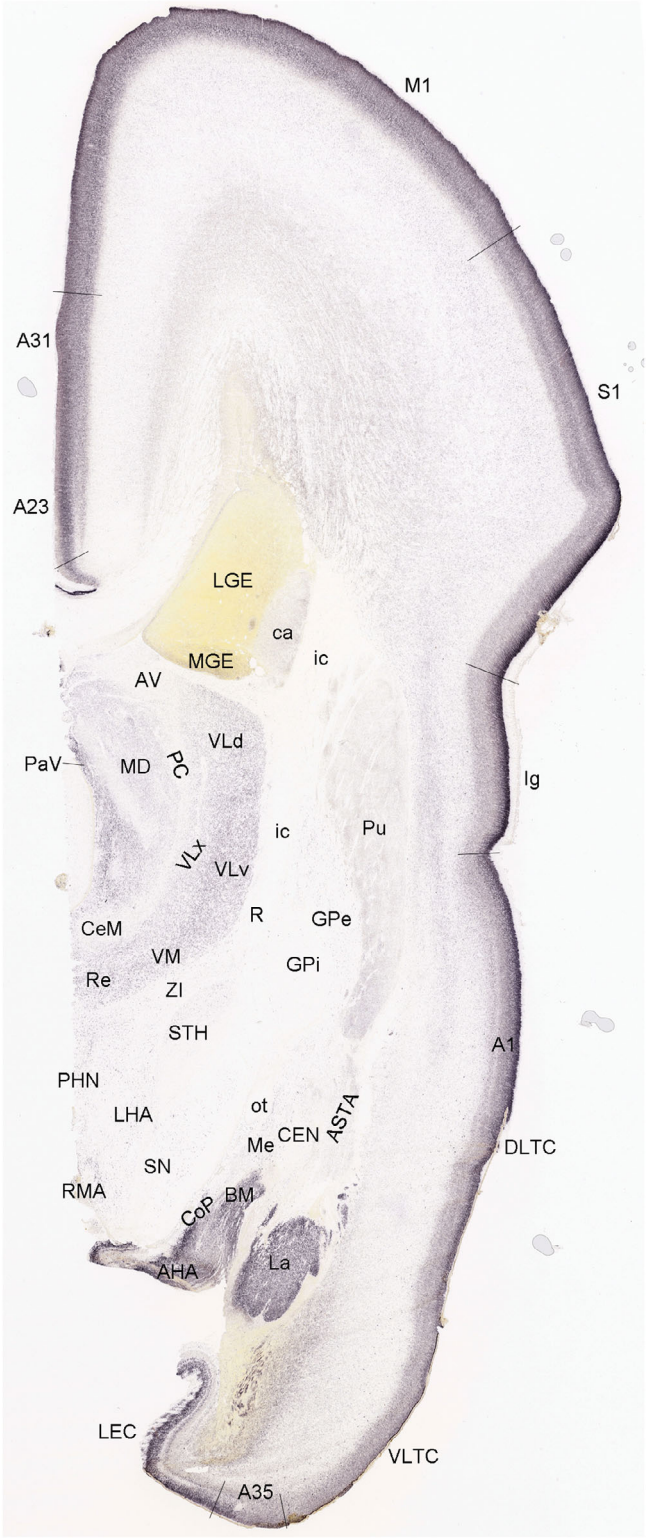

ENC1-02-589 (Level ~36)

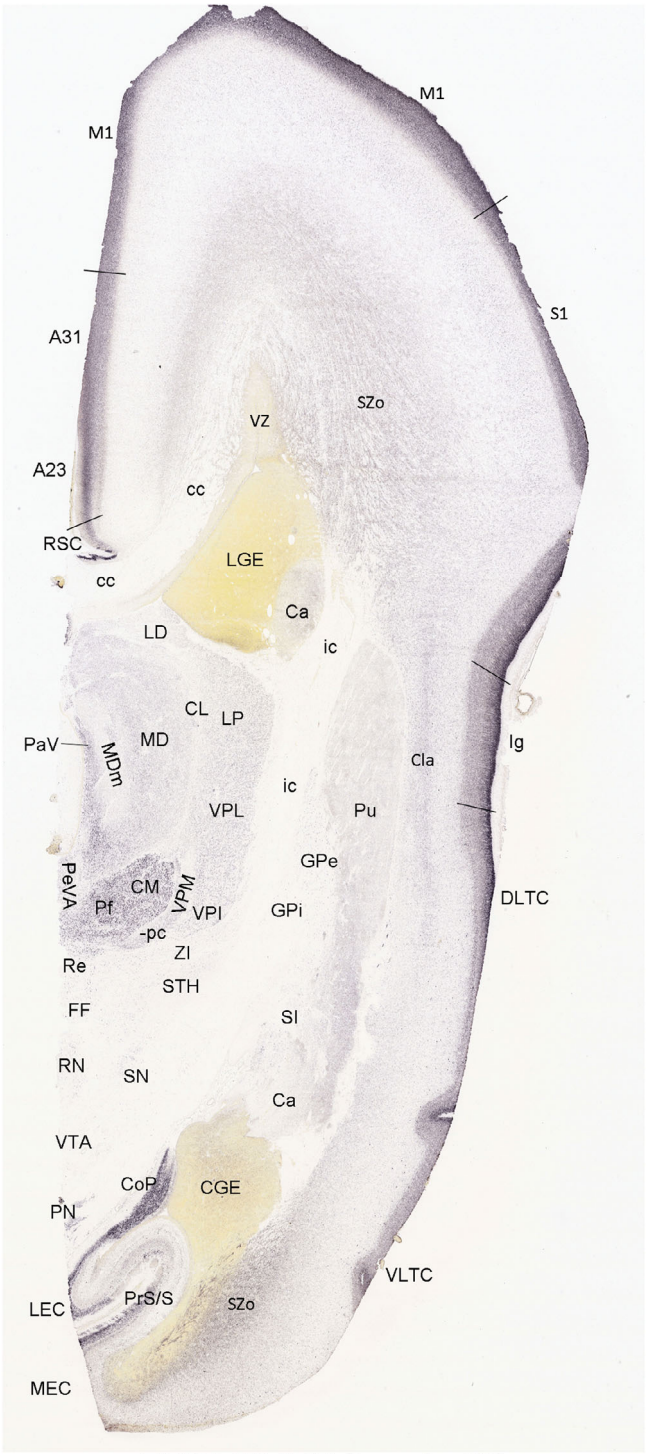

ENC1-02-640 (Level ~38)

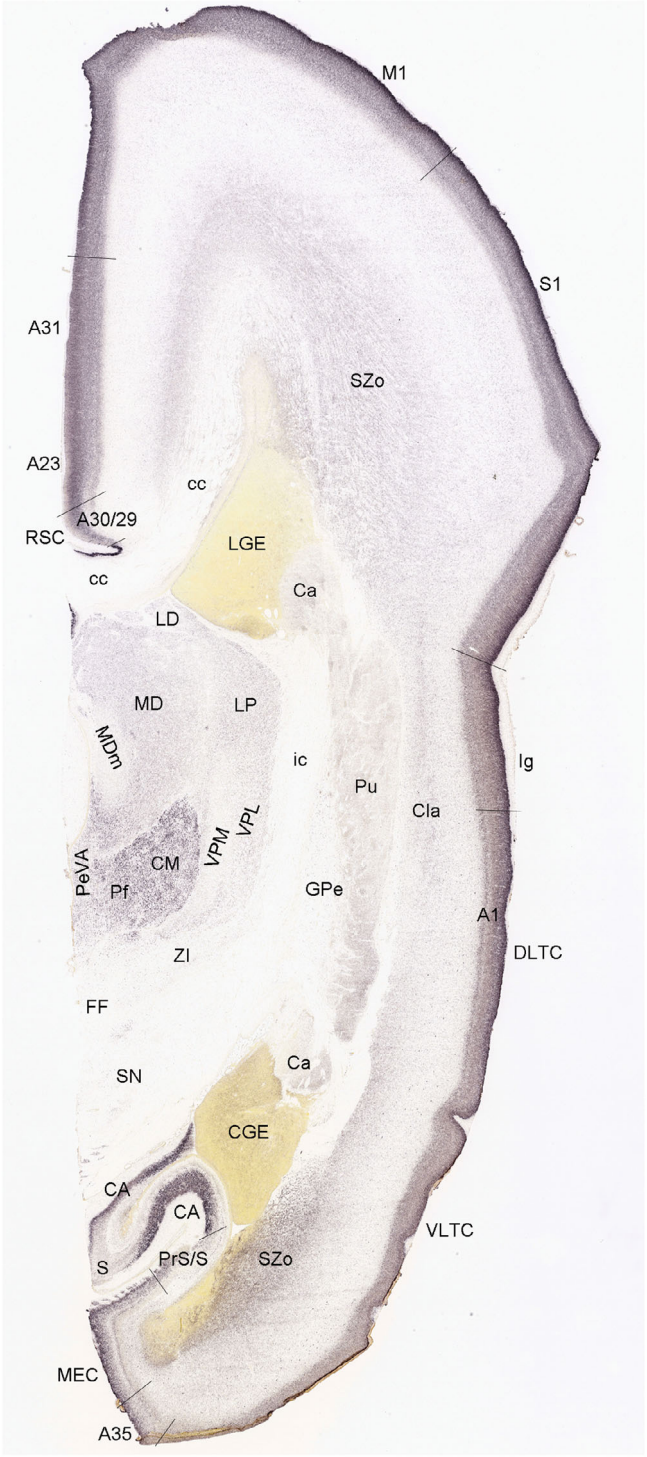

ENC1-02-691 (Level ~40)

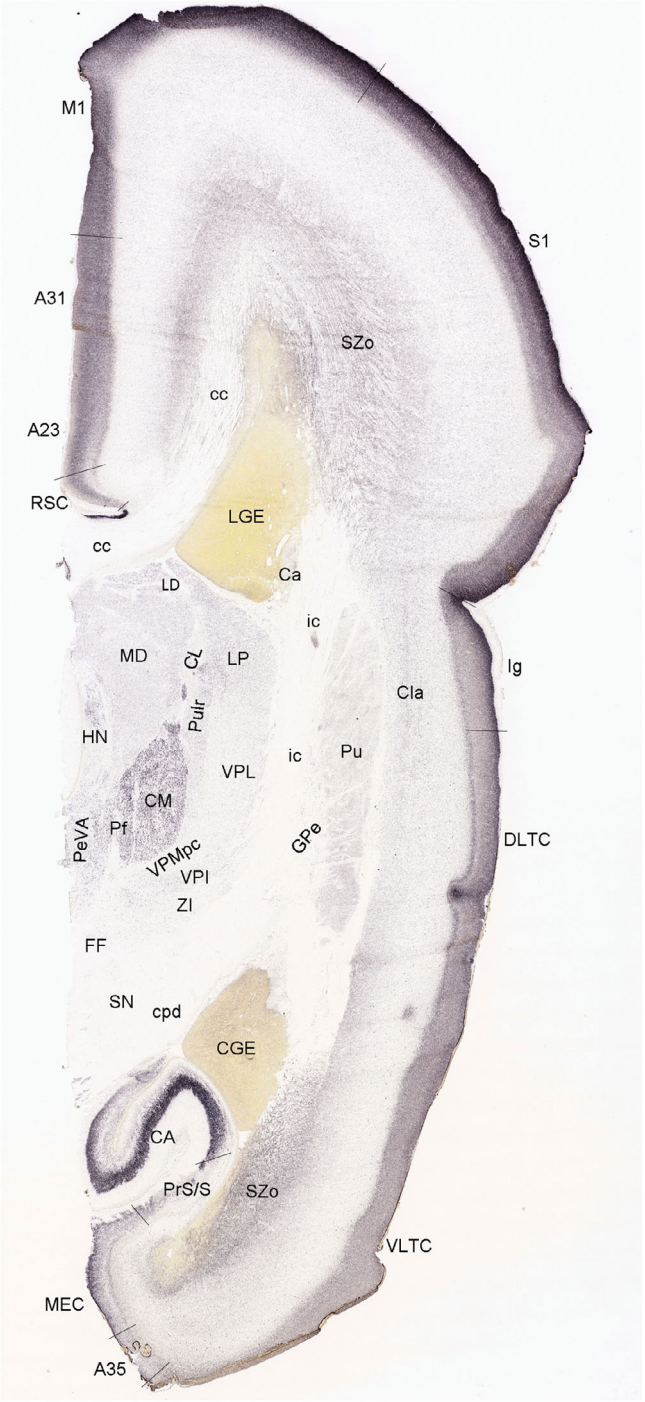

ENC1-02-742 (Level ~42)

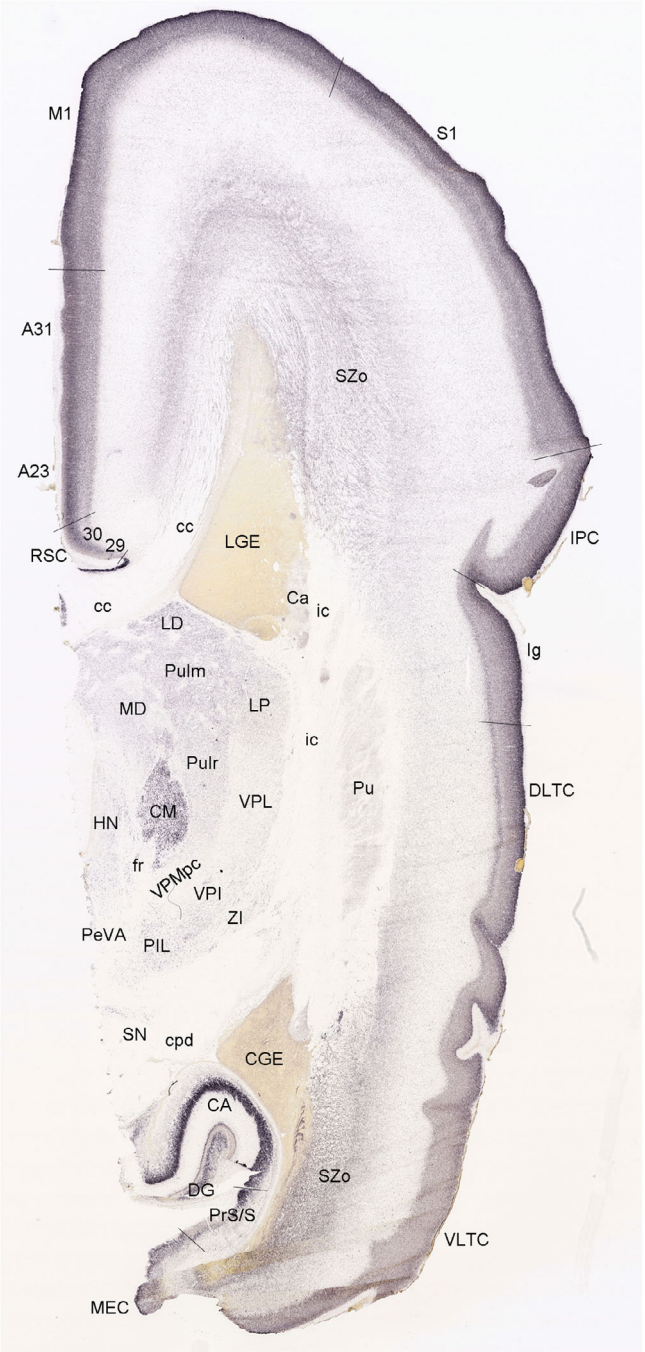

ENC1-02-793 (Level ~44)

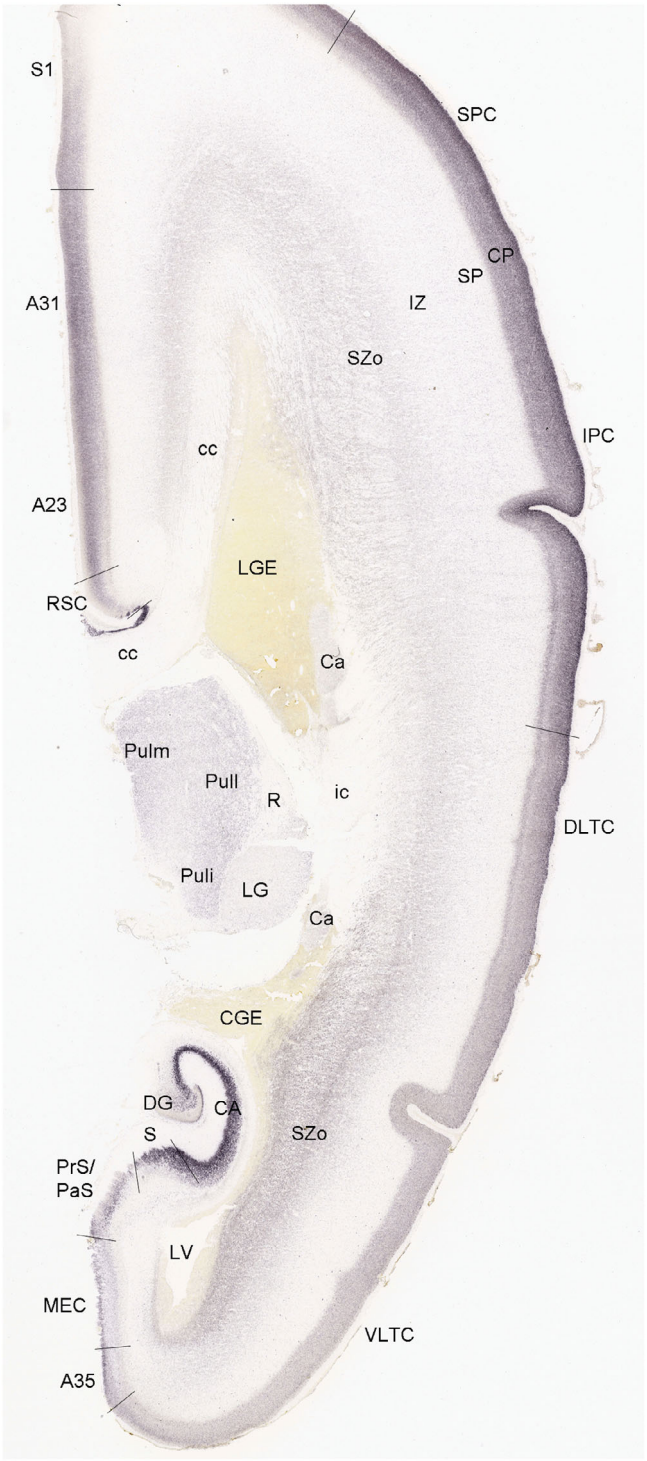

ENC1-03-079 (Level ~48)

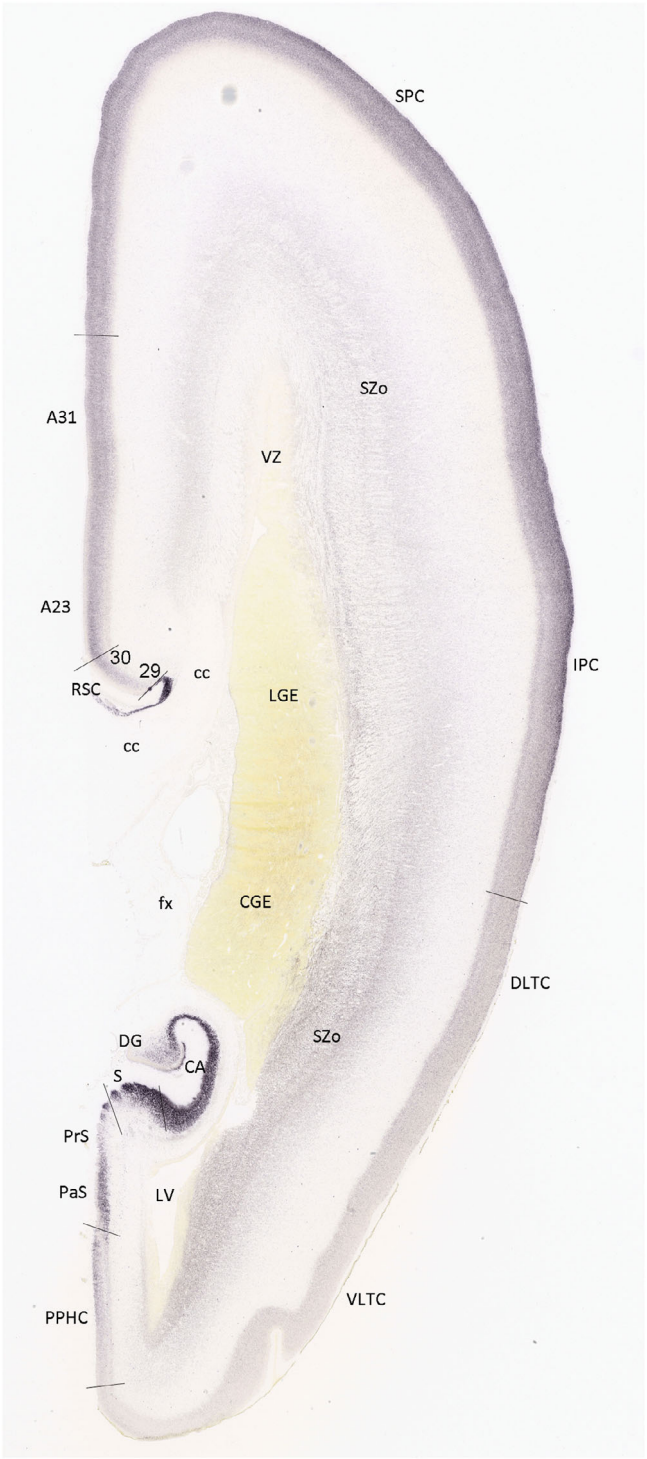

ENC1-03-232 (Level ~54)

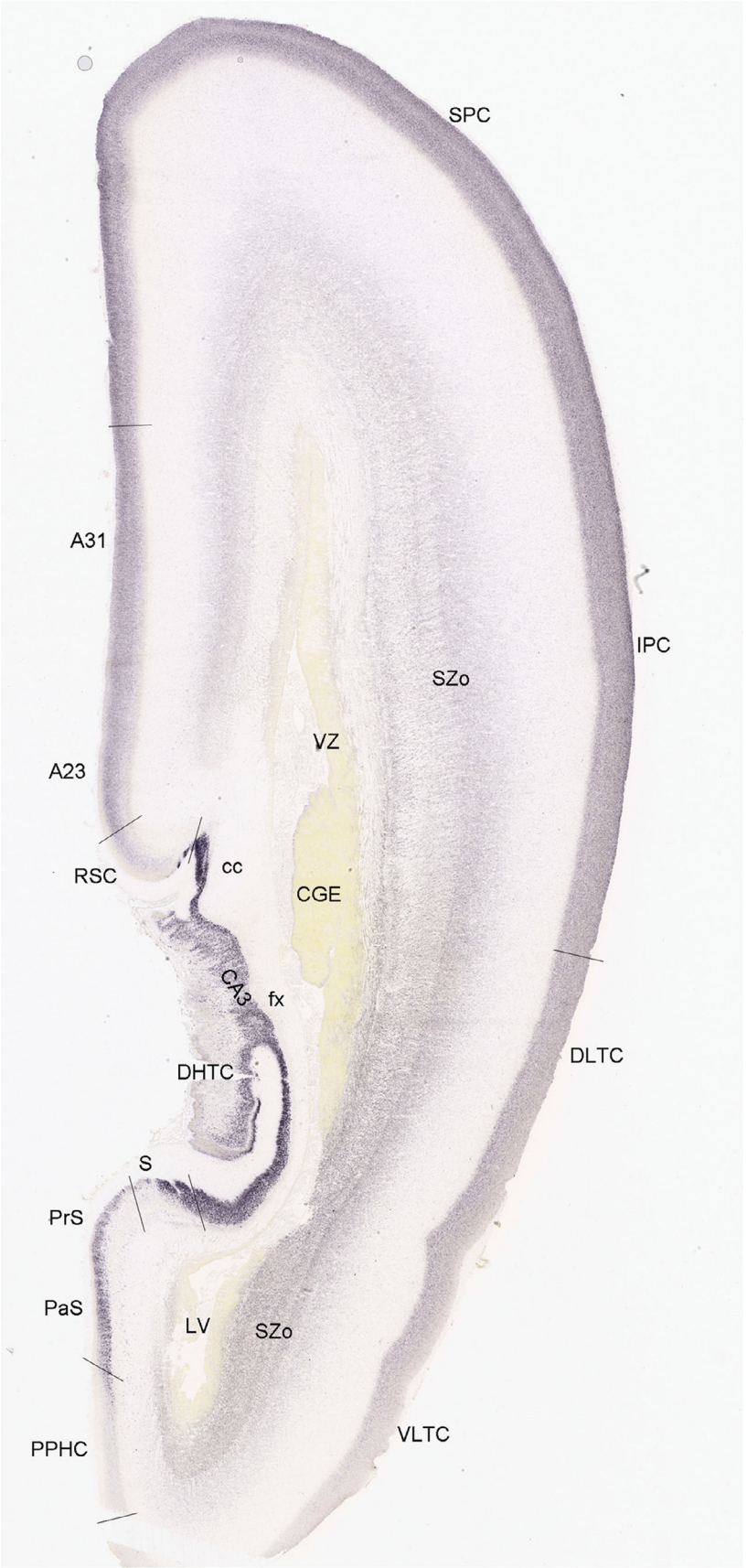

ENC1-03-385 (Level ~60)

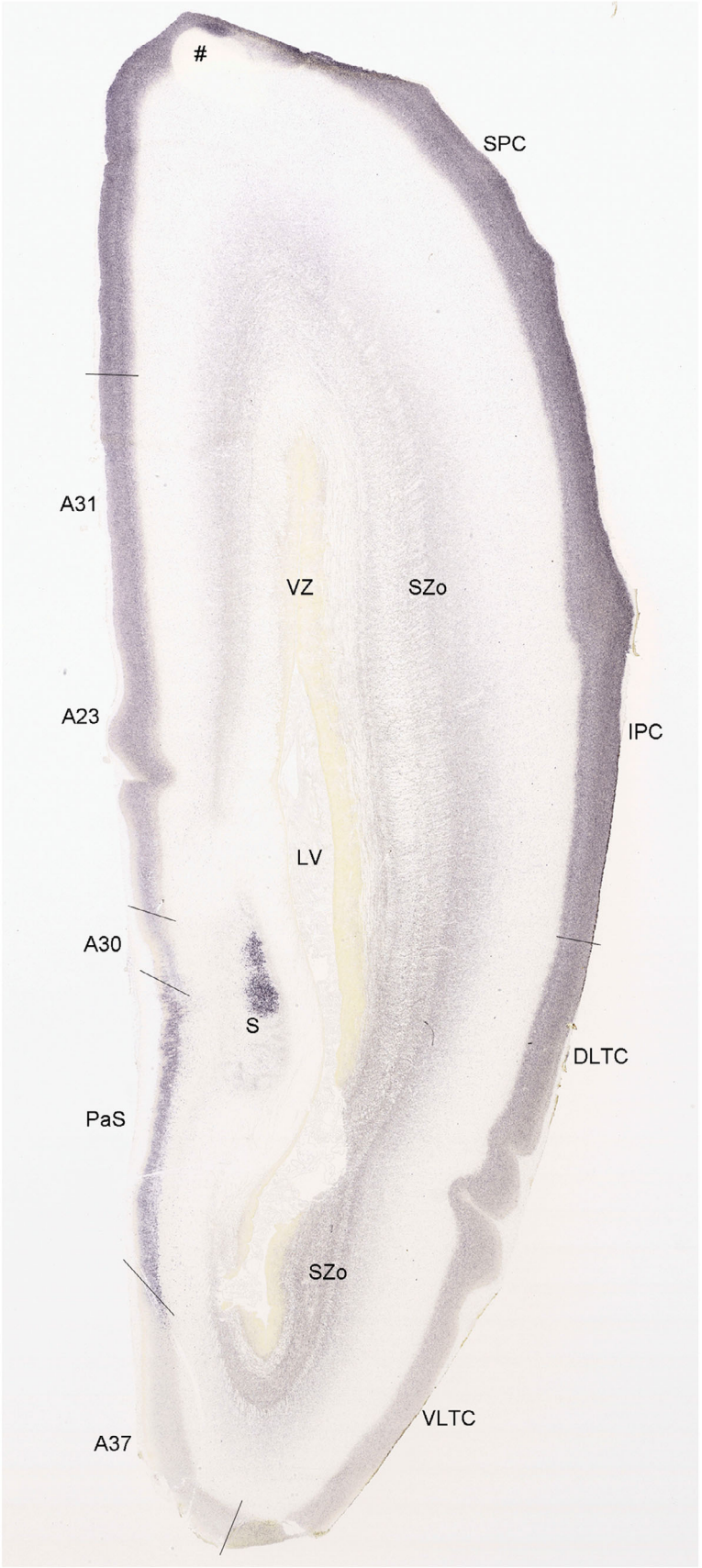

ENC1-03-487 (Level ~63)

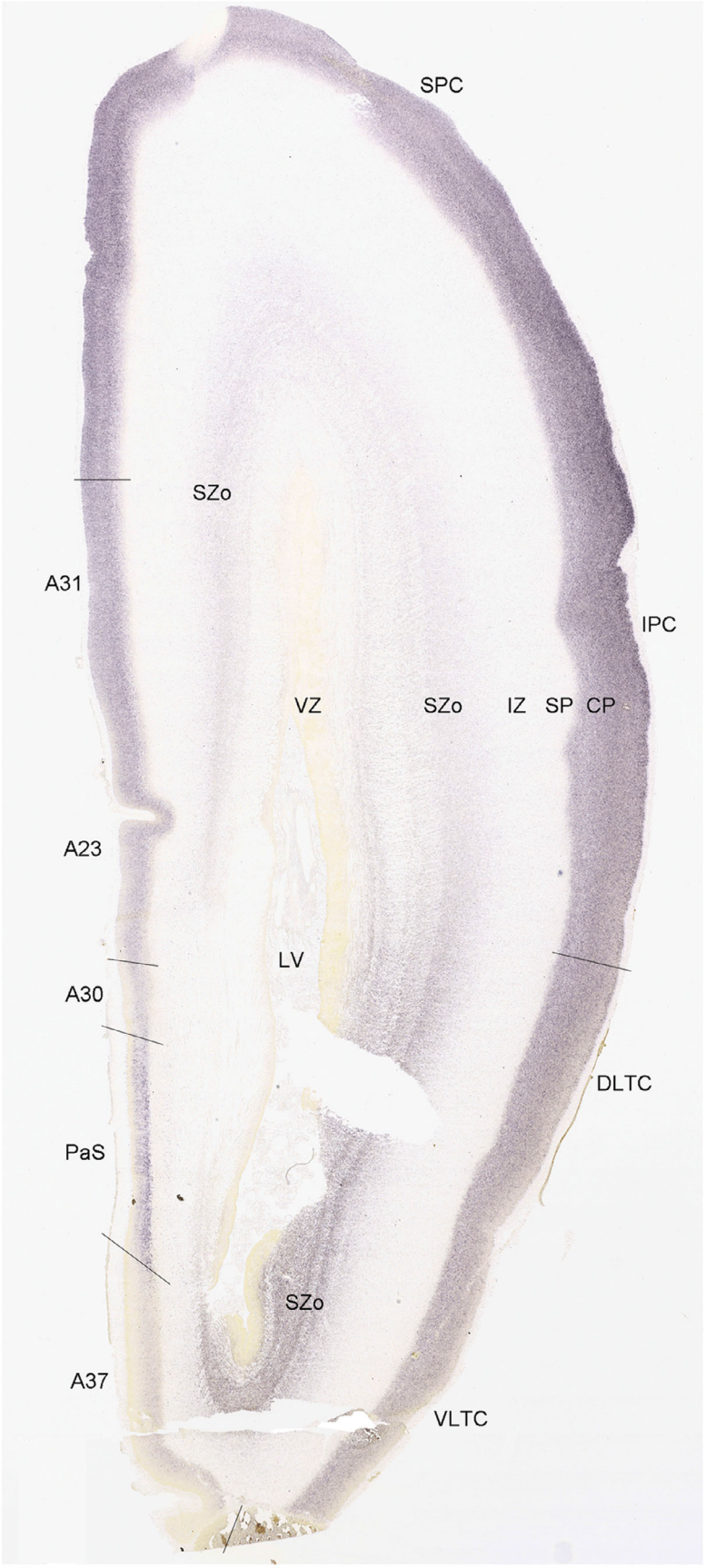

ENC1-03-538 (Level ~65)

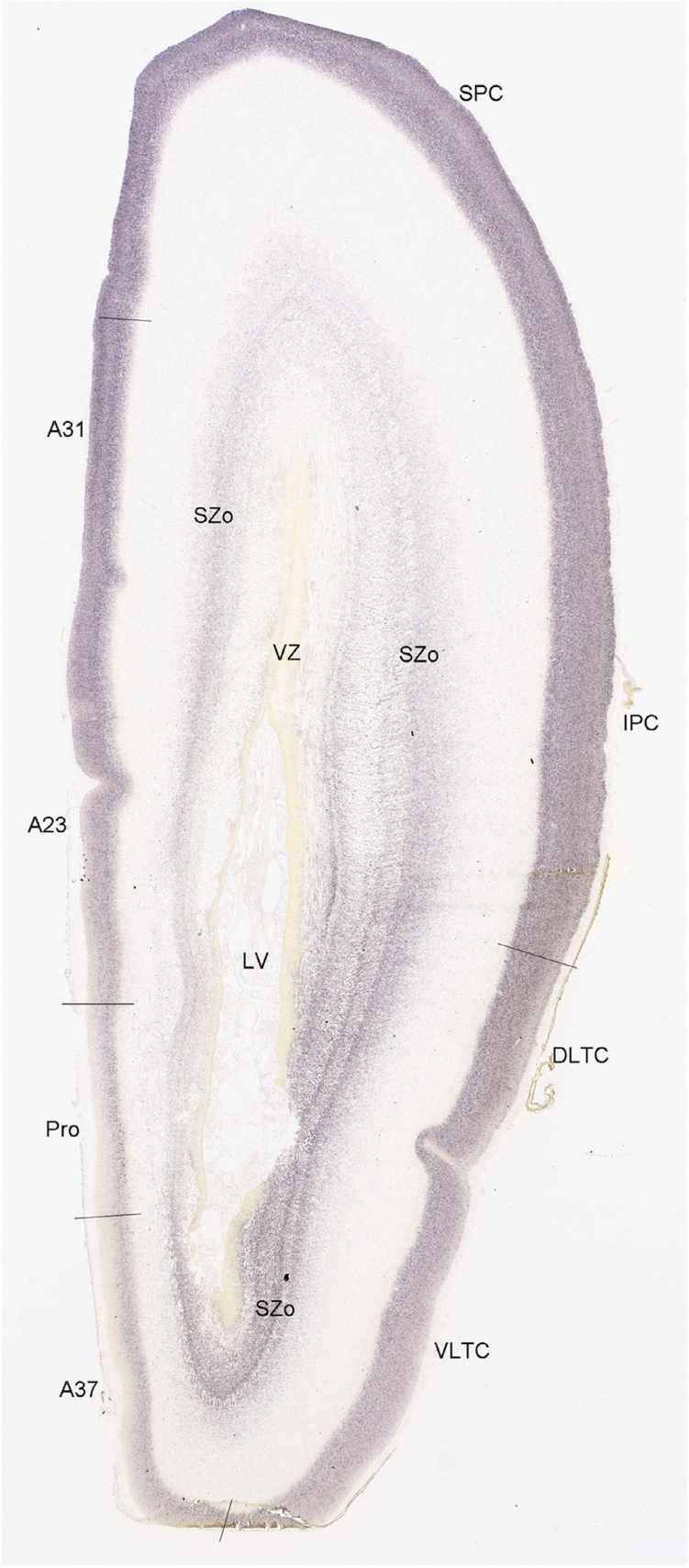

ENC1-03-589 (Level ~66)

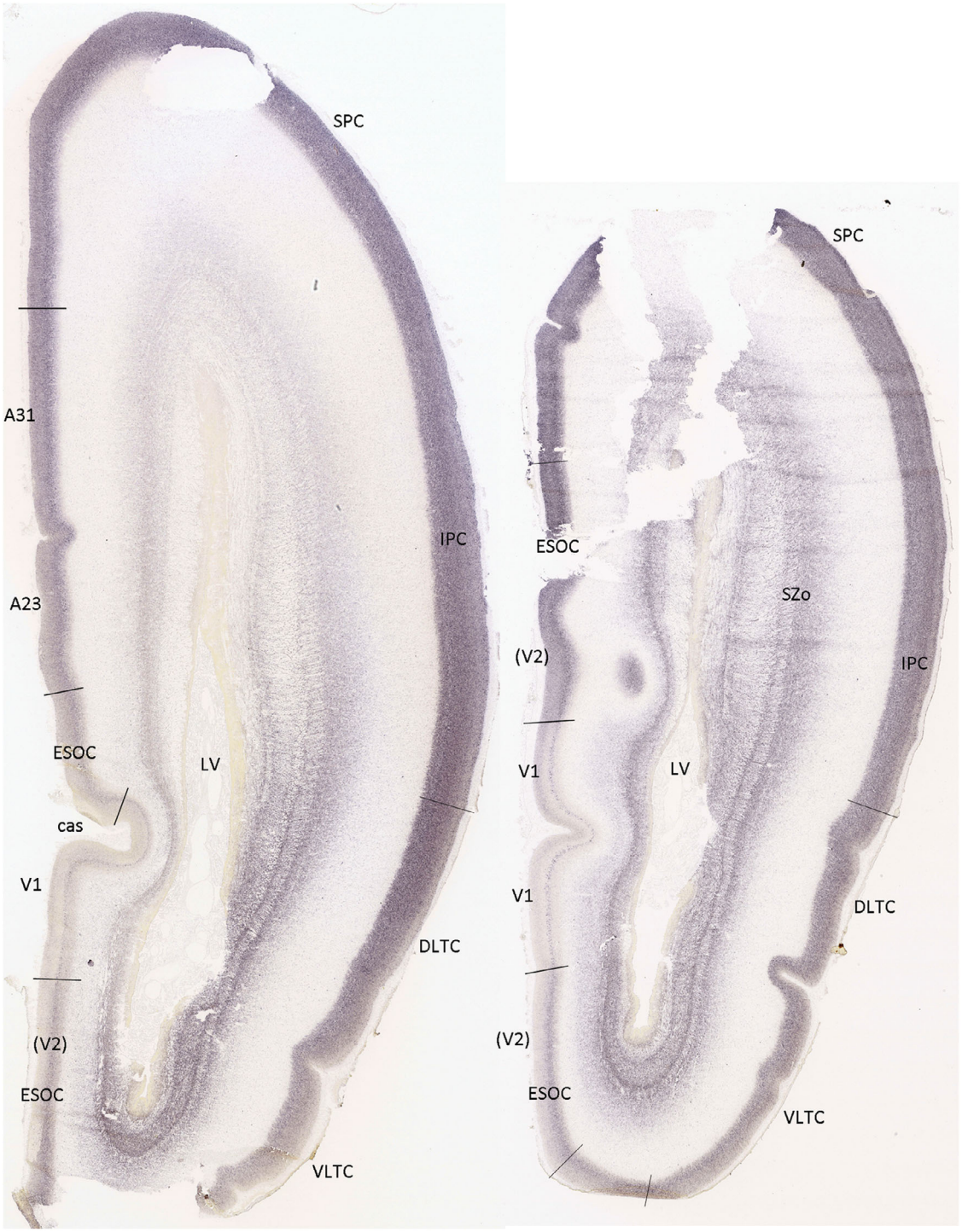

ENC1-03-640 (Level ~67) **ENC1-04-079 (Level ~69)**

ENC1-04-181 (Level ~71) **ENC1-04-334 (Level ~74-75)**

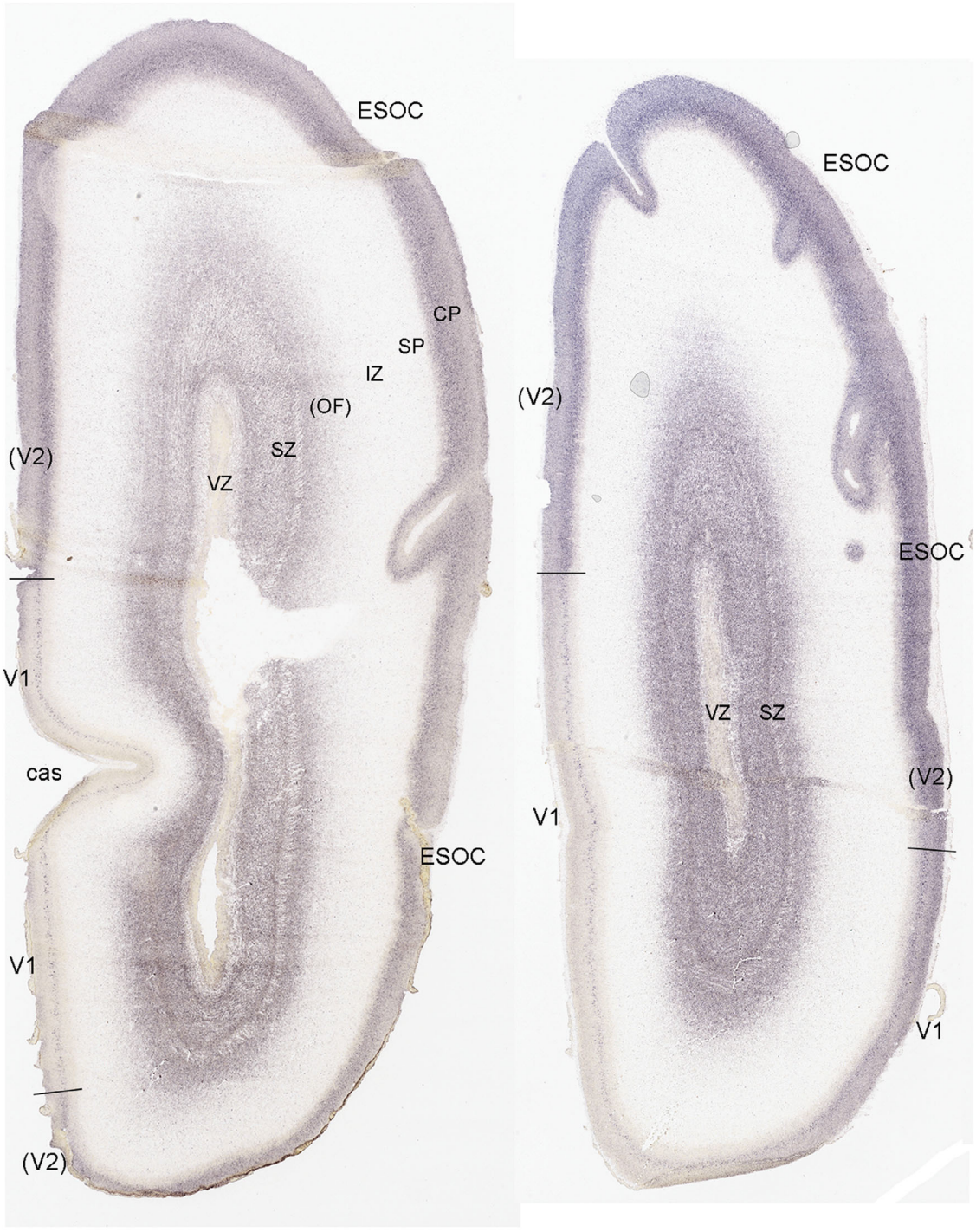

ENC1-04-436 (Level ~76-77) **ENC1-04-589 (Level ~79)**

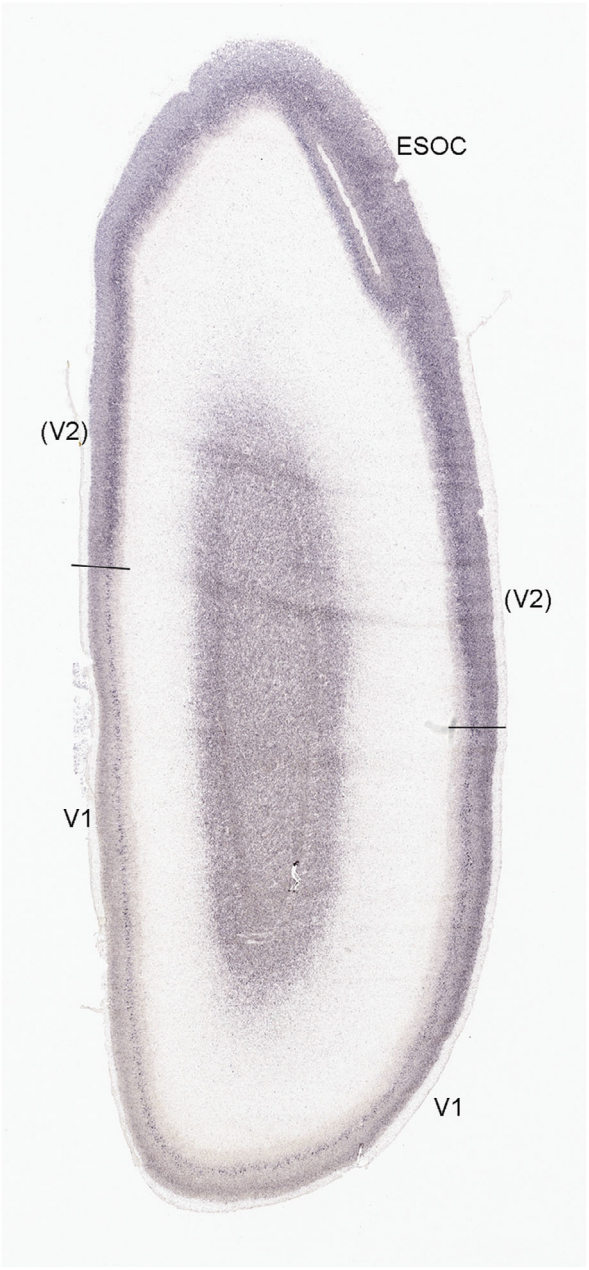

ENC1-04-640 (Level ~79-80)

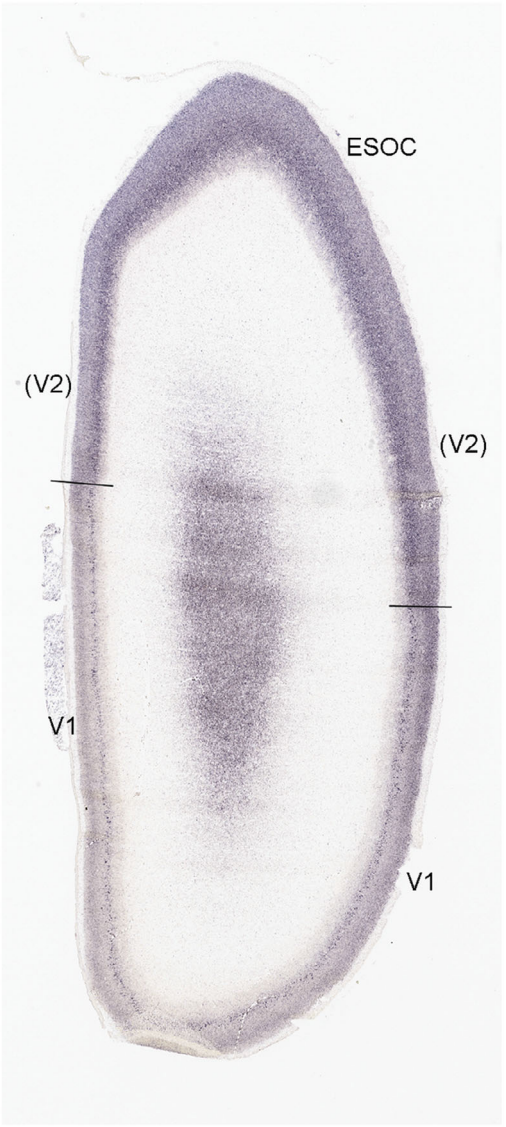

ENC1-04-691 (Level ~80-81)

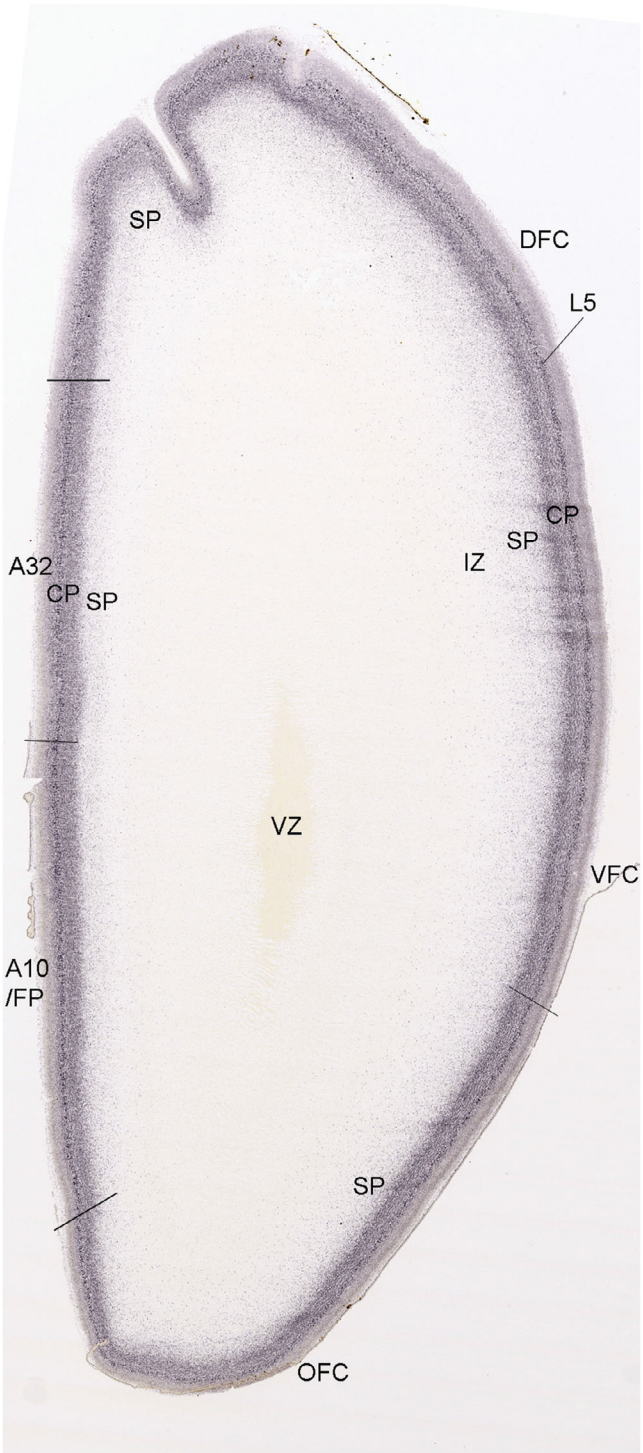

GRIK2-01-295 (Level ~5-6)

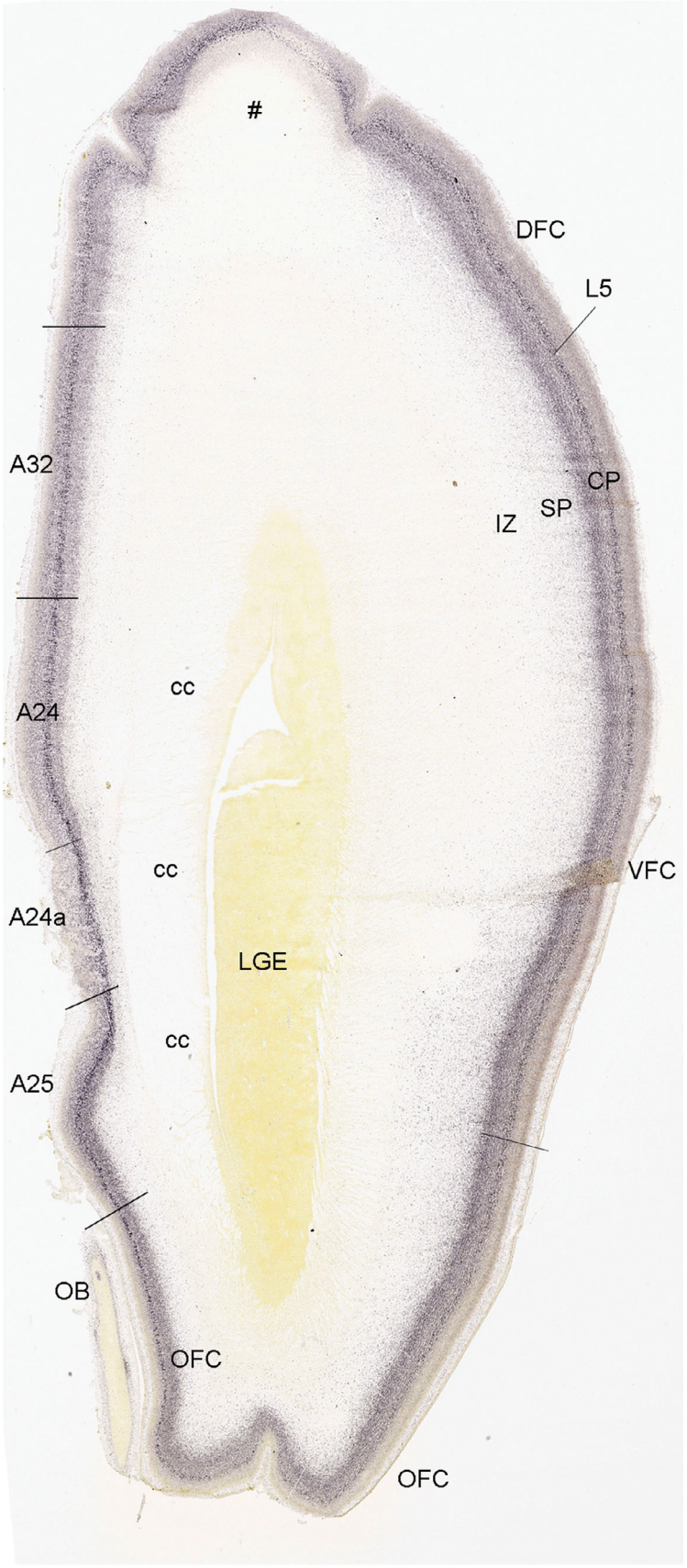

GRIK2-01-550 (Level ~11-12)

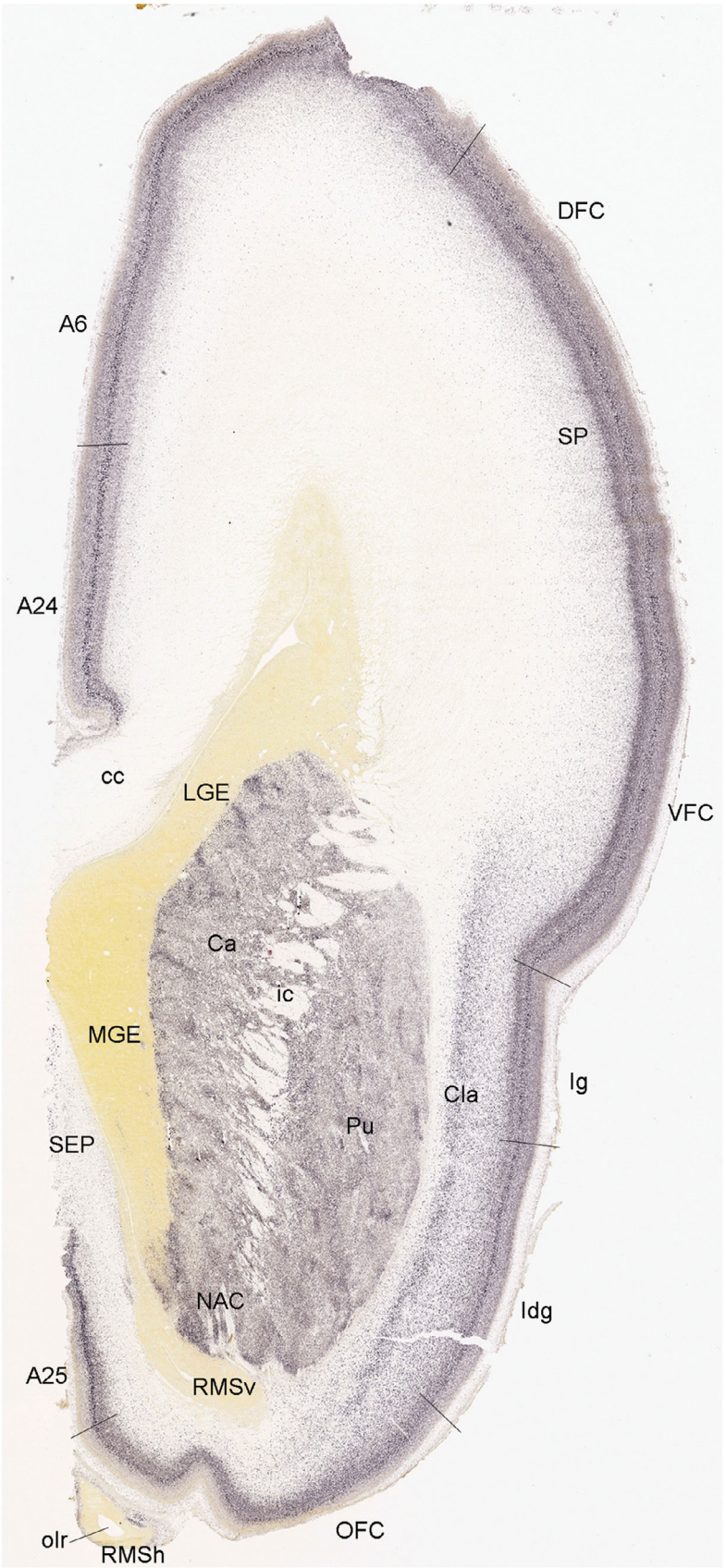

GRIK2-02-091 (Level ~18)

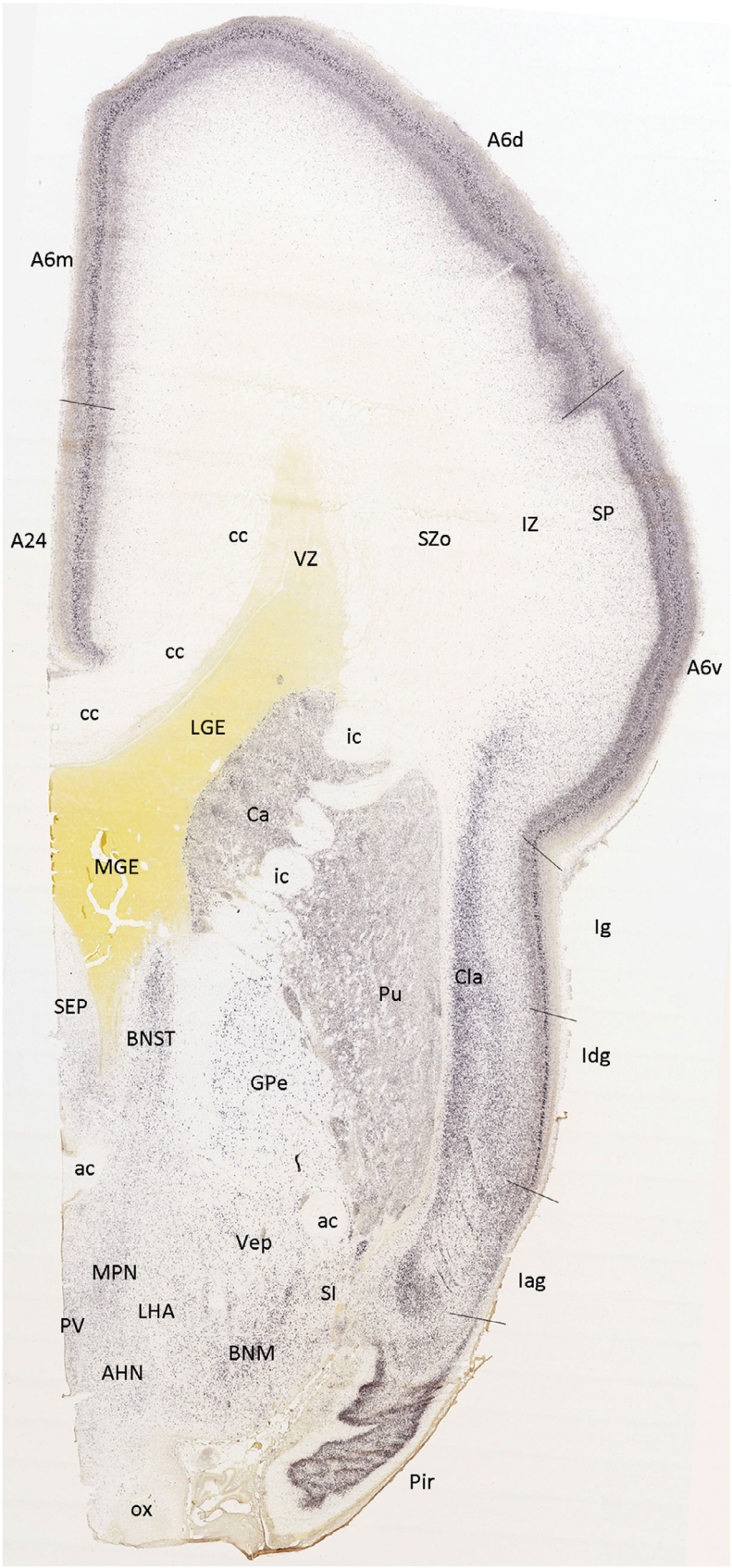

GRIK2-02-295 (Level ~24-25)

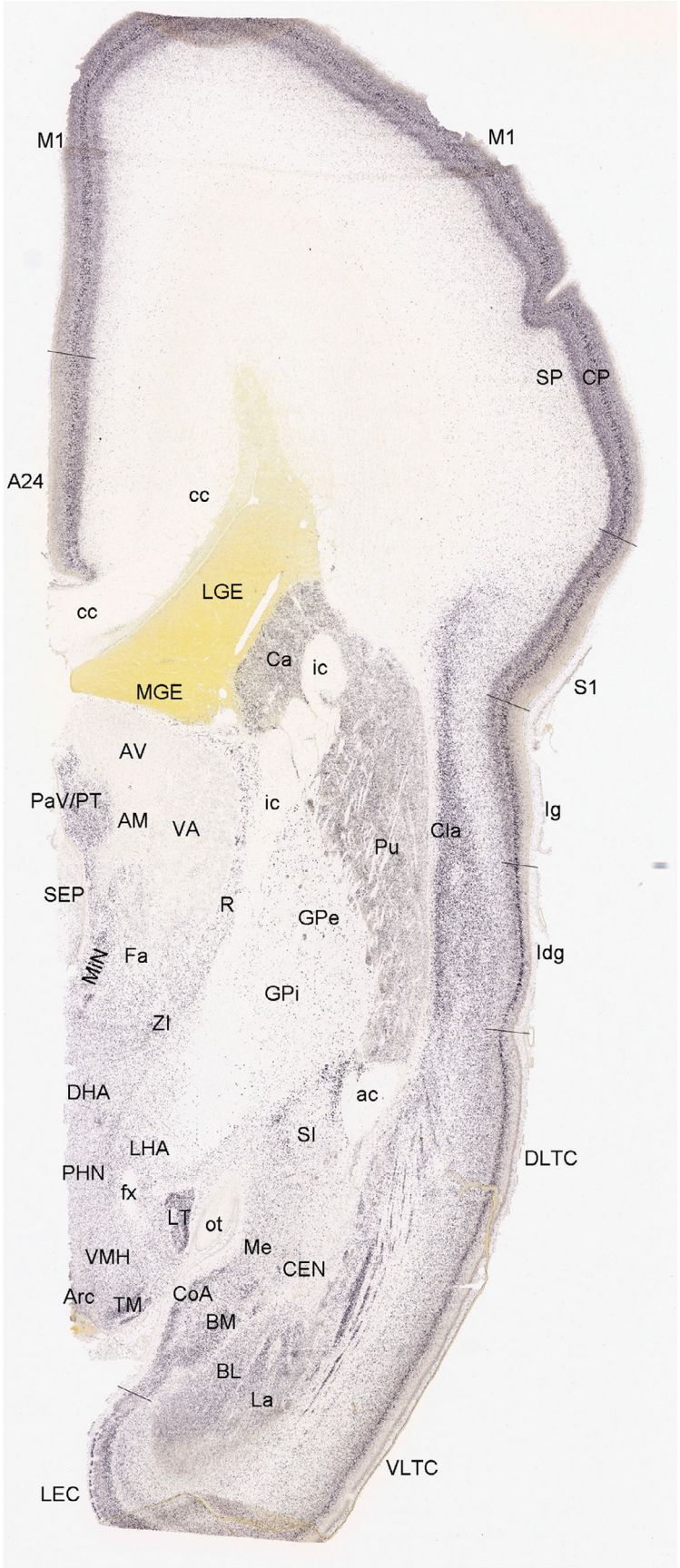

GRIK2-02-448 (Level ~30-31)

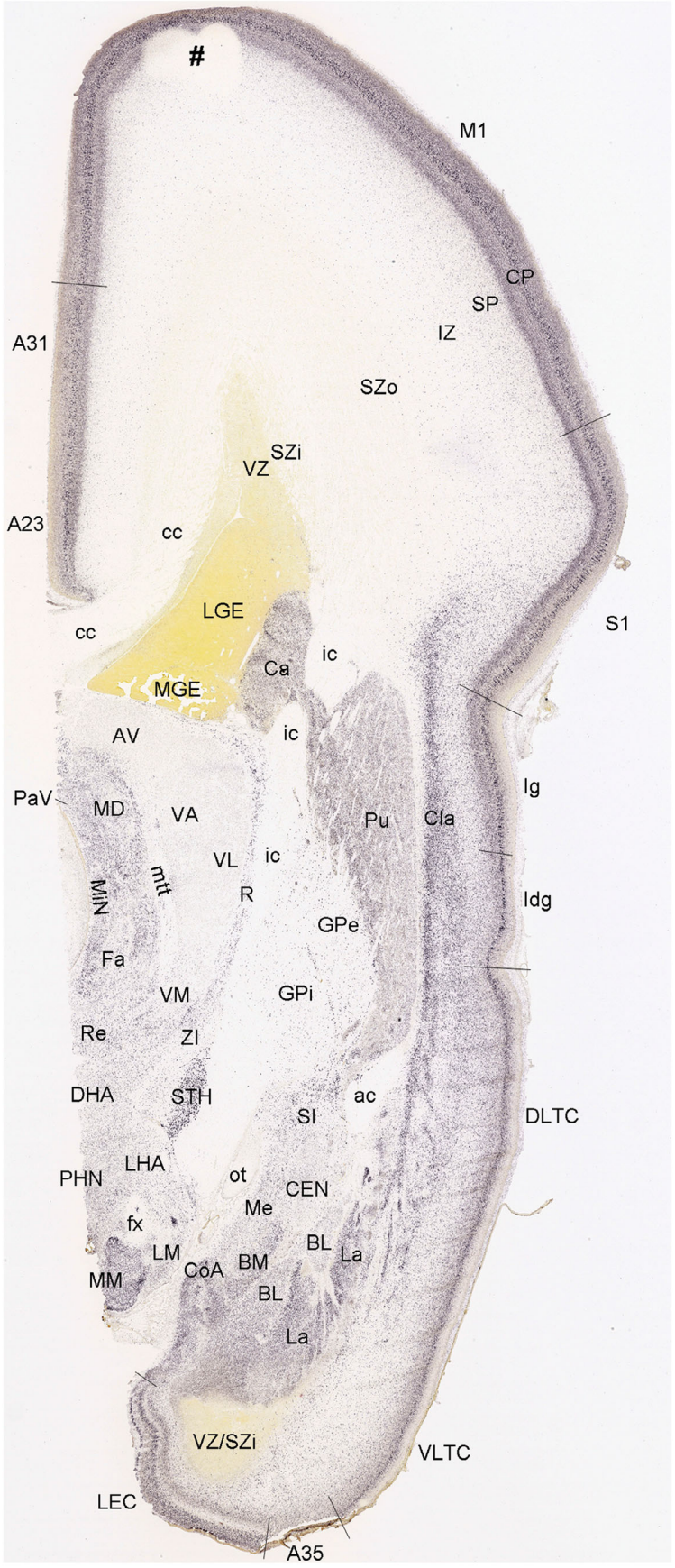

GRIK2-02-499 (Level ~32-33)

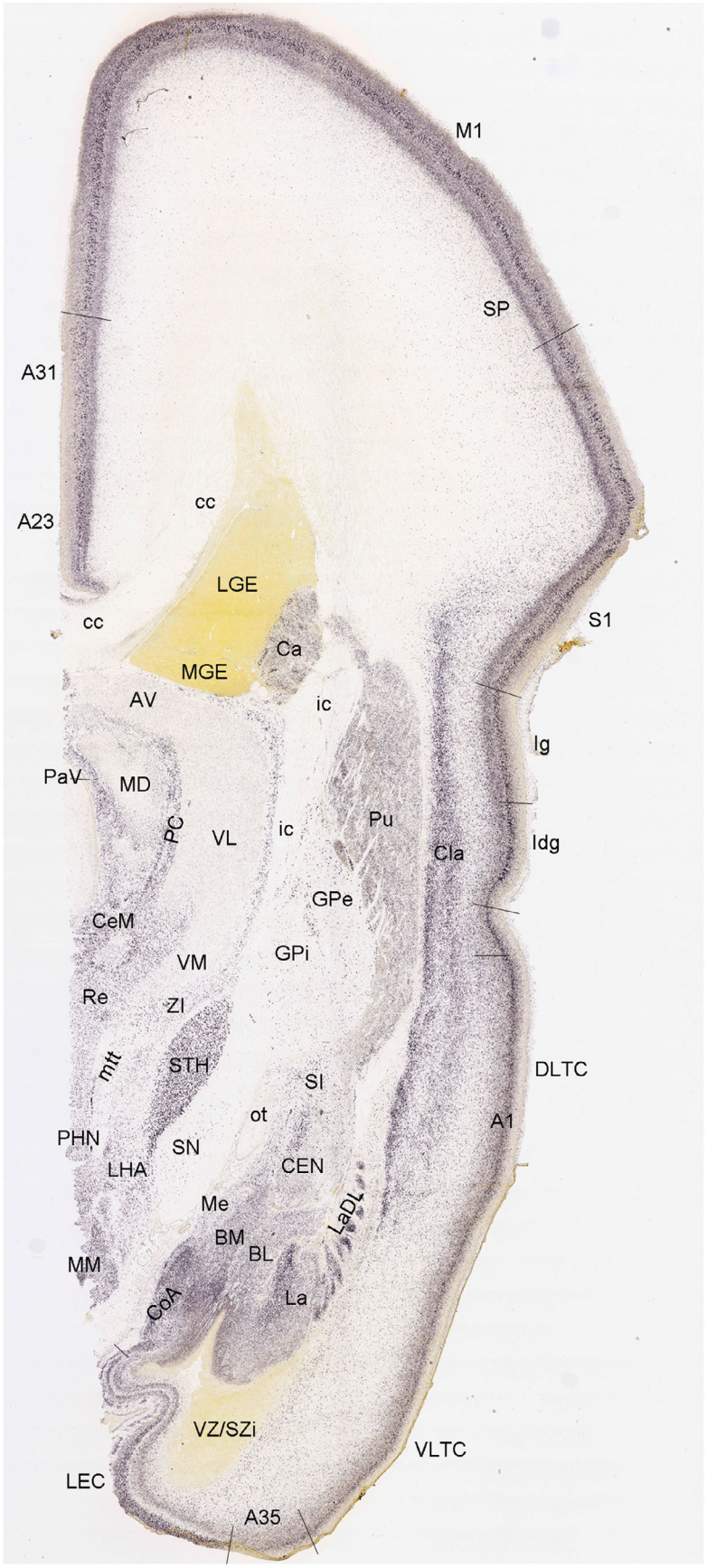

GRIK2-02-550 (Level ~35)

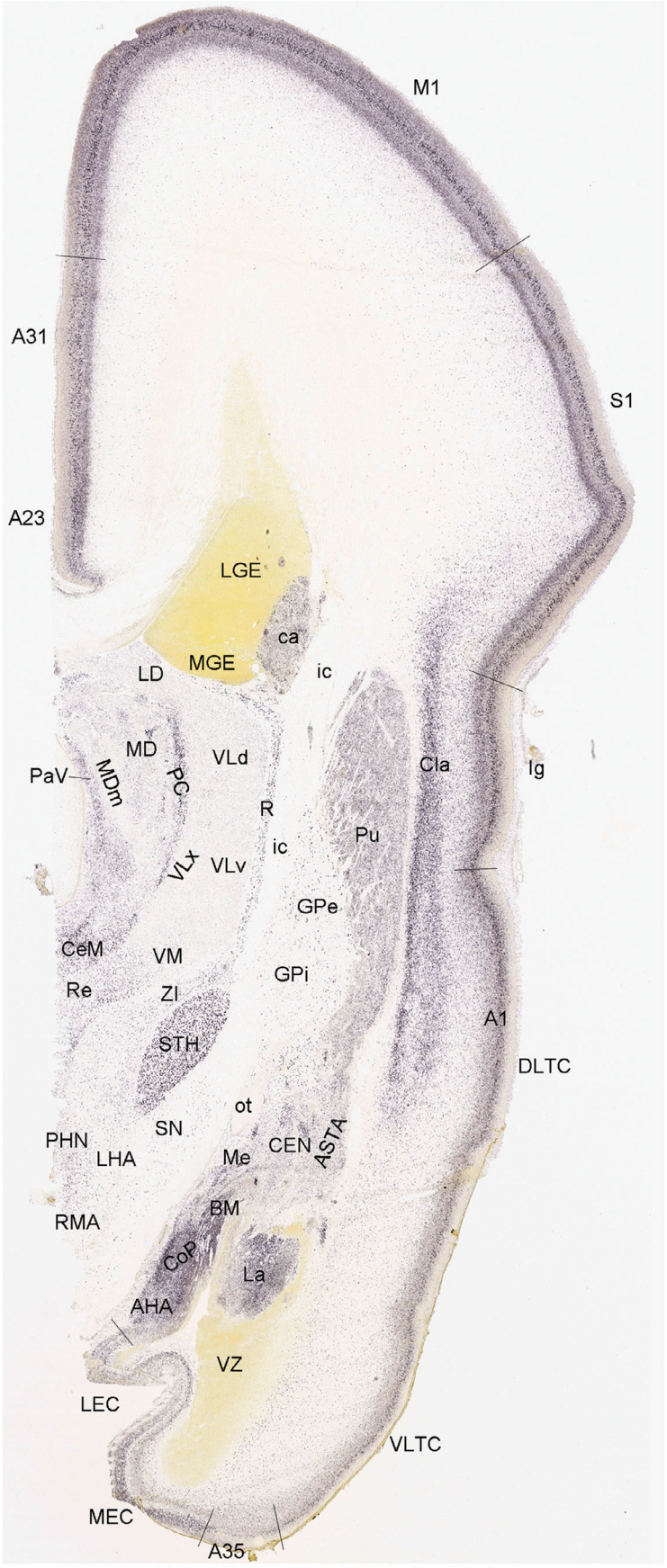

GRIK2-02-601 (Level ~36-37)

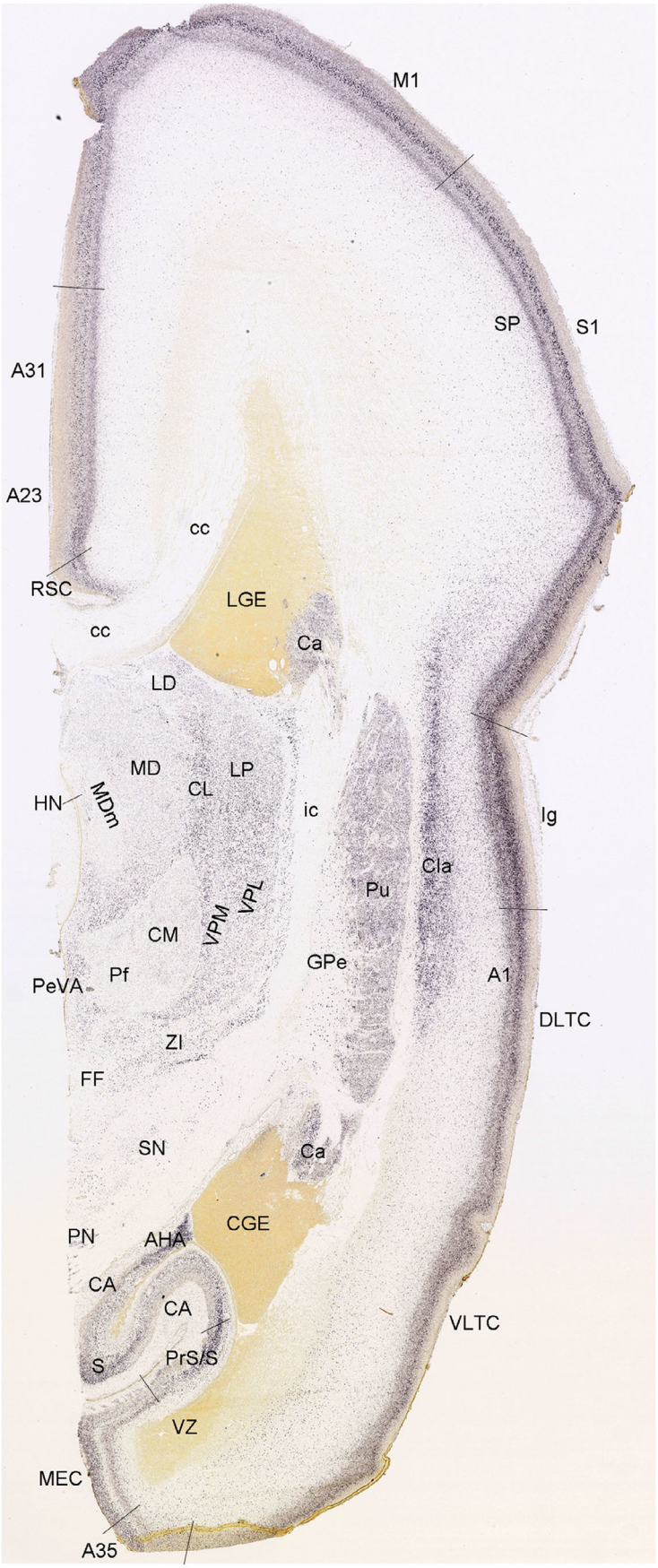

GRIK2-02-703 (Level ~40-41)

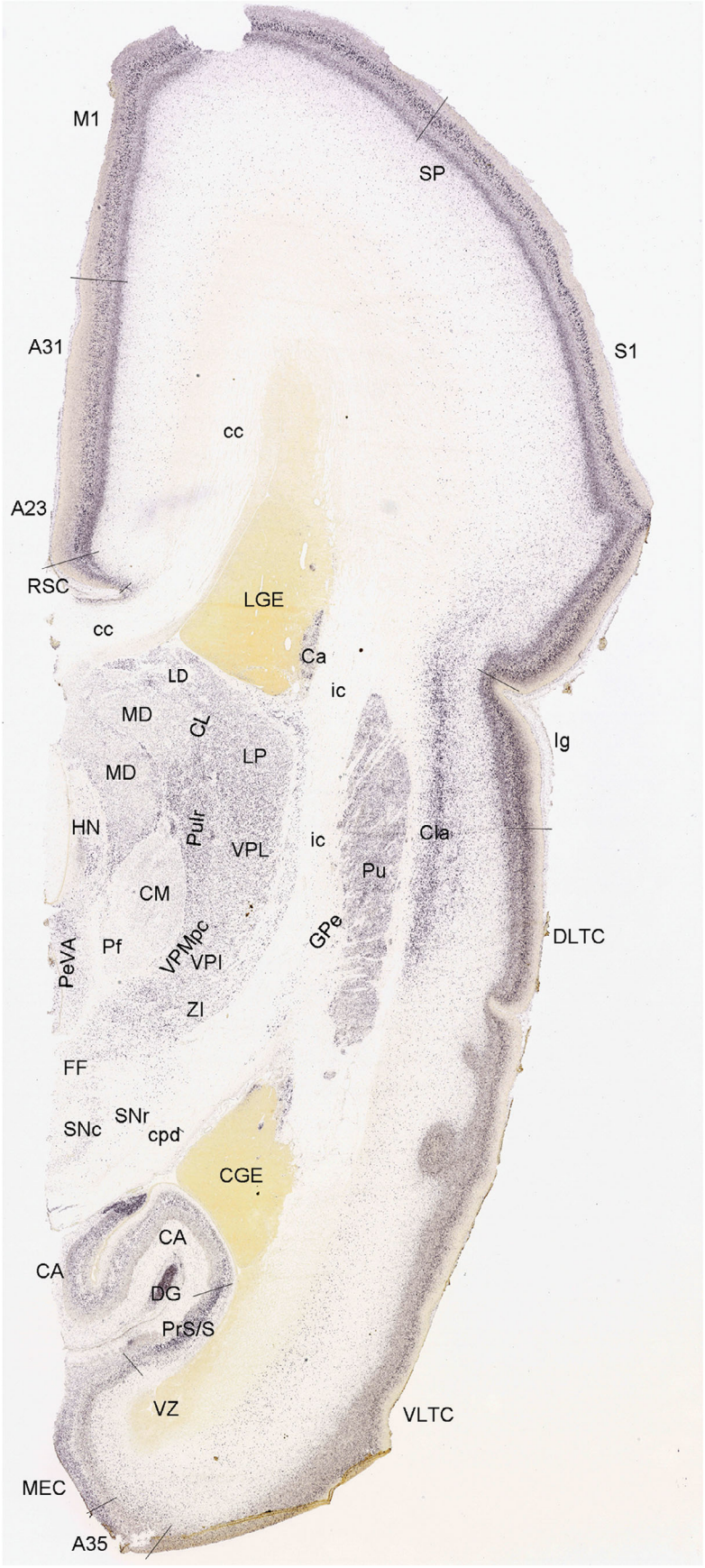

GRIK2-02-754 (Level ~42-43)

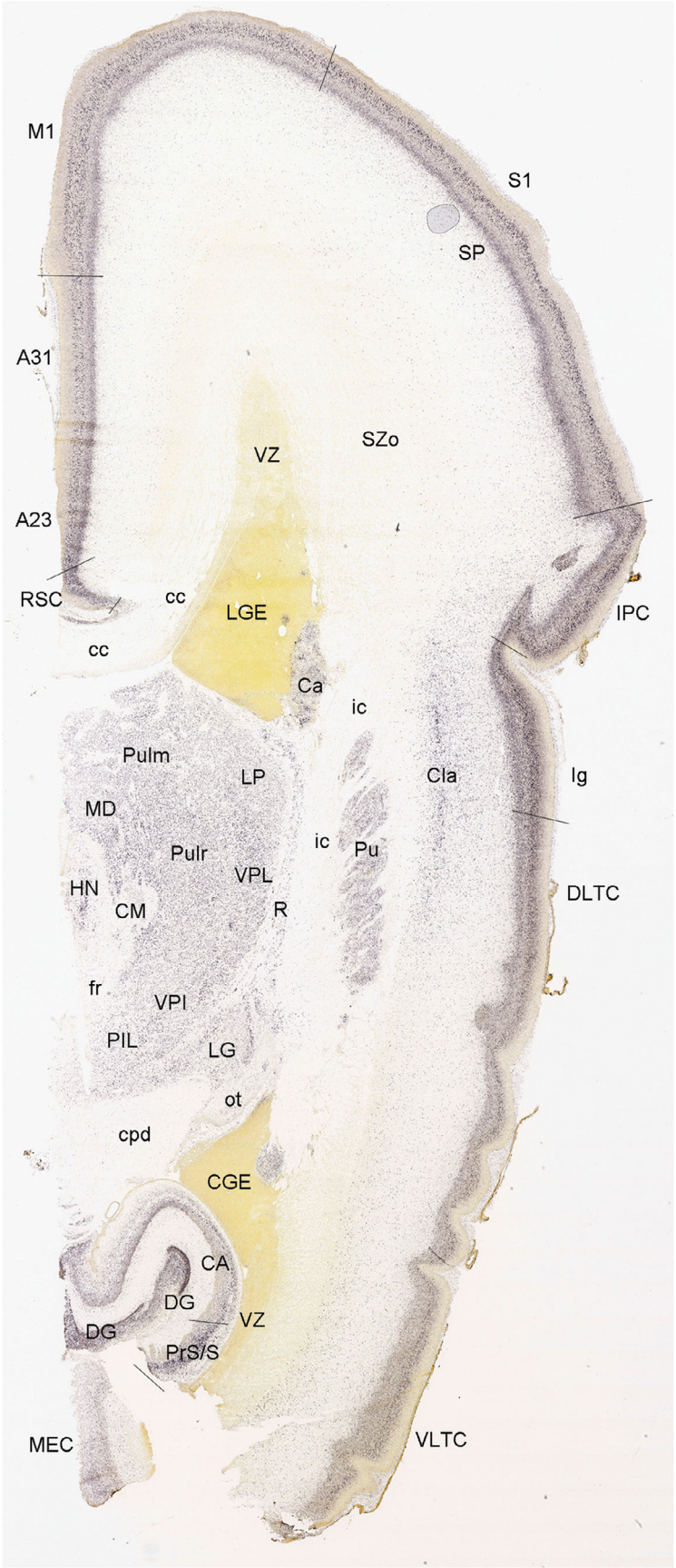

GRIK2-02-805 (Level ~44-45)

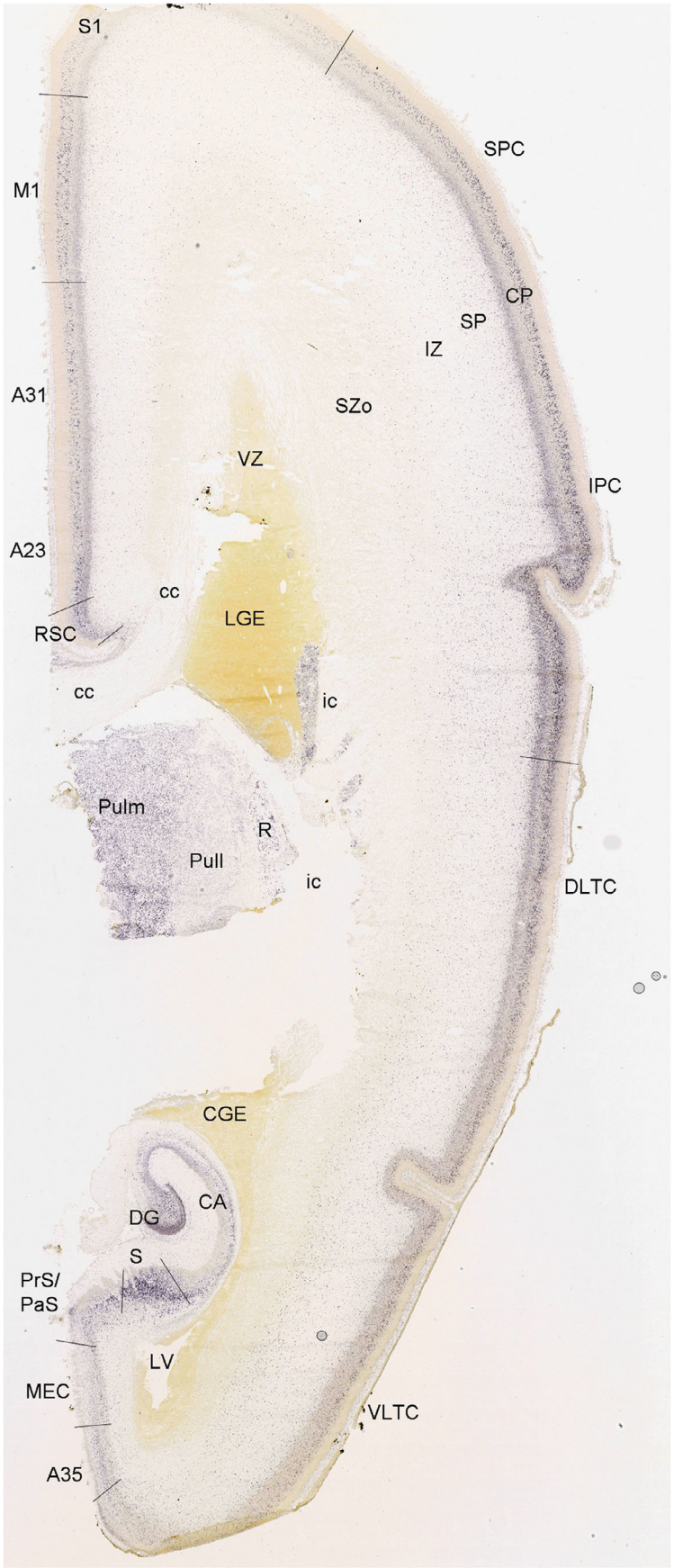

GRIK2-03-040 (Level ~47)

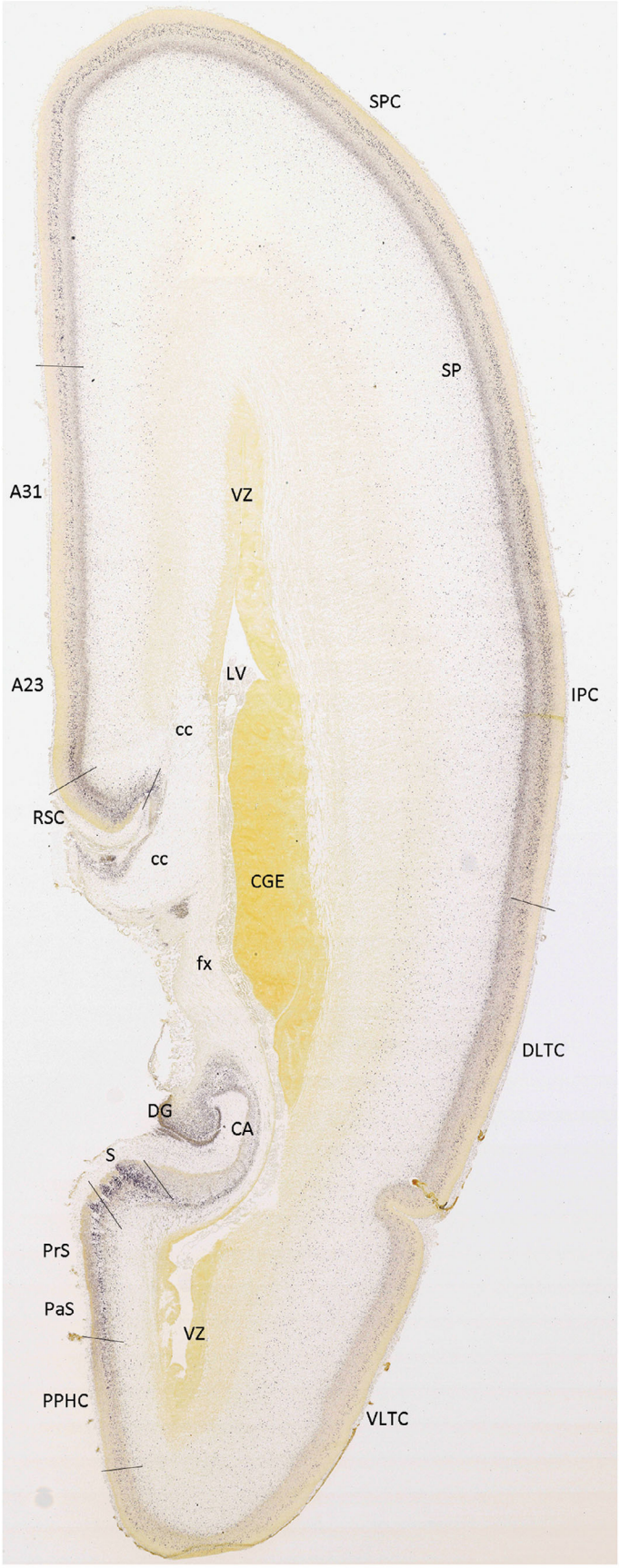

GRIK2-03-346 (Level ~58-59)

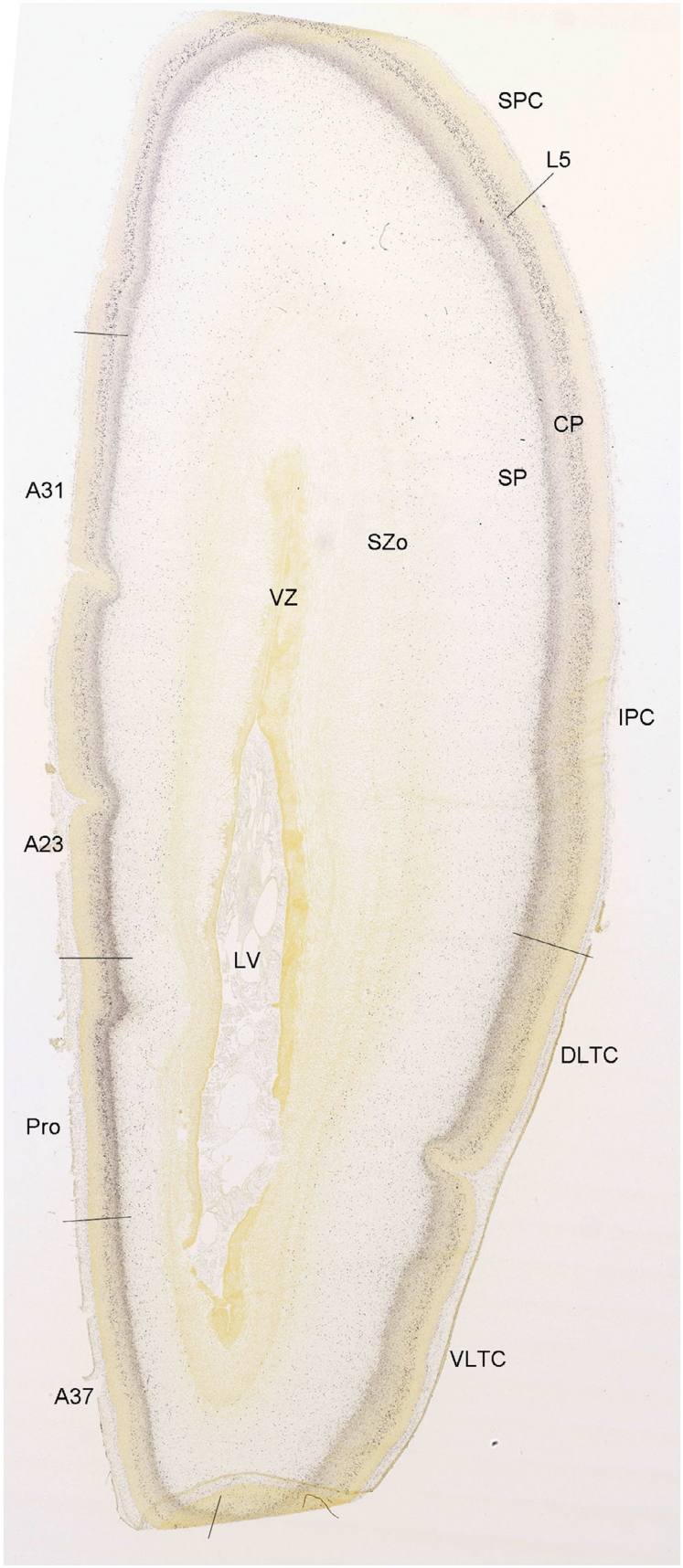

GRIK2-03-601 (Level ~66-67)

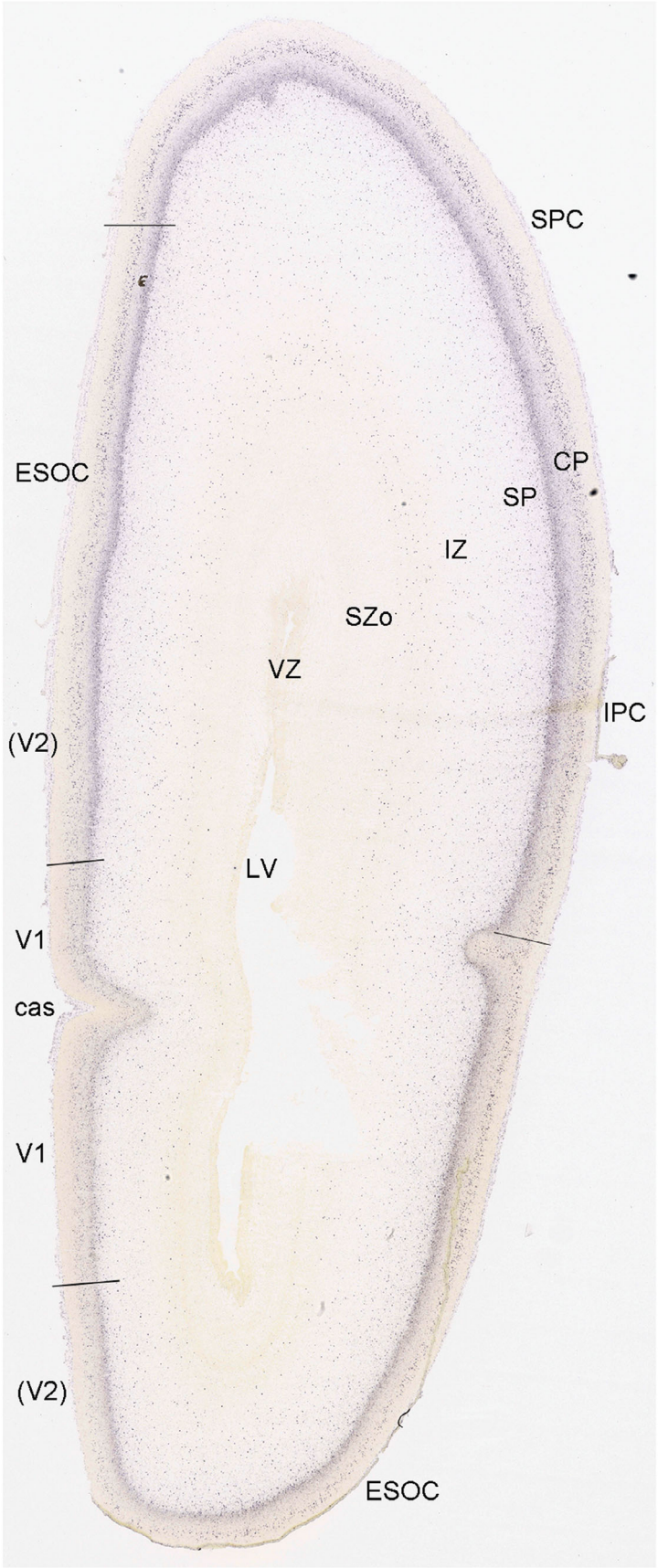

GRIK2-04-295 (Level ~73-74)

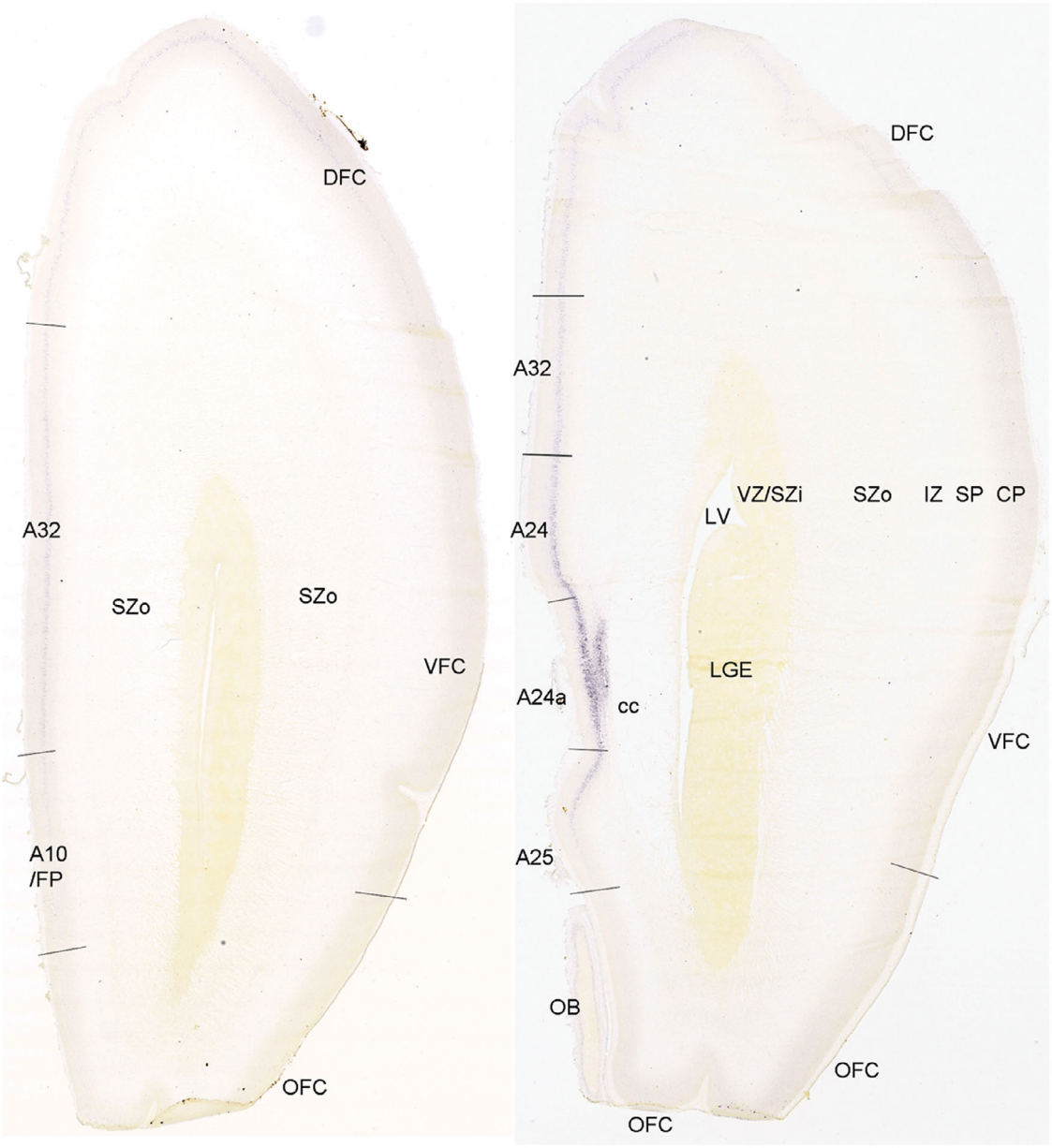

NRGN-01-405 (Level ~8) **NRGN-01-558 (Level ~11-12)**

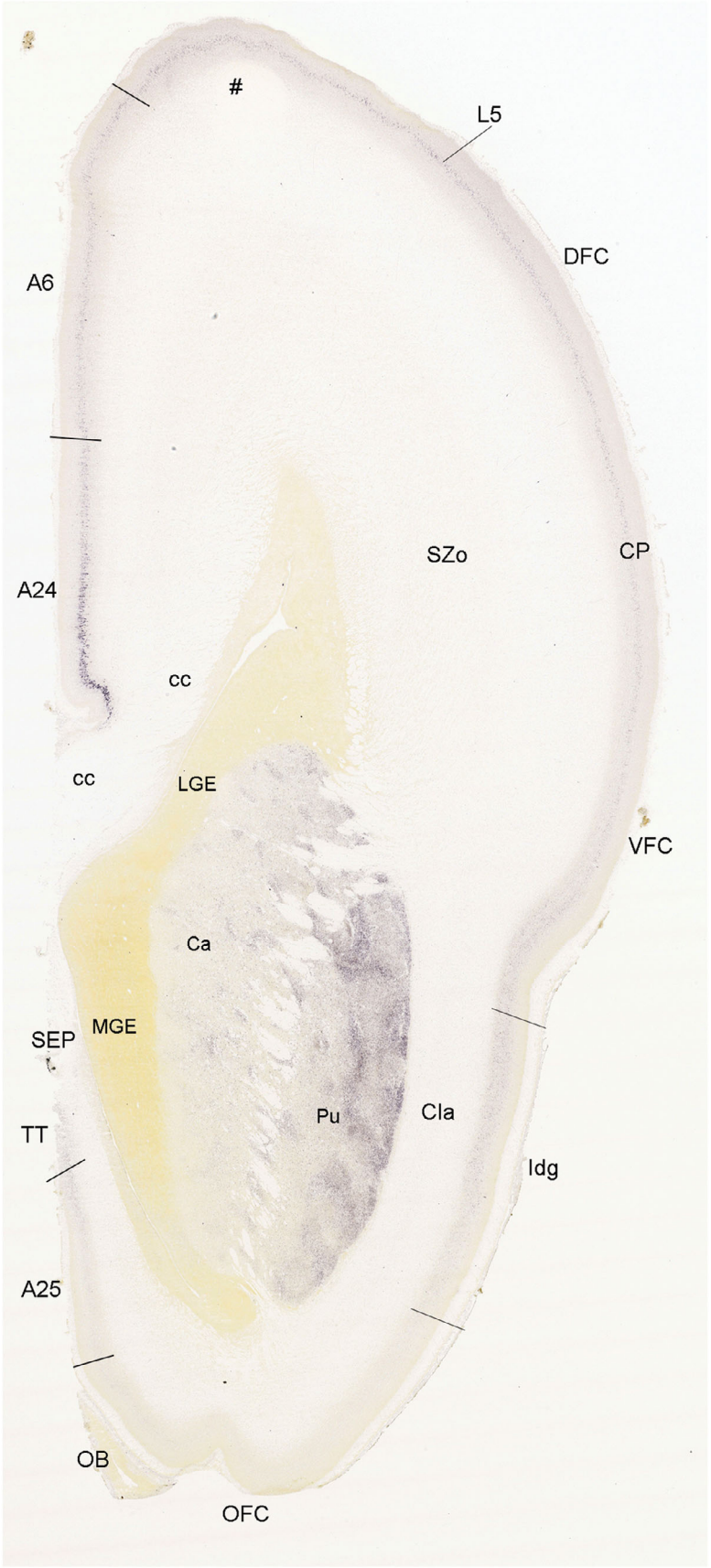

NRGN-02-048 (Level ~16)

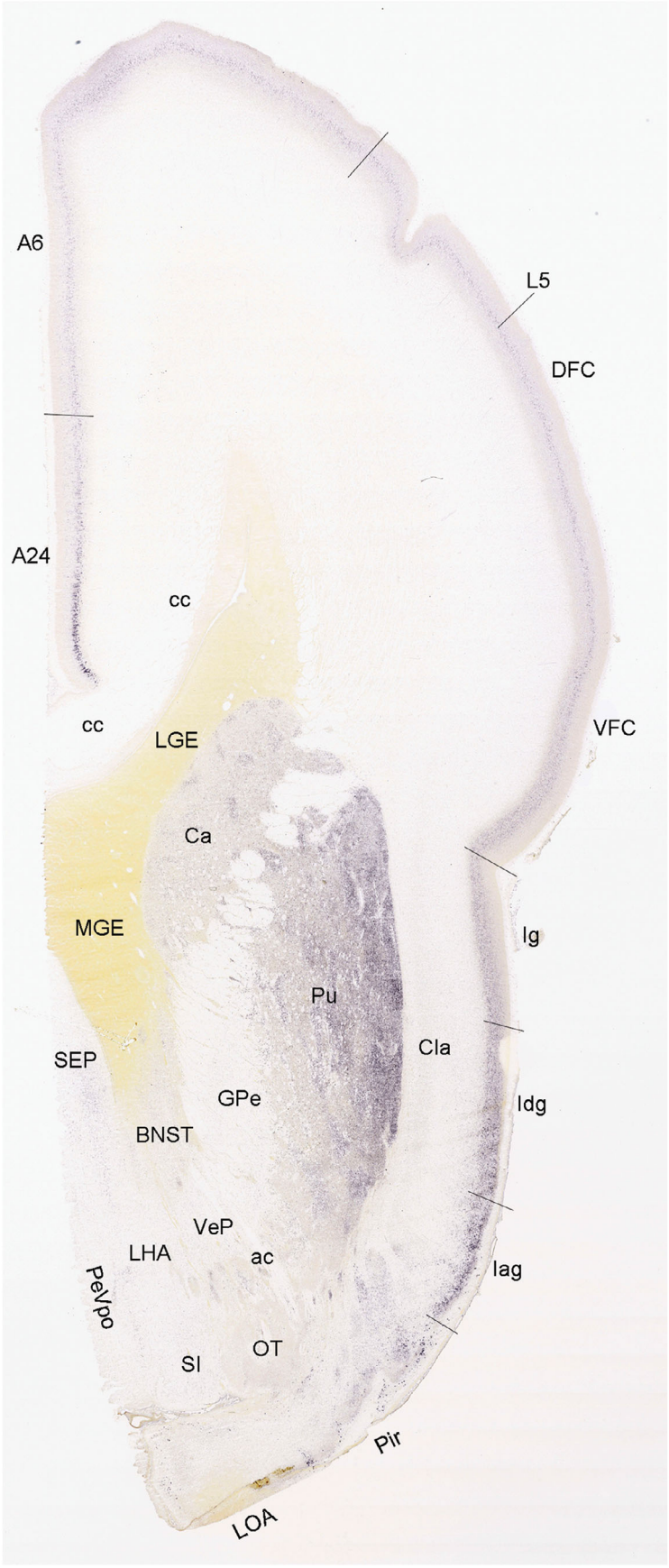

NRGN-02-201 (Level ~21)

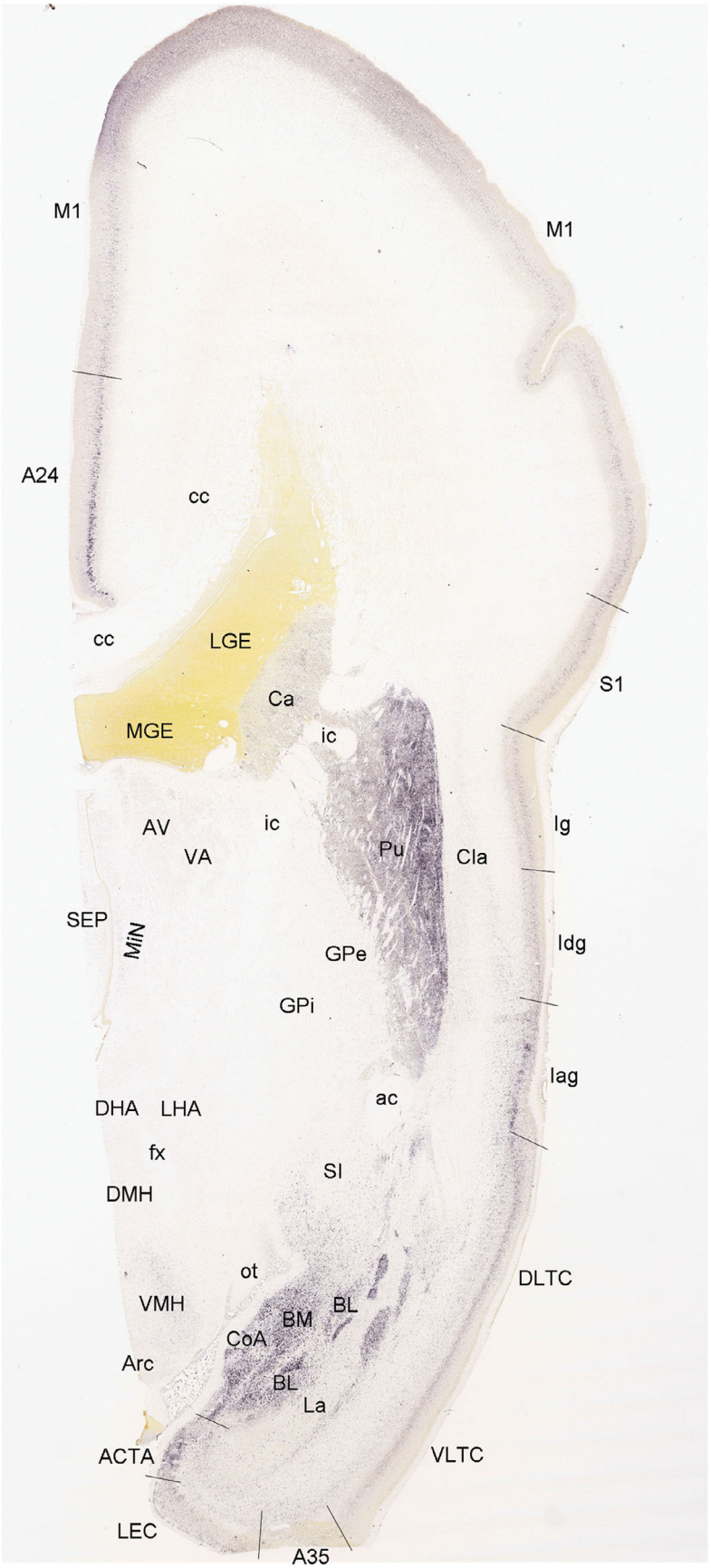

NRGN-02-405 (Level ~29)

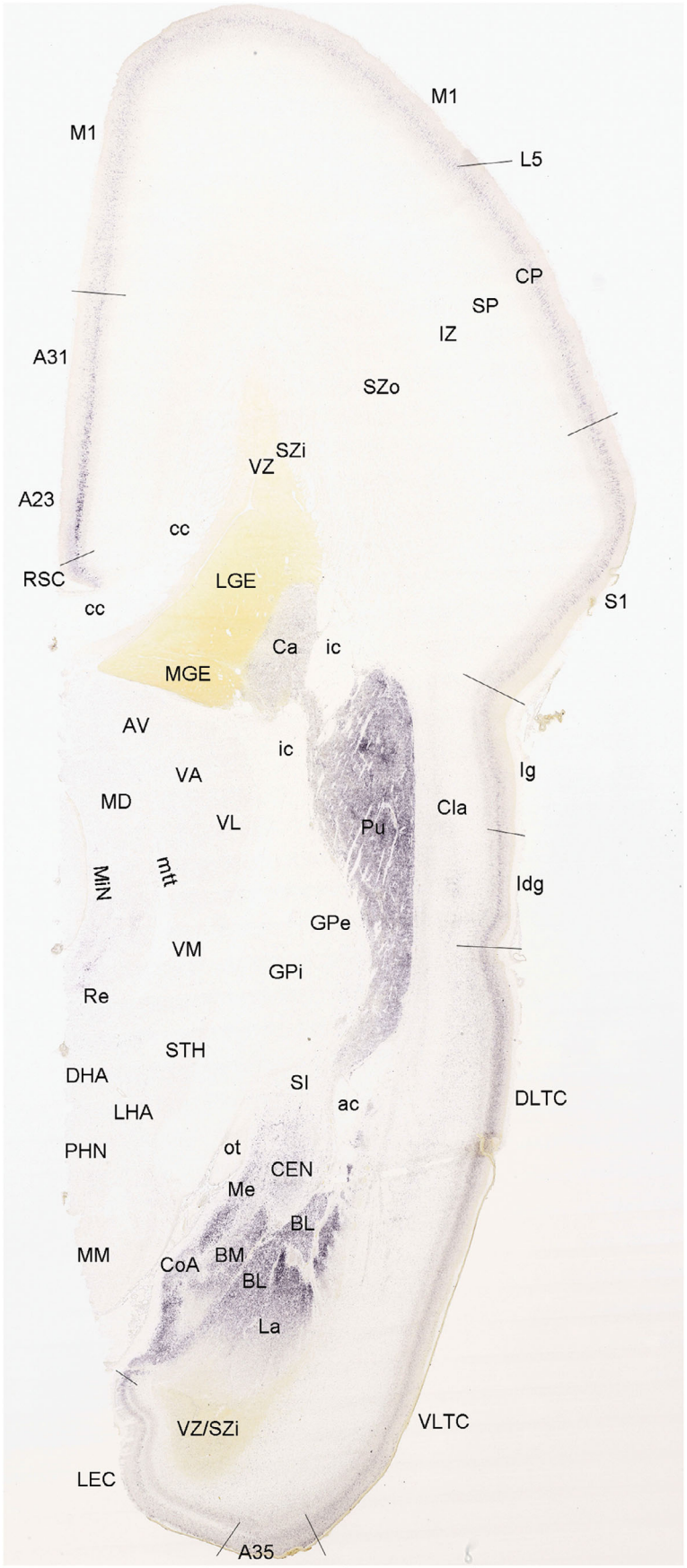

NRGN-02-507 (Level ~33)

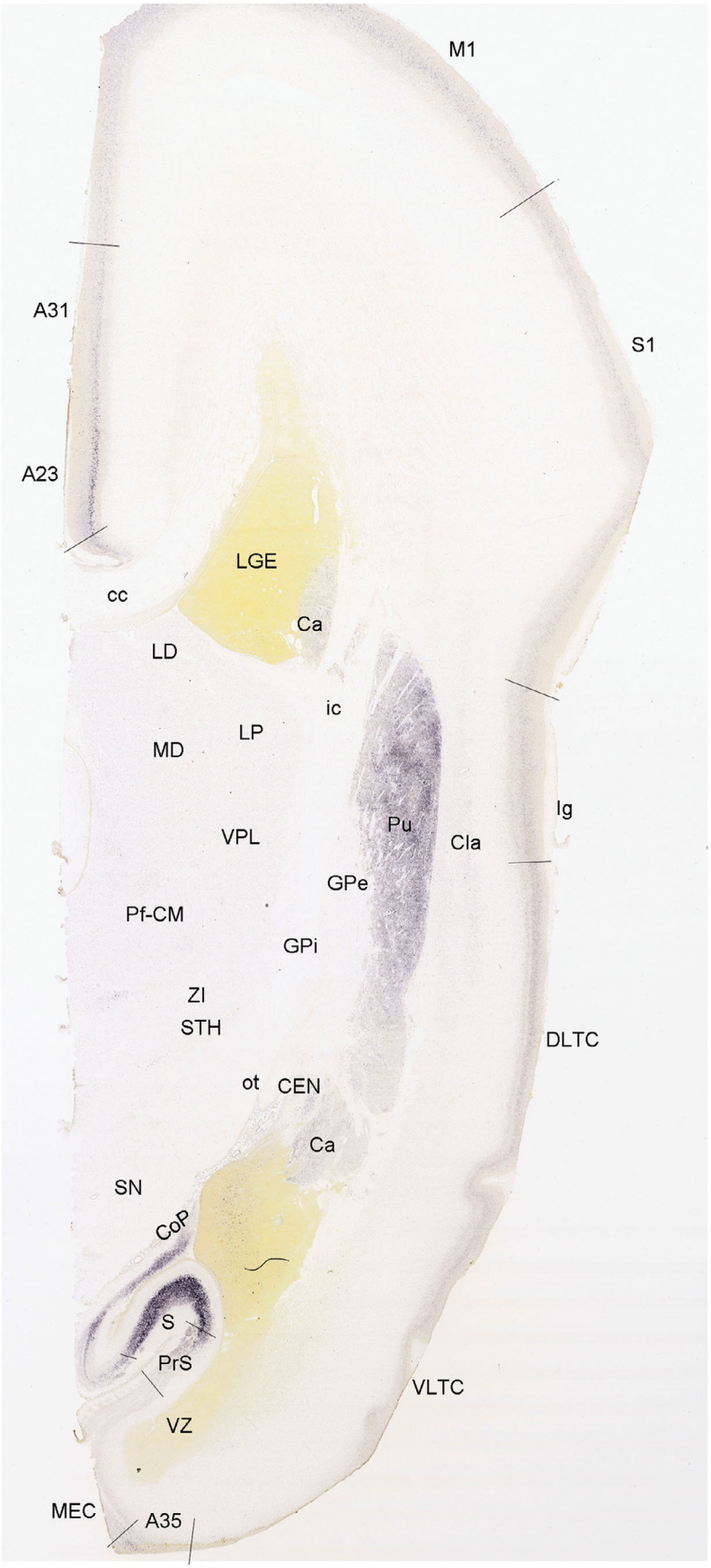

NRGN-02-660 (Level ~39)

PLXNA2-02-762 (Level ~43)

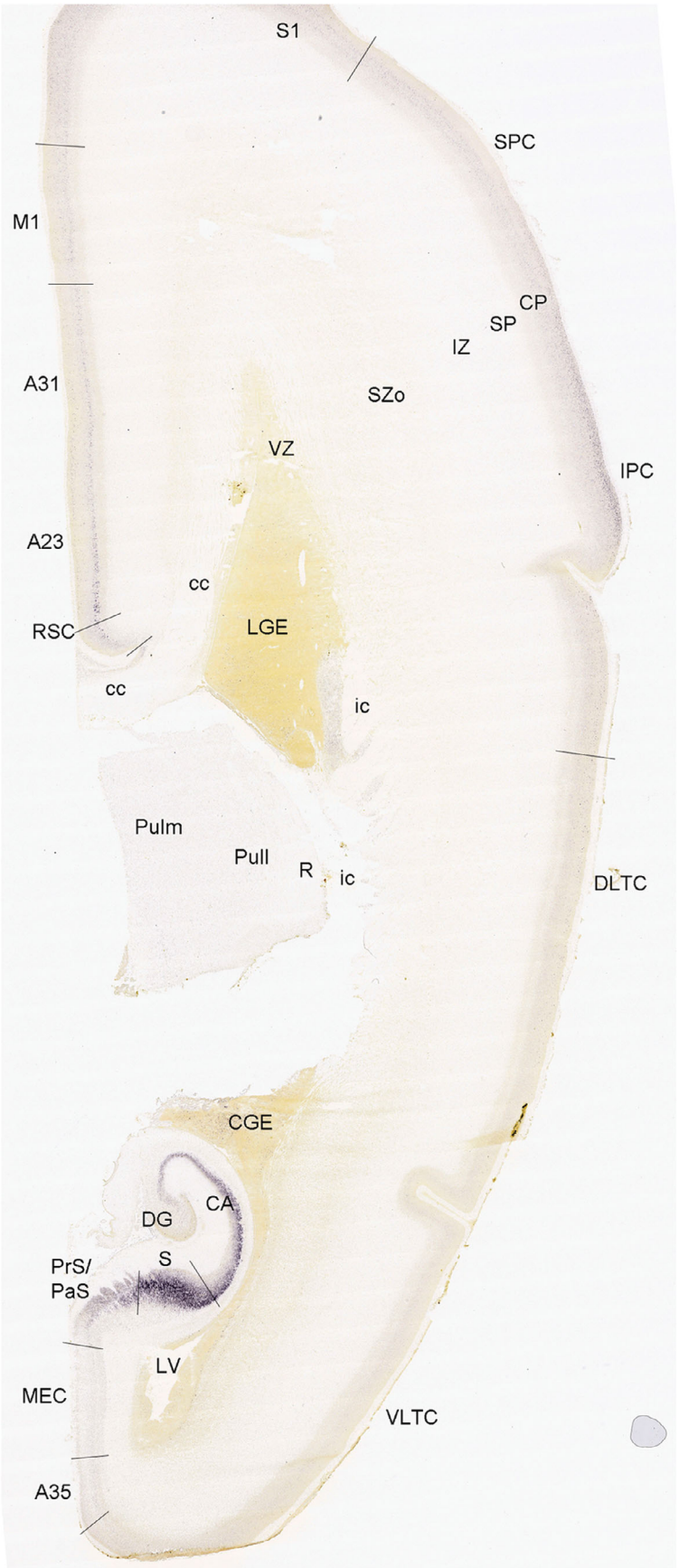

NRGN-03-048 (Level ~47)

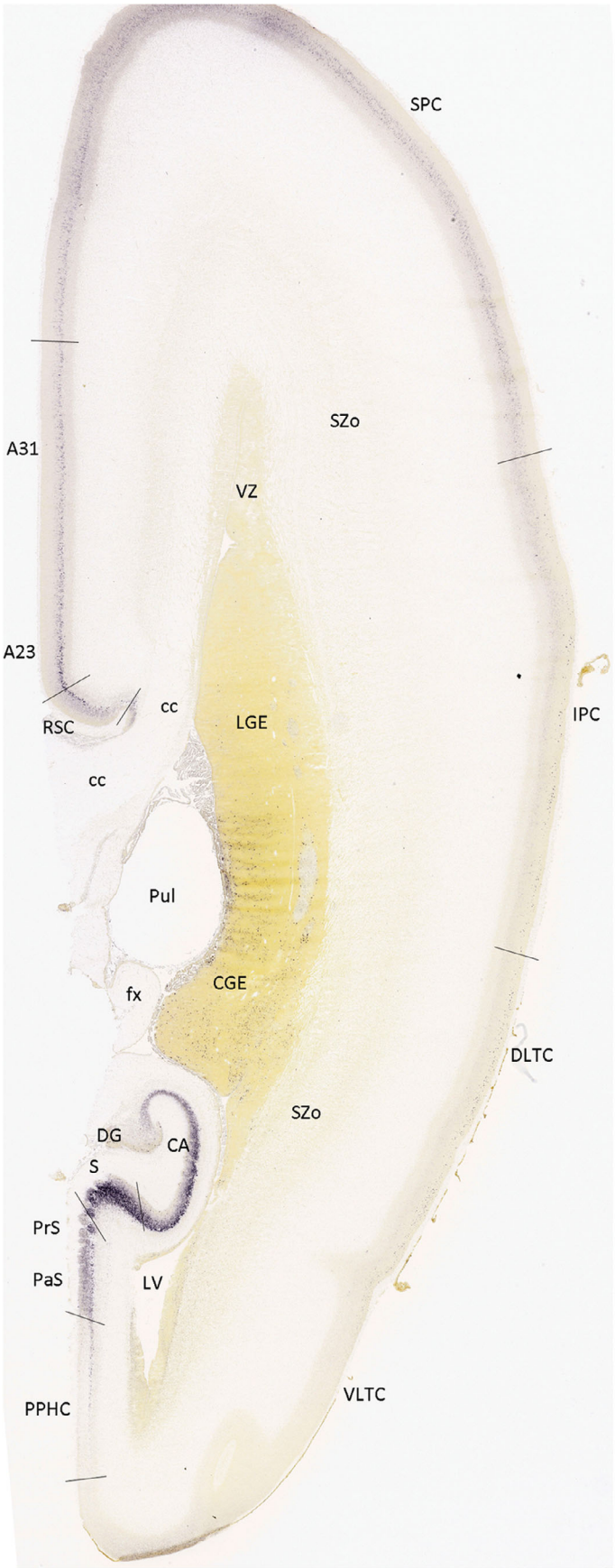

NRGN-03-201 (Level ~53)

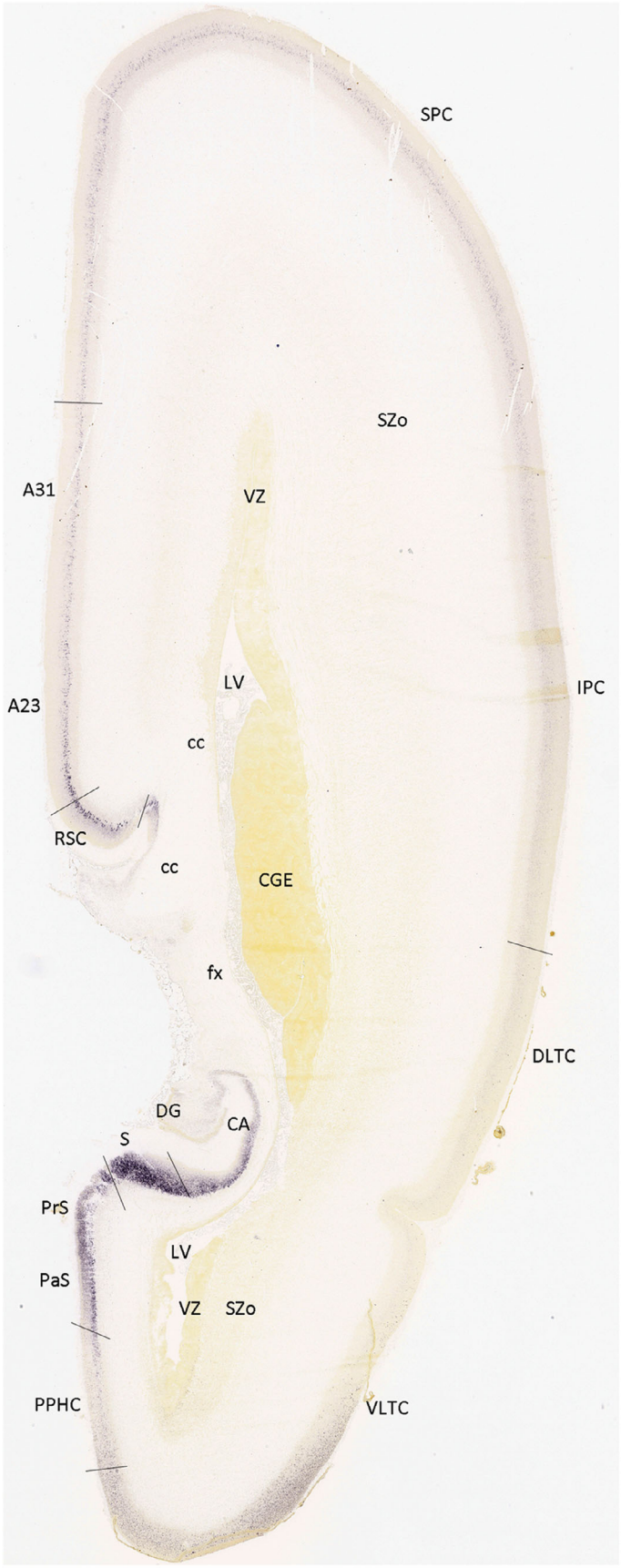

NRGN-03-354 (Level ~59)

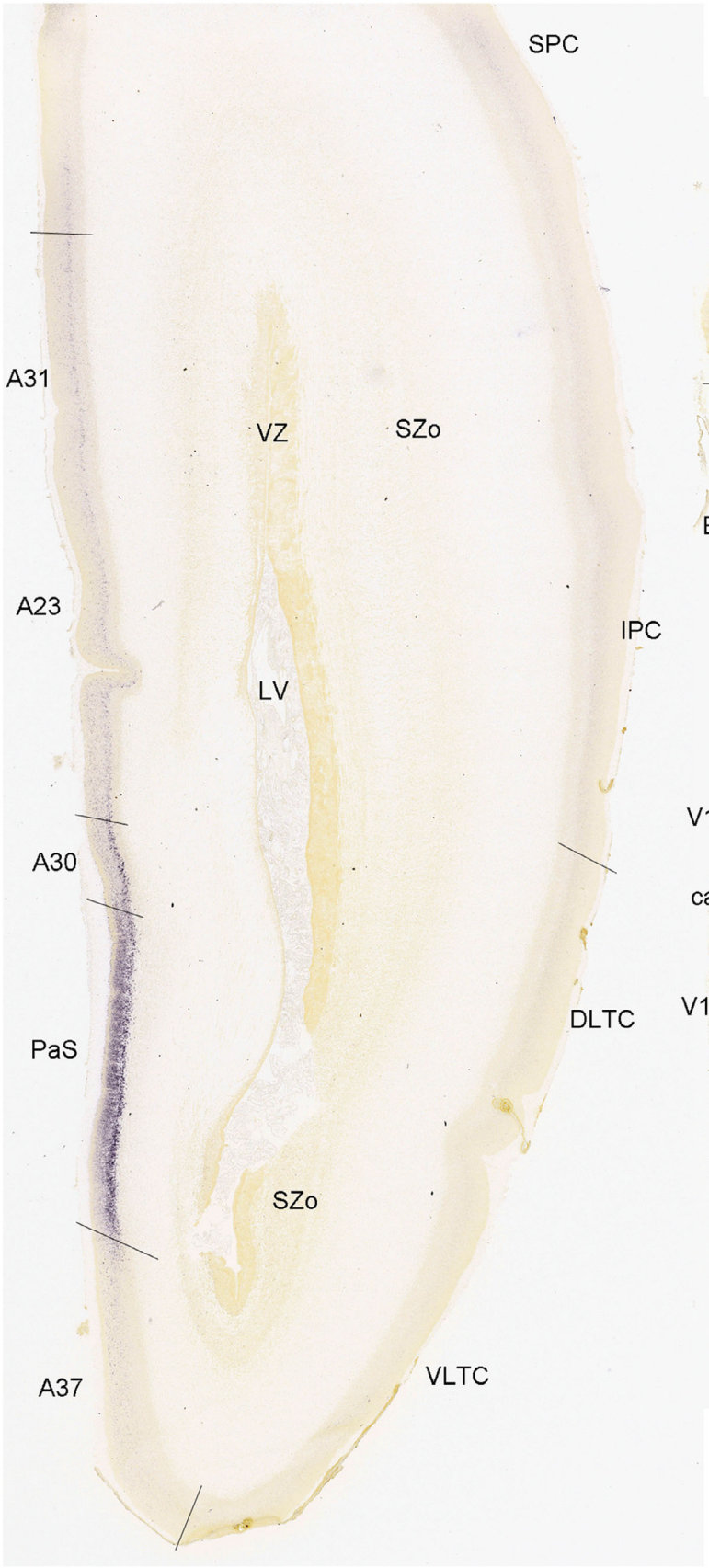

NRGN-03-507 (Level ~64)

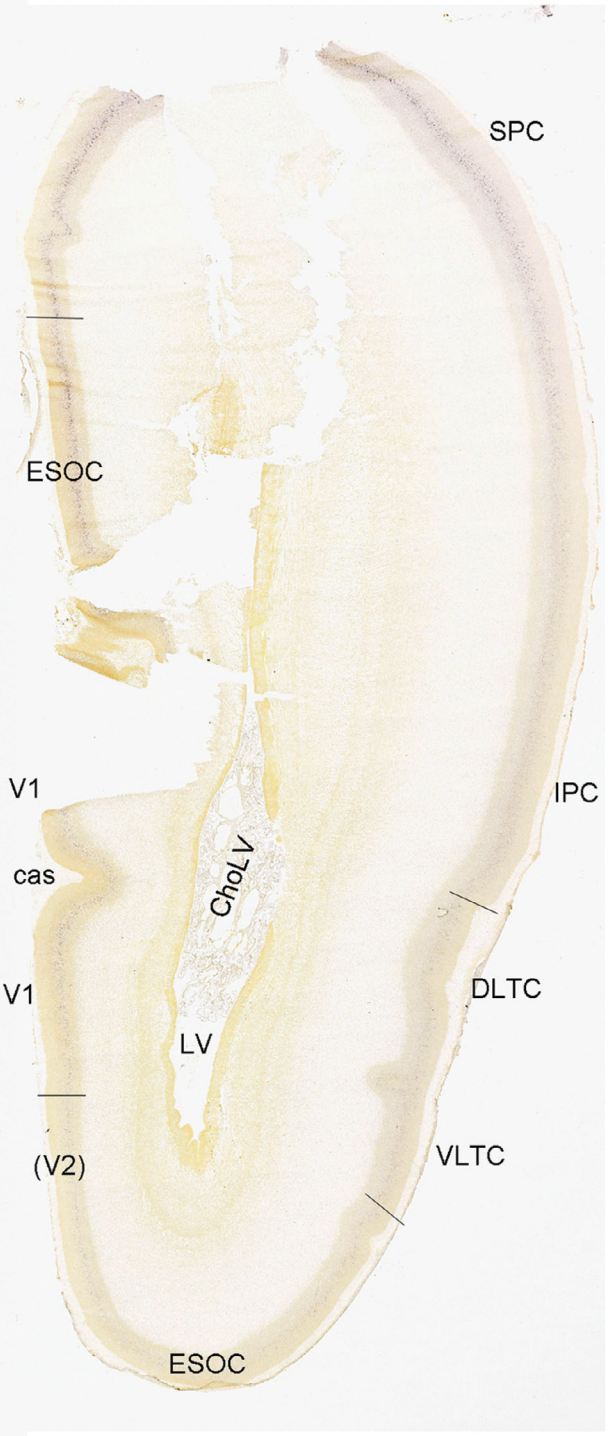

NRGN-04-150 (Level ~70-71)

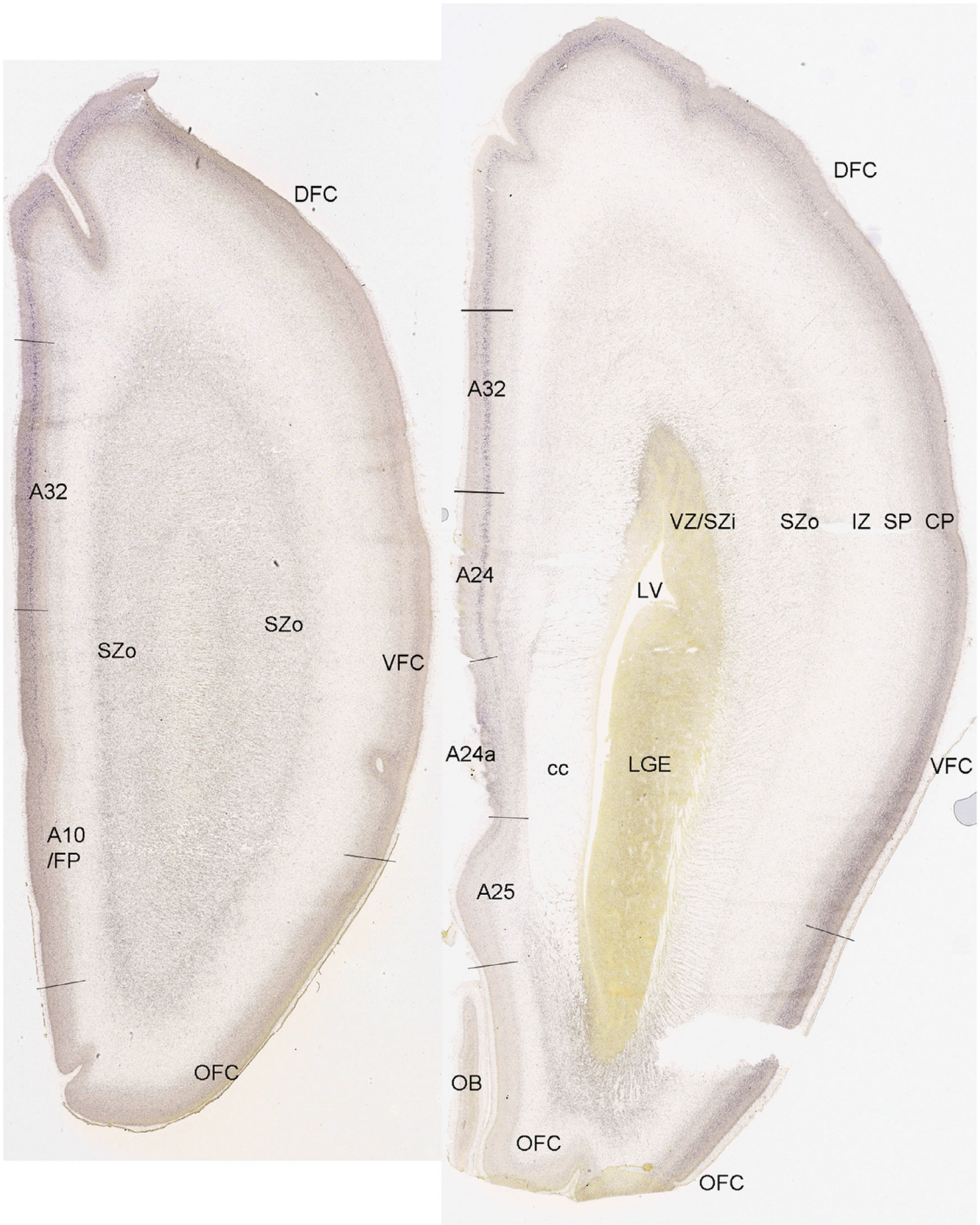

PLXNA2-01-248 (Level ~5) **PLXNA2-01-554 (Level ~11-12)**

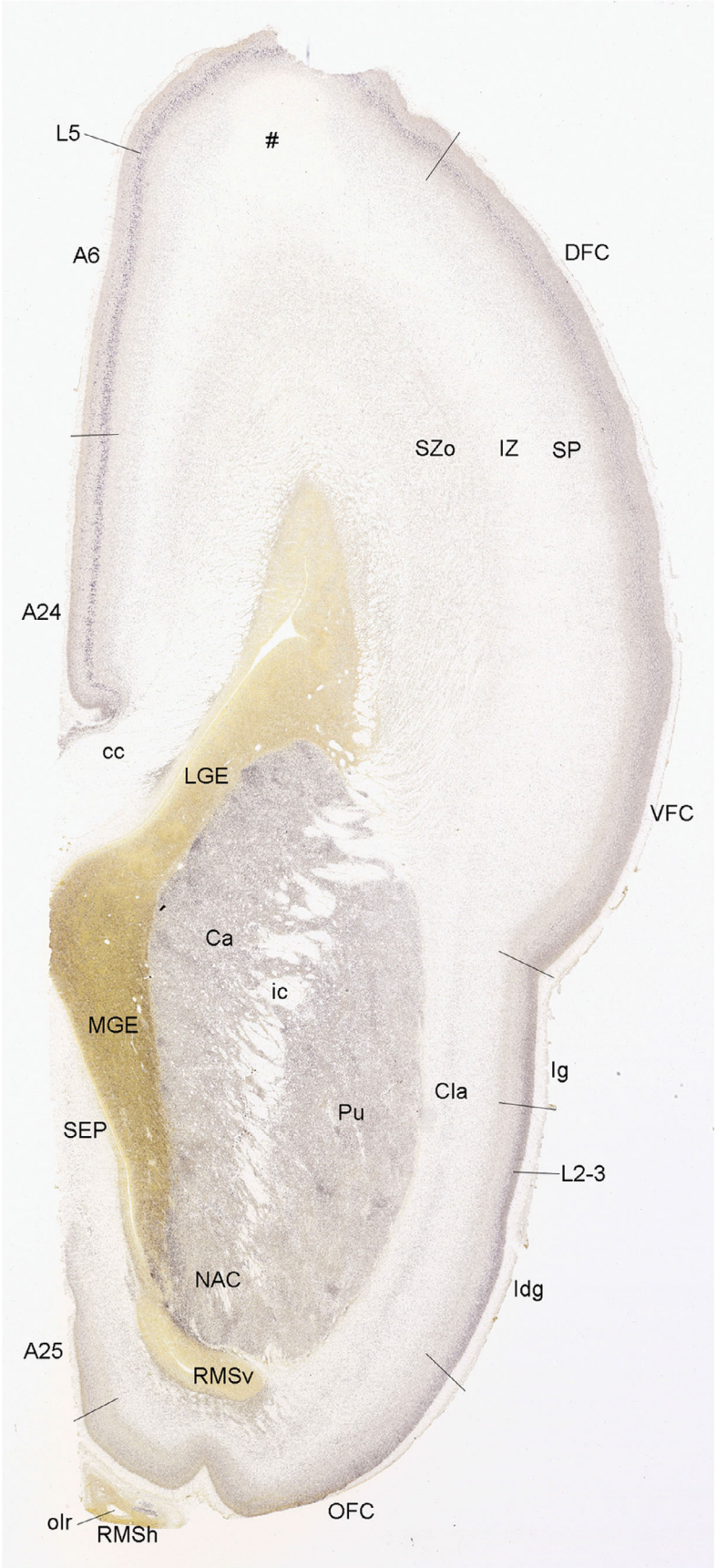

PLXNA2-02-095 (Level ~18)

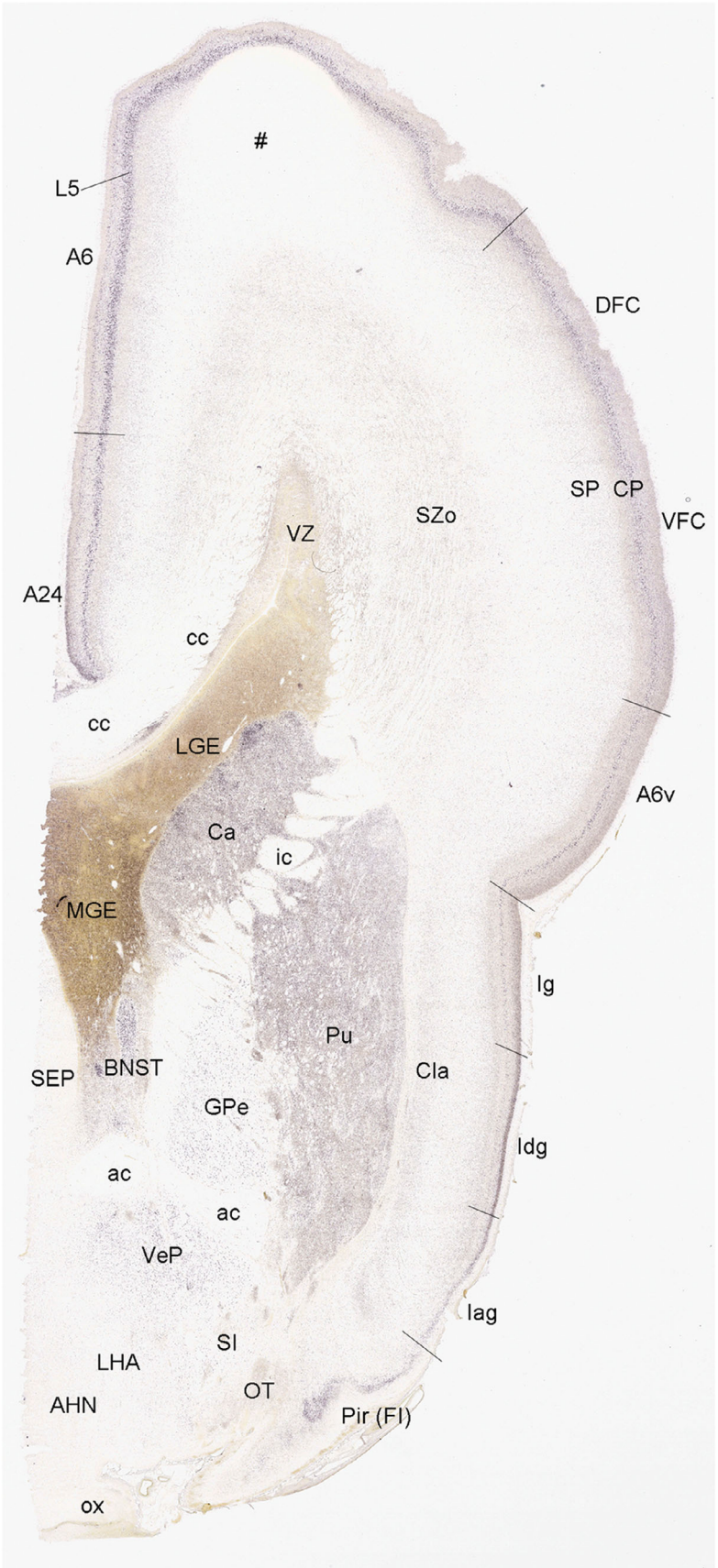

PLXNA2-02-248 (Level ~23)

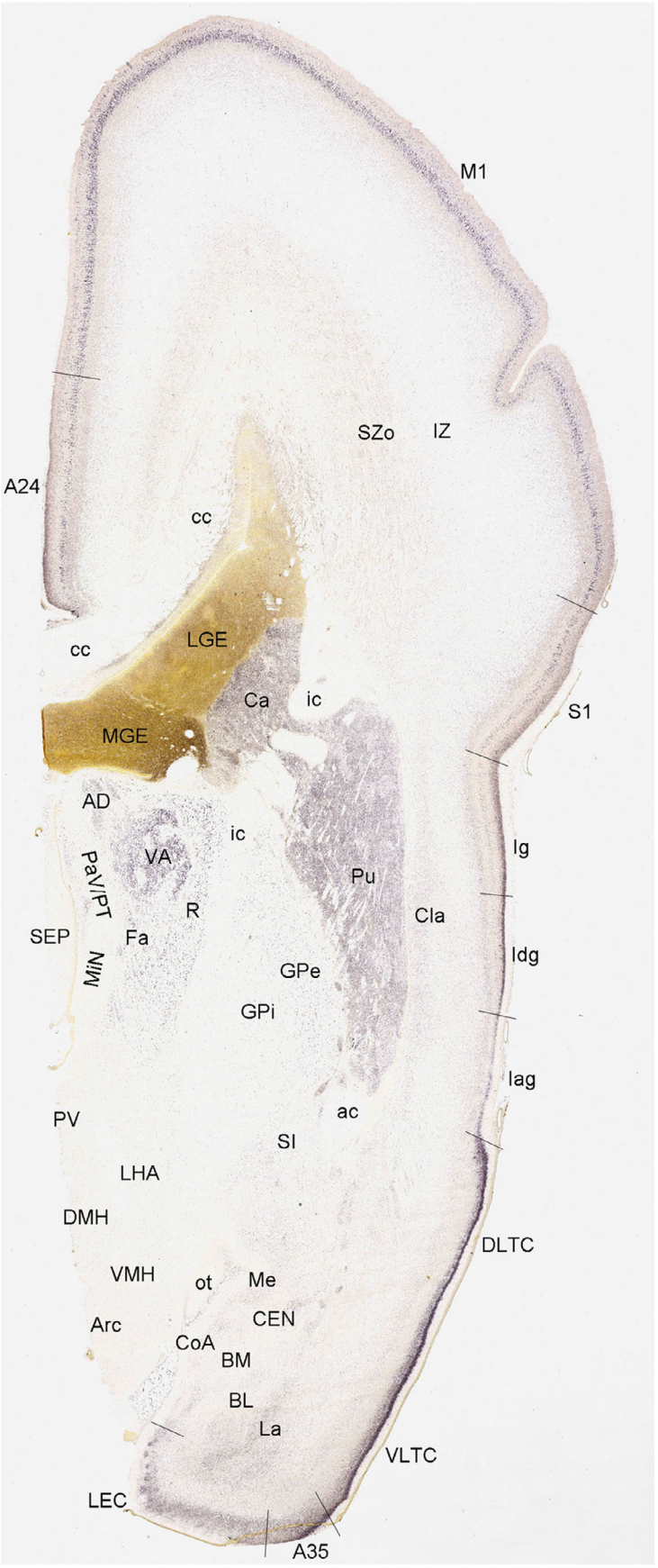

PLXNA2-02-401 (Level ~28-29)

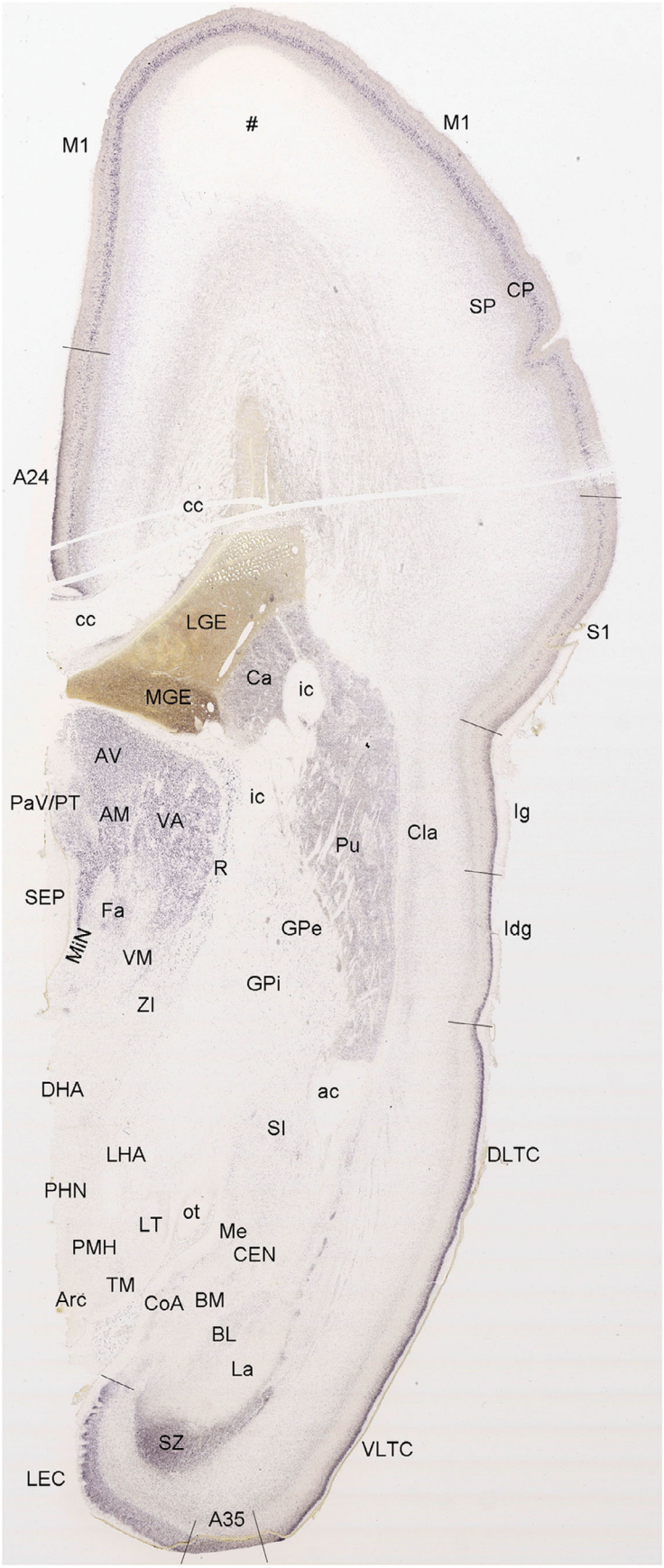

PLXNA2-02-452 (Level ~30-31)

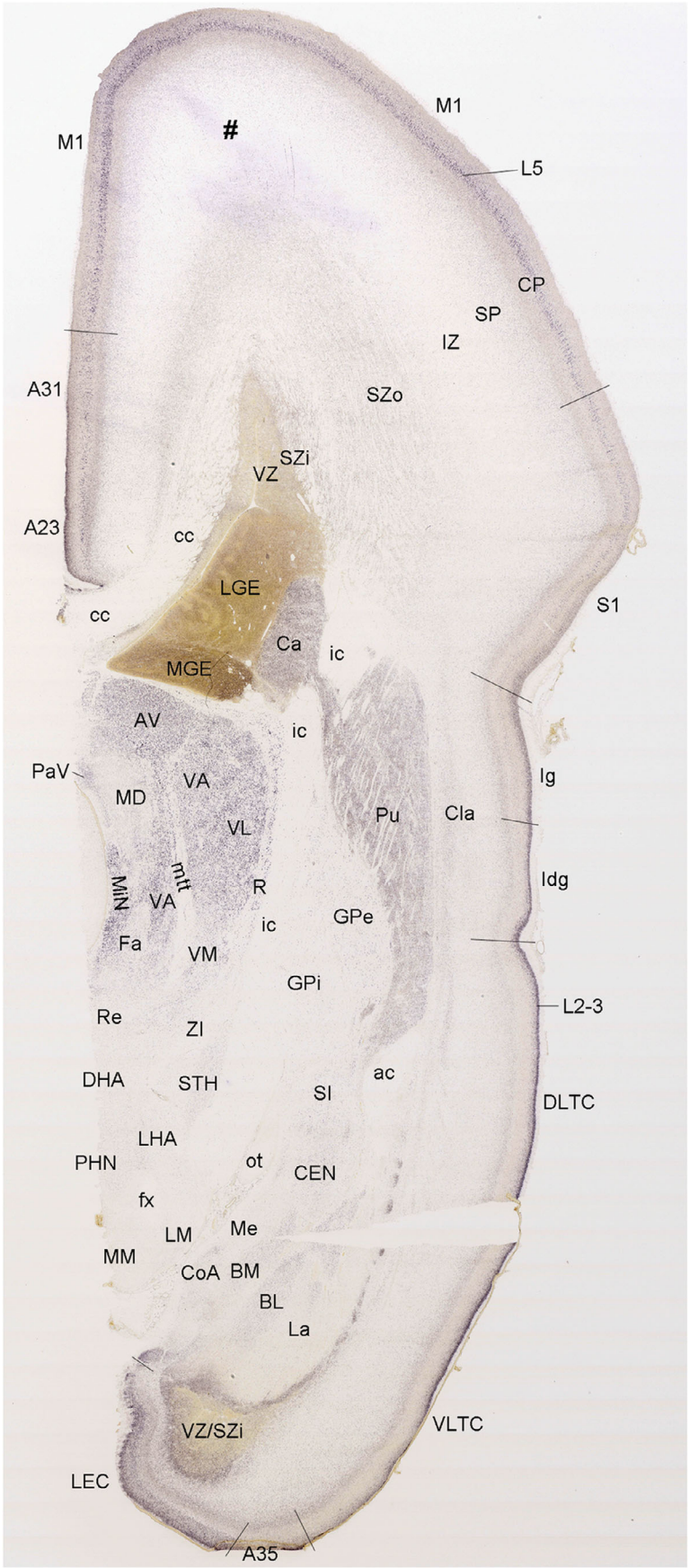

PLXNA2-02-503 (Level ~33)

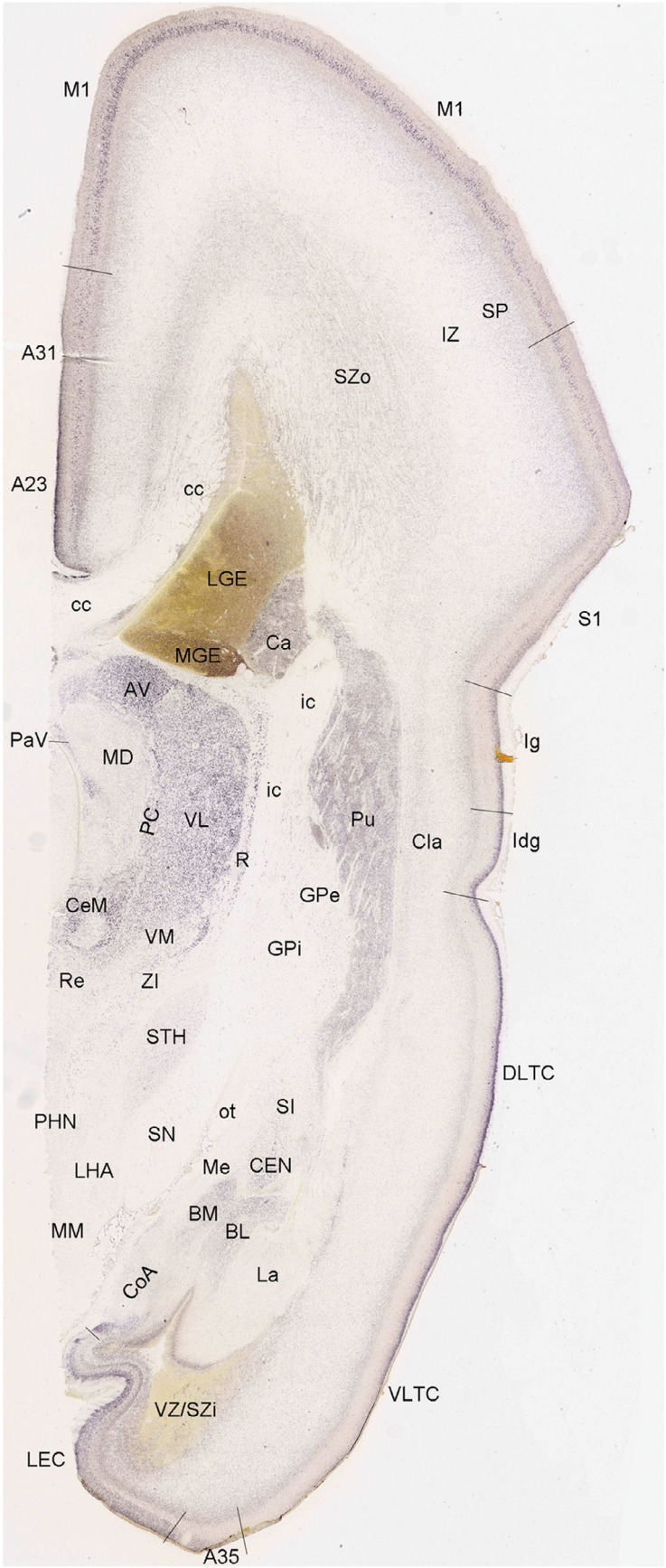

PLXNA2-02-554 (Level ~35)

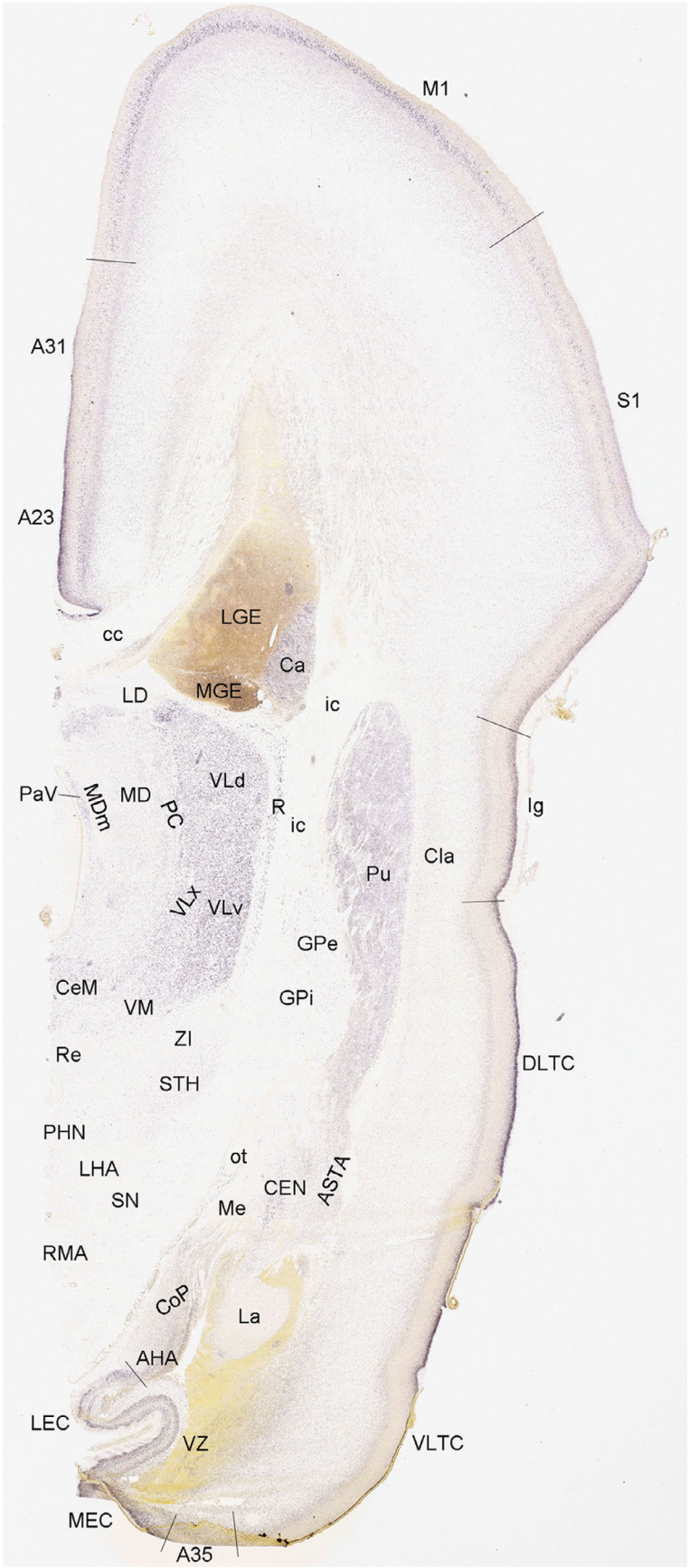

PLXNA2-02-605 (Level ~36-37)

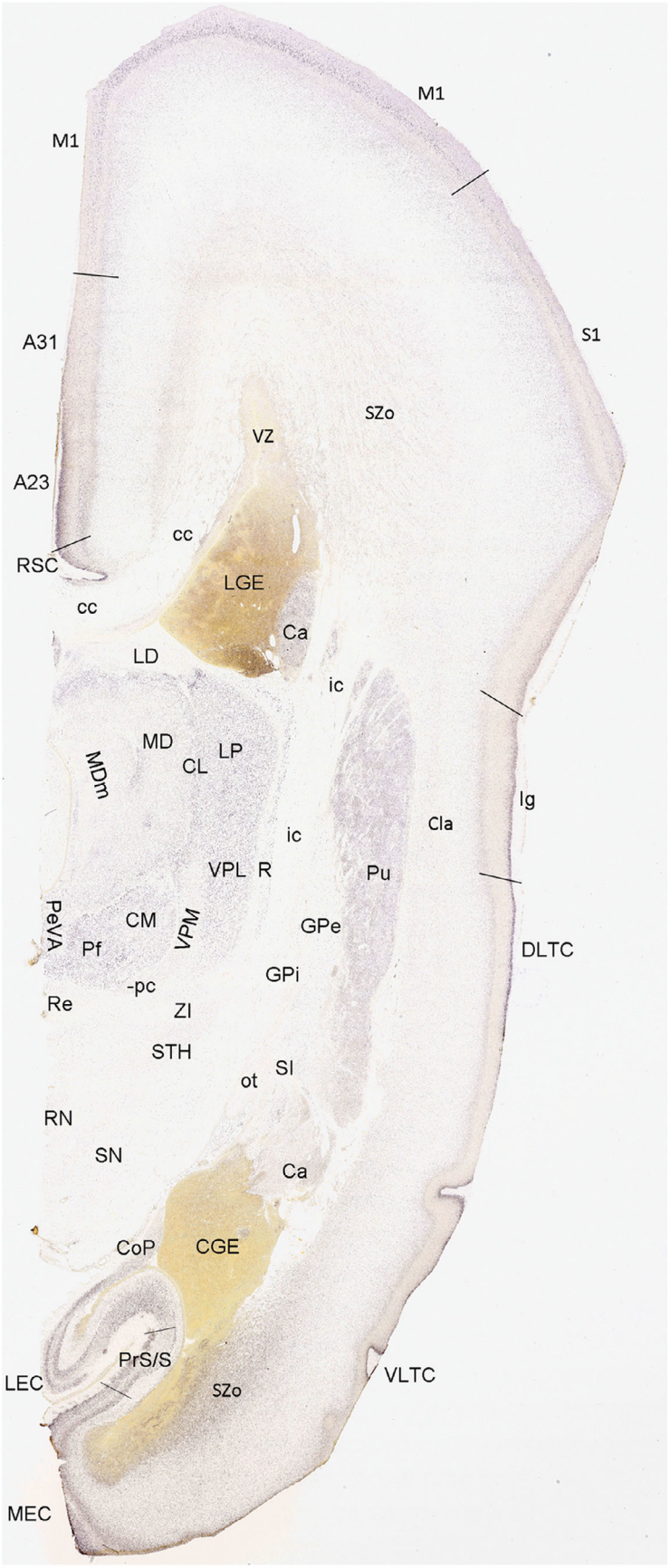

PLXNA2-02-656 (Level ~38-39)

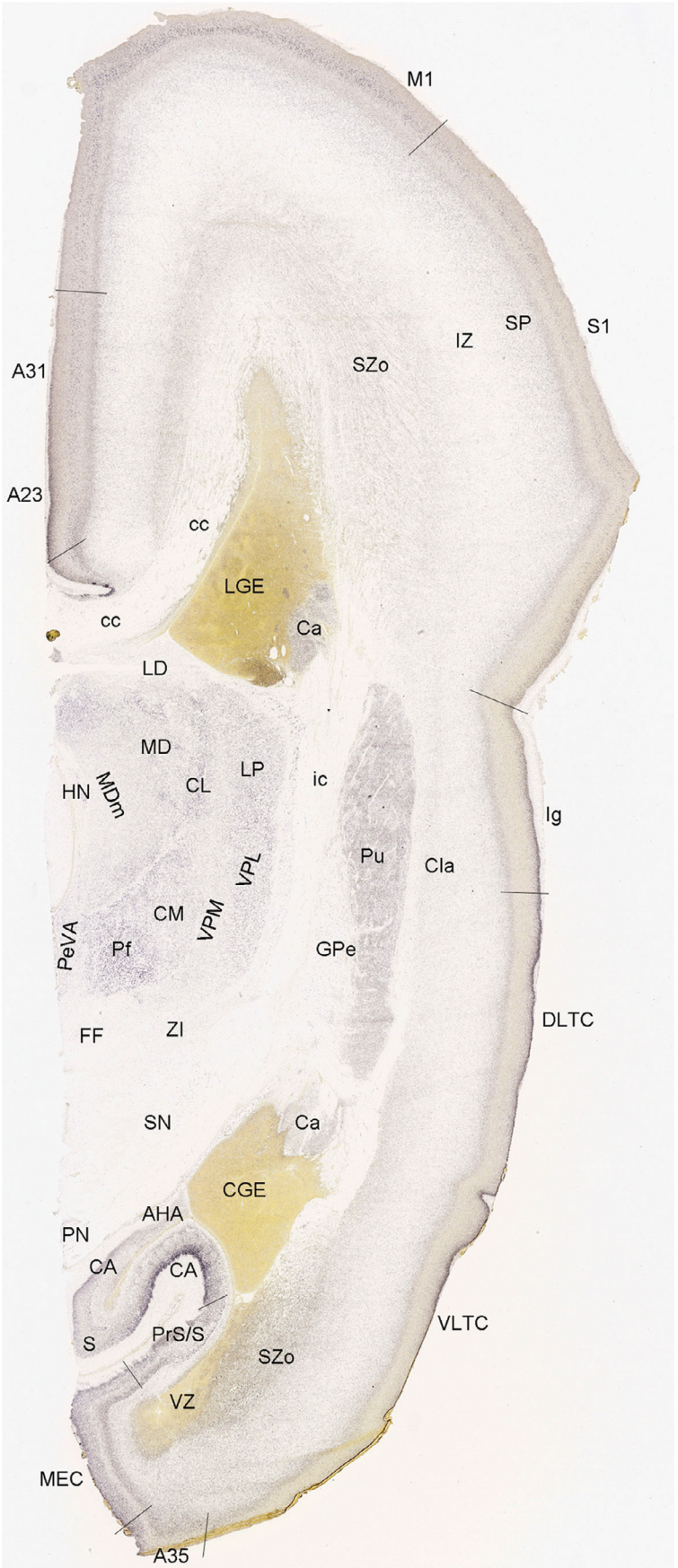

PLXNA2-02-707 (Level ~40-41)

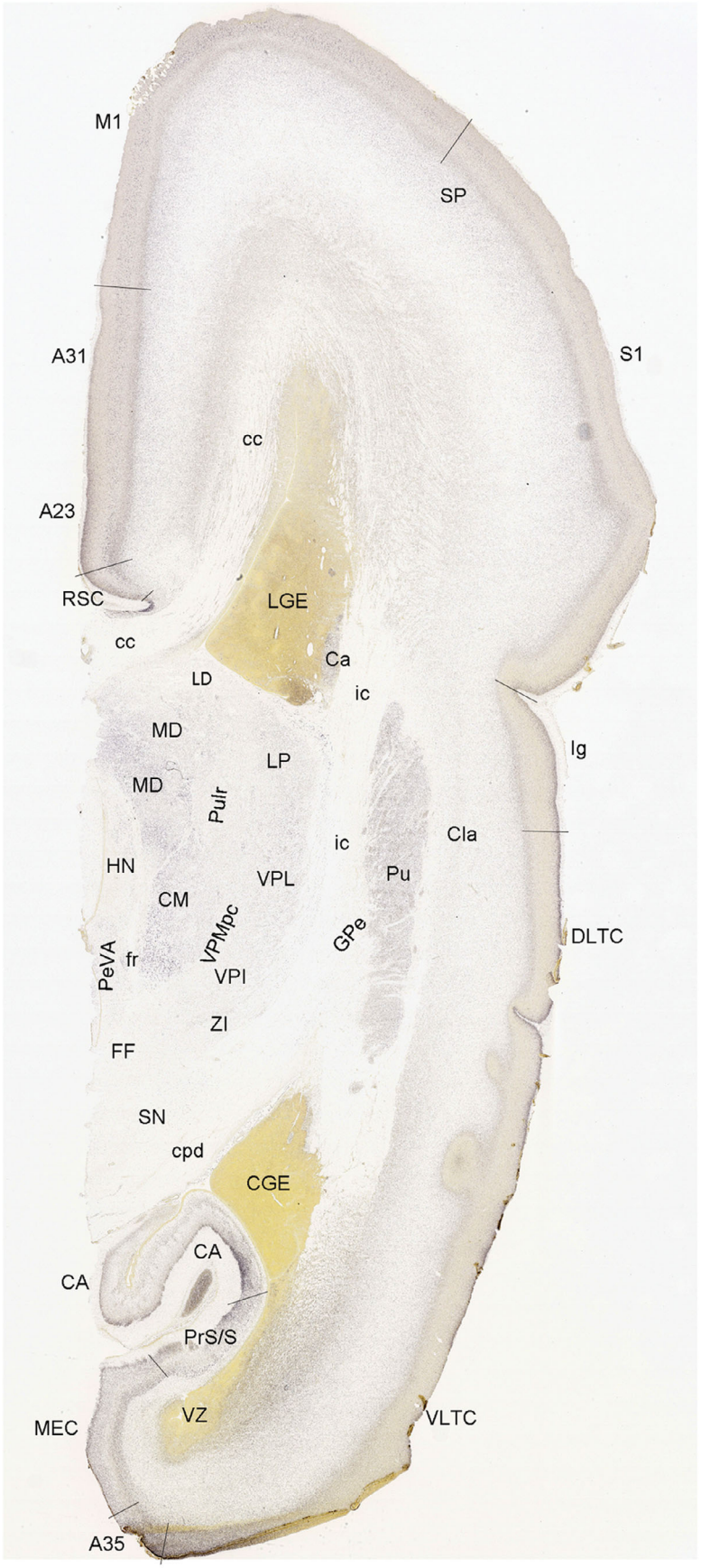

PLXNA2-02-758 (Level ~42-43)

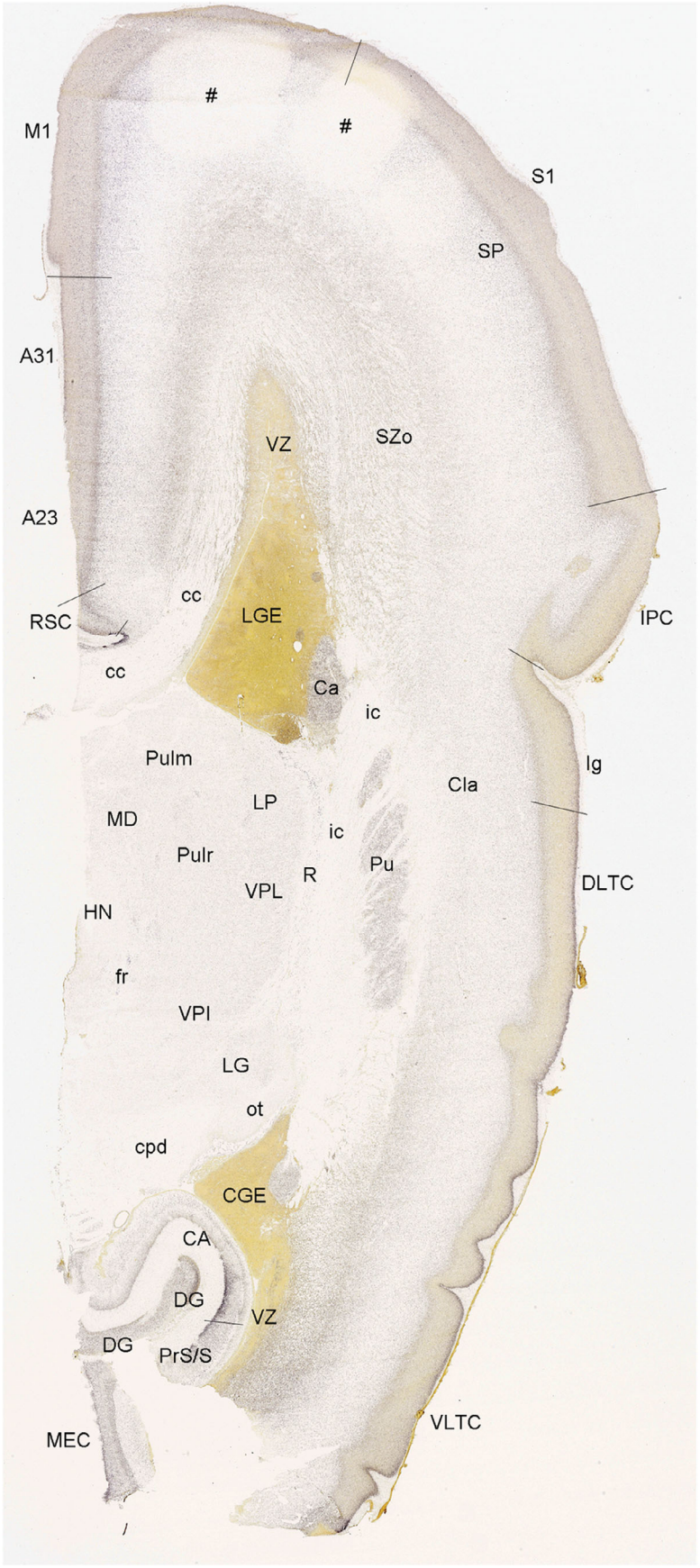

PLXNA2-02-809 (Level ~44-45)

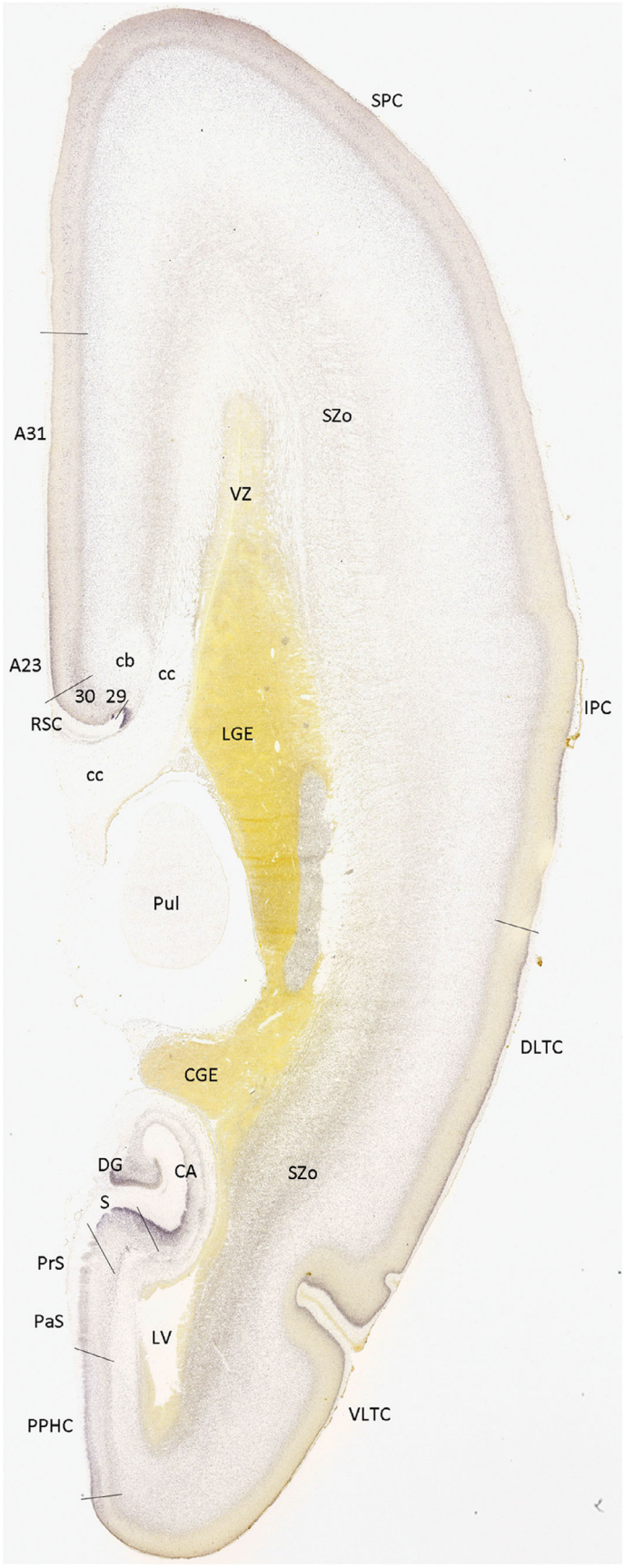

PLXNA2-03-146 (Level ~51)

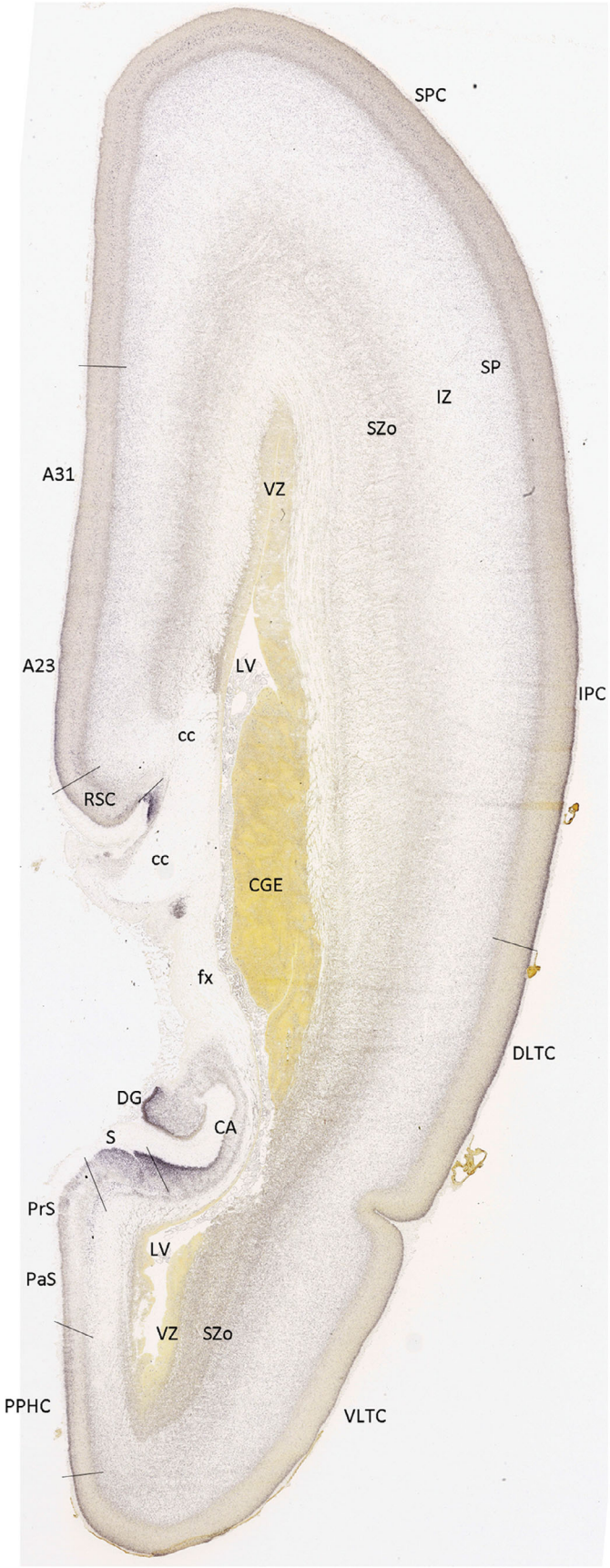

PLXNA2-03-350 (Level ~59)

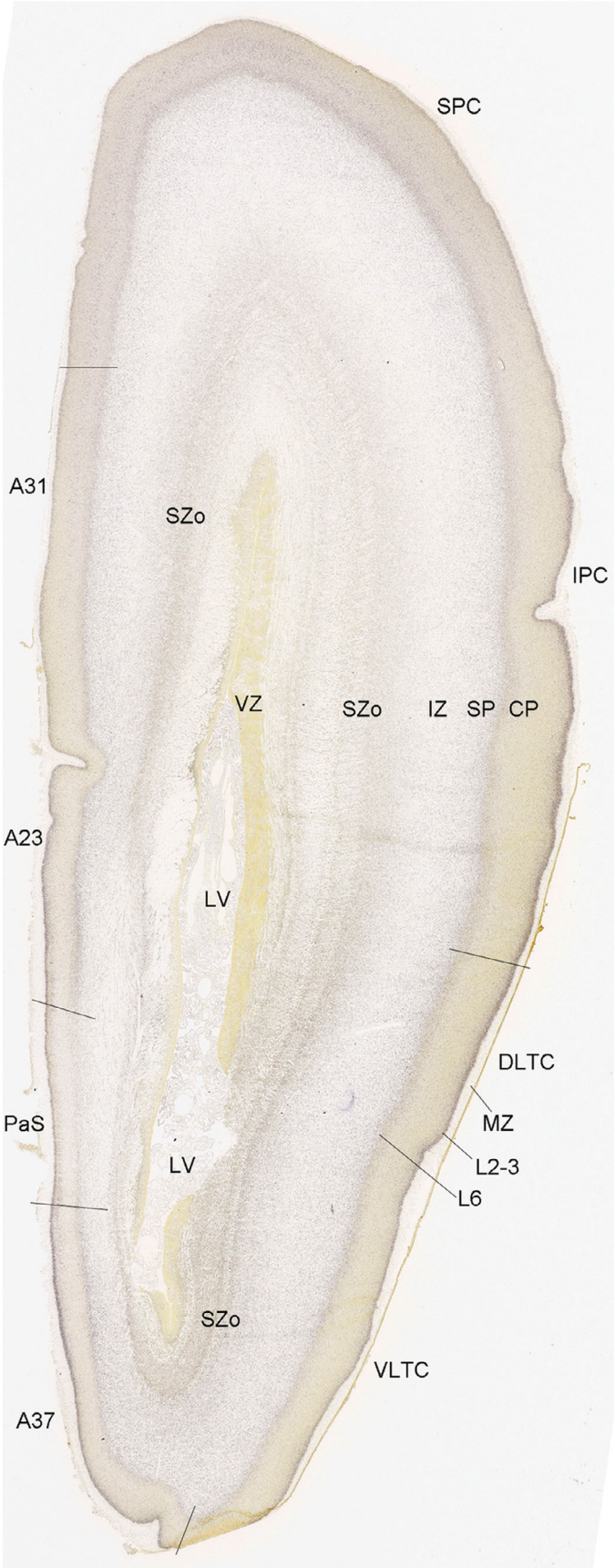

PLXNA2-03-554 (Level ~65)

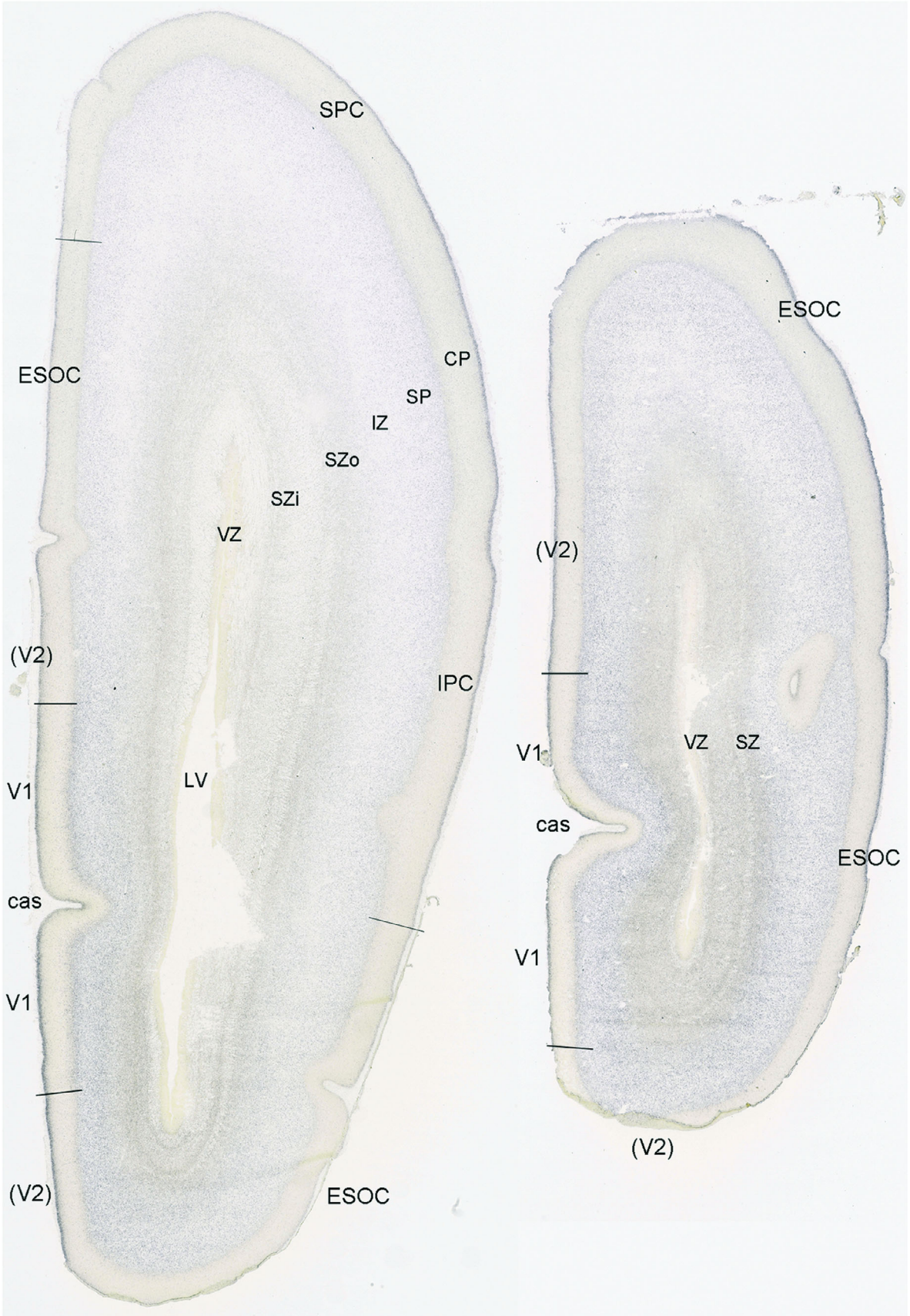

PLNA2-04-197 (Level ~71-72) **PLXNA2-04-503 (Level ~78)**

SST-01-469 (Level ~9)

SST-01-571 (Level ~11-12)

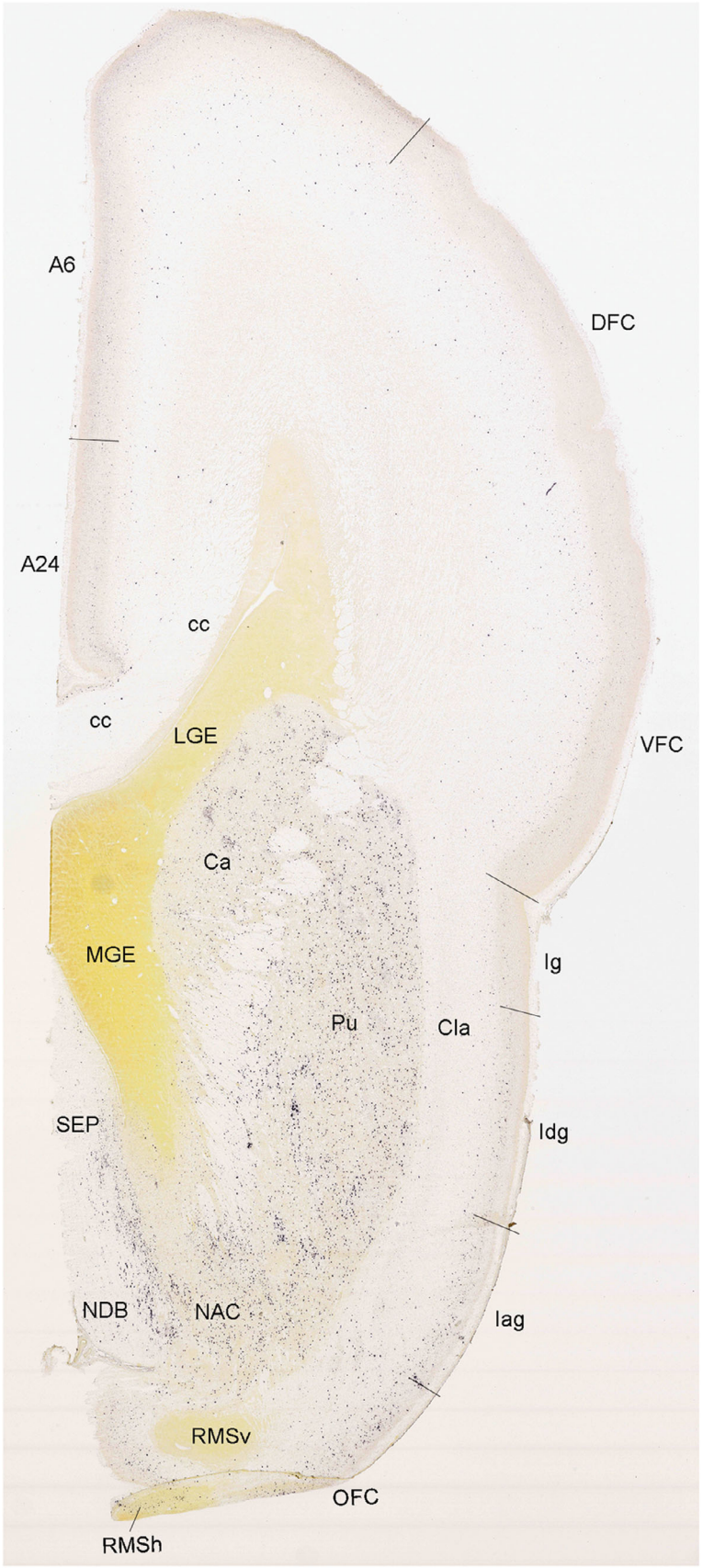

SST-02-163 (Level ~19-20)

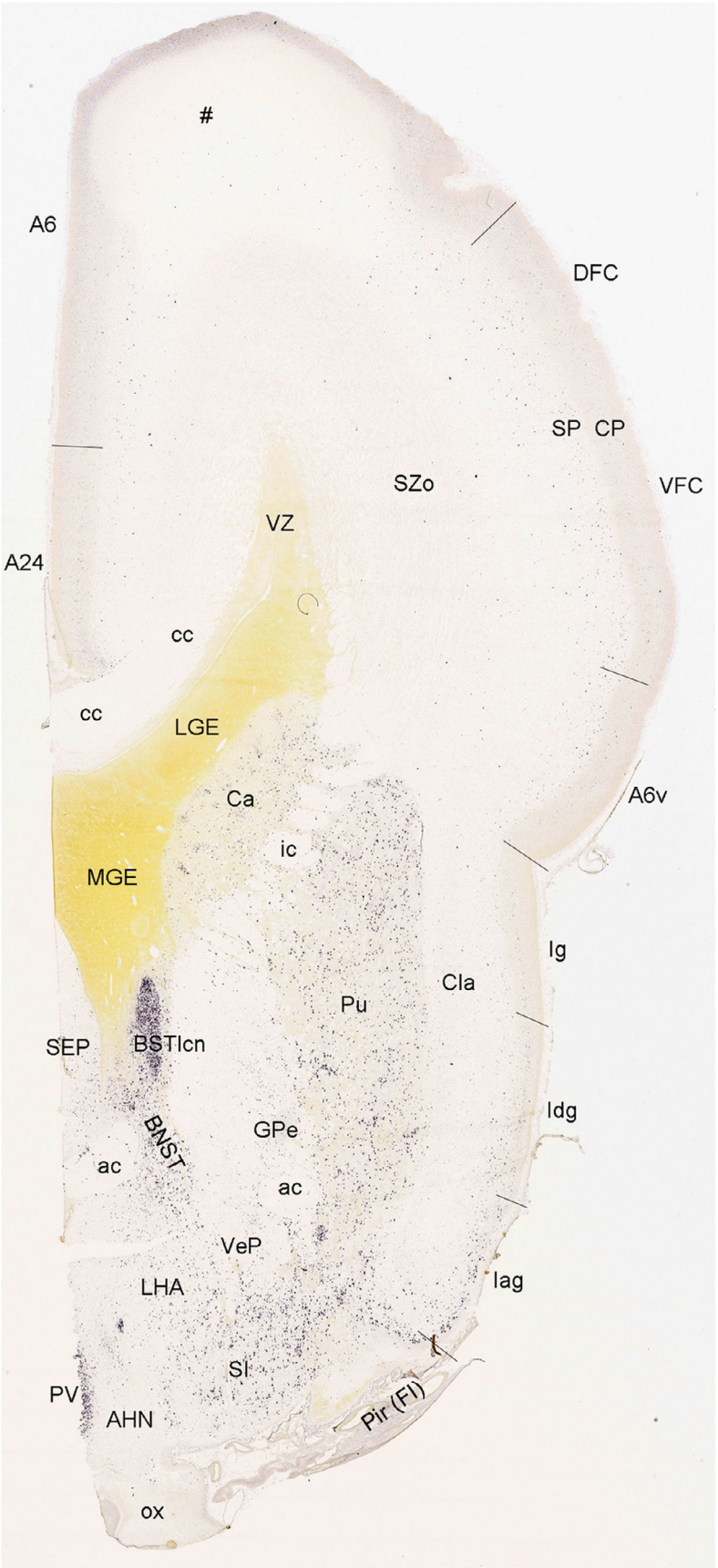

SST-02-265 (Level ~23-24)

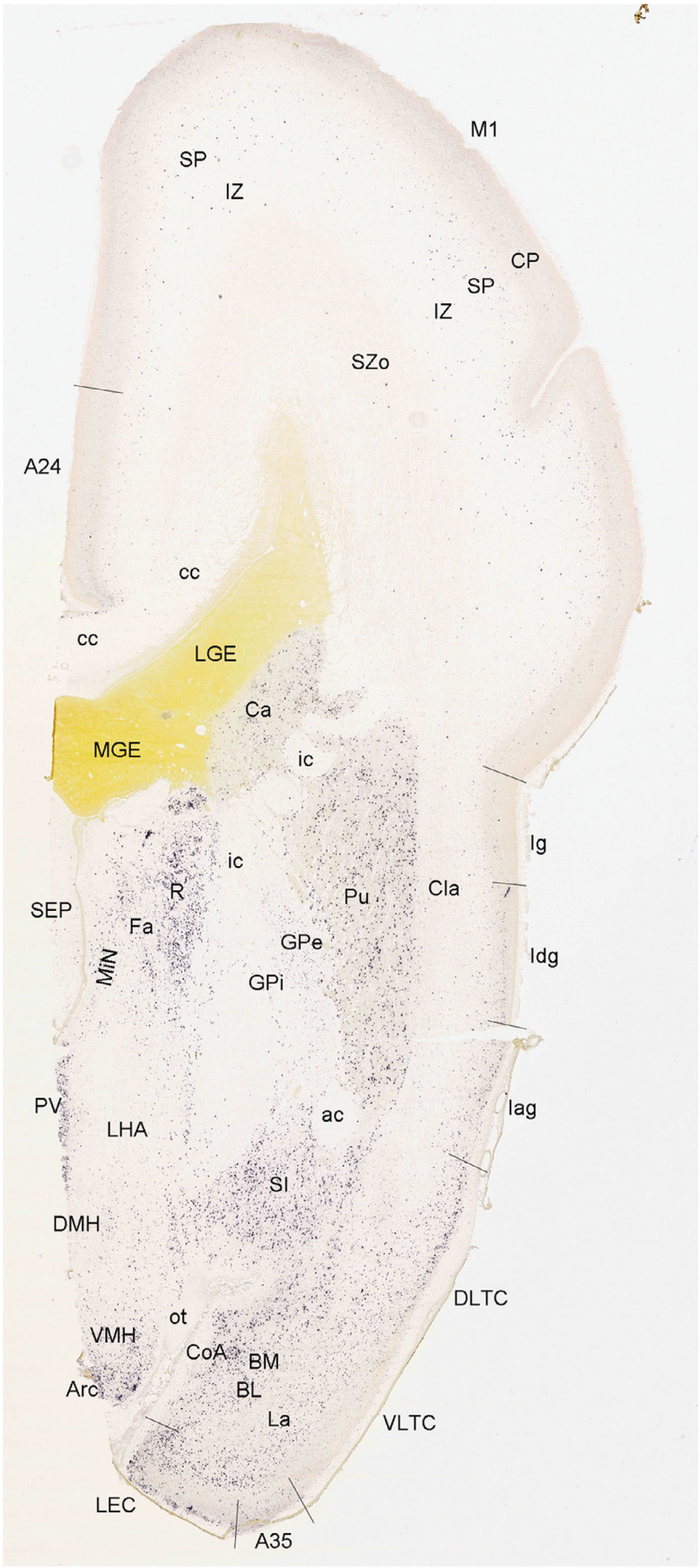

SST-02-367 (Level ~27-28)

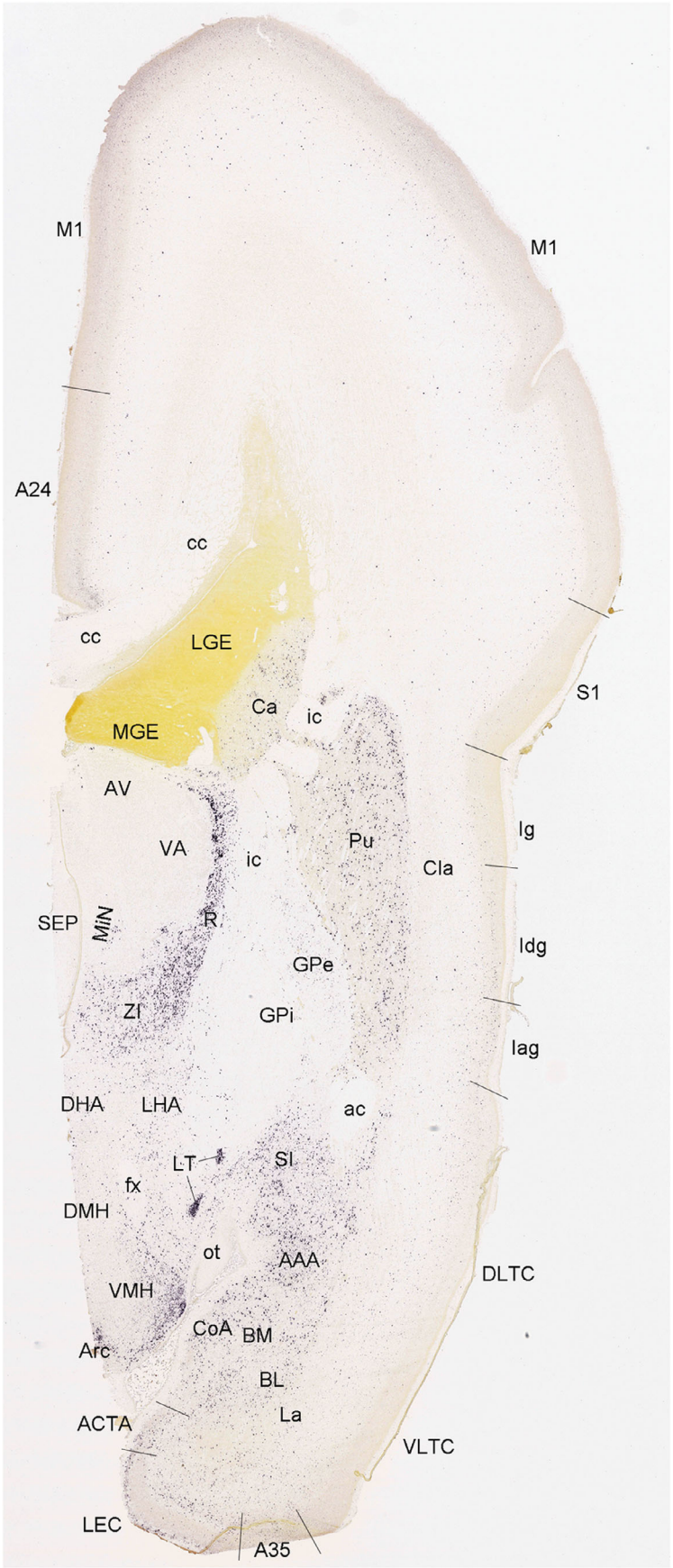

SST-02-418 (Level ~29-30)

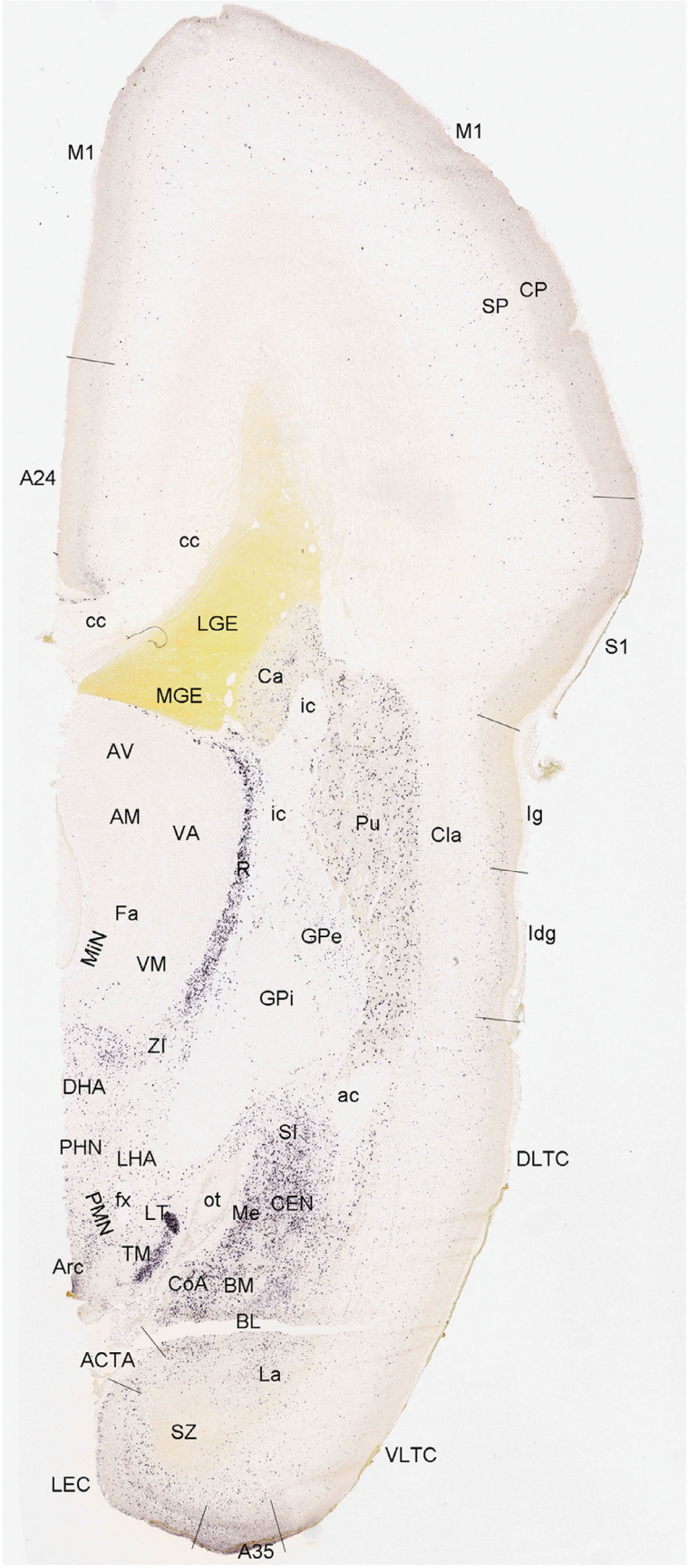

SST-02-469 (Level ~31)

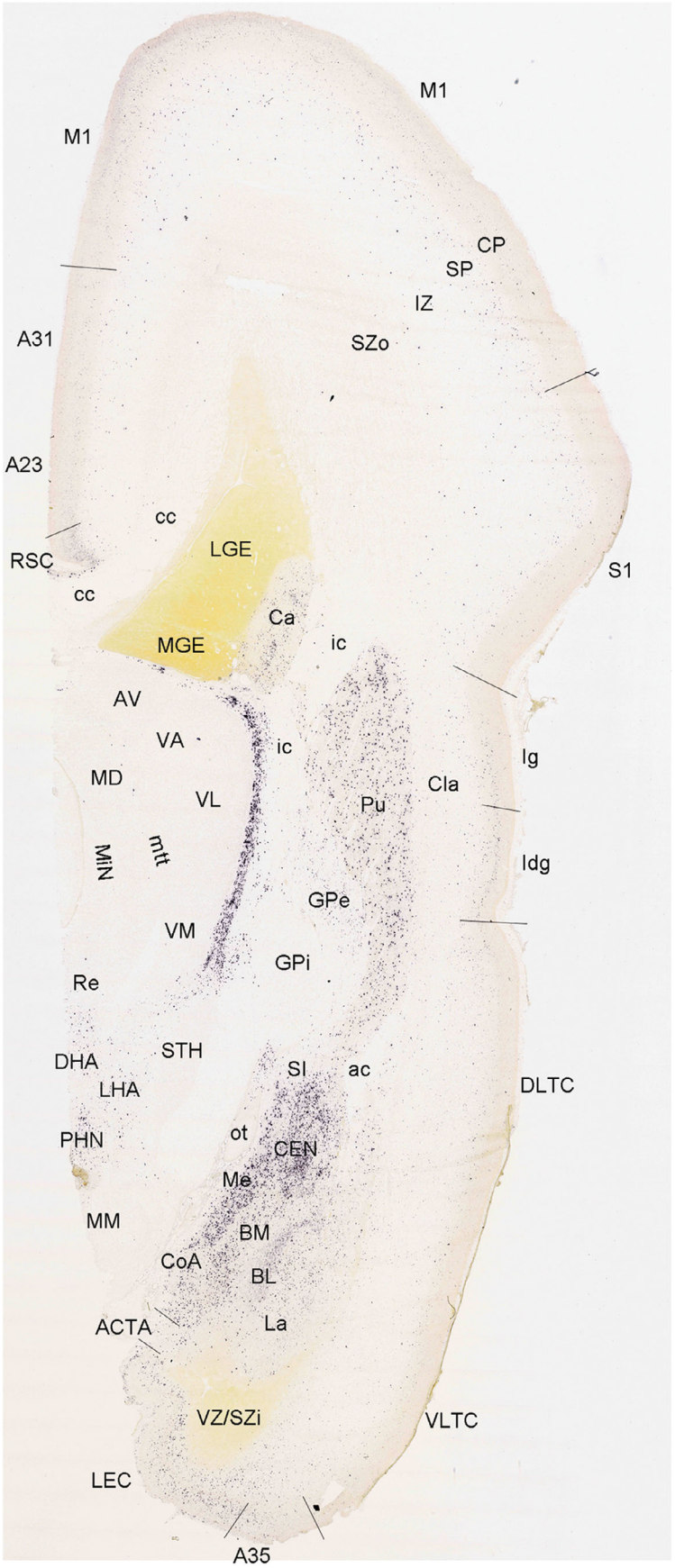

SST-02-520 (Level ~33-34)

SST-02-571 (Level ~35-36)

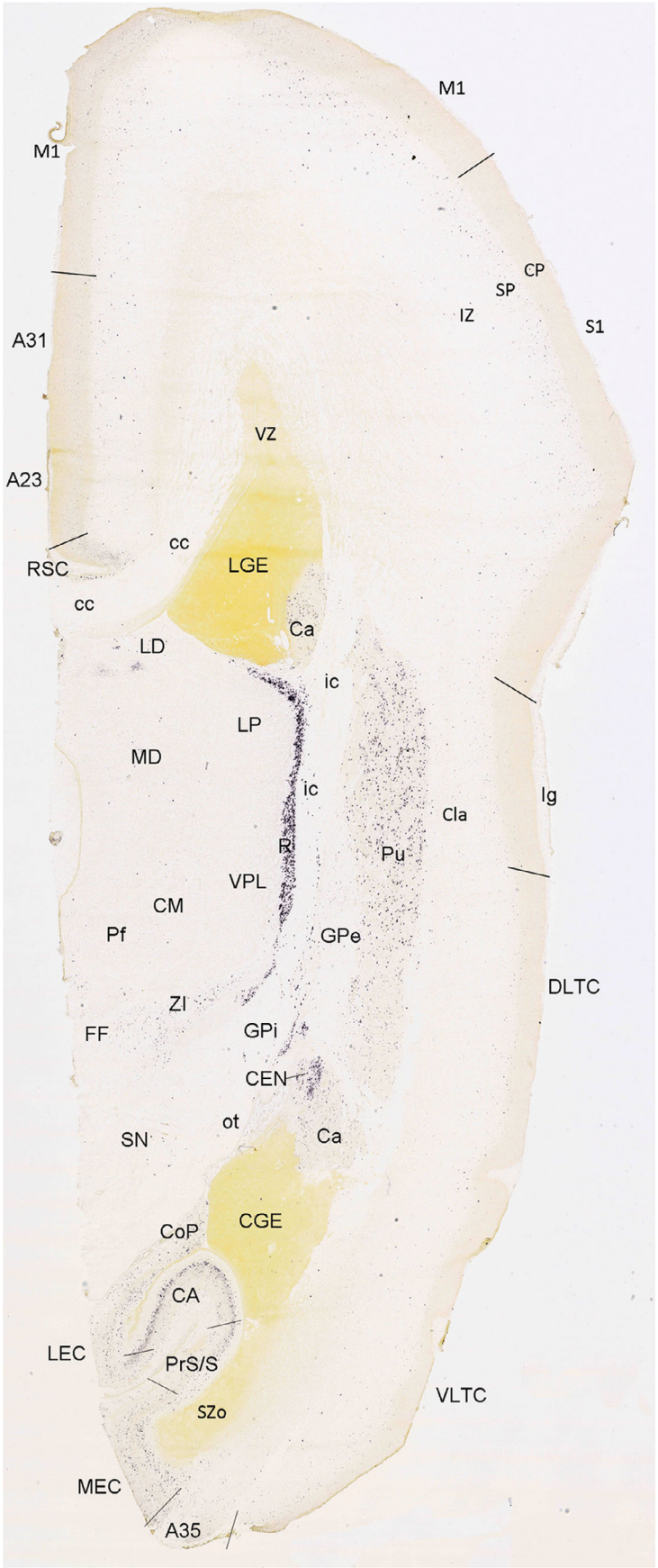

SST-02-673 (Level ~39-40)

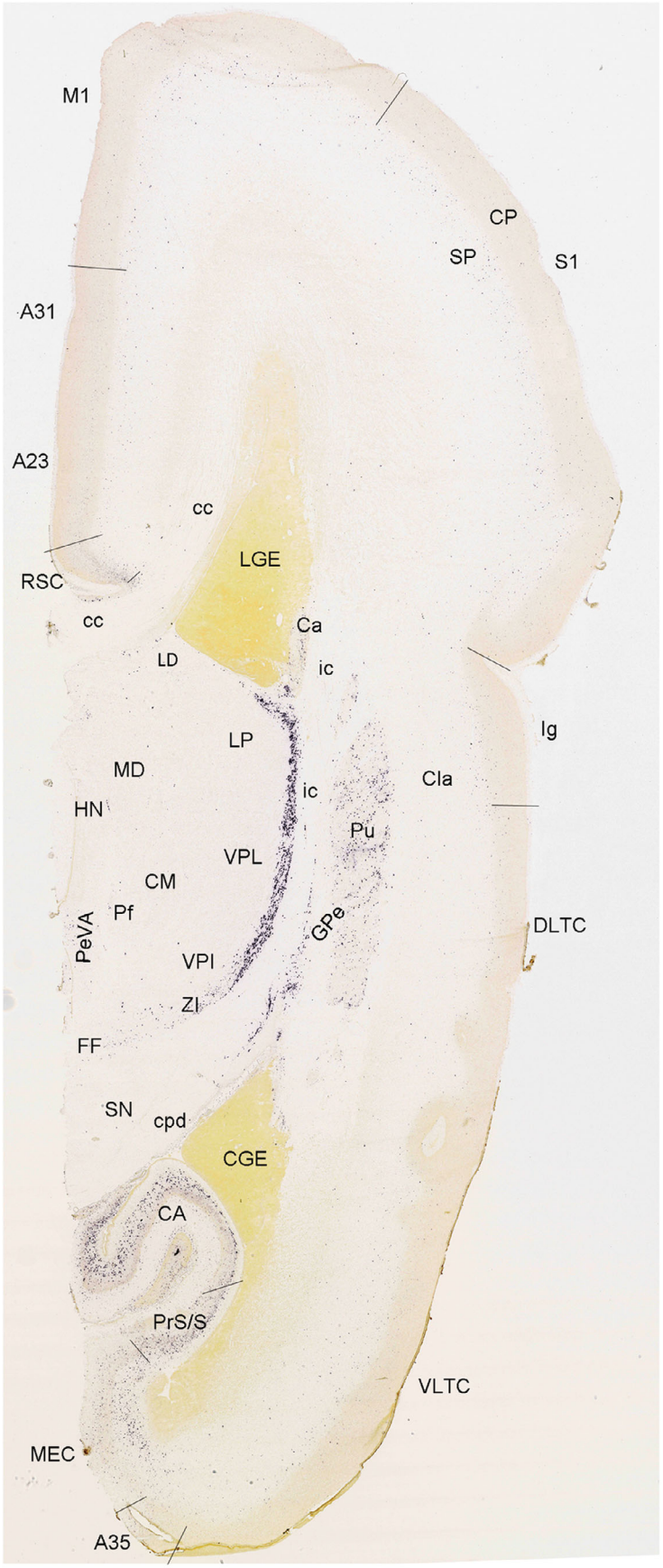

SST-02-724 (Level ~41-42)

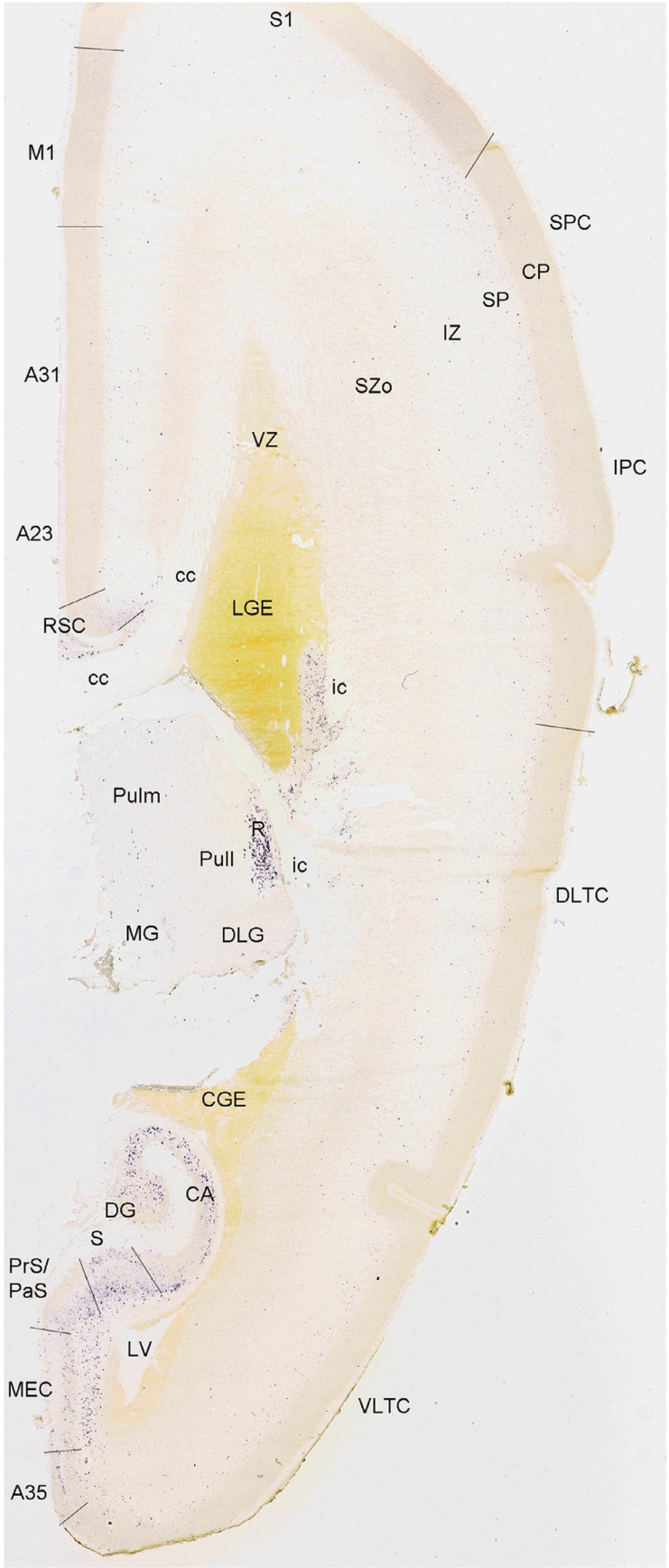

SST-03-010 (Level ~46)

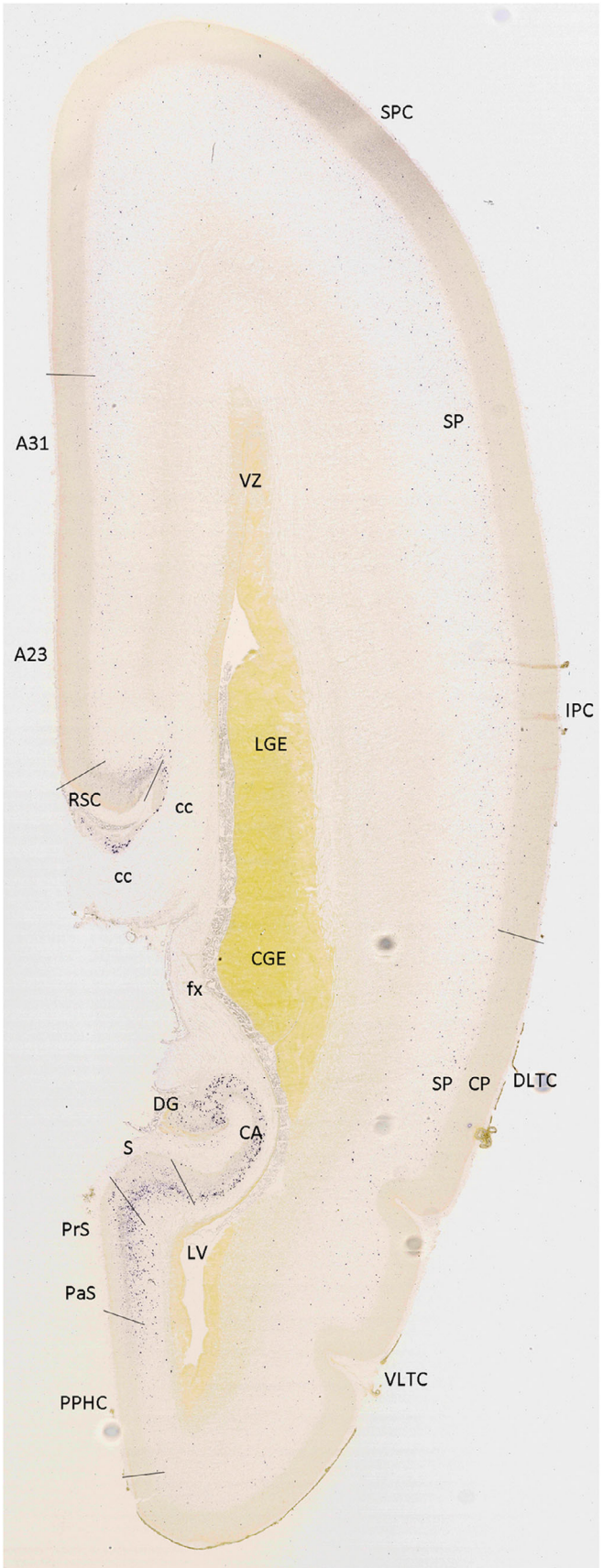

SST-03-265 (Level ~55-56)

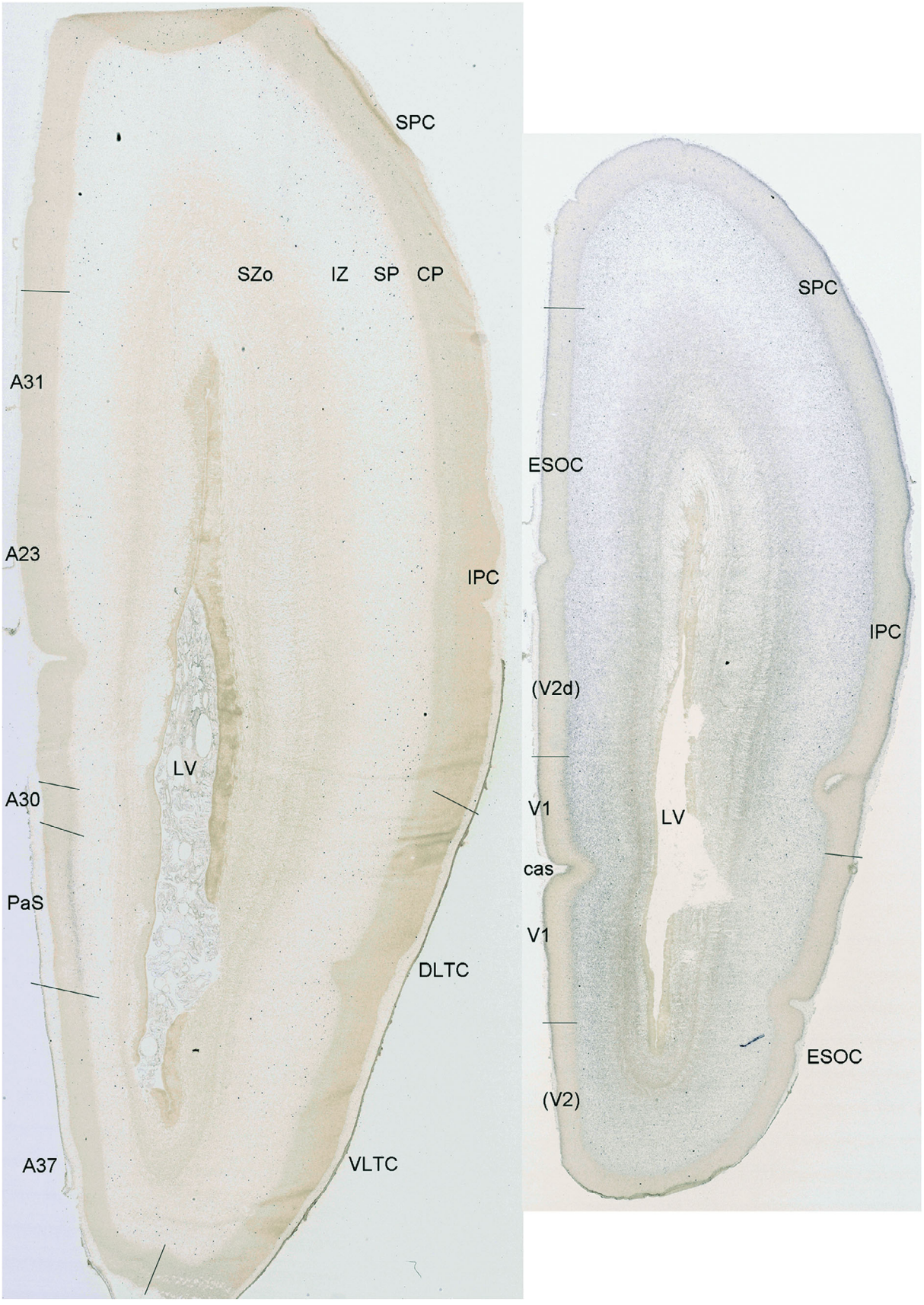

SST-03-520 (Level ~64-65) **SST-04-214 (Level ~72)**